Bone (Orthopedic Pathology)

3

A. Kevin Raymond

Introduction

Multidisciplinary should be the watchword, if not the first word, in any discussion concerning the management of bone tumors.

Even if entities arguably classified as "neoplasia" (e.g., fibrous dysplasia) are included in the analysis, primary bone tumors comprise less than 2% of neoplastic processes. Although primary bone sarcomas account for some 2–6% of childhood malignancy, they constitute less than 0.2% of malignant tumors in the general population. With some 30,000 new cases per year in the USA, multiple myeloma is the most common primary malignant bone tumor, and its study is routinely ceded to hematopathology. Osteosarcoma (1000–2000 USA new cases per year) and the half-as-common chondrosarcoma are the next most frequent primary bone sarcomas. In contrast, metastases *to* bone are at least 50–100 times more common than primary tumors of the bone.

Critical to the development of diagnostic acumen are case exposure, hands-on experience, and mentoring. The rarity of bone tumors has a negative impact on the educational and clinical experience for many. The problem of rarity is compounded by the development of consultation and referral patterns, involving both diagnosis and treatment, that results in a concentration of bone cases in a small number of institutions with a history of commitment to orthopedic oncology: an embarrassment of riches for some and virtual absenteeism for many.

As a pathologist, there is a temptation to review histological slides in the absence of so-called *biasing* clinical information. Such *blinded* review may be an interesting academic exercise, but it tends to view tumors as an abstract diagnostic problem rather than a *patient*. The histopathology of bone tumors should always be reviewed in conjunction with full knowledge of the entire clinical setting and imaging studies: the classic triad of clinical information, radiology, and pathology espoused in bone pathology. However, it should be added that with the inevitable translation of basic science to clinical application, the input of cytogenetics and molecular studies is beginning to enter clinical use and no doubt will be routinely integrated into the diagnostic armamentarium in the not-too-distant future.

Pathology-patient interaction should start at the earliest possible juncture. Patient presentation at a multidisciplinary *pre*operative conference is far superior to case presentation at a *post*operative tumor board. Preoperative presentation has the advantage of adding additional experience and varying points of view to patient evaluation before irreversible steps have been taken.

Demographics are the most basic element of necessary clinical information. With notable exceptions, all bone tumors can occur in virtually any part, of any bone, of any patient at any age. However, each primary bone tumor has *tendencies* with regard to age, gender, and skeletal site of origin. Although not absolute, these tendencies can be extremely helpful for assessment of diagnostic probabilities and aid in identifying potential avenues of clinical and pathology investigation that are most likely to be of benefit.

Anatomically, the bones may be viewed as being composed of *structures* and *compartments*. The structures include the cortex, cancellous bone, growth plates, and articular surfaces. In tubular bones formed through endochondral ossification, these structures define compartments that subdivide the medullary cavity into physis (i.e., epiphyses or apophyses), metaphysis, and diaphysis (Fig. 3.1). Epiphyses constitute compartments bounded by an articular surface and a growth plate. In contrast, apophyses are bounded by bone and a growth plate, e.g., femoral greater and lesser trochanters. The diaphysis is that part of the bone in which the cortices are parallel. The metaphysis lies between the epiphysis and diaphysis and constitutes the portion of the bone in which the cortices are nonparallel, i.e., diverging or converging. In addition, cancellous bone is essentially confined to

A. K. Raymond (✉)
Department of Pathology, The University of Texas MD Anderson Cancer Center, Houston, TX, USA

C. A. Moran et al. (eds.), *Oncological Surgical Pathology*, https://doi.org/10.1007/978-3-319-96681-6_3

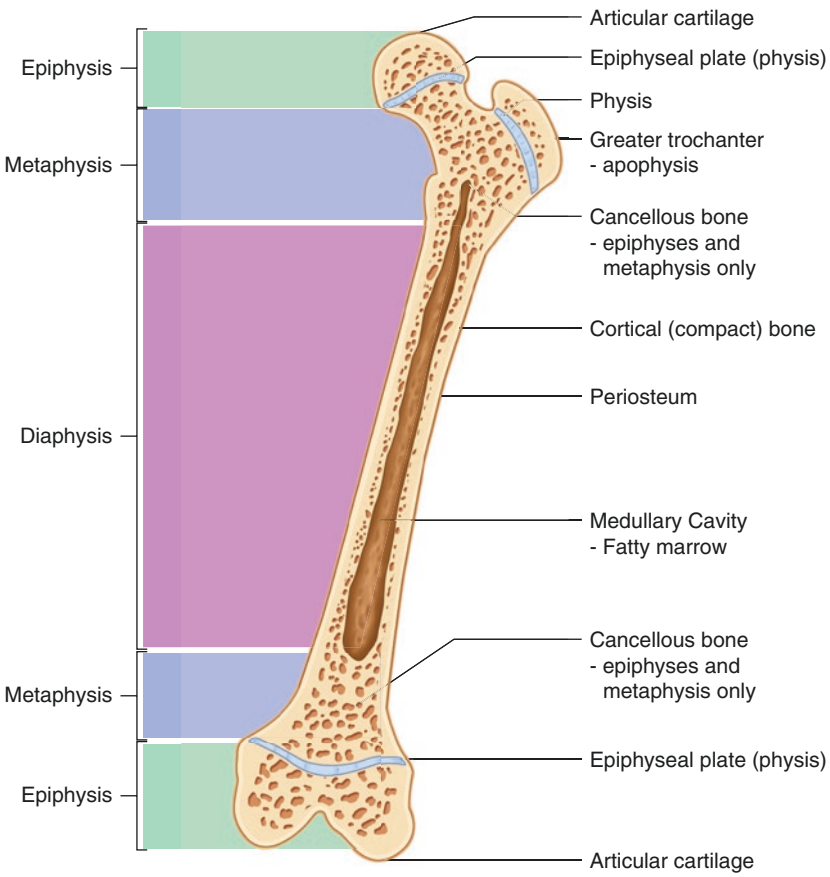

Fig. 3.1 Appendicular bone anatomy. Bones formed via endochondral ossification can largely be viewed as being composed of structures (cortex, physis, articular surface, cancellous bone) that divide the medullary cavity into compartments (i.e., epiphysis, metaphysis, diaphysis). (©2009 Encyclopædia Britannica, Inc.)

the epiphysis and metaphysis while virtually absent in the diaphysis. After skeletal maturity and growth plate involution, one of the physes defining boundaries is technically absent, and terminology becomes a bit inconsistent; for our purposes we will continue to refer to these areas as epiphyses and apophyses.

Individual primary bone tumors show preferences for particular bones, and even specific parts of those bones (Fig. 3.2). Although tumors may originate on or within the cortex, most arise within the medullary cavity. Bone tumors arising within the medullary cavity are deemed *central*, while those originating outside of the medullary cavity and cortex are frequently referred to as *peripheral* tumors.

In discussing bone tumor management, the pathology literature uniformly recommends reviewing patient imaging studies in conjunction with gross and histological materials, ignoring the likely lack of formal radiology training or experience. At the same time, it should be pointed out that the factors impacting pathology experience with bone tumors also confront radiology. Therefore, it is helpful that pathologists working with bone tumors have an elemental working knowledge of skeletal radiology. Although a detailed review of skeletal radiology is beyond the scope of this work, a number of points should be made, both theoretical and practical.

The radiographic work-up is a goal-oriented algorithm intended to characterize the primary lesion while establishing the extent of local-regional tumor as well as identifying systemic disease. The usual work-up includes plane films of the primary site, skeletal survey, computerized transaxial tomography (i.e., CT), magnetic resonance imaging (i.e., MRI), bone scan, and specialized studies as needed, e.g., arteriogram and positron emission tomography (i.e., PET scan).

Plane films, AP and lateral, remain the mainstay of skeletal radiology, particularly in the evaluation of lesions involving the appendicular skeleton. On the other hand, when working with the axial skeleton or non-tubular bones of the appendicular skeleton, plane films act more as a preliminary screening, while CT has become the definitive study. At the same time, regardless of skeletal site, CT can provide detailed information of all bone lesions, as well as assessing the status of surrounding normal bone, and reactive changes.

Much of routine, plane film bone imaging is done in a fashion that provides information concerning joints and soft

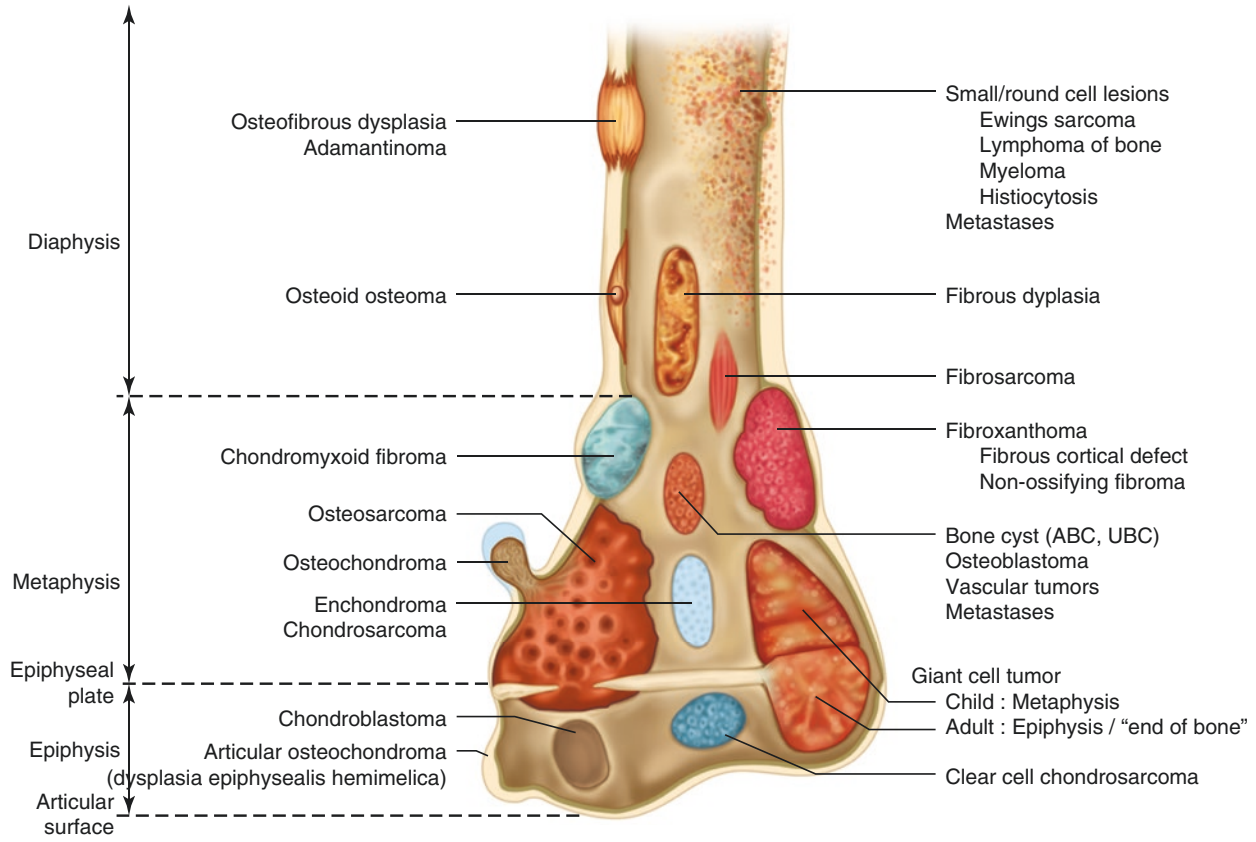

Fig. 3.2 Each bone tumor shows predilection for specific bones. In addition, each bone tumor shows preferential involvement of specific bone parts

tissues in addition to the bone. A skeletal survey is a series of plane films that includes all bones but is performed in a manner (i.e., orientation and exposure) that optimizes *bone* analysis.

A wealth of information can be provided through the skillful analysis and interpretation of CT and MRI. Perhaps, most importantly, these studies provide the most reliable, preoperative information concerning tumor size and locoregional extent of disease.

Although no longer in the central role it formerly occupied, skeletal scintigraphy (i.e., Tm^{99} bone scan) still provides information. It is a useful tool for identifying tumor multicentricity including both skip metastases and systemic dissemination. A problem with bone scan is that it combines a high degree of sensitivity with a low level of specificity. Tm^{99} bone scan will show increased radioactive tracer uptake in areas of bone remodeling and therefore will show increased activity in any area of stress, routinely around most joints. Therefore, a useful practice is to establish an initial baseline, evaluate for multicentricity, and then repeat the test after passage of a predetermined period of time with an eye toward identifying any change over time.

In reviewing imaging studies, it is useful to establish a routine (Table 3.1). Identify the site of the tumor including the specific bone(s) and the position within the bone including the end, the part of the bone, the compartment involved, and the position within the involved compartment. Establishing the plane film characteristics of the lesion usually points to the lesional tissue type and in turn a diagnosis or at least a differential diagnosis; parameters to analyze include lesion size, shape, as well as the quantitative and qualitative status of mineralization. The form and extent of the tumor/normal bone interface (i.e., *transition zone*) generally provides information concerning tumor biology and potential growth characteristics. Aggressive lesions tend to be ill-defined and have a protracted, infiltrative interface. In contrast, quiescent lesions tend to have narrow transition zones that are circumscribed and well-defined. The presence or absence and form of any reactive bone can provide additional information concerning the lesion growth characteristics.

In addition, when interpreting skeletal imaging studies, it is helpful to keep in mind a couple of other things:

- Plane films remain the anchor of skeletal radiology; however, in order to show radiolucent changes on plane films, pathological processes must involve and alter the cortex. Simply put, there is a minimum calcium density that must

Table 3.1 Skeletal radiology initial review: the table is meant as a quick checklist of items to analyze when reviewing plane films and/or CT during review of skeletal imaging studies

Location			
Bone	Specific bone		
End	Proximal	Mid	Distal
Orientation	On cortex	Within cortex	Under cortex
Compartment	Epiphysis	Metaphysis	Diaphysis
Position	Central	Eccentric	
Character			
Destructive	Cortex	Cancellous	
Mineralization	Blastic	Lytic	Mixed blastic/lytic
Blastic	Bone	Cartilage	Other
Lytic	Purely lytic	Mixed	Internal structure: Cystic Soap bubble
Interface: tumor/normal			
Geographic	Well defined	Sharply circumscribed	Sclerotic interface
Ill defined	Vague	Infiltrative	
Reactive bone formation			
Periosteal	Spiculated ("sunburn")	Finely laminated ("onionskin")	Layered
Ill-defined	Vague	Infiltrative	
Pathological fracture			

be altered to manifest lytic changes on plane films. Cancellous bone does not have sufficient calcium density for destructive changes to consistently, and significantly impact plane film images [1].

- The term "soft tissue mass" reflects a radiographic finding which may or may not have corresponding anatomical correlation. The periosteum is not easily penetrated by pathological processes and many radiographic soft tissue masses correspond to tumor outside the cortex but still confined beneath the periosteum.

Historically, open biopsy has been the diagnostic tool of choice, "big diagnosis, big tissue." Biopsy could be performed in conjunction with frozen section analysis at the time of definitive surgery or as an independent first of two procedures. Although bone frozen section analysis is frequently frowned upon by pathologists because of the consequences of cutting calcified materials, there is generally sufficient unmineralized tissue within these biopsies to allow unimpeded frozen section preparation. Also, the advent of inexpensive disposable microtome blades has greatly reduced the consequences of cutting focally mineralized tissue.

However, the incision required to provide sufficient exposure to acquire open biopsy tissue is almost always sizable, e.g., 10–20 cm. Post-biopsy, the incision must be considered entirely tumor-contaminated and removed at the time of definitive surgery to avoid the consequences of tumor local relapse. At a time when amputation was the treatment of choice for malignant bone tumors, biopsy incisions were automatically included with surgical specimens; therefore, open biopsy and its consequences posed an issue of lesser significance.

However, with the development of resection techniques, the production of functional prostheses, and the evolution of reconstruction procedures, limb-sparing surgery became the treatment of choice in appropriately selected patients, and the issue of tumor-contaminated biopsy incisions became consequential. Currently, diagnosis in the absence of soft tissue contamination is feasible in the vast majority of bone tumors through the judicious use of needle biopsy, fine needle aspiration, and/or core biopsy. It should be noted that bone needle biopsy is no longer considered an experimental procedure but, to many, the standard of care. At the same time, it must be emphasized that the most frequent reason for denial of limb-salvage surgery is an inappropriately performed open biopsy.

With knowledge of the clinical and radiographic background, pathology-patient contact frequently begins with specimen receipt. Simply put, the minimum job of the pathologist is confirmation of specimen, dissection, description, tissue fixation, decalcification, tissue processing, histological review, and reporting. In addition, there are the possibilities of specimen photography and tissue acquisition for special studies and research. Most importantly, there is the need for seamless communication; one too many conversations is far better than one too few.

Initial pathologist/specimen contact may occur at the time of intraoperative consultation. This may be in the form of diagnostic frozen section, margin assessment, or a request for immediate dissection to view the tumor with related soft tissues to expedite intraoperative planning. As already indicated, whether it be needle biopsy, curettings, resection, or amputation, there is generally sufficient tumor soft parts to allow diagnostic frozen section. Resection margin examination is generally a function of gross examination. Although all cases must be individualized, the presence of freely mobile soft tissue overlying tumor virtually assures that the corresponding margin is free of tumor; and consideration of limiting margin pursuit to gross examination is legitimate. However, if the soft tissues are fixed to tumor, in an area approaching the margin, frozen sections to document the relationship between tumor and margin are justified. It should be kept in mind that although the vast majority of bone tumors grow as a cohesive mass, there are a number of tumors renowned for having foci of tumor independent of the main mass with normal marrow between, so-called skip metastases. Tumors in which this is a recognized danger include osteosarcoma, chondrosarcoma,

adamantinoma, and vascular tumors. Therefore, margin evaluation must be done in conjunction with imaging review, focusing on those tests that reliably detect multicentricity, bone scan and more importantly MRI.

A detailed discussion of specimen dissection is beyond the scope of this chapter and has been the subject prior publications [2]. However, a number of procedural points deserve comment.

When multiple needle cores are submitted, we suggest submitting them in individual cassettes, thus eliminating the problem of cores being embedded at different depths and angles within the paraffin block(s). As a result of optimal specimen orientation, full-face sections can be cut with minimal tissue loss, and special studies can be performed selectively thus allowing maximum retention of tissue for potential future studies.

The tissue obtained in curetting/open biopsy specimens is generally immersed in blood. To see the true appearance of the specimen and optimize tissue fixation, the specimen should be washed either with water, normal saline, or formalin: selected specimen fragments to container, add fluid, shake and decant, and repeat as needed.

The dissection of major specimens should be done on fresh tissue, after radiology/pathology correlation and as close to the time of surgery as possible. The specimen should be reduced to the bone of origin, tumor and any local tumor extension by removing as much normal tissue as feasible prior to cutting the specimen with a saw. The soft tissues are removed for both esthetics and safety. Room temperature, fresh, soft tissue may catch on the saw blade, resulting in loss of control of a moving specimen and potential prosector injury.

Most prosectors incise into or immediately adjacent to tumor and spread out normal tissues as the dissection proceeds, effectively dissecting in a tight, narrow incision. Ultimately this approach leads to removing bulk tissue by cutting across tissues in a relatively random fashion, as one attempts to reduce the specimen while gaining exposure.

An alternative is suggested: first remove the skin from the specimen; this increases specimen exposure while eliminating the confining influence of skin. The overwhelming majority of further soft tissue dissection is then a matter of removing skeletal muscles in what is essentially a sequential, layered fashion allowing easier and orderly dissection.

A "bone saw" is used to make the initial longitudinal (i.e., sagittal or coronal plane) or transaxial cuts in the bone following removal of the soft tissues. A high-speed, heavy-duty meat saw with a one half inch to three quarter inch blade is preferred for making these initial cuts. The heavy-duty saw is both more dangerous and safer than lighter equipment (e.g., jigsaw, striker saw). The more powerful motor and stronger blade allow the saw to cut through bone more easily, allowing better control of specimen and greater precision in guiding the bone through the saw. In turn, this decreases the pressure required to push the bone through the saw and largely eliminates accidents caused by pushing too hard and losing control of the specimen during cutting. At the same time with the more powerful blade, any accident will likely be more damaging. When working with the bone saw, always plan for possible problems; hope for the best, but always plan for the worst by considering various negative scenarios in advance. After cutting the specimen, the resulting cut surface must be washed to eliminate bone dust that cutting may have embedded in the interstices of cancellous and cortical bone; running water and light effort with a surgical hand brush are generally adequate to the task.

Following bone saw dissection, the bone must be cut into pieces that fit the pathology processing cassettes. The Isomet® is a small, tabletop geology saw that allows bone to be cut into precise small pieces of uniform size and thickness with minimal artifacts (e.g., bone dust) and is well-suited to this task. Some laboratories fix and decalcify the large sections/slabs of bone resulting from the initial bone saw cut. After decal, the specimen can be cut by routine laboratory tools. However, we prefer using the Isomet®; we have found that cutting the mineralized bone into pieces that fit processing cassettes allows for easier and more thorough processing.

Freezing whole specimens so that the bone, tumor, and normal tissues can be viewed together and photographed is not recommended for routine use. Freezing introduces artifacts analogous to those seen in frozen sections, i.e., so-called frozen section artifact. However, if there is a pressing reason for whole surface demonstration and photography, there is a protocol. First, the plane of section/demonstration must be established; if you *need* it, you can define it. Tissue for diagnosis is obtained from planes parallel to the ultimate cut surface. Following tissue acquisition, the specimen is reassembled and frozen; a minus 70° freezer is preferable. After 2 or 3 days of freezing, the specimen can be safely cut on the band saw.

Other than "mapping" or other standardized procedures, the amount of tissue submitted for histological examination in curetting and definitive surgical specimens is somewhat arbitrary. In general pathology, tissue submission is a function of the concept of "representative sections," which in turn requires the ability to grossly distinguish between specific pathology and normal and secondary changes.

Because of their relatively non-specific gross appearance and the frequent superimposition of secondary reactive, degenerative, and/or inflammatory processes, the concept of "representative sections" is difficult to precisely define and apply to bone tumors. We generally use the soft tissue formula of one cassette per centimeter of homogeneous tumor. Additional sections are then submitted from any heterogeneous components.

Table 3.2 Classification of bone tumors. Division of tumors by tissue type and subdivided by benign vs malignant

Tissue/phenotype	Benign neoplasm	Malignant neoplasm
Cartilage	Osteochondroma Chondroma Chondroblastoma Chondromyxoid fibroma	Chondrosarcoma Conventional Variants
Bone	Osteoid osteoma Osteoblastoma	Osteosarcoma Conventional Variants
Fibrous	Metaphysical fibrous cortical defect Nonossifying fibroma Fibrous histiocytoma Desmoplastic fibroma Fibrous dysplasia Osteofibrous dysplasia	Unclassified pleomorphic sarcoma Malignant fibrous histiocytoma Fibrosarcoma
Notochord	Benign notochordal cell tumor	Chordoma and Variants
Uncertain		Ewing's sarcoma Adamantinoma
	Giant cell tumor of bone	Malignancy in giant cell tumor of bone
Hematopoietic	Plasmacytoma Histiocytosis	Myeloma Lymphoma
Vascular	Hemangioma Epithelioid hemangioma	Epithelioid hemangioendothelioma Angiosarcoma
Adipose tissue	Lipoma	Liposarcoma
Nerve sheath	Neurofibroma Schwannoma	Malignant peripheral nerve sheath tumor
Smooth muscle	Leiomyoma	Leiomyosarcoma

The cassetted tissue is then submitted for fixation, decalcification, and routine processing. We prefer fixation with a 10% solution of neutral, buffered formalin. A number of decalcification processes are available; we use dilute formic acid. We use specimen radiographs to monitor decalcification.

At some future time, cytogenetics and molecular pathology will determine appropriate tumor-specific treatment niches. However, for the foreseeable future, histopathology remains the diagnostic standard of care with special studies answering specific needs. Although there are minor differences, current classification systems are based on dividing bone into its constituent tissue types and subdividing lesions into the benign and malignant lesions expressing a given phenotype (Table 3.2). At the same time, it is recognized that there are certain tumors that are almost unique to bone, while the remaining mesenchymal lesions are more common in soft tissue tumors. This chapter will focus on the bone unique lesions.

Overall, bone tumor grading has long been a contentious topic. Historically, grading has been largely based on the semiquantitative analysis of tumor cellularity and degree of atypia, parameters that frequently progress in parallel. Mitotic activity and necrosis may impact interpretation but, for the most part, are not generally considered "hard" criteria. Admittedly, criteria for numerical grading are frequently somewhat ethereal and of questionable reproducibility. However, with the advantage of well-defined classification and subclassification criteria, grading is relegated to "another parameter" that allows rough estimation of relative tumor aggression within a given category. Grading also forms the basis for staging. For the most part, tumor grade is inherent within bone tumor classification and is reduced to an evaluation of high versus low grade (Table 3.3). Formal numerical grading is largely restricted to primary soft tissue tumors and defined osseous exceptions.

The concept of "dedifferentiation" began in skeletal pathology in reference to an unusual subset of chondrosarcoma and has now been expanded to virtually all forms of low-grade malignant bone tumors. Histologically, dedifferentiation consists of superimposition of a form of high-grade sarcoma (e.g., osteosarcoma, fibrosarcoma, unclassified sarcoma) upon an underlying low-grade sarcoma. The low- and high-grade components do not mix, and there is no transition between the two components, almost as if they were a collision of two unrelated neoplastic processes. While the low-grade tumor may be the dominant component, it is the high-grade sarcoma that determines the ultimate biological potential of a dedifferentiated sarcoma. In general, the prognosis in dedifferentiated sarcomas is poor, and they are by definition considered high grade.

Many/most orthopedic surgeons adhere to the staging system proposed by the Musculoskeletal Tumor Society (i.e., so-called Enneking system) which incorporates the terms *grade* and *stage* in an at times confounding way. Tumors are assigned a numerical stage (i.e., I–III) with alphabetic subdivisions (i.e., A vs B). The system is based on the evaluation of three parameters: tumor grade, extent of local tumor involvement at the primary site, and the presence or absence

Table 3.3 Grading of bone tumors. Bone tumor grade is largely a function of diagnosis; as indicated, there are exceptions to this general principal

Grade 1: Low grade	
	Chondrosarcoma, clear cell
	Osteosarcoma, low-grade central and parosteal
Grade 2: Intermediate grade	
	Adamantinoma
	Periosteal osteosarcoma
Grade 3: High grade	
	Chondrosarcoma, dedifferentiated and mesenchymal
	Chordoma, dedifferentiated
	Ewing sarcoma/PNET
	Giant cell tumor, "malignant"
	Osteosarcoma, conventional
	Osteosarcoma, high-grade surface and dedifferentiated parosteal OS
	Osteosarcoma, secondary
	Osteosarcoma, small cell and telangiectatic
Variable grade	
	Chondrosarcoma, conventional (grades 1–3)
	Lymphoma (grade by classification)
	Soft tissue-like sarcomas (i.e., leiomyosarcoma, angiosarcoma)
	Spindle-cell sarcoma (histological grade)
Ungraded	
	Chordoma, conventional

Modified from WHO

of metastases. In this system, all primary bone tumors are divided into low- and high-grade. In the absence of metastases, low-grade tumors assigned a numerical Stage of I, while high-grade tumors define Stage of II. The presence of systemic metastases results in Stage III assignment. Tumors confined within cortex are subdivision "A" (i.e., "intracompartmental"). Tumors extending through cortex are designated "B" (i.e., "extracompartmental").

Although frequently misrepresented as being a function of size, orthopedic specimen types are defined in terms of the extent of their resection margins: intralesional, marginal, wide, and radical. As the name would imply, *intralesional* procedures are those in which no effort is made to have a free resection margin (e.g., curettings), primarily used in "open biopsy," benign lesion treatment, and debulking procedures. *Marginal* specimens are those in which an attempt is made to remove the entire tumor, but the reactive interface between tumor and normal bone is not completely removed, and therefore the resection margin may be involved. *Wide resection margins* are those in which a tumor is completely removed, with a cuff of normal tissue, but portions of the involved compartment(s) are left in place. A *radical specimen* is one in which the tumor and the entire involved compartment are removed with a cuff of normal tissue.

Historically, the study of bone tumors has lagged behind other disciplines in the use of what might be termed special studies, e.g., special stains, immunohistochemistry, cytogenetics, and molecular studies. This is at least partially explained by the need for harsh processing procedures (i.e., decalcification) during the routine management of these specimens. However, with greater attention to detail, and an increasing interest in their use, we have entered a period of rapid advancement in this area.

Here is a final thought for the readers. Historically, there have been limited authoritative texts addressing bone tumors. We are now at a juncture where we have a wealth of riches from a broad range of investigators with an extraordinary talent for organization and presentation [1–21].

Cartilage Neoplasia (Fig. 3.3)

Osteochondroma

Definition

Solitary osteochondroma is alternately considered either a developmental anomaly [1] or benign hyaline cartilage tumor [10]. The lesion itself is a cartilage "cap" that may be either sessile or stalked. The purposes of discussion osteochondroma will be referred to as a "tumor."

Introduction

Osteochondroma comprises some 33% of benign bone tumors and 10% of all bone tumors [22]. Being largely asymptomatic, many consider these numbers a significant underestimation.

Although initial presentation may be at any age, the peak incidence of osteochondroma is in the second decade of life, with a somewhat lower incidence in the first and third decades. Men are affected more frequently than women, with the male to female ratio ranging from 5:3 to 2:1. Osteochondroma may originate from any bone formed through endochondral ossification. Some 85% of osteochondromas are "solitary osteochondromas," and they most frequently involve the distal femur, proximal humerus, and proximal tibia. The remaining 15% are forms of multiple exostosis/osteochondromatosis and tend to be multifocal [22, 23]. Rarely, osteochondroma may present as a postradiation phenomenon [1, 24].

Clinical

The natural history of osteochondroma is one of gradual growth until skeletal maturity followed by cartilage cap involution and lesional growth cessation. Osteochondroma starts as a cartilage "plug" within a cortical defect in the region of the growth plate (Fig. 3.4). With time, the lesion may: 1) stay the same, 2) enlarge through largely centrifugal growth, but

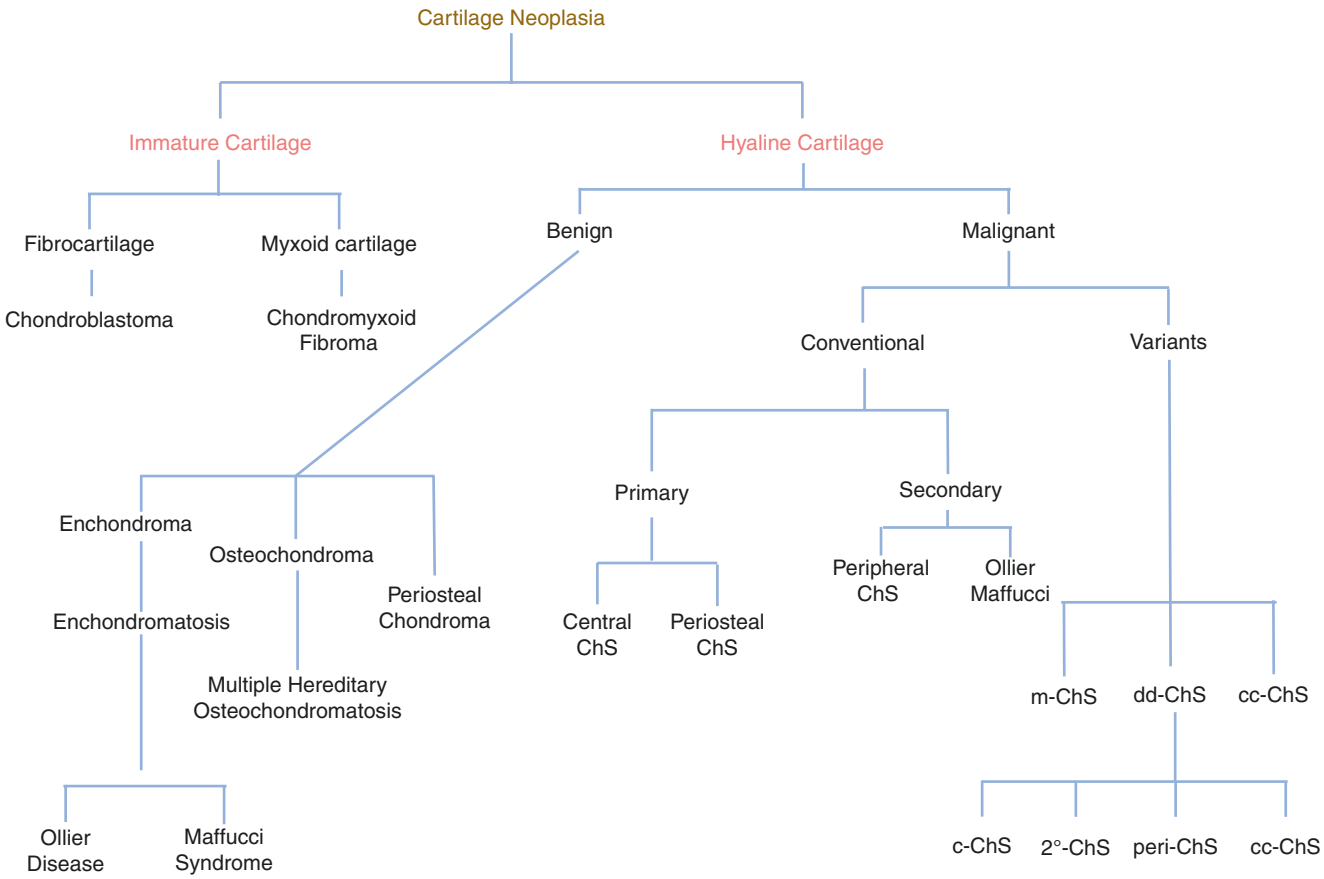

Fig. 3.3 Cartilage tree chart showing relationships in classification of cartilage neoplasia

remain largely contained by cortex and periosteum or 3) begin growing perpendicular to the long axis of the parent bone and develop a "stalk". Growth is a function of endochondral ossification of the cartilage cap resulting in the formation of a tubular stalk consisting of cortices continuous with the parent bone cortex surrounding a medullary cavity that is continuous with the parent bone medullary cavity. If stalked, early perpendicular growth is followed by sessional growth away from the nearest joint as a response to forces generated by overlying soft tissues. The cartilage cap continues to grow during skeletal development and may have surprising/worrisome radiographic and histological changes during the second growth period. However, with skeletal maturity, the cartilage component involutes, leaving behind any stalk topped by a rudimentary cartilage cap. Secondary malignancy occurs in far less than 1% of osteochondromas.

The majority of osteochondromas are asymptomatic and discovered during imaging studies performed for unrelated reasons; the majority of these go unreported, ergo the belief that the incidence of osteochondroma is underestimated. Growth of lesion may result in a slowly enlarging palpable mass. Fracture through the stalk results in pain. Symptoms may evolve as a function of tumor size and location. Mass effect with compression of neurovascular elements or other vital structures may result in local or referred symptoms. Large lesions may induce bursa formation that may then evolve bursitis-like symptoms.

In the absence of symptoms or suspicion of secondary malignancy, treatment is limited to observation. With symptomatology, complete surgical excision is the treatment of choice.

Changes that may signal the development of secondary chondrosarcoma include cartilage cap >2 cm thick after skeletal maturity, continued growth of the cartilage cap after skeletal maturity of the involved parent bone, and the appearance of new pain in the area of the osteochondroma. None of these findings are diagnostic, but their potential association with malignancy raises their significance.

Histopathology

The "cartilage cap" is the lesional tissue of the osteochondroma. It is composed of gray-blue to gray-white cartilage with architecture and cytology largely recapitulating growing cartilage (Fig. 3.4) and mimicking the appearance of the active epiphyseal plate. Older, more quiescent lesions largely mimic the appearance of an articular surface. Some lesions

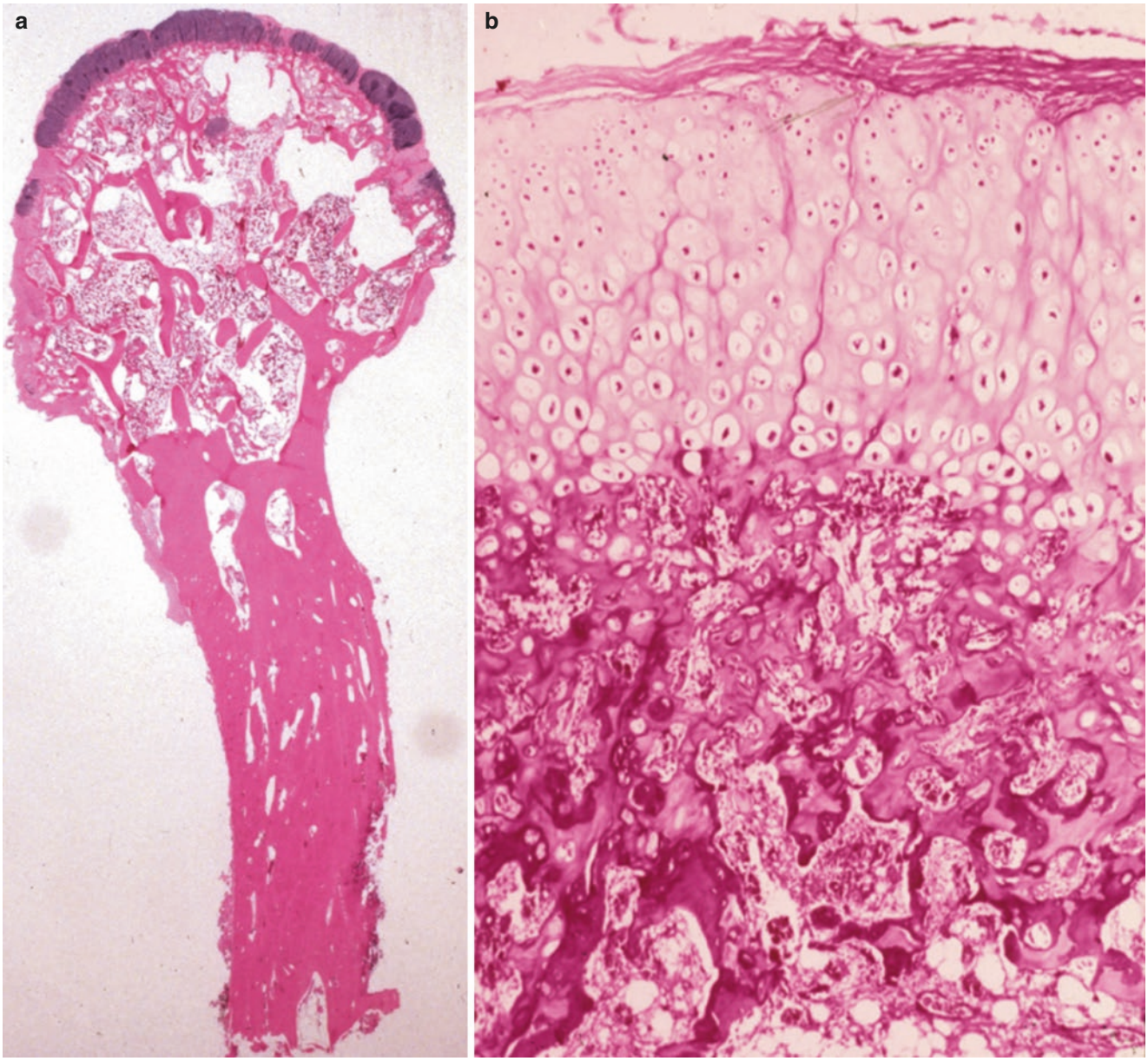

Fig. 3.4 (**a**) Osteochondroma: scan of whole mount. Stalked lesions with cartilage cap. (**b**) Osteochondroma: higher power of cartilage cap; architecture recapitulates that of growing epiphyseal plate. (Courtesy of A. Kevin Raymond, M.D.)

never develop a vertical growth phase and remained confined within the cortical defect from which the lesion originated, *sessile osteochondroma* (Fig. 3.5). However, the more typical picture is that of a stalked lesion with the cartilage cap at the apex overlying a tubular bone stalk with its cortices and medullary cavity in continuity with those of their parent bone counterparts (Fig. 3.6). The cytological features of the individual neoplastic cells reflect the presence or absence of active growth. In the mature, inactive lesion, the nuclei are small hyperchromatic blue to purple to black dots with minimal nuclear detail. Cytoplasm is also minimal. In actively growing lesions, there tends to be more nuclear detail and cytoplasmic detail; but atypia is absent. Mitoses are extraordinarily rare.

Gross Pathology

The gross appearance of osteochondroma can be difficult to appreciate in fragmented specimens, fragments of bone and cartilage, which may or may not have an obvious physical relationship to each other. However, intact osteochondromas consist of a lobulated cartilage mass atop a tubular bone stalk (Fig. 3.7). The cut surface of the cartilage component varies

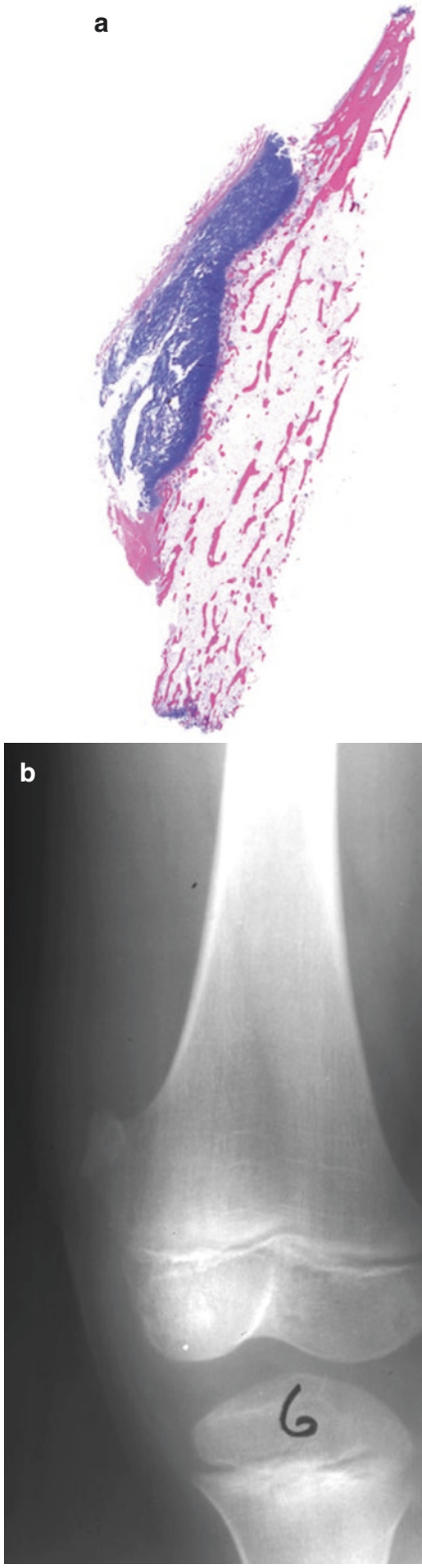

Fig. 3.5 (**a**) Osteochondroma: scan of whole mount; low power. Sessile lesion with cartilage component within a defect in the cortex. (**b**) Osteochondroma: plane film of sessile osteochondroma. (Courtesy of A. Kevin Raymond, M.D.)

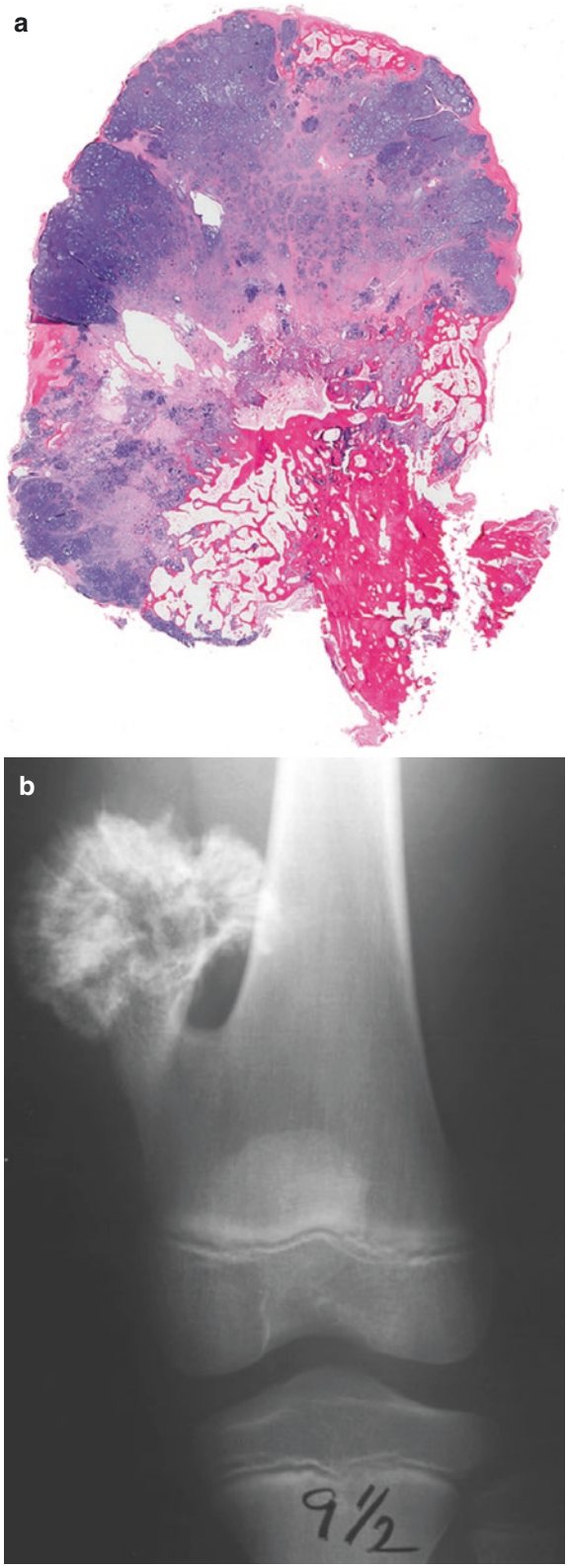

Fig. 3.6 (**a**) Osteochondroma: scan of whole mount; low power. Stalked lesion in young, growing patient with very thick cartilage cap. (**b**) Osteochondroma: plane film of stalked osteochondroma. Note continuity of osteochondroma cortices and medullary cavities of osteochondroma and parent bone. (Courtesy of A. Kevin Raymond, M.D.)

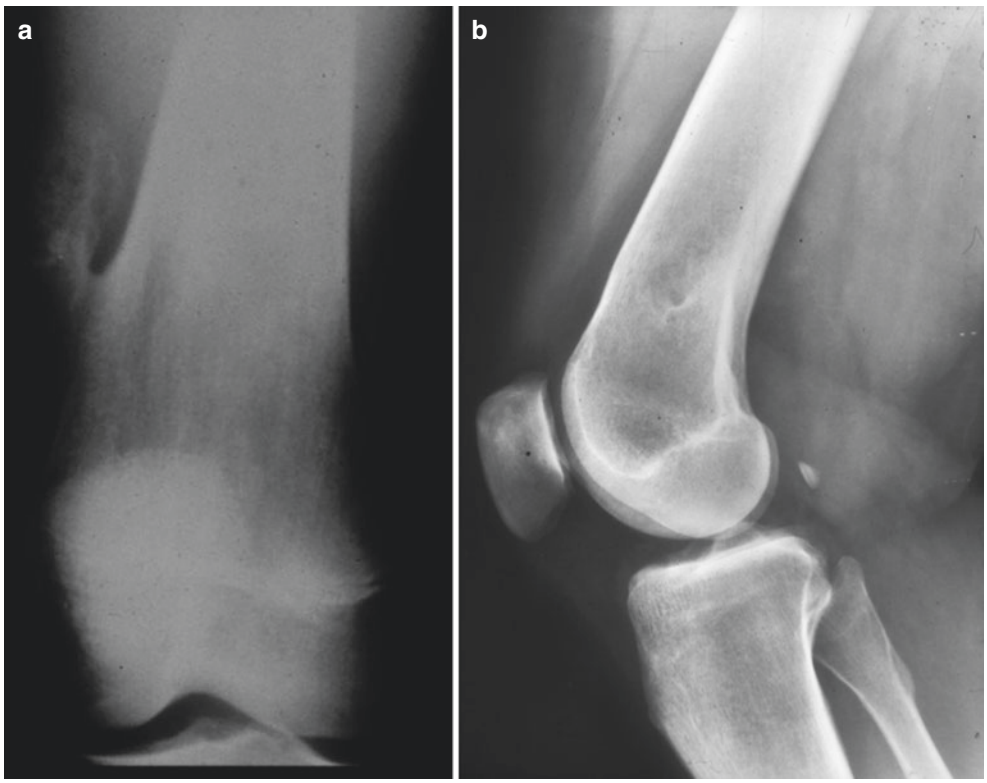

Fig. 3.7 (**a**) Osteochondroma: plane film (AP) showing osteochondroma with continuity of lesion and parent bone cortices and medullary cavities. Note that lesion has curved stalk causing lesion to "grow away from" the nearest joint. (**b**) Osteochondroma: plane film (lateral) showing osteochondroma; same case as (**a**). The patient is rotated 90°. The osteochondroma is represented by the small area of sclerosis surrounding a focus of radiolucency. The latter changes are secondary to superimposition of the cortices and medullary cavities of the osteochondroma and the parent bone. (Courtesy of A. Kevin Raymond, M.D.)

from gray-blue to gray-white to white, glistening, and semitranslucent with focal chalky white areas corresponding to mineralization. The stalk consists of cortices of lamellar bone surrounding a fatty marrow-filled medullary cavity. The gross appearance of osteochondroma is a function of patient/lesional age and proximity to skeletal maturity. In younger patients the cartilage cap will be relatively thick and may undergo thickening during the teen growth period. However, upon skeletal maturity the cartilage component begins to regress until there is little or no evidence of cartilage present. During active growth, the interface between bone and cartilage frequently consists of chalky white to yellow-white, amorphous, mineralized material corresponding to the zone of cartilage mineralization within the endochondral ossification of the osteochondroma.

Sessile osteochondromas may be difficult to appreciate in fragmented specimens, mixed pieces of bone and cartilage with normal underlying cancellous bone and overlying connective tissue. Intact lesions consist of a lobulated blue-gray cartilage with focal mineralization sitting within a defect of surrounding cortical bone (Fig. 3.5). The cartilage cap is in direct contact with the underlying parent bone medullary cavity.

Radiology

The radiographic appearance of osteochondroma varies with regard to a number of parameters including location, sessile vs stalked status, and patient/lesional age. Diagnostic features in long bone lesions are best viewed on plane films, while flat bones are best investigated with CT and MRI. In light of its high water content, the cartilage cap is best appreciated (e.g., thickness) with MRI.

Osteochondroma begins as a cartilage-filled cortical defect. With time the lesion develops a stalk resulting in a cartilage-capped stalk (Fig. 3.5). The cortices and medullary cavities of the osteochondroma and parent bone are in continuity with their respective counterparts (Fig. 3.6). Sessile osteochondromas remain largely confined within the cortex with direct exposure to the parent bone's medullary cavity. Stalked osteochondromas initially grow perpendicular to the long axis of the parent bone, and then in response to forces from overlying muscles, they appear to "bend" away from the nearest joint and grow roughly parallel to the cortical long axis.

Special Studies

Mutations in the exostosin genes (EXT1/EXT2 gene) appear to contribute to osteochondroma formation [23–27]. The mutation results in disruption of heparin sulfate proteoglycan synthesis that in turn impacts the Hedgehog and Wnt signaling pathways. These alterations affect the pattern of endochondral ossification in the growth plate resulting in defective formation of the "bone collar" that is adjacent to and surrounds the epiphyseal growth plate [28, 29]. The mutated population is thought to achieve a functional advantage and, through recruitment of other normal elements,

results in osteochondroma formation. In solitary osteochondroma, these genetic changes are confined to elements of the cartilage cap [23, 24]. In contrast these changes are heterozygotic germline mutations in patients with hereditary multiple exostosis [23–28].

Multiple Hereditary Exostosis

Definition

Multiple hereditary exostosis (MHE) is defined as a condition in which two or more osteochondromas are found in a patient with a family history of MHE or evidence of a germline mutation of one of the EXT genes [28, 30–32]. MHE is inherited as an autosomal dominant of near-complete penetration [33].

Clinical

MHE, also referred to as multiple osteochondromas or diaphyseal achalasia, may occur as an isolated orthopedic disease. Alternatively it may occur as part of a clinical syndrome: e.g., trichorhinophalangeal syndrome type II (Langer-Giedion syndrome) or Potocki-Shaffer syndrome [1, 30].

MHE tends to become evident in patients in the first and second decades of life. Although variably reported, males appear to be affected more frequently than females: male to female ratio 3:2 [30, 31]. Any bone formed via endochondral ossification may be involved. When comparing involvement between patients, even family members, the number of bones and sites of involvement can be highly variable, but the long bones of the appendicular skeleton, particularly the knee region, are frequently involved (Fig. 3.8) [28].

The presence of multiple metaphyseal osteochondromas interferes with remodeling of the affected bone and results in osseous deformities of varying degrees of severity: bowing of paired bones, leg length discrepancies, joint angulation, and short stature [33]. Patients may present with a variety of complaints referable to deformity and/or mass effect causing compression and interference of adjacent normal structures. The most serious consequence is an increased incidence of secondary peripheral chondrosarcomas arising in association with osteochondromas, estimated at 0.5–5.0% of MHE patients [22, 30, 31].

Treatment in the vast majority of cases of MHE is pointed toward excision of painful lesions, correction of functional impairments, genetic counseling, and monitoring for the development of secondary chondrosarcoma. Suspicion of secondary malignancy should be raised if an osteochondroma cap continues to grow after skeletal maturity, a cartilage cap is >2.0 cm thick, or new pain develops in the area of an osteochondroma. The treatment and prognosis of secondary chondrosarcoma in MHE is the same as that of spontaneous peripheral chondrosarcoma.

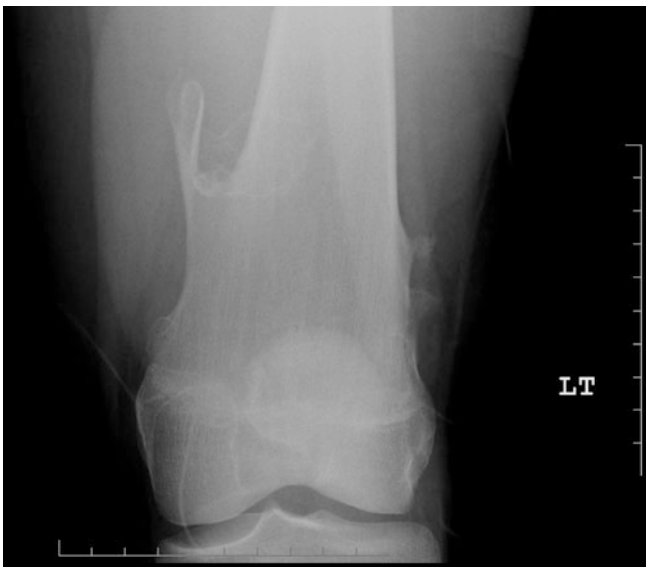

Fig. 3.8 Multiple osteochondromatosis involving the metaphysis of the distal femur. The lesions have interfered with normal metaphyseal remodeling resulting in deformity; so-called *mild bottle deformity.* (Courtesy of A. Kevin Raymond, M.D.)

Morphology

The morphological and radiographic features of these osteochondromas are similar to those of solitary osteochondromas. There appear to be two gross/radiographic configurations in MHE osteochondromas. They are the typical stalked, cartilage-capped osteochondroma. Alternatively, they may appear as broad-based sessile lesions.

At times the histological features of the osteochondromas of MHE may be somewhat atypical and at times suspect for malignancy. However, awareness of this issue and correlation with a clinical and radiographic aspect of an individual case will help in appropriate histological interpretation, atypical histology within expectations of MHE versus secondary malignancy.

Enchondroma

Definition

Enchondroma is defined as a benign intramedullary hyaline cartilage neoplasm.

Clinical

Enchondroma is one of the most common primary bone tumors, accounting for some 15.5% of benign bone tumors and 4.7% of all bone tumors. However, as with osteochondromas, most enchondromas are asymptomatic, and the incidence may be higher. Although initial diagnoses may be at any age, it is somewhat more frequent in younger patients. The male to female ratio is roughly equal, perhaps minimally

more frequent in females. Enchondromas may arise in any bone formed through endochondral ossification, becoming increasingly frequent with distal progression in the appendicular skeleton. Enchondromas are most frequent in the small tubular bones of the hands. They tend to arise within the metaphysis but may be seen in diaphyses.

Enchondromas tend to be asymptomatic and are frequently first recognized as incidental findings in imaging studies performed for unrelated reasons. Larger lesions can cause pain or result in a slowly enlarging mass lesion. In general, enchondromas are self-limited and stop growing at the time the parent bone undergoes skeletal maturity. Ultimately large portions are at least partially mineralized, and they may undergo a degree of involution.

Historically, therapy has been a sort of "benign neglect" with treatment only contemplated with the appearance of symptoms or complications, e.g., non-healing pathological fracture. The clinico-pathological situation determines therapy. When the patient is symptomatic, but without suspicion of malignancy, curettage is the treatment of choice. If there is suspicion of malignancy, biopsy may be performed prior to definitive therapy.

There remains the difficult-to-address issue concerning the association of secondary chondrosarcoma with *solitary* enchondroma. The problem results from the heterogeneity of cartilage neoplasia and the difficulty in unequivocally distinguishing between benign and "minimally malignant" (i.e., low-grade) components in a given lesion. Most authors admit that it occurs, but precise estimation awaits definition and awaits the development and availability of more precise investigatory techniques [4].

Histology

Enchondromas are composed of well-formed hyaline cartilage (Fig. 3.9). The matrix is pale blue to blue-gray with the lesion growing in a cohesive, lobular fashion. The tumor is well-defined and tends to have a sharp, lobular interface with normal bone resulting in concave cortical bone remodeling, often with cortical thinning, so-called endosteal scalloping. There may be interface reactive bone without infiltration. The neoplastic cells of enchondroma are similar to those of normal hyaline cartilage and are largely present within well-defined lacunes. Nuclei tend to be round, hyperchromatic with little or no nuclear detail, without mitotic activity and minimal heterogeneity. The cytoplasm is variable in amount, wispy or bubbly, with frequent attenuated attachments to lacunar walls. There is frequent mineralization that tends to be at the lobule peripheries where mineralized endochondral ossification may be superimposed. There may be some degenerative changes in the matrix and apoptosis of neoplastic cells; both processes tend to be centro-lobular and largely confined to older lesions. Infiltration of normal cancellous bone is minimal and largely confined to early lesions. With time lesions tend to develop peripheral mineralization and undergo endochondral ossification resulting in an appearance of cartilage lobules with a peripheral layer of the bone, so-called *encasement* [1].

The atypia of enchondroma hyaline cartilage is largely architectural in the form of hypercellularity and loss of normal organization when compared with normal hyaline cartilage (i.e., articular cartilage, epiphyseal plate). Frank cytological atypia is minimal.

Histological features that should suggest the possibility of malignancy include both architectural and cytological changes: marrow and cancellous bone permeation, entrapment and destruction of trabecular bone, myxoid matrix degeneration, marked hypercellularity, nuclear and cytoplasmic atypia and variability (i.e., increased nuclear detail, increased cytoplasm), and evidence of cellular proliferation (e.g., binuclear cells, mitoses).

Gross

Since most enchondroma surgical specimens are the product of curettage, the overall gross appearance of enchondroma may be difficult to appreciate. Grossly, they tend to be a well-defined, lobular lesion without infiltration of normal bone. When cortical bone is included, it tends to be attenuated, and the tumor/cortex interface has a scalloped configuration. The cut surface is firm, semitranslucent, shiny, and blue-gray to white. There may be randomly scattered, ill-defined chalky white to yellow-white areas corresponding to foci of mineralization and endochondral bone formation.

Radiology

Radiographically, enchondroma is a well-defined, destructive, geographic lesion [1, 34, 35]. When located in long bones, they tend to form a well-defined, central metaphyseal or diaphyseal lesions. The interface with normal bone is frequently sclerotic. The lesions tend to be largely radiolucent with punctate calcifications that may impart a stippled appearance, "ring and dot" or "arch and fleck" or "popcorn-like" mineralization. In the short tubular bones (Fig. 3.9), the lesions may be central but frequently involve the entire diameter of the meta-diaphysis resulting in a lobulated lesion that expands and thins overlying scalloped cortical bone. Unequivocal plane film distinction between enchondromas and bone infarct can be problematic.

CT and MRI may add greater detail to our ability to visualize components of the primary tumor and estimate extent of disease. Because of the high water content, enchondroma has low signal intensity on T1-weighted images. In contrast there is high signal intensity on T2-weighted images. At the same time, there has been a suggestion that MRI may help in distinguishing between enchondromas and low-grade chondrosarcoma. The absence of MRI T2 hyperintensity can help distinguish enchondroma from bone infarct [34, 35].

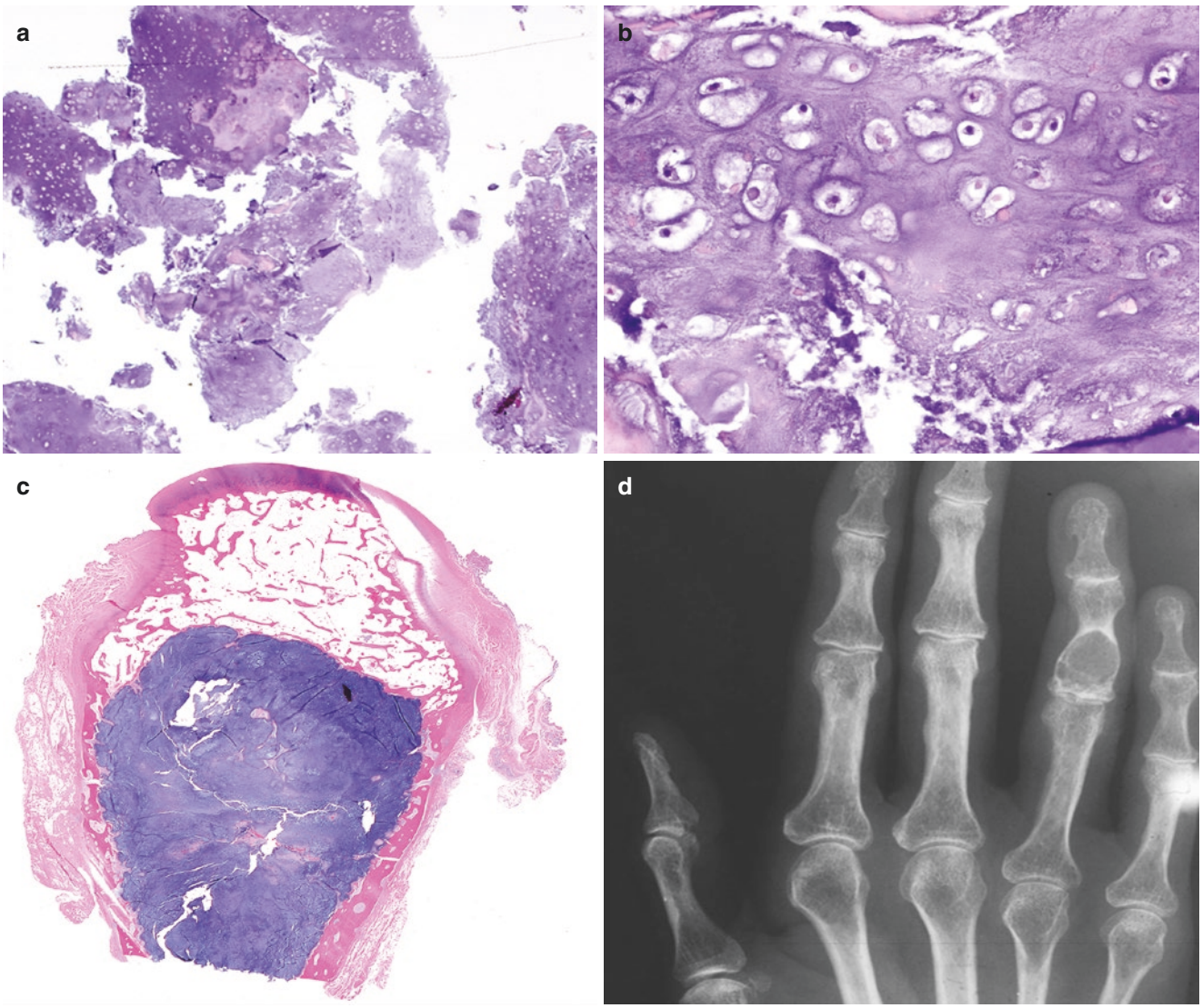

Fig. 3.9 Enchondroma: (**a**) Fragments of disorganized, hypercellular benign hyaline cartilage, with (**b**) minimal nuclear atypia and wispy cytoplasm with attachments to lacune walls. (**c**) Section of finger, scanned whole mount with cohesive, lobulated mass of hyaline cartilage. There is endochondral ossification at the tumor/normal interface; "encasement." Tumor has caused endosteal scalloping of overlying cortical bone which is thinned but intact. (**d**) Plane film (AP) of hand. There is a lobulated radiolucent expansile lesion involving the fourth digit. Endosteal scalloping by tumor has resulted in cortical thinning. (courtesy of A. Kevin Raymond, M.D.)

The question of benign versus malignant is frequently posed to the radiologist. Radiographic features that suggest the possibility of malignancy include large tumor size, infiltration of normal trabecular or cortical bone, extensive bone remodeling, cortical thickening, and tumor extension into overlying soft tissue.

Molecular and Cytogenetics

Although more frequent in syndromic enchondromas (i.e., 87%) than sporatic enchondromas (52%), enchondromas are associated with IDH1 and IDH2 mutations. Although most have a normal karyotype, structural abnormalities of chromosomes 6 and 12 have been described [20, 22, 28, 36].

Periosteal Chondroma

Definition

Periosteal chondroma (aka juxtacortical chondroma) is a benign hyaline cartilage neoplasm that arises on the cortical surface of the involved bone and beneath the periosteum [1, 10, 20, 37].

Clinical

Described by Lichtenstein (1953), periosteal chondroma represents a distinctive cartilage tumor that most frequently affects patients in the second decade of life and somewhat less frequently in third decade. Males are affected more frequently than females in a ratio approaching 2:1. Although any bone formed by endochondral ossification may be the

primary site, it most frequently arises from the proximal humerus, followed by the distal femur and fingers [1, 20, 38].

Although many may be largely asymptomatic, painless mass and pain secondary to mass effect are the most frequent presenting complaints [20, 39].

The natural history tends to be that of a lesion with limited growth potential; continued growth after skeletal maturity should at least raise the question of malignancy. In the absence of significant symptomatology, observation may be the first line of therapy. However, if treatment is required, intralesional or marginal excision (i.e., curettage) is the treatment of choice [39, 40]. Local relapse is infrequent and almost always cured by re-excision.

Histopathology

Taken out of context, periosteal chondroma may be morphologically indistinguishable from enchondroma. In general, the cytological features of enchondroma are recapitulated in periosteal chondroma (Fig. 3.10). Histologically, they consist of disorganized lobules of hypercellular cartilage. Tumor is bounded by underlying cortex with superficial reactive bone and overlying periosteum; cortex may be eroded, and periosteum may be expanded, but tumor rarely infiltrates either structure. Since the degree of atypia may exceed that of classical enchondromas and not portend a more aggressive biological behavior, it is critical to correlate morphology with radiology.

Gross Pathology

With the treatment of choice being curettage, the overall gross appearance of periosteal chondroma may be difficult to appreciate. Tumor forms a gray-blue, pale-blue, or gray-white, semitranslucent, ovoid to *lens-shaped* mass that is generally <5 cm in greatest dimension, located on the cortical surface and beneath the periosteum (Fig. 3.10). The lesion is frequently accompanied by underlying reactive bone formation that in turn is indented/eroded by the lens-shaped tumor, corresponding to radiographic *saucerization* [41]. However, curettings are composed of multiple intermixed fragments of gray-blue to white cartilage together with reactive and cortical bone.

Radiology

The plane film appearance of periosteal chondroma is fairly distinctive [39, 41–43]. The largely radiolucent, hemispherical, or *lens-shaped* lesion appears embedded within underlying reactive bone, superimposed on cortical bone (Fig. 3.10) resulting in a curvilinear cortical depression (i.e., *saucerization*). The lesion may be surrounded by a collar of reactive bone that when viewed on plane films gives the appearance of triangles of reactive bone limiting the peripheral edges of the tumor, so-called buttressing [40].

CT and MRI give better detail concerning the spatial relations of tumor. The lesion is hypointense on T1-weighted images and hyperintense on T2-weighted images [44].

Diagnostic Issue

Periosteal chondroma is notorious for unexpected histological atypia [40, 41]. Lesions that are otherwise typical of periosteal chondroma may be more hypercellular and more atypical than expected for a benign cartilage lesions (Fig. 3.10). There are a variety of features that may help distinguish benign from malignant lesions. Lesions that are <5 cm, which do not invade through cortex into underlying medullary cavity, do not infiltrate through periosteum into true soft tissue, and do not have metastases, are almost assuredly benign [40]. Nevertheless, treatment should be aimed at complete tumor removal while minimizing normal tissue contamination.

Enchondromatosis

Definition

"Enchondromatosis" is the presence of multiple skeletal chondromas, enchondromas and periosteal chondromas.

Introduction

Enchondromatosis refers to a group of rare conditions, with the shared property of multiple skeletal chondromas. The various subtypes are defined by chondroma sites of involvement, associated pathology, symptoms, and possible mode of inheritance. The most common forms are Ollier disease and Maffucci syndrome; both are non-inherited conditions that present in early childhood without apparent gender difference. Less common chondromatosis forms include metachondromatosis, genochondromatosis, cheirospondyloenchondromatosis, and dysspondyloenchondromatosis [1, 45, 46].

Ollier disease is defined as the presence of multiple chondromas in the absence of any other consistent, associated pathology. It is almost always polyostotic, and there may be preferential involvement of anatomic region (e.g., one extremity, dermatomal distribution) or body laterality, one side of the body. Lesions tend to involve bones of the appendicular skeleton, where they involve the metaphyses of the tubular bones and over time interfere with normal bone remodeling, resulting in skeletal deformities, limb length discrepancies, and impaired function. The clinical impact of the enchondromas is a function of their number, size, and location. The resulting functional impairments frequently necessitate surgical intervention (Fig. 3.11).

Although the incidence of Ollier disease in unknown, the incidence of secondary c-chondrosarcoma (c-ChS) in recognized cases of Ollier disease [47] is estimated as approaching 40%, most frequently involving appendicular long bones. In

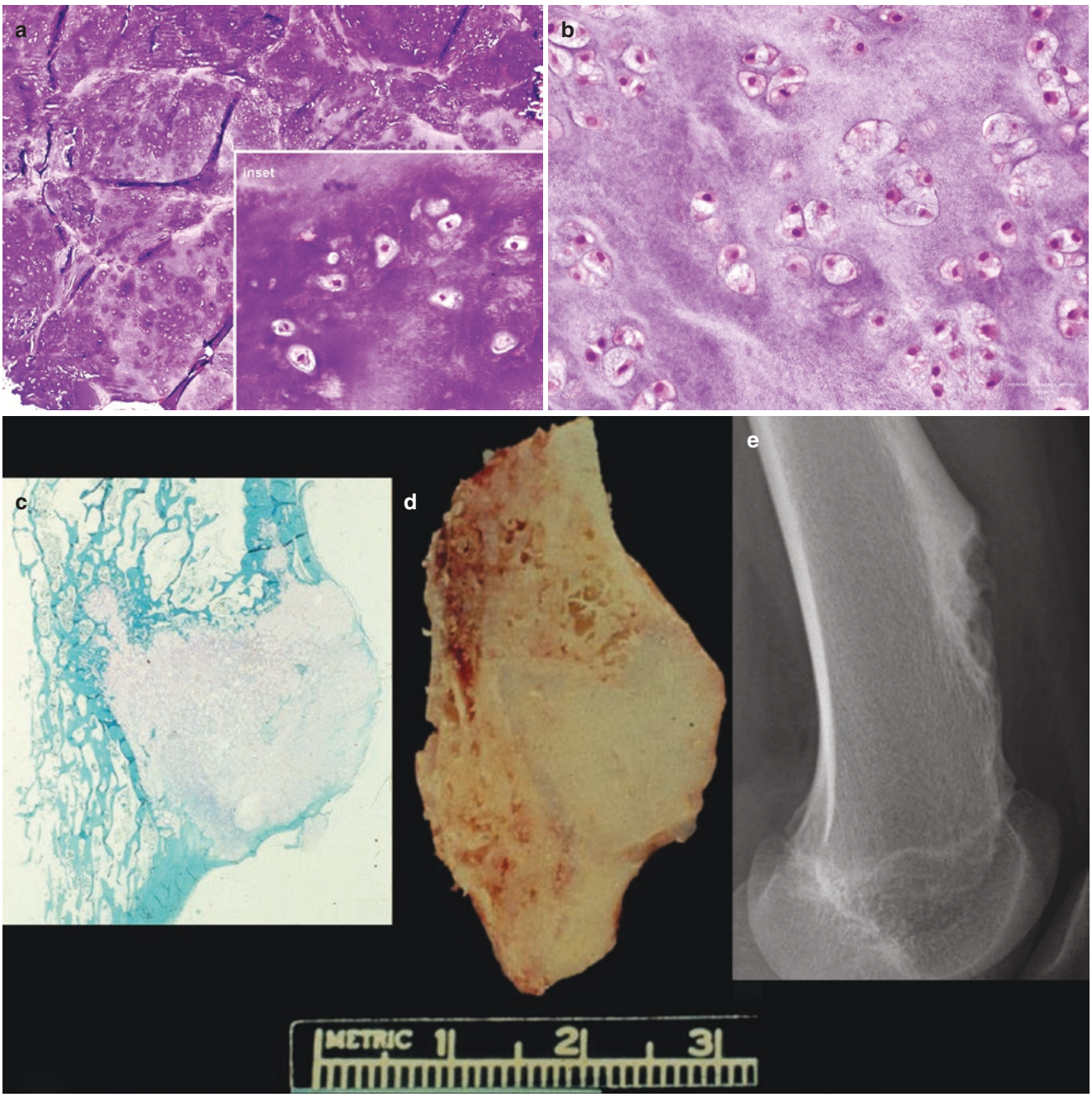

Fig. 3.10 Periosteal chondroma. (**a**) hypercellular, disorganized hyaline cartilage with (inset) minimal atypia and bi-nuclear cell, (**b**) periosteal chondroma with significant atypia: hypercellular, disorganized, increased nuclear detail but retained lobular organization (i.e., retention of lobular array) and without significant binuclear cells, (**c**) Whole mount: hypercellular, gray, hyaline cartilage neoplasm embedded in cortex, (**d**) Gross specimen: pale gray, semi-translucent chondroid lesion embedded in cortex (same case as [c]), (**e**) plane film (lateral): lytic lesion arising from distal femur cortex resulting in periosteal scalloping (i.e., so-called saucerization) of cortex

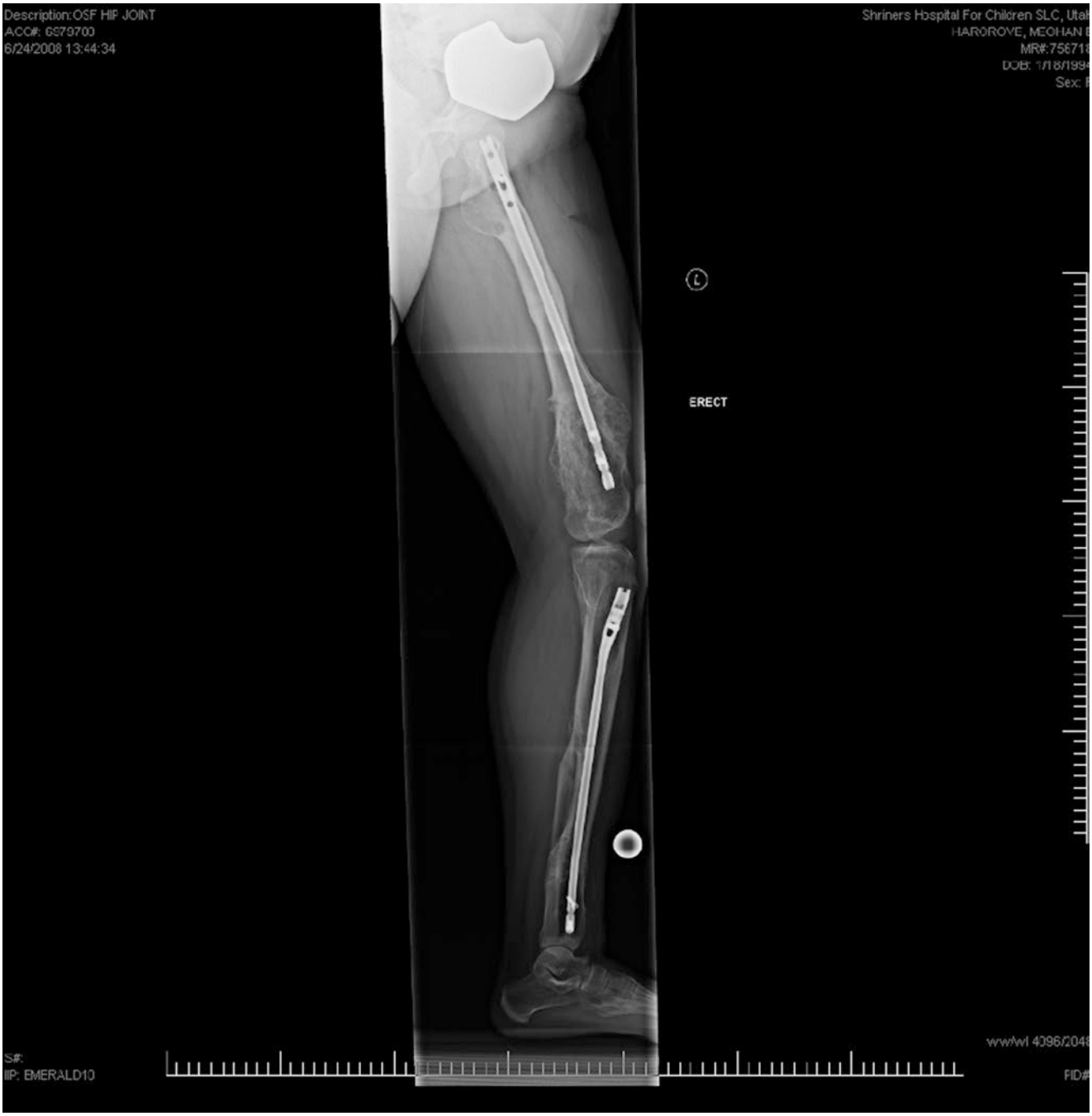

Fig. 3.11 Olliers disease: plane film (lateral). Patient with enchondromatosis largely confined to one lower extremity. There is severe involvement of the proximal and distal femur and tibia. The enchondromas have interfered with normal remodeling resulting in severe anatomical distortion and functional compromise requiring orthopedic intervention. (Courtesy of A. Kevin Raymond, M.D.)

contrast the incidence of secondary ChS in the small bones of the hands and feet is much lower (15%). Of those who develop ChS, an estimated 25% of patients develop multiple ChS.

Maffucci syndrome consists of cartilage lesions indistinguishable from Ollier disease together with vascular lesions, both hemangioma and spindle-cell hemangioendothelioma [48].

The vascular lesions may involve bone, soft tissues, or internal organs. Patient presentation may be a function of either the cartilage or vascular lesions. As with Ollier disease, Maffucci patients suffer skeletal deformities and consequent functional disabilities.

Both chondroid and vascular malignancies are associated with Maffucci syndrome. The incidence of secondary ChS may be as high as 50%, and there is a suggestion that they are more aggressive than spontaneous ChS. In addition, Maffucci patients have a much higher than expected incidence of epithelial malignancies. The high proportion of patients reported without follow-up impedes detailed prognostic analysis of Maffucci syndrome.

Histopathology

Overall, the histological appearance of enchondromatosis chondromas is similar to solitary chondromas albeit frequently somewhat more cellular and atypical. They tend to be more cellular and less organized, and the cytology of individual neoplastic cells includes increased nuclear detail and increased cytoplasm that approach fulfillment of minimal ChS criteria.

Taken out of the enchondromatosis context, there is danger of overcalling these atypical cartilage lesions chondrosarcoma. The presence or absence of tumor infiltration through cortex into overlying soft tissues serves as a fairly reliable indicator of malignancy.

Gross

The overall appearance of the lesions of enchondromatosis is similar to their solitary intramedullary and periosteal counterparts. Lesions are present in multiple bones and may be multiple within a single bone, both intramedullary and periosteal. Lesions tend to be well-defined but vary greatly in size and shape: multi-lobulated, round to oval, etc. Smaller lesions may align in a linear or curvilinear pattern imparting an appearance that evokes an image of a series of lesions being seemingly "cast off" from an underlying growth plate. Lesional cut surfaces are gray-blue to white and semitranslucent. Older lesions tend to mineralize.

Radiology

Bone scans can serve as a quick evaluation of the extent of polyostotic involvement. However, plane films are generally considered diagnostic, and a "skeletal survey" (i.e., plane films of all bones) is generally performed to assess all lesions. The plane film appearance of individual enchondromas tends to be similar to their monostotic counterparts, lobulated, largely radiolucent lesions with variable intralesional ring and fleck calcification and well-defined transition zone which may be sclerotic. However, the presence of multiple small lesions within a long bone metaphysis can impart the appearance of confluent lobulated lesions or a striated radiolucent area.

CT can give additional information pertaining to qualitative analysis and together with MRI the standard for evaluation of extent of disease of individual lesions. Vascular studies can give added information concerning the vascular lesions of Maffucci syndrome.

New symptoms or changing symptomatology may point toward secondary malignancy. However, radiographic monitoring of existing lesions is mandatory follow-up. An existing lesion having evidence of new growth, cortical erosion, or extension into soft tissue should immediately raise suspicion of secondary malignancy.

Molecular

The vast majority of both Ollier and Maffucci patients have mutations in isocitrate dehydrogenase genes (i.e., IDH1 or IDH2) in the majority of their tumors. Interestingly, the various tumors within the same patient tend to contain the same mutation, while the mutation is virtually absent in normal tissues from the same patient. A small fraction of Ollier patient may have mutations in the parathyroid hormone-like hormone (PTHLH) gene [49–54].

Primary Central Chondrosarcoma

Definition

Primary central conventional ChS is a form of ChS that arises de novo within the medullary cavity of the involved bone in the absence of a previously existing lesion or predisposing conditions. These tumors produce hyaline cartilage without additional neoplastic histopathology or matrix forms.

Clinical

Primary central c-ChS is what Jaffe and Lichtenstein originally described and what most people think of as *chondrosarcoma* [55]. Central c-ChS affects patients over a broad age range, but most frequently patients in the fourth to seventh decades, and is rare in patients under the age of 20 years. Men are affected twice as often as women. Central c-ChS may arise within any bone, but most frequently in bones formed all, or in part, through endochondral ossification. The most frequently involved sites are the pelvic and shoulder girdles, femur, ribs, spine, and tibia. In the long

bones, the metaphyses and metadiaphyses are preferentially involved. In essence central c-ChS is a disease of the axial skeleton and long tubular bones above the ankles and wrists. ChS rarely involves the small bones of the hands and feet; and when it does, it tends to be a relatively indolent disease [1, 4, 10, 20].

Pain with or without slowly enlarging mass is the most frequent presentation. Depending on location and size, symptoms secondary to mass effect, referred pain, and reduced range of motion may be present. Tumors that arise in the skull base or spine may result with a wide range of neurological findings.

Central chondrosarcoma tends to be a disease of predictable, locally aggressive growth combined with less frequent and less predictable metastatic potential [1, 4, 56]. The treatment of choice is surgery. Currently, there are no forms of adjuvant therapy (e.g., chemotherapy) that are effective in the treatment of c-ChS. The prognosis is largely a function of tumor grade, size, and location, as well as surgical accessibility and completeness of surgery.

Historically, central-ChS is graded using a three-tiered system. In most series, grades 1 and 2 tumors each account for ≥40% of central-ChS with grade 3 ChS accounting for the remaining <10% of c-ChS [20].

Although subject to much criticism for lack of absolute criteria and resulting inconsistencies in observer and interobserver evaluation, grading is one of the few tools available to assess potential biological behavior and thus attempts to logically approach therapeutic decisions [1, 10, 20, 57, 58].

Less than 10% of grade 1 tumors exhibit aggressive behavior, virtually all in the form of local growth and relapse after incomplete surgery.

Grade 2 tumors are somewhat less innocuous, with some 20% of tumors having aggressive behavior; locally aggressive growth and relapse are an issue, but metastases become a problem of some significance in this patient group.

Grade 3 lesions constitute <10% of central-ChS but have a high incidence of aggressive behavior in the form of both local growth and a substantial risk of potentially lethal systemic metastases.

In one series [58], the 5-year survival in grades 1, 2, and 3 ChS was 90%, 81%, and 43%, while the 10-year survival in the same groups was 83%, 64%, and 29%, respectively. No metastases were seen in the grade 1 ChS, while metastases occurred in 10% of grade 2 ChS and 71% of grade 3 ChS.

Additional factors having a negative impact on survival include local relapse after definitive surgery, progression of grade on relapse, and the development of clinically evident systemic metastases.

And it should be emphasized that a large percentage of patients with tumors in symptomatically silent areas tend to present with large tumors in surgically challenging sites. The threat of systemic metastases may not be a high probability, but death due to the consequences of uncontrolled local disease is.

The accrual of large numbers of patients and multi-institutional experience has led to an evolution in the thinking regarding ChS therapy. Historically, the treatment of choice was complete tumor extirpation, resection when possible and ablation/amputation when necessary. Currently, complete surgical resection with negative margins remains central to the treatment of grade 2 and grade 3 ChS [4, 10, 59].

However, the recognition of the relatively indolent behavior of grade 1 ChS, combined with the difficulty in providing unequivocal histological discrimination between "atypical enchondromas" and grade 1 ChS, has resulted in a movement toward combining these minimally atypical lesions into a single treatment group, i.e., *atypical cartilaginous tumor* (ACT). The consequent emphasis is pointed toward individualized minimal surgical intervention. Patients are reviewed on a case-by-case basis, and appropriately selected patients are subject to either close clinical follow-up or extended curettage and cementation. The incidence of local relapse using this approach is reported as <5% in this treatment group [4, 59].

Pathology

The morphological features of ChS at the level of light microscopy, gross examination, and imaging studies are a function of complex, admixed, and superimposed processes. The base features are those of a hypercellular, hyaline cartilage lesion lacking normal chondroid organization. Superimposed is calcification and endochondral ossification of tumor produced cartilage, as well as reactive bone and admixed normal bone. There may be degenerative processes with attendant reactive changes, especially in higher-grade lesions. Infiltration of normal cancellous and/or cortical bone is present at the normal/tumor interface and implies active lesional growth. Although tumor tends to grow as a lobulated, cohesive mass, skip metastases may be present in something approaching 1% of patients, an incidence similar to that seen in osteosarcoma and necessitating careful interpretation of extent of disease to assure surgical adequacy. ChS skip metastases are best appreciated preoperatively through careful review of T2-weighted MRI studies [60].

Histopathology

Lobular and *blue* are terms generally ascribed to the appearance of ChS. At low power, ChS appears as sheets of blue to blue-gray homogeneous, amorphous material with an overall lobular configuration interrupted by numerous randomly arranged lacunes. From low power, the number and organization of lacunes (i.e., cells) *hint* at tumor grade; roughly, the higher the number of randomly organized cells, the higher the grade.

From low power, tumor forms a relatively well-defined lobular interface with normal bone. Higher magnification may reveal normal trabecular bone embedded within tumor implying that cancellous bone had been infiltrated, overrun, and then encompassed by growing ChS, as opposed to the

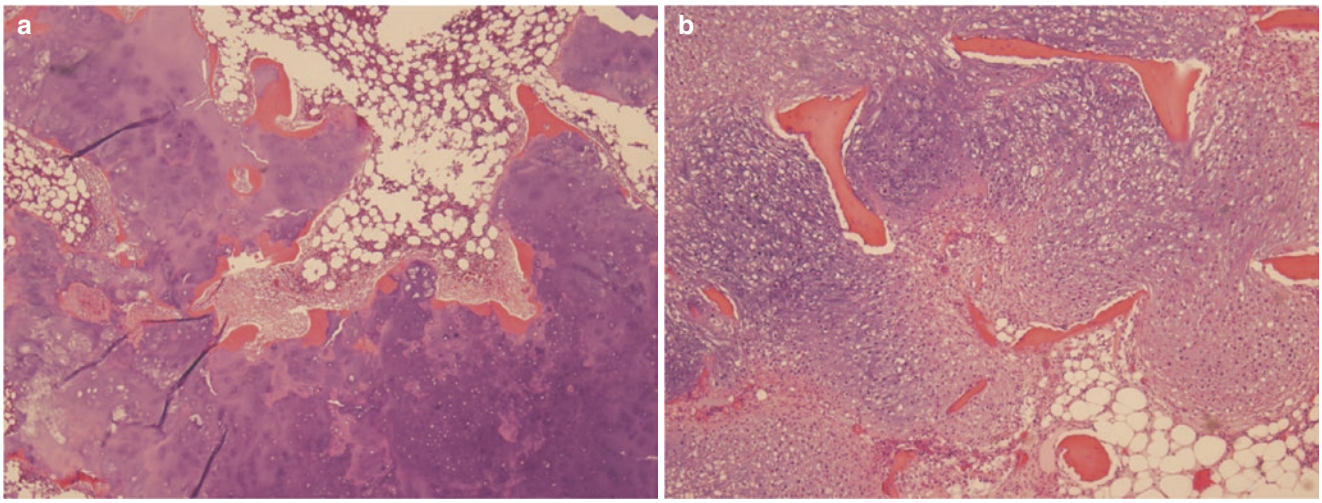

Fig. 3.12 Conventional chondrosarcoma: (**a**) and (**b**) from the same case. (**a**) Lobules of low-grade chondrosarcoma with endochondral ossification involving some lobule peripheries. (**b**) Chondrosarcoma infiltrating between and surrounding pre-existing trabecula of cancellous bone (H&E. 20×)

encasement seen in enchondromas. At the tumor/normal interface, microscopic tumor lobules infiltrate between trabecula of normal cancellous bone (Fig. 3.12a, b). The tumor/cortical interface is usually well-defined with an overall lobular appearance and lobular erosion of overlying cortical bone, i.e., *endosteal scalloping*. Cortex is frequently thickened but may be infiltrated and ultimately eroded. Lobule peripheries may be accentuated by pink material or bone and lined by normal osteoblasts, reflecting endochondral ossification similar to encasement seen in enchondromas.

The basic histological criteria for distinguishing malignant from benign hyaline cartilage neoplasia were originally proposed by Jaffe and Lichtenstein [55], and although refinements have been suggested [1, 4, 10, 20, 58, 59, 61], they have largely remained unchanged and barely adequate to the task. There are four criteria that compare histological/architectural and cytological properties of cartilage neoplasia to normal cartilage and set the so-called minimal criteria for malignancy [1, 4].

Cellularity The lesion should be hypercellular when compared to normal cartilage. This is a property that may be seen in both benign and malignant lesions. However, increasing cellularity roughly corresponds to increasing probability of malignancy and increasing grade.

Organization The lesion should be disorganized when compared with normal cartilage, neither the layered array of articular cartilage nor the sequential maturation zones of the growth plate. Again, at the lower end of disorganization, benign and malignant lesions share this property. And again increasing degrees of disorganization correlate with increased probability of malignancy and increasing histological grade.

Increased nuclear detail The normal chondrocyte is essentially a small hyperchromatic nucleus with minimal if any recognizable cytoplasm at the level of routine light microscopy. Outside certain well-defined circumstances, any euchromatin in cartilage nuclei is considered abnormal; the ability to discriminate a nuclear membrane distinct form the chromatin constitutes a minimum of increased nuclear detail. In truth, increased nuclear detail is almost always accompanied by increased cytoplasm, a helpful feature for initial low-power evaluation. Increased nuclear detail is unusual in benign cartilage neoplasia.

Binuclear cells *There are "more than occasional binuclear cells."* This is felt to be a reflection of active growth and ongoing mitotic activity. Although rare in benign cartilage neoplasia, taken within the appropriate context, this is a helpful discriminator between benign and malignant.

Other criteria are championed to augment those historical. Infiltration of normal bone is a reflection of active tumor growth. Most ChS appear after skeletal maturity. In contrast, under normal circumstances, solitary enchondromas arise in the young, and any growth takes place before skeletal maturity. In essence, enchondromas are relatively self-limited and either cease growing or begin some degree of involution with skeletal maturity. Therefore, growth after skeletal maturity as reflected by tumor infiltration of normal bone suggests malignancy.

For the most part, benign hyaline cartilage lesions and low-grade ChS do not undergo significant, spontaneous necrosis or degeneration. The presence of degenerative changes suggests malignancy and appears more frequent with increasing grade. In these cases there is a transition between intact, homogeneous, amorphous, lobulated, blue hyaline cartilage with matrix that is going through, or has gone through, dissolution into wispy, filamentous

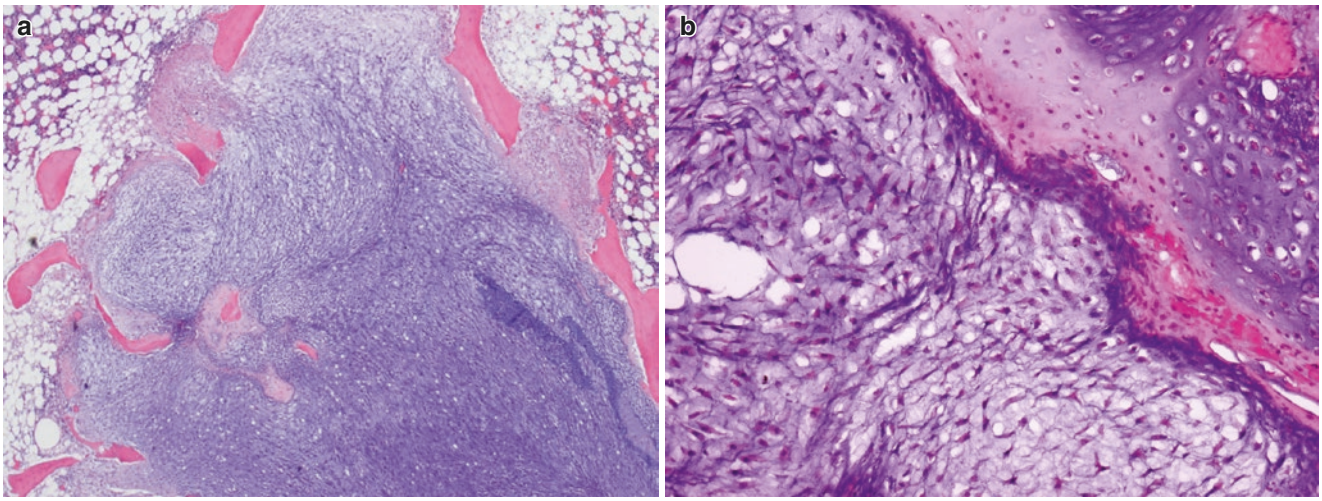

Fig. 3.13 Conventional chondrosarcoma: normal cartilage for comparison. (**a**) Normal articular cartilage. (**b**) Normal epiphyseal plate. *R* resting cartilage, *P* proliferating cartilage, *H* hydropic change, *D* mineralization, *S* bone deposition. (H&E). (Courtesy of A. Kevin Raymond, M.D.)

strands admixed with granular matrix debris, so-called myxoid degeneration or myxoid change (Fig. 3.13a, b). Intact, viable cells are present in the areas retaining hyaline cartilage areas, while those in the degenerating matrix are either apoptotic or hypereosinophilic.

Caution As imprecise/ambiguous as they are, the above are the diagnostic criteria for ChS. However, it should be noted that they only hold, with any degree of consistent biological implication, for lesions of the axial skeleton and long bones of the appendicular skeleton. These criteria are not necessarily applicable for cartilage lesions arising in the small bones of the hands and feet, lesions arising in synovium (e.g., synovial chondromatosis), lesion arising on the cortical surface, and soft tissue lesions. Add to this list the chondromas of enchondromatosis and the osteochondromas of multiple hereditary exostoses. Cartilage lesions in the latter areas may have a higher degree of atypia without being malignant. In these latter areas, lesion size and invasive properties, in addition to histological evidence of malignancy, are factors necessarily incorporated to arrive at parameters predictive of malignancy and aggressive behavior [1, 4, 10, 20].

Historically, the goal of grading in ChS has been an attempt to predict the probability of systemic dissemination, generally in the form of pulmonary metastases. As indicated earlier, ChS grading has been traditionally based on a three-tiered system, with increasing grade corresponding to increasing potential for aggressive biological behavior.

As with other organ systems and tissues, the criteria for grading used with ChS are at times seemingly vague and arbitrary. Many authors merely refer to increments of atypia progressing from well-differentiated (grade 1) to moderately differentiated (grade 2) and then high-grade or poorly differentiated (grade 3) chondrosarcoma [1].

However, since grading would appear to have significant therapeutic implications, the issue of grading criteria lingers.

There are a number of potential answers:

- The most used systems bases discrimination between grade 1 and grade 2 based on relative cellularity and atypia. Grade 3 designation is a function increasing atypia and so-called peripheral spindling. Peripheral spindling occurs with zonated cartilage lobules in which there is a transition from central, matrix dominant hyaline cartilage through matrix depletion to a periphery where there is a virtual absence of matrix, just layers of encircling compressed (i.e., *spindled*) neoplastic cells [4, 20, 61].
- In an alternate system, tumor grade is a function of mitotic index: grade 1 having <1 mitosis per 10 high-power fields (HPF), grade 2 having <2 mitoses per 10 HPF and grade 3 having >2 mitoses per 10 HPF [58]. Of interest, in higher-grade lesions, mitoses are generally found within areas of peripheral spindling. However, the system has the advantage of identifying highly aggressive tumors that lack peripheral spindling and would be otherwise inappropriately down-graded; i.e., lesions that would otherwise be included with grade 2 chondrosarcoma. This system helps to more completely identify the group of patients most likely to be at risk for systemic metastases.

The issue of grading has been reassessed and redirected toward determining the form of surgery for the primary tumor, rather than acting as the harbinger of metastases. Orthopedic surgeons demand a system in which ChS is divided into low and high grade. Low-grade ChS is being defined as tumors which *never* metastasize; and therefore, it identifies tumors that can be adequately managed with obser-

vation or extended curettage and cementation. In contrast, high-grade tumors are those in which there is *any* chance of metastases and which require definitive complete tumor extirpation via resection or ablation followed by follow-up to monitor for potential systemic metastases and further therapy.

In the past, the emphasis of grading was to identify the patients with the highest probability of developing metastases. There has been a change. The emphasis has now shifted to more accurately identifying low-grade lesions to appropriately minimize surgery. There have been a number of suggestions for establishing grading criteria.

- In one system atypical enchondromas and minimally diagnostic chondrosarcomas are defined as "low-grade" or atypical cartilage tumors (i.e., ACT) and everything else is "high-grade." [4, 59]
- Another suggestion has been to define low-grade as lesions that are histologically benign but have an aggressive radiographic appearance. All lesions that are histologically malignant are classified as high-grade.

Personal Comment

Despite its central role, criteria for grading at times appear ethereal. However, there are investigators actively pursuing avenues aimed at great objectivity [59, 61]. But until then grading remains with us. As a matter of the practical, I use a combination of criteria that involve histological analysis together with integration of clinical information including age, gender, bone involved, lesion size and configuration, and most importantly radiographic appearance. These histological criteria include:

- *Grade 1*: These are those tumors that barely fulfill minimal Jaffe and Lichtenstein criteria for malignancy. In addition, lesions have a mitotic index <1 mitosis per 10 HPF, there is minimal myxoid change, and there is no peripheral spindling (Fig. 3.14a–c).

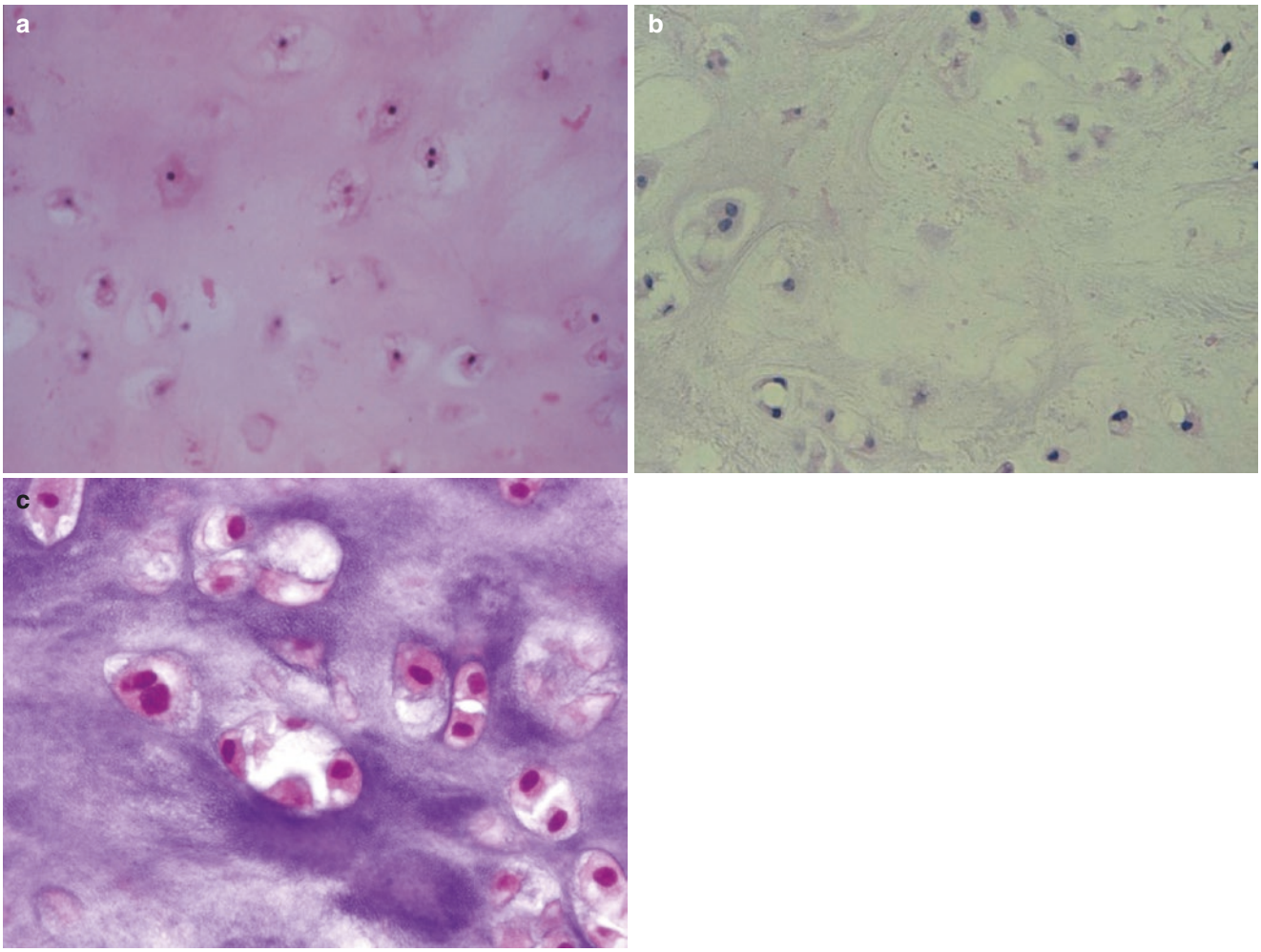

Fig. 3.14 Conventional chondrosarcoma: grade 1 chondrosarcoma (**a–c**). Hypercellular, disorganized hyaline cartilage with increased nuclear detail and more than occasional binuclear cells, features increasing from (**a–c**) ((**a**) 40×, (**b**) 100×, (**c**) 250×) (Courtesy of A. Kevin Raymond, M.D.)

- For treatment purposes, I combine grade 1 lesions with atypical enchondromas and benign lesions with aggressive imaging features. This combined group is then referred to as *low-grade cartilage neoplasm or low-grade chondrosarcoma*. The absence of the word "chondrosarcoma" may decrease confidence in the diagnosis.
- *Grade 2*: These are those cartilage lesions that clearly fulfill the Jaffe and Lichtenstein minimal criteria for malignancy: they are clearly hypercellular, very disorganized, and have increased nuclear detail and easily detectable binuclear cells. Myxoid change/degeneration is a frequent finding. At the same time, these are lesions in which more conventional pathology criteria begin to apply: inverted nuclear/cytoplasmic ratio, nuclei with varying shapes and sizes, chromatin condensation within the nucleus and along the nuclear membrane, nucleoli of varying sizes and prominence, and cytoplasm of varying amounts and staining characteristics. These are the lesions that have overall histological features that might be described as "typical" or "classical" chondrosarcoma. At the same time, these are lesions with more than none but <2 mitoses per 10 HPF and lack peripheral spindling (Fig. 3.15A–D).
- *Grade 3*: These are rare (i.e., ≤10% of ChS) and share histological features with grade 2 lesions that may extend to a histological extreme. However, they also have >2 mitoses per 10 HPF and/or peripheral spindling (Fig. 3.16a, b).
- For treatment purposes lesions classified as either grade 2 or grade 3 chondrosarcoma are included in the term *high-grade chondrosarcoma*.

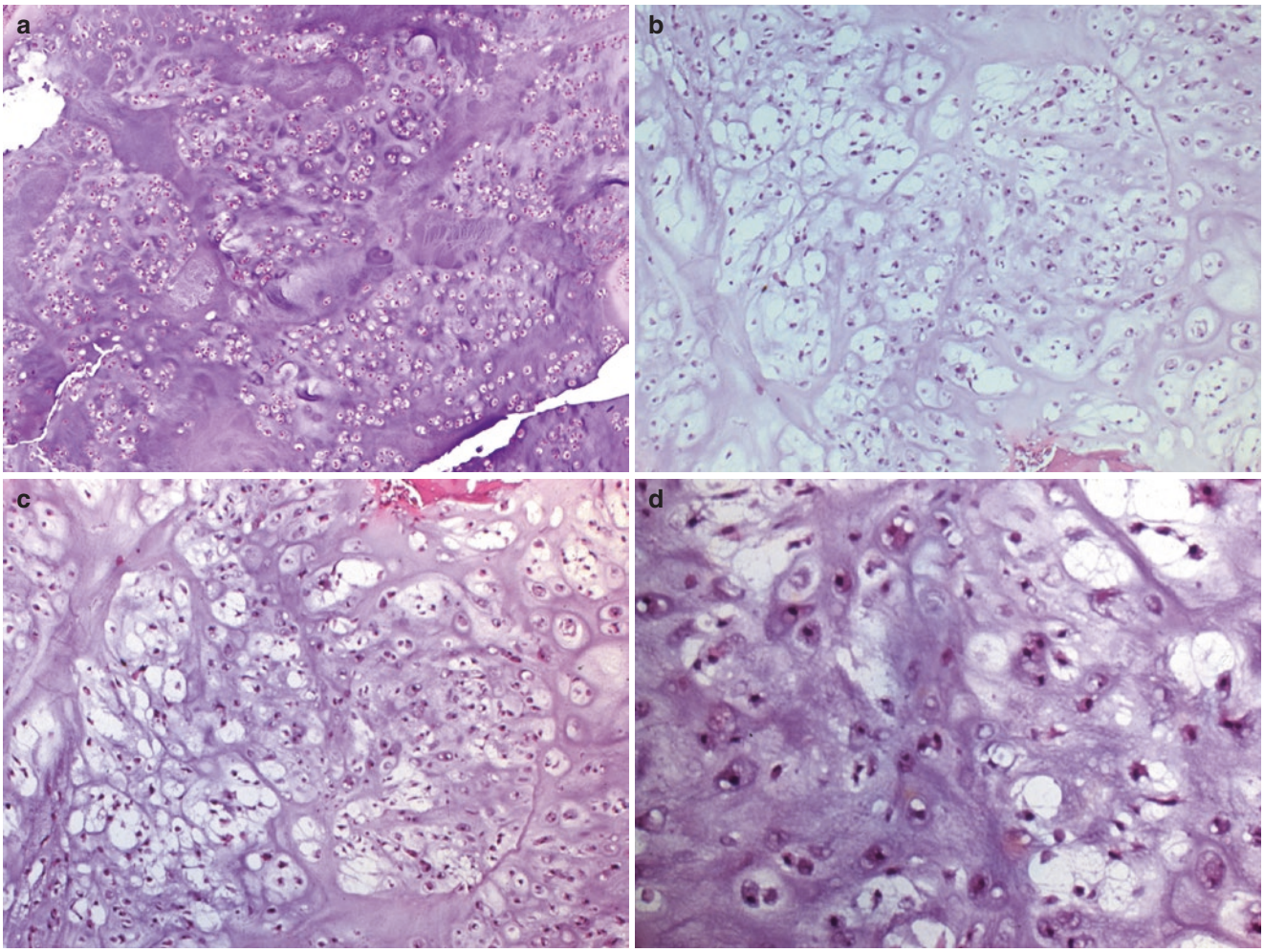

Fig. 3.15 Conventional chondrosarcoma (**a**–**d**): grade 2 conventional chondrosarcoma. In addition to hypercellularity, disorganization, increased nuclear detail, and binuclear cells: neoplastic cells show changes of significant pleomorphism and atypia. Occasional mitoses are present. Varying degrees of myxoid change are present. (Courtesy of A. Kevin Raymond, M.D.)

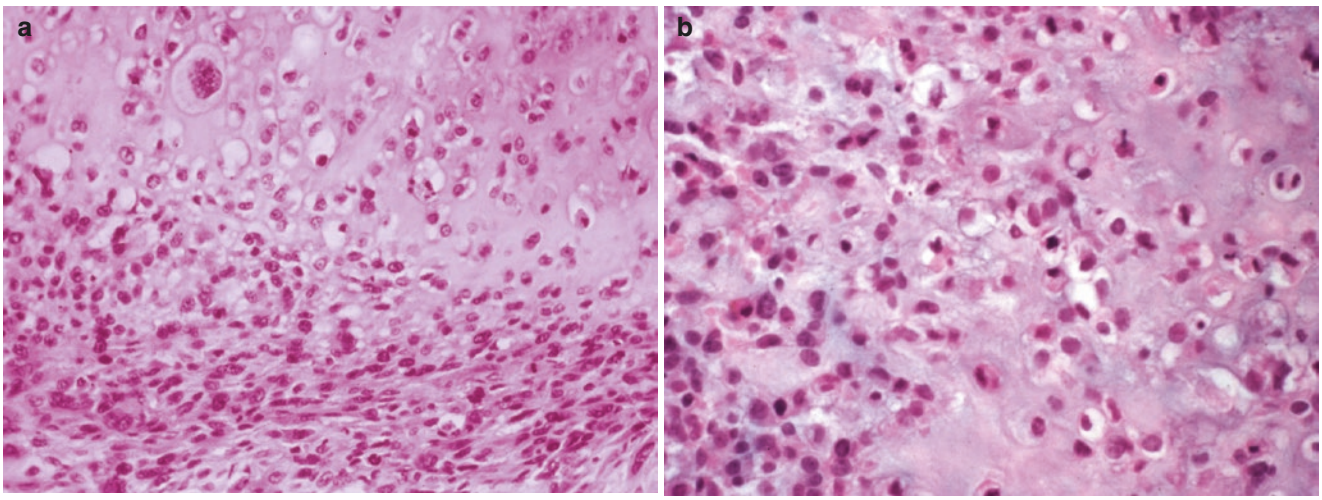

Fig. 3.16 Conventional chondrosarcoma: grade 3 chondrosarcoma. (**a**) Grade 3 conventional chondrosarcoma. The upper portions of the slide have typical hyaline cartilage with a significant degree of atypia. There is a progressive decrease in matrix toward the middle of the field. There is virtually no chondroid matrix at the bottom of the slide where cells approximate one another and the cells have a pronounced spindle configuration; peripheral spindling (200×). (**b**) The degree of atypia is significant but in and of itself is insufficient to merit a diagnosis of grade 3 chondrosarcoma. However, the presence of mitotic activity >2 mitoses per 10 HPF qualifies for grade 3 grading. (Courtesy of A. Kevin Raymond, M.D.)

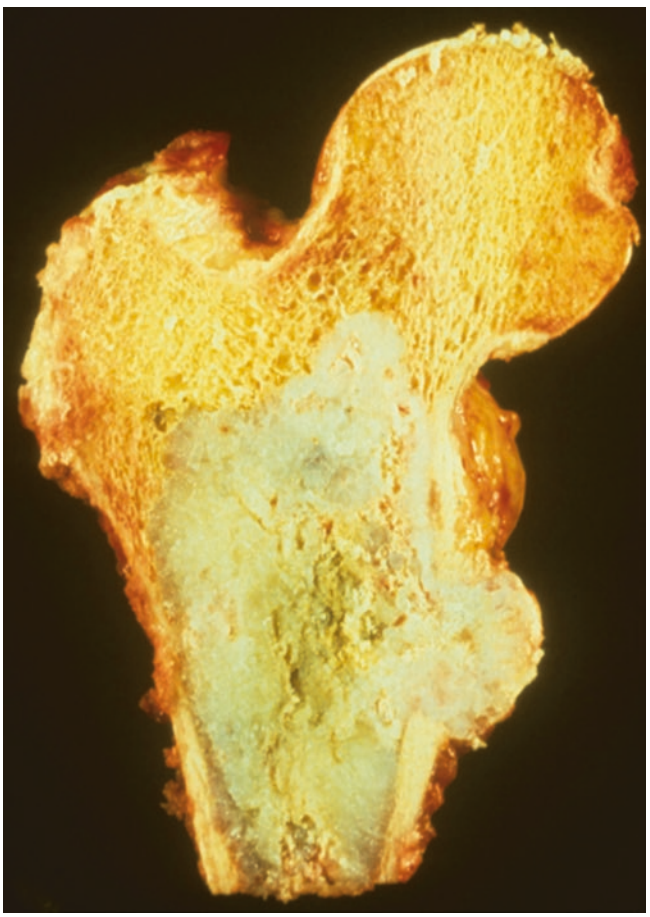

Fig. 3.17 Conventional chondrosarcoma: gross specimen. Grade 2 chondrosarcoma consists of a lobulated gray-white to blue-gray to white firm lesion involving the intertrochanteric proximal femur. Tumor is well-defined, and tumor infiltration is not appreciated. There are focal gray-green central degenerative changes. Tumor has grown through the open biopsy site on the medial aspect. (Courtesy of A. Kevin Raymond, M.D.)

Gross

Grossly, c-ChS forms a cohesive, lobulated, blue-gray to off-white, semitranslucent to opalescent, firm and homogeneous mass (Fig. 3.17). Foci of calcification and/or endochondral ossification of tumor matrix are rock-hard, serpiginous to solid, white to yellow-white, and granular. The interface with normal cancellous and cortical bone is lobulated and results in endosteal scalloping of cortex and small lobular infiltration of cancellous bone. Tumor may infiltrate and/or destroy cortex and extend into overlying subperiosteal tissue or true soft tissue. Rarely, skip metastases may be identified (Fig. 3.18).

Higher-grade lesions tend to have varying amounts of degenerative changes that impart a semisolid, mucoid, or even frankly necrotic consistency to the affected areas. These tumors tend to be pale-gray, semitranslucent with scant admixed finely granular white to gray-green material or with red to red-black hemorrhage (Fig. 3.19).

Radiology

On plane films, c-ChS appears as a destructive, mixed lytic/blastic, relatively well-defined geographic lesions (Figs. 3.20a–c and 3.21). The tumor lobulations result in cortical endosteal scalloping that appear on plane films and CT. The tumor is mineralized in the form of small rings/arcs and flecks/dots (i.e., so-called popcorn calcification), reflecting mineralization and endochondral ossification of cartilage lobule peripheries. Unlike enchondromas, mineralization is characteristically heterogeneous. In addition, although cortical thinning is frequently present, the presence of ChS characteristically results in the widening of the involved bone and cortical

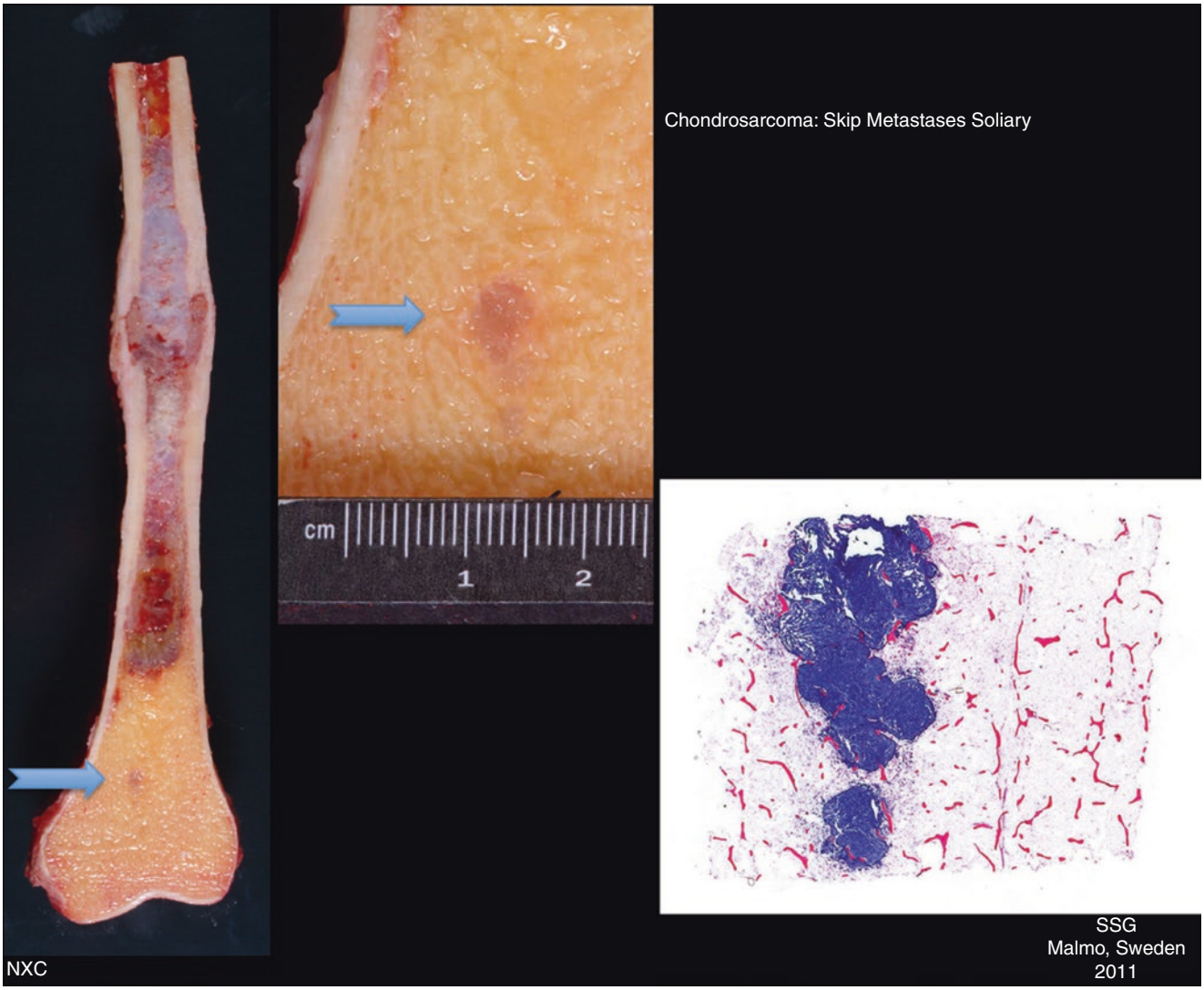

Fig. 3.18 Conventional chondrosarcoma: skip metastasis. Grade 2 chondrosarcoma involves the femoral diaphysis. Tumor forms a well-defined blue-gray intramedullary mass with endosteal scalloping. There is a healing mid-femoral pathological fracture. There is an 8 mm skip metastasis (arrow head) distal to the tumor within the distal femoral metaphysis (see Fig. 3.22). (Courtesy of A. Kevin Raymond, M.D.)

thickening, perhaps the result of slowly growing tumor allowing accommodation by the host bone. Soft tissue tumor extension tends to have the same mineralization characteristics as the intramedullary component. When soft tissue components are less mineralized than the intramedullary component, a high-grade component or dedifferentiation should be questioned. CT scan can add to qualitative assessment of tumor, but together CT and MRI are best for evaluating extent of disease. ChS tends to be hypointense on T1-weigthed imaging while hyperintense on T2-weighted scans. The possibility of skip metastases [60] is best evaluated with MRI (Fig. 3.22a–c and Table 3.4) [62].

Periosteal Chondrosarcoma

Introduction

Periosteal chondrosarcoma (peri-ChS) is a form of primary chondrosarcoma arising directly upon the intact cortical surface of the involved bone.

Clinical

Peri-ChS was described by Lichtenstein in 1955 [63] and has been the subject of subsequent investigation [1, 20, 40, 64–68] and controversy [20].

Although affecting patients over a broad age range, peri-ChS is somewhat more common in patients in the

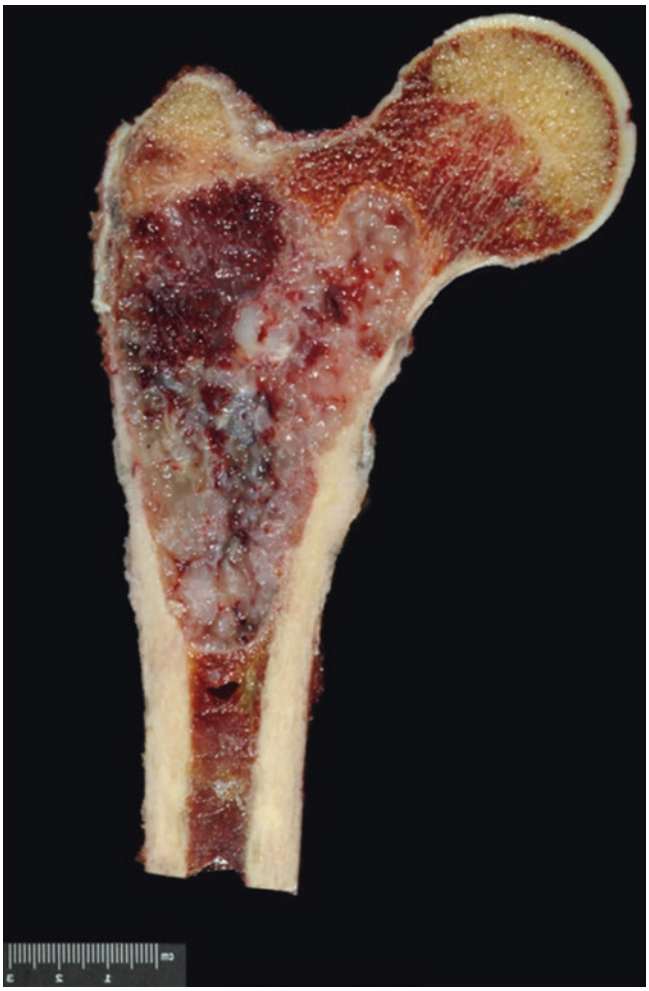

Fig. 3.19 Conventional chondrosarcoma: Grade 2 conventional chondrosarcoma with extensive myxoid degenerative changes. The underlying tumor is formed by a lobulated blue-gray mass with endosteal scalloping. There are superimposed degenerative changes resulting in dissolution of the usual hyaline cartilage and the appearance of a semi-solid mass that varies from yellow-green to red-brown depending on the ratio of myxoid/mucoid degeneration to hemorrhagic degeneration. (Courtesy of A. Kevin Raymond, M.D.)

second through fourth decades of life with a peak incidence in the fourth decade. Males are affected twice often as females. As with other forms of primary cartilage neoplasia, bones formed through endochondral ossification are preferred primary sites, most frequently involving the femur and proximal humerus. Although the vast majority of tumors are >4 cm in greatest dimension, one large series reported tumor sizes ranging from 1.5 to 27 cm, mean 8.1 cm [67].

The signs and symptoms of peri-ChS are relatively nonspecific and frequently of months to years duration [64, 67, 69]. Palpable mass, which may or may not be painful, is the most frequent presenting complaint.

Although long felt to a *less aggressive* form of chondrosarcoma, the rarity of this tumor together with noncomparable reporting makes it difficult to make confident judgment concerning the prognosis of peri-ChS; ultimate survival has been reported at 75–100% [64, 67]. In the only large clinical series [67], the form of surgery, local relapse, and tumor grade were found to influence survival. The vast majority of local relapses and all systemic metastases occurred in patients who underwent intralesional (i.e., curettage) or marginal excision. At the same time, metastases were more frequent in patients having local relapse. When viewed as a function of tumor grade, patients with grade 1 ChS were 71% local relapse-free and 94% metastasis-free. In contrast patients with grade 2 lesions were 67% local relapse-free and 50% metastasis-free. Metastases were generally pulmonary but could appear in lymph nodes (Fig. 3.23a, b) and could appear late in the disease course [63, 68]. Dedifferentiation, i.e., superimposition of a high-grade non-chondroid sarcoma upon a low-grade periosteal chondrosarcoma, has been reported [69].

The current treatment of choice is excision with wide margins of normal tissue, resection when possible and amputation when necessary. No effective forms of adjuvant therapy are currently available.

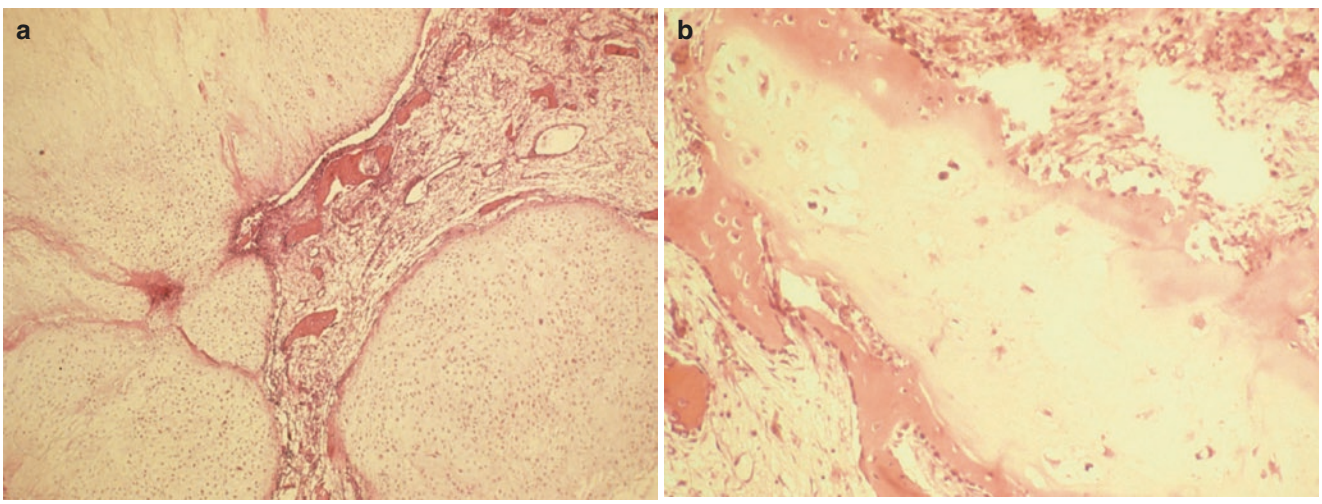

Fig. 3.20 Conventional Chondrosarcoma. (**a**–**c**) This sequence of photos emphasizes the lobular nature of cartilage that is fundamental to the histological appearance of tumor (**a**) that undergoes calcification and endochondral ossification at the lobule periphery (**b**) and results in the gross appearance of cartilage tumors

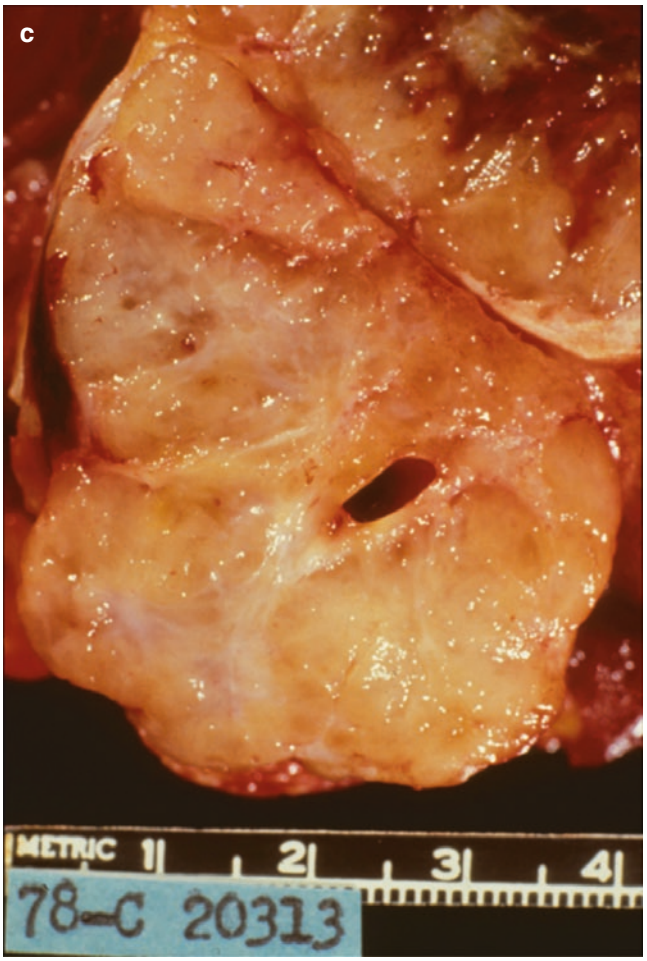

Fig. 3.20 (continued) (**c**) These are the morphological factors that underlie the typical radiological appearance of chondrosarcoma (see Fig. 3.21). (Courtesy of A. Kevin Raymond, M.D.)

- Geographic lesion
- Endosteal scalloping
- Cortical thinning
- Cortical thickening
- Calcifications
  - Ring/Arc
  - Flecks/Dots
  - Heterogeneous

Fig. 3.21 Conventional chondrosarcoma. Plane film radiograph. The typical radiographic appearance of conventional chondrosarcoma: a well-defined, destructive, mixed lytic/blastic geographic lesion. The underlying growth parameters result in widening of the bone and cortical thickening. Calcification at the center and periphery of tumor lobules results in the typical arc/dot, ring/fleck, or popcorn mineralization pattern seen on plane films and CT of chondrosarcoma. As opposed to enchondroma where lesional calcification tends to be uniform, it is heterogeneous in malignant cartilage. (Courtesy of A. Kevin Raymond, M.D.)

Histopathology

The histological features of peri-ChS are the same as those of conventional intramedullary ChS [1, 20, 40, 63, 64, 66–68]. The overwhelming majority of tumors are grade 1 or grade 2 chondrosarcoma, composed of typical gray-blue hyaline cartilage lobules (Fig. 3.24). Matrix degeneration (e.g., myxoid change) may be seen and is generally associated with increasing tumor atypia and grade. Focal calcification and endochondral ossification typical of cartilage neoplasia may be present. Tumor generally overlies periosteal reactive bone; infiltration of the reactive bed may occur over time. Intact and frequently thickened periosteum almost always bounds the tumor at the peripheral tumor/normal soft tissue interface.

Gross

Peri-ChS generally forms a broad-based mass arising on the cortical surface overlying the metaphysis or meta-diaphysis. Initially, tumor limits are defined by the intact underlying cortex and the overlying periosteum. Advanced lesions tend to grow circumferentially around the parent bone forming a so-called "wraparound" lesion (Fig. 3.25). Focal cortical erosion and/or invasion may be seen.

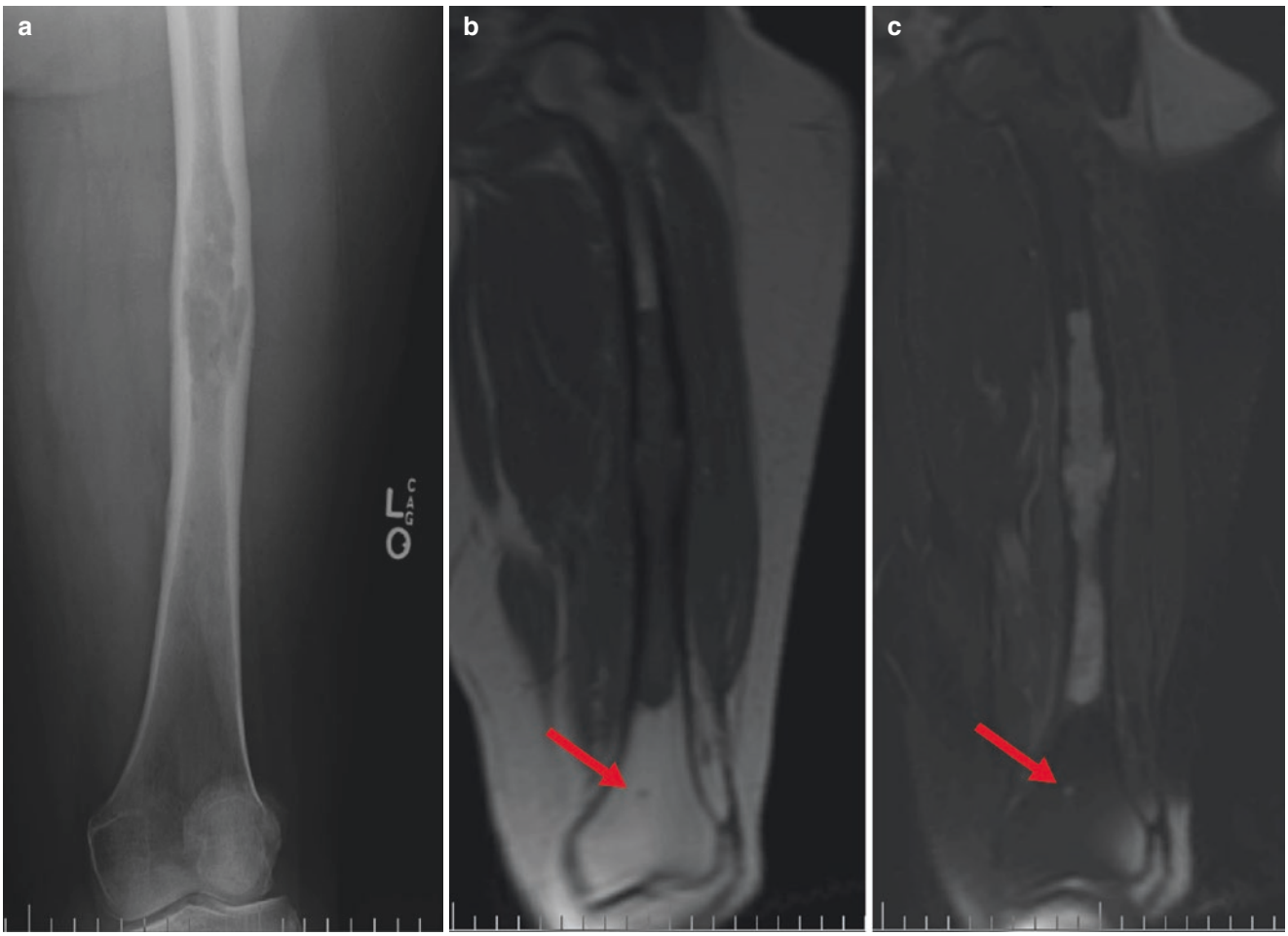

Fig. 3.22 Conventional chondrosarcoma: skip-metastasis (same case as Fig. 3.18). (**a**) Although plane film identifies the diaphyseal chondrosarcoma, there is no evidence of the skip metastasis on plane film. (**b**, **c**) MRI clearly shows the skip metastasis on both T1- and T2-weighted images (arrow). (Courtesy of A. Kevin Raymond, M.D.)

Table 3.4 Comparison of criteria for diagnosis of enchondroma and conventional chondrosarcoma

Criteria	Benign	Malignant
Age	Broad	Older (fourth to seventh decade)
Gender	Equal	Male/female (3:2)
Location	Acral	Central
Radiology	Chondroid	Chondroid
	Quiescent	Aggressive
Architecture (histology)	Hypercellular	Hypercellular
	Loss or organization	Loss of organization
		Infiltration
		Increased nuclear detail
		Increased cytoplasm
Histology/ cytology		More than occasional
		Binuclear cells
		Typical histologic criteria of malignancy
		Mitoses

There are differences at the level of clinical, radiographic, and histological level that must be considered. From the perspective light microscopy, both enchondroma and chondrosarcoma have significant architectural changes. Histological discrimination between them lies largely within cytological parameters.

As with central c-ChS, cut surface is composed of lobules of hyaline cartilage with color, consistency, and texture being a function of tumor grade and degenerative changes. Low-grade peri-ChS having few degenerative changes tends to be firm to rock-hard, lobular, homogeneous, smooth, blue to blue-gray, glassy, and semitranslucent. Smudgy or speculated chalky white to yellow-white areas correspond to areas of mineralization and endochondral ossification.

In higher-grade peri-ChS the above features are generally maintained but accompanied by secondary changes. Higher-grade tumors tend to be less homogeneous with the cut surface being granular, focally semisolid, with the blue-gray becoming cloudy or opalescent and potentially of green-gray discoloration together with white to yellow-white patches of calcification (Fig. 3.25). Rare lymph node metastases may be seen (Fig. 3.23).

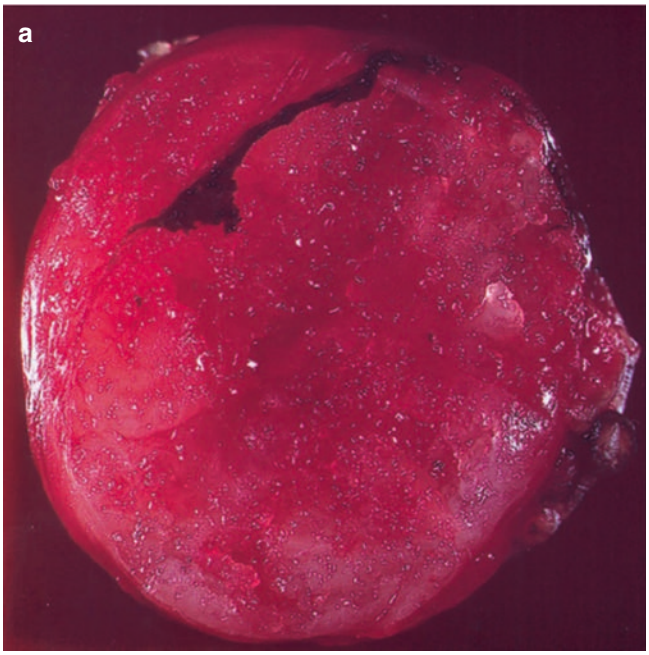

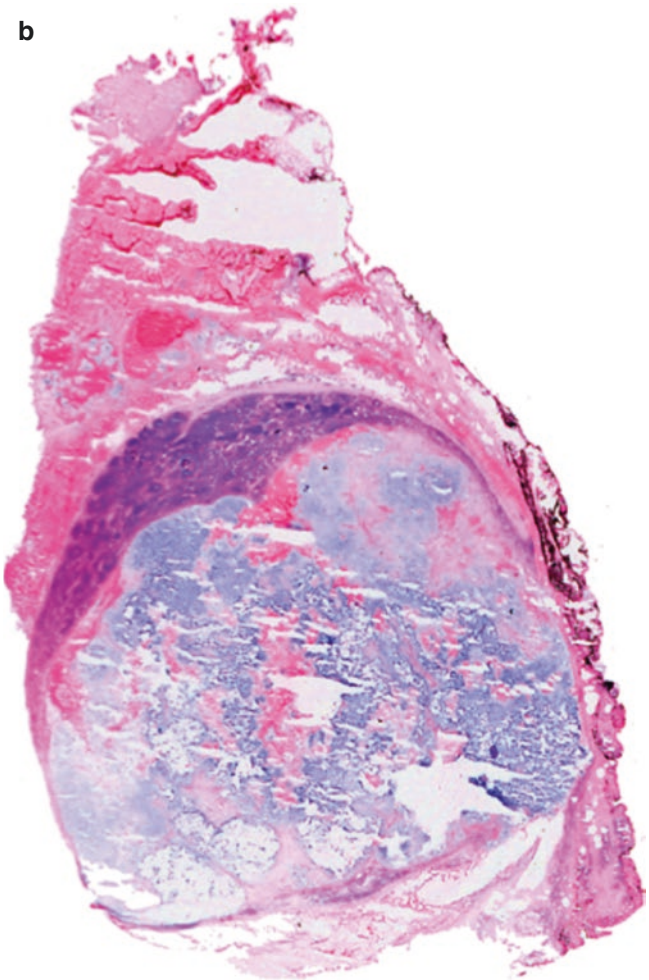

Fig. 3.23 Periosteal chondrosarcoma. (**a**) Metastatic chondrosarcoma involving lymph node (gross specimen: cut surface). (**b**) Metastatic chondrosarcoma involving lymph node (whole mount frozen section). (Courtesy of A. Kevin Raymond, M.D.)

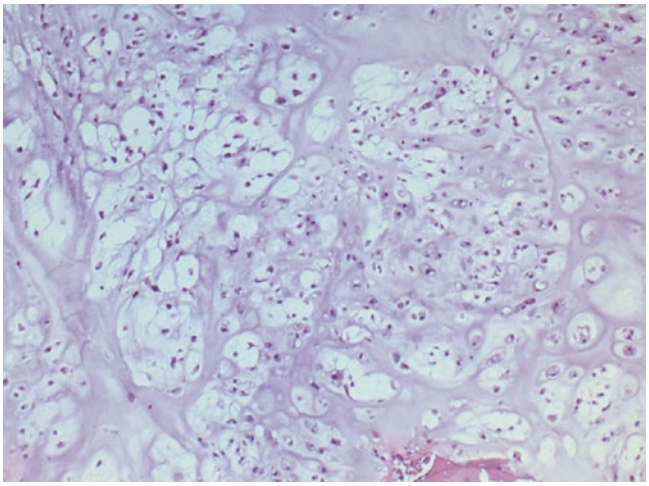

Fig. 3.24 Periosteal chondrosarcoma. The histological features are those of grade 2 chondrosarcoma (40×)

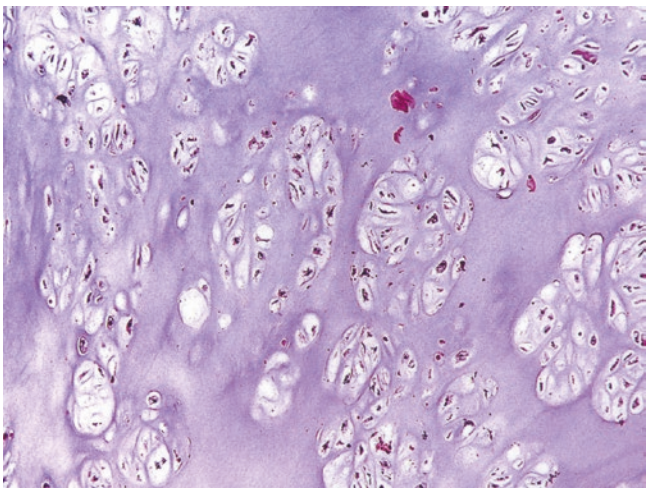

Fig. 3.25 Periosteal chondrosarcoma. The histological features are those of grade 2 chondrosarcoma (100×)

Radiology

Peri-ChS forms relatively well-defined, broad-based, mixed lytic/blastic lesion centered on the cortical bone surface. There is frequently cortical erosion alternating with laminated periosteal bone formation. The interface with overlying normal soft tissues tends to be well-defined by irregularity, corresponding to unmineralized tumor and entrapped normal tissues. Mineralization is in the usual "popcorn" and "ring/arc and fleck" pattern [1, 64, 69, 70]. Caution should be taken in interpreting these, since mineralization may so profound as to mimic other forms of surface neoplasia (e.g., parosteal osteosarcoma) (Figs. 3.26 and 3.27). CT and MRI

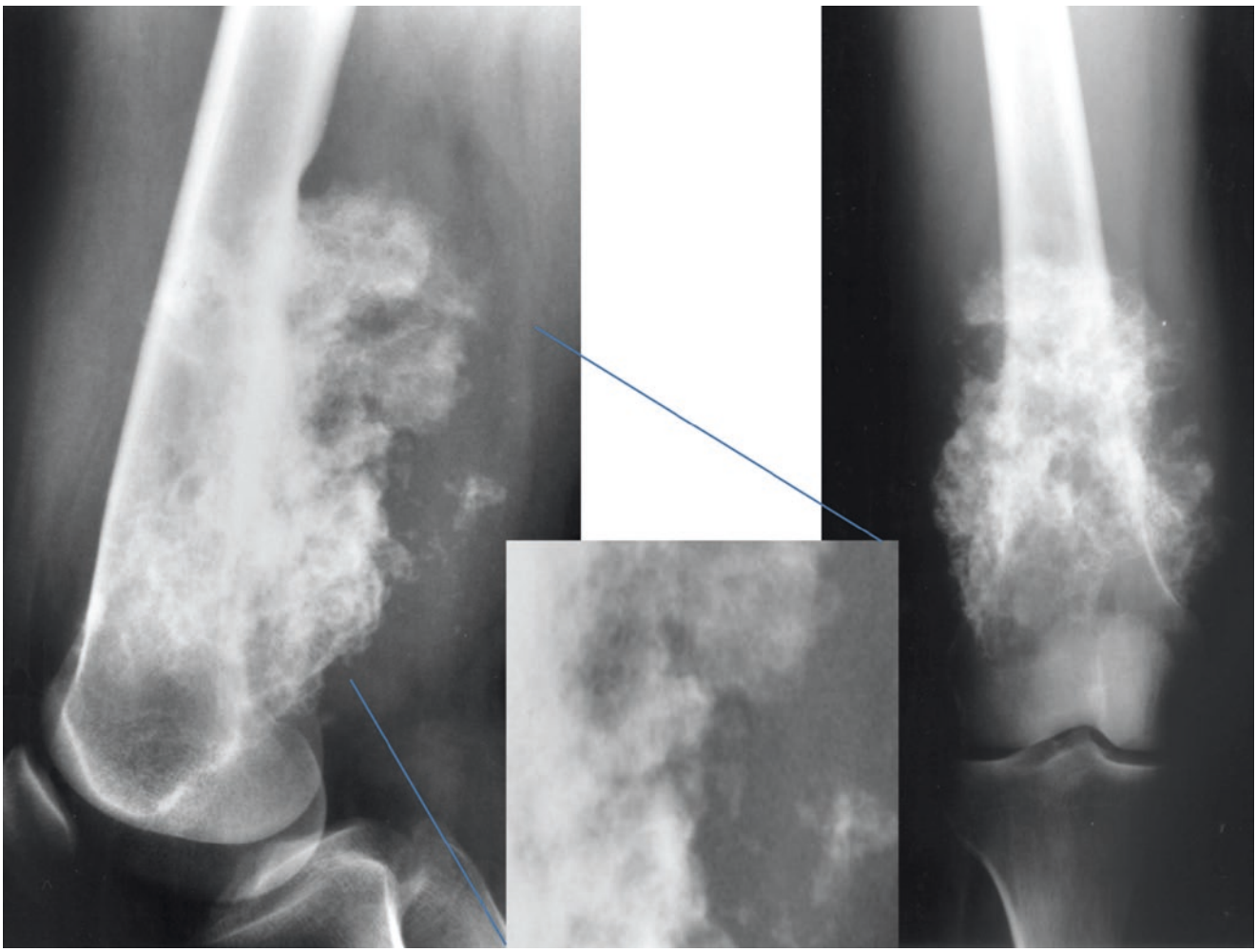

Fig. 3.26 Periosteal chondrosarcoma. Radiographs (plane films: lateral and AP) of periosteal chondrosarcoma involving distal femoral metaphysis. The mineralization density raised the question of parosteal osteosarcoma. However, close examination (magnified inset) shows the typical cartilaginous "popcorn" mineralization pattern

provide greater detail concerning extent of disease and normal/tumor interface. Peri-ChS tends to be hyperintense in T2-weighted images.

The differential diagnosis of peri-ChS casts a broad net and depending on a variety of factors (e.g., age, location, histology, imaging features) includes periosteal chondroma, periosteal osteosarcoma, parosteal osteosarcoma, periosteal Ewing's sarcoma, dedifferentiated peripheral chondrosarcoma, Ollier's disease, Nora's lesion, florid reactive periostitis, subungual exostosis, and avulsion reaction. However, most of these are easily dealt with; the most critical are summarized in (Table 3.5).

Secondary Chondrosarcoma

Definition

Chondrosarcoma is arising as a secondary phenomenon in the setting of an underlying, previously existing condition.

Clinical

Secondary chondrosarcoma (secondary ChS) is generally regarded as representing those forms of conventional ChS arising in association with previously existing cartilage lesions: solitary/multiple osteochondromas, solitary/multiple chondromas, and synovial chondromatosis [1, 10, 20, 71, 72]. Although

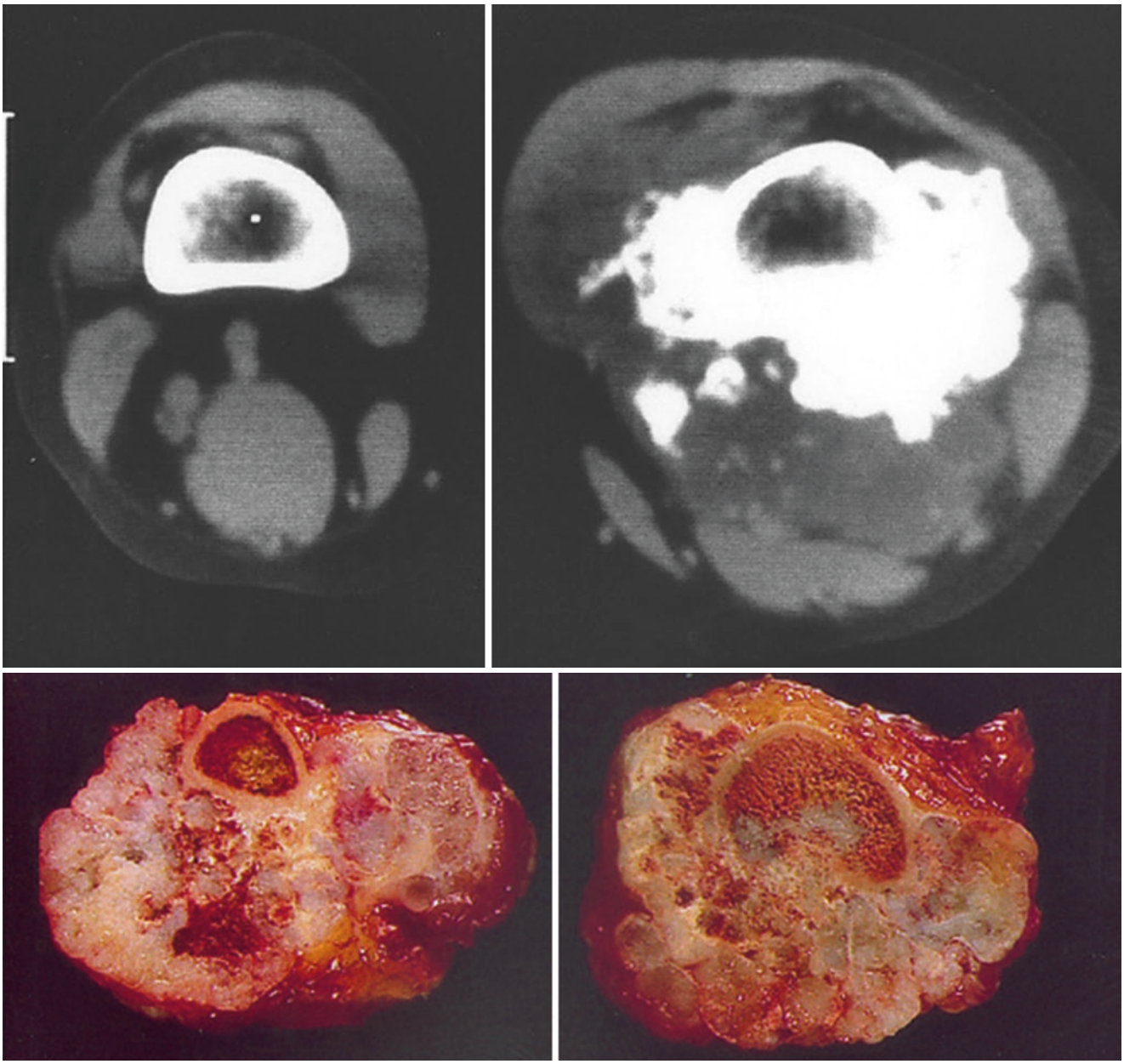

Fig. 3.27 Periosteal chondrosarcoma. Tumor forms a wraparound lesion as seen on both CT scan and cross-sectional specimen sectioning. The cut surface of the tumor is that of a largely blue-gray lobulated mass that engulfs the posterior, lateral, and medial aspects of the femur

Table 3.5 Surface neoplasia. Differential diagnosis chondroid surface lesions

	Diagnosis			
Parameter	Periosteal chondroma	Periosteal chondrosarcoma	Periosteal osteosarcoma	Parosteal osteosarcoma
Age (decades)	2 > 3	2 > 4	2 > 3	3 > 4
Gender (M/F)	5:3	2:1	3:2	1:2
Location	Humerus, femur	Femur, humerus	Femur, tibia	Femur, tibia, humerus
Part	Metaphysis	Meta-diaphysis	Diaphysis	Meta-diaphysis
Size	<4 cm	>4 cm	>5 cm	>5 cm
Imaging	Lytic, hemisphere	Irregular, broad-based, popcorn	Spiculated hemisphere with collar	Mushroom lucent line wraparound
Histology	Enchondroma	g1/g2 ChS	g2 zonated COS	Low-grade spindle cells well-formed bone ± cartilage cap

much less frequent than osteosarcoma and fibrosarcoma, secondary ChS can arise as a form of postradiation sarcoma.

Secondary ChS tends to occur in a somewhat younger patient population than primary c-ChS. Patients tend to be in the second to fifth decades with a peak incidence in the third decade. Males are affected more often than females, with male to female ratio of 3:2. The most frequent bones involved include the bones of the pelvic and shoulder girdles, femur, spine, and ribs.

Secondary ChS affects less than 1% of patients with solitary osteochondromas and probably and equally small number of patients with solitary enchondromas. The estimated incidence associated with MHE rises to at least 5% of MHE patients. However, a much higher proportion of patients with multiple enchondromatosis suffer secondary ChS, 40% of Ollier and 50% of Maffucci patients [10].

Patients tend to present with pain. Swelling and enlarging of mass are frequent, especially when ChS arises in association with an osteochondroma. Mass affect can result in symptoms dependent on tumor location. New pain, a change in the character of previously existing pain, new growth, or a cartilage cap thickness of >2.0 cm in a skeletally mature patient should raise suspicion of secondary ChS.

Although the presence of underlying benign cartilage lesion may add an element of complexity to therapy, the treatment of secondary ChS is similar to primary ChS, resection when possible and amputation when necessary. That fact that these tumors arise secondary to a pre-existing benign cartilage lesion or within the context of a defined syndrome does not impact ultimate ChS prognosis. Patient survival remains a function of tumor location, size, and grade. Maffucci's syndrome is associated with an increased incidence of a wide variety of tumors, and prognostic significance is in question; the lack of adequate follow-up complicates data interpretation.

In light of the anatomical differences, interpretation of origin from a specific enchondroma is more difficult than cases associated with osteochondroma. In the case of osteochondroma, ChS arises from the cartilage cap. The latter may be completely replaced by tumor. However, the stalk, or in the case of sessile osteochondromas the cortical defect, remains, allowing interpretation. In the case of enchondromas, the histological similarities between "atypical" enchondroma and chondrosarcoma impede unequivocal interpretation of benign versus malignant. Prior imaging studies documenting a preexisting enchondroma add confidence to interpretation. Generally, enchondromatosis patients have long medical histories with a long history of imaging studies that can be used for comparison.

Histopathology

Other than the presence of the underlying benign cartilage lesion, the histological appearance of secondary ChS is identical to de novo chondrosarcoma. The vast majority of tumors are grade 1 or grade 2 chondrosarcoma; grade 3 lesions are vanishingly rare.

Gross

As with histology, other than the presence of the underlying benign cartilage lesion, the gross appearance of secondary ChS is identical to de novo chondrosarcoma. Key is identifying the underlying benign lesion. In the case of osteochondroma, tumor generally arises from the periphery of the cartilage cap and extends outward into soft tissues, initially beneath the perichondrium/periosteum and ultimately involving true soft tissues (Fig. 3.28).

Unequivocal gross identification of an underlying enchondroma can be difficult. Benign and malignant lesions are similar. However, secondary degenerative changes are infrequent in enchondroma and frequent in ChS. In the case of enchondromatosis, it is the presence of coexisting enchondromas adjacent or near ChS which allows association.

Radiographs

Secondary ChS appears as enlarging chondroid-mineralized mass. In the case of underlying osteochondromas, tumors tend to arise from the cartilage cap surface. Tumor then extends outward toward soft tissues (Fig. 3.29). The size and extent of involvement of ChS arising with osteochondroma is largely a function of location and proximity to structures that will give rise to symptoms when compress. At the same time, ChS growth often destroys the pre-existing cartilage. The presence of the osteochondroma stalk and/or the cortical defect caused by the site of origin of the osteochondroma remains and allows diagnosis [1]. Of course, if there are prior imaging studies, evidence of new growth of the cartilage cap is circumstantial evidence of superimposed malignant change.

A similar approach applies to enchondromas. In the absence of prior imaging studies, a definitive statement concerning the possible presence of a previously existing enchondroma underlying a ChS may be problematic. However, patients with enchondromatoses inevitably have prior imaging studies documenting their multiple destructive and distortive enchondromas. Secondary ChS appears as a destructive, enlarging lesion superimposed on a previously existing enchondroma.

Mesenchymal Chondrosarcoma

Definition

Mesenchymal chondrosarcoma (m-ChS) is a bimorphic malignant neoplasm with elements of conventional chondrosarcoma juxtaposed to a population of malignant small cells. Tumor shows some tendency to preferentially involve the non-appendicular skeleton and has a poor prognosis.

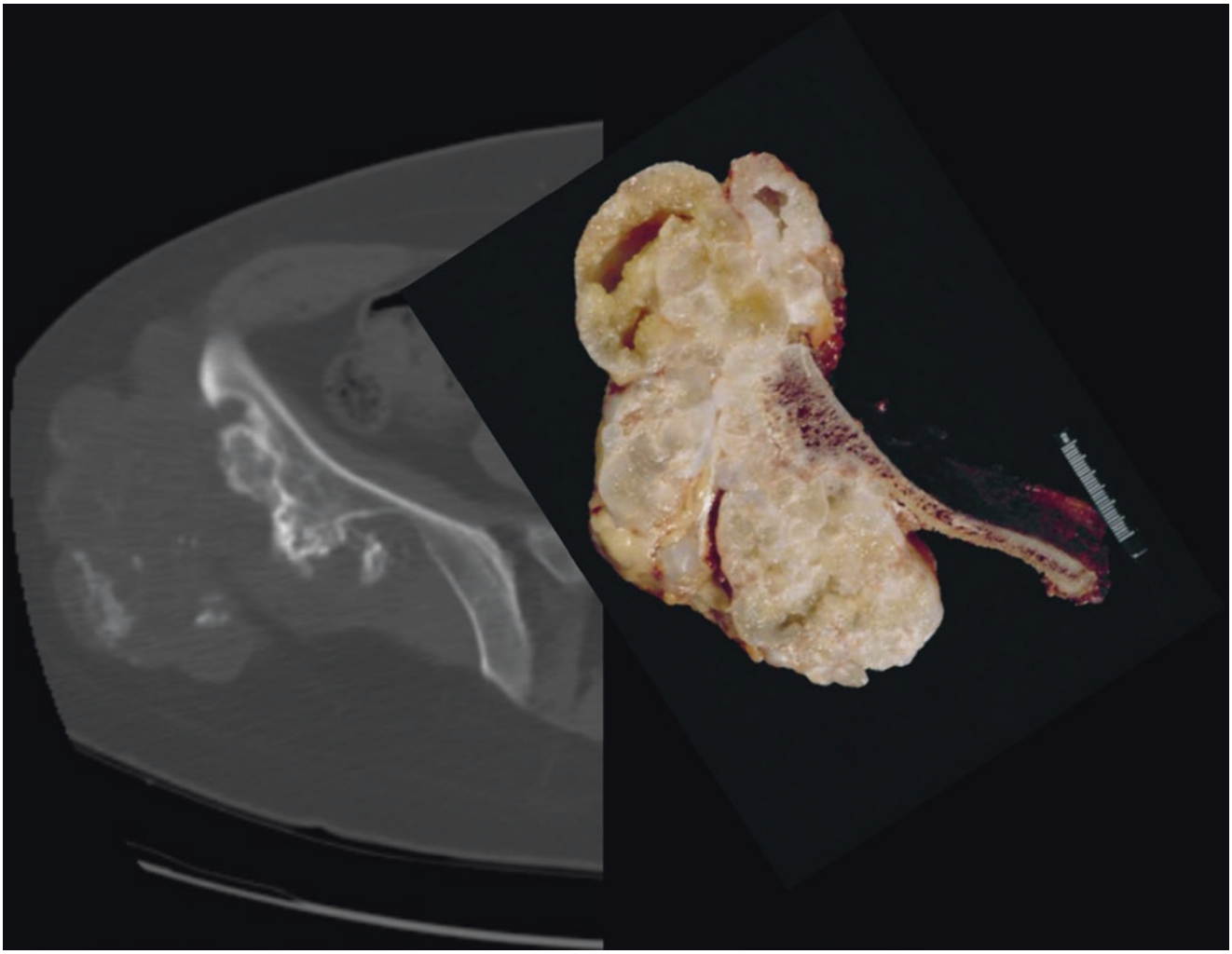

Fig. 3.28 Secondary chondrosarcoma. CT and gross specimen. Same case as Fig. 3.29. CT shows a large soft tissue mass overly the lateral aspect of the iliac wing. Note the area of cortical discontinuity at the base of the osteochondroma stalk. Gross specimen correlates and confirms the findings of the CT imaging. The tumor is composed of lobulated gray-blue to white, semitranslucent mass. The foci of green-gray change correspond to areas of degenerative change, particularly toward the anterior end where there is cystification

Fig. 3.29 Secondary chondrosarcoma. Plane film (AP) shows a large largely lytic mass overlying the iliac wing. Tumor is finely stippled with fine ring and fleck (i.e., popcorn) calcification. Inset: close-up on chondroid popcorn calcification

Clinical

m-ChS was originally described by Lichtenstein and Bernstein in 1959 [73] in a paper describing diagnostic issues involving a number of unusual cartilage lesions. The observations were subsequently confirmed and expanded by a number of subsequent investigators [1, 74–78].

m-ChS tends to affect patients in the second and third decades and somewhat less frequently in the fourth decade. The incidence in men and woman is roughly equal. Although appendicular bones may be a source, m-ChS most frequently involves more central bones: head and neck, especially the jaws, ribs, pelvis, and spine. When arising in appendicular lone bones, m-ChS tends to originate in the metaphyses.

Pain and slowly enlarging mass are most frequent. Although symptoms may have a sudden sever onset, they tend to arise over a prolonged course of time.

The natural history of m-ChS is one of the local, repeated aggressive relapses and eventual lethal systemic metastases.

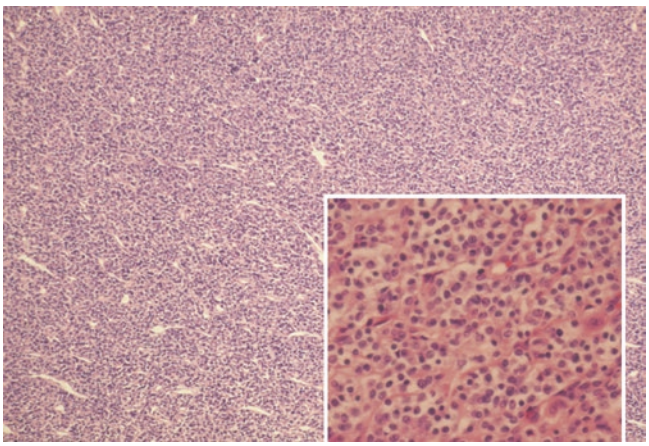

Fig. 3.30 Mesenchymal chondrosarcoma: tumor is composed of sheets of small blue cells through which there are arcades of dichotomous branching small vessels; *hemangiopericytoma-like pattern*. (40×). Inset: small blue cells with minimal ill-defined cytoplasm (100×)

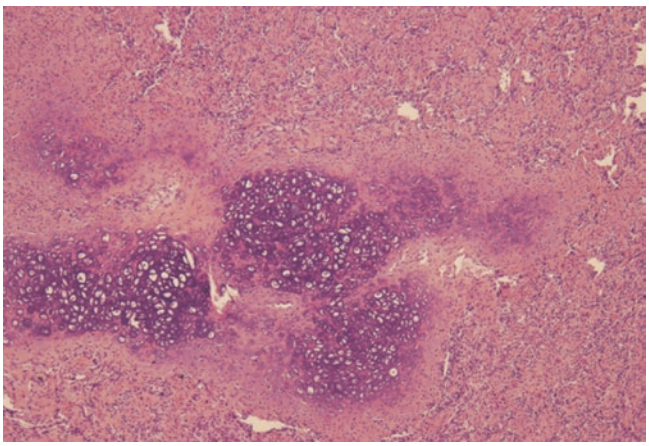

Fig. 3.31 Mesenchymal chondrosarcoma: photomic. Cellular phase composed of sheets of small blue cells juxtaposed to low-grade malignant hyaline (40×)

Historically, complete surgical removal of the primary tumor was the mainstay of therapy, with near uniformly poor results. The addition of re-excision of local relapse(s) and pulmonary metastases together with external beam radiation therapy and various forms of systemic (e.g., chemotherapy) therapy has shown little, if any, impact on prognosis. In a recent review [77], the overall survival at 5, 10, and 20 years was 55%, 43.5%, and 15.7%, respectively. However, event-free survival was found to be 45%, 27%, and 8.1% at 5, 10, and 20 years, respectively.

Histopathology

m-ChS is bimorphic tumor, with both cellular and matrix-producing components (Fig. 3.30). The matrix component is made up of well-defined, variably sized, gray-blue, lobules of hyaline cartilage. This chondroid component is made up of hypercellular, disorganized hyaline cartilage with variable degrees of cellular atypia, usually relatively low-grade (i.e., grade 1 or grade 2) ChS. The cellular component is composed of sheets of "small blue cells." Slit-like, delicate vessels/capillaries with a tendency toward dichotomous branching (i.e., so-called "staghorn" pattern) frequently course through these sheets of neoplastic cells imparting a hemangiopericytoma-like appearance. At the same time, the vessels with apparent retraction artifact may impart an organoid appearance to the cellular tumor component. The individual cells, within the cellular phase, are usually round to oval with minimal cytoplasm and may have either hyperchromatic or open nuclei. When non-hyperchromatic, tumor nuclei tend to have well-defined nuclear membranes that may be irregular and encase unevenly distributed coarse and clumped chromatin, small nucleoli may be present. Mitotic activity may or may not be appreciable. At times the "small cells" may be short spindle cells. The cytological features of m-ChS may mimic those of Ewing sarcoma, malignant neuroendocrine tumors, or lymphoma. There is a sharp interface between the cellular and matrix component; they do not mix nor is there transition between the cellular and matrix elements (Figs. 3.31 and 3.32).

Neoplastic cells has immunoreactivity for SOX9, CD99, and desmin [79, 80], while immunohistochemical studies for FLI-1 and CD45 are negative [81].

Molecular studies have potentially added to our diagnostic armamentarium when dealing with m-ChS. Over time a variety of abnormalities have been reported in association with chromosome 8. Recently, the HEY1-NCOA2 fusion appears to be a potentially defining gene fusion in m-ChS [19, 82]. At the same time, IDH1 and IDH2 point mutations associated with more typical hyaline cartilage neoplasia are not present [83].

The differential diagnosis of m-ChS versus osteosarcoma (e.g., small cell osteosarcoma) can present significant problems. A largely unspoken issue is the fact that m-ChS is a tumor in which neoplastic cells may produce osteoid. With the discovery of immunoreactivity for SOX9 and a unique molecular marker, this problem may recede from significance and have an answer more substantial than that of personal histological interpretation.

Gross

The gross appearance of m-ChS reflects its histological composition (Fig. 3.33a, b). The color and texture of the cut surface are functions of the relative amounts of matrix- and non-matrix-producing components. When hyaline cartilage is dominant, it imparts and overall lobulated,

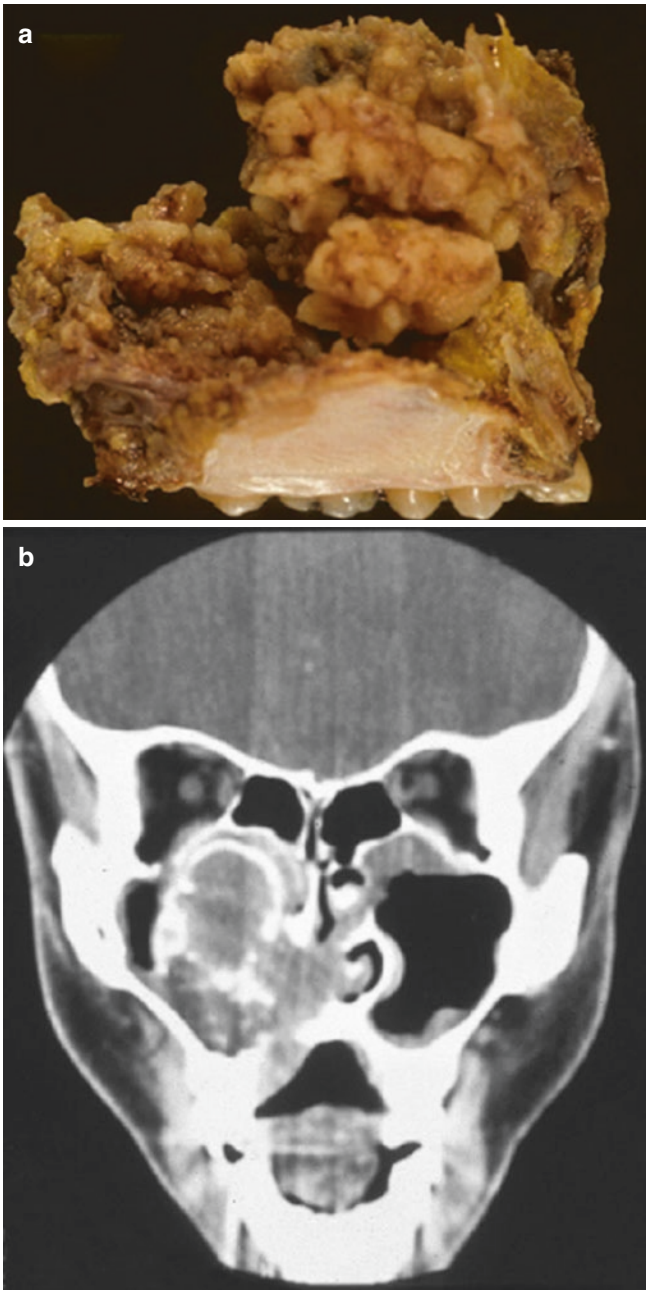

Fig. 3.32 Mesenchymal chondrosarcoma: gross and CT. (**a**) Maxillectomy gross specimen: the cut surface of tumor is a characteristic lobulated fawn brown. (**b**) CT shows the maxilla replaced by a lobulated, hazy, minimally opaque lesion with focal popcorn calcification

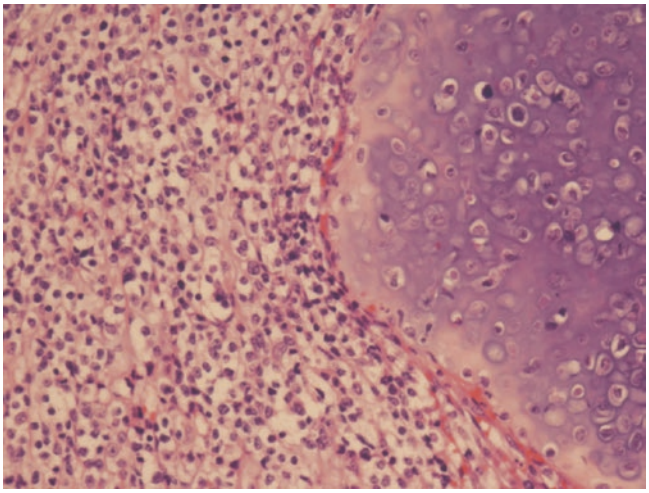

Fig. 3.33 Mesenchymal chondrosarcoma: biphasic neoplasm. Interface between small blue cells and low-grade hyaline cartilage. There is no mixing or transition between the cellular and matrix phases (200×)

blue-gray to silver semitransparent appearance, and the lesions are correspondingly solid (Fig. 3.33a, b). In contrast, when the majority of the lesion is composed of sheets of small cells, the m-ChS is predominantly pale brown, a color shade not unlike parathyroid tissue, i.e., so-called fawn brown (Fig. 3.33a, b). In this latter situation, there tend to be small islands of blue-gray hyaline cartilage that impart a granular quality to an otherwise homogeneous soft/firm tumor. The lesions are generally highly destructive, eliminating trabecular bone in the involved area. There tends to be endosteal scalloping of overlying cortex and cortical destruction in areas of tumor extension into overlying soft tissue. It has been our experience that the fawn brown color is the more common appearance. Although relatively well-defined, the interface with normal bone tends to be infiltrative.

Radiology

These lesions are largely radiolucent and destructive. Although relatively well-defined the tumor/normal interface tends to be infiltrative. The involved bones frequently have changes of endosteal scalloping and reactive cortical thickening alternating with areas of cortical destruction where

tumor extends into overlying soft tissues. Lesions frequently show nonhomogeneous intralesional calcification similar to c-ChS, i.e., punctate calcification with a ring and fleck pattern (Fig. 3.32a, b). CT may add detail to the analysis of tumor composition. m-ChS is hyperintense on T2-weighted MRI images. Again the combination of CT and MRI best estimates the extent of disease [10, 20].

Dedifferentiated Central Chondrosarcoma

Definition

Dedifferentiated ChS (dd-ChS) is a biphasic form of ChS in which there is a low-grade cartilage neoplasm juxtaposed to a form of high-grade non-cartilaginous sarcoma. dd-ChS is associated with a very poor prognosis.

Clinical

dd-ChS was introduced as a unique entity by Dahlin in 1976 [1] as recognition of a particularly aggressive form of intramedullary (i.e., central) ChS in which contemporary forms of therapy were ineffective, an observation confirmed by subsequent investigators [1, 84–86]. In the original description, high-grade sarcoma was juxtaposed to a low-grade intramedullary chondrosarcoma. Since then these observations have been confirmed, and the concept of *dedifferentiation* has been described in association with a number of primary cartilage lesions including peri-ChS, peripheral secondary ChS, clear cell ChS [10, 20], and even on occasion enchondroma, periosteal chondroma, or osteochondroma.

dd-ChS tends to affect an older population with a peak incidence in the sixth to eighth decades and slightly more common in males than female. The femur, especially the proximal femur, the ilium, and humerus are the most frequent primary sites.

Pain, swelling, and enlargement of mass are frequent. The frequency of mass effect with attendant symptomatology is a function of tumor size and location.

dd-ChS is an extremely aggressive form of chondrosarcoma, both in relentless invasive local growth and the rapid development of lethal systemic metastases. Historically, treatment was focused on the primary tumor, resection when possible and amputation when necessary. Surgery-only therapy was followed by near-uniform failure, rapid clinically evident systemic metastases, followed by death within 2 years [10, 87]. Contemporary therapy employs protocols similar to those used in the treatment of osteosarcoma, preoperative chemotherapy, followed by surgery, followed by response-dependent postoperative chemotherapy (see section "osteosarcoma"). Survival is still suboptimal with most patients dead of disease within 2 years [10, 88].

Histopathology

Histologically, dd-ChS is a biphasic lesion composed of low- and high-grade components. The bulk of the intramedullary lesion generally corresponds to an underlying form of low-grade (i.e., grade 1 or grade 2) chondrosarcoma or even chondroma or osteochondroma [86]. Juxtaposed to the low-grade cartilage neoplasm is a form of high-grade sarcoma, most frequently osteosarcoma, fibrosarcoma, malignant fibrous histiocytoma, or unclassified sarcoma [10, 87]. Other forms of high-grade sarcoma, e.g., rhabdomyosarcoma, leiomyosarcoma, and telangiectatic osteosarcoma, have been reported [89–91]. Interestingly the reported association between a low-grade cartilage neoplasm with superimposed giant cell tumor of the bone also has an extremely poor prognosis [92].

Discrimination from cartilage predominant osteosarcoma (i.e., chondroblastic osteosarcoma) is key. In chondroblastic osteosarcoma, the various histological constituents are all high-grade, liberally mix together, and frequently have areas of transition between the various components.

In contrast, there is a sharp interface between the low- and high-grade components in dd-ChS; the two elements do not mix nor is there transition between them (Fig. 3.28).

Tumor mineralization is variable and related to the type of matrix. Tumor forms largely cohesive sheets that have an infiltrative interface with normal trabecular bone. In areas in which the chondroid component interfaces with endosteal cortex, the resulting interaction results in endosteal scalloping typical of cartilage lesions. Either the cartilage or non-cartilaginous component may infiltrate cortical bone and extend into overlying soft tissues. Periosteal reactive bone may be extensive (Fig. 3.34).

Gross Pathology

dd-ChS remains a bimorphic neoplasm at the level of gross examination. In general, there is a region of well-defined and easily recognized chondrosarcoma/cartilage neoplasia: blue to blue-gray, lobulated, semitranslucent, firm, compressible, focally calcified chondroid tissue with a scalloped cortical interface. Superimposed on this is a non-chondroid component whose gross appearance reflects the underlying histopathology. The secondary component may be a highly mineralized, bone-producing component of osteosarcoma. The non-matrix-producing secondary forms (e.g., fibrosarcoma, malignant fibrous histiocytoma, rhabdomyosarcoma) have an off-white to beige to tan fish-flesh appearance. Although the secondary component may be within the medullary cavity, it is frequently at the peripheral tumor/soft tissue interface.

Radiology

The overall radiographic appearance largely simulates conventional chondrosarcoma. However, the superimposition of a second non-chondroid component results in a bimorphic (Fig. 3.35a–c) appearance referred to by one investigator as *tumoral dimorphism* [93]. In most cases there is a large intra-

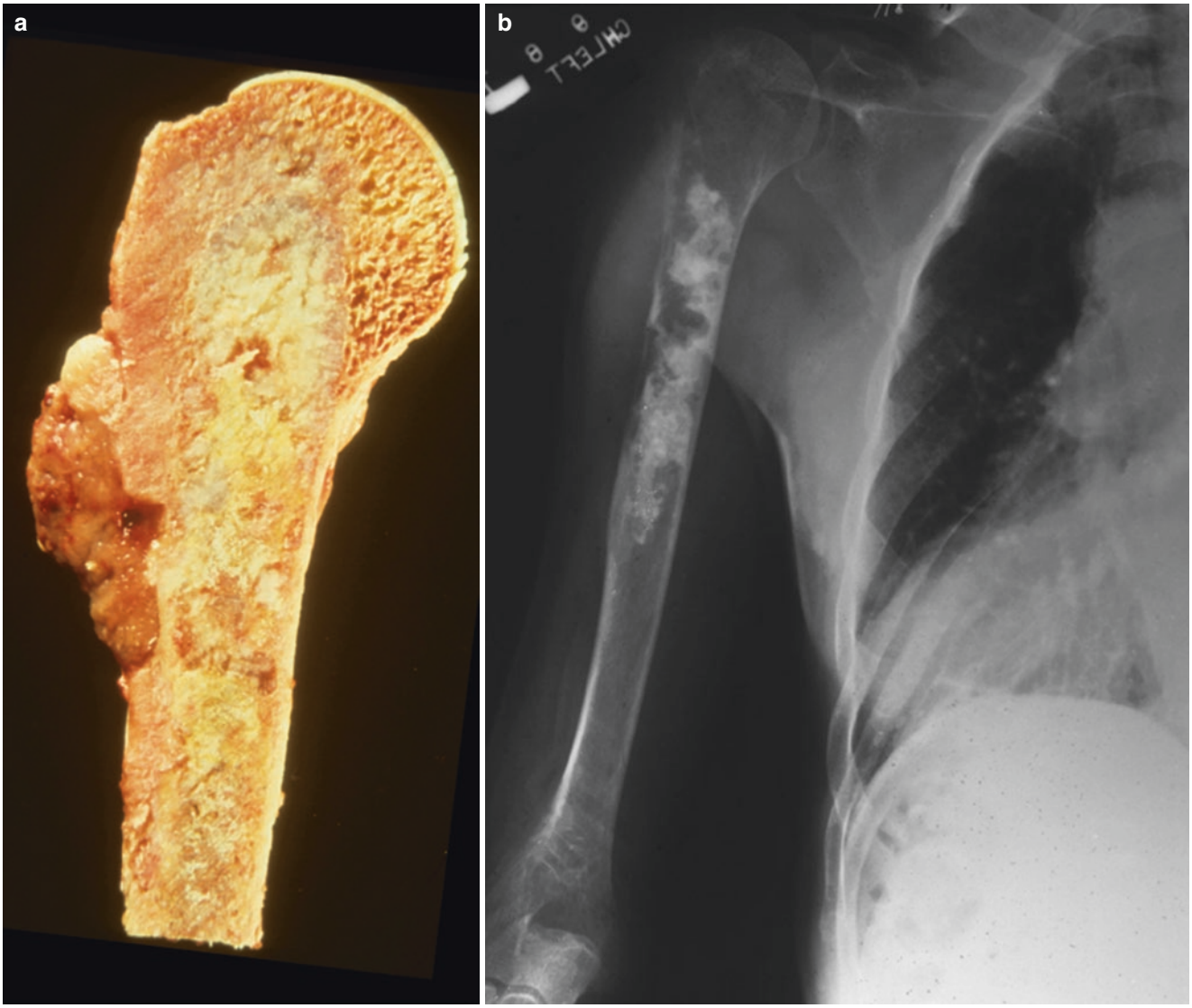

Fig. 3.34 Dedifferentiated chondrosarcoma: gross specimen and plane film. Dedifferentiated chondrosarcoma forms a bimorphic lesion with a lobulated gray-blue to yellow intramedullary chondrosarcoma component. Immediately adjacent to the chondrosarcoma component is a tan hyperemic, fleshy tumor component that has eroded through cortex into adjacent soft tissue

medullary lesion with a typical aggressive chondroid appearance: heterogeneous, lobulated lesion with endosteal scalloping, nonhomogeneous popcorn calcification, cortical thickening, and cortical breakthrough. Superimposed on this is a secondary lesion with features typical of osteosarcoma or a non-mineralized sarcoma.

This tumoral dimorphism will vary as a function of the underlying previously existing lesion. The possible underlying lesions so far described include periosteal chondroma, periosteal ChS, osteochondroma with or without a secondary ChS, and clear cell ChS.

Clear Cell Chondrosarcoma

Introduction

Clear cell chondrosarcoma (cc-ChS) is biphasic variant of chondrosarcoma. The hallmark is the presence of neoplastic cells with clear cytoplasm. The tumor has a marked propensity for epiphyseal origin.

Clinical

cc-ChS was originally described by Unni, Dahlin et com [94] and constitutes some 2% of chondrosarcoma. Although it may occur at virtually any age, it most frequently affects patients in the third and fourth decades of life. Men are affected more frequently than women, with male to female ratio of 3:1. Although virtually any bone may be involved, it most frequently arises from the epiphyses of the long bones of the appendicular skeleton, in particular the proximal femur (55%) and proximal humerus (17%). Since most patients are skeletally mature resulting from growth plate involution, these are technically not epiphyses, and some authors refer to the site as merely the *end of the bone.* For simplicity we refer to these as *epiphyses* or *apophyses.*

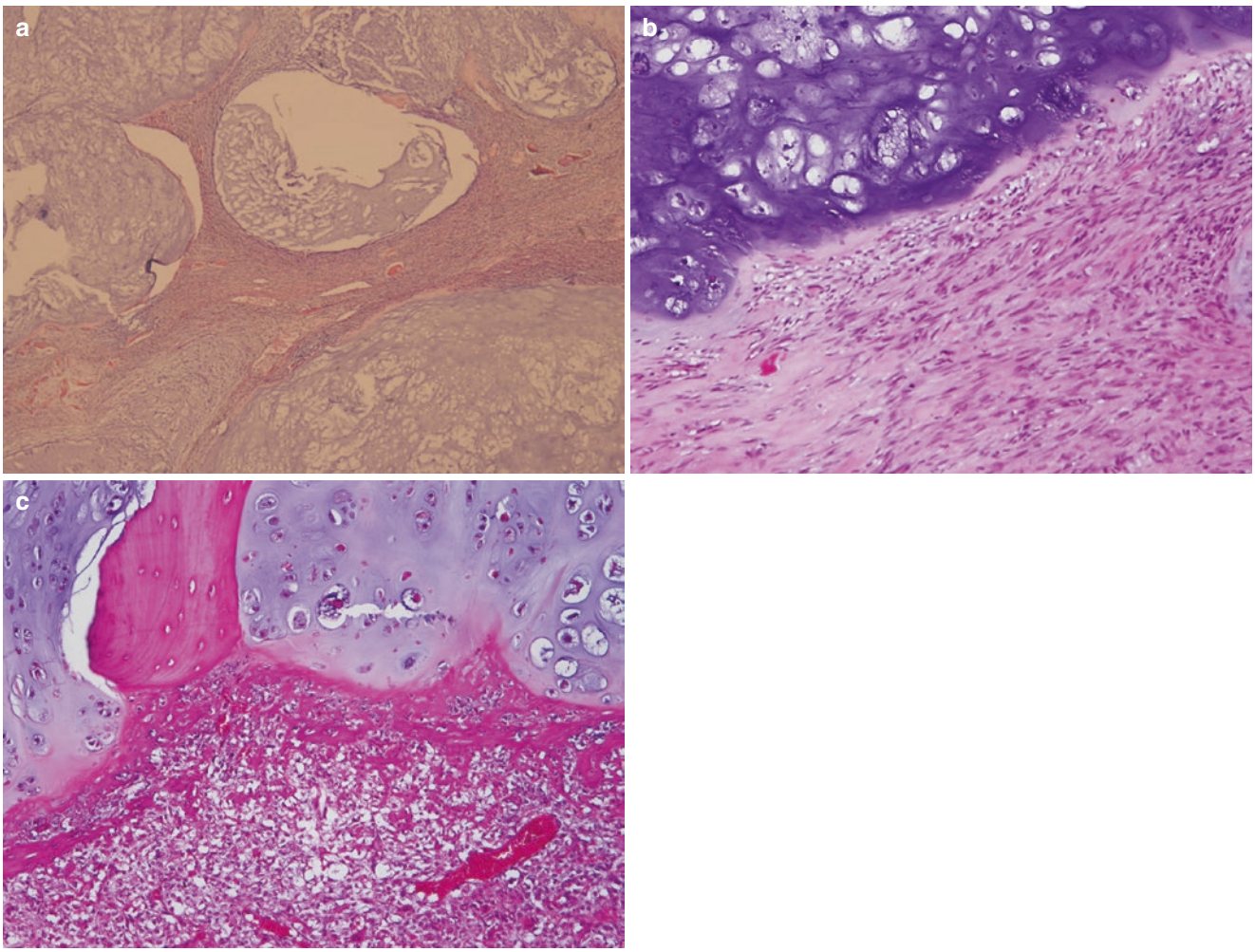

Fig. 3.35 Dedifferentiated chondrosarcoma: photomics. (**a**) High-grade spindle-cell sarcoma juxtaposed to grade 2 chondrosarcoma. Each component is well-defined and circumscribed; there is no mixing or transition between the two components (20×). (**b**) High-grade spindle-cell sarcoma juxtaposed to grade 2 chondrosarcoma. Each component is well-defined and circumscribed; there is no mixing or transition between the two components (200×). (**c**) High-grade osteosarcoma juxtaposed to grades 1–2 chondrosarcoma. Each component is well-defined and circumscribed; there is no mixing or transition between the two components. There is appositional deposition of tumor-produced osteoid on both the chondrosarcoma and normal trabecular bone (200×)

Pain is the most frequent chief complaint. In a slow-growing tumor, symptoms are frequently present and evolve over months or years [95, 96].

The natural history of cc-ChS is one of local growth, extension into overlying soft tissue, and eventual systemic dissemination. Prior to its description and confirmation [94], many cases were misdiagnosed as chondroblastoma leading to incomplete treatment (e.g., curettage), local relapse, metastases, and death. Occasional examples of multi-focal cc-ChS have been reported.

The treatment of choice for cc-ChS is wide local resection with a margin of normal tissue. Even when including misdiagnosed/inappropriately treated patients, the expected survival is in excess of 80% [94, 95].

Histopathology

Histologically, cc-ChS may be a biphasic lesion composed of clear cells and low-grade chondrosarcoma (Fig. 3.36). The clear cells are large with abundant well-defined cytoplasm that is either optically clear or finely granular and eosinophilic. The nuclei of the clear cells are round to oval and may have a linear groove or kidney bean configuration. The chromatin tends to be finely divided and mitoses are infrequent. Multinucleated osteoclast-like giant cells are frequent, and aneurysmal bone cyst-like change may be present. Intralesional reactive bone formation is frequent, and osteoblast-lined osseous trabecula are routinely present. Low-grade chondrosarcoma is a variable finding and may be abundant or focal and require extensive sampling to detect.

Special Studies

cc-ChS has immunoreactivity with a wide variety of antibodies, most importantly, SOX9 and collagen type II, confirming the cartilage lineage of this neoplasm [97, 98]. In addition tumor may show immunoreactivity for S-100 protein, vimentin, alpha-1 antichymotrypsin, lysozyme, wheat germ agglu-

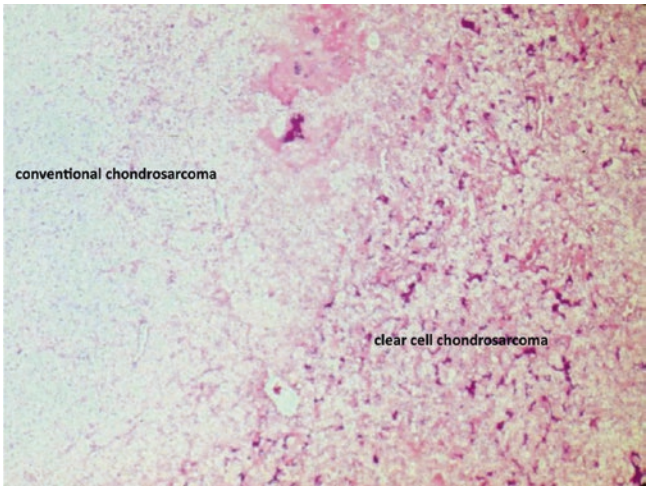

Fig. 3.36 Clear cell chondrosarcoma. Biphasic components of clear cell chondrosarcoma. The left half of the field is typical low-grade chondrosarcoma. The right side has the histological features of typical clear cell chondrosarcoma (10×)

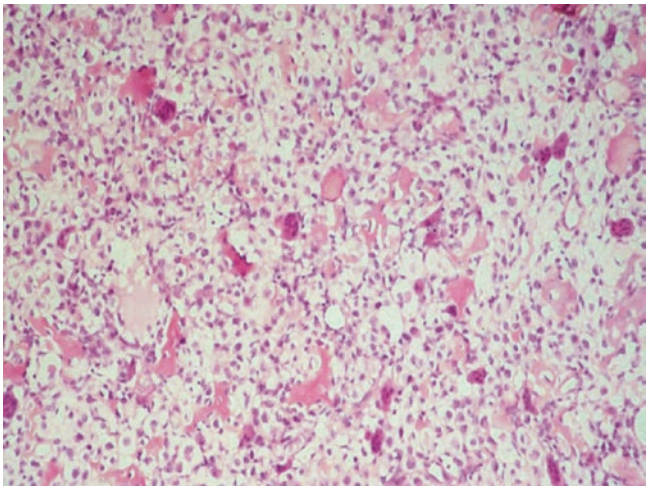

Fig. 3.38 Clear cell chondrosarcoma: photomic. Sheets of clear cells. There are multiple foci of focally mineralized osteoid that are lined by both flat and activated osteoblasts. Multiple osteoclasts are present (100×)

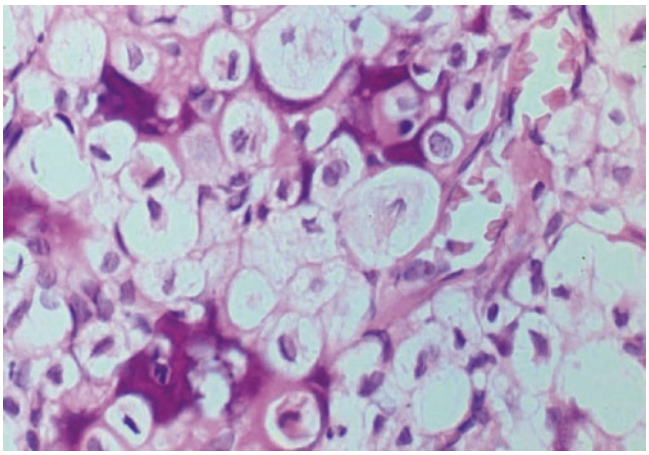

Fig. 3.37 Clear cell chondrosarcoma: photomic. Sheets of clear cells with abundant clear or finely granular pink cytoplasm. The nuclei are round to oval with finely distributed chromatin. There are small foci of mineralized osteoid (200×)

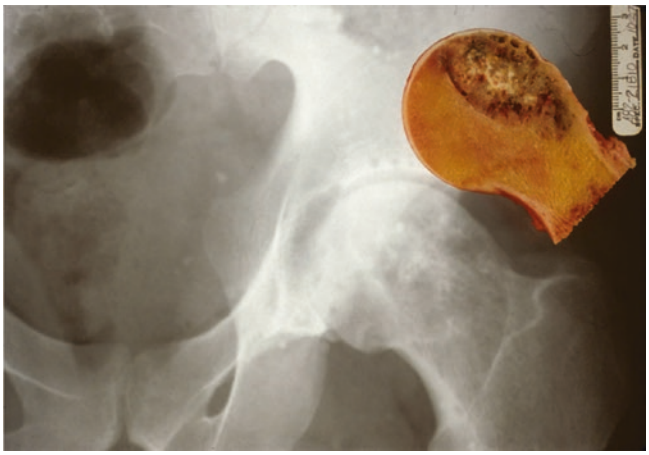

Fig. 3.39 Clear cell chondrosarcoma: gross and plane film. The capital epiphysis of the proximal femur contains a variegated lesion. The cut surface has central mineralized, granular white cartilage. The cartilage is surrounded by a beige to tan fleshy component that is hyperemic, focally cystic, and well-defined from surrounding normal bone. Plane film (AP) shows a destructive mixed lytic/blastic lesion with focal intralesional popcorn-like mineralization within the femoral head epiphysis

tinin, concanavalin A, and aggrecan. At the same time, there is no immunoreactivity for type I collagen.

PAS and ultrastructural studies show evidence of intracytoplasmic glycogen. Neoplastic cells show immunoreactivity for S-100, SOX 9, and collagen II. Interestingly, cc-ChS does not have mutations of IDH1 and IDH2.

Gross Pathology

The gross appearance of cc-ChS is to an extent a function of lesional cartilage content (Fig. 3.37). Those cases with large amounts of cartilage look chondroid. However, cartilage is generally small in amount, and the lesions frequently do not look cartilaginous. Rather because of the predominance reactive bone, the lesions vary from granular yellow-white to tan with red-black intertrabecular hyperemia/hemorrhage. There may be superimposed aneurysmal bone cyst-like change.

Radiology

The vast majority of cc-ChS arise within the long bone epiphyses, where they tend to form relatively well-defined, ovoid, geographic, mixed lytic/blast lesions (Figs. 3.37, 3.38, and 3.39). The tumor/normal interface is frequently sclerotic. Approximately one-third have evidence of chondroid matrix, lobulated with popcorn calcification. The remainder has a relatively non-specific lytic/blastic quality. There may

be bone expansion and cortical thinning with an absence of periosteal reactive bone formation [99].

CT may better show details of cortical destruction and allow more accurate characterization of mineralized tumor matrix, cartilage versus bone versus non-specific.

On MRI cc-ChS tends to be hypointense on T1-weighted images while having moderate to strong hyperintense signal on T2 images. Areas of signal heterogeneity on T1 and T2 would appear to correspond to variable matrix mineralization, intralesional hemorrhage, and cystic changes.

Chondroblastoma

Definition

Chondroblastoma is a biphasic benign cartilage neoplasm represented by a cellular phase of mononuclear cells and a chondroid matrix component that preferentially involves epiphyses.

Clinical

Chondroblastoma (ChB) was first described by Codman [100] who described it as a subset of giant cell tumor of the bone and then revisited by Jaffe who likened the cytological features of the neoplastic cells to immature chondrocytes and coining the term chondroblastoma [101, 102]. It is estimated to comprise 4–5% of benign bone tumors and 1.5% of all bone tumors. Roughly 75% affect patients under the age of 30 years with a sharp peak in the second decade. Males are affected more frequently than females (male to female ratio, 2:1). Tumor most frequently arises in the distal femur, proximal humerus, and proximal tibia. ChB almost exclusively arises within secondary ossification centers, epiphyses and apophyses.

Pain is generally the presenting complaint. However, epiphyseal localization frequently results in joint referable symptoms.

The treatment of choice is curettage and packing when possible and resection when necessary. When treated via curettage and packing, the frequency of local relapse ranges from 5 to 25%. In general follow-up curettage is curative. Rare examples of metastases from otherwise typical chondroblastoma have been reported [103].

A subset of ChB is referred to as *aggressive chondroblastoma* [10, 104, 105]. So far no unique cytological/histological features have been associated with this ChB subset. Anecdotally, the few cases we have reviewed have had a dominant cellular phase, with only small amounts of tumor-produced matrix. This is a group of tumors that is defined by its biological behavior: local relapse occurs more frequently and aggressively than expected. Although rare, metastases may occur, and they vary from innocuous phenomena to lethal.

Some institutions are attempting radio-frequency ablation as first-line treatment for selected cases of ChB; but follow-up is too short to judge efficacy.

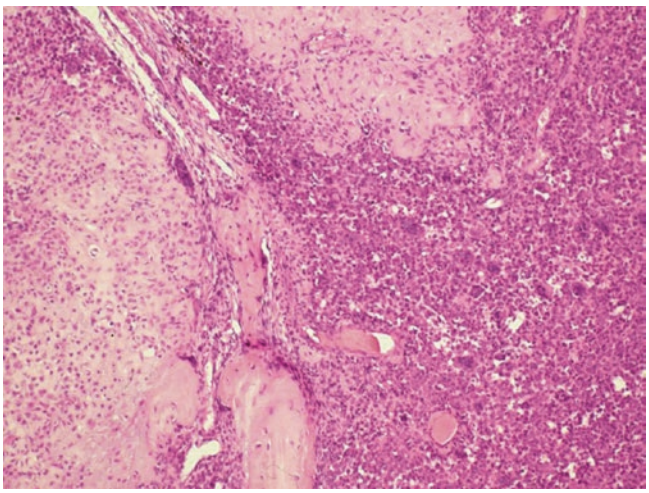

Fig. 3.40 Chondroblastoma is a biphasic tumor with matrix and cellular components. (Courtesy of A. Kevin Raymond, M.D.)

Histopathology

Overall, ChB has a cohesive, lobular configuration and a relatively well-defined, pushing interface with normal structures. It is a biphasic lesion consisting of juxtaposed and intermixing cellular and matrix components (Fig. 3.40). The individual cells have well-defined round- to oval- to cigar-shaped nuclei with thin, well-formed nuclear membranes encompassing finely distributed chromatin. There may be small, inconspicuous nucleoli. Mitoses tend to be infrequent. Many nuclei have linear, longitudinal grooves. Alternatively the nuclei may have a "kidney-bean" configuration. In the cellular areas, the neoplastic cells tend to have abundant, well-defined, dense, eosinophilic cytoplasm. This combination of features may impart a *fried-egg* appearance to the neoplastic cells (Fig. 3.41). At the same time, individual cells are uniformly surrounded by a narrow clear zone that may reflect a lack of desmosomes, resulting in retraction of cells from each other during fixation imparting an overall *cobblestone* appearance to the cellular regions. Frequently, there are small weblike pink, amphophilic to basophilic intercellular areas containing finely stippled calcification, so-called chicken-wire calcification (Fig. 3.42a, b). This finding is not specific for ChB and may be seen in osteosarcoma, conventional chondrosarcoma, and mesenchymal chondrosarcoma.

The matrix-dominant areas of ChB tend to be amorphous, lobular, and more frequently pink than blue, and frequently with a "cotton candy-like" consistency. The neoplastic cells within the matrix are contained within lacunes and, although frequently possessing minimal cytoplasm, are otherwise identical to the neoplastic cells in the cellular areas (Fig. 3.43).

Osteoclasts are frequently present in the cellular areas, particularly near areas of hemorrhage. Aneurysmal bone cyst-like change (Fig. 3.42) is a relatively frequent event and has no bearing on prognosis.

Although immunohistochemical studies are rarely necessary, the neoplastic cells of ChB frequently exhibit immuno-

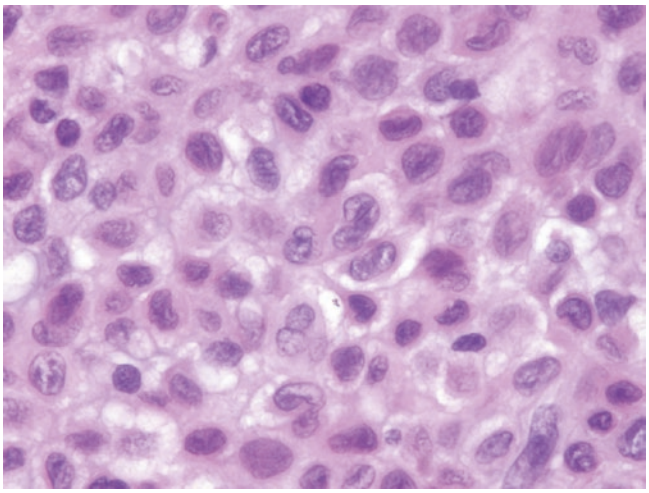

Fig. 3.41 Chondroblastoma cellular phase. Neoplastic cells have round to oval nuclei with finely nuclear grooves or kidney-bean shape. There is abundant eosinophilic to amphophilic cytoplasm. The absence of desmosome leads to cell to cell cytoplasmic retraction leaving a clear zone around neoplastic cells and imparting a cobblestone appearance to chondroblastoma. (Courtesy of A. Kevin Raymond, M.D.)

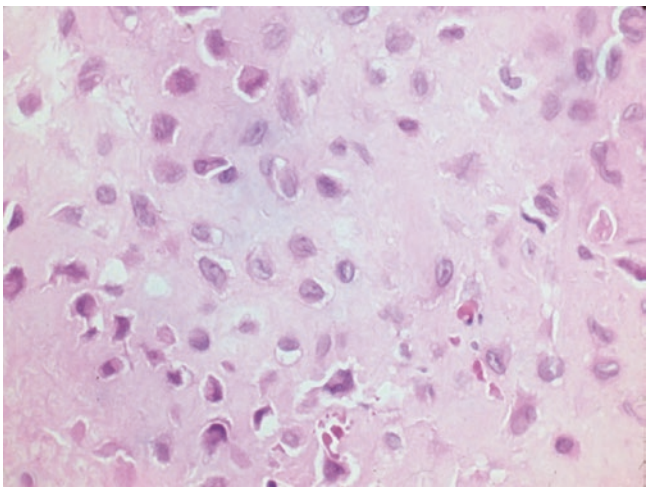

Fig. 3.43 Chondroblastoma matrix phase with neoplastic cells in lacunes; cells are similar to those in cellular phase. (Courtesy of A. Kevin Raymond, M.D.)

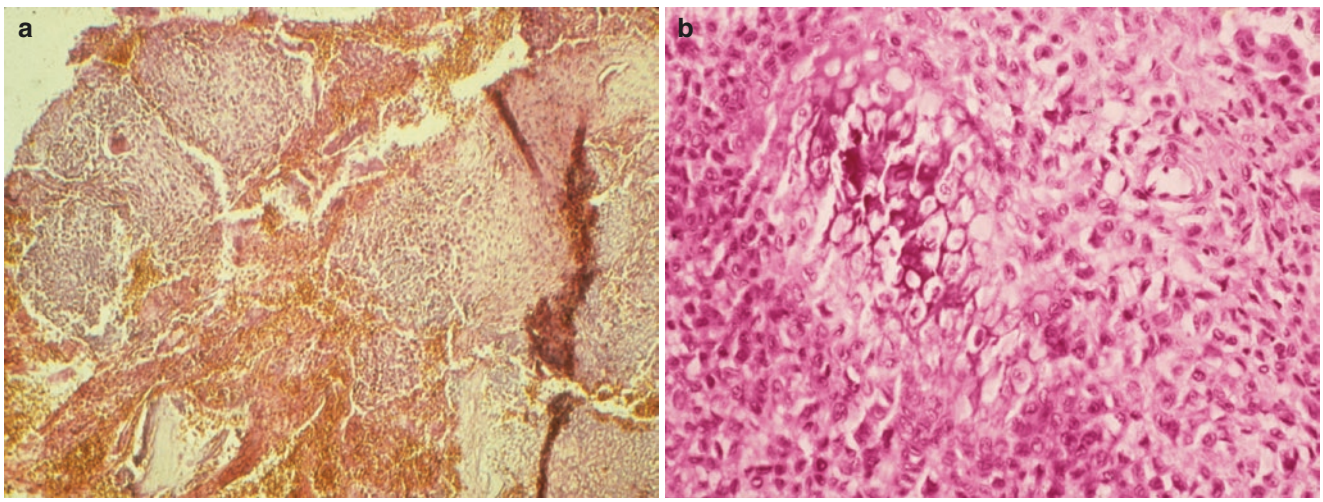

Fig. 3.42 Chondroblastoma. (**a**) Chondroblastoma with secondary aneurysmal bone cyst-like change. (**b**) Chondroblastoma with tumor necrosis leaving mineralized matrix; so-called "*chicken-wire calcification*." (Courtesy of A. Kevin Raymond, M.D.)

reactivity for both S-100 and the cartilage lineage regulator SOX9 [106]. There may be immunostaining for CK8, CK18, and CK19 [101, 107].

Gross Pathology

With curettings being the usual surgical specimen, the gross appearance of ChB is difficult to appreciate. In the latter cases, the specimen consists of irregular fragments of hemorrhagic, finely granular, mineralized tissue that includes both tumor and normal tissues. In those cases undergoing resection, the tumor has an appearance referred to as *pebbles on the beach.* The dominant color is a particular pale brown (i.e., *fawn brown* similar to parathyroid tissue) corresponding to the cellular portions of the tumor, the beach. Scattered throughout the cellular areas are small foci of white mineralized tissue (i.e., the so-called pebbles) corresponding to the tumor matrix (Fig. 3.44).

Radiology

Radiographically, ChB forms an eccentric, destructive, largely radiolucent lesion situated within epiphyses/apophyses of the involved bone (Fig. 3.45). Small, punctate, randomly distributed, intralesional calcifications are frequent and may range from few to numerous. The tumor/normal bone interface is generally both well-defined and sclerotic.

CT and MRI can be used to better localize the lesion. ChB tends to be hypointense on T1-weighted views and hyperintense on T2-weighted images. These findings reflect the high water content of the ChB cartilage. However, either

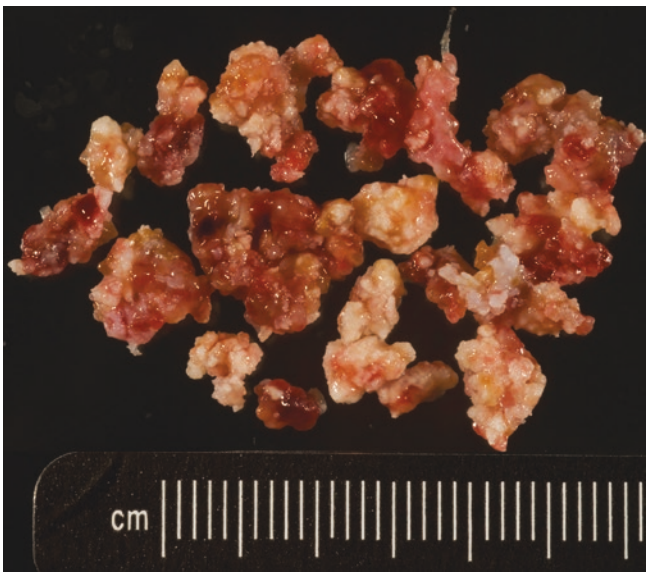

Fig. 3.44 Chondroblastoma gross specimen. The washed specimen consists of multiple fragments of *fawn-brown* to tan tissue interrupted by small white lobules; the so-called *pebbles on the beach* appearance. (Attributed to Crawford Campbell, M.D.) (Courtesy of A. Kevin Raymond, M.D.)

T1- or T2-weighted images may become more or less intense with increasing amounts of mineralization of tumor cartilage.

Tumor may extend through the physis to involve adjacent metaphysis. It may extend through articular cartilage to involve the adjacent joint. With increasing size, tumor can extend through soft tissue to form a subperiosteal and occasionally a true soft tissue mass.

In the few observed cases of aggressive ChB, tumor tends to form a large, radiolucent mass that may extensively distort the parent bone and extend into soft tissues [22, 108, 109].

Chondromyxoid Fibroma

Definition

Chondromyxoid fibroma (CMF) is a rare benign, cartilage neoplasm most frequently arising within the metaphyses of long and short tubular bones in which a histological hallmark is zonated myxoid cartilage.

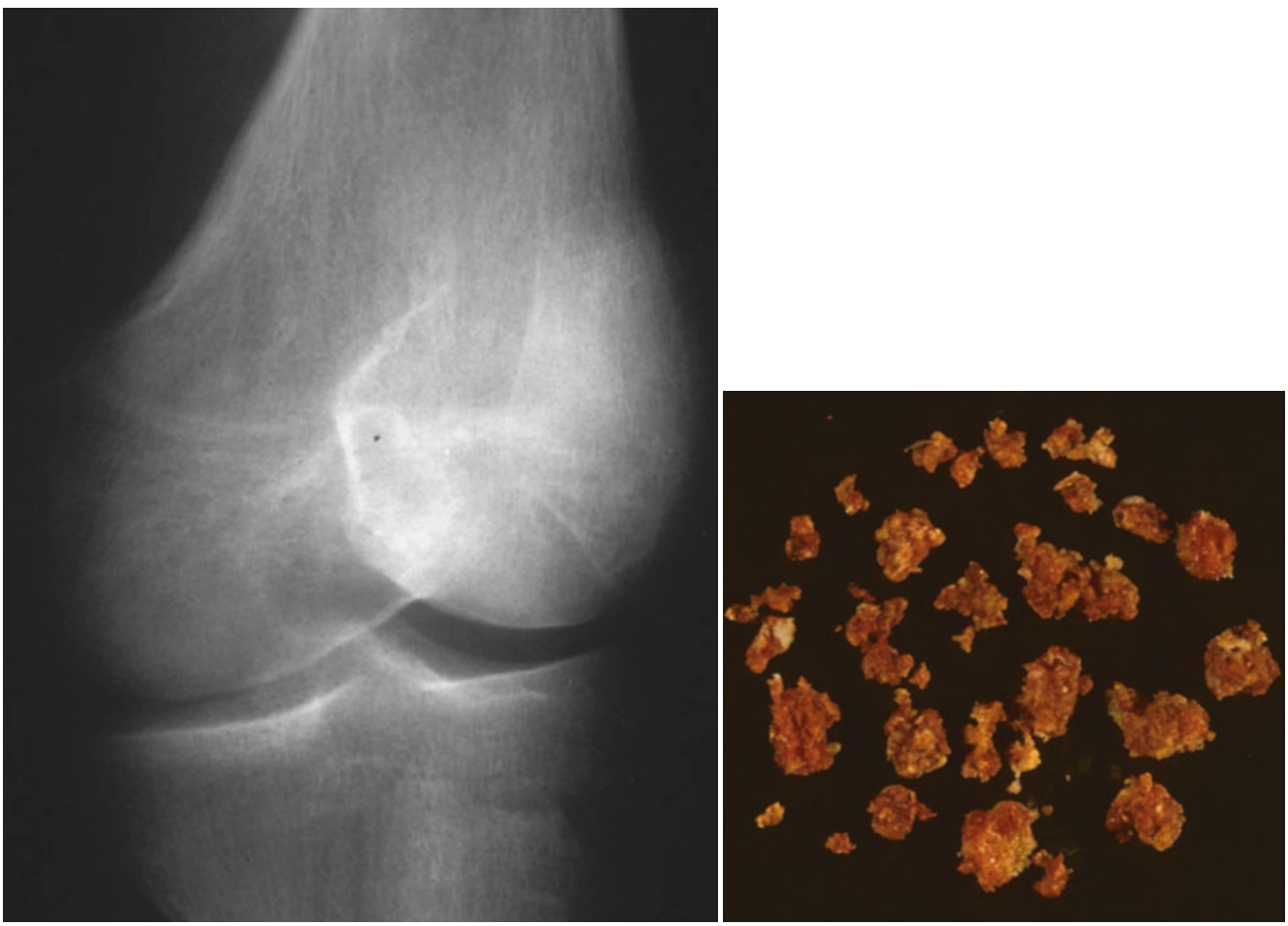

Fig. 3.45 Chondroblastoma plane film and gross. (**a**) Tumor forms a well-circumscribed area of radiolucency within the distal femoral epiphysis. Tumor has fine stippled calcification. (**b**) Gross: fragments of fawn brown tumor with alternating yellow-white foci of mineralization

Clinical

CMF was first described by Jaffe and Lichtenstein in 1948 [110] as a diagnostic pitfall in the differential diagnosis of chondrosarcoma. Subsequent investigations have expanded this concept and clarified its clinico-pathological significance. Comprising some 1.6% of benign bone tumors and <0.5% of all primary bone tumors, CMF is rare even by bone standards [22, 106, 111–115]. Some 75% of CMF affects patients under the age of 30 years, with roughly equal distribution over the first three decades, unlike chondroblastoma where there is a significant peak in the second decade [115]. Males are affected more frequently than females, with male to female ratio ranging from 2:1 to 3:2. The most frequently involved bones are the proximal tibia and distal femur together with the small bones of the feet. Although other sites are described, CMF preferentially involves the metaphyseal medullary cavity of involved bones. Tumor tends to grow in the long axis of the involved bone, and by direct extension CMF may extend into adjacent epiphyses and diaphysis or erode cortex and occasionally involve overlying soft tissues.

Pain with or without swelling is the most common presentation. Functional limitation may occur. The treatment of choice is curettage and packing where possible and resection when necessary [22, 111, 113, 115]. Local relapse can be expected in some 25% of cases and may be somewhat more frequent with lesions involving the small bones of the foot [112]. Relapse may be confined to the host bone or result from soft tissue implantation with regrowth. Long-term (e.g., 20 year) relapse has been reported [115]. The latter may reflect anatomic considerations and limited availability of local reconstructive tissues. Aggressive behavior in CMF is anecdotal.

Histopathology

In contrast to chondroblastoma, CMF is a monophasic, matrix-producing lesion. The matrix is composed of lobulated, zonated myxoid cartilage (Fig. 3.46). The lobules are hypercellular at the periphery, where the cells are larger, plumper, much more numerous, and closer together. In contrast the lobule centers are hypocellular, where the cells are small, shorter, far more slender, far less numerous, and further apart. In either case, the neoplastic cells can be described as stellate, spindle cells with well-defined round-to-elongate nuclei with finely distributed chromatin and few if any mitoses. The cytoplasm is fusiform in shape, variable in amount by zonation, and mildly eosinophilic. In some 10–20% of cases, amorphous deposits of basophilic calcified material can be identified. Osteoclast-like giant cells may be present within the lesion, tending to congregate around areas of hemorrhage and the interface with normal bone. Areas with features mimicking chondroblastoma are not infrequent, and aneurysmal bone cyst-like changes may be present.

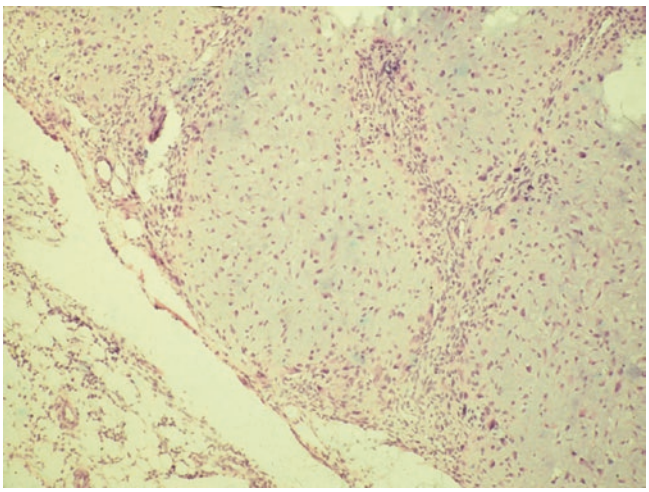

Fig. 3.46 Chondromyxoid fibroma formed by zonated lobules of myxoid cartilage. The periphery of the lobules is hypercellular: the cells are larger, plumber, more numerous, and closer together. The lobule centers are hypocellular: the cells are more slender and fewer in number. (Courtesy of A. Kevin Raymond, M.D.)

Gross Pathology

Inasmuch as its treatment of choice is generally curettage and packing, it can be difficult to gain an appreciation of the gross features of CMF, other than fragments of mucoid, focally calcified material. However in resection specimens (Fig. 3.47), the gross appearance of CMF is that of a lobulated, cohesive mass with a sharp interface with normal bone. The cut surface is a semitranslucent, gray to gray-blue, soft gelatinous material that may have an element of fine granularity.

Radiology

As expected, the radiographic appearance reflects the gross specimen. CMF tends toward eccentric, lobulated involvement of the metaphyses of appendicular tubular bones (Fig. 3.47). CMF presents as a destructive, geographic radiolucent lesion with frequent pseudotrabeculation and endosteal scalloping of overlying cortex. Small, punctate, intralesional calcifications may be present. The tumor/normal bone interface tends to be well-defined but neither calcified nor sclerotic. CT and MRI confirm the latter impressions. The lesion tends to be hypointense on T1-weighted images and zonated with peripheral lobular increased signal intensity on T2-weighted images.

Fig. 3.47 Grossly chondromyxoid fibroma forms a shiny gray, semitranslucent, semisolid lobulated mass. Radiographically, tumor forms a well-defined, eccentric lobulated radiolucent mass with cortical thinning. There is virtually no evidence of intralesional mineralization, and although the transition zone with normal is well-defined, it is not sclerotic. (Courtesy of A. Kevin Raymond, M.D.)

Synovial Chondromatosis

Definition

Synovial chondromatosis (SynCh) is a benign nodular hyaline cartilage lesion arising within synovial surfaces.

Clinical

SynCh is generally regarded as a form of cartilage metaplasia involving the synovial tissues of joints and/or adjacent tendon sheath. The peak incidence of SynCh is variably reported as being in the second to third decades (WHO), third to fourth decades (Wold), and fifth decade [1]. On the other hand, there is general agreement that the male to female ratio is 2:1 [1, 10, 21]. Although any joint may be involved, SynCh most frequently involves the large weight-bearing joints, in particular the knee (70%) and hip [1].

In general, SynCh patients present with a months to years history of pain, swelling, and decreased range of motion involving the affected joint. Rarely, SynCh may be multifocal. Surgical excision is the treatment of choice. Local relapse necessitating additional surgery is frequent. Secondary malignancy is extraordinarily rare, far more written about than seen (Fig. 3.48a, b).

Histopathology

The cytological features of SynCh at medium to high power can be worrisome. The neoplastic cells frequently have a significant degree of atypia including generally enlarged cells with significant cytoplasm, variable size and shaped nuclei with increased nuclear detail, and binuclear forms. Mitoses are generally not present.

However, although hypercellular, SynCh has a characteristic, highly reproducible, and organized architecture: *lobules-within-lobules pattern* (Raymond AK, unpublished work). The blue-gray cartilage nodules vary from a few cells to centimeter lobules. Each synovium-embedded cartilage nodule is composed of multiple smaller, similar-sized lobules (Fig. 3.49a, b). In turn each of these lobules is composed of smaller lobules that encompass multiple lobules containing lobules of progressively decreasing size until they are composed of individual and double lacunes containing lesional cells, lobules within lobules.

Gross

In general, the gross specimen is a partial or complete synovectomy and consists of generally edematous, and inflamed boggy synovium with embedded, white cartilage nodules. The nodules range from near microscopic up to 1 or even 2 cm. The smallest nodules are composed of gray-white semitranslucent plaques on the synovial surface. Close examination of larger gray-white, firm to rock-hard nodules reveals a lobular, raspberry-/blackberry-like architecture and external surface reflective of the lobule-within-lobule microscopy. Some nodules may become detached from the involved synovium and form intra-articular loose bodies that may be submitted separately. The lobules are usually calcified with increasing mineralization roughly correlating with lesional age. With long-standing massive joint involvement or relapse, SynCh nodules may become adherent forming sheets of nodular cartilage.

When photographing synovectomy specimens from SynCh patients, meticulous dissection of the nodules free from the synovium yields specimens for easy histological processing but with little clinico-pathological correlation. In

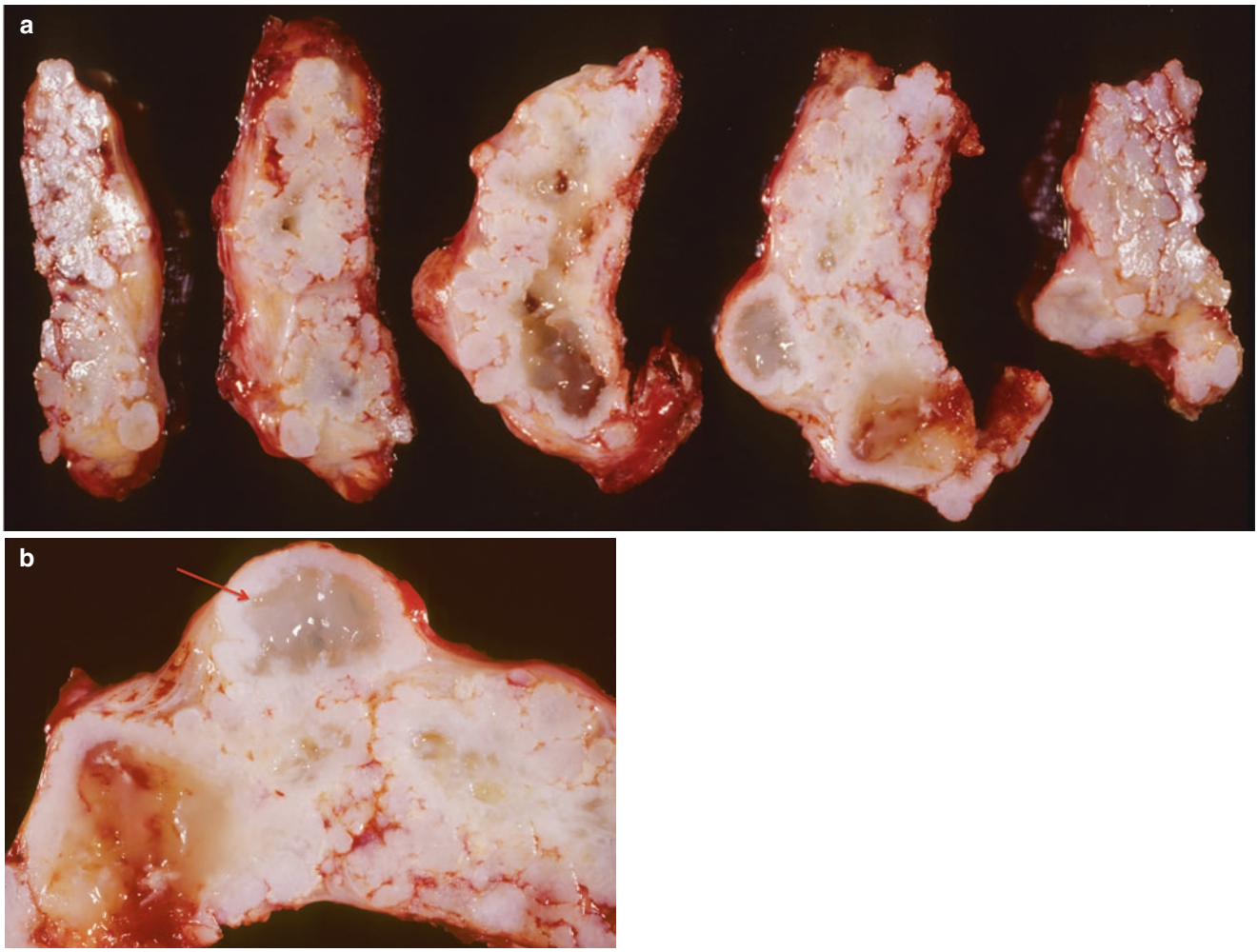

Fig. 3.48 Synovial chondromatosis with secondary chondrosarcoma. (**a**, **b**) Resected specimen from a patient with a long-standing history of synovial chondromatosis and multiple prior procedures. Resection for current growing mass. One piece (red arrow) is suspicious for secondary chondrosarcoma. (Courtesy of A. Kevin Raymond, M.D.)

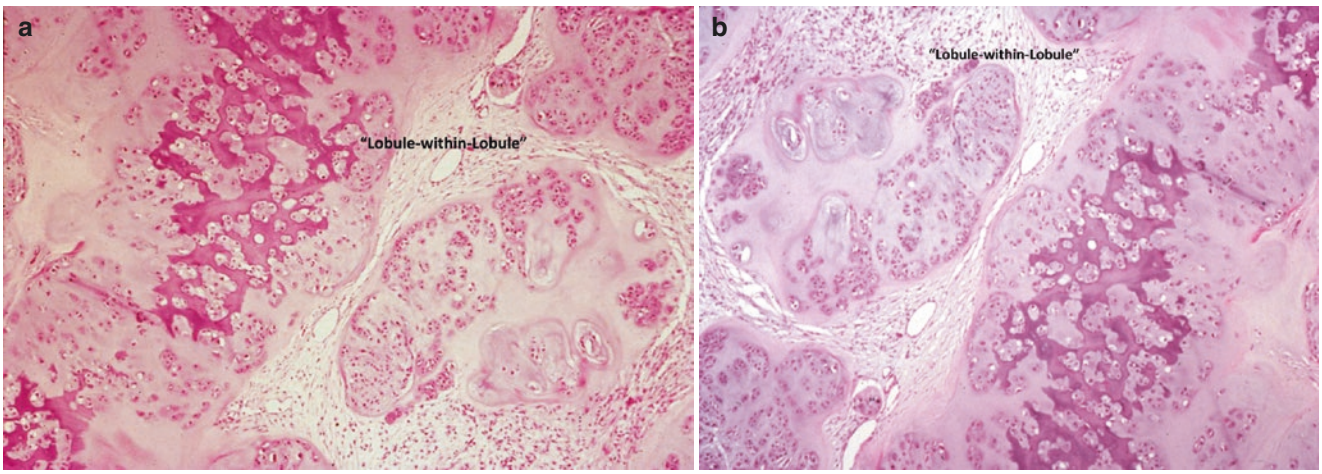

Fig. 3.49 Synovial chondromatosis. (**a**, **b**) Synovial chondromatosis is composed of numerous cartilage lobules covered by and immersed in synovium. The tumor cells have varying degrees of atypia, which may be significant; increased nuclear detail, nuclear variability, and increased cytoplasm. However, the lesional cells remained arranged within a well-defined lobular architecture. However, on closer inspection, each lobule is composed of a concentric network of lobules-within-lobules-within-lobules extending from the microscopic-to-the-gross and reflected in imaging studies (H&# 20×, 100×). This lobule-within-lobule organization is strongly associated with synovial chondromatosis. (Courtesy of A. Kevin Raymond, M.D.)

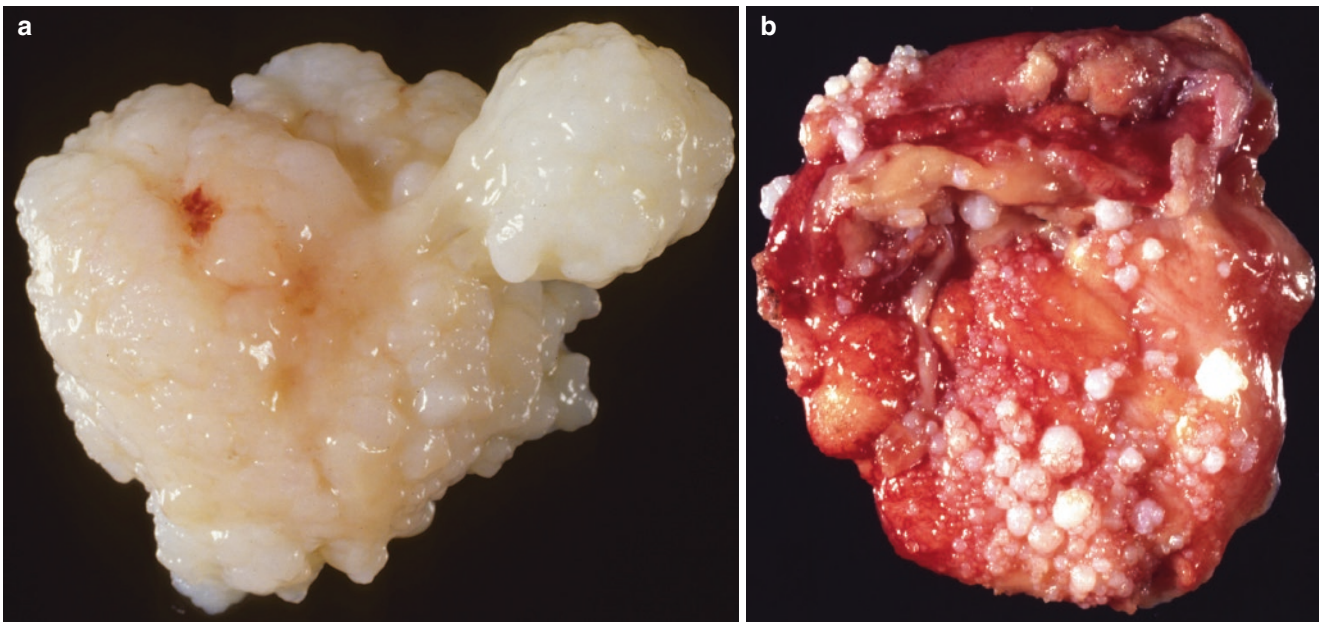

Fig. 3.50 Synovial chondromatosis. (**a**) A small aggregate of synovial chondromatosis has been dissected free of the larger mass. The lobule within lobule architecture has been retained. (**b**) Subtotal synovectomy specimen. There are numerous lobules of synovial chondromatosis present. Lobules vary from the near microscopic to fractions of a centimeter and are embedded in synovium. (Courtesy of A. Kevin Raymond, M.D.)

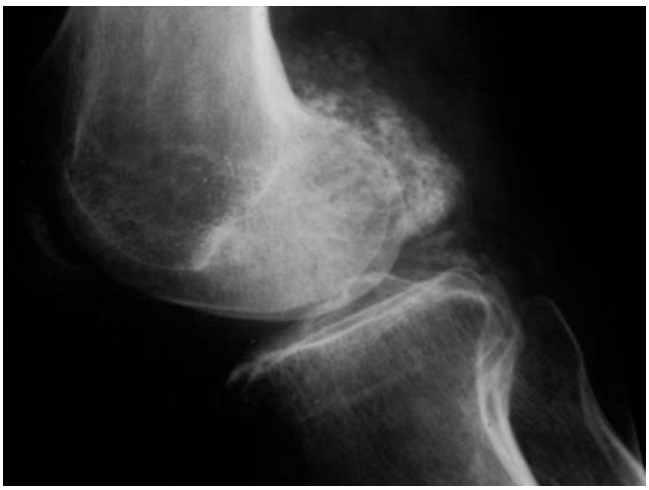

Fig. 3.51 Synovial chondromatosis. Plane film (lateral) of the knee showing innumerable foci of popcorn-like calcification. The appearance is consistent with synovial chondromatosis. Care must be taken not to over-read or under-read the possibility of bone involvement; primary or secondary. (Courtesy of A. Kevin Raymond, M.D.)

contrast, leaving the nodules in situ will result in a photograph reflecting the gross appearance of the lesion as seen through an arthroscope (Fig. 3.50a, b).

Radiology

Inasmuch as the cartilage lobules of SynCh are usually mineralized, the radiographic appearance on plane films is that of numerous individual and confluent nodules with ring and fleck calcification (Fig. 3.51).

Being synovial-based, the lesions are located outside of the bone and may appear to fill and expand the involved joint space. Increased lesional detail may be garnered from CT studies. Extent of disease is best evaluated using CT and MRI. When viewed with MRI, lobules of SynCh appear as dark foci on T1-weighted images and hyperintense nodules on T2-weighted images. High-resolution studies may help identify early lesions.

A classic error in plane film interpretation is to identify the extraosseous, mineralized cartilage lesions involving soft tissue and to automatically interpret them as representing chondrosarcoma extending from the bone into soft tissues. The presence or absence of intraosseous tumor is key in the clinical discrimination between SynCh and chondrosarcoma and may be difficult to assess on the basis of plane films alone, emphasizing the need for full radiological work-up including CT and MRI.

Osseous Neoplasia

Introduction

Osseous neoplasia (aka osteogenic neoplasia) comprises a complex family of biologically diverse lesions. The heterogeneity is such that without some organization one is facing what amounts to a random list of disparate disease processes. Histologically, the common factor connecting these entities is the production of osseous matrix by neoplastic cells. From a purely histological point of view, the first organizational step might be to take into account the form of matrix they produce: lamellar bone versus woven bone.

Pathological processes producing fully mature lamellar bone are rare. The benign lesions are referred to as osteomas. These include *parosteal osteoma* (so-called ivory exostosis) and its intramedullary histological "cousin," the *enostosis*, i.e., *bone island*. There are also malformations (e.g., *torus palatinus*), which, although of different origin, are histologically similar.

In each case, bland, innocuous spindle cells produce well-formed lamellar bone, in one case on the cortical surface and the other within the medullary cavity. Each of these lesions tends to be relatively self-limited, but it is the exceptions that are drawn to medical attention. Parosteal osteomas occur almost exclusively in bones formed through membranous ossification (e.g., craniofacial bones) or parts of bones formed through membranous ossification (e.g., diaphyses). Although most are asymptomatic, they can result in mass lesions, which may become symptomatic or at least unpleasant. Osteomas are a component of Gardner syndrome, an inherited autosomal dominant condition. In general, no treatment is necessary or at least limited by symptomatology.

Bone islands can occur as small, radiopaque solitary lesions or multifocal in *osteopoikilosis* (Buschke-Ollendorff syndrome). Their main concern in being excluded from the differential diagnosis of osteosclerotic metastases.

The malignant tumors producing lamellar bone are parosteal osteosarcoma and low-grade central osteosarcoma. For convenience's sake they are considered with the osteosarcoma family.

Woven bone is produced by the overwhelming majority of primary bone tumors. The benign lesions include the various manifestations of osteoid osteoma and osteoblastoma. The dominant matrix pattern in osteosarcoma is woven osteoid and bone. However, matrix maturation or remodeling can be seen in limited amounts in most forms of osteosarcoma. Such maturation tends to be in the older parts of the tumor. In general the peripheral portions of osteosarcoma have the least mature matrix, while the most mature is found at the center, the opposite of myositis ossificans. However, the vast majority of osteosarcoma tumor-produced matrix is woven osteoid and bone. The subtypes of this basic division form the basis of the remainder of this chapter (Fig. 3.52).

Fibrous dysplasia and osteofibrous dysplasia produce woven bone. Following this division by matrix form, they might be included with osteogenic tumors. However, these two lesions are generally considered appropriately included with fibrous lesions.

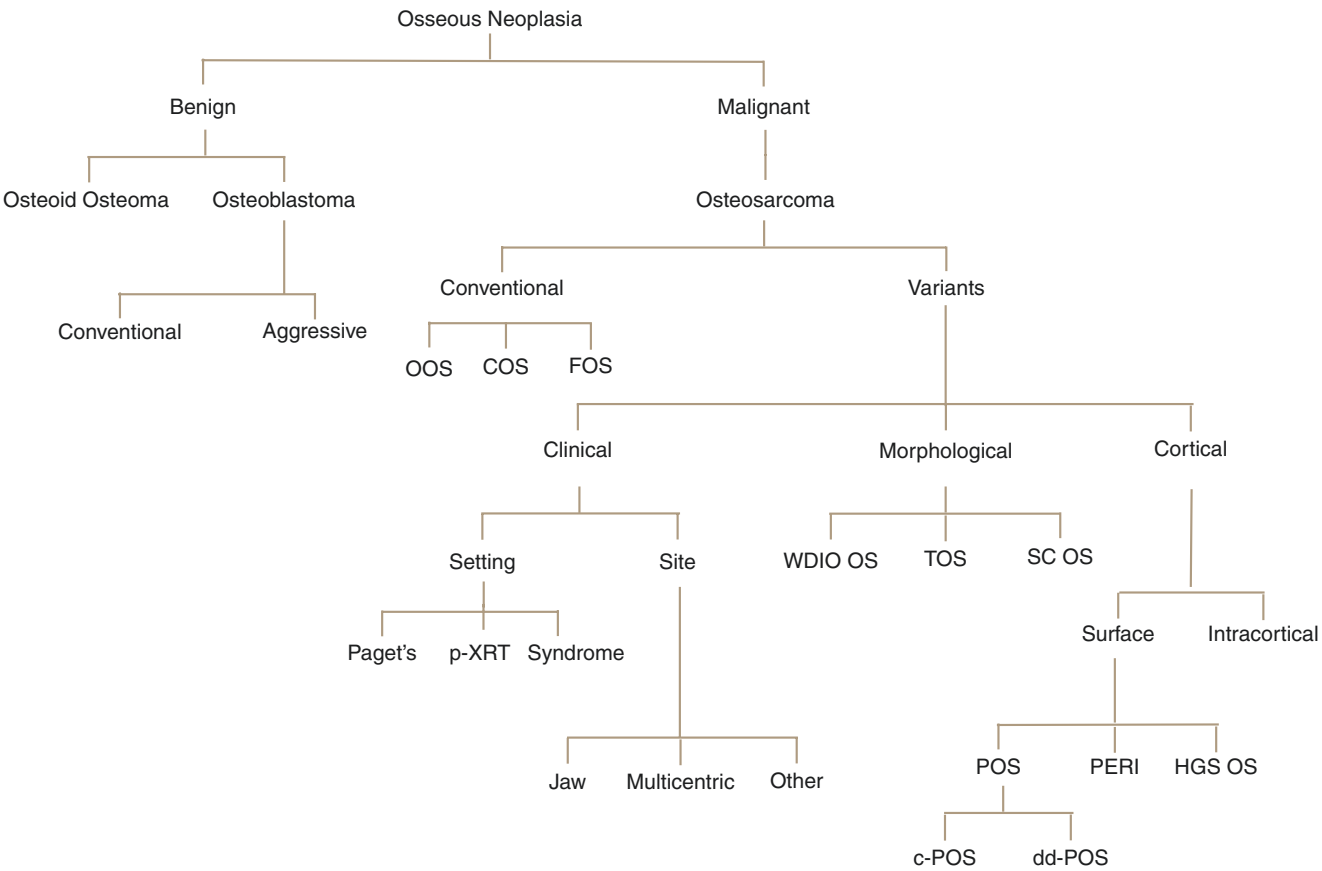

Fig. 3.52 Osseous neoplasia

Osteoid Osteoma

Definition

Osteoid osteoma is a small, benign, bone-producing primary bone tumor of limited growth potential.

Clinical

Since its first description by Jaffe in 1934, a large body of literature has arisen concerning the diagnosis and treatment of osteoid osteoma. The lesion is referred to as a "nidus" and is by definition less than 2 cm in greatest dimension. Osteoid osteoma occurs most frequently in the first three decades of life, with a significant peak in the second decade. The male to female ratio is profoundly skewed toward males and variously reported being between 3:1 and 5:1. Although any part of any bone may be affected, osteoid osteoma occurs most frequently in the long bones of the appendicular skeleton, in particular the femur, tibia, and humerus. Although less generally recognized, the spine is also a frequent site of origin. In the long bones, the tumor usually arises within cortex or immediate subcortical bone in the diaphysis or metadiaphysis of the affected bone. Occasional origin from the epiphysis and periosteal surface are well described, and a rare intra-articular form has been reported [1, 10, 20, 116].

Severe pain is the hallmark of osteoid osteoma. A classic triad of pain that is worse at night and relieved by salicylates has been long taught. The specificity and frequency of the triad have been questioned with one investigator noting that pain is a constant finding with virtually all bone tumors, virtually all pain is worse at night, and aspirin relieved most forms of pain. Pain may result in disuse phenomenon, while pain involving the spine may result in splinting.

As indicated, osteoid osteoma growth is self-limited with an upper limit of size being somewhat investigator-determined between 1 and 2 cm, with a recent suggestion of 1.3 cm. However, pain is a constant and does not diminish with time. Although spontaneous regression has been reported, it is vanishingly rare [20].

Until recently, complete open surgical extirpation of tumor was the treatment of choice. However, cortical curettage and cortical resection are not without complications, e.g., immobilization in a long-leg cast. Worse yet, in the best of hands, 25% of lesions can be missed during the first surgical approach. Apparently, translating lesional location from measured radiographs to the realities of the operating room table and flesh-covered bone is not without difficulty [20, 116].

Currently, the treatment of choice in most institutions is radio frequency ablation (RFA), in which an instrument is introduced into the lesion under radiographic visualization, electrical current applied and the lesion destroyed. This may or may not be preceded by core biopsy. Local relapse is reported as less than 5%. Alternate forms of limited therapy are available, but each has limitations [117–120].

Histopathology

The nidus is composed of an interweaving tangle of randomly oriented, relatively slender woven osteoid and bone (Fig. 3.53). The osseous matrix is lined by osteoblasts and occasional osteoclasts. The osteoblasts may be either the flat-inactive or plasmacytoid-activated forms. The lined osseous matrix is embedded in a minimally cellular fibrovascular background stroma. The noninfiltrating nidus is sharply demarcated from the juxtaposed adjacent normal trabecular, cortical, or reactive bone.

Gross

Grossly, the nidus consists of a sharply demarcated lesion either adjacent to or embedded within dense normal or reactive bone (Fig. 3.53). The lesion itself is an osseous sphere with a finely granular, ivory white to tan bone surface that is generally hyperemic or hemorrhagic when compared with surrounding normal or reactive bone. The mineralized lesion is gritty on sectioning.

Radiology

The osteoid osteoma nidus forms a sharply circumscribed radiolucent lesion on plane films (Fig. 3.53). The nidus may be surrounded by intramedullary reactive bone and/or periosteal reactive bone formation. The lesion itself may become variably mineralized. The nidus is better visualized with CT or MRI examination. The nidus is hypervascular on arteriogram. The hallmark of osteoid osteoma on Tm99 bone scan is a focus of intense hyperactivity surrounded by a zone of lesser activity, i.e., so-called "double density" sign [10].

Molecular Biology

Structural chromosomal alterations involving 22q13 [del(22)(q13.1)] have been described. The latter involves a region of chromosome 22 where genes related to cell cycle regulation have been mapped [118]. Of interest, the intense pain associated with osteoid osteoma is thought to be a function of the production of high levels of prostaglandin E2 mediated by cyclooxygenases (i.e., COX-1 and COX-2) [121–123].

Osteoblastoma

Definition

Osteoblastoma is a benign, bone-producing primary tumor of the bone without limited growth potential and by definition >2 cm in greatest dimension.

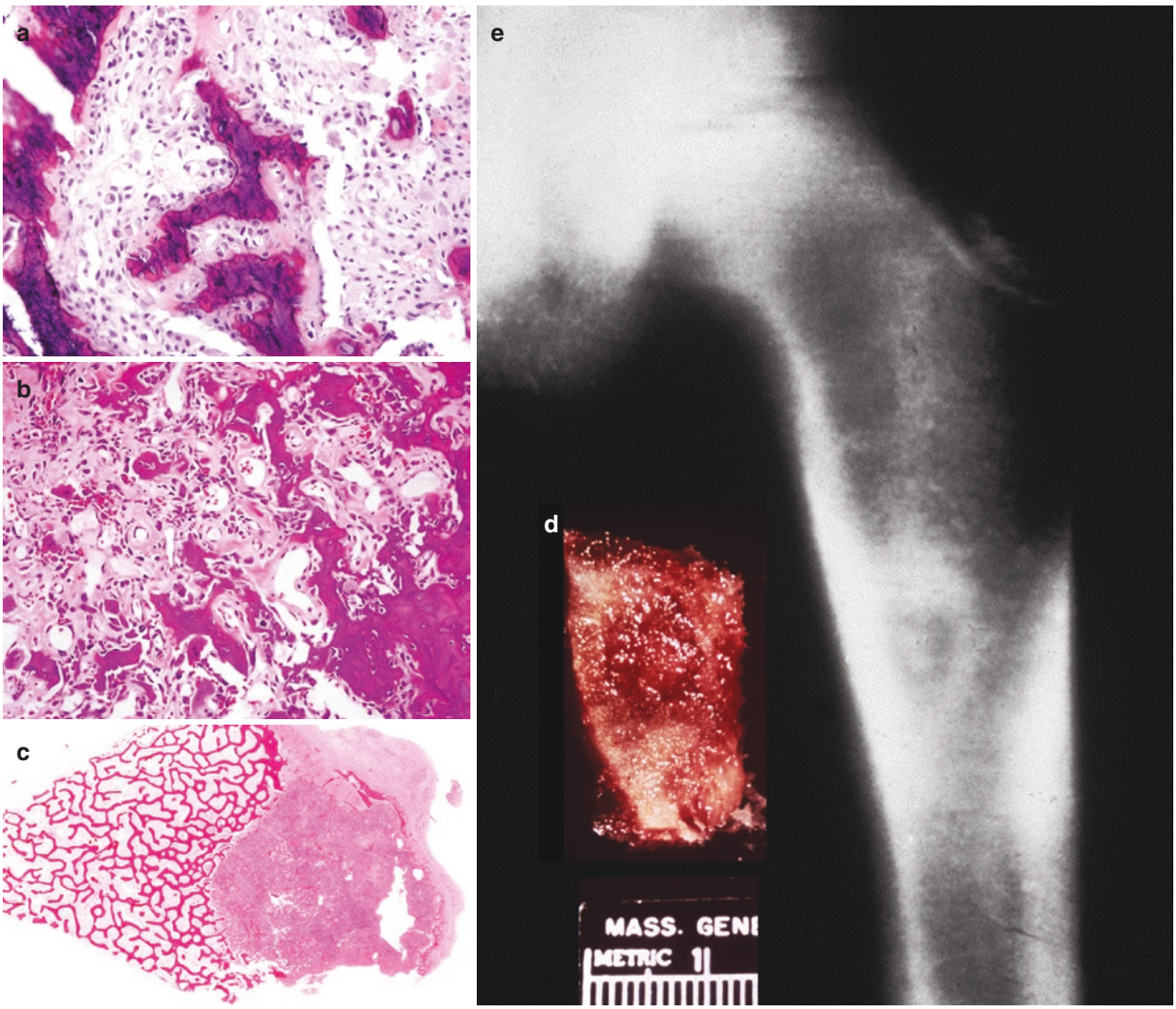

Fig. 3.53 Osteoid osteoma. (**a**, **b**) anastomosing trabecula of osteoid and bone lined by osteoblasts, occasional osteoclasts set in a loose capillary stroma [(**a**) frozen section, (**b**) formalin-fixed paraffin embedded, H&E. 100x), (**c**) Whole mount: intra-cortical osteoid osteoma next, (**d**) Gross: intra-cortical, hemorrhagic berry-like lesion (so-called "nidus"), (**e**) plane film (AP): periosteal and intra-medullary reactive bone formation in addition to tumor mineralization has resulted in a targetoid-appearance for this lesion. (courtesy of A. Kevin Raymond, M.D.)

Clinical

Originally described by Dahlin [124] as "giant osteoid osteoma," the term "osteoblastoma" was subsequently, *independently* suggested by Jaffe [125] and Lichtenstein [126]. Osteoblastoma is rare in patients over the age of 40 years and most frequent affects patients in the second and third decades. Males are affected twice as often as females. Although osteoblastoma may originate in any part of any bone, the spine/vertebra is the most frequently involved bone, in particular the spinous and transverse processes, i.e., the so-called posterior elements. The metaphyses of long tubular bones are also frequently involved. Surface origin is rare but is recognized, periosteal osteoblastoma.

By definition osteoblastoma is greater than 2 cm in greatest dimension. In contrast to osteoid osteoma, there is no intrinsic limited growth potential. Intuitively, osteoblastoma must start as a "small" lesion (i.e., <2 cm) that then grows to diagnostic size (i.e., >2 cm). Interestingly, lesions that are clinically identified as osteoid osteoma do not grow. Documented transition between small and large lesions is an

extremely rare event, justifying the separation into two distinct entities despite histological similarities [127–129].

Severe dull aching pain with or without mass is the cardinal symptom of osteoblastoma. When originating in the spine, there may be neurological symptoms.

The natural history of osteoblastoma is one of local growth resulting in increased symptoms referable to mass effect, compression of vital structures and interference with normal function. Pathological fracture may occur. Metastases are an extraordinarily rare event and demand investigation of the possibility of osteosarcoma, e.g., osteosarcoma resembling osteoblastoma [130].

The absence of metastatic potential focuses treatment on complete extirpation of the primary tumor. Curettage with packing and resection are the therapeutic options with the choice being determined by clinical factors, e.g., tumor size, location, and accessibility. Local relapse following curettage is variously reported between 15% and 25% and almost uniformly cured by recurettage [131, 132].

Histopathology

Histologically, osteoblastoma is composed of interweaving and anastomosing trabecula of woven osteoid and/or bone that is lined by osteoblasts and occasional osteoclasts (Figs. 3.54 and 3.55). The cellular osseous matrix is embedded in a loose fibrovascular background. As with osteoid osteoma, the appearance of osteoblasts varies from flat inactive cells to the tall, epithelioid appearance of activated osteoblasts. Individual cells have well-defined, eccentric nuclei with finely divided chromatin, inconspicuous nucleoli, and rare but non-atypical mitoses. Cytoplasm is eosinophilic, and larger *activated* cells frequently have a *perinuclear hoff*. The osteoblasts line osseous trabecular in a near-continuous line. The cytology of these osteoblasts is such that they all look virtually identical, inspiring Texan observers to liken them to *crows on a fence*, while German pathologists saw them as *soldiers in a row.*

Occasionally, the chromatin of individual osteoblasts may be condensed or *smudged*. This is a degenerative change analogous to that seen in *ancient Schwannoma*. Tumor tends to grow as a cohesive mass, and although infiltrative, the tumor/normal interface appears relatively well defined.

Rarely, minimally atypical osteoblasts with bizarre distorted nuclei may be present. The overall appearance of the nuclei might be described as smudged and is analogous to changes that may be seen in schwannomas (Figs. 3.56 and 3.57). Familiarity with this histological possibility is required to avoid a misdiagnosis of osteosarcoma in cases that are actually a form of osteoblastoma, *ancient osteoblastoma* also referred to as *pseudomalignant osteoblastoma* [133].

Although contradicting historical teaching, recent work suggests that cartilage may be occasionally produced by osteoblastoma [134]. However, the presence of cartilage in a bone-producing lesion should be viewed with extreme caution since it is more typical of malignant lesions, i.e., osteosarcoma.

Gross

With curettage and packing the treatment of choice, the gross appearance of osteoblastoma is frequently obscured by superimposed, adherent hemorrhage (Fig. 3.58). The lesion is hard and gritty and has finely granular or lacy cut surface reflecting the underlying randomly anastomosing bone trabecula. The lesion is frequently hyperemic and secondary degenerative changes, including aneurysmal bone cyst-like change may be present.

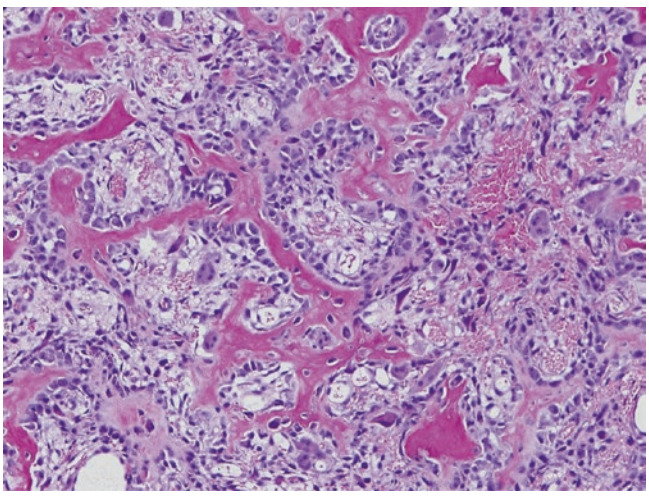

Fig. 3.54 Osteoblastoma: randomly anastomosing trabecular of woven bone and osteoid lined by a near-continuous layer of activated osteoblasts alternating with occasional osteoclasts set in a loose fibrovascular stroma (100×). (Courtesy of A. Kevin Raymond, M.D.)

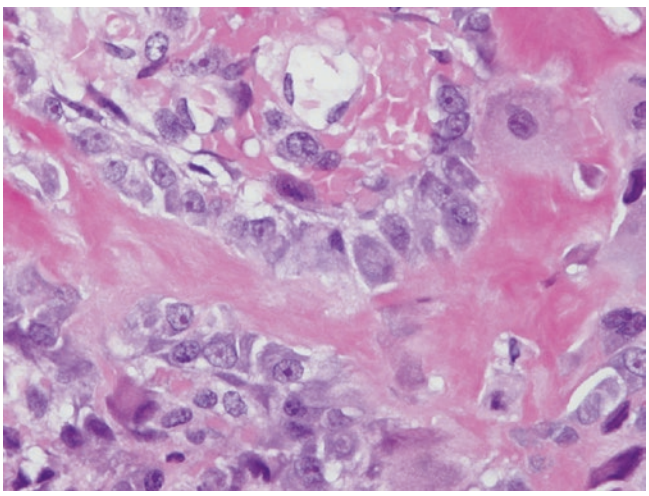

Fig. 3.55 Osteoblastoma: randomly anastomosing trabecula of woven bone and osteoid lined by a near continuous layer of activated osteoblasts alternating with occasional osteoclasts set in a loose fibrovascular stroma (400×). (Courtesy of A. Kevin Raymond, M.D.)

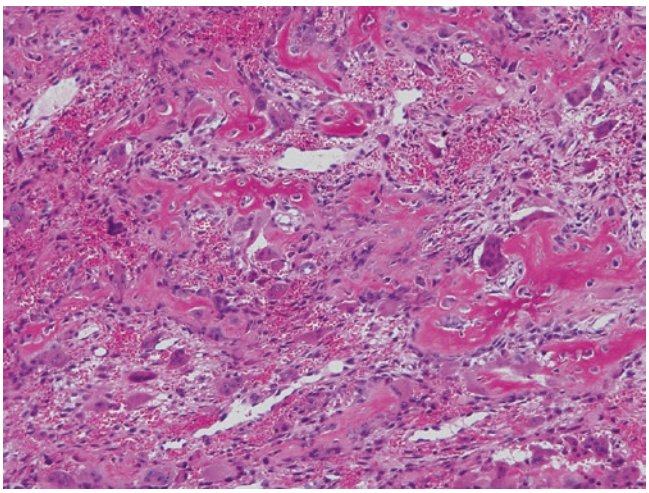

Fig. 3.56 Ancient osteoblastoma: randomly anastomosing trabecular of woven bone and osteoid lined by a near-continuous layer of activated osteoblasts alternating with occasional osteoclasts set in a loose fibrovascular stroma. Note that there are multiple bizarre-shaped, enlarge nuclei with *smudged* chromatin (100×). (Courtesy of A. Kevin Raymond, M.D.)

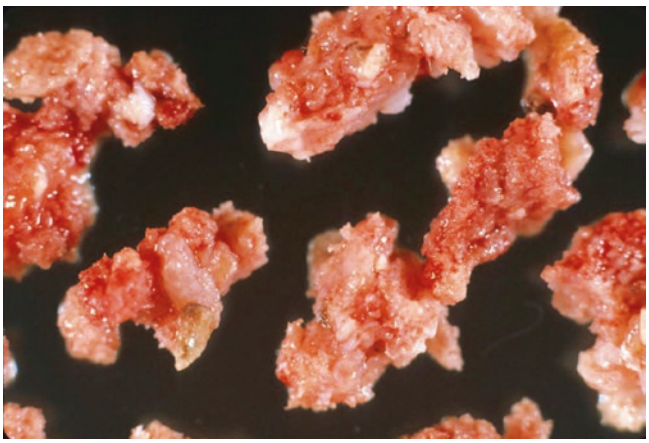

Fig. 3.58 Osteoblastoma: fragments of tumor from curettings. The oriented and organized trabecular architecture of normal bone is replaced by tumor whose exposed surface is hyperemic tan, with a granular to nodular consistency. Specimen is gritty on cutting. Note that specimen was washed before examination. (Courtesy of A. Kevin Raymond, M.D.)

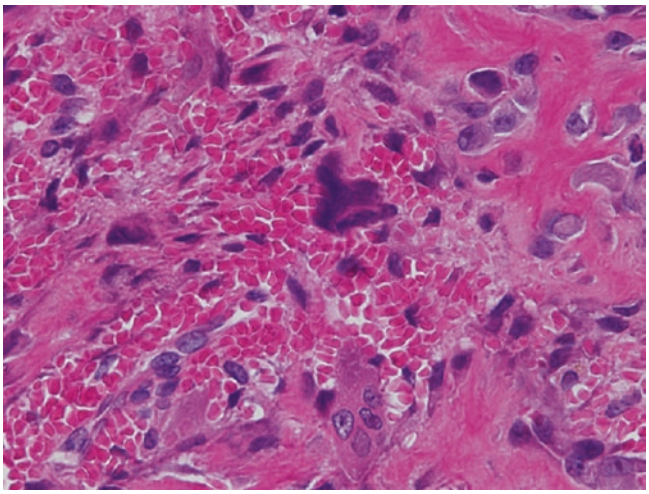

Fig. 3.57 *Ancient osteoblastoma*: randomly anastomosing trabecula of woven bone and osteoid lined by a near continuous layer of activated osteoblasts alternating with occasional osteoclasts set in a loose fibrovascular stroma. Note that there are multiple bizarre-shaped enlarged nuclei with smudged chromatin (400×). (Courtesy of A. Kevin Raymond, M.D.)

Fig. 3.59 Osteoblastoma: plane film (AP). There is an expansile, mixed lytic/blastic lesion involving the transverse process of T-11. Note that you should not be able to see the transverse processes on this view; to see it indicates that it is abnormal. (Courtesy of A. Kevin Raymond, M.D.)

Radiology

The resulting radiographic appearance is that of a mixed lytic/blastic lesion with destruction of normal trabecular architecture, cortical thinning and expansion, and potential extension into overlying tissues (Figs. 3.59 and 3.60) [135]. These features are readily appreciable in plane films of lesions involving tubular bones. However, spine lesions are better characterized with CT (Fig. 3.61). The combination of CT and MRI serves to define the extent of disease [128, 129, 136].

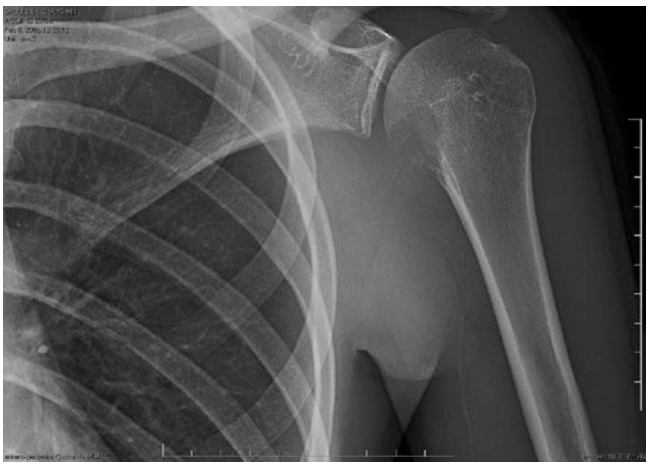

Fig. 3.60 Ancient osteoblastoma: plane film (AP). There is a destructive, largely lytic lesion involving the proximal metaphysis of the humerus. There are foci of cloud-like amorphous mineralization within the lesion

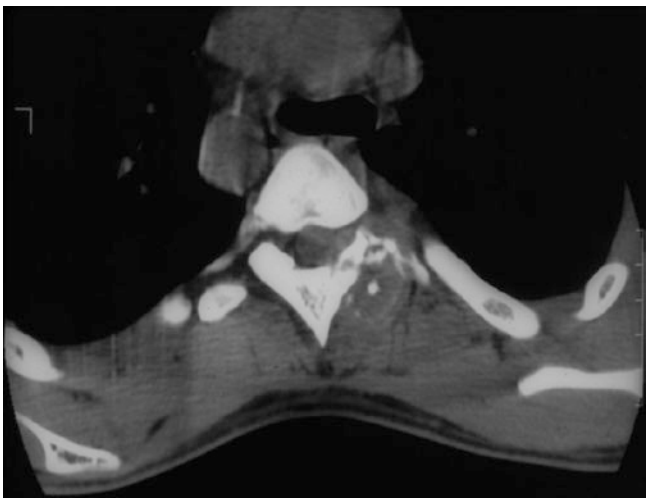

Fig. 3.61 Osteoblastoma: CT shows an expansile mixed lytic/blastic lesion involving the transverse process

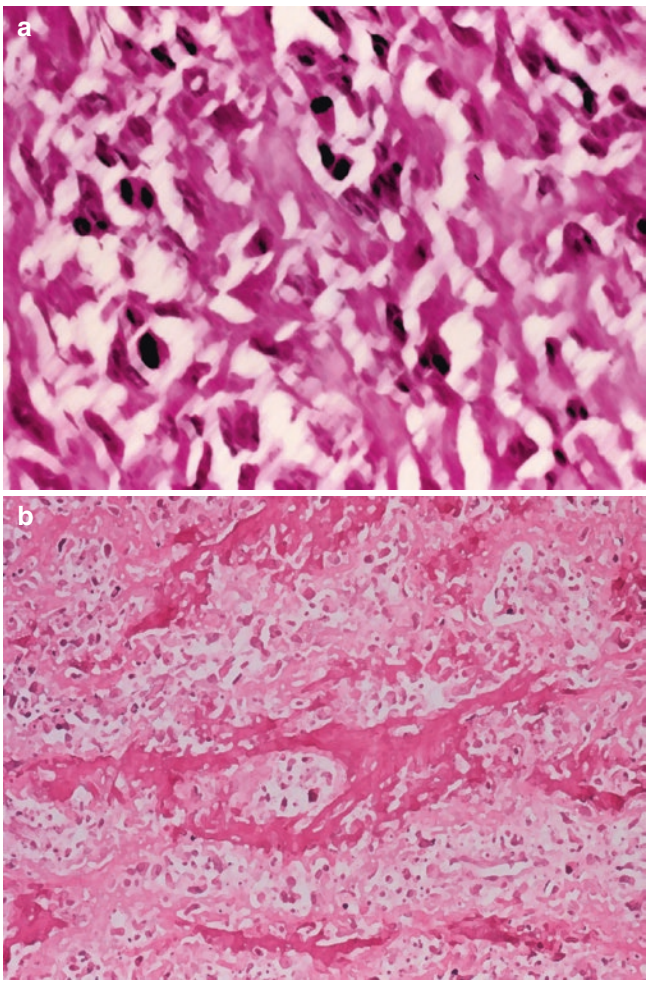

Fig. 3.62 Osteosarcoma. (**a**) High-grade malignant cells producing abundant osteoid (H&E, 200×). (**b**) High-grade low high-grade malignant cells producing abundant osteoid and bone (H&E, 100×). (Courtesy of A. Kevin Raymond, M.D.)

Molecular

Molecular specificity has not been defined for osteoblastoma. However, a unique three-way translocation involving chromosomes 1, 2, and 14 has been identified: [t(1;2;14)(q42;q13;q24)] [137].

Osteosarcoma

Definition

Osteosarcoma (aka osteogenic sarcoma) is defined as a primary malignant tumor of the bone in which the neoplastic cells produce osteoid and/or bone even if only in small amounts (Fig. 3.62a, b) [1, 138–140].

Excluding multiple myeloma, osteosarcoma (OS) is the single most common primary malignant tumor of the bone. However, OS is not a single, stereotypic entity. Rather, it is a complex family of malignancies in which the production of osseous matrix is the single unifying parameter. OS can be divided into two major groups: *conventional* osteosarcoma (c-OS) comprises 65–75% of cases, and the remaining 25–35% represent *variants* [10, 141–145].

Clinical

Although the demographics pertaining to OS may vary as a function of special circumstances, a number of generalizations apply. Overall, OS has a very broad age distribution but most frequently affects patients in the second decade of life and to a lesser extent those in the third and first decades. One series includes a second peak in older individuals thought to be secondary to diseases specific to that age group [1]. Males

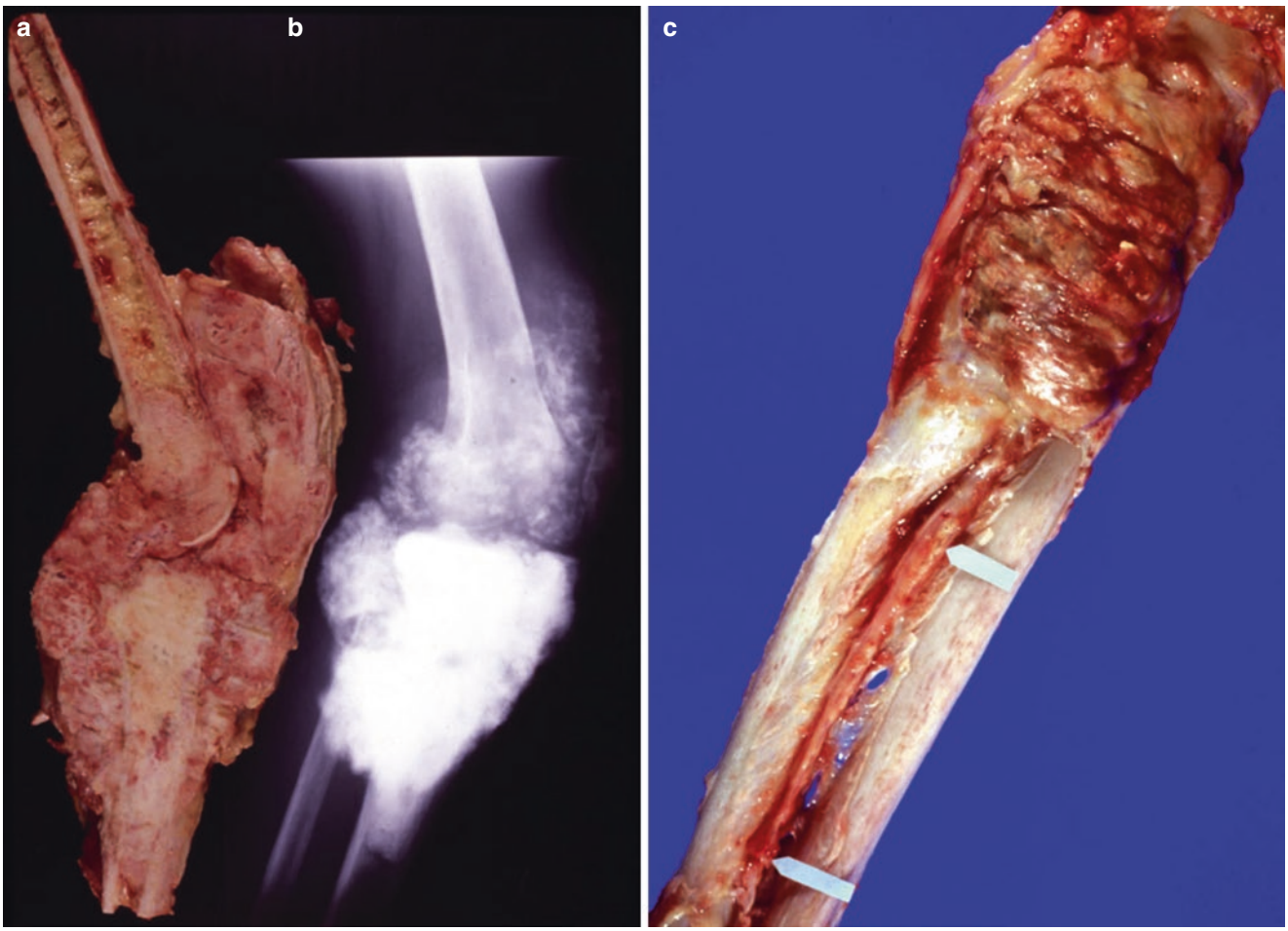

Fig. 3.63 Osteosarcoma. (**a**) Gross specimen: high-grade osteosarcoma arising and replacing the proximal tibia has circumferentially invaded through cortex into overlying soft tissue. Tumor has invaded the knee join, obliterated the patellar compartment, and invaded the posterior aspect of the distal femur. (**b**) Plane file (lateral): a radiopaque mass with cumulous cloud-like quality involvement corresponding to the gross specimen (**a** and **b** are the same case). (**c**) Osteosarcoma encasing the distal radius and ulna. Tumor has invaded the draining veins (blue arrow). (Courtesy of A. Kevin Raymond, M.D.)

are affected more frequently than females, with male to female ratio variously reported as 2:1 to 3:2.

Any part of any bone may be the primary site for OS. However, the vast majority (>90%) of OS arise within the medullary cavity, while <10% originate on the cortical surface and <1% arise within the cortex itself. Among the intramedullary tumors, roughly 90% arise within the metaphysis, while some 10% arise in the diaphysis, and far less than 1% originate within epiphyses. As a rule of thumb, the most frequent sites of origin are within the major growth centers of the long bones of the appendicular skeleton: distal femur, proximal tibia, and proximal humerus. The latter skeletal distribution is being fairly typical of tumors with second decade predominance.

Symptom onset in c-OS is relatively rapid, in general less than a year prior to presentation. Severe, progressive pain in the region of the primary tumor is the cardinal symptom of OS. Other symptoms include localized tenderness, swelling, palpable then visible enlarging mass, mass effect, referred pain, decreased range of motion, warmth on palpation, and occasional bruit on auscultation. Pathological fracture may be present in 5–10% of patients [146].

The natural history of OS is one of potential unrestrained aggressive local growth and early lethal systemic dissemination (Fig. 3.63a–c). When tumor is left untreated, or improperly treated, clinically evident systemic metastases tend to appear within 9–12 months followed by death due to systemic dissemination within 18–24 months [1, 138].

Sites of metastases are fairly predictable. In those patients suffering metastases, virtually 100% of patients have pulmonary metastases. Although pulmonary metastases can be centro-lobar, many are subpleural (Fig. 3.64a–c). Bone is a fairly frequent site of clinically significant metastasis and is extremely common as a preterminal event. After that, the sites of systemic dissemination appear somewhat arbitrary,

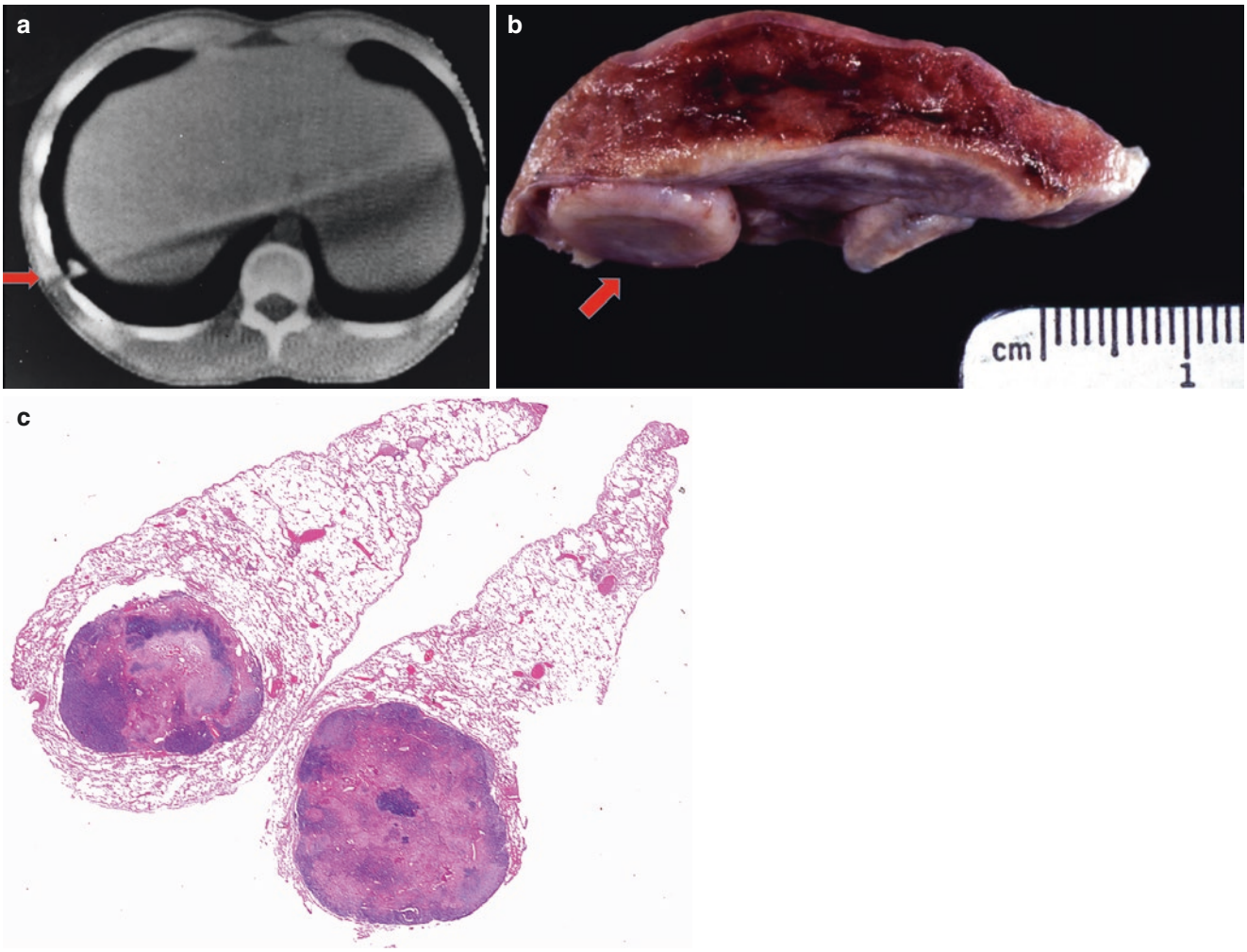

Fig. 3.64 Osteosarcoma: lung metastases. (**a**) CT of chest: there is a radiopaque subpleural mass (red arrowhead). (**b**) Lung wedge resection with subpleural lung metastasis with button-like configuration (red arrowhead) (**a** and **b** are the same case). (**c**) Whole mount sections of subpleural osteosarcoma lung metastasis. Peripheral portions of tumor are dark blue and consist of sheets of neoplastic cells with little matrix. The central portions of the tumor contain larger amounts of osseous matrix resulting in the pink coloration. (Courtesy of A. Kevin Raymond, M.D.)

although kidney may be affected somewhat more frequently than expected.

Historically, treatment focused on the primary tumor with complete tumor extirpation, amputation being the usual treatment of choice. The goal was removal of a potentially lethal tumor and the *prevention* of systemic metastases. The expected 5-year survival with surgery-only protocols was in the range of 10–20% [138, 147] with one exception reporting a survival of some 40% [146].

The evolution of OS treatment has been a multidisciplinary endeavor with contributions from radiology, pathology, oncology, and surgery. Critical to the evolution of OS treatment has been the recognition that systemic metastases occur at a much earlier point in time than historically appreciated. The recognition of the existence of early, subclinical, micrometastases in OS and the need to view OS as a systemic disease at the time of initial presentation shepherded the development of successful OS treatment [140, 145, 148].

The introduction of chemotherapy to the treatment of OS was at best a contentious decision [140, 141, 144]. Initially, chemotherapy was given postoperatively, and the available agents (e.g., 5-fluorouracil, cyclophosphamide, mitomycin C, phenylalanine mustard) were at best ineffective. A major drawback of giving all chemotherapy in the postoperative setting is that the first sign of treatment failure is the development of clinically evident systemic metastases. However, the development of newer therapeutic agents (i.e., Adriamycin, cisplatin, ifosfamide, methotrexate) and protocol evolution demonstrated both the potential and necessity of systemic therapy in the treatment of OS.

At the same time, combining a better understanding of OS with the evolution of more sophisticated surgical techniques and the development of more user-friendly prostheses

allowed the extension of limb-salvage procedures into more generalized use.

The original prostheses used for resection reconstruction were so-called *custom prosthesis* whose manufacture was time-consuming (i.e., weeks to months) thus leaving a treatment void between biopsy and resection. This pre-surgical time period provided an opening for the introduction of preoperative chemotherapy. In essence it is a test, a test to determine if there is response to preoperative chemotherapy in the primary tumor that is going to be removed anyway and, more importantly, to investigate whether the response in the primary tumor predicts response in micro-metastases as measured in patient survival.

Ultimately, development of so-called *neoadjuvant* or *primary* chemotherapy showed that multidisciplinary therapy, encompassing preoperative chemotherapy, followed by surgery and followed by administration of response-determined postoperative chemotherapy is the best, currently available therapeutic option [145, 148–152]. At the core of primary chemotherapy is the concept that while treatment is aimed at metastatic disease, the primary tumor acts as a measurable gauge of response to therapy, response to therapy as measured in terms of histological evidence of tumor necrosis seen in the primary tumor. Following this principle, it was found that if response to preoperative therapy is good (i.e., tumor necrosis ≥90%), then the same agents used preoperatively are employed postoperatively. If response to preoperative therapy is poor (i.e., tumor necrosis <90%), then an alternate chemotherapy protocol is used in the postoperative setting.

There are a number of prognostic factors related to the patient, tumor, tumor biology, and treatment that impact OS patient survival [4, 141]. These prognostic factors include patient age and gender, the presence of clinically evident transarticular or systemic metastases on presentation, size and site of tumor, tumor respectability, local relapse following initial therapy, and the treatment regimen. In addition, there are a number of factors that can be employed to monitor the patient for relapse (e.g., serum alkaline phosphatase). However, the most powerful indicator of patient survival is response to preoperative chemotherapy. Tumor necrosis ≥90% is associated with 80–90% long-term survival. Depending on the protocol, tumor necrosis <90% portends a survival of <12%. However, with the appropriate adjustment of postoperative therapy in patients with poor response to preoperative therapy, survival can be made to approximate that of good responders [145].

Systemic metastases are the primary therapeutic target of preoperative chemotherapy. However, experience has shown that there is also clinical benefit resulting from therapy effect on the primary tumor. There is almost immediate relief of symptoms referable to the primary tumor, e.g., marked decrease or elimination of pain and swelling. More importantly, local response to therapy usually results in the so-called downstaging of the primary tumor, i.e., local tumor regresses, and marginates in a form and to a degree that increases patient eligibility for limb-salvage surgery. In the absence of preoperative chemotherapy, <10% of OS patients are eligible for limb-sparing surgery, while after preoperative chemotherapy >90% of treated patients are eligible for limb-salvage surgery [19, 145].

Histopathology

Although frequently referred to as *spindle cells*, the neoplastic cells of OS generally have a very broad spectrum of diversity, usually including a high degree of both anaplasia and pleomorphism. Neoplastic cells may well be spindle in shape, long or short or in between. However, they may also be round, oval, epithelioid, plasmacytoid, small or large, bizarre angulated shapes, with variable numbers of nuclei including multinucleated malignant giant cells. Cytoplasm may be minimal to abundant, eosinophilic, amphophilic, or clear. Nuclei may have finely divided or coarsely clumped chromatin with or without nucleoli that vary from innocuous to prominent. Mitotic activity is highly variable and atypical forms frequent. There is nothing cytologically unique or specific about the cells of OS (Fig. 3.65a, b).

By definition, OS is a tumor in which the neoplastic cells produce osteoid and/or bone. In truth, the neoplastic cells produce osteoid that may or may not undergo mineralization resulting in conversion to bone; mineralization is an extracellular event. Technically, neoplastic cells only *produce* osteoid. However, the definition has largely remained as given to emphasize the histological *appearance* of tumor-produced matrix in OS as seen through light microscopic examination.

The presence of osseous matrix is obviously central to the concept and diagnosis of OS. Inquiries are frequently made as to the markers for osteoid. Osteoid *is the marker*, and therefore, it is important to be familiar with its morphological characteristics. Osteoid is an extracellular matrix. It is a form of collagen, a form of type I collagen. Therefore, the frequently encountered query, osteoid versus collagen, is the wrong question. The issue revolves around being able to discriminate between osseous and non-osseous collagen; and at this point-in-time, this remains within the purview of the surgical pathology.

Tumor-produced osseous matrix is abundant and readily evident in the vast majority of OS cases, even in small biopsies (Fig. 3.65a). However, there are cases in which the identity of intercellular pink material can be called to question (Fig. 3.62a).

Therefore, it is important to be familiar with the morphological characteristics of osteoid.

Osteoid is eosinophilic, while tending to be both homogeneous and amorphous (Fig. 3.66a). This is in contrast to collagen produced in fibrous tumors, e.g., desmoplastic fibroma, which is heterogeneous and fibrillar (Fig. 3.66b).

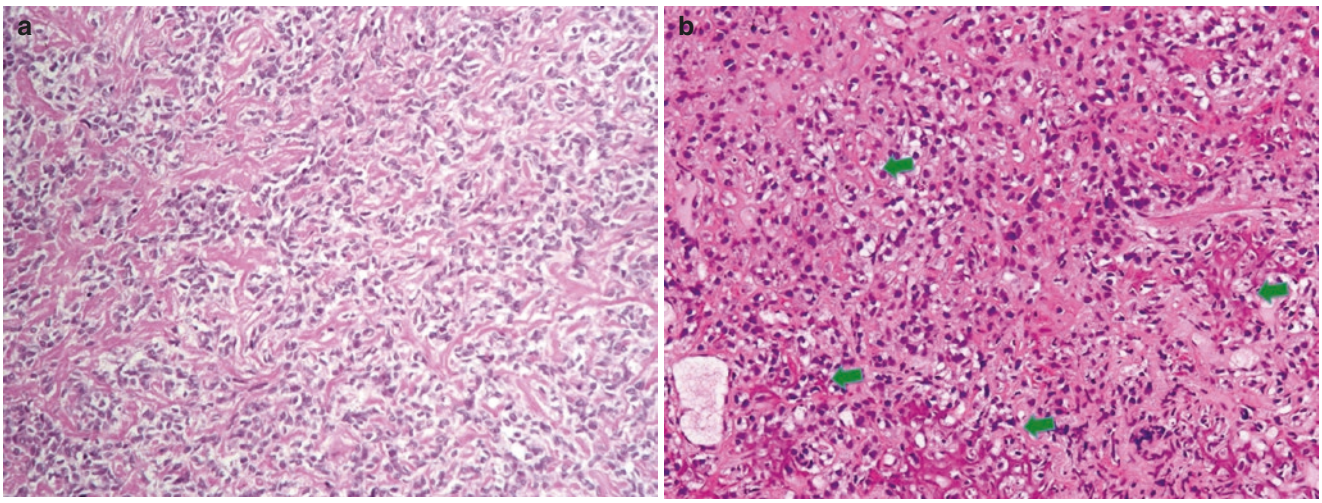

Fig. 3.65 Osteosarcoma. (**a**) High-grade sarcoma with abundant, easily recognized osseous matrix: osteosarcoma (H&E, 100×). (**b**) High-grade grade sarcoma with fine lines of pink intercellular material (green arrowheads): query osteoid. Osteosarcoma vs other malignant tumor (H&E, 100×). (Courtesy of A. Kevin Raymond, M.D.)

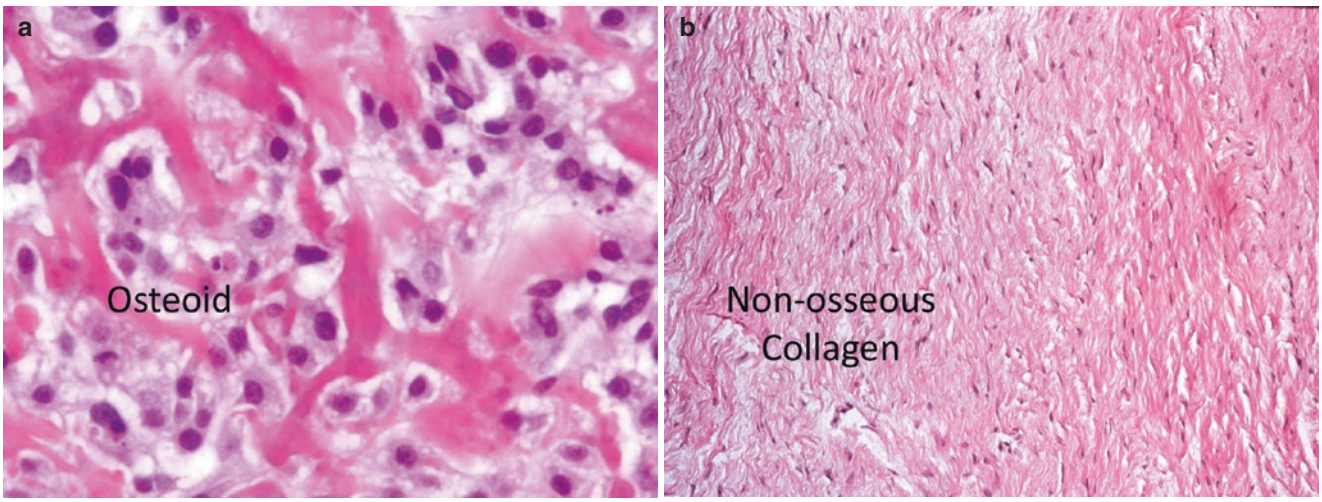

Fig. 3.66 Osteosarcoma. (**a**) Osteoid: well-defined, amorphous, homogeneous pink intercellular matrix (H&E ×250). (**b**) Non-osseous collagen: ill-defined, wispy intercellular, fibrillar material with internal structure and variability. Desmoplastic fibroma (H&E 100×). (Courtesy of A. Kevin Raymond, M.D.)

Osteoid tends to be refractile, almost mirror-like with focusing under the microscope. It is curvilinear rather than straight; in some ways the architecture of osteoid appears to recapitulate lacune formation (Fig. 3.67a, b). Tumor matrix deposition on previously existing normal or tumor bone is inevitably present and mimics the normal appositional deposition of bone matrix, *scaffolding*. Lastly, tumor-produced osteoid is randomly oriented (Fig. 3.68). The latter is contrast to normal or "reactive bone" that is produced in response to stress and is therefore oriented in response to stress. Osseous matrix produced in OS is not produced in response; rather it is deposited randomly (Fig. 3.69).

The earliest forms of mineralization consist of small blue dots scattered through the otherwise pink osteoid. Further mineralization results in rhomboid crystalline structures (Fig. 3.70a–c). Since decalcification removes calcium from tissue, mineralized matrix is best view in non-decalcified tissue, e.g., frozen section.

Gross

The bulk of any given tumor tends to form a cohesive mass with destruction of underlying osseous structures in the involved area. The interface with residual normal trabecular and cortical bone is both infiltrative and destructive. Tumor may extend through cortex into overlying soft tissue either as

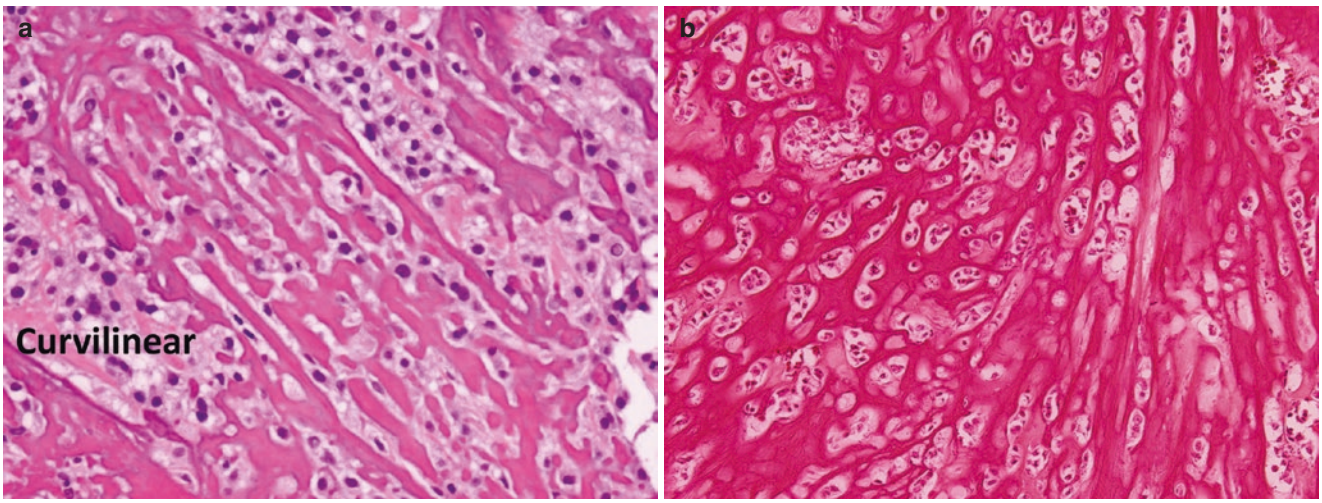

Fig. 3.67 Osteosarcoma. (**a**) Osteoid: pink, homogeneous, amorphous material is not linear; rather it is curvilinear reminiscent of lacune formation (H&E 100×). (**b**) Osteoid and bone: abundant pink, homogeneous, amorphous, curvilinear material is refractile under the microscope (H&E 100). (Courtesy of A. Kevin Raymond, M.D.)

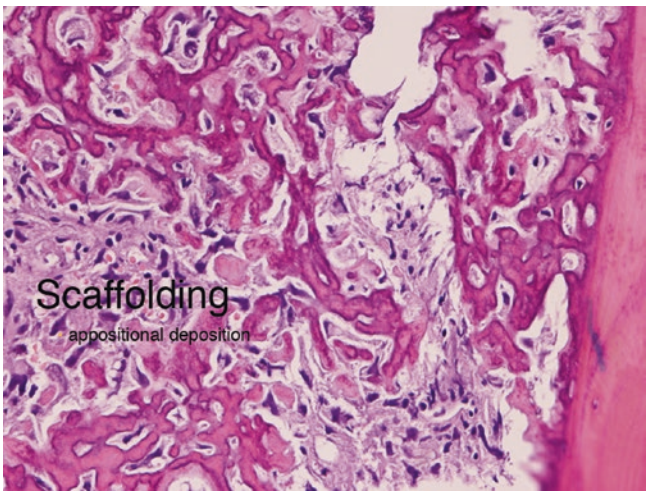

Fig. 3.68 Osteosarcoma. Malignant cells depositing osseous matrix on previously existing trabecular bone; so-called *scaffolding* (H&E 100×). (Courtesy of A. Kevin Raymond, M.D.)

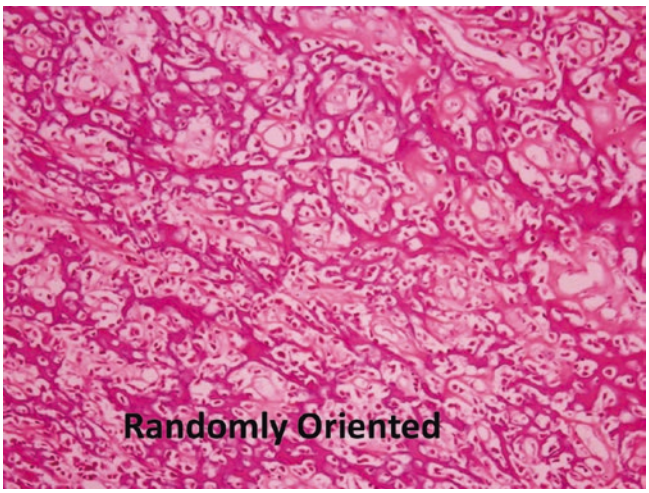

Fig. 3.69 Osteosarcoma. Osseous matrix is randomly oriented (H&E 40×). (Courtesy of A. Kevin Raymond, M.D.)

an infiltrative process through intact cortex or by destroying cortex. The vast majority of tumors remain confined beneath the periosteum until late in the course of disease. Although OS tends to grow as a relatively cohesive mass, intramedullary *skip metastases* may be present [1, 143, 145]. Skip metastases are discrete foci of intramedullary tumor separated from the primary tumor by normal tissue and come in two forms. *Intramedullary skip metastases* occur when both the primary OS and metastasis are present in the same bone but separated by normal bone marrow (Figs. 3.71 and 3.72).

Transarticular skip metastases occur when the primary OS and metastasis are present in an adjacent bones separated by an opposing common joint.

Grossly, the color, consistency, and texture of OS are a reflection of the cell to matrix ratio, the form of matrix, and the superimposed secondary degenerative changes. The non-matrix-predominant areas of OS tend to be soft but firm and vary from tan to pale cream color (i.e., "fish flesh"). Frequently, there are superimposed changes of hyperemia, hemorrhage, inflammation, necrosis, fibrosis, cystification, aneurysmal bone cyst-like change, pathological fracture, and/or preoperative chemotherapy. Whether periosteal, cortical, or intramedullary, osseous matrix produced by normal bone elements in response to a pathological process (i.e., "reactive bone") may quantitatively range from minimal to dramatic. Reactive bone can display a

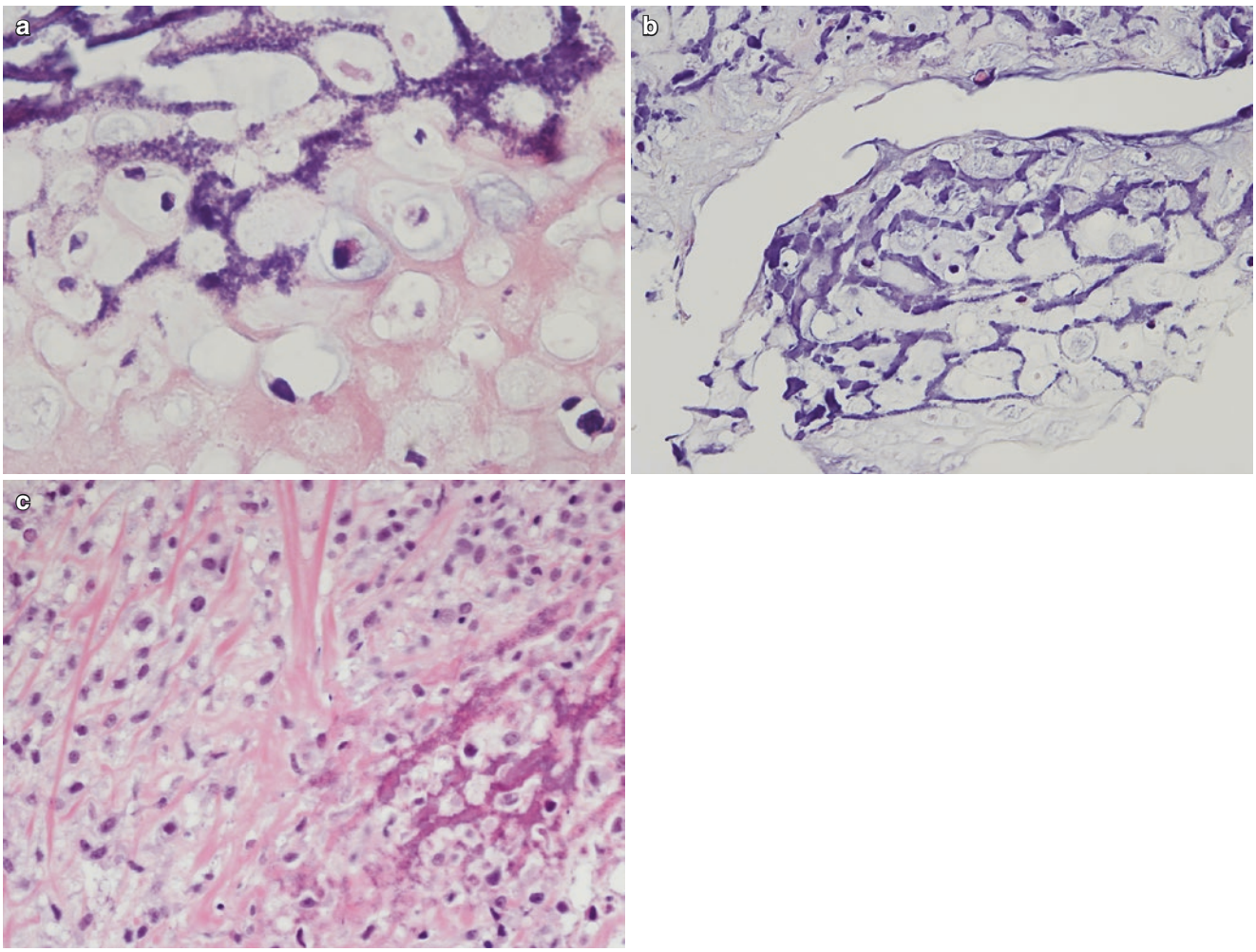

Fig. 3.70 Osteosarcoma. (**a**) Frozen section: malignant cells producing osteoid. The fine purple stippling is early mineralization, osteoid being converted to bone (H&E, 400×), (**b**) Frozen section: malignant cells producing osteoid that has a pinkish-blue quality and has considerable mineralization, rhomboid crystals (H&E, 400×). (**c**) Formalin fixed permanent section: malignant cells producing osteoid and bone with relatively early mineralization (H&E, 100×). (Courtesy of A. Kevin Raymond, M.D.)

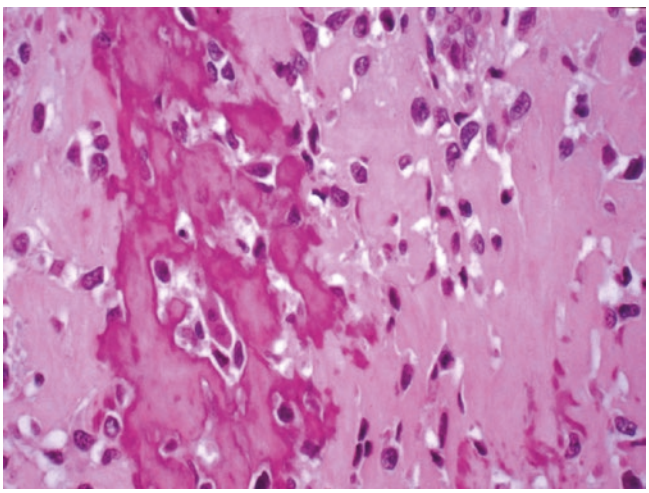

Fig. 3.71 Osteosarcoma. High-grade osteosarcoma with abundant osteoid and bone production (H&E, 100×). (Courtesy of A. Kevin Raymond, M.D.)

wide variety of manifestations, e.g., trabecular or cortical thickening, laminated matrix deposited longitudinally on the cortical surface (so-called onionskin), or spiculation radiating outward from the bone surface (so-called sunburst).

Radiographically, the plane film (i.e., AP and lateral) remains the mainstay of qualitative OS evaluation. OS tends to be a destructive, relatively well-defined, mixed lytic/blastic neoplasm with an infiltrative normal/tumor bone interface. Lesional radiodensity reflects a combination of factors: content of mineralized tumor-produced matrix, destruction of underlying normal bone, and the presence of reactive bone formation. CT including high-resolution and three-dimensional reconstruction adds detail to plane film examination. In general, OS tends to be hypointense on T1-weight scans and hyperintense on T2-weighted images. CT and MRI are the tools of choice for evaluating extent of disease,

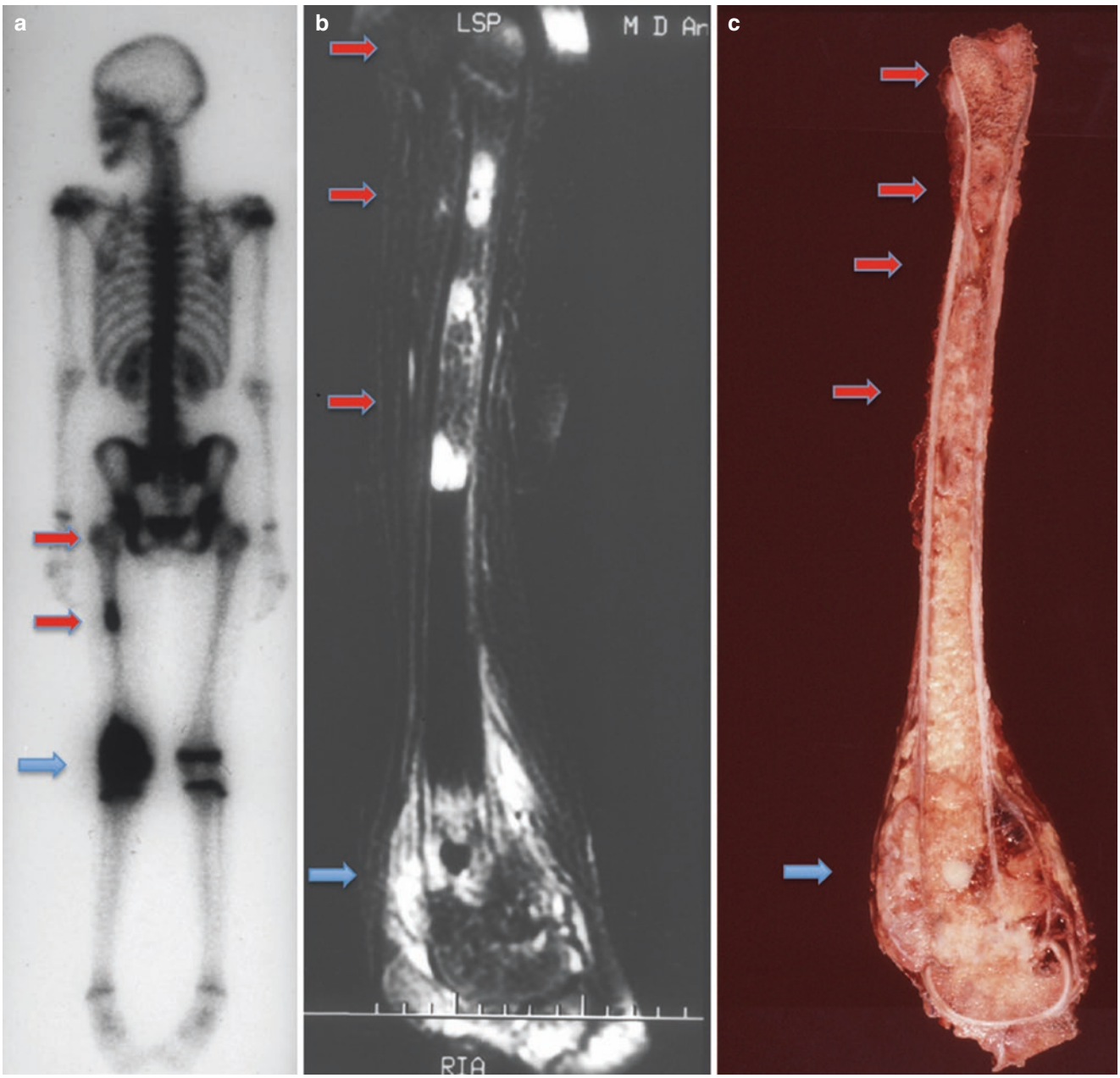

Fig. 3.72 Osteosarcoma. (**a**) Tm99 bone scan showing increased uptake in the primary tumor involving the distal femur (blue arrow). There is also increased uptake in more proximal areas of the femoral diaphysis and proximal metaphysis/epiphysis corresponding to intramedullary skip metastases (red arrows). (**b**) MRI T2-weighted image: region of hyperintensity in the primary tumor involving the distal femur (blue arrow). There are also areas of hyperintensity in more proximal areas of the femoral diaphysis, proximal metaphysis, and epiphysis, corresponding to intramedullary skip metastases (red arrows). (**c**) Gross specimen: primary osteosarcoma involving the distal femur (blue arrow). There are skip metastases involving the more proximal femoral diaphysis, metaphysis, and epiphysis (red arrows). (Courtesy of A. Kevin Raymond, M.D.)

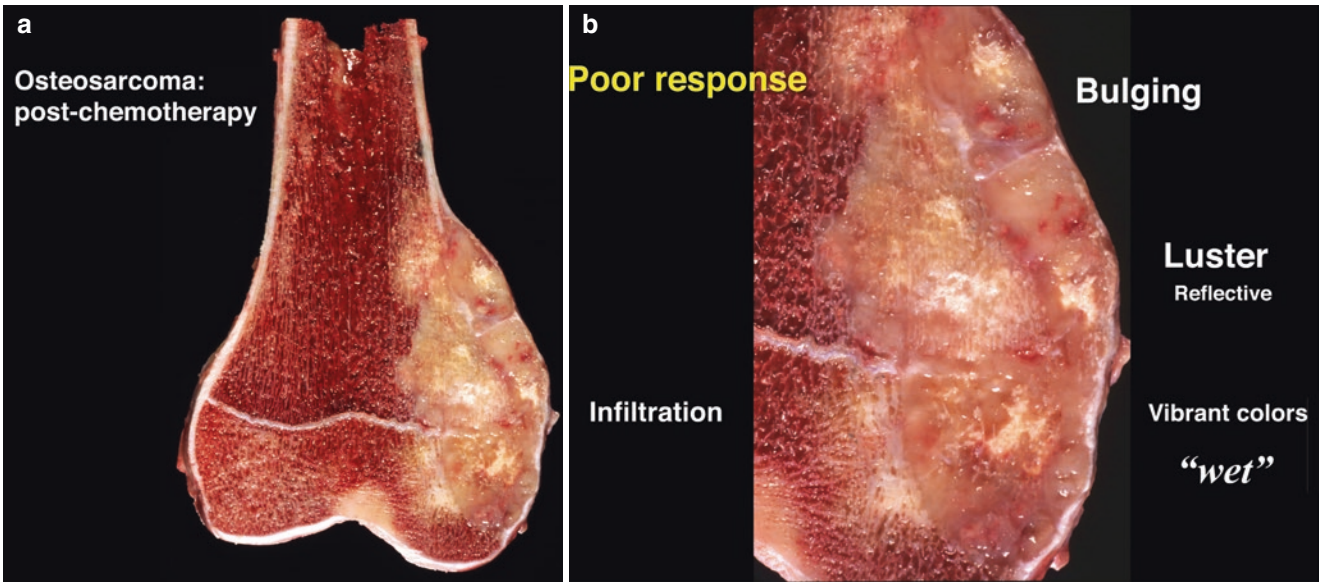

Fig. 3.73 (**a**, **b**) Osteosarcoma. Specimen from patient who has undergone preoperative chemotherapy. The tumor has vibrant, bright colors, which have luster and reflect light. The tumor has a bulging cut surface, and there is infiltration of adjacent cancellous bone. The overall appearance is that of "wet" specimen. These changes are consistent with a poor response to preoperative chemotherapy. (Courtesy of A. Kevin Raymond, M.D.)

in particular soft tissue involvement and resection margin estimation. Tm^{99} bone scan and MRI allow for reliable detection of skip metastases. Detection of systemic disease is the domain of the "skeletal survey," Tm^{99} bone scan, and high-resolution CT of the lungs.

Response to Therapy

The quantitative evaluation of response to preoperative chemotherapy has become central to the management of the OS patient. The details of specimen management have been the subject of detailed reports [145, 153–157] but will be summarized here. The essence of pathology specimen processing is the ability to recognize, select, and submit "representative sections" for histological examination [158], that is, the ability to reproducibly and confidently submit a very limited number of tissue sections that they will allow accurate diagnosis and evaluation of prognostic factors. When dealing with OS, there are several problems, the foremost being the lack of consistency in gross versus histological findings. Viable tumor (Fig. 3.73a, b) is solid with vibrant colors and luster. Non-mineralized soft elements have bulging cut surfaces, and the entire viable lesion has an overall *wet* appearance. Necrotic tumor tends to be nonhomogeneous, with dull suppressed colors. Necrotic tumor has tissue retraction from matrix. The overall appearance of necrotic OS is that of a tumor that looks *dry* and desiccated (Fig. 3.74a, b). However, inflammatory infiltrate and reactive elements can add to luster and make the otherwise necrotic tumor appear wet (Fig. 3.75a, b). Therefore, while dry is relatively specific for tumor necrosis, the *wet look* may be seen with either viable or necrotic tumor. Therefore, in the absence of gross specificity allowing representative sections, we rely on the consistency of protocol-dictated tissue sampling, at a minimum, submitting a full cut surface (i.e., sagittal, coronal, oblique) of the involved bone. In general, an anatomic record of tissue submission is kept. This may be done in any of a variety of techniques: specimen x-ray, labeled specimen photograph, or diagram. Additional tissue may be submitted per protocol (Fig. 3.76a, b).

Fundamental to the histological analysis of response to therapy is the ability to evaluate tumor necrosis, or more properly tumor *apoptosis*. The hallmark of "tumor necrosis" is tumor cell dropout. Analysis of tumor necrosis in OS is somewhat more straightforward than other tumor types because of tumor matrix production. Tumor cells are eliminated in response to successful therapy; however, tumor matrix is non-resorbable and acts a marker for tumor-involved areas. Areas of tumor response consist of residual tumor-produced matrix devoid of neoplastic cells. There is also background supporting tissue with an appearance of embryonic areolar tissue and adipose tissue. There may be some element of non-specific chronic inflammation (e.g., lymphocytes, lipid, and hemosiderin -laden macrophages) and detritus of degenerated cells. Using these materials

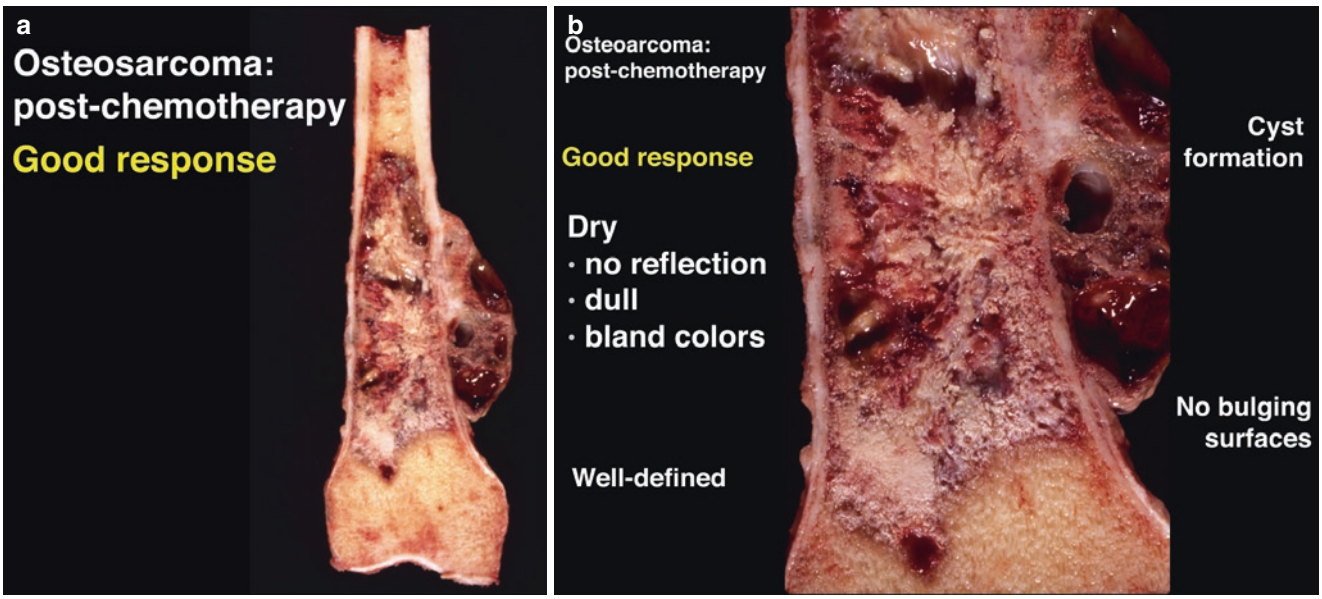

Fig. 3.74 (**a**, **b**) Osteosarcoma. Whole specimen from patient who has undergone preoperative chemotherapy. The tumor has dull, bland colors, which lack luster and do not reflect light. The tumor has a flat cut surface with focal cystification and absent infiltration of adjacent cancellous bone; tumor appears marginated. The overall appearance is that of "dry" specimen. These changes are indicative of a good response to preoperative chemotherapy. (Courtesy of A. Kevin Raymond, M.D.)

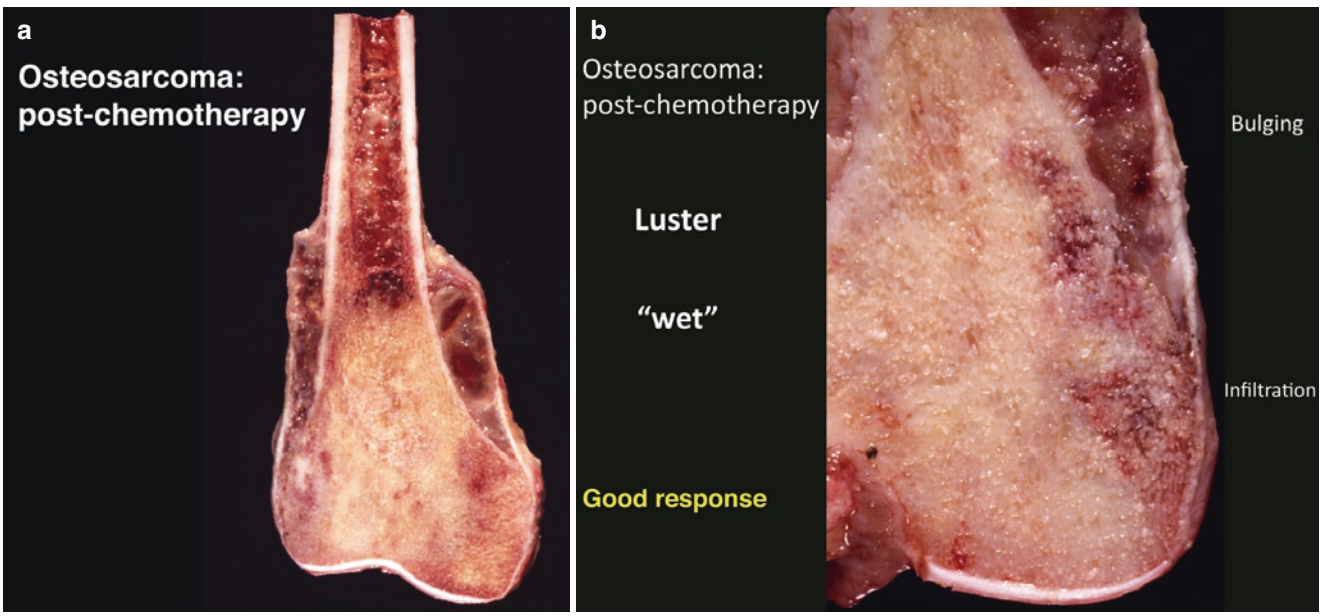

Fig. 3.75 (**a**, **b**) Osteosarcoma. Specimen from patient who has undergone preoperative chemotherapy. The tumor has vibrant, bright colors, which have luster and reflect light. The tumor has a bulging cut surface, and there is infiltration of adjacent cancellous bone. The overall appearance is that of "wet" specimen. Although these changes suggest a poor response to preoperative chemotherapy, this patient had a good response to chemotherapy. The changes suggestive of viability are thought to reflect inflammatory changes. (Courtesy of A. Kevin Raymond, M.D.)

Fig. 3.76 Osteosarcoma. Specimen mapping. (**a**) Post-chemotherapy osteosarcoma specimen cut in the coronal plane. (**b**) Post-chemotherapy osteosarcoma *slab section* has been *"mapped"* using the Isomet™. (Courtesy of A. Kevin Raymond, M.D.)

response to therapy can be calculated and expressed in terms of percent tumor necrosis (Fig. 3.77a, b).

As previously indicated, OS is not a single disease, but a family of biologically diverse malignancies with a common histological finding of osseous matrix production by neoplastic cells. Attempts at structuring a classification system are almost as numerous as the involved investigators [1, 139, 141, 143–145]. For the most part, all of the systems recognize the same specific entities; the differences are largely in how those entities are arranged or grouped. The system presented here was initiated at MD Anderson Cancer Center in 1983 and presented in 1987 [145]. The essence of the system is to recognize common factors that potentially impact OS survival and separate those off from the "classical," "typical," or what is commonly referred to as "conventional osteosarcoma." The potential benefit is to establish a means to more accurately evaluate protocol treatment results.

Conventional OS (c-OS) constitutes the majority (i.e., 60–80%) of cases, with the remainder being so-called variants. In turn, the many variants can be distributed among three major groups subdividing OS in terms of cases defined

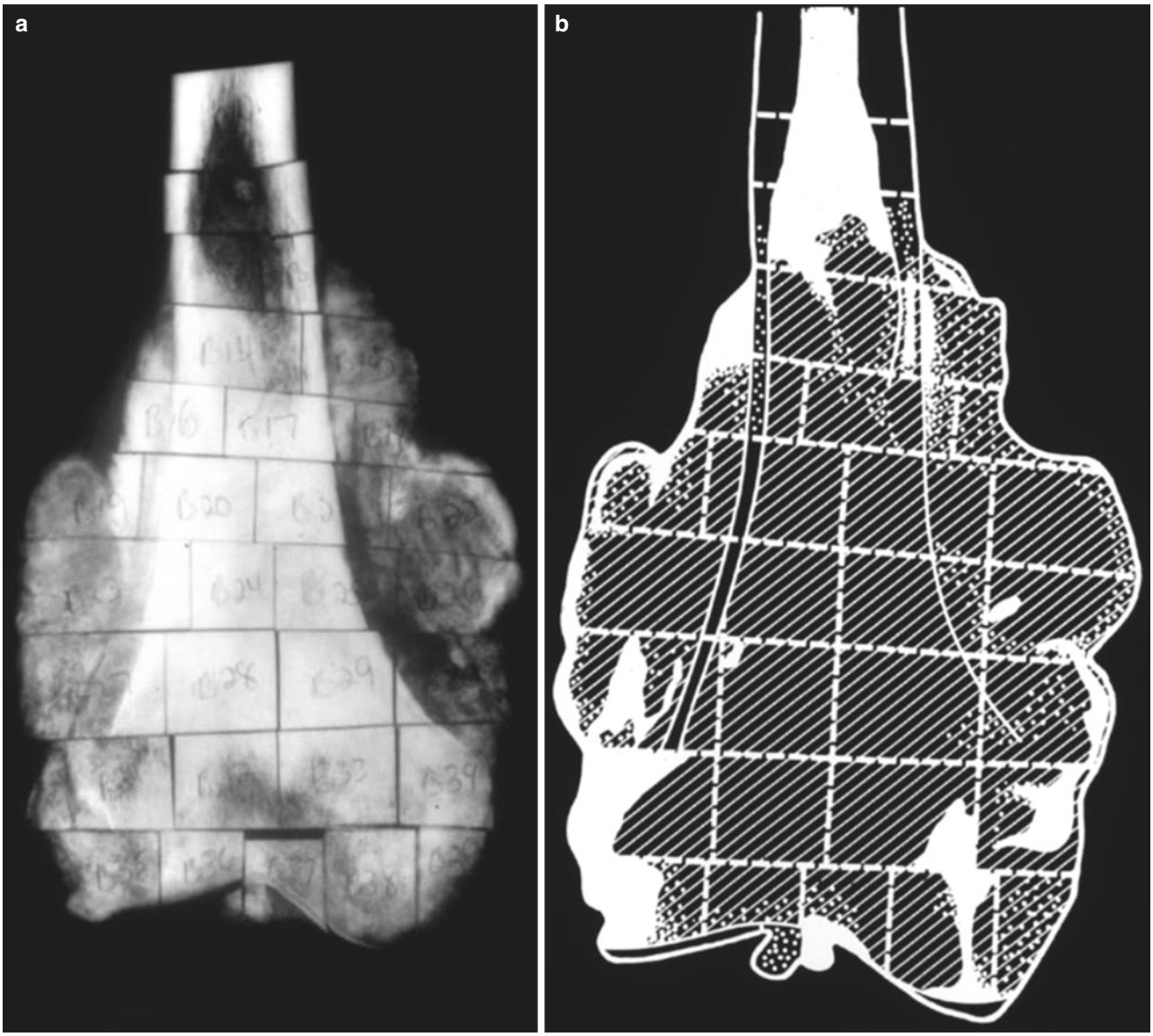

Fig. 3.77 Osteosarcoma. Specimen mapping. (**a**) Labeled specimen x-ray of a mapped slab section of a specimen from a treated osteosarcoma patient. (**b**) Post formal-mapping record. The specimen x-ray has been used to create a diagram upon which areas of viable and nonviable tumor can be recorded. (Courtesy of A. Kevin Raymond, M.D.)

in terms of clinical factors versus those determined by histological parameters versus those that arise within/on cortex.

The *clinical variants* can be further subdivided into those forms defined in terms of clinical setting versus site of origin. Those cases defined in terms of a clinical setting, i.e., Paget's disease, postradiation and those arising in association with specific genetic syndromes may also viewed as *secondary* OS. In each case, there are specific criteria allowing reproducible classification.

Site of origin is not generally considered grounds for classification. However, it is recognized that certain anatomic sites are associated with OS that is intrinsically different from c-OS (i.e., jaws, multicentric OS). On the other hand, successful treatment of OS requires complete surgical removal of the primary tumor. There are anatomic sites (e.g., skull, vertebra, pelvis) where complete tumor removal is at best difficult if not impossible, and these cases should not be included in any overall treatment analysis.

Morphological variants are forms of OS defined in terms of histological features and include low-grade central OS, telangiectatic OS, and small cell osteosarcoma.

At times malignant fibrous histiocytoma and those forms of dedifferentiated chondrosarcoma in which the high-grade component is osteosarcoma have been included here. Although care must be exercised to avoid misdiagnosis, these tumors are best viewed within spindle cell/fibrous and cartilage tumors, respectively.

Other histological subtypes have been described and include sclerosing OS, chondroblastoma-like OS, chondromyxoid fibroma-like OS, epithelioid OS, plasmacytoid OS, osteoblastoma-like OS, and giant cell-rich osteosarcoma. However, the rarity of these tumors together with a lack of demonstrable unique clinical differences makes their separation from c-OS a matter of opinion. Currently, their importance lies in recognizing that they exist and may represent diagnostic pitfalls in terms of discriminating them from the entities with which they share histological features. At this point in time, for purposes of data analysis, we include them as subsets of conventional osteosarcoma determined by the dominant matrix or lack of matrix.

Cortical variants include two groups of tumors. There are those that originate within the cortex: *intracortical osteosarcoma*. Alternatively, there are those forms of OS that originate on the cortical surface beneath the periosteum: *surface osteosarcoma* [157]. In turn surface osteosarcoma is divided into three subtypes: *parosteal* osteosarcoma, *periosteal* osteosarcoma, and *high-grade surface* osteosarcoma.

An extreme body of work has evolved investigating the cytogenetic and molecular properties of osteosarcoma. It is a complex disease the underlying biological mechanisms appear to be a measure of that complexity. The work relating to molecular properties of some of the low-grade forms of osteosarcoma shed new light on old problems. However, as we approach the complex genetic aberrations consequent to chromothripsis and kataegis, there is all the more respect for a challenging problem.

Conventional Osteosarcoma

Definition

Conventional osteosarcoma (c-OS) is a primary malignant tumor bone in which the neoplastic cells produce osteoid and/or bone even if only small amounts. These are forms of OS that arise within the medullary cavity and are not associated with unique genetic, clinical, or morphological features. There are three subsets of c-OS: osteoblastic osteosarcoma (OOS), chondroblastic osteosarcoma (COS), and fibroblastic osteosarcoma (FOS). c-OS is what most people think as osteosarcoma [4, 10, 138, 141, 145].

Clinical

The clinical features are largely those given above. c-OS tends to occur in the second and third decades of life, more frequently in men than women (3:2). It shows a strong predilection for the metaphyses and metadiaphyses of the long tubular bones of the appendicular skeleton, in particular the distal femur, proximal tibia, and proximal humerus. Pain followed by pain and enlarging mass is the cardinal symptomatology.

c-OS constitutes some 75% of OS, and despite some variability; c-OS represents a fairly homogeneous clinical group. Clinical experience regarding the biology and treatment of OS is a function of our understanding of c-OS.

Skip metastases occur in something less than 1% of cases. Intramedullary skip metastases, independent foci of OS within a single bone separated by normal marrow, have no impact on prognosis unless surgery is inadequate to include them in the definitive specimen. In contrast, transarticular skip metastases consist of a dominant tumor in one bone separate from a smaller focus (i.e., skip metastasis) in an adjacent bone separated by a joint. The biological significance of transarticular skip metastases is similar to systemic metastases.

c-OS is subclassified on the basis of the predominant matrix present within the tumor. Accounting for some 50% of c-OS is bone predominant (osteoblastic) osteosarcoma. Cartilage-predominant (chondroblastic) osteosarcoma and spindle cell-predominant (fibroblastic) osteosarcoma each comprise roughly 25% of c-OS [138, 145].

Histologically, *osteoblastic osteosarcoma* (OOS) is typically composed of highly anaplastic and pleomorphic malignant cells producing large amounts of osseous matrix. Osteoid can have many forms ranging from slender, interlacing lines (filigree pattern) of varying length, to thicker separate osteoid seams of highly variable configuration to thick aggregates of matrix appositionally applied to one another and underlying normal bone (Fig. 3.78a–d).

The gross appearance of OOS is a function of the cell to matrix ratio and superimposed secondary processes. When large amounts of rock-hard matrix are present in OOS, the predominant color ranges from off-white to yellow-white to white to tan or pink-tan. The cut surface consistency ranges from granular to layered to homogeneous rock-hard tumor. At the tumor normal interface, the advancing edge of tumor infiltrates normal cancellous and cortical bone. At the extreme edge, tumor appears as thickening of normal trabecula secondary to tumor matrix deposition on underlying cancellous bone, scaffolding (Fig. 3.79). More proximally, tumor begins to fill the spaces between bone trabecular, until the more central portions form a homogeneous mass. Cortical involvement can vary from outright destruction to infiltration leaving the cortex largely intact, while in either case tumor extends into overlying connective tissues. Soft tissue involvement ranges from amorphous masses to radiating spicules. When involving the distal femur, always examine the intercondylar notch, an apparent anatomic weak point where subtle joint invasion can take place.

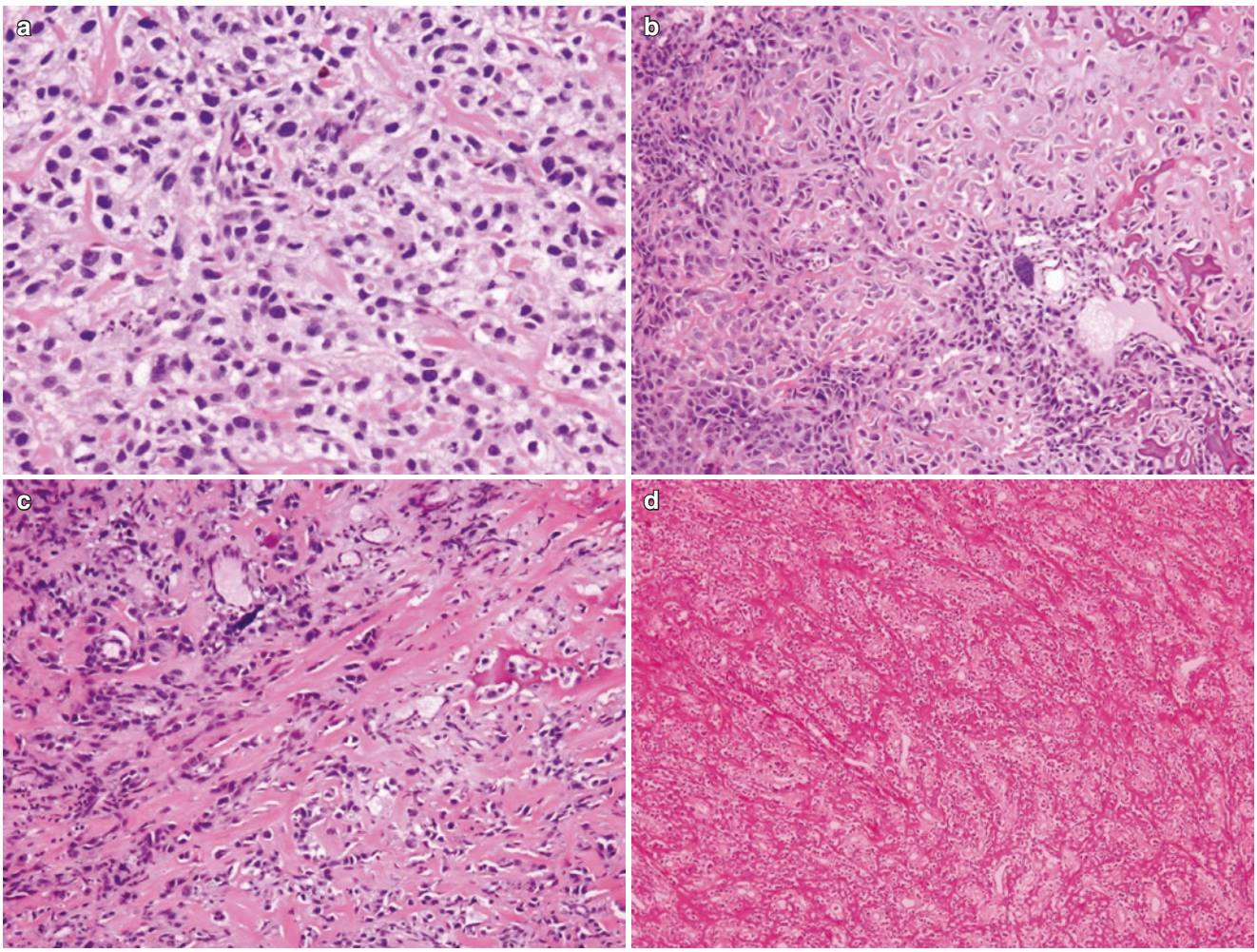

Fig. 3.78 Conventional osteosarcoma. Osteoid patterns. (**a**) Varying thicknesses of filigree pattern osteoid (H&E, 100×). (**b**) Basket weave pattern of osteoid and bone (H&E, 100×). (**c**) Early sclerosing pattern of osteoid: thick layers of osteoid and bone superimposed on one another (H&E, 100×). (**d**) Late sclerosing pattern of osteoid: thick layers of osteoid and bone densely applied to each other (H&E, 40×). (Courtesy of A. Kevin Raymond, M.D.)

The imaging features are those of a radiopaque lesion replacing the metaphysis or metadiaphyseal region of the involved bone. The lesion may be present as a solid radiopaque mass or a less dense *cumulous cloud-like* density. The radiographic appearance of tumor extension through cortex into overlying soft tissue ranges from cortical destruction to infiltration. Soft tissue extension ranges from amorphous masses to radiating fine lines (i.e., *sunburst* appearance). Periosteal elevation with reactive bone or tumor bone extension can result in formation of the so-called Codman's triangle at the juncture of normal and tumor-involved subperiosteal tissues. CT confirms the presence of tumor and with MRI provides a better measure of both intramedullary and soft tissue extent of disease (Fig. 3.80a–c).

For purposes of data analysis, rare histologically defined forms of OS without apparent unique biological properties but significant osteoid/bone production might be included with OOS. *Sclerosing osteosarcoma* refers to forms of OOS with massive amounts of tightly packed osseous matrix. As the name implies, *osteoblastoma-like osteosarcoma* is a form of OS in which the cytological/histological features closely simulate osteoblastoma. Osteosarcoma with rosettoid osteoid is a rare form of OS in which the hallmark is a unique pattern of osteoid production whose histological appearance is reminiscent of rosettes seen in primitive neural tumors (Fig. 3.81).

In *chondroblastic osteosarcoma* (COS), the predominant matrix is cartilage, and tumors are composed of lobules of high-grade malignant cartilage with admixed osteoid and/or bone (Fig. 3.82a–e). The cartilage of enchondroma and chondrosarcoma may undergo endochondral ossification causing peripheral lobular mineralization and ossification that result in encasement of the chondroid matrix; but the

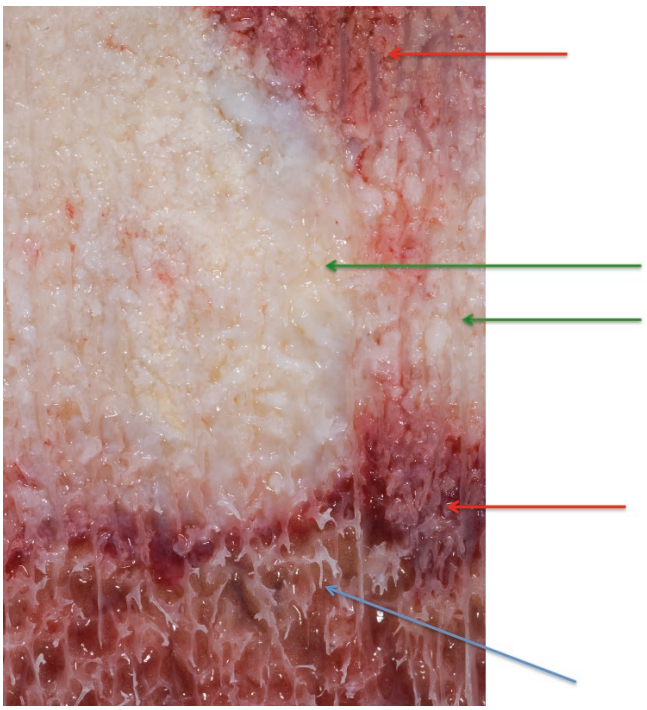

Fig. 3.79 Osteoblastic osteosarcoma. Osseous matrix. Cut surface of osteosarcoma specimen. Blue arrow: early tumor matrix deposition on the surfaces of normal cancellous bone. Red arrows: tumor beginning to fill intertrabecular spaces. Green arrows: tumor has completely filled intertrabecular spaces and destroyed pre-existing trabecular bone. (Courtesy of A. Kevin Raymond, M.D.)

bone-producing cells are normal osteoblasts. In contrast, the osseous matrix of COS is produced directly by the neoplastic cells, cells that are generally much more anaplastic and diverse than those present in cartilage lesions. The growth characteristics are similar to OOS, but with large amounts of intermixing tumor-produced cartilage in addition to osteoid.

In many cases the gross appearance (Fig. 3.82a–e) reflects the histological appearance in the expected fashion, resulting in a tumor that is largely composed of lobules of gray-blue, semitranslucent cartilage. Both ChS and OS are infiltrative at the histological level. In contrast, infiltration of normal cancellous bone is easily grossly appreciated in COS. In contrast, ChS usually appears well-circumscribed to all but the closest scrutiny. Areas of osseous matrix and chondroid mineralization appear as granular off-white to yellow-white to white geographic areas. Alternatively, the cut surface of COS is rubbery and appears as a beige, tan, or sickly off-white fish-flesh appearance. The latter areas may be homogeneous and smooth or have a layered, feather-like configuration.

There are several other histologically defined forms of OS with unusual forms of chondroid matrix. These subtypes are much more frequent in osteosarcoma of the jaw, where they appear to be part of a biologically unique form of OS. However, their rarity in the appendicular skeleton prohibits a definitive statement concerning prognostic significance. These are osteosarcoma with features mimicking benign and malignant primary cartilage tumors: *chondroblastoma-like osteosarcoma*, *chondromyxoid fibroma-like chondroblastic osteosarcoma*, *clear cell chondrosarcoma-like osteosarcoma*, and *myxoid chondroblastic osteosarcoma*. Although these rare subtypes do not appear to impart unique biological significance in the extragnathic skeleton, there histological appearance at any site can cause diagnostic difficulties for the unfamiliar.

As a group c-OS is defined in terms of the predominant tumor-produced matrix or, in the case of *fibroblastic osteosarcoma* (FOS), a relative absence of matrix. By definition, the neoplastic cells of FOS produce osteoid/bone. However, also by definition, the majority of tumor is matrix-free. The neoplastic cells of FOS *tend* to be elongated spindle cells mimicking those of fibrosarcoma or malignant fibrous histiocytoma (Fig. 3.83a–c). Other than the absence of significant amounts of tumor-produced matrix, the growth characteristics of FOS are similar to the other forms of c-OS. Tumor is composed of sheets of neoplastic cells that diffusely infiltrate and replace normal marrow, surrounding and then causing the destruction of underlying normal bone. In as much as the neoplastic cells of FOS lack specific characteristics, the cytological/histological spectrum of FOS can be extremely diverse. For purposes of data analysis, some of the rarer forms of matrix-poor OS (e.g., *giant cell-rich osteosarcoma*) might be included here.

Grossly, the absence of matrix in FOS results in a tumor with the sarcoma characteristics similar to soft tissue tumors. Tumors are fleshy and tend to be fish-flesh gray-white to tan or beige. Small areas of tumor-produced matrix may be present as firm to rock-hard, granular areas. Pathological fracture may be present and superimpose changes secondary to hemorrhage, necrosis, reactive bone formation, and cystification.

Radiographically, in keeping with the relative absence of gross matrix formation, FOS presents as a radiolucent lesion with focal mineralization on plane films and CT. FOS tends be hyperintense on MRI T2-weighted images.

Postradiation Sarcoma

Definition

Postradiation sarcomas (aka radiation-induced sarcomas) are sarcomas arising within bones subject to prior irradiation.

Clinical

Malignant tumors originating in the bone and/or soft tissue as a consequence of radiation exposure have been long recognized. In the absence of alternative sources of radiation,

the vast majority of postradiation sarcomas (p-XRT-sarc) arise as a consequence of exposure to external beam radiation therapy. The criteria to be classified as a p-XRT-sarc were originally put forward by Cahan in 1948 [1, 20, 141, 159–164] and have changed little over time.

1. There is a documented history of radiation exposure.
2. The bone exposed to radiation was normal, or if abnormal, there is histological documentation that the original lesion was substantively different from the subsequent p-XRT-sarc.
3. The postradiation tumor arises within the radiation field or immediately adjacent to it; there is a suggestion that due to interface scatter, the bone immediately adjacent to the radiation field is at greater risk.
4. There is a latent period between the time of radiation exposure and the development of sarcoma. Initially, a 5-year latent period was suggested to assure that occult spontaneous tumors were excluded from consideration. With the development of more sensitive imaging techniques and more thorough baseline assessment, it is felt that a 2-year latent period is adequate. In general latency period is not an issue since the mean latent period is 15 years in several large series [160, 161, 164].
5. There is histological documentation of the p-XRT-sarc.

Patient demographics are a reflection of the population at risk, patients receiving and surviving therapeutic irradiation. Although p-XRT-sarc may occur in younger patients, most patients are older, most frequent in the fourth to sixth decades of life. Women are affected more frequently than men, with male to female ratio approximating 1:2. The bones most frequently involved reflect the irradiated anatomic regions and include bones of the pelvis, head and neck, shoulder, and knee.

Patients tend to present with new pain with or without mass. The treatment of choice depends on the classification of the p-XRT-sarc. However, multidisciplinary therapy similar to osteosarcoma is the therapy of choice in the majority of patients. Historically, the survival in p-XRT-sarc has been reported as poor, in one series 18% 5-year survival [160]. Although there is some disagreement, more recent literature

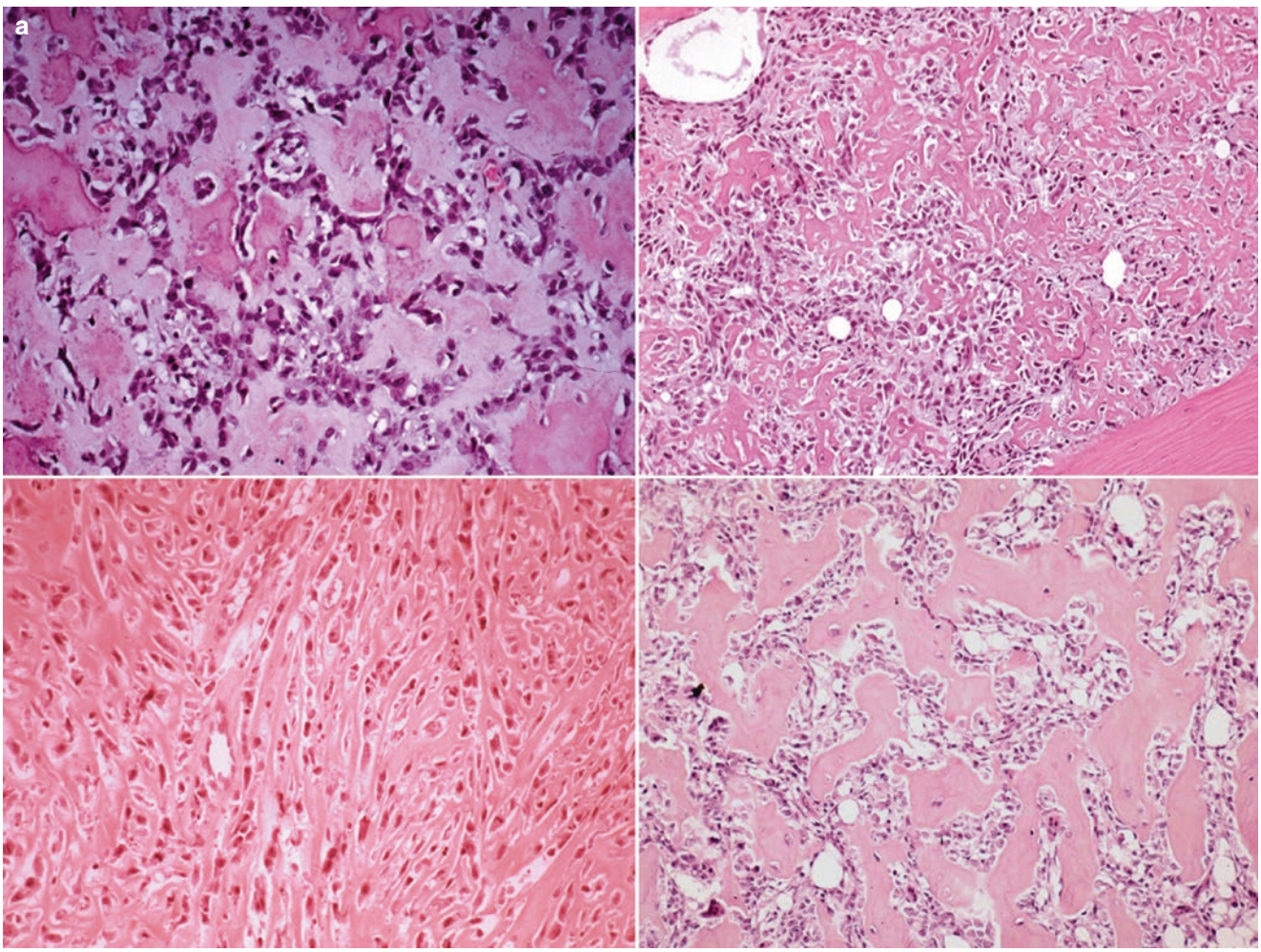

Fig. 3.80 Osteoblastic osteosarcoma. (**a**) Pre-chemotherapy: viable osteoblastic osteosarcoma; variety of histological patterns.

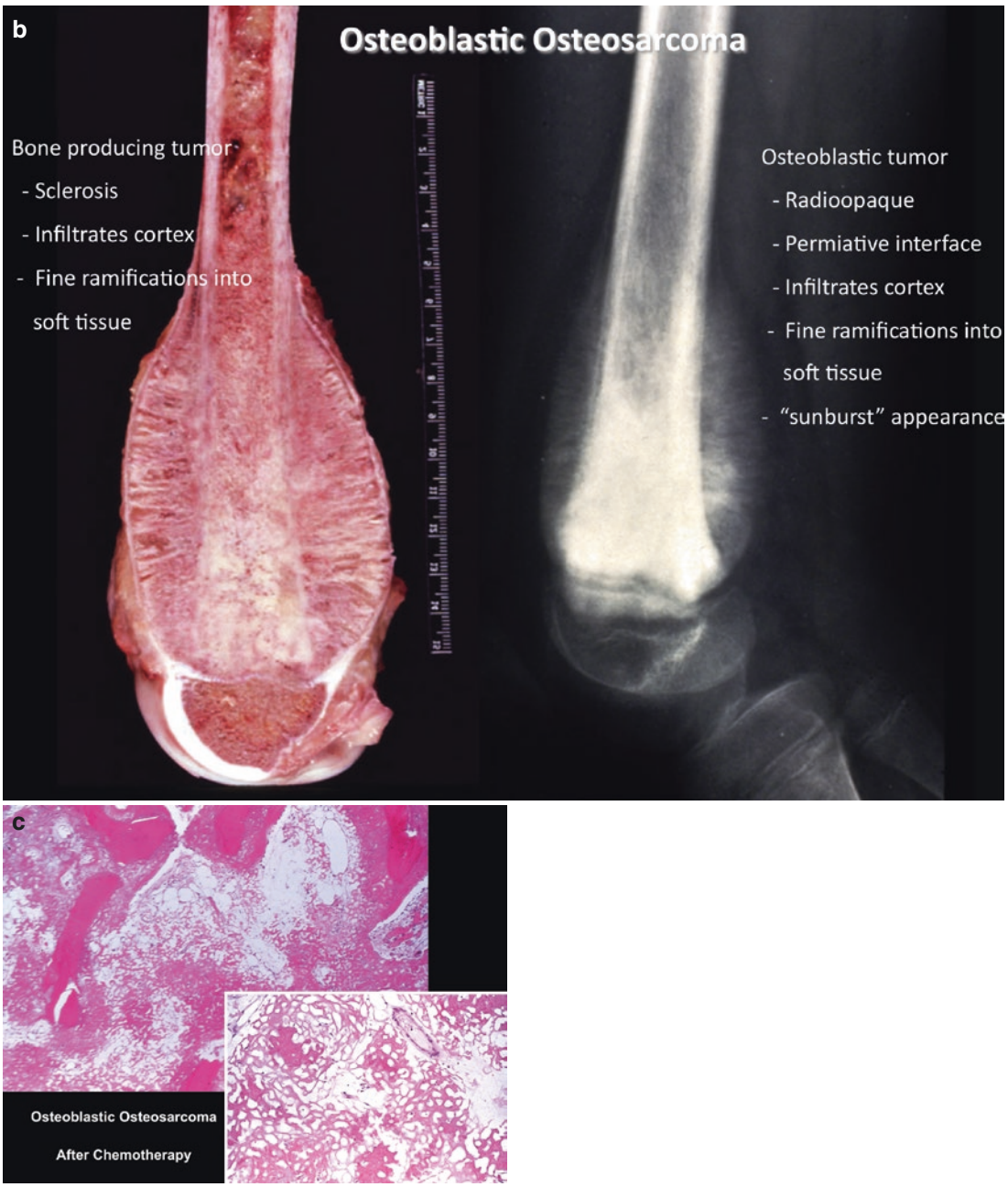

Fig. 3.80 (continued) (**b**) Gross and plane film. Grossly, tumor forms a solid, rock-hard, sclerotic white to tan mass replacing the distal femoral metaphysis invading cortex and radiating into overlying connective tissues. The plane film shows a radiopaque mass corresponding to the gross specimen forming a "sunburst" pattern. (**c**) Post-chemotherapy: complete response to preoperative chemotherapy—no tumor cells are present. Only residual osseous matrix remains. (Courtesy of A. Kevin Raymond, M.D.)

suggests that survival in p-XRT-sarc in patients with resectable "peripheral" tumors is not significantly worse than c-OS and is at least partially a function of the potential for complete surgical tumor extirpation with negative margins [161, 162]. In addition, a recent study suggests that the relationship between response to preoperative chemotherapy, as measured in terms of tumor necrosis, and survival described in c-OS does not apply to postradiation sarcomas [162].

Histopathology

p-XRT-sarc exhibits a spectrum of histological forms including osteosarcoma, fibrosarcoma, malignant fibrous histiocytoma (MFH), chondrosarcoma, angiosarcoma, and Ewing sarcoma and lymphoma [20]. However, the vast majority is either high-grade osteosarcoma or fibrosarcoma; in one series 60% were OS, and 95% of cases fell within the triad of OS, fibrosarcoma, and

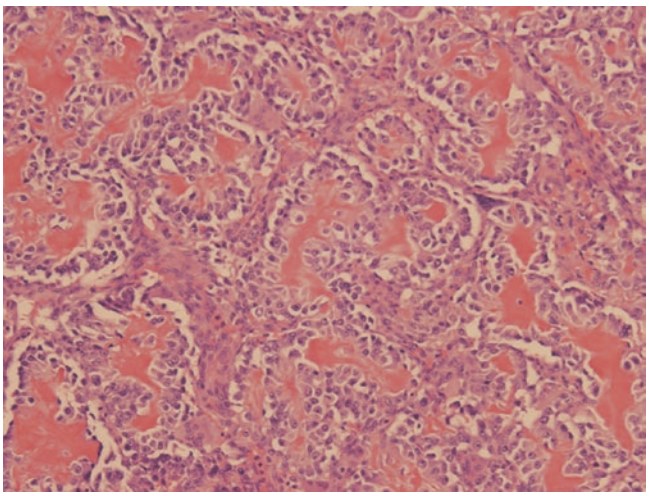

Fig. 3.81 Osteoblastic osteosarcoma with rosetoid osteoid. Osteosarcoma producing osteoid in a pattern mimicking the rosettes associated with neuroblastoma. (Courtesy of A. Kevin Raymond, M.D.)

MFH. Although the full histological spectrum of OS subtypes may be seen in p-XRT-sarc, most are morphologically similar to high-grade c-OS, in particular OOS and FOS. Underlying changes reflective of prior radiation therapy (e.g., osteonecrosis, fibrosis) may be present or overrun by the p-XRT-sarc. Secondary degenerative changes may be superimposed.

Gross Pathology

The gross appearance will reflect the histopathology of the p-XRT-sarc and should be similar to their spontaneous counterparts, sarcoma with varying amounts and forms of matrix production, with varying mineralization, and with superimposed degenerative changes. Depending on the extent of the superimposed sarcoma, there may be residual changes secondary to direct radiation damage together with fibrosis and pathological fracture.

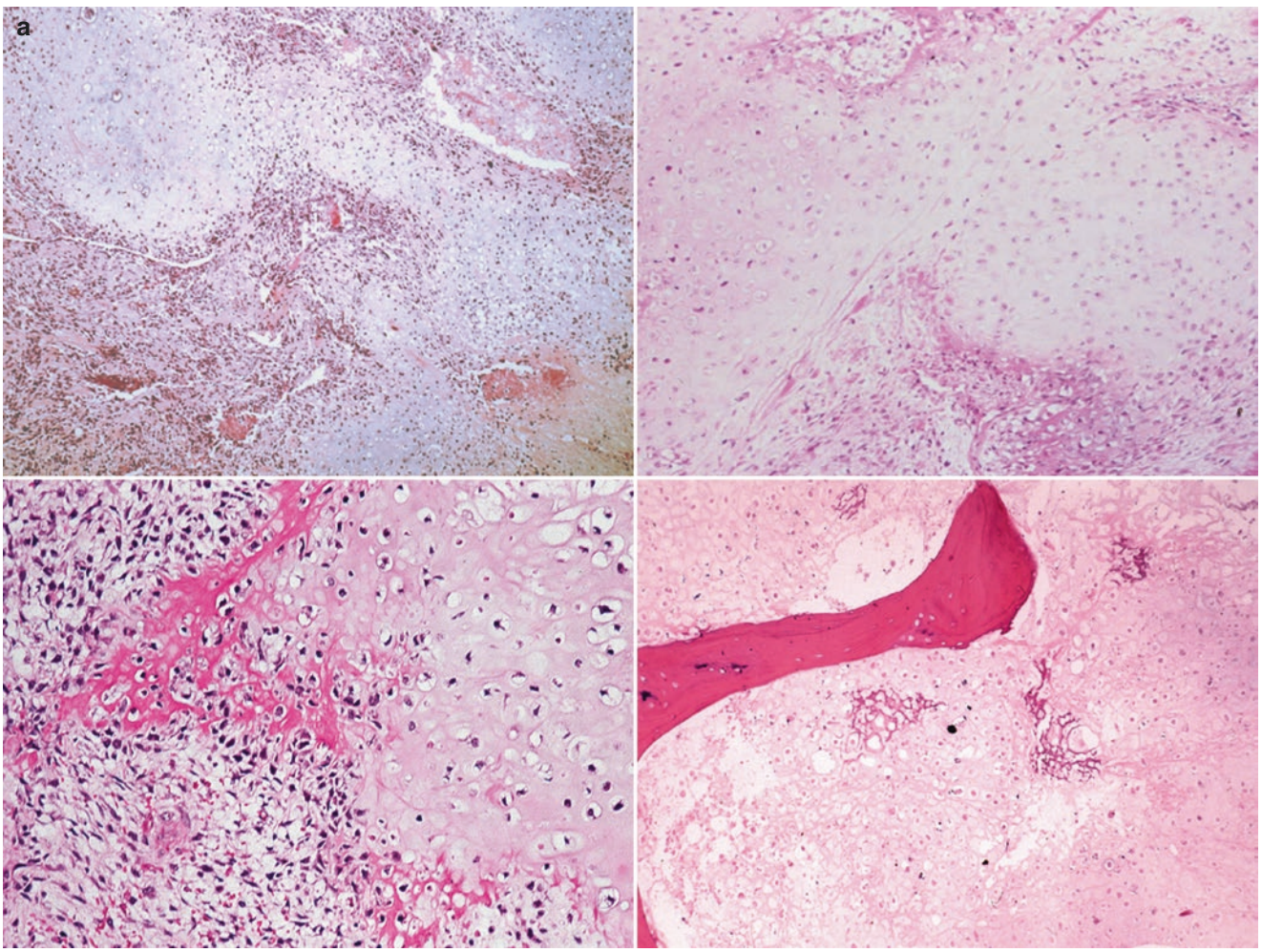

Fig. 3.82 Chondroblastic osteosarcoma. Pre-chemotherapy: viable chondroblastic osteosarcoma, variety of histological patterns.

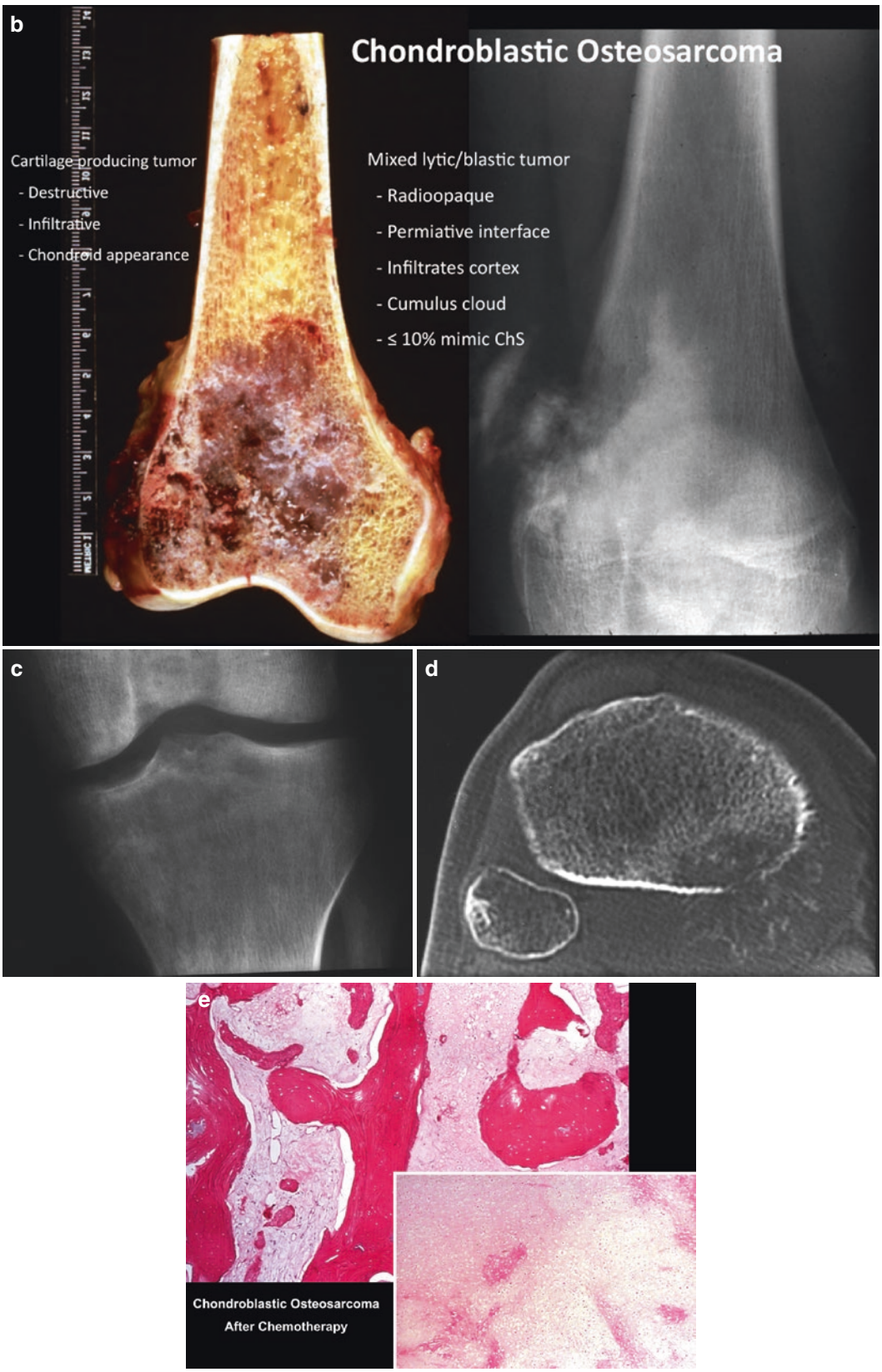

Fig. 3.82 (continued) (**b**) Gross and plane film. Grossly tumor forms a solid, gray-blue to tan mass with areas of pink-white bone production replacing the distal femoral metaphysis. Tumor invades cortex and radiation into overlying connective tissues. The plane film shows a radiopaque mass corresponding to the gross specimen infiltrating cortex. (**c**) Plane film (AP) shows a destructive largely lytic mass with focal popcorn-like calcifications involving the proximal tibia. Rare case of chondroblastic osteosarcoma with cartilage-like imaging features. (**d**) CT shows a destructive largely lytic mass with focal popcorn-like calcifications. Rare case of chondroblastic osteosarcoma with cartilage-like imaging features. (**e**) Post-chemotherapy: Complete response to preoperative chemotherapy: no tumor cells are present. Only residual cartilage matrix with small amounts of osteoid remain. (Courtesy of A. Kevin Raymond, M.D.)

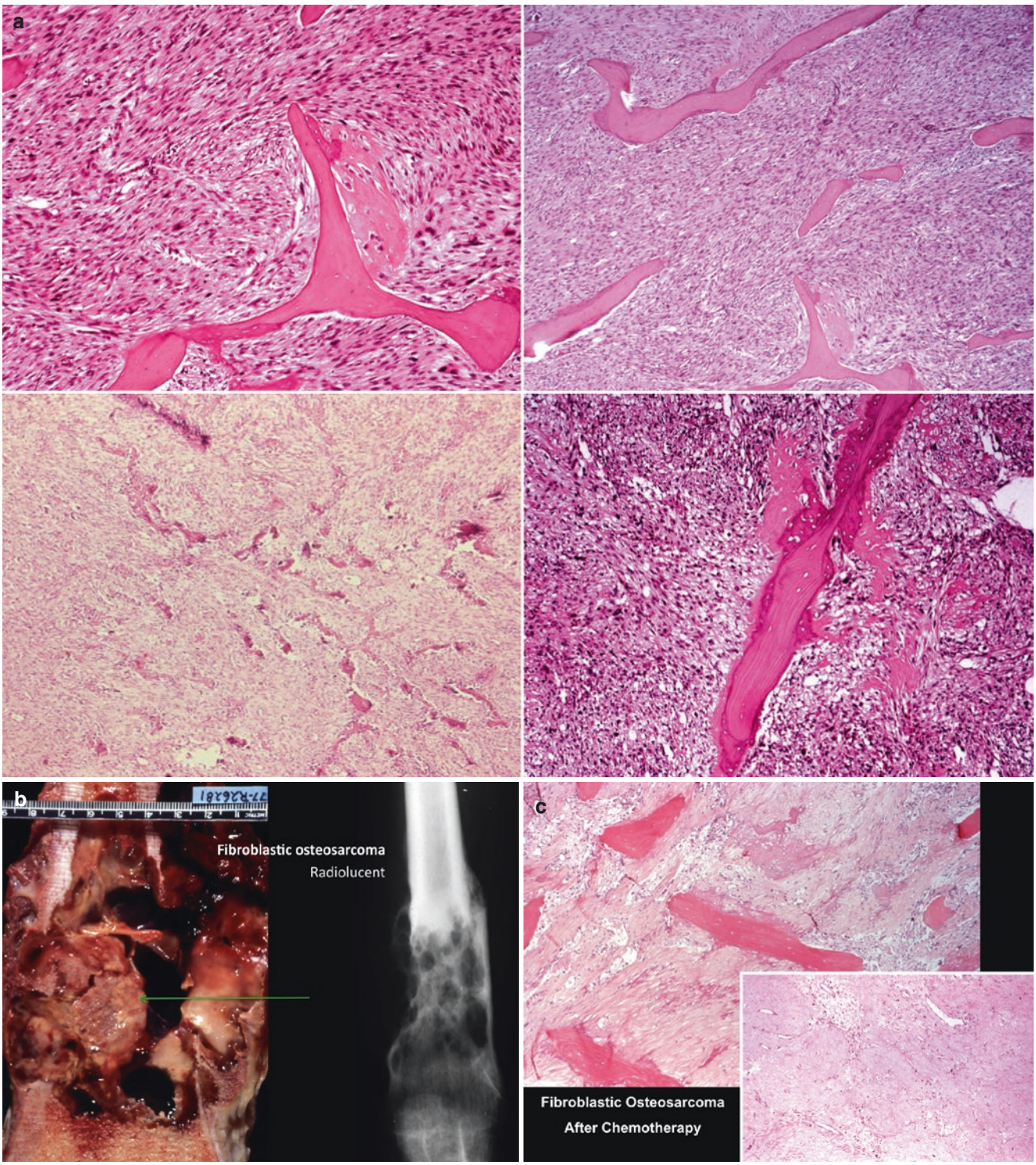

Fig. 3.83 Fibroblastic osteosarcoma. (**a**) Pre-chemotherapy: viable fibroblastic osteosarcoma, variety of histological patterns with high-grade spindle cells producing variably small amounts of osseous matrix. (**b**) Gross and plane film. Grossly, tumor forms soft, fleshy, beige mass with pathological fracture and resulting hemorrhage involving the distal femoral metaphysis. There is a small focus (green arrow) of tumor-produced osseous matrix. The plane film shows a radiolucent lesion with cortical erosion and destruction with superimposed pathological fracture. (**c**) Post-chemotherapy: complete response to preoperative chemotherapy—no tumor cells remain. Only residual edematous areolar-like tissue is present. (Courtesy of A. Kevin Raymond, M.D.)

Radiology

As with the histopathology and gross pathology, the imaging features of p-XRT-sarc are similar to c-OS; most are mixed lytic/blastic lesions and may extend from the bone into soft tissue (Fig. 3.84a, b). Again, there may be changes that suggest prior radiation damage [1, 163].

Paget's Sarcoma

Definition

Sarcoma arises in a patient with Paget's disease of bone (*osteitis deformans*).

Clinical

Secondary bone sarcomas are a long-recognized complication of Paget's disease of the bone (i.e., PDOB) [1, 165–169]. The demographics of Paget's sarcoma reflect the population at risk, an older population with a peak incidence in the seventh and eighth decades of life. Men are affected more frequently than women, with male to female ratio of 2:1. Tumors arise in bones involved by PDOB. Although there is some variation between published series, PDOB most frequently involves the axial skeleton (spine and skull), pelvis, and femur [169, 170]. The distribution of Pagetic sarcomas shows some variation between series, and although its distribution is similar to PDOB, it is not identical: pelvis, femur, humerus, skull, and tibia.

Older literature would suggest that 10% of patients with PDOB develop sarcomas [1, 166, 171]. However, with the accrual of larger numbers of patients, it is apparent that the incidence of secondary sarcoma complicating PDOB is much lower, 0.7–0.9% of Paget's patients [165, 172]. Most series report that 50–70% of patients with Paget's sarcoma have polyostotic PDOB. Although tradition says that patients with long-standing PDOB are more likely to develop secondary sarcomas [170], this has not been borne out by recent large

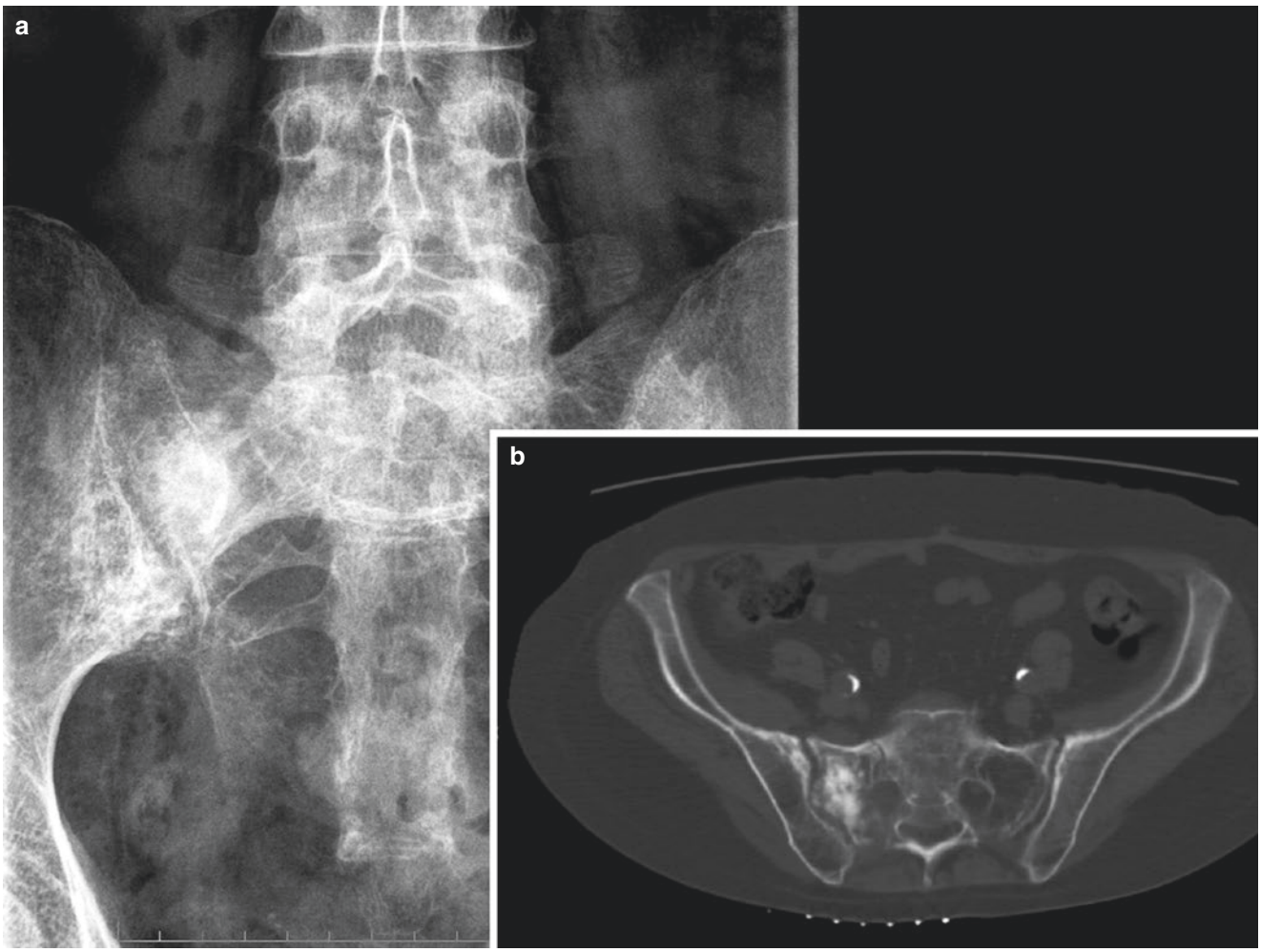

Fig. 3.84 Postradiation sarcoma. Imaging in a patient with a previously irradiated gynecological malignancy. Now complains of hip and back pain. (**a**) Plane film show and ill-defined radiopaque lesion overriding the region of the sacral ala and the adjacent sacroiliac joint. (**b**) CT shows a largely radiopaque lesion replacing much of sacral ala. Tumor appears to encroach on the sacroiliac joint

series [1]. In one series >50% of Pagetic sarcomas were diagnosed simultaneous to or within 1 year of their diagnosis of PDOB.

In of itself, PDOB is associated with bone pain. A classic symptom of secondary sarcoma is the development of new pain or changing pattern of existing symptoms. Pathological fracture is seen in 33–50% of Paget's sarcoma [173, 174].

Paget's sarcoma is extremely aggressive with the rapid development of lethal systemic metastases even in the face of immediate ablative surgery. Although the number of patients treated is small, adjuvant therapy appears to have little impact on prognosis. The expected 5-year survival is <10%. Defying expectations, patient age, as well as tumor size, location and stage do not appear to impact the prognosis of Pagetic sarcoma. Rather, it would appear that these lesions are intrinsically more aggressive than c-OS and largely nonresponsive to currently available systemic therapy [165, 172].

It is of interest that giant cell tumor of the bone arising in patients with PDOB is a much more aggressive tumor than spontaneous GCT. The estimated mortality of GCT associated with PDOB is 50%.

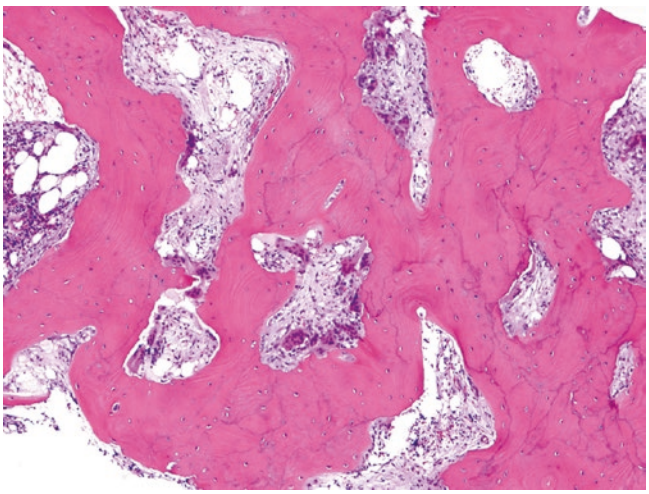

Fig. 3.85 Pagetic bone. Bone shows evidence of Paget's disease of bone: atypical osteoclasts, bone production, and bone resorption on the same surface, hypervascular bone marrow, marrow fibrosis, and pagetic mosaic pattern of lamellar bone organization. (40×). (Courtesy of A. Kevin Raymond, M.D.)

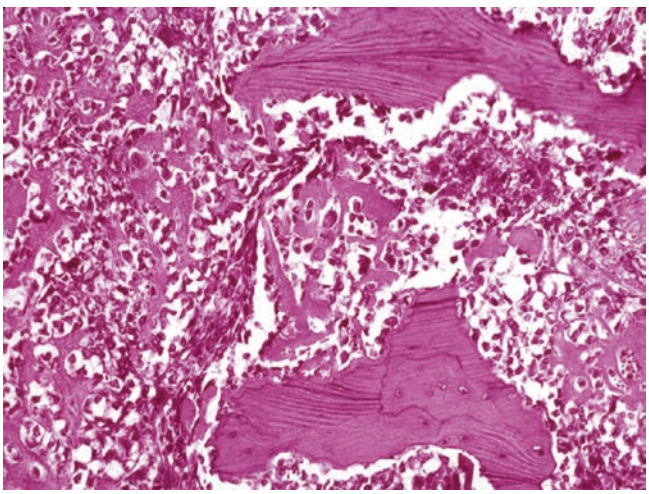

Fig. 3.86 Paget's sarcoma. High-grade osteoblastic osteosarcoma infiltrating between fragments of pagetic bone (100×). (Courtesy of A. Kevin Raymond, M.D.)

Histopathology

Virtually all Paget sarcomas are either osteosarcoma (80–90%), malignant fibrous histiocytoma, or fibrosarcoma [10, 165, 175, 176]. The histological appearance of the vast majority of the osteosarcomas falls within the histological spectrum of c-OS (Fig. 3.85). In one series, the histological subtype break- down of OS was OOS (61%), FOS (31%), and COS (5%). Tumor is composed of anaplastic, matrix-producing spindle cells forming a mass lesion infiltrating normal and Pagetic bone. The hallmark of PDOB is thickening of cortical and cancellous with the so-called mosaic pattern of lamellar bone reflecting the altered metabolic activity and rapid turnover of Pagetic bone. However, there are other histological changes associated with PDOB: atypical osteoclasts with randomly oriented nuclei, bone deposition and resorption on the same surface, marrow fibrous, and marrow hypervascularity (Fig. 3.86).

Gross Pathology

Tumor forms a relatively well-defined infiltrative mass within the surrounding thickened Pagetic bone [10, 177]. The gross parameters reflect the underlying histological sarcoma type and subtype as well as superimposed reactive and degenerative changes together with underlying Pagetic bone (Fig. 3.87a).

Radiology

The plane film hallmark of PDOB is thickening of cortical and trabecular bone that results in blurring of cortical/cancellous interface [171]. This results in increased bone density and enlargement of the affected bone. There may be bowing of involved bones, probably reflecting inappropriate weight-bearing properties (Fig. 3.87b).

In essence, the radiological hallmark of Paget's sarcoma is a *change in the appearance* of the Pagetic bone. More specifically, it is the appearance of a defined mass lesion within the Paget-altered bone. These lesions may be radiopaque, radiolucent, or combinations of radiolucency and opacity.

Because of the extreme density of Pagetic bone, localized tumor frequently appears as an area of *relative* radiolucency.

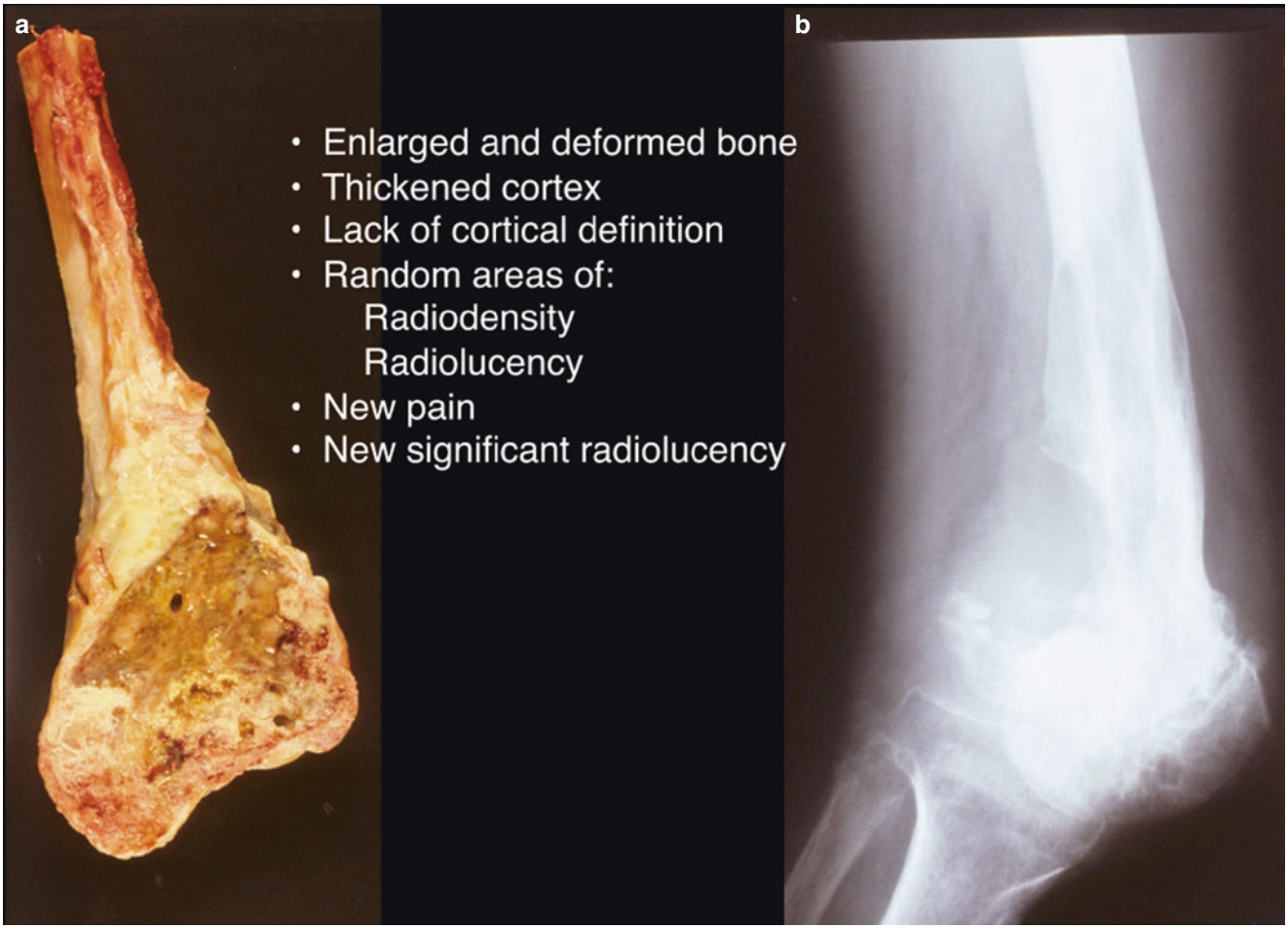

Fig. 3.87 Paget's sarcoma gross and imaging. (**a**) Gross specimen shows replacement of the medullary cavity by a tan to brown fleshy tumor. The specimen has been cut to a fashion that the presence of Paget's cannot be assessed. (**b**) Plane film shows a diffuse increased thickness of cortical bone with loss of definition of between the cortex and medullary cavity. In addition, there is a large radiolucent mass replacing the metadiaphyseal medullary cavity and destroying overlying cortex

Molecular

There is some indication that Paget's sarcoma is associated with in loss of constitutional heterozygosity (LOH) of a putative tumor-suppressor gene that maps to chromosome 18q [170, 177].

Jaw Osteosarcoma

Definition

Osteosarcoma of jaw (OSj) is defined as OS involving the mandible or maxilla.

Clinical

OS involving the gnathic bones, i.e., the mandible and maxilla, comprises some 6–8% of OS [178, 179]. Although affecting patients over a wide range of ages, OSj appears to have something of a peak in the second to fourth decades of life. Although varying from series to series, the male to female ratio is near equal, as is the relative distribution between mandible and maxilla [179–183].

Mass and pain tend to be the most frequent presentation and may be accompanied by a variety of coexisting symptoms: paresthesias, infection, bleeding, and dental problems, e.g., alveolar widening and lose teeth.

Radical surgery is the treatment of choice with an expected 5-year survival of 50–60%. However, inasmuch as metastases are only encountered in 10–20% of patients [183], it is apparent that local disease/relapse comprises the greatest threat to life. Therefore, the need for pathology-confirmed negative margins is critical. Because of their frequency and subclinical presentation, careful preoperative examination for skip metastases is mandatory in OSj to ensure appropriate intraoperative margin estimation followed by complete pathology evaluation. When margins are positive or questionable, one series has shown significant benefit of postoperative radiation therapy [184]. The role of chemotherapy has not been established in the treatment of OSj.

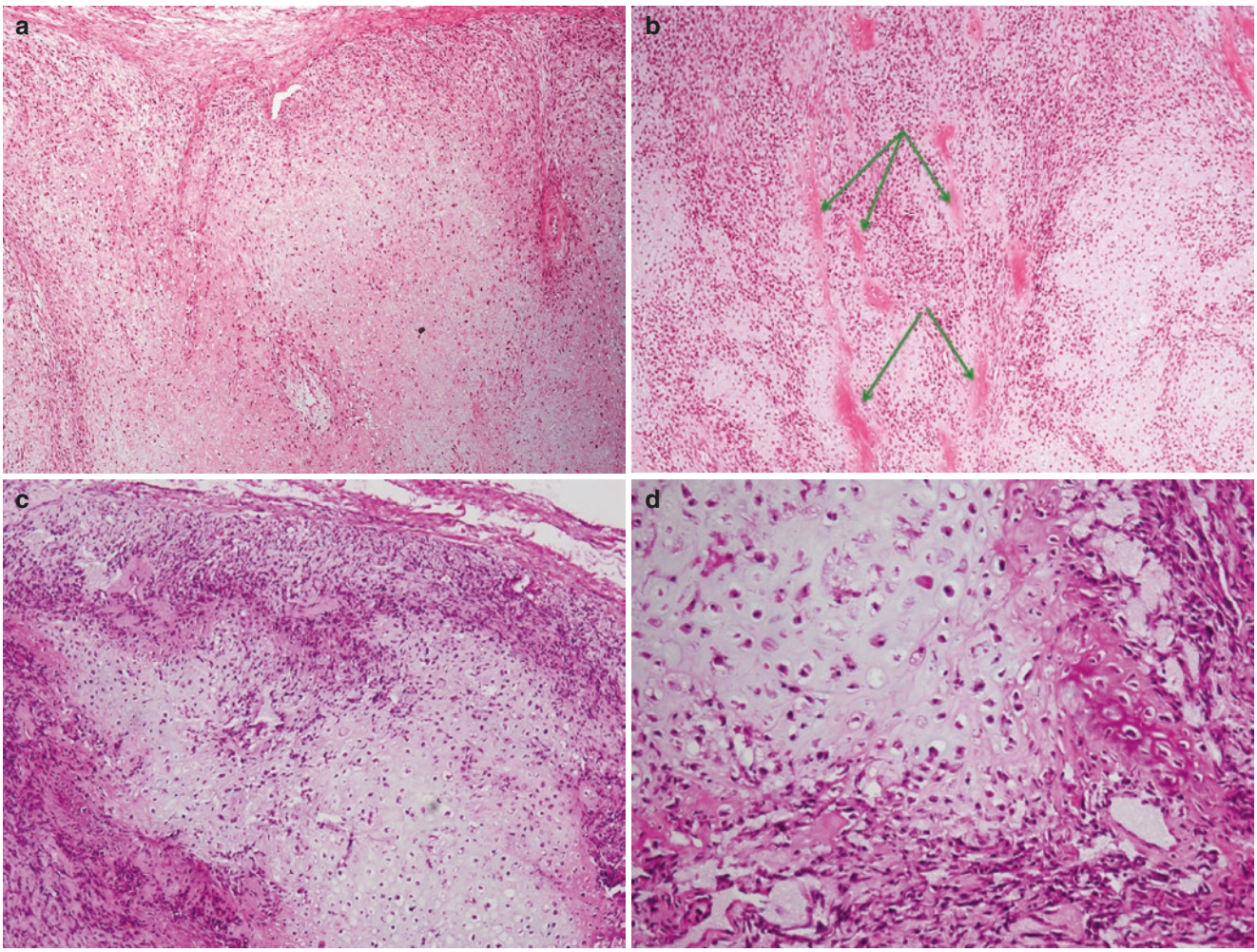

Fig. 3.88 Jaw osteosarcoma: periosteal osteosarcoma-like chondroblastic osteosarcoma. (**a**–**d**) Zonated lobules of chondroblastic osteosarcoma. The lobule centers are hypocellular, while the lobule peripheries are hypercellular with larger, plumber cells that are closer together and produce osteoid. Note osteoid seams (arrows) in the interlobular septa (H&E. 20×, 40×, 100×, 200×). (Courtesy of A. Kevin Raymond, M.D.)

Histology

OSj has the same histological findings and spectrum as non-gnathic OS. However, there are significant differences in the frequency of the various histological subtypes. In many OSj series, chondroblastic OS (COS) is the most frequent histological form. COS has four seldom-discussed histological patterns (i.e., subtypes): hyaline-COS, myxoid-COS, a pattern mimicking periosteal OS or chondromyxoid fibroma (PERI-like), and clear-cell COS [183]. Hyaline cartilage COS is the dominant form seen in appendicular OS, the other COS subtypes being extremely rare in the extra-gnathic skeleton. In contrast, PERI-like and myxoid-COS are the most frequent forms in jaw-COS followed by occasional clear cell and less frequent hyaline cartilage COS. In addition, well-differentiated intraosseous OS (i.e., low-grade central OS) is somewhat more frequent in the jaw than their appendicular counterparts [185]. In all cases, the neoplastic cells form diffuse, infiltrating sheets accompanied by their respective matrices. Tumor infiltrates cancellous and cortical bone. Extension into overlying soft tissue is virtually always present. OSj is notorious for intramedullary skip metastases.

The cytological features of the neoplastic cells are typical of OS in general, pleomorphic and anaplastic. Although difficult to quantify, there is frequently a suspicion that the cells of OSj appear somewhat better differentiated than expected in c-OS. The combination of diminished anaplasia and unusual chondroid matrix forms appears to contribute to misinterpretation. The differential diagnosis is broad and includes benign tumors and reactive processes.

The PERI-like variant of COS has a distinctive zonated-lobular architecture that mimics that pattern seen in periosteal osteosarcoma, but on the inside of the bone (Fig. 3.88a–d). The mimicry is analogous to the similarities between parosteal OS and well-differentiated intraosseous OS. The periphery of the lobules is distinctly more cellular, and the cells are larger,

plumper, closer together, and more anaplastic, while the cells of the lobule centers tend to be smaller, thinner, and further apart. Osseous matrix in the form of comparatively thin trabecula of osteoid and/or bone accompanies viable cells toward the lobule peripheries. Osteoid is frequently most easily identified as slender *streamers* in an arcade-like pattern at the extremes of lobule peripheries. Some lobule centers may be frankly necrotic and have acellular areas that may contain dense bone dissecting the otherwise chondroid matrix.

The myxoid-COS is as the name implies dominated by myxoid cartilage with randomly scattered islands of anaplastic cells accompanied by variably fine streams of osseous matrix (Fig. 3.89a–c). There may be mixtures of the PERI-like and myxoid-COS patterns.

Gross

The gross appearance reflects the histological components. However, the unusual patterns of COS may have an unexpected appearance. Rather than the blue-gray of hyaline cartilage, the lesions are off-white to cream-colored. Depending on the degree of mineralization, lesions tend to be rubbery and have an overall lobulated, feather-like appearance (Fig. 3.90). Tumors infiltrate the medullary cavity and extend through cortex into overlying subperiosteal and true soft tissues. Soft tissue margins are generally easily assessed, while bone margins tend to be "close" secondary to anatomical/functional considerations imposed on surgery. At the same time, bone margins can be difficult to evaluate intraoperatively. We suggest that jaw specimens be cut in a coronal plane (i.e., superior/inferior plane) with the parts including resection margins then cut perpendicular to the true margin (i.e., transverse plane). OSj can have insidious extension or skip metastases that might be otherwise missed without such attention to detail at the time of surgery (Fig. 3.91).

Radiology

The plane film appearance of OSj tends to be that of a destructive lesion that is either mixed lytic/blastic or purely osteolytic

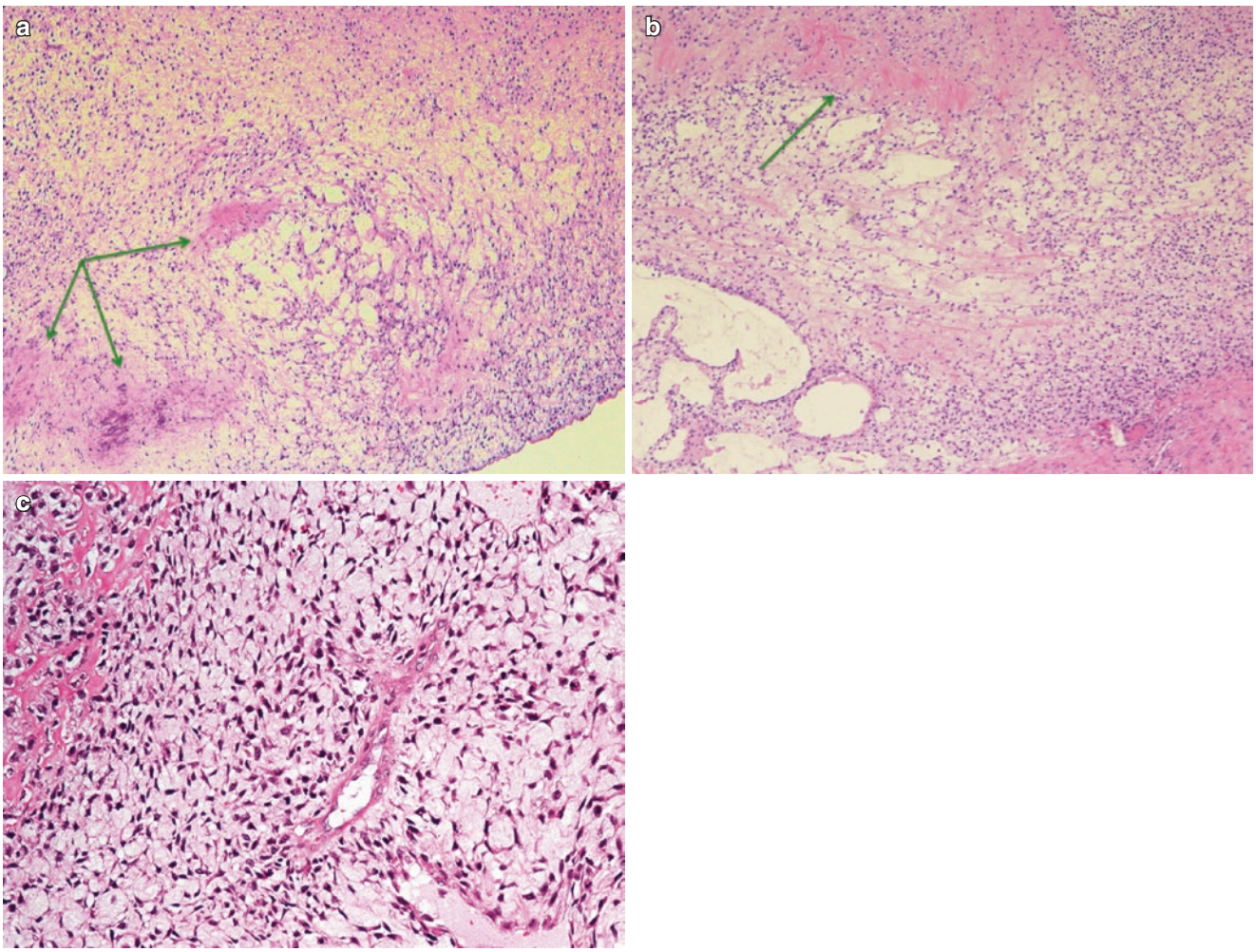

Fig. 3.89 Jaw osteosarcoma: myxoid chondroblastic osteosarcoma. (**a**–**c**). Lobules and sheets of chondroblastic osteosarcoma in which the matrix is composed of myxoid cartilage. The neoplastic cells are randomly dispersed and have nuclei that vary from round- to cigar-shaped which are surrounded by wispy, ill-defined clear to pink cytoplasm. There are randomly scattered foci of osteoid and bone production by tumor (arrows) (40×, 40×, 100×). (Courtesy of A. Kevin Raymond, M.D.)

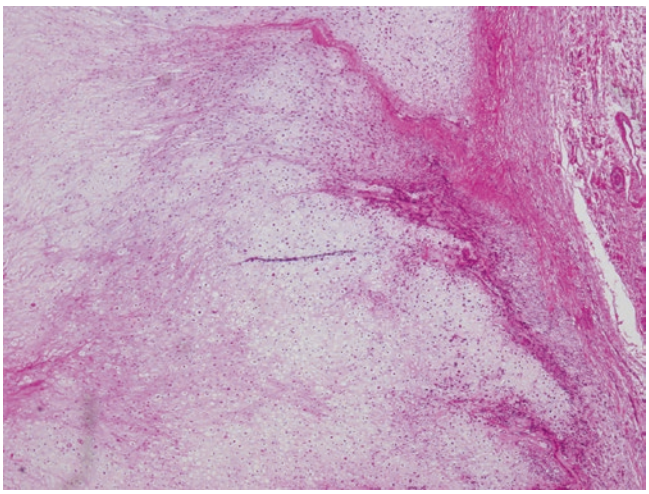

Fig. 3.90 Jaw osteosarcoma. Mixed periosteal-like osteosarcoma and myxoid chondroblastic osteosarcoma (40×). (Courtesy of A. Kevin Raymond, M.D.)

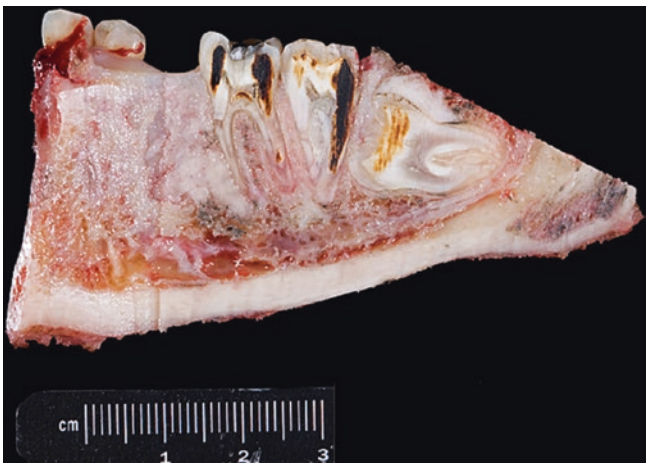

Fig. 3.91 Jaw osteosarcoma. Longitudinal section of the jaw showing intramedullary gray-white, lobulated tumor forming an anterior mass with invasion of adjacent marrow and infiltration between teeth. Given the narrow width and sharp angles of the mandible, this can be a difficult dissection. (Courtesy of A. Kevin Raymond, M.D.)

(Fig. 3.92) with minimal reactive bone. The osteoblastic "sunburst" appearance common to the appendicular skeleton is rare in OSj. CT scans are critical to the qualitative evaluation of OSj. CT and MRI provide complimentary tools for the evaluation of extent of disease and margins in OSj, as well as providing better assessment of intramedullary skip metastases.

Multicentric Osteosarcoma

Definition

Multicentric osteosarcoma (mf-OS) is a rare, particularly aggressive form of osteosarcoma in which multiple bones are involved without contemporary involvement of visceral organs.

Clinical

mf-OS was first described by Silverman in 1936 in a single-patient case report [186]. mf-OS is estimated to comprise some 1–1.5% of osteosarcoma and as such constitutes one of the rarest forms of OS. Since the first description, subsequent publications have largely consisted of case reports, a brief review [187, 188] and a recent review of 56 cases from 2 institutions with a long commitment to orthopedic oncology [189].

mf-OS can affect patients over a broad age range but most frequently affects patients under the age of 30 years. Males are affected more frequently than females, with male to female ratio of 3:2. Patients present with pain with or without swelling. Additional symptoms are a function of tumor site and size.

There appear to be two major subgroups: synchronous and metachronous mf-OS. Synchronous OS includes those cases in which patients have multiple bones involved by OS without visceral (e.g., lung) involvement on presentation. Lesions in patients with synchronous mf-OS tend to involve the long bones and the spine.

Metachronous mf-OSs are those cases in patients present with a solitary-involved bone and over time develop additional involved bones without visceral disease. The interval between initial OS and the first metachronous lesion ranged from 7 months to 14 years [189]. The lesions of metachro-

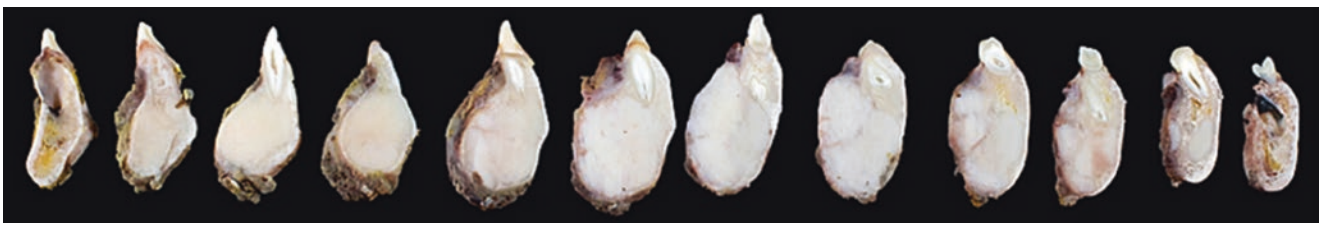

Fig. 3.92 Jaw osteosarcoma. The jaw has been serially cut in coronal sections which allows confident dissection and viewing of the vast majority of the tumor while keeping intact the surrounding tissues. The two end pieces constitute the bone resection margins, and they in turn are inked and cut perpendicular to the true margin and submitted in toto. (Courtesy of A. Kevin Raymond, M.D.)

nous mf-OS tend to show a predilection for the long bones of the appendicular skeleton. Some patients with synchronous OS develop metachronous lesions.

Clinically, mf-OS is an extremely aggressive form of OS. Survivors of synchronous mf-OS regardless of treatment form are extraordinarily rare, far less than 5%. However, with aggressive combined therapy, including multiple surgeries, long-term survivorship in metachronous mf-OS may reach 20%.

Pathology

The morphological features of the vast majority of mf-OS fall within the spectrum of high-grade conventional OS, in particular OOS (Fig. 3.93).

Fig. 3.93 Jaw osteosarcoma. Single slab section from coronal section mandible. The tumor is relatively homogeneous but has a lobulated peripheral surface. The cut surface varies from finely granular to smooth, and the tumor has an overall rubbery consistency, typical jaw chondroblastic osteosarcoma. (Courtesy of A. Kevin Raymond, M.D.)

Radiology

The imaging features of each of the lesions of metachronous mf-OS are those expected of primary osteosarcoma, large destructive lesions, with a broad transition zone and mixed osteoblastic/osteolytic features with cloud-like mineralization (Fig. 3.94).

In contrast, the lesions of synchronous mf-OS have the appearance of a dominant lesion with features consistent with primary OS. In contrast, the additional lesions are relatively small, well-defined, and sclerotic, suggestive of a metastatic process. Too few cases have undergone more sophisticated studies to develop generalizations.

Well-Differentiated Intraosseous Osteosarcoma

Definition

Well-differentiated intraosseous osteosarcoma (WDIO OS) is a form of low-grade osteosarcoma arising within the medullary cavity (aka low-grade central osteosarcoma).

Clinical

WDIO OS is a rare, indolent form of OS that was first described by Unni and Dahlin in 1977 [190] and has been the subject of limited subsequent literature [191–195]. There is a peak incidence in the third decade, less frequently affecting patients in the second and fourth decades of life. WDIO OS affects men and women equally. More than 80% of tumors involve long bones of the appendicular skeleton, in particular the distal femur, and proximal tibia. Localized pain with or without mass is the presenting symptom.

Left untreated WDIO OS is a disease of slow progression with eventual systemic dissemination. The treatment of choice is complete surgical extirpation with documented negative margins, resection when possible and amputation when necessary. When appropriately treated, the expected long-term survival exceeds 85% [20, 190, 191]. Because of its relatively indolent behavior, there may be temptation to perform surgical procedures less than resection with WDIO OS; the increased probability of local relapse, dedifferentia-

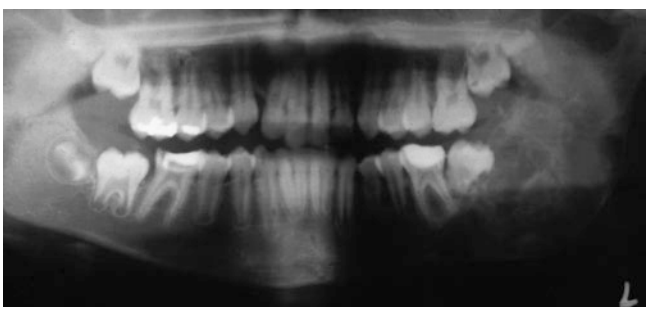

Fig. 3.94 Jaw osteosarcoma. Panorex plane film. Typically, tumor (right side) forms a destructive, radiolucent mass with little if any reactive bone formation. (Courtesy of A. Kevin Raymond, M.D.)

tion, and metastases speaks against this. Chemotherapy does not appear to have a place in the treatment of WDIO OS.

However, 15–20% of WDIO OS undergo dedifferentiated in either the primary, local relapse or metastases. In cases of dedifferentiation, the biological behavior assumes the aggressive characteristics of high-grade c-OS resulting in a poor survival [190]. In the face of dedifferentiation, multidisciplinary therapy similar to c-OS including chemotherapy is warranted.

Histopathology

WDIO OS has a small spectrum of histological diversity that is a function of the form and quantity of tumor-produced matrix and the appearance of the neoplastic cells [20, 191, 194]. The neoplastic cells are minimally atypical, minimally pleomorphic spindle cells. The cells have fairly well-defined cytoplasm and spindle- to cigar-shaped nuclei with chromatin varying from finely dispersed to clumped. Neoplastic cells tend to be infiltrative of adjacent normal structures, marrow or cortex. Where matrix is minimal, the neoplastic cells tend to form interlacing bundles. Matrix varies from quantitatively minimal in a bland spindle-cell lesion to randomly disposed fascicles of woven bone without osteoblastic rimming to long trabecula of well-formed lamellar bone, thus mimicking desmoid, fibrous dysplasia or parosteal osteosarcoma, respectively [190]. The presence of a degree of atypia, mitotic activity, and infiltrative growth pattern supports a diagnosis of malignancy and WDIO OS. Other than location, the morphological features of WDIO OS are virtually identical to parosteal osteosarcoma (Fig. 3.95).

Gross

WDIO OS tends to form large tumors that are relatively well-defined, infiltrative, and destructive which in the absence of degenerative change have a pale yellow to yellow-white cut surface (Fig. 3.96). The overall appearance generally mimics parosteal osteosarcoma, only on the inside of the bone. The density and consistency are a function of the amount and form of osseous matrix, together with its mineral content. Many tumors have cut surfaces that are rock-hard, sclerotic, well-defined masses with either a relatively homogeneous marble-like or granular cut surfaces. With less bone formation, the cut surface takes on a feathery or rope-like or swirled configuration. With lesser amounts of matrix, secondary changes (e.g., hemorrhage, cystification) may be present.

Radiology

WDIO OS tends to form fairly large lesions within the metadiaphysis of long bones. They tend to be a destructive and

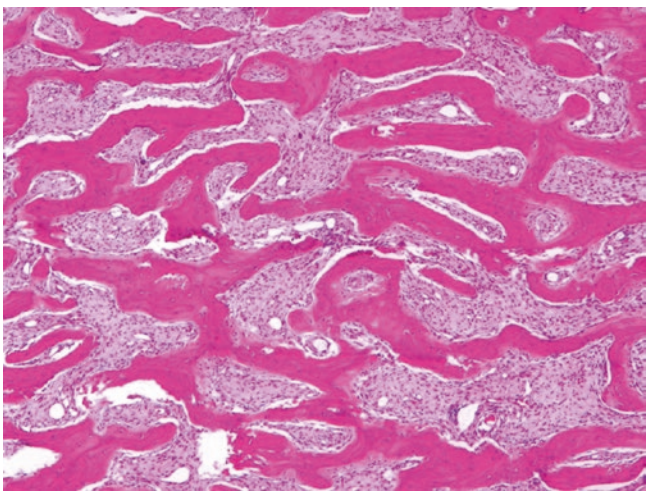

Fig. 3.95 Well-differentiated intraosseous osteosarcoma. Tumor is composed of sheets of uniform, minimally anaplastic spindle-cells accompanying well-formed lamellar bone. Osseous matrix tends to form long continuous trabecula-like structures (H&E. 20×)

Fig. 3.96 Well-differentiated intraosseous osteosarcoma. Tumor forms a relatively homogeneous, rock-hard ivory white mass. While the intramedullary component is large, there is a disproportionally small extraosseous component. (Courtesy of K.K. Unni M.D.)

infiltrative, but relatively well-defined but poorly marginated. Frequently, there is a large intraosseous tumor with little extension outside of cortex. The radiographic features of WDIO OS are a function of the amount and form of osseous matrix and the amount of mineralization. Extent of disease is best evaluated with CT and MRI.

Molecular

Recently cytogenetic studies have shown a supernumerary ring chromosome including amplification of 12q13-15, which includes the cyclin-dependent kinase (CDK4) and murine double-minute type 2 (MDM2) gene regions [195], which are seen in both forms of low-grade osteosarcoma, i.e., WDIO OS and parosteal osteosarcoma. At the same time, these findings are not present in the other elements of the differential diagnosis, e.g., fibrous dysplasia, desmoid, and reactive fibrous proliferation.

Telangiectatic Osteosarcoma

Definition

Telangiectatic osteosarcoma (TOS) is a form of high-grade OS heralded by a triad of findings: a radiolucent lesion, a grossly hemorrhagic mass that is formed by anaplastic cells that produce minimal osseous matrix and form the lining membranes of blood-filled cysts.

Clinical

Although it may occur at any age, TOS has a profound tendency to affect patients in the second decade of life. Males are affected more often than females, with male to female ratio of 1.5:1. The most frequently involved sites are the distal femur and proximal humerus where it tends to originate within the metaphysis but often extends into the diaphysis and/or epiphysis as well as overlying soft tissues. Patients present with severe pain and enlarging mass of short duration. This is a form of OS in which rapid increase in tumor size may be secondary to degenerative changes or tumor growth.

The original discussions pertaining to the current concepts of TOS can be found in sequential publications by Huvos et al. [196] and Dahlin et com [197]. The authors reached very different conclusions, but their study designs and intentions were also very different. One group sought to review all cases previously diagnosed as *telangiectatic sarcoma* in their institution. The other group sought to develop criteria that would reproducibly define a subset of OS with a predictably poor prognosis that could be excluded from survival data analysis of c-OS.

One school [197] held that when treated with surgery alone, TOS was a particularly aggressive form of OS that quickly resulted in near-uncontrollable local growth, rapid systemic dissemination, and death due to disease. Pathological fracture was a frequent (>25% of cases) complication. In this series all but one patient were dead of disease at the time of manuscript submission, and the final patient was dead of disease shortly after publication. The major objection to this study was the long period of time from which the cases were drawn and the resulting therapeutic inconsistencies.

The second school [196] found that per their criteria, TOS did not impart survival advantage/disadvantage when treated on a surgery-alone protocol. However, they found that TOS appeared to be more responsive to available chemotherapy than c-OS and that response translated into better survival.

Subsequent studies have supported these findings. Although information regarding surgery-alone treatment is limited, another group reports near-uniform lethal outcome when TOS is treated with surgery alone [145]. At the same time, there is virtual universal agreement that TOS is more sensitive to contemporary chemotherapy than c-OS and that the ultimate survival in these patients is better than c-OS [1, 10, 145, 196, 198–203].

In light of these observations, the current therapy of choice in TOS is preoperative chemotherapy followed by surgery. The results of tumor necrosis evaluation determine the form of subsequent postoperative therapy. Excellent response to preoperative therapy is so routine that poor response to preoperative therapy immediately triggers a call for diagnosis review.

A few cases of TOS have been subject to cytogenetic and/or molecular analysis to reach sweeping conclusions. However, the limited data has so far failed to identify recurrent chromosomal rearrangements and suggests the absence of any currently recognized sarcoma-related translocations [10].

Histopathology

Histologically, TOS is composed of interlacing and superimposed membrane-bound blood-filled cysts (Fig. 3.97). The membranes are composed of neoplastic cells that produce minimal amounts of osteoid (Fig. 3.97). In and of themselves, the neoplastic cells of TOS are among the most anaplastic and pleomorphic seen in any form of OS (Fig. 3.97). The neoplastic cells run the spectrum from small to large to giant and exhibit a wide array of configurations: round, oval, epithelioid, irregular, grooved, twisted, spindle cells as well as anaplastic giant forms. Tumor cells may be mononuclear or multinuclear. Nuclear membranes may have irregular contours. The chromatin is highly variable: finely distributed, clumped, condensed, fragmented, and/or smudged. Nucleoli may be present, small or large, and prominent. Mitotic activity may be brisk, and abnormal mitoses are generally present. The cytoplasm may vary from barely discernible to abundant and range from amphophilic to deeply eosinophilic.

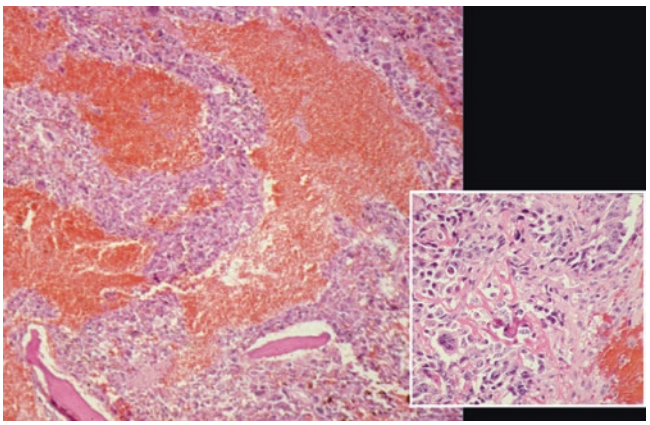

Fig. 3.97 Telangiectatic osteosarcoma histopathology without chemotherapy. Blood-filled membrane-bound cysts composed of malignant cells. Inset: malignant cells producing filigree pattern osteoid. (Courtesy of A. Kevin Raymond, M.D.)

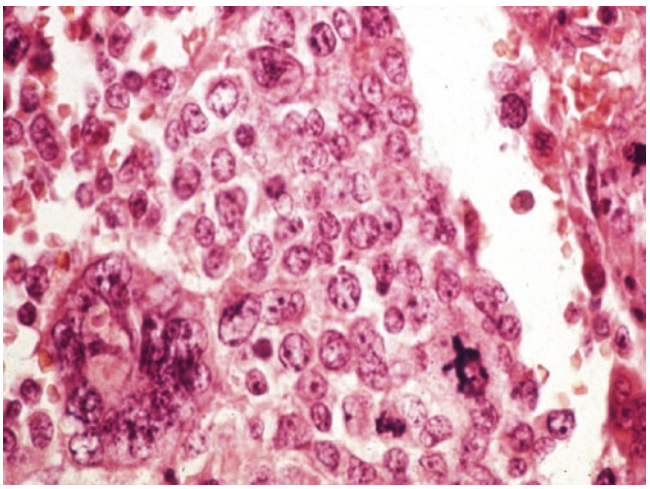

Fig. 3.98 Telangiectatic osteosarcoma histopathology without chemotherapy. High-power of highly anaplastic cells. (Courtesy of A. Kevin Raymond, M.D.)

Post-chemotherapy, the histological appearance of TOS retains the architectural properties of interconnecting, membrane-bound, blood-filled cysts. However, successful therapy is manifest by a virtual, complete absence of neoplastic cells (Fig. 3.97). The membranes are composed of collagen and minimal numbers of nonneoplastic stromal cells accompanied by low-level non-specific chronic inflammation.

The histological features may be complicated by the presence of superimposed reactive or degenerative processes. Osteoclast-like giant cells may be present and frequently abundant, particularly near areas of hemorrhage. Blood breakdown products may result in a wide variety of reactive processes. Pathological fracture may superimpose normal healing processes upon pre-existing tumor.

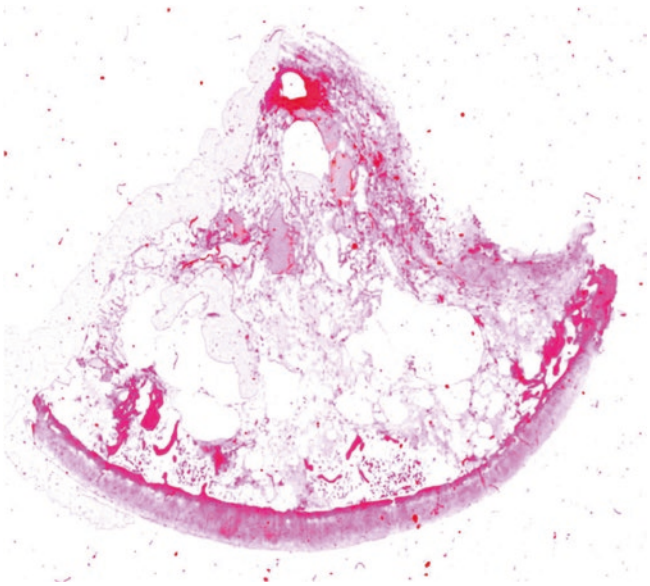

Fig. 3.99 Telangiectatic osteosarcoma post-chemotherapy. Blood-filled membrane-bound cysts with an absence of neoplastic cells. (Courtesy of A. Kevin Raymond, M.D.)

Gross

Grossly, TOS forms a destructive, hemorrhage mass, so-called *bag of blood*. The tumor itself is composed of multiple, membrane-bound, blood-filled cysts (Fig. 3.98). Cancellous bone is destroyed, and the interface with normal bone is infiltrative and ill-defined. Tumor may erode cortical bone and extend into overlying subperiosteal tissue and ultimately into true soft tissues.

Radiology

On plane films, TOS forms a highly destructive, lytic, or almost purely lytic tumor (Figs. 3.98, 3.99, and 3.100) with a permeative interface. Pathological fracture may be present. Fluid levels may be identified on CT and MRI. TOS is hyperintense on T2-weighted images, which provide accurate estimation of extent of disease [204, 205].

Small Cell Osteosarcoma

Definition

Small cell osteosarcoma (SC OS) is a form of high-grade OS in which the histological hallmark is the presence of a relatively homogeneous population of osteoid producing small "round" cells.

Clinical

Described by Sim et al. in 1979 [206], SC OS is a rare form of OS and the subject of a limited number of subsequent publications [207]. Nearly half of cases are patients in the second decade of life with the majority of the remaining cases in the third, fourth, and first decades

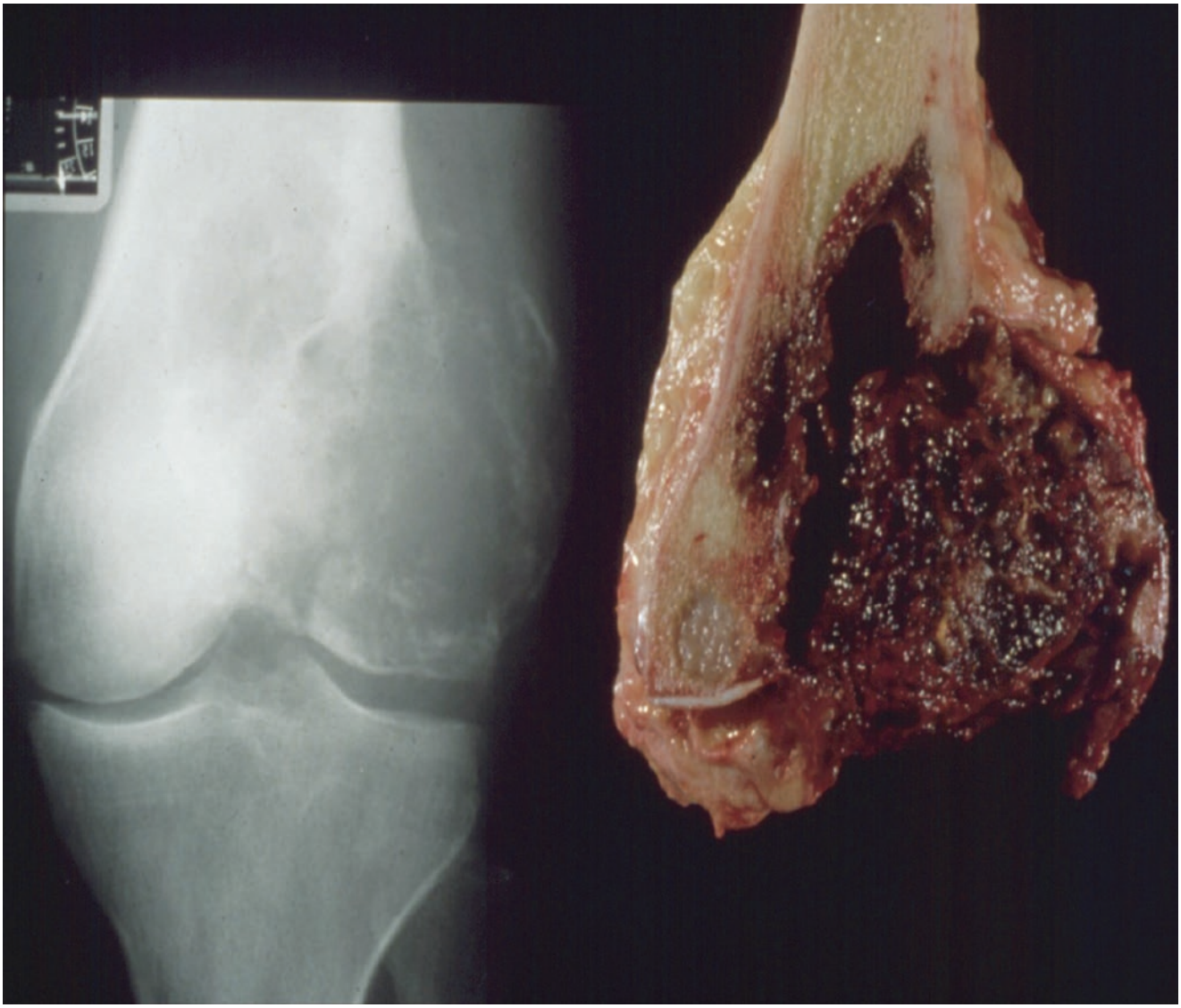

Fig. 3.100 Telangiectatic osteosarcoma plane film and gross specimen. Plane film: the distal femur is replaced by a destructive purely radiolucent lesion. The corresponding gross specimen: distal femur replaced by a hemorrhagic mass composed of blood-filled membrane-bound cysts. (Courtesy of A. Kevin Raymond, M.D.)

[206]. Men and women are affected equally. The bones most frequently involved are the femur, proximal humerus, and proximal tibia. Pain with or without mass is the cardinal presentation.

SC OS is a particularly aggressive form of OS with rapid progression to systemic involvement and few survivors when treated with surgery alone. Standard OS chemotherapy protocols have not achieved the same level of success seen in c-OS. Therefore, treatment protocols frequently utilize a hybrid of OS and Ewing's sarcoma multidisciplinary protocols with some improved survival [208]. Despite aggressive multimodality therapy, survival rarely exceeds 20%, and the histological response to preoperative therapy does necessarily correlate with prognosis.

Histopathology

Histologically, SC OS is composed of sheets of diffusely infiltrating malignant small cells. The cells are usually 3–5 times the size of red blood cell with well-defined nuclei and minimal cytoplasm (Fig. 3.101). Although there is some heterogeneity of cell type between cases, tumor cells tend to be relatively uniform within a given lesion. The neoplastic cells frequently have minimal cytoplasm surrounding round to oval nuclei with well-defined nuclear membranes encompassing finely distributed chromatin thus mimicking Ewing sarcoma. Less frequently they may mimic large cell lymphoma. Occasionally the neoplastic cells are relatively nondescript, small, oval spindle cells. Osseous matrix formation can be extremely variable but tends to be abundant. In some cases there is distinct zona-

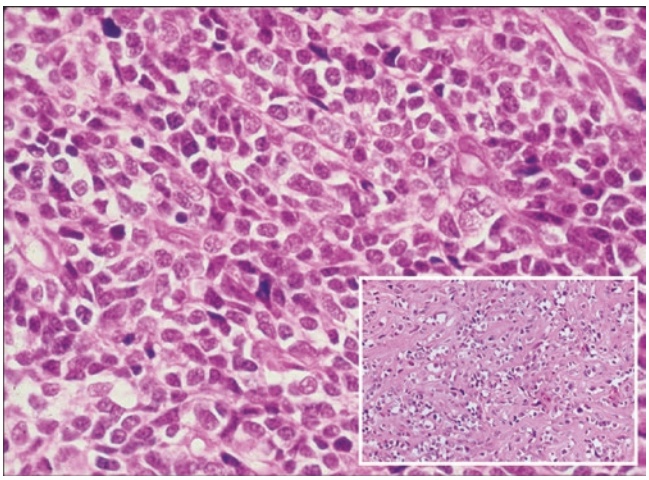

Fig. 3.101 Small cell osteosarcoma: at intermediate power, tumor is composed of sheets of uniform small cells mimicking Ewing's sarcoma. Inset: osteoid production by neoplastic cells of small cell osteosarcoma. (Courtesy of A. Kevin Raymond, M.D.)

tion with areas of minimal matrix-producing tumor sharply set off from tumor with abundant osteoid.

Special studies are variable. There may be diastase sensitive positive staining for glycogen with PAS stain. There tends to be immunostaining for CD-99. Tumor cells may show staining for osteocalcin, SMA, and CD-34. Negative staining for Fly1 may be useful in discriminating SC OS from Ewing's sarcoma in cases with minimal or questionable matrix production [10]. At least one case has been shown to have a t(11;22) translocation [207, 209].

Gross

The gross features reflect the histological composition. If the lesion is a relatively consistent mixture of neoplastic cells with evenly distributed matrix, the lesions tend to mimic OOS. However, several of our cases [208, 210] had regional variation within the tumor. The intraosseous tumor may have an inconsistent infiltrative pattern with unmineralized fleshy tumor alternating with a mixture of reactive and tumor-produced bone. Juxtaposed with latter were areas lacking significant matrix production, appearing as an off-white to tan fleshy mass (Fig. 3.102). Tumor may form a large subperiosteal extramedullary soft tissue mass.

Radiology

Radiographically, the tumors are generally mixed lytic/blastic lesions similar to c-OS. In other cases they may have a bimorphic appearance with an intramedullary moth-eaten permeative component and an unmineralized extraosseous mass (Fig. 3.102). CT confirms the plane film findings while giving more detail as to the tumor/normal interface. Tumors tended to be hyperintense on T2-weighted MRI [211–213].

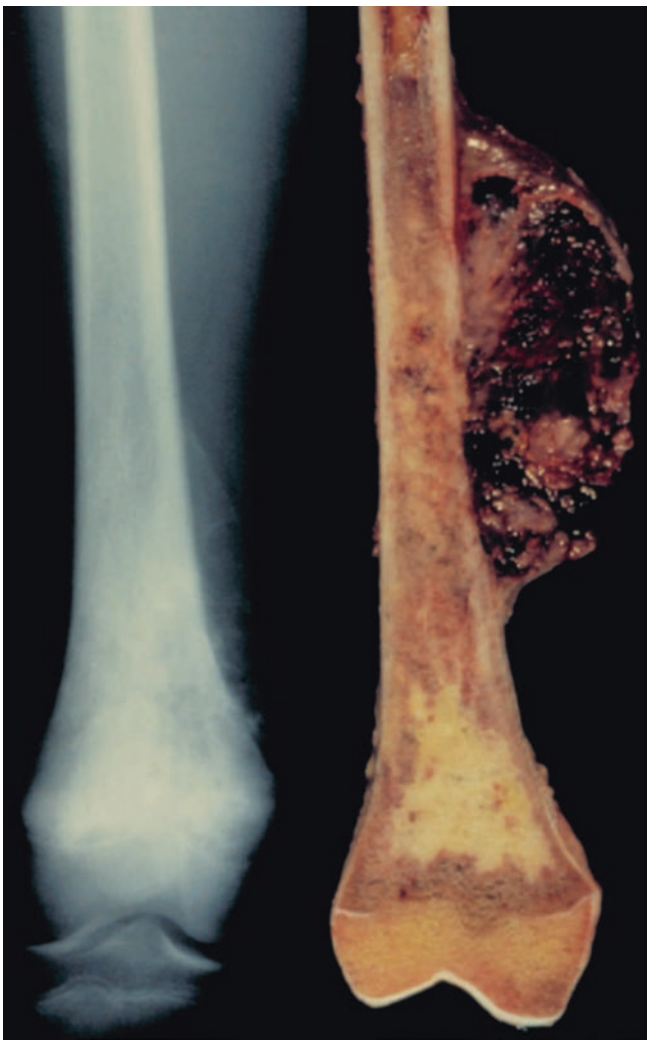

Fig. 3.102 Small cell osteosarcoma. Plane film and gross specimen. The plane film shows a largely bimorphic tumor. The distal portion of the intramedullary component is largely radiopaque, suggestive of osteosarcoma. The diaphyseal component has a moth-eaten permeative pattern suggestive of a small cell process. The extraosseous component is radiolucent. The gross specimen confirms a largely matrix-producing intraosseous component, while the extraosseous portion is a fleshy tan tumor with extensive hemorrhage. (Courtesy of A. Kevin Raymond, M.D.)

Conventional Parosteal Osteosarcoma

Definition

Conventional parosteal osteosarcoma (c-POS) is a form of low-grade osteosarcoma arising on the cortical surface consisting of relatively innocuous spindle cells producing well-formed lamellar bone.

Clinical

c-POS is the form of surface OS originally described by Geschickter and Copeland in 1948 [214]. Not fully convinced of its malignancy, the authors' initially referred to it as "parosteal osteoma." With accrual of additional cases and experience

[13, 215, 216], it was apparent that POS is a fully malignant tumor. The modifier "conventional" is appended to the name to distinguish this group of low-grade tumors from a high-grade subset: "dedifferentiated parosteal osteosarcoma" [156].

c-POS most frequently affects patients in the third and fourth decades of life and occurs more frequently in women (male to female ratio, 1:2). Tumors most frequently arise from long bones of the appendicular skeleton, in particular the distal femur, proximal tibia, and proximal humerus. It should be noted that while any bone may serve as the origin of c-POS, in some series as many as 75% originate from the posterior aspect of the distal femur [156, 217].

A painless, enlarging mass of long duration is typical of c-POS. It is not unusual for patients to report a known slowly growing mass of several years' duration. Patients with known lesions of 7 and 13 years have been reported [156]. With increasing size tumors may reach tremendous proportions resulting in mass effect-related symptoms, and significant decreased range of motion ensues.

Arising from the subperiosteal aspect of cortical bone, initial growth of c-POS is confined to the cortical surface; growth is both linear and circumferential. Circumferential growth may eventually become near complete, resulting in a so-called "*wraparound*" lesion. Invasion of underlying cortex with focal extension into medullary cavity eventually occurs in most patients. This raises question regarding differentiating c-POS invading bone from WDIO OS extending out from medullary cavity into soft tissue. Although there is disagreement as to the upper limit of involvement, investigators agree that no more than 10% [156, 218] or 25% [219] of a surface tumor can involve medullary cavity and the tumor still considered surface in origin.

If left untreated c-POS will continue to grow locally and eventually result in systemic metastases. Of interest, if uncomplicated by "dedifferentiation," the metastases of c-POS are also low grade and slow-growing. Death due to metastases or complications of local disease are the consequences of untreated tumor.

With metastases being a long-term event, generally expected only after known years of tumor growth, treatment is focused on complete removal of the primary tumor, resection when possible and amputation when necessary. Wide local excision of the primary tumor with a 1–2 cm margin of normal bone can be carried out in some patients but adds a significant level of difficulty to surgery. In general, en bloc resection of the involved segment of bone with a wide cuff of normal tissue is the treatment of choice when technically feasible [218, 220]. Complete local resection is mandatory since residual tumor results in a 100% local relapse and potential 25–80% dedifferentiation with its attendant precipitous decline in prognosis. However, successful treatment results in a long-term survival in access of 90–95% [156, 217, 221].

Although c-POS does not show the extensive complex changes seen in conventional osteosarcoma, molecular analysis shows a number of interesting findings [10, 222, 223]. Cytogenetically, c-POS is characterized by supernumerary ring chromosomes that contain amplified DNA from the 12q13-15 region. Genes typically amplified include mouse double-minute 2 (MDMD2) and cyclin-dependent kinase 4 (CDK4) in >85% of cases. Of interest, these changes are common in the histologically similar low-grade central osteosarcoma but are rare in conventional high-grade osteosarcoma and may add a useful tool enabling discrimination between c-POS and other pathological processes, e.g., fibrous dysplasia.

Histopathology

Histologically, the neoplastic cells of c-POS are minimally atypical spindle cells, largely oriented in parallel fascicles producing osseous matrix [156, 215, 218, 224]. There is minimal cellular pleomorphism with the individual cells being blunt-ended or pointed spindle cells varying somewhat in length. The nuclei vary from round to fusiform and frequently have irregular nuclear membranes with variably condensed chromatin. Mitoses are infrequent.

One of the hallmarks of c-POS is the production of long, roughly parallel trabecula of well-formed lamellar bone. There may be areas that suggest that matrix originates as unoriented woven osteoid that remodels into lamellar bone, i.e., *normalization* [156]. Overall, the lesion consists of relatively broad sheets of bone-producing tumor (Fig. 3.103). There may be some variation of the cell-to-matrix ratio, but in general it is relatively consistent within a given lesion, with the understanding that matrix volume frequently decreases toward the periphery of the tumor. The tumor/normal interface is confined beneath periosteum, but uneven growth can result in entrapped normal tissues. Cartilage may be found at the lesional periphery, so-called *cartilage cap*. The latter term is an organizational analogy drawn from osteochondroma and is without significance other than the changes it may impart to the tumor roentgenograms and the diagnostic conundrum it may present when seen in small biopsy specimens.

Gross Pathology

The overall gross appearance depends on the stage of tumor growth (Fig. 3.104). Initially, c-POS starts as a hemispherical lesion arising from and adherent to cortical bone with intact overlying periosteum. As tumor develops, it grows vertically and radially in both linear and circumferential planes frequently resulting in a mass with an overall mushroom configuration. The slow rate of tumor growth results in accommodation (i.e., stretching) of normal tissues (e.g., periosteum, tendon attachments, skeletal muscle) that become attenuated and trapped between overlying growing

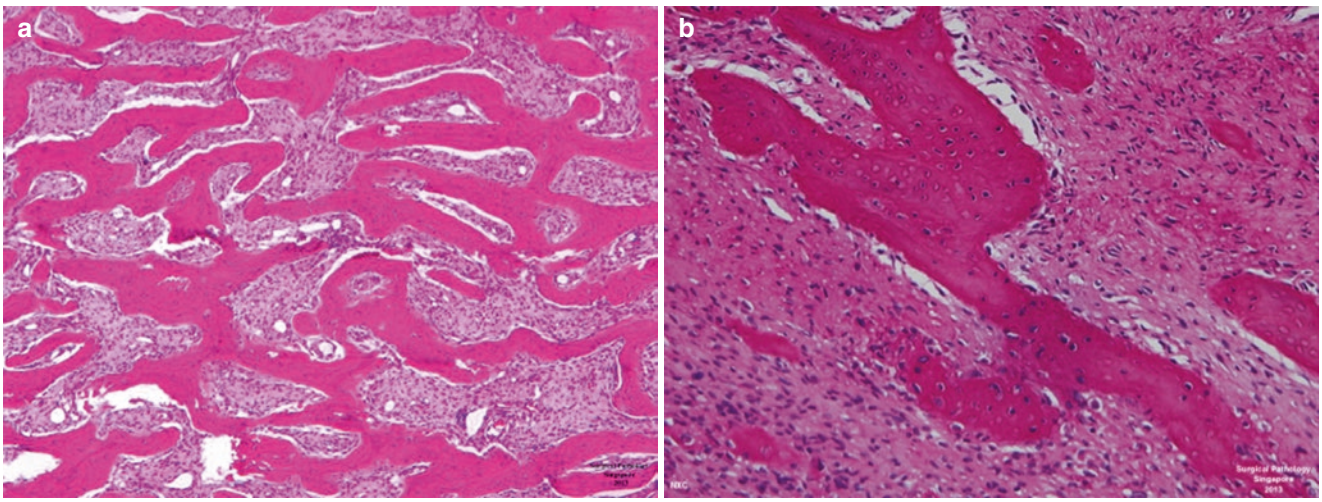

Fig. 3.103 Conventional parosteal osteosarcoma. (**a**) Tumor is composed of long trabecular of lamellar bone produced by innocuous spindle cells (low power). (**b**) Conventional parosteal osteosarcoma. At higher magnification, the details of innocuous spindle cells produce well-formed bone. (Courtesy of A. Kevin Raymond, M.D.)

tumor and underlying cortex. Rather than invaded, overlying normal tissues (e.g., neurovascular bundles, skeletal muscle) are usually pushed ahead of the tumor. These residual normal tissues result in a buffer zone of normal soft tissues between the underlying cortex and overlying tumor. The latter corresponds to the *radiolucent line* frequently seen on imaging studies of POS. Over time, c-POS tumor gradually surrounds the parent bone, i.e., *wraparound lesion*. The periosteum may be distorted but is almost always intact.

c-POS appears as a rock-hard mass adherent to the cortical surface via a narrow attachment. Tumor preferentially grows along the cortical surface both linear and circumferential (Fig. 3.104). In most cases the lesion is rock-hard and bosselated and has a relatively homogeneous yellow-white to white sclerotic cut surface that is either very finely granular, fibrillar, or glass-like smooth. Some cut surfaces have a feathery configuration, while others have a rubbery whorled cut surface. The degree of mineralization may vary somewhat from area to area within a given lesion.

Although historically an exclusionary criterion, medullary cavity invasion is now well-recognized in c-POS and has no prognostic significance. As indicated earlier, distinction between c-POS invading medullary cavity and low-grade central osteosarcoma extending through cortex is viewed as a function of the amount of medullary cavity involvement. Up to 10% or 25% tumor volume is the accepted cutoff; the limit, a function of investigator [156, 219].

Radiology

The radiographic features of c-POS are a reflection of the gross characteristics [156, 216, 225]. c-POS forms a radiopaque lesion situated on the bone surface. The specific features are a function of the lesion age and growth characteristics. Early lesions appear as a small opaque hemisphere (Fig. 3.104). With vertical and radial growth, it may appear as a radiodense lesion with a mushroomlike configuration and narrow attachment base. With further growth c-POS appears as a radiopaque lesion surrounding the bone but retaining a narrow attachment (Fig. 3.105). That is, regardless of size, there is only a small area attached to the cortical bone. Rather, as indicated above, the majority of tumor, other than the attachment point, has a layer of normal tissue (e.g., tendon, skeletal muscle, etc.) between tumor and cortex resulting in a thin radiolucent area between the radiopaque tumor and cortex, the so-called *radiolucent string sign*. Overall, lesions tend to be radiopaque, but there may be some variability. Small ill-defined areas of radiolucency corresponding to entrapped tendon, adipose tissue, and skeletal muscle may be seen at the lesion periphery [156, 226, 227]. CT confirms the plane film findings and allows more detailed analysis of cortical and potential medullary cavity involvement [228]. Together with CT, MRI allows more detailed examination of medullary cavity invasion and establishes the relationship between tumor and overlying soft tissues. Arteriogram shows c-POS to be a hypovascular or avascular lesion. This is an important observation since it may allow for the preoperative discrimination between c-POS and dedifferentiated POS; the latter lesion is hypervascular [227].

Fig. 3.104 Conventional parosteal osteosarcoma. (**a**) Plane film: tumor appears as a radiopaque mass originating from the cortical surface. (**b**) Gross external surface: tumor growth along the surface of the involved bone, both linear and circumferential. (**c**) Gross cut surface: tumor appears as a pale-tan lesion growing on the cortical surface without involvement of the medullary cavity. (Courtesy of A. Kevin Raymond, M.D.)

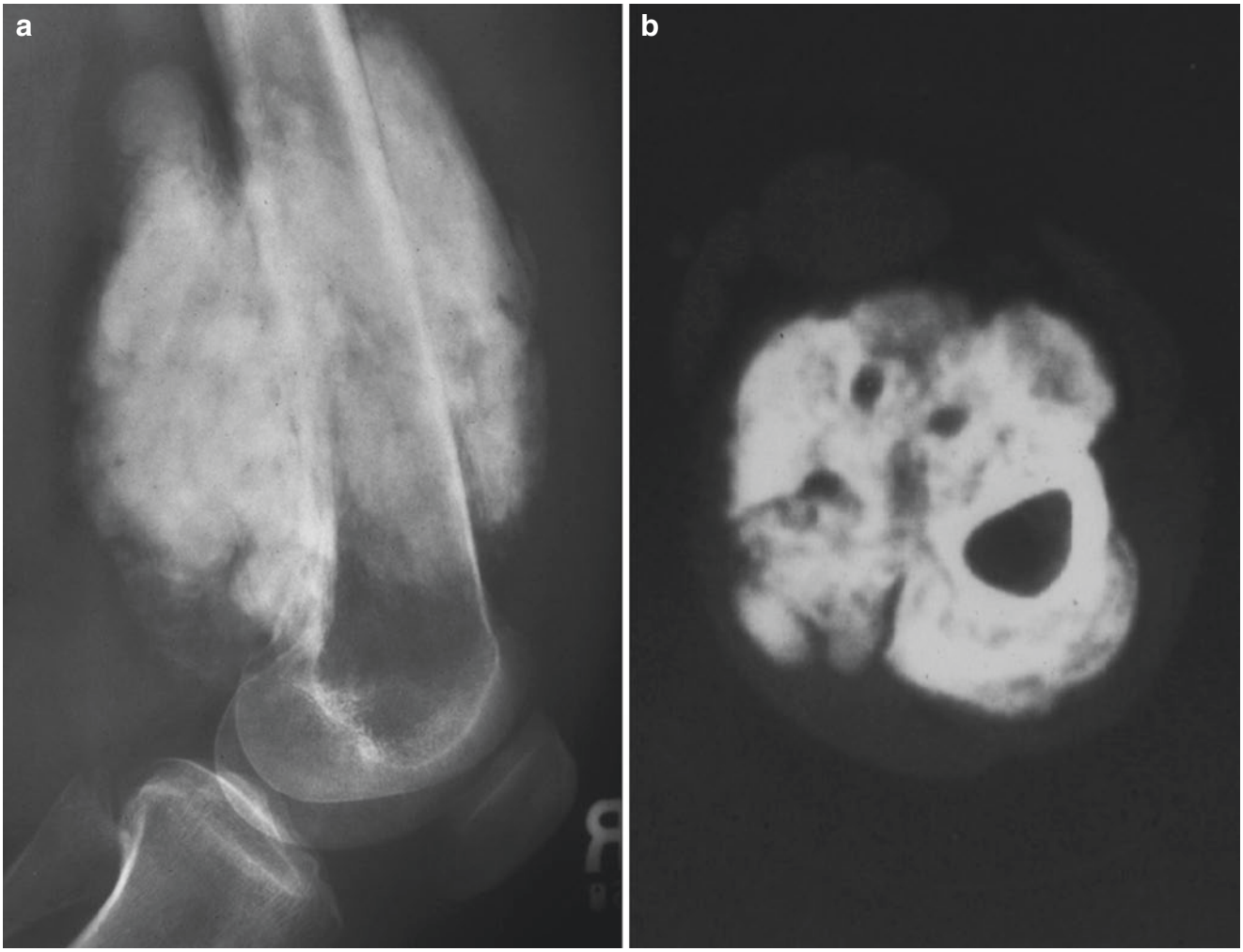

Fig. 3.105 Conventional parosteal osteosarcoma imaging. (**a**) Plane film: tumor has grown circumferentially along the cortex. Note the small area of tumor cortical attachment and the extensive radiolucent zone between tumor and normal bone. (**b**) CT: same case as A. Tumor has grown circumferentially around femur without involving the medullary canal

Dedifferentiated Parosteal Osteosarcoma

Definition

Dedifferentiated parosteal osteosarcoma (dd-POS) is a subset of parosteal OS in which there are synchronous and/or metachronous elements of both typical low-grade POS and high-grade sarcoma.

Clinical

First described in 1984 by Wold et al. [229], dd-POS affects skeletally mature young- to middle-aged patients with a peak incidence in the third and fourth decades. The male to female ratio is 1:2. dd-POS may arise from any bone but is significantly more frequent in long bones, most frequently the femur, in particular the posterior aspect of the distal femur. dd-POS occurs in both primary and secondary forms [156, 227, 229, 230]. In the primary form, the low- and high-grade components coexist in the initial tumor. Alternatively, in secondary dd-POS, the high-grade component first appears in a local relapse or systemic metastases.

The clinical presentation of primary dd-POS is similar to c-POS, painless enlarging mass of long, known duration. Secondary tumors give a history of either prior c-POS or dd-POS in addition to any signs or symptoms of local relapse or metastases.

Untreated, the natural history of dd-POS is similar to high-grade conventional osteosarcoma (c-OS) with early systemic dissemination and resulting in death in more than 89% of patients. In light of its potential aggressive behavior, the treatment of dd-POS is similar to c-OS: multidisciplinary therapy including both surgery and chemotherapy.

Histology

Histologically, the primary form of dd-POS is a biphasic tumor [156]. In general, the dominant component is an otherwise typical example of low-grade POS. Neoplastic cells

are minimally atypical, long or short spindle cells. The nuclei vary from round/oval to cigar shaped with well-defined nuclear membranes and variably dispersed chromatin. Nucleoli may be present but tend to be small and inconspicuous. Mitoses are rarely seen in the low-grade component. The cytoplasm of neoplastic cells is both qualitatively and quantitatively variable but tends to well-defined and abundant. The overall appearance of tumor-produced matrix is that of long trabecula of well-formed lamellar bone.

Superimposed on this picture is a form of high-grade sarcoma: generally a form of osteosarcoma, spindle-cell sarcoma, or otherwise unclassified sarcoma (Figs. 3.106, 3.107, and 3.108a, b). Sarcoma forms other than conventional OS have been described in the high-grade component, e.g., telangiectatic osteosarcoma-like, and giant cell-rich osteosarcoma differentiation has been described. The high-grade component typically forms a relatively well-defined, destructive mass central within the tumor [231–233]. In the secondary forms, high-grade sarcoma is present, with or without the low-grade component in either local relapse or systemic metastases.

Of interest, metastases may contain either the low-grade or high-grade components or both. Knowledge of this potential for mixed histological metastases may help in interpretation of imaging studies employed to follow response to chemo-

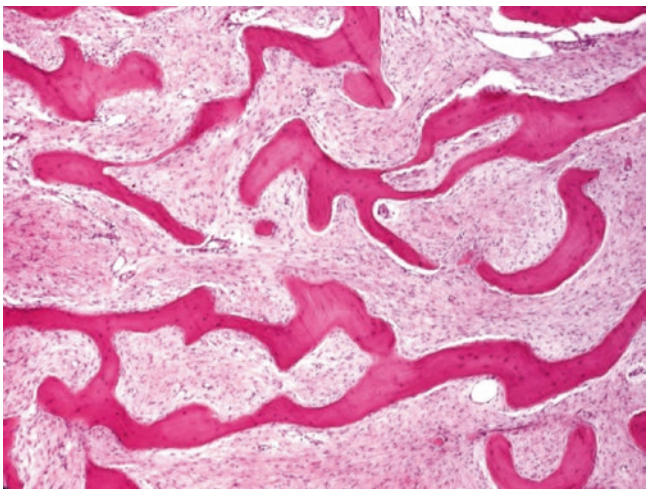

Fig. 3.106 Dedifferentiated parosteal osteosarcoma. Tumor is composed of innocuous spindle cells producing well-formed lamellar bone diagnostic of parosteal osteosarcoma (H&E, 40×). (Courtesy of A. Kevin Raymond, M.D.)

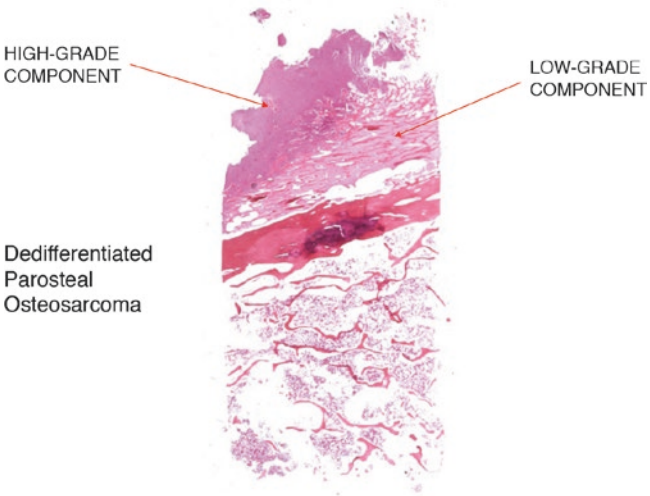

Fig. 3.107 Dedifferentiated parosteal osteosarcoma. Whole mount preparation of interface between the low-grade and high-grade components of dedifferentiated parosteal osteosarcoma. Tumor is present on cortical surface overlying uninvolved bone marrow (H&E 1×). (Courtesy of A. Kevin Raymond, M.D.)

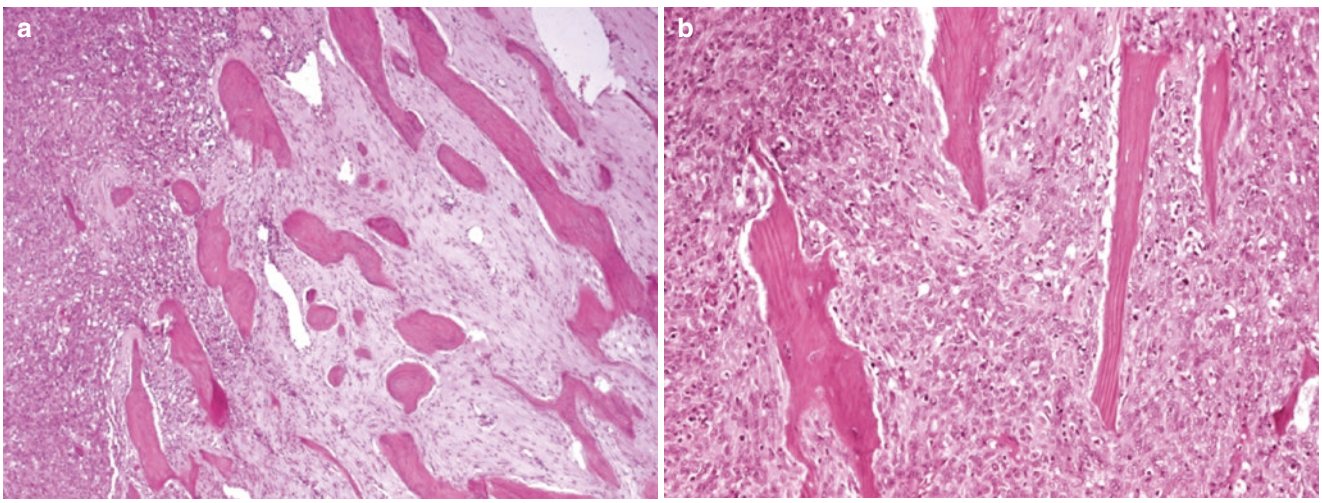

Fig. 3.108 Dedifferentiated parosteal osteosarcoma. (**a**) Low-power view of interface between the low-grade and high-grade components of dedifferentiated parosteal osteosarcoma. This is the same case with the same orientation as Fig. 3.107 (H&E. 40×) (**b**) High-grade component of dedifferentiated parosteal osteosarcoma (same case as Fig. 3.107) (H&E. 100×). (Courtesy of A. Kevin Raymond, M.D.)

therapy: high-grade components respond, while low-grade components do not. And mixed lesions have mixed response. Therefore, the significance of a lack of response to therapy is unknowable preoperatively; it may represent a high-grade tumor in which therapy is ineffective or a low-grade tumor or tumor component that is not expected to respond to chemotherapy (Raymond AK, unpublished work) [156].

Gross

As might be surmised, the overall appearance of dd-POS is largely similar to c-POS. The bulk of the tumor forms a relatively well-defined rock-hard mass beneath the periosteum and attached to the underlying parent bone by a narrow base. The peripheral surface of the mass is frequently undulating with the periosteum and adherent connective tissues following the indentations. Early tumors generally form a mushroom-shaped mass attached to the parent bone. With time tumor may grow on the bone surface both in linear and circumferential. Ultimately, tumor may completely surround the parent bone, so-called wraparound lesion. However, other than the cortical attachment, there is a layer of connective tissue between the tumor and cortex. Over time there may be cortical erosion and invasion of the underlying medullary cavity. Investigators suggest that 10–25% of the tumor may be intramedullary and still considered having origin from the cortical surface if all other parameters fulfill c-POS definitions.

The cut surface of tumor is biphasic. The bulk of the tumor is generally the low-grade component represented by a rock-hard, sclerotic, yellow to yellow-white mass. The cut surface is generally, relatively homogeneous with a finely granular to ivory smooth surface. On occasion, the cut surface may have a feather-like stranded appearance. In addition, there may be a chondroid component mimicking the cartilage cap of an osteochondroma.

The high-grade component forms a well-defined relatively soft, fleshy mass that appears discrete from the underlying c-POS. The appearance of the high-grade component is either fish flesh in quality or a function matrix production (e.g., tan, hyperemic, white, yellow-white) and secondary changes (e.g., hemorrhage, necrosis, cystification, necrosis).

Radiology

Radiographically, dd-POS has features of an altered POS. On plane films and CT, the dominant features are those of a radiopaque mass with a narrow base of attachment on the cortical surface. Early lesions have mushroom configuration which with time extends superior and inferior while wrapping around the parent bone (Figs. 3.109 and 3.110). A radiolucent zone between tumor and cortex corresponds to periosteum and musculotendinous attachments. Radiolucent areas may be present. Those that are small, ill-defined and peripheral correspond to connective at the tumor/normal interface. Those that are large, well-defined, and central tend to correspond to areas of high-grade sarcoma. In essence, nothing is as radiodense as c-POS; by default anything else would be at least relatively radiolucent [227, 234].

Arteriograms may allow preoperative identification of high-grade tumor. c-POS is avascular with arteriogram. In contrast, high-grade areas correspond to localized hypervascular areas in an otherwise avascular tumor [227].

Periosteal Osteosarcoma

Definition

Periosteal osteosarcoma is a form of low- to intermediate-grade chondroblastic arising on the cortical surface with relatively unique radiographic and histological characteristics [64, 156, 235].

Clinical

Periosteal osteosarcoma was described by Unni et al. in 1976 in one of two back-to-back articles readdressing the issue of osteosarcoma arising on the cortical surface, periosteal osteosarcoma vs parosteal osteosarcoma. Subsequent confirmatory studies were carried out [64, 236, 237]. PERI tends to affect younger patients than c-POS, most frequently in the second decade, and to a lesser extent the third decade. Males are affected somewhat more often than females. The most frequently involved sites are the proximal and distal meta-diaphyses of the femur, and the tibia both proximal and distal. Clinically, pain and enlarging mass are the most frequent presentation.

Historically, the treatment of choice has been surgery. Incomplete surgery is followed by inevitable local relapse and increased probability of systemic metastases and death [238]. The role of chemotherapy in PERI treatment is still in question [156, 238]. Therefore, contemporary therapy consists of wide local resection with or without chemotherapy [156, 239] with an expected 5-year survival of 80–89% [156, 236, 238, 240] and long-term survival of >80% [238, 241].

Histopathology

Histologically PERI is a form of low- to intermediate-grade chondroblastic osteosarcoma (i.e., COS) arising upon the cortical surface and beneath the periosteum of the involved bone [235, 236]. In some, tumor consists of typical randomly organized chondroblastic osteosarcoma. However, typically PERI is a form of zonated chondroblastic osteosarcoma [156] in which the lobulated tumor is hypercellular at the periphery of the lobules, while hypocellular at the lobule centers. Neoplastic cells are condensed at lobule peripheries where they are more numerous, longer, larger, plumber, more closely packed with little intervening matrix and tumor is largely viable (Fig. 3.111). In contrast the lobule centers have a higher matrix-to-cell ratio with many empty

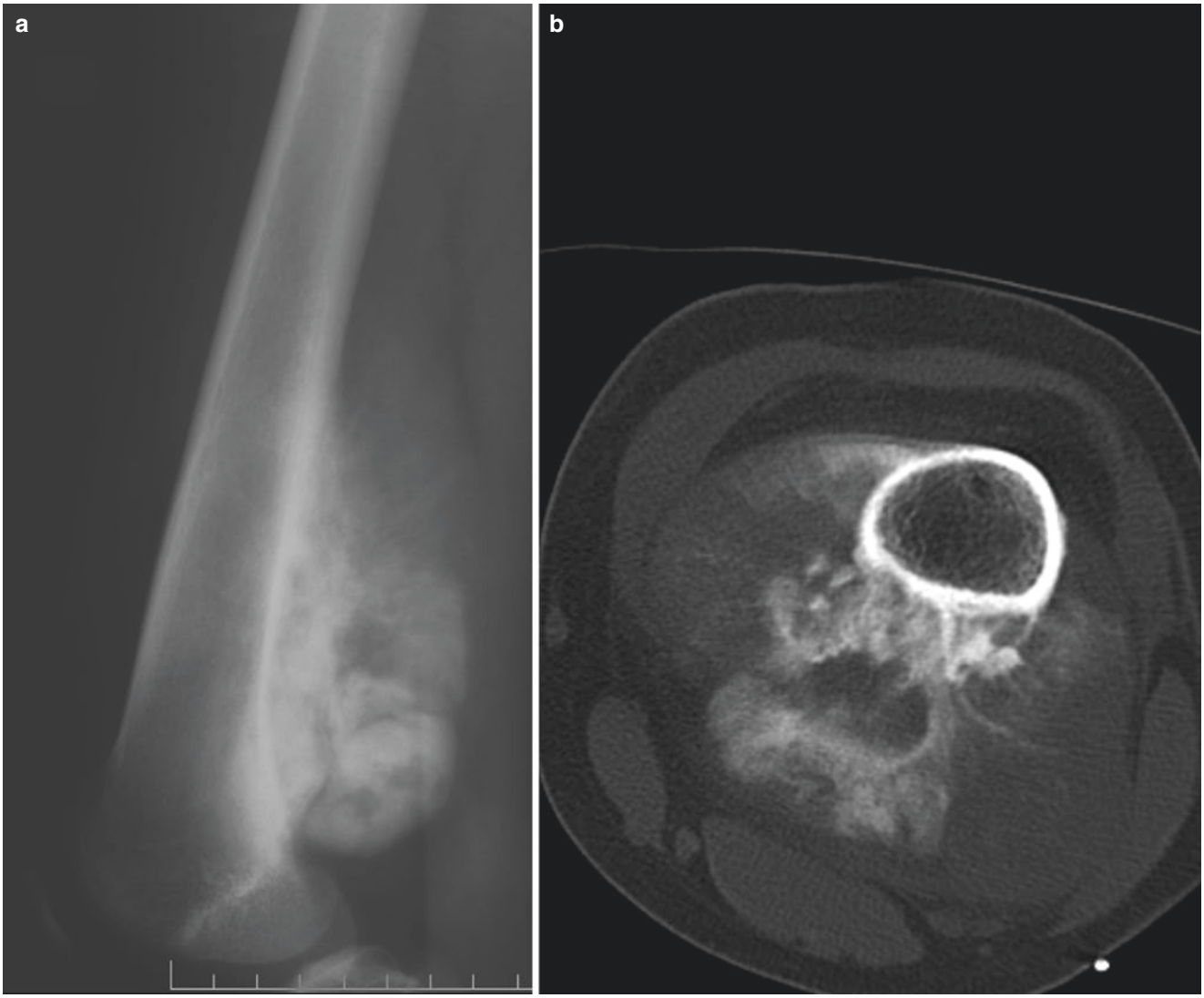

Fig. 3.109 Dedifferentiated parosteal osteosarcoma. (**a**) Plane film, lateral view of dedifferentiated parosteal osteosarcoma. Tumor has a narrow base of attachment to the posterior aspect of the distal femur, with a proximal radiolucent line. There is a large central area of radiolucency. (**b**) CT confirms the plane film findings including the wraparound growth pattern, lack of invasion of the medullary cavity, and the large central area of radiolucency. The latter corresponds to part of the tumor with the high-grade component. (Courtesy of A. Kevin Raymond, M.D.)

lacunes and frequent areas of apoptosis. Although the architecture of PERI may mimic CMF, the cytological features of the neoplastic cells are those malignancy: anaplastic cells varying significantly in size and shape with inverted nuclear/cytoplasmic ratio, irregular chromatin distribution, nucleoli, and mitoses including atypical mitoses. Tumor-produced osteoid is present as slender trabecula of osteoid and/or bone at the superficial and peripheral lobular edges.

In general, the base of the tumor rests on a dense mass of reactive bone. Frequently course, relatively thick spicules of reactive bone and admixed tumor-produced bone extend perpendicularly from the reactive base and parent bone through the lobulated tumor [64, 156, 236]. Unlike c-POS and WDIO OS, periosteal osteosarcoma does not show MDM2 genetic aberration.

Gross

PERI has a fairly stereotypical gross appearance [237, 241–243]. Tumor forms a lobulated chondroid mass affixed by a broad base to the underlying bone (Fig. 3.112). The overlying periosteum remains intact until advanced disease.

PERI forms a hemispherical mass in which the cut surface consists of blue-gray to translucent gray-white tumor with bone spicules radiating through it. Tumor may erode underlying cortex, but the defect is largely filled by a bed of dense, layered reactive bone that forms a base for the tumor. Tumor is inevitably surrounded by a raised collar of reactive bone. As with c-POS tumor grows in both the linear and circumferential axis; the resulting tumor may wrap around as much as 50–90% of the involved bone [242].

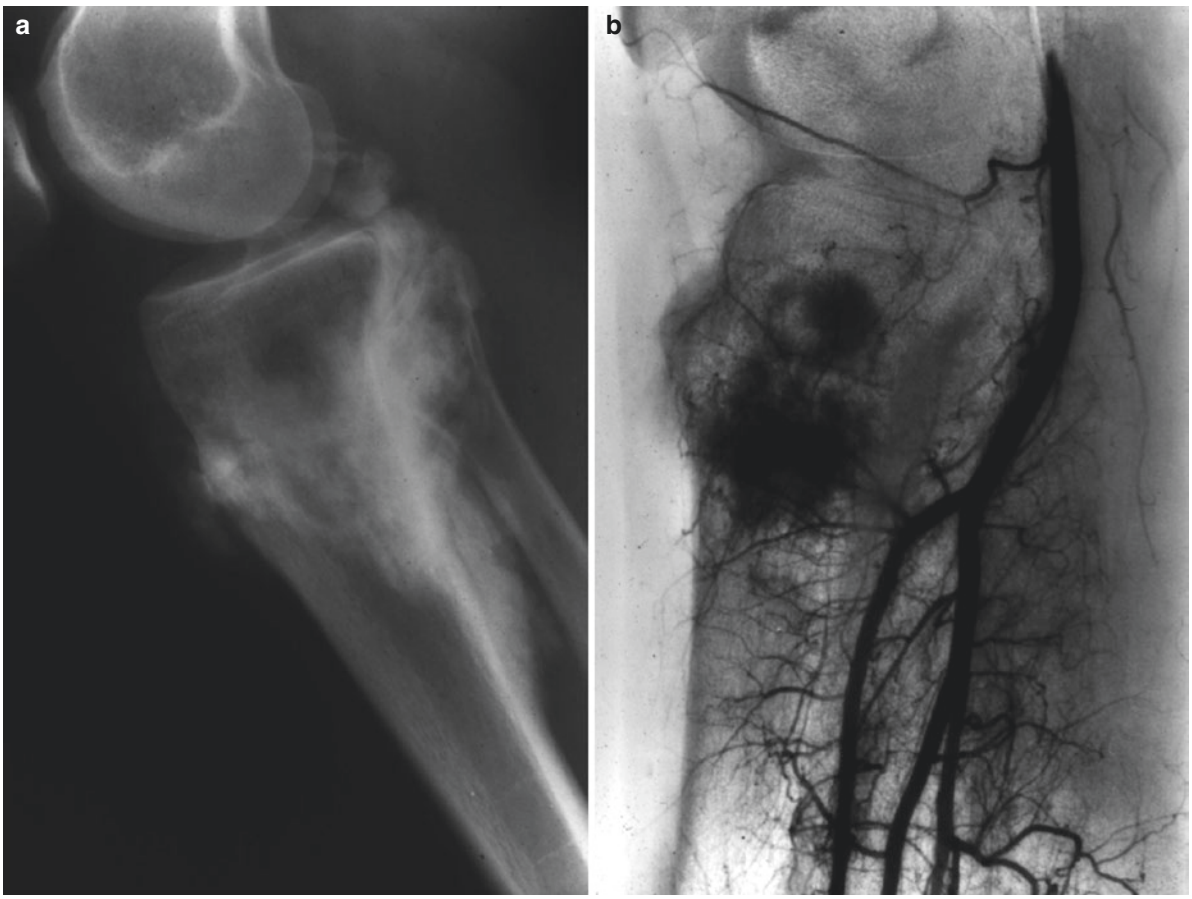

Fig. 3.110 Dedifferentiated parosteal osteosarcoma. (**a**) Plane film, lateral view of dedifferentiated parosteal osteosarcoma. Tumor has a narrow base of attachment to the posterior aspect of the proximal tibia, with a distal radiolucent line. Tumor has grown in both the linear and circumferential axes. (**b**) Arteriogram reveals an area of hypervascularity corresponding to the high-grade component of this dedifferentiated parosteal osteosarcoma. (Courtesy of A. Kevin Raymond, M.D.)

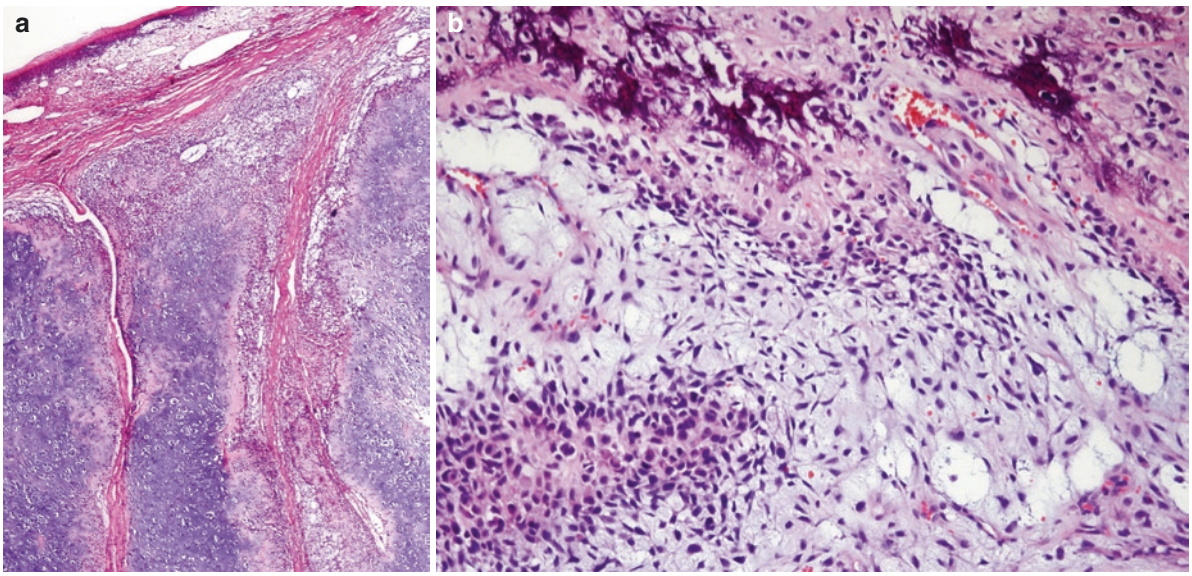

Fig. 3.111 Periosteal osteosarcoma. (**a**) Tumor is made up of zonated lobules of chondroblastic osteosarcoma. The lobule peripheries are hypercellular with larger, plumber more pleomorphic cells that more densely packed. The lobule centers are hypocellular, and the cells are more slender and loosely packed (low power). (**b**) Lobule periphery with neoplastic cells producing osteoid with focal mineralization. (Courtesy of A. Kevin Raymond, M.D.)

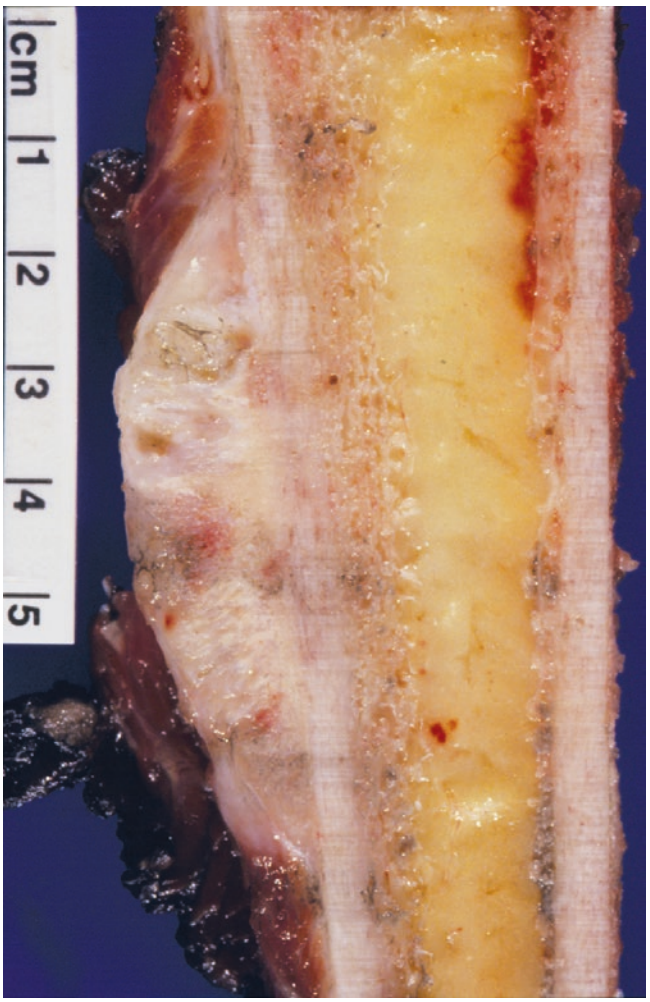

Fig. 3.112 Periosteal osteosarcoma. Gross specimen with lens-shaped chondroid lesion on bone surface. The lobulated mass contains linear mineralized spicules oriented perpendicular to the long axis of the bone. (Courtesy of A. Kevin Raymond, M.D.)

Fig. 3.113 Periosteal osteosarcoma. Plane film with lens-shaped lesion on bone surface. These are fine lines of mineralized matrix- oriented perpendicular to the long axis of the bone. Note the dense reactive bone formation underlying the tumor and forming peripheral sclerosis. (Courtesy of A. Kevin Raymond, M.D.)

Radiology

Again, the radiographic appearance recapitulates the tumor gross and for the most part is stereotypical [235–238, 242–244]. Tumor appears as a broad-based, radiolucent, hemispherical mass arising on the bone surface with linear spicules of mineralized matrix projecting through the lesion perpendicular to the long axis of the bone (Fig. 3.113). There is dense underlying reactive bone with a concave defect that frequently erodes underlying superficial cortex. The reactive bone forms a dense radiopaque collar that surrounds the tumor and ascends it, analogous to a circular Codman triangle.

CT may more clearly define the tumor/bone relationship and extent of disease while examining the possibility of marrow cavity invasion. Tumor has high signal intensity on T2-weighted MRI imaging, reflecting the high water content of the predominantly cartilage matrix [156]. The underlying medullary cavity may also show a degree of increased signal intensity, that in the vast majority of cases, this represents reactive changes.

Comment

There is some difference in opinion as to the appropriate classification of high-grade chondroblastic osteosarcoma arising on the cortical surface. There are some who feel that the criteria of periosteal OS are all-or-nothing. That is, all cases of chondroblastic OS arising on the cortical surface should be classified as periosteal OS. Others feel that PERI is a low- to intermediate-grade COS on the surface and that the high-grade COS should be classified as high-grade surface OS [243]. In the limited number of cases in which this parameter has be reviewed, high-grade tumors behaved more aggressively and had a worse prognosis. The "appropriate" classification is less important than mutual understanding between pathologist and clinician as to biological probabilities and appropriate therapy.

High-Grade Surface Osteosarcoma

Definition

High-grade surface osteosarcoma (HGS OS) is defined as a form of OS histologically and biologically similar to conventional intramedullary OS but arising on the cortical surface of the bone.

Clinical

First described by Wold et al. [156, 245, 246] and the subject of subsequent reports [246, 247], HGS OS is one of the rarest recognized variants of OS. Occurring in males more frequently than females (male to female ratio of 2:1), HGS OS tends to affect patients in the second, and less frequently the third, decade of life. HGS OS most frequently arises on the cortical surface of long bones of the appendicular skeleton, in particular the mid and distal femur followed by the tibial diaphysis.

Localized pain and enlarging mass are the cardinal presentation of HGS OS.

Untreated or treated with surgery alone, HGS OS is a locally aggressive tumor that will develop systemic metastases and have a poor prognosis [245, 246, 248]. However, HGS OS appears to respond well to contemporary multimodality therapy with an expected survival similar to c-OS [248, 249].

Histopathology

Histologically, HGS OS is indistinguishable from c-OS; in particular osteoblastic OS and fibroblastic OS only confined to the cortical surface of bone. Examples of tumors mimicking telangiectatic OS and giant cell-rich OS have been described (Fig. 3.114).

Gross

As with the other forms of surface OS, HGS OS preferentially grows along the cortical surface, beneath the periosteum. Like PERI, HGS OS tends to have a broad base of cortical attachment. Tumor preferentially grows along the periosteal cortical surface without involving medullary cavity until very late in the disease course, and medullary involvement should be less than 25% of tumor volume [249]. The appearance of the cut surface is similar to c-OS subtypes and a function of the type and amount of tumor matrix production and its mineralization. In general, the cut surface is firm to rock-hard, granular, and off-white to tan with focal areas of hyperemia. The consistency ranges from fleshy to granular to sclerotic depending on matrix production. In those cases in which the tumor histology is high-grade FOS or one in which tumor matrix does not mineralize, the cut surface is beige to tan and fleshy (Fig. 3.115).

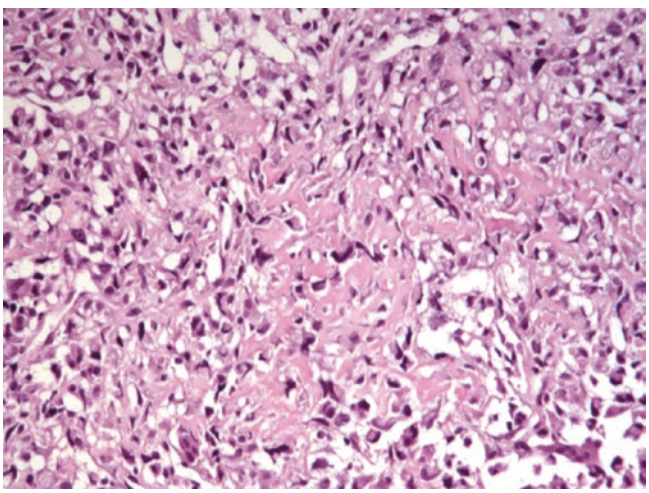

Fig. 3.114 High-grade surface osteosarcoma: osteoblastic osteosarcoma

Radiology

The radiographic appearance varies with the histological tumor composition (Fig. 3.115). Tumor tends to be mineralized with cloud-like intralesional densities. Radiopaque speculation may be present, and in some cases the appearance can mimic PERI [249]. The question of marrow involvement is best approached through the use of CT and MRI.

Comment

As indicated earlier in the discussion of periosteal osteosarcoma. A source of some disagreement is the appropriate classification of cases of high-grade chondroblastic osteosarcoma arising on the cortical surface. There are those who believe that all high-grade OS originating on the cortical surface, regardless of histological subtype, should be grouped together for treatment purposes, HGS OS. Others feel that all COS arising on the cortical surface should be classified as periosteal OS. The specifics of classification are less important than appropriate therapy. Whether grouped with PERI or HGS OS, examples of high-grade COS originating on the cortical surface should benefit from multimodality therapy including contemporary primary chemotherapy [217, 250–252].

Small Cell Neoplasia

Introduction

Historically, the main considerations in the differential diagnosis of small cell tumors were largely confined to Ewing's sarcoma, primary lymphoma of the bone, metastatic rhabdomyosarcoma, and metastatic neuroblastoma.

However, the differential diagnosis is much longer and must be kept in mind when dealing with the individual case (see Table 3.6). Paramount considerations are hematological entities, largely systemic with secondary involvement of bone. These include plasmacytoma localized to bone with a high (>60%) incidence of evolution to multiple myeloma and a change from a relatively indolent process to an almost inevitably lethal malignancy. There are the disseminated lymphomas and leukemias. Histiocytoses including Langerhan cell histiocytosis and Erdheim-Chester disease enter the differential diagnosis.

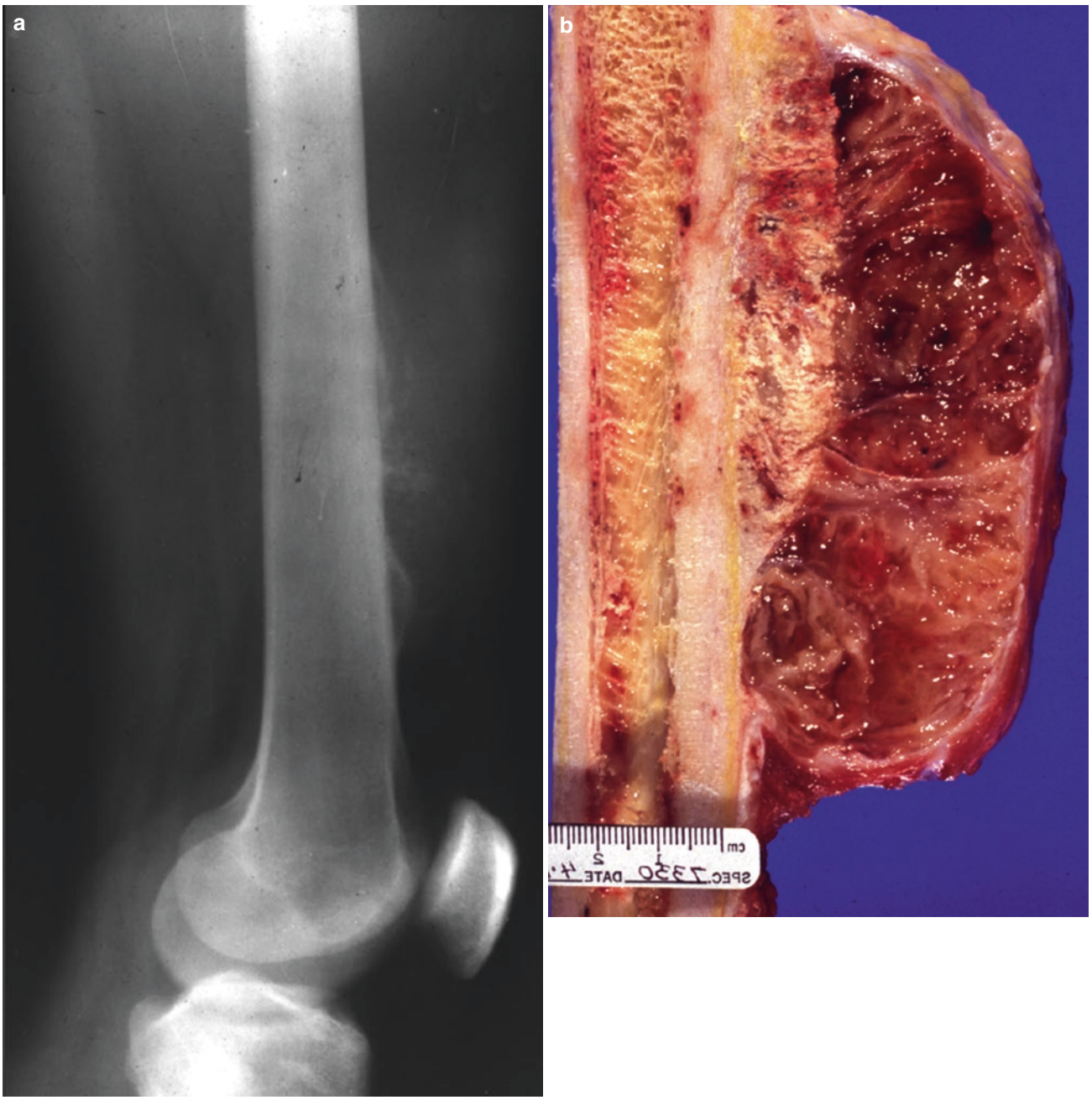

Fig. 3.115 Radiographic appearance and histological tumor composition: The consistency ranges from fleshy to granular to sclerotic depending on matrix production. In those cases in which the tumor histology is high-grade FOS or one in which tumor matrix does not mineralize, the cut surface is beige to tan and fleshy

Table 3.6 Small cell tumors

Ewing sarcoma
Lymphoma
Rhabdomyosarcoma
Neuroblastoma
Hematological:
Plasmacytoma/myeloma
Leukemia/lymphoma
Histiocytosis
Langerhans cell histiocytosis
Erdheim-Chester disease
Small cell variants
Sarcoma
Carcinoma
Inflammatory processes

Small cell variants of a wide variety of both primary and secondary malignancy are of prime concern. Primary tumors include the aforementioned Ewing sarcoma and primary lymphoma of the bone but also small cell osteosarcoma and mesenchymal chondrosarcoma. A wide variety of carcinomas can also present as small cell malignancies involving the bone.

Inflammatory phenomena enter into the differential and range from recognized specific processes to osteomyelitis.

With advances in fixation techniques and processing the use of routine light microscopy, special stains, a broad range of ever increasingly specific immunohistochemical studies, cytogenetics and molecular investigation can be brought to bear to work through these complex and frequently critical medical issues.

Langerhans Cell Histiocytosis

Definition

Langerhans cell histiocytosis is now thought to represent a neoplastic proliferation of Langerhans cells.

Clinical

Langerhans cell histiocytosis (LCH) replaces the older-term histiocytosis X the latter being a term coined by Lichtenstein and Jaffe as a unifying concept encompassing eosinophilic granuloma, Schüller-Christian disease, and Letterer-Siwe disease [253, 254]. It is now felt that eosinophilic granuloma and Schüller-Christian disease represent the monostotic and polyostotic forms of a single disease, Langerhans cell histiocytosis, while Letterer-Siwe disease is an unrelated process [20, 255].

LCH may affect patients of any age. However, the majority of patients are in the first decade of life, and >80% are under the age of 20 years [256]. The male to female ratio ranges from 3:2 to 2:1. Much of the literature indicates that the skull, jaw, and pelvis are the most frequently involved bones. Although pain is a frequent complaint, a broad spectrum of findings may be present and are a function of tumor size and location, in particular lesions involving the base of the skull and vertebra. Pathological fracture may complicate larger lesions.

Treatment is a largely a function of tumor size and location. Accessible lesions can confidently be treated with either curettage or intralesional installation of corticosteroids. External beam radiation therapy is generally curative in surgically inaccessible lesions. In the cases of disseminated disease, chemotherapy may be necessary, and the prognosis is uncertain [10, 255].

Histopathology

The cytological/histological hallmark of LCH is the Langerhans cell (Fig. 3.116a, b). It is a histiocytic cell 2–4 times the size of a red blood cell, with round- to oval- to cigar-shaped nuclei with well-defined, prominent nuclear membranes encompassing finely divided chromatin that may condense along the nuclear membrane. Small inconspicuous nucleoli may be present, as can mitoses. Cells are usually mononuclear, but multinucleated forms may be present. Langerhans cell nuclei typically have either a linear, longitudinal groove or a kidney-bean configuration. Langerhans cells have variable amounts of abundant eosinophilic, clear, or amphophilic cytoplasm.

Langerhans cells tend to be part of a polymorphous infiltrate that includes lymphocytes, neutrophils, plasma cells, and large numbers of eosinophils. In addition, Langerhans cells are not generally evenly distributed through the lesions. Rather, they seem congregate in clusters and small groups.

Langerhans cells characteristically show immunoreactivity for CD-45, CD-68, S-100, and the more specific CD-1a and CD-207 (i.e., langerin) [17]. The ultrastructural hallmark is the tennis racket-shaped cytoplasmic Birbeck granule.

Gross Pathology

Gross specimens other than fine needle aspirates and needle biopsies are infrequent. In those rare instances in which an intact specimen is available for examination, LCH takes the form of a yellow semisolid mass indistinguishable from abscess (Fig. 3.117a, b).

Radiology

As seen on plane films and CT, LCH typically forms a well-defined lytic lesion with negligible reactive bone formation (Fig. 3.117b). Flat bone lesions (e.g., skull, pelvis) are usually asymmetric involving one cortex more than the other resulting in the defect of one cortex being smaller than the other and imparting a *hole within hole* or *beveled edge* appearance of the well-defined punch-out lesion (Fig. 3.118). Larger lesions may be more infiltrative, less well-defined, and in appendicular long bones associated with dense laminated reactive bone formation (Fig. 3.119) [257].

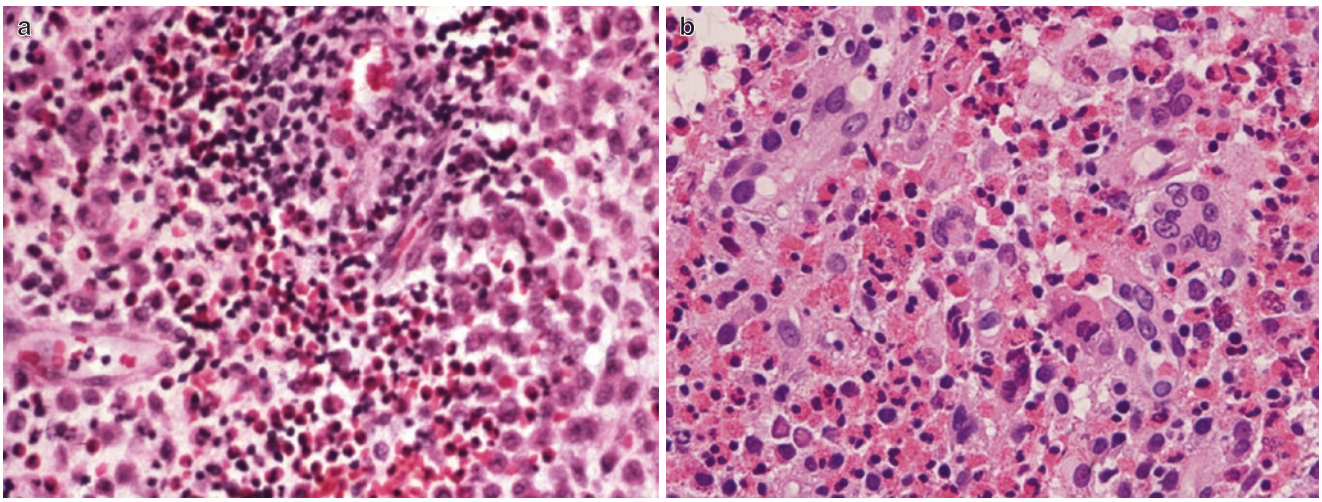

Fig. 3.116 (**a**, **b**) Langerhans cell histiocytosis. Tumor consists of a mixed inflammatory infiltrate with lymphocytes, plasma cells, and eosinophils. Langerhans histiocytosis with cigar-shaped nuclei with linear grooves or kidney-bean configuration. Occasional multinucleated giant cells are present (H&E, (**a**) 200×, (**b**) 400×). (Courtesy of A. Kevin Raymond, M.D.)

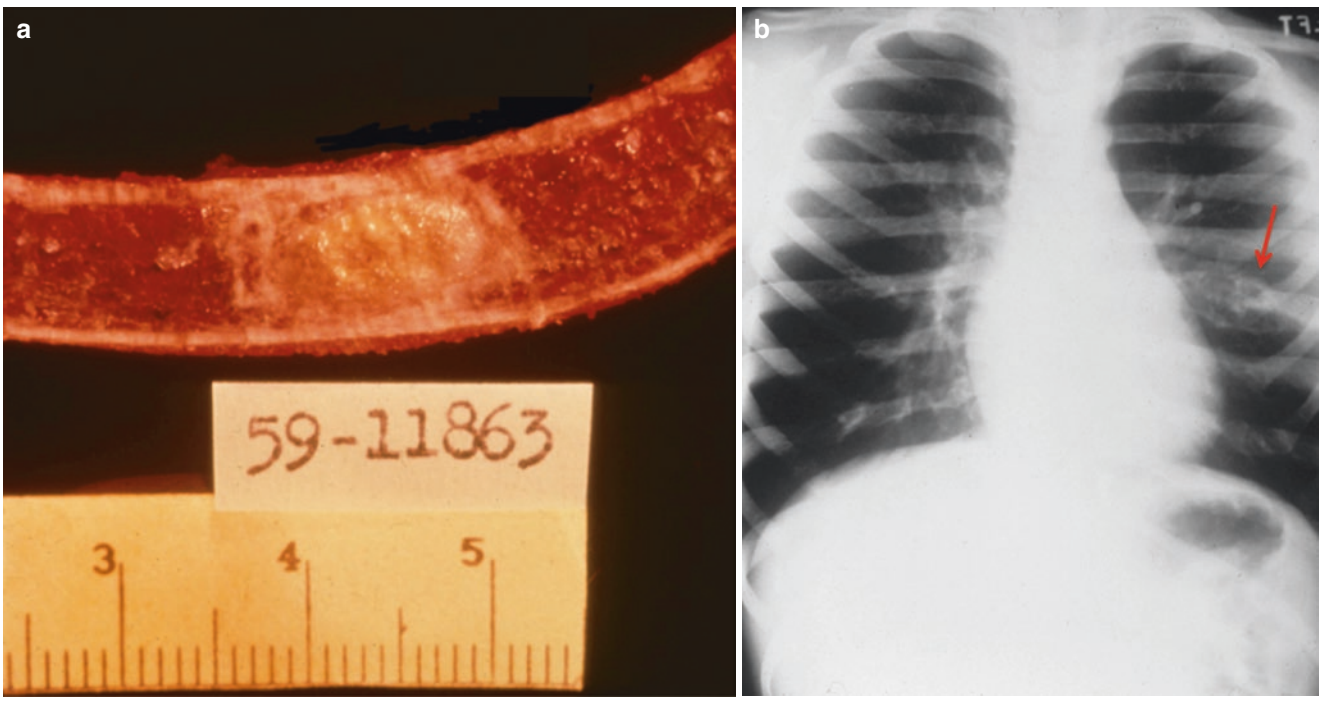

Fig. 3.117 Langerhans cell histiocytosis. (**a**) Rib resection: tumor forms a soft yellow to cream-colored relatively well-defined mass within the medullary cavity with an abscess-like appearance similar to many small cell lesions. (**b**) Chest x-ray plane film (AP): tumor forms an expansile, radiolucent lesion involving the sixth rib. There is cortical erosion with reactive bone formation. (Courtesy of A. Kevin Raymond, M.D.)

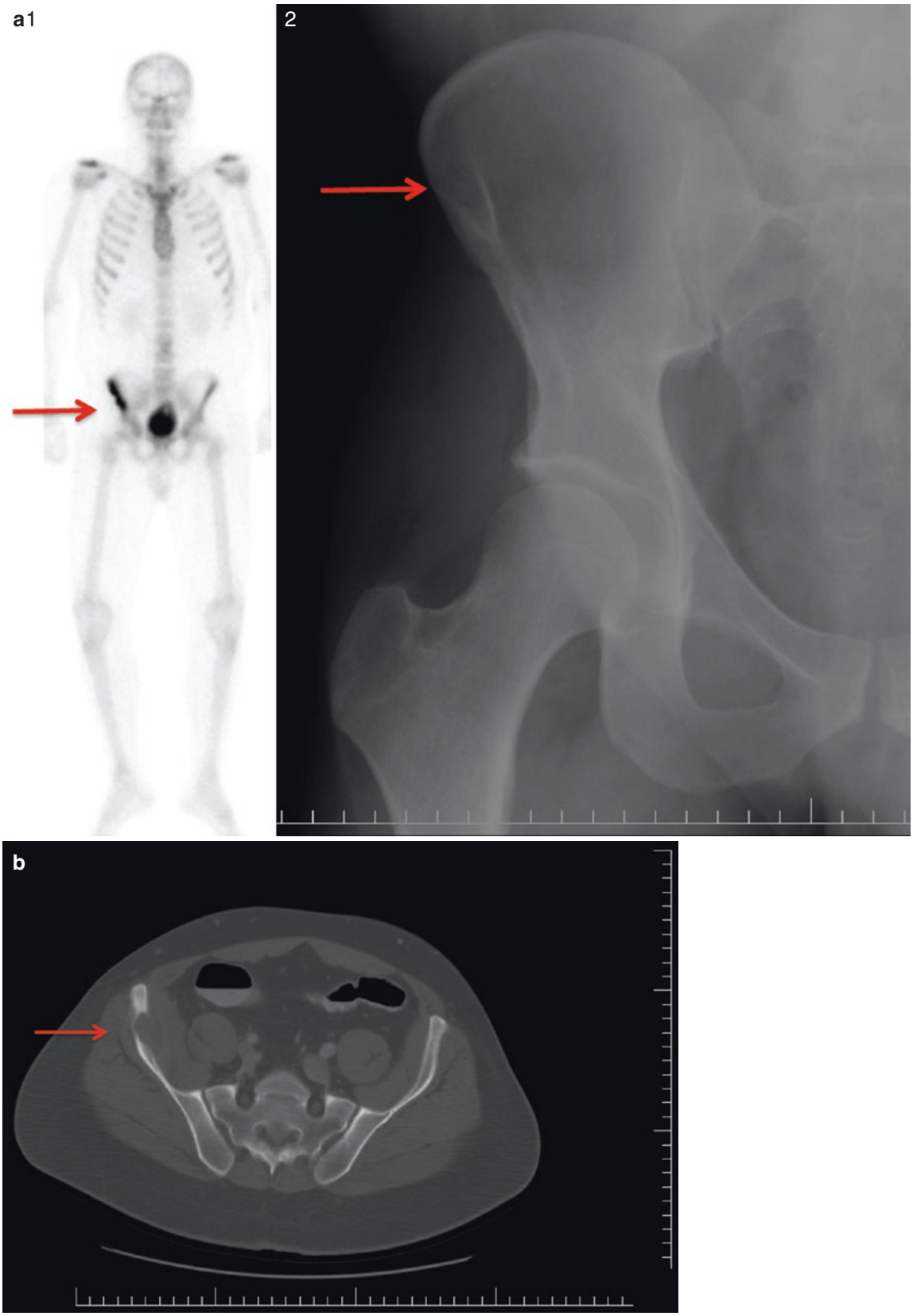

Fig. 3.118 (**a**) Langerhans cell histiocytosis [1]. Tm^{99} bone scan: the right iliac crest shows an area (red arrow) of increased isotope uptake [2]. Plane file (AP) of the pelvis shows a radiolucent punched-out lesion (red arrow) with peripheral sclerosis, hole-within-hole appearance. (**b**) Langerhans cell histiocytosis. CT pelvis. Tumor forms an eccentric destructive, radiolucent lesion involving the iliac wing. The expansile lesion is still encased by a thin shell of cortical bone. (Courtesy of A. Kevin Raymond, M.D.)

Fig. 3.119 Langerhans cell histiocytosis. Plane films (AP and Lateral): lesion involving the femoral mid-diaphysis forms a relatively well-defined intramedullary lesion. There is layered dense reactive periosteal new bone formation. (Courtesy of K.K. Unni, M.D.)

Primary Lymphoma of Bone

Definition

Primary lymphoma of bone (PLB) is defined as lymphoma arising in the bone without contemporary nodal or independent extraosseous involvement.

Clinical

Although originally described by Oberling [258], Jackson and Parker are generally credited with introducing *reticulum cell sarcoma of bone*, as it was then known, into American medicine. Subsequent observations confirmed the existence of the entity and showed it to be a form of malignant lymphoma [259–262]. The vast majority of osseous involvement by lymphoma represents a process secondary to nodal lymphoma. Even with osseous presentation, only a small percentage of bone involvement represents malignant lymphoma Stage I-E_{BONE}.

PLB is defined as malignant lymphoma that after staging is found to be confined to bone without involvement of lymph node or distant soft tissue at presentation. A small number of cases are polyostotic on presentation [10]. It is a rare tumor account for <5% of primary malignant bone tumors and <5% of extranodal lymphomas. Nodal and systemic dissemination may take place during the clinical progression of PLB. However, by definition, extraosseous involvement should not take place within the first 4–6 months following patient presentation to allow distinction between primary and secondary bone involvement [20, 260].

In the past, some suggested that all lymphomas are nodal in origin and that bone involvement represented sec-

ondary disease. The introduction of progressively more sophisticated staging techniques together with a 50% survival with localized therapy alone (i.e., external beam radiation therapy) confirmed the possibility of osseous origin [260, 261].

PLB involves patients over a broad spectrum of age, but most series show a bimodal distribution with a small peak in the second and third decades and a larger peak in the fifth and sixth decades of life. Men are affected more frequently than women: male to female ratio is 3:2. The most frequently involved sites include distal femur, ilium, proximal humerus, and proximal tibia. In the long bones, tumor involvement tends to be metaphyseal or metadiaphyseal [20].

Localized pain and swelling are the most frequent presentation. A small minority of patients may have constitutional symptoms: fever, anemia, and tiredness.

Contemporary therapy consists of multi-agent chemotherapy with or without external beam radiation therapy to the primary tumor. The expected survival is approximately 75% at 10 years [10, 17].

Histopathology

With only exceptionally rare confirmed cases of primary Hodgkin's disease of the bone, non-Hodgkin's lymphoma (NHL) makes up the overwhelming majority of PLB [20, 263]. Virtually all forms of NHL have been reported primarily in the bone (Table 3.7). However, diffuse large B-cell lymphoma (Fig. 3.120) is far and away the most common form (Fig. 3.121) with an estimated 90% being the germinal center subtype. Although uncommon, lymphoblastic lymphoma is the second most common form being relatively frequent in children and uncommon in adults. Again infrequent, anaplastic large cell lymphoma is the most common form of primary T-cell lymphoma of the bone. In contrast, primary follicular/nodular lymphoma and small lymphocytic lymphoma are at most decidedly rare in the bone. The immunohistochemical profiles for bone lymphoma are analogous to their nodal counterparts.

From low power, PLB appears as a cellular mass replacing medullary cavity with infiltration into adjacent normal tissues. As opposed to ES, small amounts of reticulum-staining connective tissue are frequently present between the

Table 3.7 Primary lymphoma of the bone

	Studies					
Classification	Heyning (n = 60) % 1999	Geanelli (n = 28) % 2002	Zinzani (n = 52) % 2003	Hsieh (n = 14) % 2006	Alencar (n = 53) % 2010	Demircay (n = 63) % 2013
DLBCL	92	93	85	50	83	93.7
FL	3	0	3.8	0	5.7	4.8
SLL/MZL/LPL	1.5	0	3.8	7	5.7	0
B-cell other	0	0	3.8	0	7.5	0
ALCL	3	3.6	3.8	36	0	1.6
T-cell other	0	3.6	0	7	3.8	1.6

Courtesy of A. Kevin Raymond, M.D.
Summary of the incidence of recognized forms of malignant lymphoma in published series concerning primary lymphoma of bone [264]
DLBCL diffuse large B-cell lymphoma, *FL* follicular lymphoma, *SLL* small lymphocytic lymphoma, *MZL* marginal zone lymphoma, *LPL* lymphoplasmacytic lymphoma, *ALCL* anaplastic large cell lymphoma.

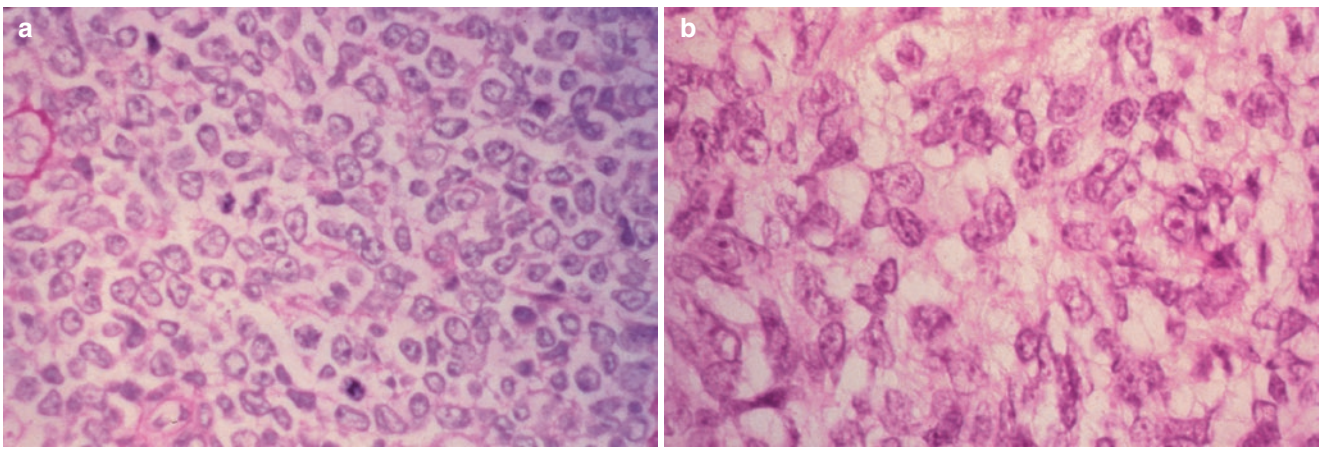

Fig. 3.120 Primary lymphoma of bone. (**a**) Diffuse large cell lymphoma infiltrating bone (H&E, 200×). (**b**) Diffuse large cell lymphoma infiltrating bone (H&E, 400×). (Courtesy of A. Kevin Raymond, M.D.)

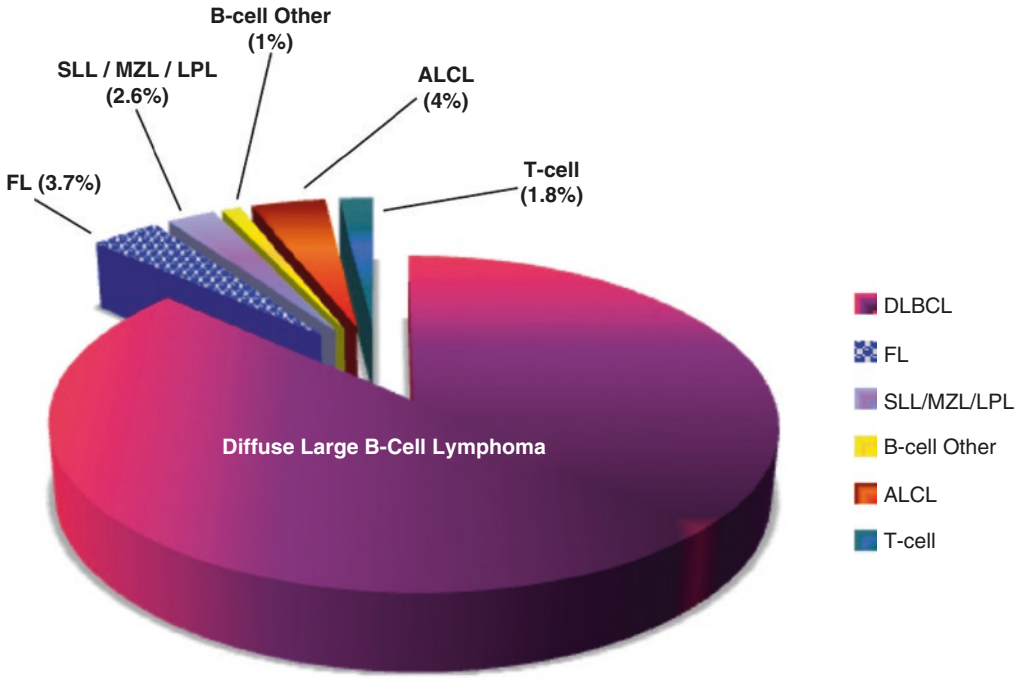

Fig. 3.121 Primary lymphoma of bone. Data abstracted from Table 3.7 summarizing the relative incidence of recognized forms of malignant lymphoma from published series concerning primary lymphoma of bone [264]. (Courtesy of A. Kevin Raymond, M.D. *DLBCL* diffuse large B-cell lymphoma, *FL* follicular lymphoma, *SLL* small lymphocytic lymphoma, *MZL* marginal zone lymphoma, *LPL* lymphoplasmacytic lymphoma, ALCL anaplastic large cell lymphoma)

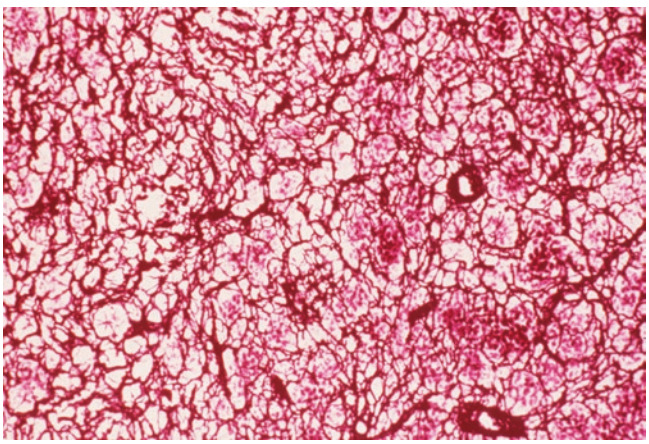

Fig. 3.122 Primary lymphoma of bone. Primary lymphoma infiltrating bone. Although an outdated and marginally contributory test, silver stain confirms the presence of reticulum fibers surrounding individual neoplastic cells and small group of cells in addition to vessels. Although a nonspecific finding, it adds some support to a diagnosis of lymphoma over other diagnostic considerations in the absence of immunohistochemical or molecular studies (H&E, 40×). (Courtesy of A. Kevin Raymond, M.D.)

neoplastic cells of PLB (Fig. 3.122), while intracytoplasmic glycogen is characteristically absent. *Crush artifact* is a frequent finding in PLB.

Gross

It is rare to see large specimens from the primary tumors of PLB except in the setting of treatment failure and/or complications. The cut surface of tumor tends to be typically sarcoma-like, semitranslucent, fish-flesh sickly-white to gray-white (Fig. 3.123). There may be superimposed degenerative changes.

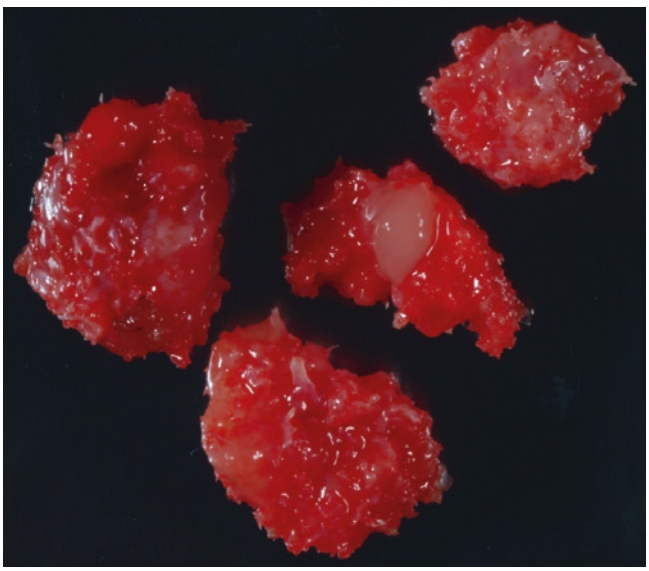

Fig. 3.123 Primary lymphoma of the bone. A washed open bone biopsy specimen (i.e., curettings) to establish a diagnosis of primary lymphoma of bone. Tumor is represented by shiny, semitranslucent gray to gray-white soft, semisolid material adherent to underlying cancellous bone (gross specimen). (Courtesy of A. Kevin Raymond, M.D.)

Radiology

PLB has an extremely wide spectrum of radiographic appearances. However, PLB is typically a radiolucent lesion resulting in an overall moth-eaten permeative appearance similar to ES (Fig. 3.124). However, soft tissue masses when present tend to be small until disease is very advanced. There may be reactive bones of various forms. CT and MRI establish details of tumor/normal interface and establish the true extent of disease [265].

Fig. 3.124 Primary lymphoma of the bone. Plane film (AP) of the humerus shows an infiltrative moth-eaten permeative, mixed lytic/blastic lesion. There is virtually no associated soft tissue mass. (Courtesy of A. Kevin Raymond, M.D.)

Ewing's Sarcoma: PNET

Definition

Ewing sarcoma (ES) is a form of "small cell" malignancy usually primary within or on bone with relatively unique clinical, morphological, and molecular features.

Clinical

Ewing sarcoma was originally described by James Ewing in 1921 [266, 267] using the rubric *diffuse endothelioma* of the bone. Comprising some 6–10% of malignant bone tumors, ES is the third most common primary malignant bone tumor following OS and ChS. It affects patients over a fairly wide age range but has a profound predilection for patients in the second decade of life, and 80% of patients are <20 years old. Males are affected somewhat more frequently than females [1, 4, 17, 268]. ES can arise in any bone but most frequently in the femur, pelvis, ribs, and shoulder. In long bones, ES preferentially involves the metaphysis or meta-diaphysis of involved bones. ES shows preferential involvement of Caucasians (incidence 3 per million) and is rare in Africans, Asians, and Native Americans (incidence 0.2 per million) [4].

There has a long been debate concerning a number of underlying fundamental issues pertaining to ES. Resolution of the lineage of ES (i.e., mesenchymal stem cells versus neural crest-derived stems cells) depends on the consulted source [4, 19]. As to the relationship between ES and primitive neuroectodermal tumor (i.e., PNET), they are for all intents and purposes clinically indistinguishable, leading some to use the terms interchangeably and some pathologist to collectively refer to the tumor as simply *Ewing's sarcoma/PNET.*

As with virtually all bone tumors, pain is the cardinal symptom. Primary tumors tend to be rapidly enlarging and therefore frequently associated with mass, local tenderness, warmth, and dilated vessels. ES is frequently accompanied by systemic symptoms, e.g., fever and elevated sedimentation rate [4, 19].

Historically, left untreated or inadequately treated, the clinical behavior of ES was one of rapidly enlarging mass, quick systemic dissemination, and almost uniform death from disease in less than 2 years [1]. In light of the fulminating course of disease, despite early surgery and negative staging, the presence of systemic micrometastases must be assumed present at the time of initial presentation in the majority of patients. An estimated 25% of patients have clinically evident metastases on presentation. In many primary bone tumors, the onset of sudden growth acceleration is frequently secondary to degenerative changes and consequent intralesional hemorrhage (e.g., secondary aneurysmal bone cyst-like change). However, in ES sudden growth may be a manifestation of the primary tumor growth.

ES sarcoma is a radiosensitive tumor. However, despite the use of high-dose external beam radiation therapy, long-term survival with radiation therapy alone is <10%, similar to surgery alone [269]. Contemporary ES treatment employs multidisciplinary therapy utilizing surgery or external beam radiation therapy for control of local disease and chemotherapy for management of systemic metastases: preoperative chemotherapy, local treatment, and postoperative chemotherapy. In the past, external beam radiation therapy occupied a central role in ES treatment. However, the frequency of postradiation sarcomas (Fig. 3.125a, b) in protocol survivors of several institutions has led many therapists to avoid radiation therapy whenever surgery is a viable option [266, 270].

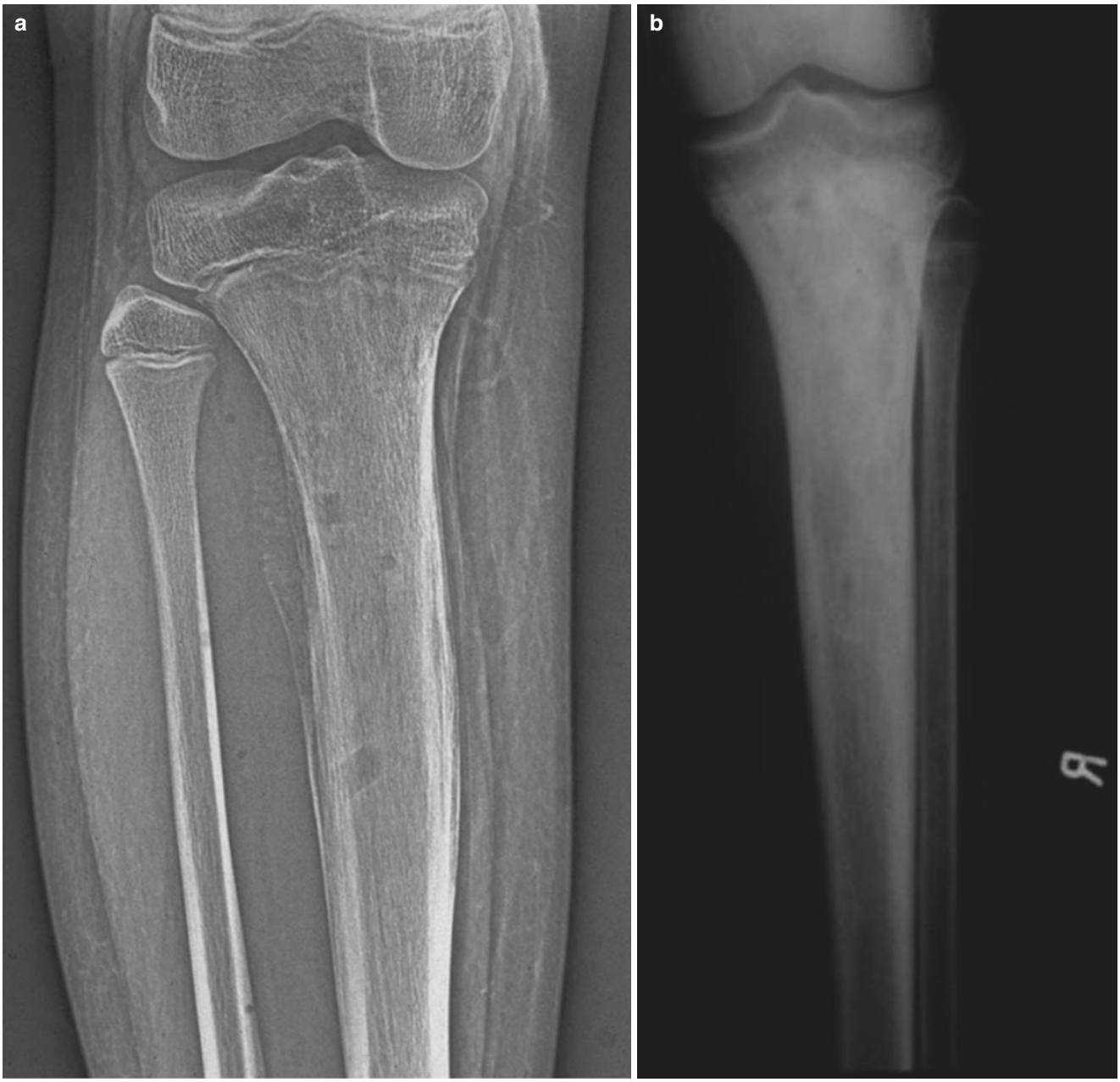

Fig. 3.125 Ewing's sarcoma. (**a**) Plane film (AP) of Ewing's sarcoma at initial presentation. The plane film shows a large mixed lytic/blastic lesion involving the tibial diaphysis with an overall moth-eaten permeative pattern and periosteal onion-skinning. (**b**) Plane film (AP) of "Ewings's sarcoma" 12 years following multi-agent chemotherapy and external beam radiation therapy to the primary tumor. However, the plane film now shows a largely radiopaque tumor involving the tibial metadiaphysis. The subsequent lesion is a post-radiation osteosarcoma. (Courtesy of A. Kevin Raymond, M.D.)

The pathologist's role in specimen management is similar to that in osteosarcoma: establish the diagnosis and subsequently evaluate the extent of disease establish the adequacy of resection margins and evaluate response to preoperative chemotherapy. Although ≥90% tumor necrosis is considered a good response to preoperative therapy, the relationship between response to therapy and ultimate survival is not necessarily as linear as seen with OS [4].

Prognosis in ES is a function of complex interrelationship of factors: tumor size/volume, location, stage, patient age, and response to preoperative therapy. Bad prognostic factors include large tumor, axial localization, older patient, poor response to preoperative therapy, early relapse, and clinically evident systemic metastases on presentation. Currently, the expected survival in ES treated with contemporary multimodality therapy is 65–80% [1, 4, 19].

Histopathology

ES forms a mass lesion originating within the medullary cavity or on the cortical surface, with cortical infiltration and tumor extension from one compartment into others. From low power, ES appears as a relatively homogeneous, royal blue sheet of small cells (Fig. 3.126a–d). At the tumor/normal interface, tumor insinuates between and around pre-existing trabecula of cancellous bone as well as infiltrating haversian systems and Volkmann's canals of cortex. Ultimately tumor causes destruction of both cancellous and cortical bone. Tumor extends into subperiosteal soft tissues and ultimately may invade through periosteum into true soft tissue.

Tumor necrosis may be present and can be highly variable. In neglected larger lesions, tumor necrosis can be extensive and viable tumor confined to small perivascular collars and nests, the feature that led Ewing to propose endothelial origin of the tumor bearing his name [266, 267].

Viable tumor is made up of sheets of small cells that are 2–3 times the size of a lymphocyte with extreme cytological monotony, every neoplastic cell closely resembling every other cell (Fig. 3.126a–d). Viable cells consist of well-defined round to oval nuclei with sharply circumscribed, smooth, thin nuclear membranes encompassing nuclei with finely divided, uniform euchromatin. Occasional small nucleoli may be present. Despite the growth characteristics of ES, mitoses are not frequently detected. When identifiable, cytoplasm tends to be minimal, consisting of a very thin rim of ill-defined minimally eosinophilic or clear material surrounding the nucleus. There may be some cytological variability in the form of sheets of "light staining" cells as described, with occasional scattered hyperchromatic "dark" apoptotic cells. In a minority of cases, the cells of ES can be found to encircle small amounts of central eosinophilic material imparting a rosette-like appearance suggesting neural differentiation (Fig. 3.127). These cases may also show some immunohistochemical properties suggestive of neural differentiation, some staining with NSE or CD-57 (Leu-7).

Special studies of progressive sophistication have been an integral component of small cell pathology for decades. Depending on a number of parameters (e.g., fixation), ES has evidence of intracytoplasmic glycogen (i.e., PAS-positive, diastase-sensitive material) and an absence of stainable intercellular/interstitial tissue, i.e., negative reticulum in almost all cases (Fig. 3.128a–c). However, the presence of membranous immunostaining with CD-99 has become a useful sen-

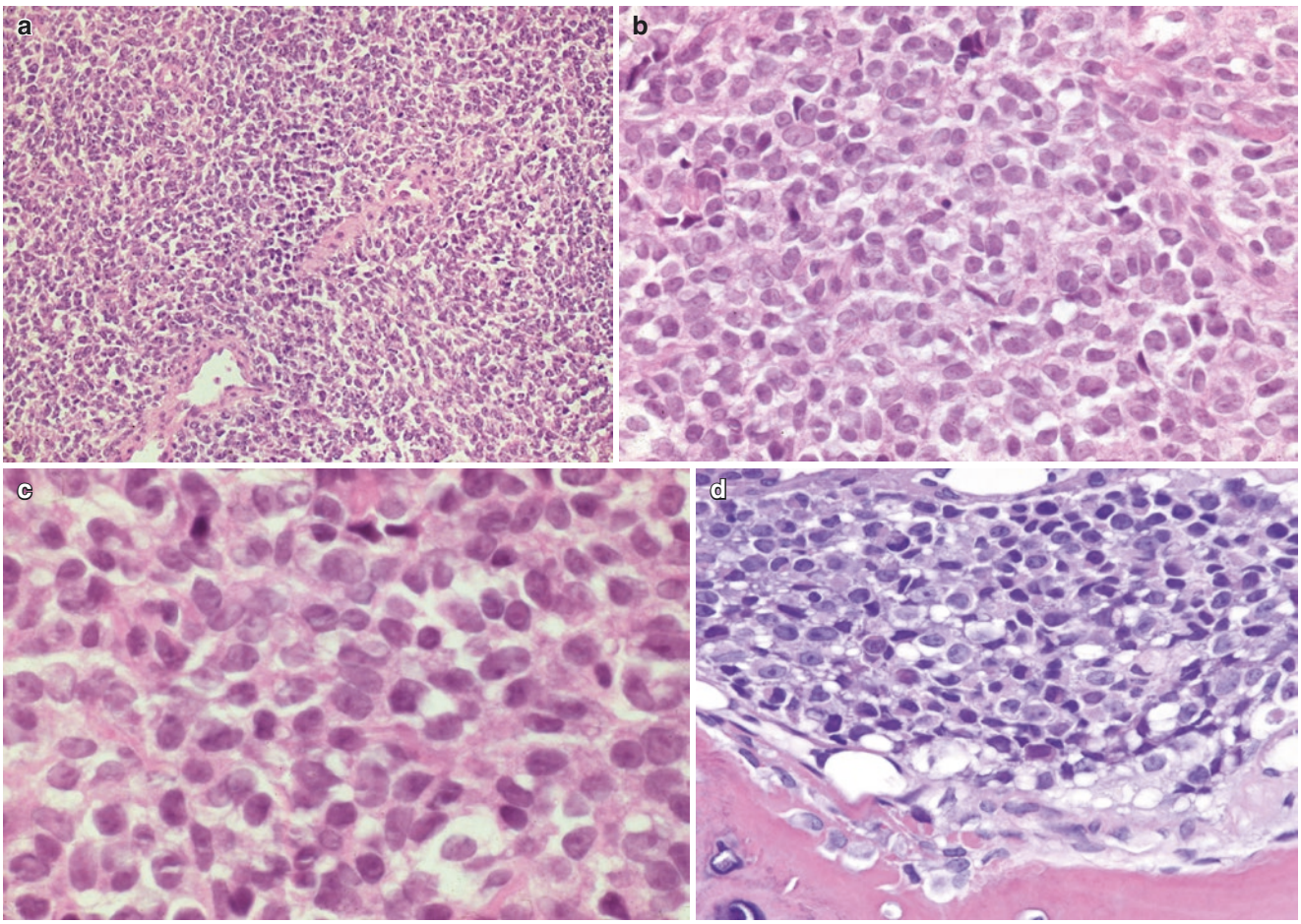

Fig. 3.126 Ewing's sarcoma. (**a**, **b**) Ewing's sarcoma consists of sheets of neoplastic small cells that in some cases may show evidence of "*rosette*" formation (H&E. (**a**) 40×, (**b**) 100×). (Courtesy of A. Kevin Raymond, M.D.)

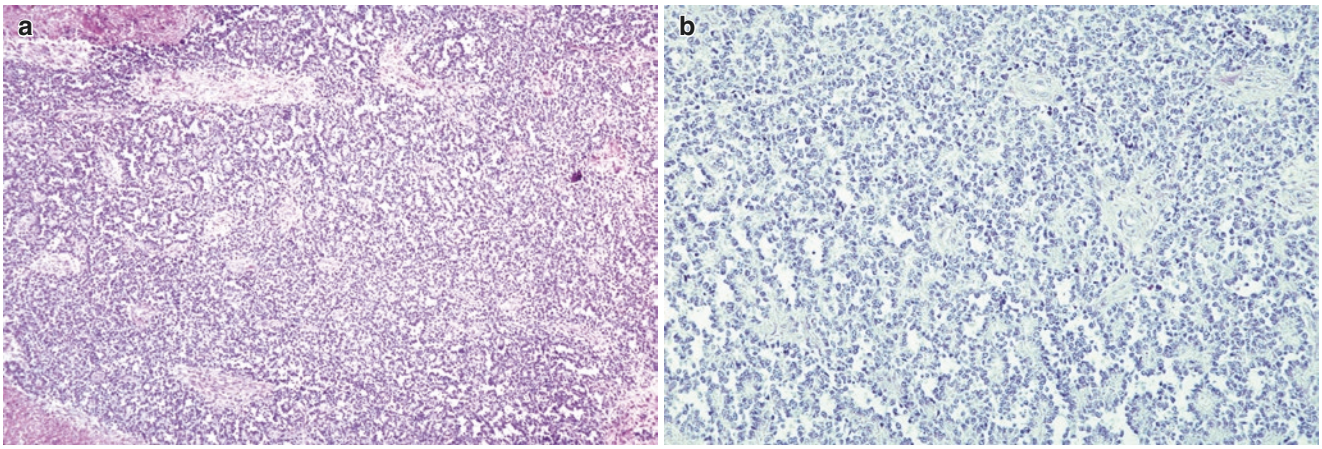

Fig. 3.127 Ewing's sarcoma. (**a**, **b**) Low Ewing's sarcoma consists of sheets of neoplastic small cells with extensive rosette formation (H&E, (**a**) 40×, (**b**) 100×). (Courtesy of A. Kevin Raymond, M.D.)

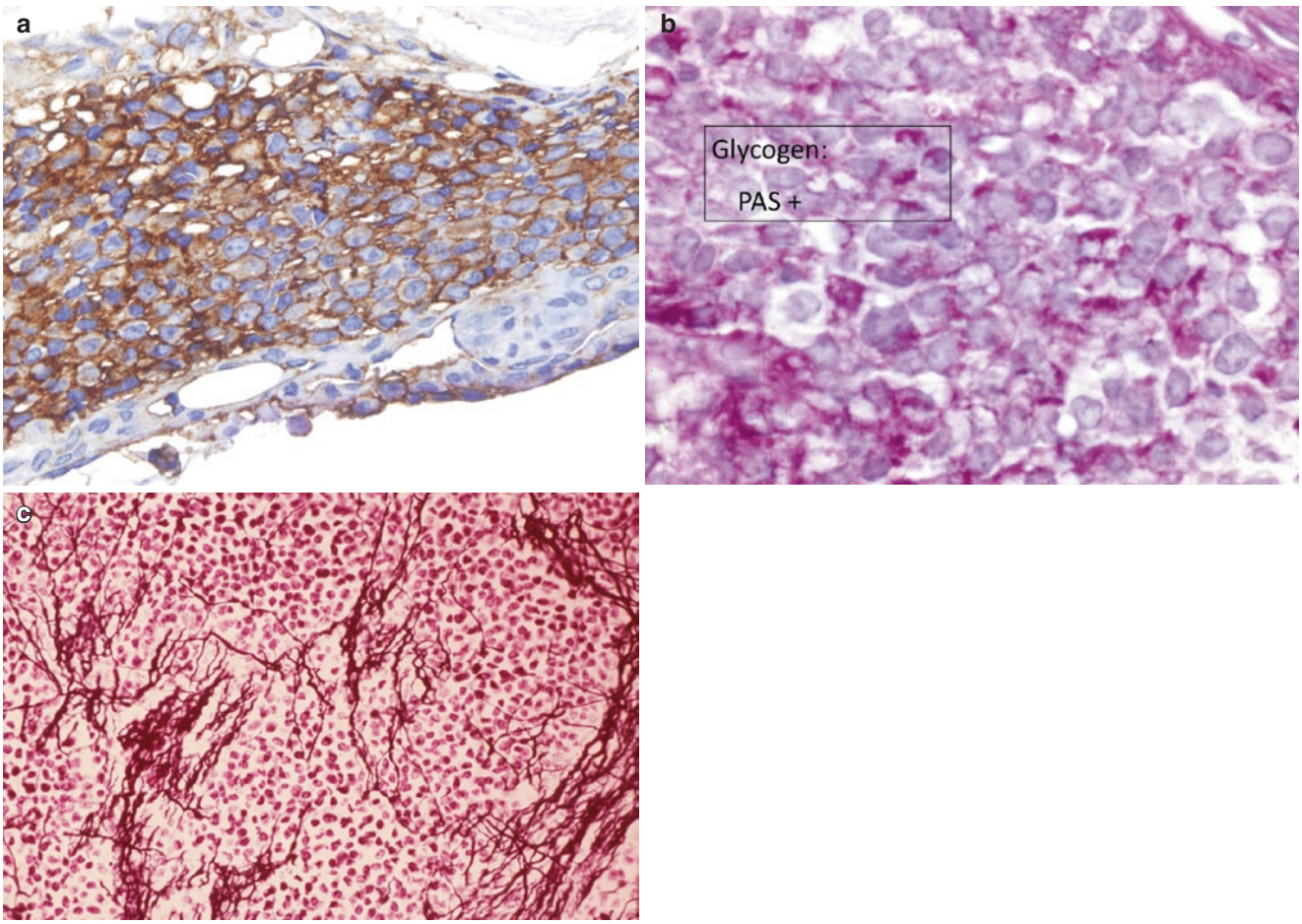

Fig. 3.128 Ewing's sarcoma. (**a**) Immunohistochemical staining shows diffuse membrane pattern for CD99 in Ewing's cells (CD99. 200×). (**b**) ES shows positive PAS staining (diastase sensitive) for intracytoplasmic glycogen (PAS. 400×) (courtesy of A. Kevin Raymond, M.D.). (**c**) ES shows positive reticulin staining confined to normal capillaries. There is no staining around individual cells (reticulin stain, 400×). (Courtesy of A. Kevin Raymond, M.D.)

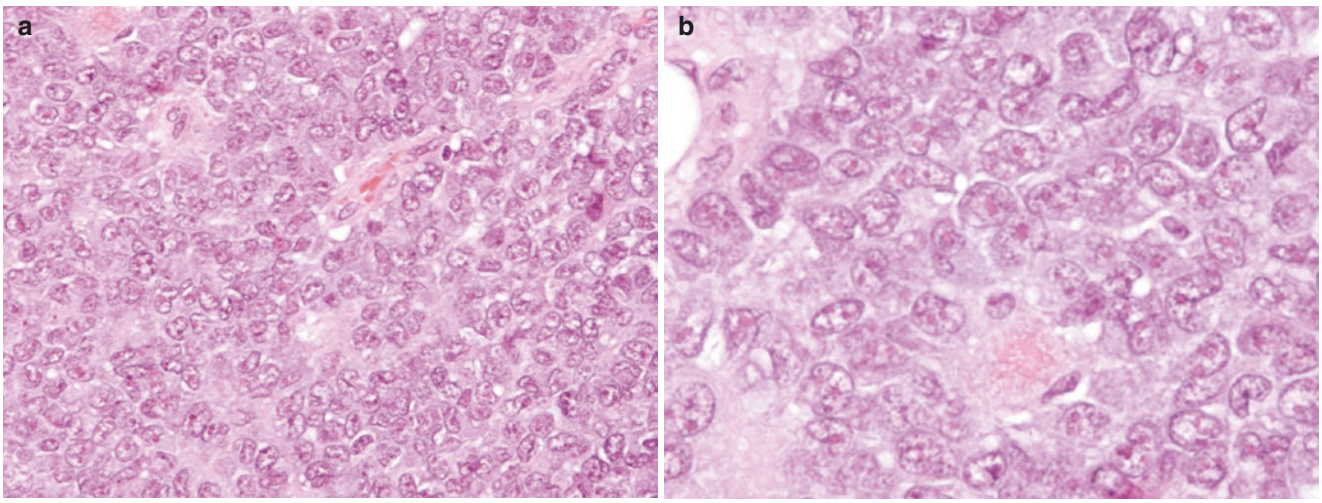

Fig. 3.129 Ewing's sarcoma. Atypical/large cell form. (**a**, **b**) Immunohistochemical ES composed of larger than expected neoplastic cells. The cell contain large nuclei many with large, angulated nuclei, coarsely clumped and vesicular chromatin. Cells have abundant cytoplasm. These findings can be seen in either atypical or large cell variant of Ewing's sarcoma or following sublethal chemotherapy effect (H&E (**a**) 200× (**b**) 400×). (Courtesy of A. Kevin Raymond, M.D.)

sitive, though non-specific, diagnostic tool in the evaluation of ES, especially when coupled with the less sensitive but more specific tests for Fly 1 [17]. However, at this point in time, it is not unreasonable to consider detection of the appropriate balanced chromosomal translocations as the standard of care: t(11;22)(q24,q12) or t(21;22)(q22,q12) and their consequent fusion proteins EWSR1-FLI-1 and EWSR1-ERG [4, 19, 271].

Although fairly stereotypical, there is some spectrum of histological findings in ES. In cases of so-called *large cell Ewing's sarcoma* or *atypical Ewing's sarcoma* [17, 272], neoplastic cells tend to be somewhat larger; nuclei are larger and cytoplasm is significantly more abundant. The nuclei are less monomorphic with angulation, nuclear membrane thickening, chromatin clumping and frequently prominent nucleoli. The results of special studies are inconsistent in large cell Ewings sarcoma. Similar findings can be seen when response to preoperative chemotherapy is suboptimal (Fig. 3.129). There are also cases in which Ewing's cells are arranged in an organoid pattern separated by connective tissue and potentially immunoreactive for cytokeratin: so-called adamantinoma-like Ewing's sarcoma (Fig. 3.130).

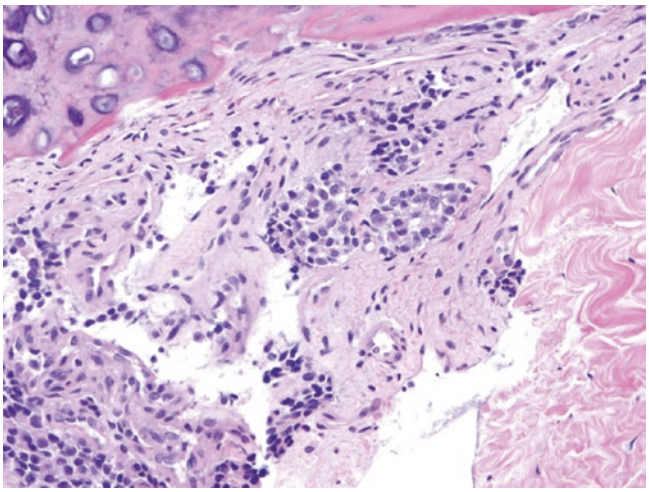

Fig. 3.130 Ewing's sarcoma. Adamantinoma-like Ewing's sarcoma. Ewing's cells form small epithelioid and gland-like aggregates (H&E, 100×). (Courtesy of A. Kevin Raymond, M.D.)

Gross Pathology

In the absence of preoperative therapy or secondary degenerative changes (e.g., fracture, necrosis), the gross appearance of ES is the quintessential fish-flesh sarcoma. Currently, intact viable tumor is a rare specimen (Figs. 3.131 and 3.132a, b) with needle or open biopsy more probable. The tumor cut surface is smooth, homogeneous, sickly-white to beige to pale-tan, and soft though compressible. Tumor luster imparts a wet veneer. Foci of necrosis, whether biological or therapeutic, are matt-yellow and granular. In long bones of the appendicular skeleton, tumor tends to involve the metaphysis, diaphysis, or both (i.e., meta-diaphysis). Tumors tend to be large and may involve more of the medullary cavity than expected. Large extraosseous soft tissue components are typical of ES. Reactive bone may be present in any number of ways including fine layers of periosteal new bone formation, so-called *onionskinning*.

Radiology

The plane film appearance of ES has a very broad spectrum ranging from purely radiolucent to radiopaque mimicking the sunburst appearance of OOS. However, ES tends to form

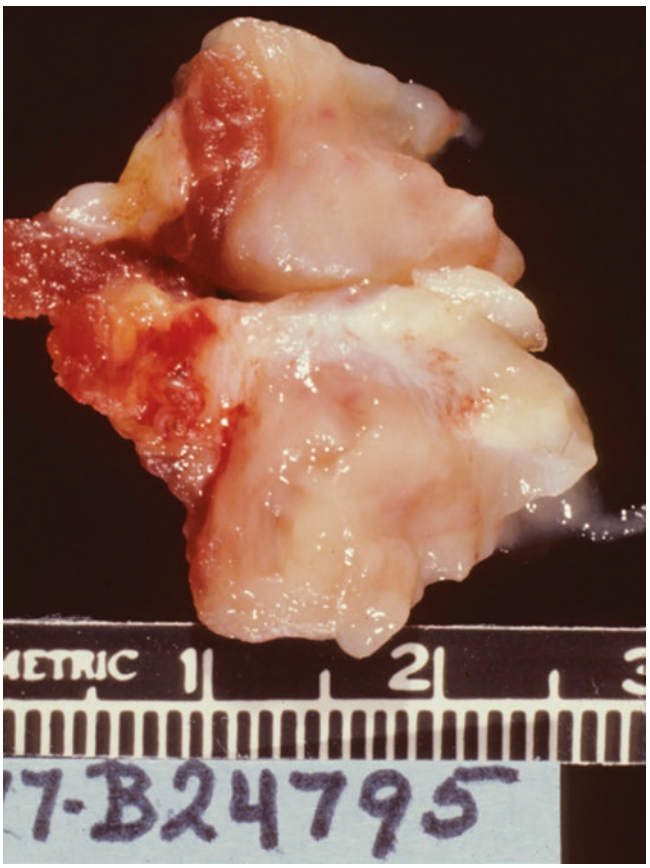

Fig. 3.131 Ewing's sarcoma: open biopsy specimen. Tumor is composed relatively soft beige to tan soft tissue. Notice how specimen has oozed fluid onto the glass suggesting a role for aspiration. (Courtesy of A. Kevin Raymond, M.D.)

a destructive, mixed lytic/blastic lesion (Figs. 3.125 and 3.132). The so-called *moth-eaten permeative* appearance is most frequent and radiographically correlates to small geographic areas of cortical destruction alternating with fine linear foci of cortical erosion.

Lesions of ES tend to be large with radiolucent soft tissue components frequently much larger than might be expected considering the extent of intramedullary involvement. Although perhaps an exaggeration, the *rule-of-75* is an old adage referable to ES and a warning not to underestimate the primary tumor size, i.e., 75% of ES tumors involve 75% of the bone of origin. CT and MRI better define the extent of intramedullary involvement as well as the overall extent of disease. Similarly, imaging studies can be used to follow response to preoperative therapy.

Although not absolute, when attempting to discriminate between ES and primary lymphoma of bone (PLB), the presence of a disproportionally large soft tissue mass favors a diagnosis of ES. In contrast, minimal or absent soft tissue mass in a small cell tumor favors a diagnosis of PLB [273].

Fibrous Neoplasia

Introduction

Fibrous neoplasia has long been a most enigmatic and difficult portion of bone pathology. Lacking classifying matrix and specialized structures (e.g., vasoformative capacity), the spindle-cell group has been a long source of diagnostic frustration. However, with the development of increasingly specific and sensitive immunohistochemical techniques together with the potential for cytogenetic contribution and molecular definition, new doors are opening.

For the purposes of this chapter, fibrous neoplasia has been subdivided into three major groups (see Tables 3.8 and 3.9):

Fibrohistiocytic lesions are those tumors that have a seemingly bimorphic cell population. The basic population consists of typical spindle cells with elongate nuclei accompanied by elongate cytoplasm of varying amounts. Alternating with these are cells that are more round to oval and an overall histiocytoid appearance or even infiltrated by histiocytes. The benign lesions are the histologically similar metaphyseal fibrous cortical defect, nonossifying fibroma and benign fibrous histiocytoma. The malignant counterpart is malignant fibrous histiocytoma.

Fibrous lesions have historically included periosteal desmoid, desmoplastic fibroma, and fibrosarcoma. Although there may be an exception somewhere, the so-called periosteal desmoid, which occurs with some frequency in the area of the posterior aspect of the distal femur, is not a neoplastic process. Rather it represents a response to trauma. It is the consequence of tendon evulsion. *Desmoplastic fibroma* (aka desmoid) is a benign collagen producing spindle-cell lesion. In contrast, *fibrosarcoma* represents spindle-cell malignancy in its most elemental form.

Fibro-osseous lesions include fibrous dysplasia and osteofibrous dysplasia. Although histologically similar, they appear to represent two very different lines of tumor development.

The current presentation gives a historical approach to classification of malignant spindle-cell neoplasia. The use of precise light microscopic criteria results in groups of patients with a number of consistent associations and is useful for treatment options. However, there are a large number of patients who do not fall within these definitions. As a result, many of these cases are labeled forms of *unclassified spindle-cell* or *unclassified high-grade sarcoma.* However, a number of studies have shown that with the appropriate use of advancing, increasingly specific immunohistochemical studies, cytogenetics and molecular analysis insights are possible into more accurate and appropriate diagnosis. Of interest, there appears to be increasing evi-

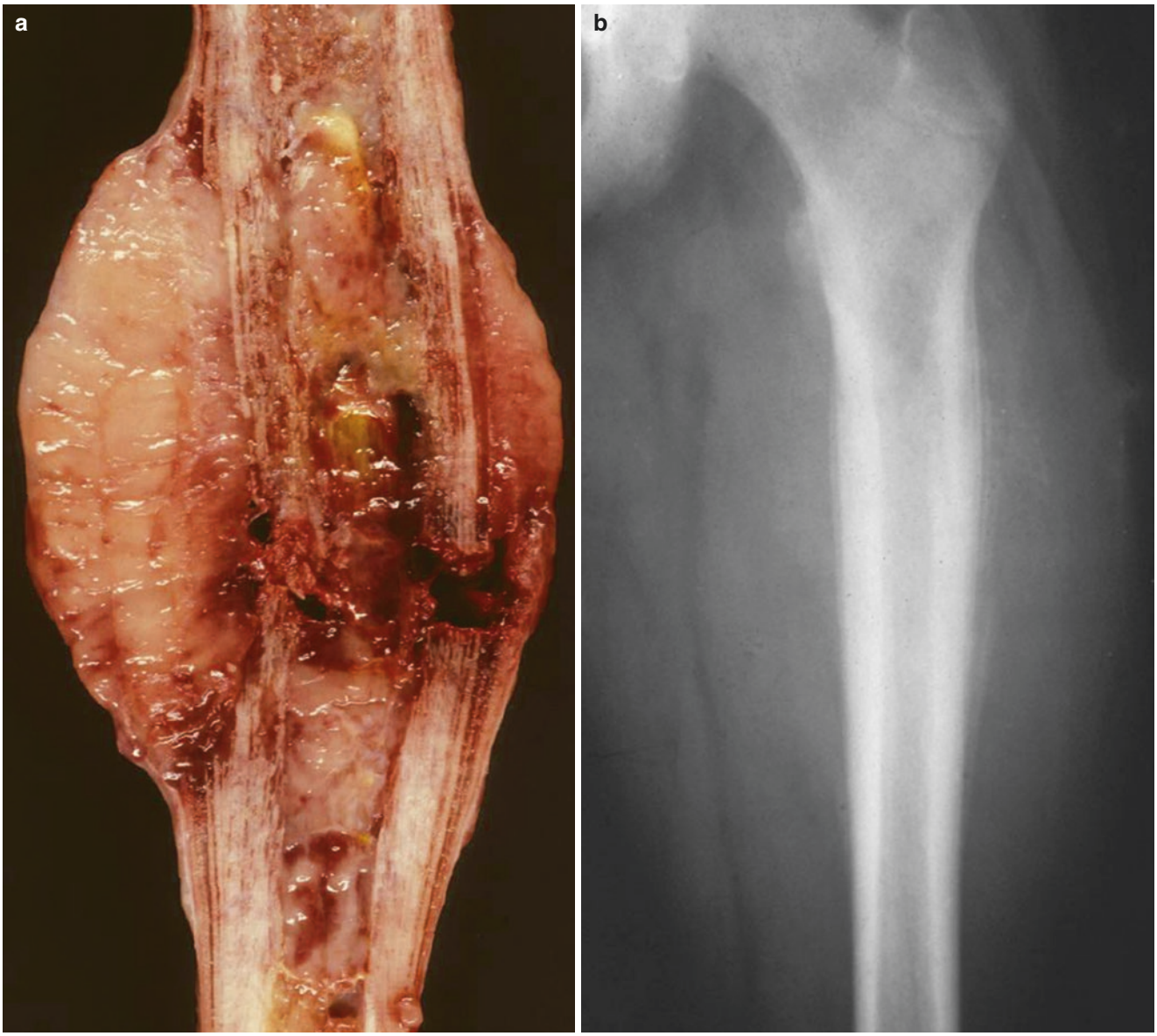

Fig. 3.132 Ewing's sarcoma. (**a**) Gross specimen: ES form a fish flesh-like intramedullary mass that has extended into overlying soft tissues. There are fine longitudinal layers of reactive bone formation, i.e., onionskinning. Pathological fracture is present. (**b**) Plane film (AP) shows a large mixed lytic/blastic lesion involving the femoral diaphysis with an overall moth-eaten permeative pattern and onionskinning pattern. Note the extremely large soft tissue mass. (Courtesy of A. Kevin Raymond, M.D.)

Table 3.8 Fibrous neoplasia

Fibrohistiocytic	Fibrous	Fibro-osseous
Metaphyseal fibrous cortical defect	Cortical irregularity syndrome (periosteal desmoids)	Fibrous dysplasia
Nonossifying fibroma	Desmoid	Osteofibrous dysplasia
Benign fibrous histiocytoma	Desmoplastic fibroma	
Malignant fibrous histiocytoma	Fibrosarcoma	

Table 3.9 Secondary fibrosarcoma: predisposing conditions

Condition	Number of patients
Radiation therapy	46
Paget's disease	7
GCT without radiation therapy	4
Bone infarct	3
Fibrous dysplasia	1
Ameloblastic fibroma	2
Odontogenic myxoma	1
Total	64

dence of forms of smooth muscle differentiation in many of these up-until-now unclassifiable tumors. To be sure, there will be changes in diagnosis; the issue is the possible endpoint(s) [264, 274].

Desmoplastic Fibroma

Introduction

Desmoplastic fibroma (DF) is a rare, benign, intramedullary spindle-cell neoplasm most frequently involving the mandible and femur. It is a tumor of destructive local growth and a penchant for relapse after incomplete therapy, but without the intrinsic capacity for metastases [1, 10, 20, 275].

Clinical

Since the original description of DF, attributed to Jaffe in 1958 [276], less than 270 cases have been reported in the world's accumulated literature [277]. DF most frequently affects patients in the second and third decades of life. Gender distribution is variously reported in the small number of reported series and case reports but does not appear to have a dramatic preference. The bones most frequently affected are the jaw, skull, femur, and pelvis.

For many years, there were questions and disagreements concerning the terms *desmoplastic* fibroma and *desmoid* as they applied to bone, two entities versus two terms for a single entity. Recent publications have been entitled desmoplastic fibroma but use the two terms interchangeably within the text, two terms for one entity [275].

The clinical history tends to be relatively non-specific, localized pain with or without accompanying swelling. The natural history of DF is one of progressive, local, destructive growth with eventual invasion through cortex and extension into overlying soft tissues. Metastases have not been reported.

The treatment of choice is complete surgical tumor extirpation. Intralesional, so-called marginal resection, is followed by near-uniform local relapse and is recommended only in those cases in which more complete therapy is not possible. The treatment of choice is wide local resection with uninvolved margins. There appears to be no effective adjuvant therapy at this time.

The small number of cases available for cytogenetic and molecular studies makes unequivocal interpretation difficult. But although DF shares many morphological parameters with primary soft tissue desmoid, the role of the ß-catenin pathway does not appear to be resolved [10, 277, 278].

Histopathology

The cytological/histological features of DF [275, 276, 279] are those of a proliferation of minimally atypical, innocuous, slender spindle cells. The nuclei are somewhat variable: round to oval or fusiform. The chromatin is finely divided, and there are few if any mitoses. The cytoplasm is eosinophilic, linear, ill-defined, and may be wavy. The cells are accompanied by abundant independent fibers and bundles of dense collagen. The cells and collagen are oriented in either a linear or swirling configuration (Figs. 3.133 and 3.134). No matrix other than residual normal bone or the sequelae of pathological fracture is present. Tumor may erode cortex and may extend into soft tissue.

Gross

Grossly, DF consists of a well-defined mass, metaphyseal in long bones (Fig. 3.135). The appearance of the cut surface is a function of the amount and distribution of collagen. At one end of the spectrum, tumors may be firm to rubbery, homo-

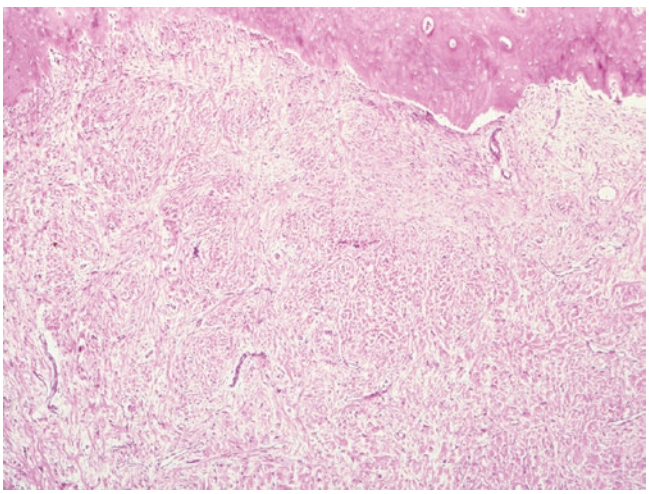

Fig. 3.133 Desmoplastic fibroma. Tumor is composed of innocuous short, slender spindle-cells accompanied by abundant extracellular collagen. Tumor is eroding cortical bone (H&E. 20×)

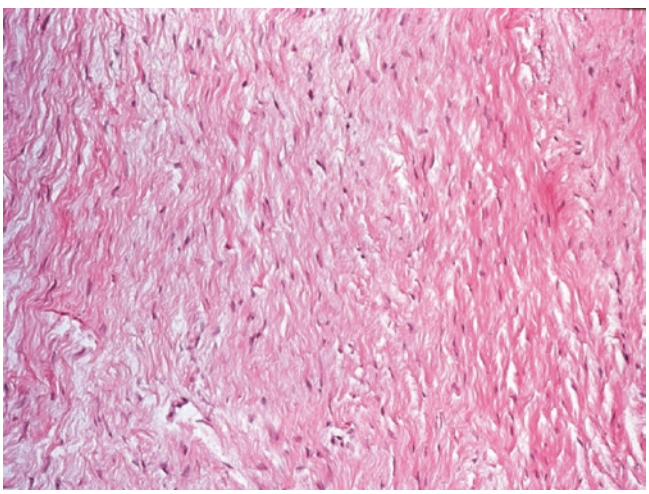

Fig. 3.134 Desmoplastic fibroma. Minimally atypical spindle-cells accompanying enormous amounts collagen (H&E. 100×)

Fig. 3.135 Desmoplastic fibroma. (**a**) Grossly tumor is composed of beige to pale-tan firm homogeneous, rubbery tumor involving the proximal tibial metaphysis with extension into proximal tibial epiphysis. The cortical defect represents an open biopsy site. (**b**) Radiographically tumor forms an eccentric, radiolucent mass involving the proximal tibia metaphysis with extension into contiguous epiphysis. Uneven cortical destruction has resulted in alternating radiodense and radiolucent areas imparting the appearance of pseudotrabeculations

geneous, and beige to tan. At the other end of the spectrum, the cut surface may be fibrous or swirling, yellow-white, and may have a distinctly hard "woody" consistency. Advanced tumors may thin or even erode through cortex and extend into overlying soft tissue.

Radiology

The radiographic appearance [275, 277, 279] of DF is that of a well-defined, radiolucent lesion, metaphyseal when involving long bones (Fig. 3.135). The cortex may be thinned and expanded. Bone erosion tends to be uneven resulting in pseudotrabeculation that may be seen on plane films and CT. CT and MRI are best for evaluating extent of disease and therefore surgical planning. The reported MRI findings in DF are somewhat unusual; tumor tends to hypointense on *both* T1- and T2-weighted images [20, 280].

Fibrosarcoma

Definition

Fibrosarcoma (FS) is defined as an intermediate- to high-grade spindle-cell sarcoma in which the neoplastic cells are disposed in interlacing fascicles and have a high degree of anaplasia but low level of pleomorphism. Tumor does not produce matrix nor is there evidence of other specialized differentiation.

Clinical

Accurate contemporary generalizations concerning FS are difficult to assess since few institutions have used this diagnosis with any frequency since the description of malignant fibrous histiocytoma. At the same time, review of cases utilizing contemporary investigatory techniques has resulted in reclassification of as many as 25% of cases [264, 274].

Two institutions have a long history of consistent use of the FS diagnosis, and most generalizations concerning FS are drawn from that data [20, 281, 282]. As defined, FS accounts for 4% of primary malignant bone tumors with osteosarcoma being seven times as common and MFH being one-third as frequent as FS. The demographics of FS and MFH are similar. Other than being rare in the first decade, the age distribution forms a bell-shaped curve with a peak in the fourth to seventh decades. Males and females are affected near equally. The sites most frequently involved are the distal femur, proximal tibia, pelvis, proximal humerus, and jaws. Some 25% of FS are secondary sarcomas with underlying conditions including prior radiation therapy, Paget's disease of the bone, giant cell tumor of bone, bone infarct (Table 3.8), and as the high-grade component of dedifferentiated sarcomas [17, 20, 283].

Pain, swelling, and mass are the most frequent presenting symptoms and tend to be of short duration, weeks to months. In secondary tumors, these new symptoms are superimposed on those of the underlying condition.

The natural history of FS is one of local growth, frequent pathological fracture, and lethal systemic metastases. Historically, the treatment of choice has been complete surgical extirpation, usually amputation. Survival is related to tumor grade. Mayo Clinic data show the overall 5-year survival is reported as 34%, while 5-year survival in grade one, two, and three tumors is 64%, 41%, and 23%, respectively [20]. Data from the Rizzoli Institute indicate an overall 5-year survival of 42% with low-grade and high-grade tumors having 5-year survivals of 83% and 34%, respectively [283]. The impact of alternative therapy is not known.

Histopathology

In many ways, FS is a sarcoma defined by an absence of findings. Although collagen may be produced by the neoplastic cells, it is a malignant spindle-cell tumor that does not produce a specialized matrix, i.e., osseous or cartilage. The neoplastic cells do not form specialized structures (e.g., vessels) or possess a specific identifying immunohistochemical profile. In essence, it is a diagnosis of exclusion [10, 17]. Cohesive tumor sheets infiltrate adjacent cancellous and cortical bone. Ultimately, tumor extends into overlying soft tissues.

The "spindle cells" are fusiform-shaped and arranged in interweaving bundles that frequently oppose one another at a 45° angle, the so-called "*herringbone*" pattern (Fig. 3.136) [283]. The nuclei range from fusiform cigar-like with blunted or pointed ends, to needle-like to oval and various combinations therein. Inasmuch as cells form opposing bundles, nuclei in cross section are a frequent finding, and they may appear round. Although some nuclei may be hyperchromatic secondary to irregularly condensed chromatin, equal numbers may have finely distributed chromatin. Mitotic activity is highly variable and atypical forms may be present. Cytoplasm can be highly variable. Some cells have abundant dense cytoplasm; however most have wispy, linear eosinophilic cytoplasm running parallel to the long axis of the nucleus. Cells cut in cross section may appear to have minimal cytoplasm and could be confused with a form of small cell malignancy. Grading is somewhat subjective, based on cellularity, degree of atypia, and mitotic index; most tumors tend to be intermediate to high grade. There may be superimposed necrosis, reactive changes, and inflammation. In addition, there may be residual changes of any underlying pathology, e.g., bone infarct and Paget's disease of bone.

Gross Pathology

The gross appearance of FS is a function of cellularity, collagen content, grade, secondary changes, and any previously existing pathology. Low-grade tumors tend to have a relatively high collagen content that causes them to be hard, firm, or rubbery and have a swirling or trabeculated cut surface. These low-grade lesions tend to be off-white to pale yellow-white. Higher-grade lesions tend to be softer, fleshy and tend from beige to tan.

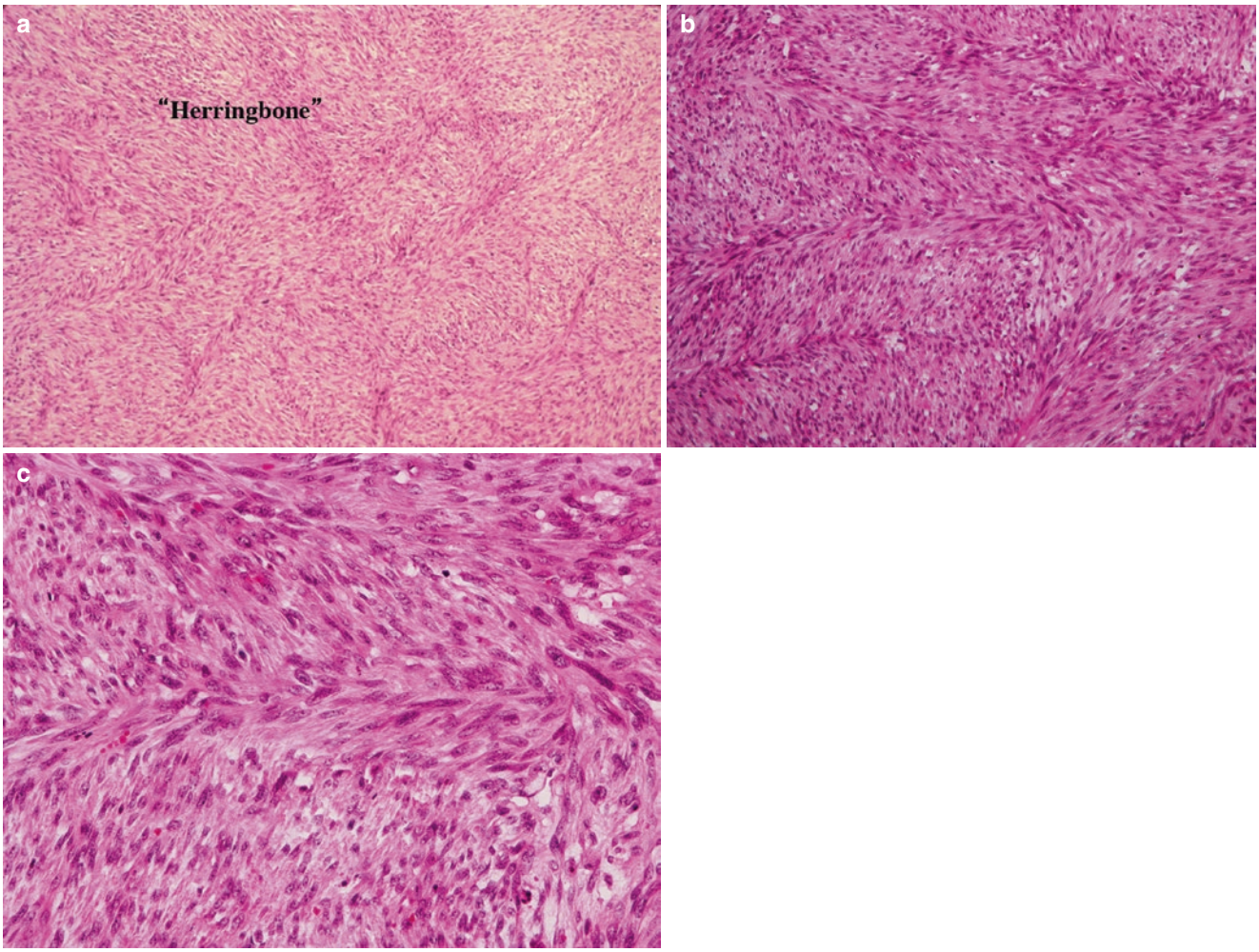

Fig. 3.136 Fibrosarcoma. (**a**–**c**). The tumor consists of malignant spindle cells arranged in bundles and fascicles that intersect at 45° angles; so-called *herringbone pattern*. There is minimal pleomorphism but a high degree of anaplasia. Numerous mitoses and apoptotic cells are present (H&E, 40×, 200×, 400×). (Courtesy of A. Kevin Raymond, M.D.)

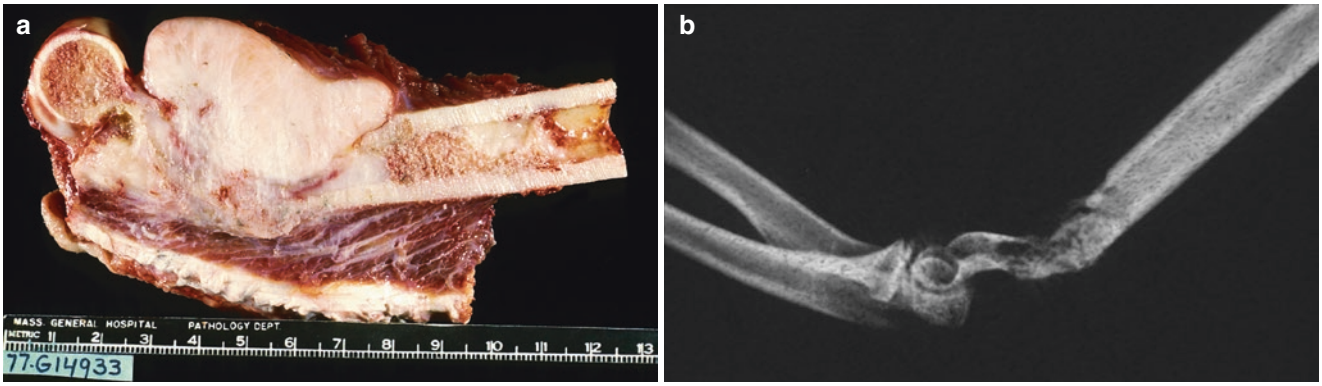

Fig. 3.137 Fibrosarcoma. (**a**) Tumor forms a variegated mass within the distal humeral metaphysis. The rubbery intraosseous component is cream-colored to white with superimposed changes of necrosis and hemorrhage. Tumor has extended through cortex into overlying soft tissue where it forms an off-white, rubbery mass with a striated to smooth cut surface (gross specimen). (**b**) Plane film (lateral): tumor forms and ill-defined, destructive radiolucent replacing the distal humerus. (Courtesy of A. Kevin Raymond, M.D.)

Fig. 3.138 Fibrosarcoma. Plane films (AP and lateral): tumor forms a well-defined purely radiolucent lesion involving the proximal metadiaphyseal tibia. The tumor has an infiltrative margin resulting in a long transition zone

Fig. 3.139 Fibrosarcoma. (**a**) CT (trans-axial plane) shows a destructive lesion involving the proximal humeral metaphysis. Tumor is ill-defined with infiltration of adjacent cancellous bone and destruction of overlying cortex with an ill-defined soft tissue component (same case as 3.138). (**b**) MRI T1-weighted image, sagittal plane. Tumor forms a hypointense lesion involving the proximal tibia with cortical destruction and extension into soft tissue. (Courtesy of A. Kevin Raymond, M.D.)

Degenerative changes result in foci of hyperemia, hemorrhage, necrosis, and myxoid degenerative changes (Fig. 3.137).

Radiology

Plane films and CT show FS to be a purely osteolytic lesion without evidence of tumor-produced matrix (Figs. 3.137, 3.138, and 3.139). Intermediate- to high-grade lesions tend to have a broad infiltrative transition zone, and cortical erosion is frequent. MRI and CT may be used to better define details of imaging features as well as evaluating extent of disease.

Metaphyseal Fibrous Cortical Defect, Nonossifying Fibroma, and Benign Fibrous Histiocytoma

Definition

Sharing a common set of histological findings, metaphyseal fibrous cortical defect (MFCD), nonossifying fibroma (NOF), and benign fibrous histiocytoma (BFH) are diagnostic entities defined by clinical and radiographic criteria [1, 20, 268]. MFCD is the term employed when this common lesion is small and confined within long bone, metaphyseal

cortex. Larger lesions that have eroded through endosteal cortex and involve medullary cavity are referred to as NOF, while BFH is the name applied to those rare lesions that occur in older, frequently asymptomatic patients and arise in odd locations (e.g., epiphyses) or flat bones.

Clinical

MFCD was first described by Jaffe and Lichtenstein in 1942 [284]. Together with NOF it is a lesion primarily seen in patients in the first three decades of life: in particular the second decade and to a lesser degree the first and third decades. The incidence in females and males is roughly equal. MFCD/NOF most frequently arise in the metaphyses of appendicular long bones, in particular the distal femur, distal tibia, and proximal tibia. MFCD/NOF may be multifocal [1, 268, 285]. Multiple MFCD/NOFs can be seen in neurofibromatosis type I and are a component of the Jaffe-Campanacci syndrome [285, 286].

The vast majority of MFCD/NOF is asymptomatic and detected during imaging studies performed for unrelated reasons. While the true incidence of MFCD/NOF is unknown, one study has estimated that 30–40% of children have one or more lesions [268].

Although unproven, the natural history of MFCD appears to follow one of the three courses: they are self-limited and remain the same (Fig. 3.140), they undergo spontaneous regression at the time of skeletal maturity (Fig. 3.141), or they progress to involve the medullary cavity, i.e., NOF. In the typical, uncomplicated case, observation with expectation of lesion resolution at skeletal maturity is the usual therapeutic avenue. When lesions progress, are symptomatic, or there is likelihood of pathological fracture (i.e., so-called pending fracture), surgical intervention is indicated [287, 288]. Curettage and packing/cementation (Fig. 3.142) are generally sufficient [289]. However, in rare cases with very large lesions complicated by pathological fracture, resection may be considered (Figs. 3.143 and 3.144).

In contrast, with less 100 described cases, BFH is a very rare lesion [268, 288]. Although they may affect patients of any age, most are adults. BFH may involve long bones, but when they do, they tend to involve the diaphysis, metaphysis, or contiguous epiphysis (Fig. 3.145). BFH occurs with some frequency in the bones of the pelvis and spine. The natural history is one of continued local growth with danger of pathological fracture. Curettage is the treatment of choice. Although questioned [268], there are rare reports of secondary malignancy [290]. However, at best it is extremely rare. Although too few to make sweeping statements, limited cytogenetic and molecular studies have been reported [291].

Pathology

Histologically, MFCD/NOF/BFH generally consists of a very heterogeneous cellular process in which a swirling population of innocuous spindle cells is the underlying lesion (Fig. 3.146a–c). The spindle-cell nuclei are round to oval to fusiform with well-defined nuclear membranes and finely dispersed chromatin. Small inconspicuous nucleoli and mitoses may be present; abnormal mitoses should be absent. The tumor cell cytoplasm tends to be abundant, eosinophilic, and ill-defined. Unaltered by degenerative changes, the neoplastic cells tend to be oriented in a "storiform" pattern (Fig. 3.146). Additional cellular elements are frequently present and may obscure the underlying pathology: red blood cells, osteoclasts, foamy macrophages, hemosiderin-laden macrophages, lymphocytes, as well as cellular debris and hemosiderin deposition. In addition, superimposed secondary aneurysmal bone cyst formation may be present (Fig. 3.147a–c).

Although speculative, a reasonable way of conceptualizing this potentially complex histological picture is to think in terms of benign storiform spindle-cell process (i.e., fibroma) that has undergone intralesional hemorrhage. The red blood cells break down releasing hemosiderin and lipids together with a variety of activating factors. The latter attract osteoclasts and inflammatory cells that ingest this material.

Inasmuch as most lesions are treated by curettage, and therefore covered in blood, the gross appearance of MFCD/NOF may be difficult to appreciate. The lesions tend to be tan to reddish-brown. The ovoid to lens-shaped lesions of MFCD are well-defined by surrounding rim of thinned, intact, residual cortical bone (Fig. 3.148). With further growth and erosion through cortex into medullary cavity, NOF retains the tan to reddish-brown qualities (Fig. 3.143). In addition, there may be yellow areas of varying sizes corresponding to lipid accumulations and red to reddish-black regions reflecting hemorrhage.

Radiology

MFCD forms an eccentric, destructive, radiolucent metaphyseal lesion. The interface with normal tissue is

Fig. 3.140 Metaphyseal fibrous cortical defect. Plane films (AP): the lesion forms a lytic intracortical lesion with a soap bubble configuration. There is a sclerotic interface. The images include the primary lesion (left) and 10-year follow-up. Initial lesion was an asymptomatic, incidental finding. (Courtesy of A. Kevin Raymond, M.D.)

Fig. 3.141 Metaphyseal fibrous cortical defect. The area of sclerosis (red arrow) represents a metaphyseal fibrous cortical defect that has undergone spontaneous involution and healing. (Courtesy of A. Kevin Raymond, M.D.)

Fig. 3.142 Metaphyseal fibrous cortical defect. The metaphyseal fibrous cortical defect that has been treated by curettage and packing with bone chips. (Courtesy of A. Kevin Raymond, M.D.)

well-defined and frequently sclerotic. The lesion itself is generally lobulated and has an overall "soap bubble" appearance. NOF shows similar features but on a larger scale as tumor erodes through cortex and involves the medullary cavity where it may extend to involve the diaphysis (Fig. 3.149).

CT and MRI may better define the extent of disease with the lesion being hypointense on both T1-weighted images and hypointense in most T2-weighted images. However, NOF shows various degrees of enhancement with contrast. The signal intensity and enhancement appear to be a function of the cellular and matrix composition [292–295].

Malignant Fibrous Histiocytoma: Unclassified High-Grade Pleomorphic Sarcoma

Definition

Malignant fibrous histiocytoma (i.e., MFH) is an aggressive intermediate- to high-grade spindle-cell sarcoma in which the neoplastic cells are characterized by a high degree of both anaplasia and pleomorphism while frequently organized in a swirling *storiform* pattern. Both the concept and terminology regarding MFH are in flux, and "unclassified high-grade pleomorphic sarcoma" is considered an alternative and perhaps preferred term by many.

Clinical

Originally proposed as a primary soft tissue tumor, MFH has been the topic of extensive publication since the 1960s [296, 297]. Suggested as a primary bone tumor by radiologists [298] and subsequently discussed by bone pathologists [299, 300], the appropriate classification of this group of

Fig. 3.143 Nonossifying fibroma. The nonossifying fibroma complicated by pathological fracture. Treated with open reduction and fixation. (Courtesy of A. Kevin Raymond, M.D.)

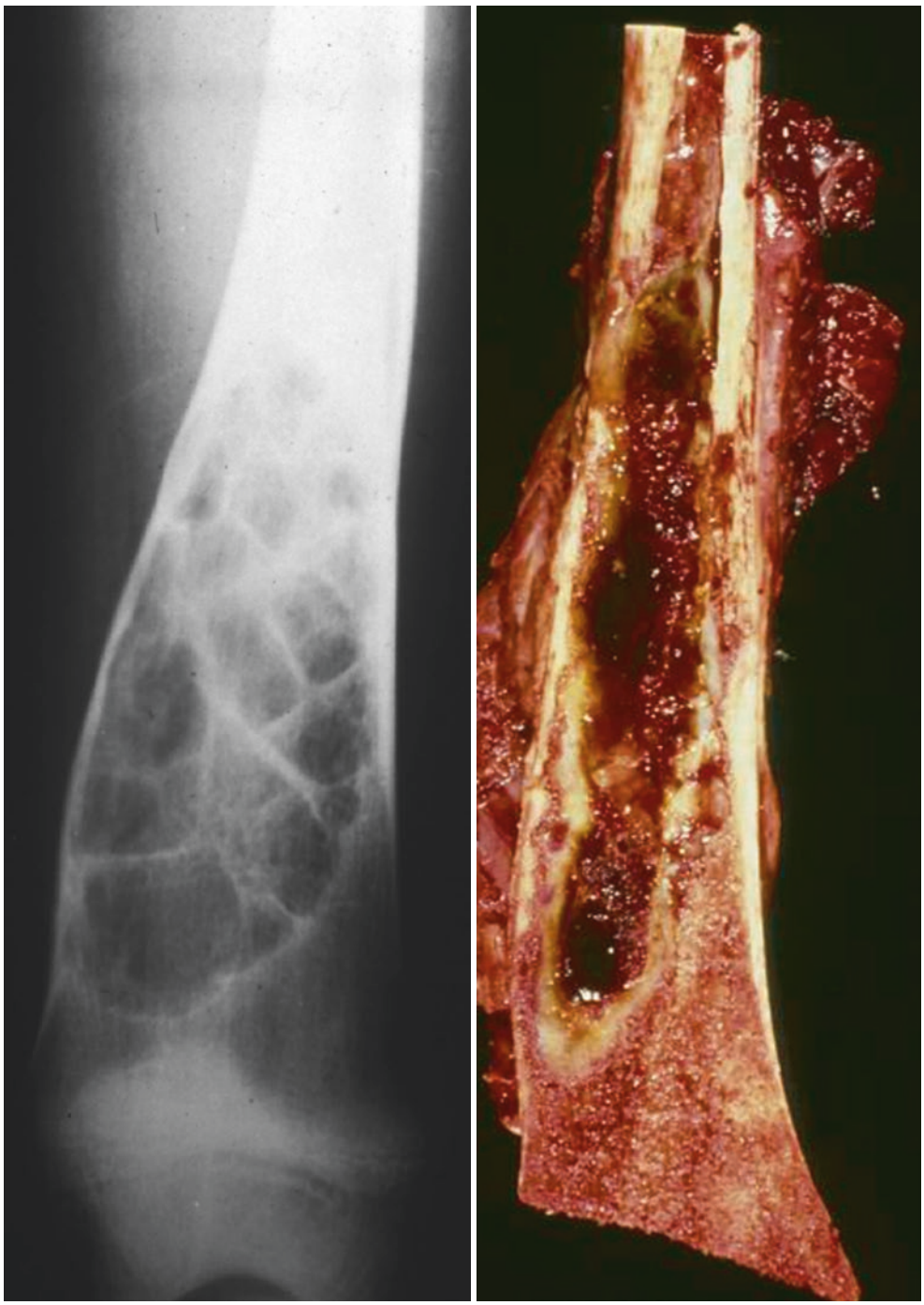

Fig. 3.144 Nonossifying fibroma. The overall features are similar to metaphyseal fibrous cortical defect; just larger. The lesion is radiolucent with a *soap bubble pattern* and sclerotic interface with normal bone. However, the lesion involves greater than 50% of the bone diameter; i.e., so-called *pending fracture*. (Courtesy of A. Kevin Raymond, M.D.)

Fig. 3.145 Metaphyseal fibrous cortical defect. (**a**) Innocuous spindle cells with round to oval nuclei and abundant eosinophilic cytoplasm. The spindle-cells are organized in a *storiform* pattern, consistent with fibroma (H&E. 40×). (**b**) Higher magnification of the spindle cells. The cells have round to oval nuclei with finely distributed chromatin and occasional mitoses. The cells have abundant cytoplasm, and there is extracellular collagen, consistent with fibroma (H&E. 200×) (**c**) Innocuous spindle cells in storiform pattern together with foamy macrophages and small numbers of lymphocytes, consistent with fibroma with nonspecific inflammatory changes (H&E. 200×) (Courtesy of A. Kevin Raymond, M.D.)

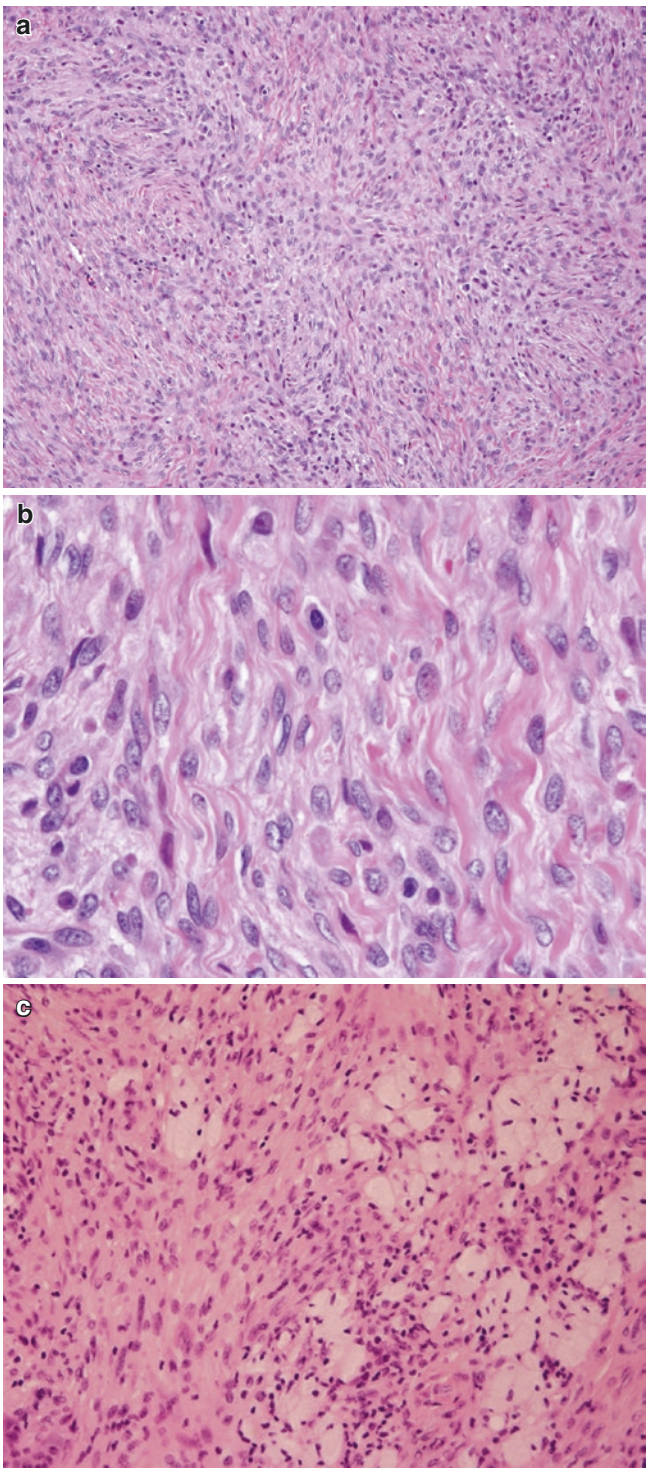

Fig. 3.146 Metaphyseal fibrous cortical defect. (**a**) Innocuous spindle cells with round to oval nuclei and abundant eosinophilic cytoplasm. The spindle cells are organized in a storiform pattern, consistent with fibroma (H&E, 40×). (**b**) High-grade higher magnification of spindle cells. The cells have round to oval nuclei with finely distributed chromatin and occasional mitoses. The cells have abundant cytoplasm, and there is extracellular collagen, consistent with fibroma (H&E, 200×). (**c**) Innocuous spindle cells in storiform pattern together with foamy macrophages and small numbers of lymphocytes. Consistent with fibroma with non-specific inflammatory changes (H&E, 200×). (Courtesy of A. Kevin Raymond, M.D.)

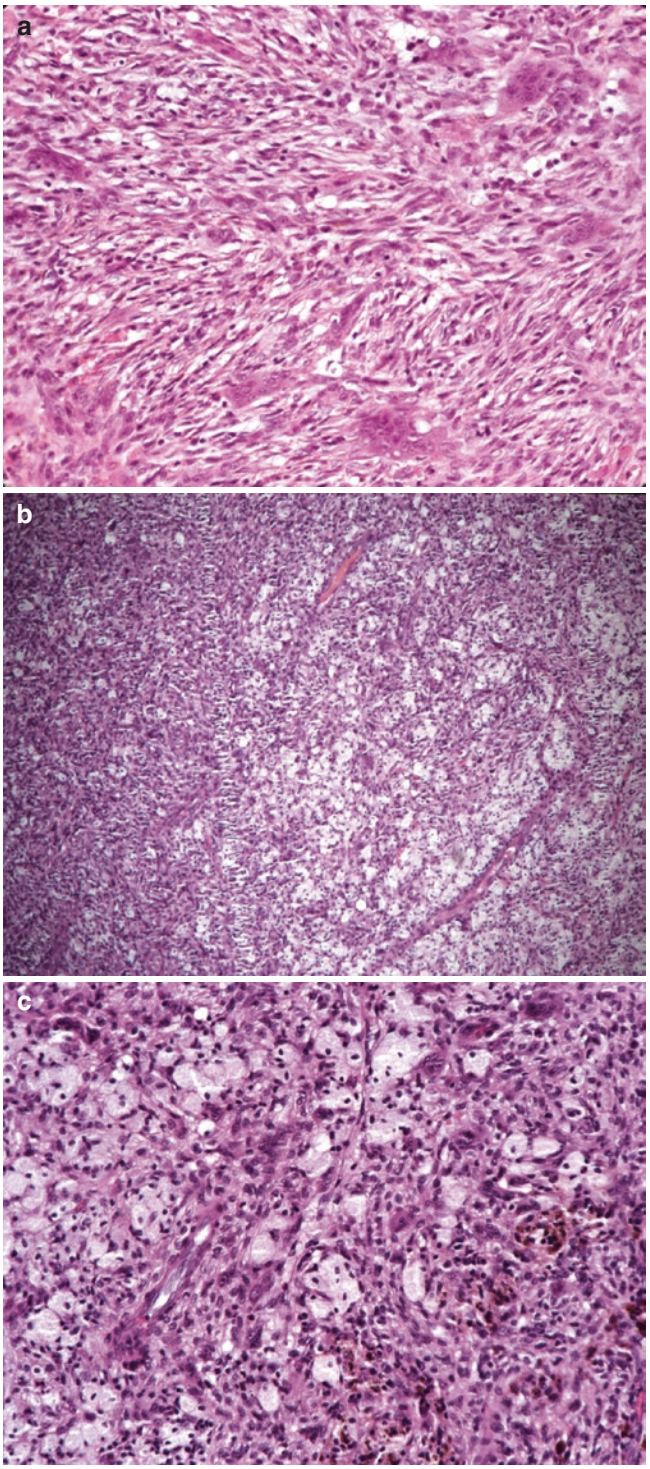

Fig. 3.147 Metaphyseal fibrous cortical defect. (**a**) Innocuous spindle cells in a storiform pattern together with significant degenerative and inflammatory changes including lymphocytes and foamy and hemosiderin-laden macrophages and osteoclasts (H&E, 200×). (**b**) Innocuous spindle cells in a storiform pattern together with significant infiltration by foamy macrophages and hemosiderin deposition (H&E, 20×). (**c**) Innocuous spindle cells largely overrun by degenerative and inflammatory changes including hemorrhage, hemosiderin deposition, lymphocytes, and foamy and hemosiderin-laden macrophages (H&E, 200×). (Courtesy of A. Kevin Raymond, M.D.)

tumors has been the source of consternation [17, 264, 274, 297, 301].

MFH affects people across a broad age range, rare in patients under the age of 30 years while peaking in the fourth to seventh decades. The male to female ration ranges from near equal to 3:2. The skeletal distribution is similar to fibrosarcoma with the most frequently affected bones being the distal femur, proximal tibia, proximal femur, and pelvis. In long bones, tumor tends to arise within the metaphysis or meta-diaphysis [20].

A significant proportion of MFHs arise as secondary phenomena superimposed on previously existing pathology. In one series only 70% of MFH were primary tumors, and the tendency toward secondary origin appears age related: secondary tumors occurring in older patients. Conditions underling MFH include radiation therapy, bone infarct, Paget's disease of bone, fibrous dysplasia, and metal endoprosthesis implantation [10, 20, 299, 302]. Although classified as variants of the low-grade component (e.g., chondrosarcoma, chordoma), the high-grade elements of dedifferentiated tumor variants frequently fulfill the histological criteria of MFH.

As with most bone tumors, the cardinal signs and symptoms are pain, swelling, tenderness, decreased range of motion, and mass. Additional symptoms are a function of tumor location and proximity to vital structures and the potential for mass effect. Pathological fracture may be present in as many as 30–50% of patients. The duration of presenting symptoms is generally short and measured in weeks to months.

MFH of bone tends to be a highly aggressive tumor, both local growth and early systemic metastases. Historically, treatment was complete surgical removal, usually ablative surgery, with poor long-term survival ranging from 0% to 40% [20]. The Rizzoli institute reports a 34% 5-year and 28% 10-year survival when treatment is limited to surgery alone. Survival with osteosarcoma-like preoperative chemotherapy is highly variable with one group reporting a survival of 57%, while Mayo reports similar early survival with long-term attrition, survival of 67.5% at 2 years, 58.9% at 5 years, and 46.0% at 10 years. Survival tends to be better with younger patients, probably representing a greater ability of the young to tolerate aggressive multimodality therapy.

Histopathology

Histologically, MFH is composed of sheets of highly anaplastic, highly pleomorphic malignant "spindle cells." Rather than the linear array associated with fibrosarcoma, the spindle cells of MFH are arranged in interlacing bundles that tend to be organized in a cartwheel/pinwheel or *storiform*

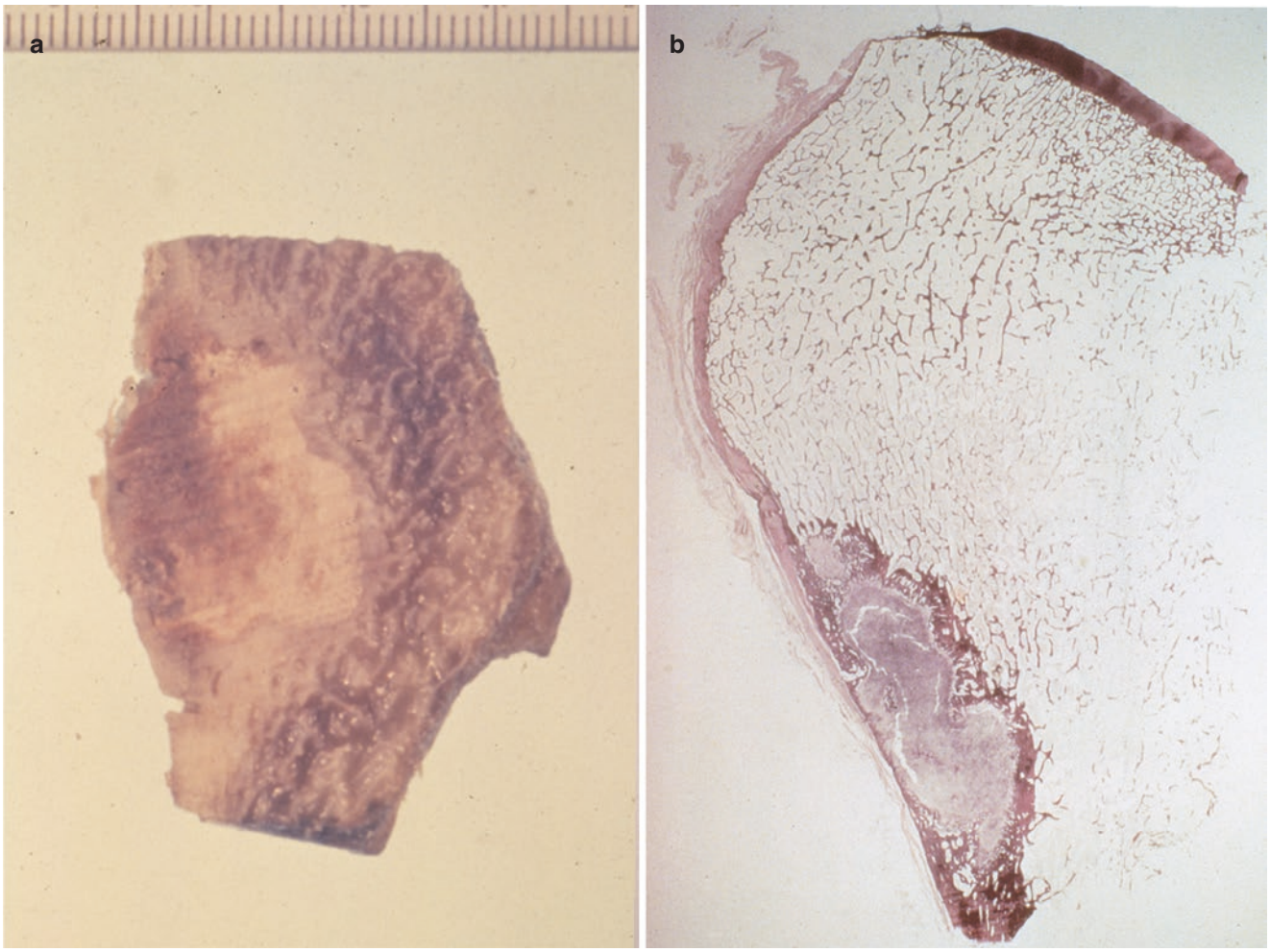

Fig. 3.148 Metaphyseal fibrous cortical defect: resection. (**a**) Formalin-fixed cut surface of metaphyseal fibrous cortical defect, involving and expanding cortex with sclerotic interface and rim of normal cancellous bone. (**b**) Whole mount section. The lesion forms an intracortical mass with thickening of the endosteal aspect corresponding to the sclerosis seen on imaging studies (H&E. 1×)

pattern and associated with variable amounts of intercellular collagen (Fig. 3.150).

The cytological features of individual neoplastic cells are highly variable. However, there is frequently a bimorphic "baseline" or background of pleomorphic cells [20]. One population has fusiform nuclei surrounded by abundant, linear-oriented cytoplasm imparting overall spindle shape resembling fibroblasts. The second group has nuclei that are more round-to-oval, some with indentations and smaller amounts of cytoplasm imparting a histiocytic phenotype. In both groups, nuclear membranes vary in thickness and contour. Nuclei frequently have both euchromatin and irregular or dense heterochromatin with random chromatin nuclear membrane condensation. Bizarre nuclear forms, giant nuclei, and multinucleated forms are frequent. Mitoses including atypical forms are frequent.

Cytoplasm ranges from eosinophilic to amphophilic and ranges from amorphous to vacuolated. Lesions are frequently accompanied by a mixed reactive and inflammatory populations including osteoclasts. Necrosis is a frequent finding, in particular accompanying pathological fracture.

Immunohistochemical studies for vimentin, alpha 1-antitrypsin, alpha 1-antichymotrypsin, and lysozyme are usually positive. However, studies for S-100 and marrow elements are negative. Immunoreactivity for more specific immunohistochemical studies (e.g., desmin, SMA) suggests the possibility of alternative classification [17, 264, 274, 300, 301].

Fig. 3.149 Metaphyseal fibrous cortical defect: resection. (**a**) Plane film (AP). Nonossifying fibroma (same as in case Fig. 3.144). (**b**) Wide resection of nonossifying fibroma involving the distal femoral meta-diaphysis. The lesion consists of a tan to brown, hemorrhagic lesion with a sclerotic interface involving 90% of the femur diameter. The lesion itself is tan; the remaining colors are a function of degenerative changes. (Courtesy of A. Kevin Raymond, M.D.)

Tumor infiltrates cancellous and cortical bone with encasement and destruction of both. There is neither tumor-produced matrix nor specialized structures present.

The histological hallmark of response to chemotherapy is cell dropout. After successful preoperative chemotherapy, responding tumor is replaced by loose connective tissue resembling embryonic areolar tissue and mild non-specific chronic inflammation. There may be lipid-filled and hemosiderin-filled histiocytes. Residual tumor may or may not show degenerative changes.

Gross Pathology

In the absence of secondary changes, the cut surface of MFH ranges from off-white to tan usually with a fish-flesh quality (Fig. 3.151). Tumors tend to grow as a cohesive mass infiltrating adjacent cancellous and cortical bone; extension through cortex is frequent. The less common white lesions tend to herald lower-grade tumors and have large amounts of extracellular collagen that make the tumor firm to rubbery and may impart a whirling, trabecular quality to the cut surface. Higher-grade tumors tend to be somewhat softer fleshy lesions varying from beige to tan and often have foci of hyperemia, hemorrhage, necrosis, and/or cystification. Lipid accumulation corresponds to yellow foci. Secondary changes tend to be more significant with fracture.

Radiology

On plane films and CT, MFH appears as a destructive, radiolucent lesions (Fig. 3.152) arising eccentrically in the metaphysis or meta-diaphysis of long bones and infiltrating adjacent cancellous and cortical bone. Secondary changes may include: variation of the imaging features, tumor extension through cortex into soft tissue, and pathological fracture. Once again, CT and MRI are best for

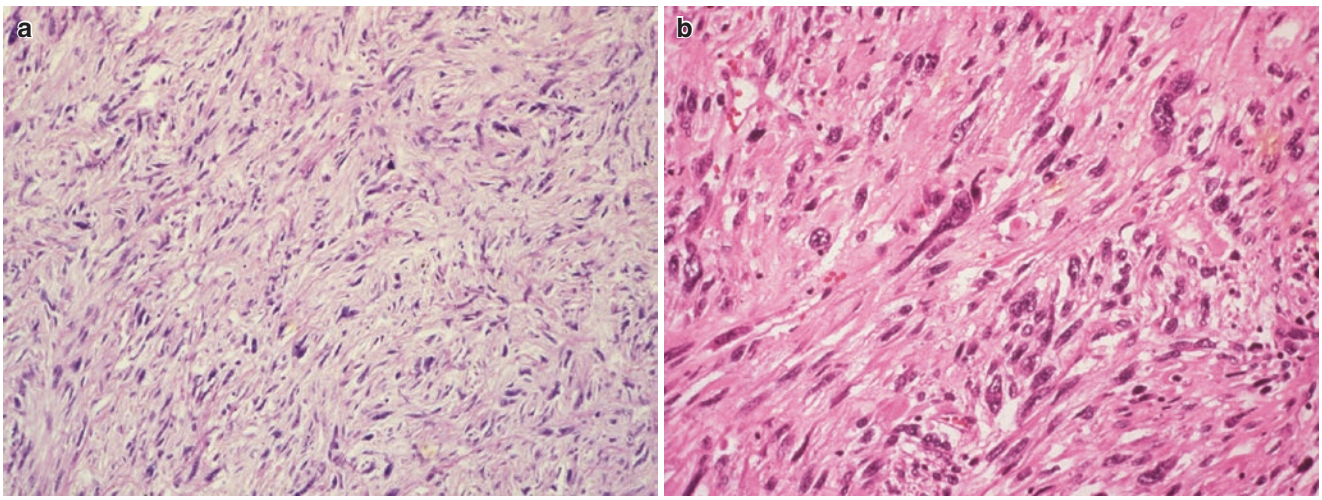

Fig. 3.150 Malignant fibrous histiocytoma. (**a**) Pleomorphic malignant spindle-cell tumor with whirling *storiform* architecture (H&E, 100×). (**b**) Higher magnification of spindle cells in intersection of whirling cell bundles. There is a high degree of both pleomorphism and anaplasia. There are both elongate malignant spindle cells along with more round to ovoid cells with a histiocytoid aura (H&E, 200×).

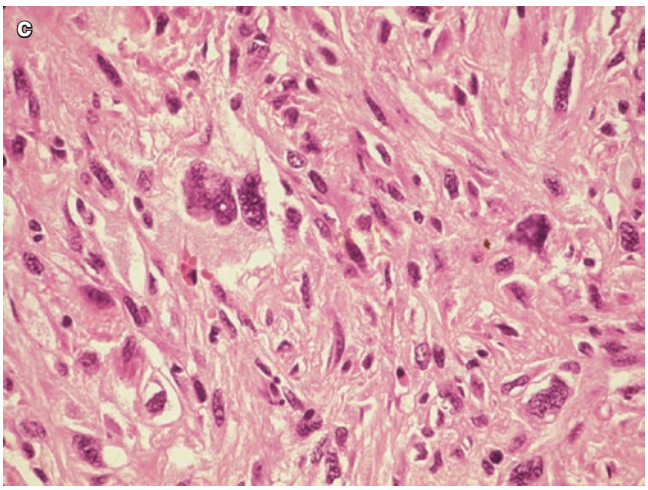

Fig. 3.150 (continued) (**c**) High magnification on a population of highly anaplastic, pleomorphic cells which include both mononuclear and multinucleated malignant giant cells (H&E, 200×). (Courtesy of A. Kevin Raymond, M.D.)

establishing the precise relationship between tumor, cortex, soft tissue, and margins, estimating extent of disease. Lesions are hyperintense on MRI T2-weighted images. Response to preoperative therapy tends to correspond to a decrease in tumor size and bone changes suggesting healing.

Fibrous Dysplasia

Introduction

Fibrous dysplasia (FD) is a fibro-osseous lesion composed of a whorled proliferation of innocuous spindle cells and randomly oriented woven bone trabecula that are lined by spindle cells rather than active osteoblasts [19, 20, 303]. FD may involve a single bone (i.e., monostotic FD) or multiple bones (i.e., polyostotic FD) and is associated with a number of systemic conditions and a relatively specific genetic aberration.

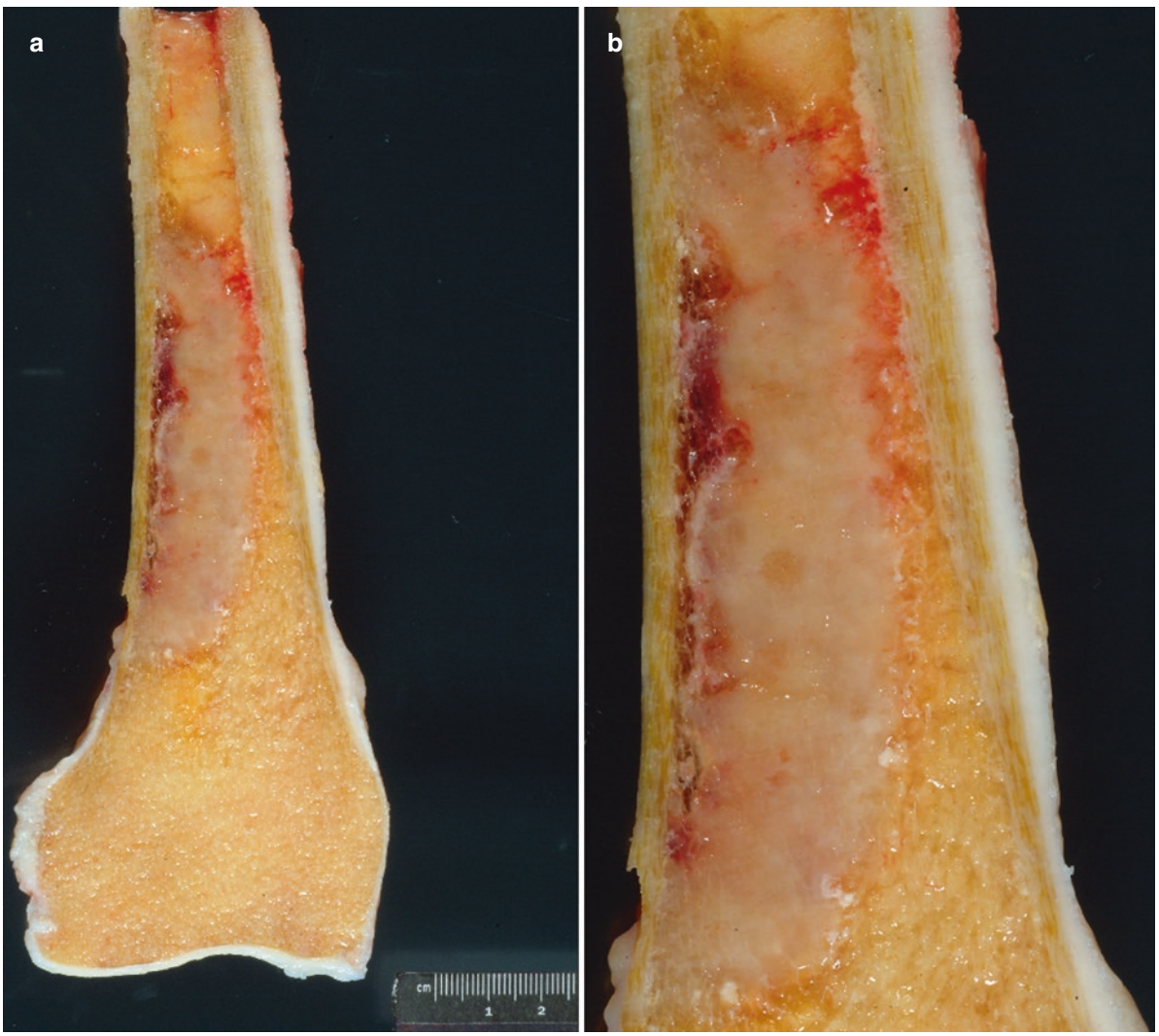

Fig. 3.151 Malignant fibrous histiocytoma. (**a**) Tumor forms an eccentric, semitranslucent, beige, focally hyperemia mass within the medullary cavity of distal metadiaphyseal region of the femur (gross: distance view). (**b**) Higher from "low power," the shiny, firm, semitranslucent tumor infiltrates both normal cancellous and cortical bone (gross: closer). (Courtesy of A. Kevin Raymond, M.D.)

Fig. 3.152 Malignant fibrous histiocytoma/high-grade pleomorphic sarcoma. Plane film (AP) shows a highly destructive, radiolucent lesion involving the proximal humeral meta-diaphysis. Pathological fracture is present. (Courtesy of A. Kevin Raymond, M.D.)

Clinical

FD was first described as a unique osseous condition by Jaffe and Lichtenstein in seminal articles in 1938 and 1942 [303–305]. Although frequently thought of as a disease of the young, initial presentation of FD has a very broad age distribution. However, the peak incidence of monostotic FD is in the second decade with somewhat lower frequencies in the first, third, and fourth decades. Males and females are affected equally. The most frequent primary sites are the femur, tibia, ribs, and craniofacial bones. Polyostotic FD tends to affect a somewhat younger population.

Fibrous dysplasia (FD) represents a genetically determined failure of bone remodeling in which immature woven bone is not "transformed" to mature lamellar bone [22, 304]. The failure to complete remodeling leads to a residuum of randomly oriented woven bone trabecula embedded in dysplastic fibrous stroma resulting in loss of normal weight-bearing/transference and structural/functional integrity.

Unless unusually large or in a critical location, monostotic FD tends to be relatively asymptomatic and discovered when imaging studies are performed for other reasons. When larger it may present as a localized mass, pain, or fracture. Lesional presence may interfere with normal bone remodeling resulting in deformities or limb length discrepancy. There are a number of named deformities associated with FD: coxa vara, shepherd's crook deformity of the proximal femur, tibial bowing, Harrison's groove, and protrusion acetabula [306]. Although they can present at any age, polyostotic lesions tend to be more disfiguring and more frequently associated with syndrome-related findings.

The treatment of choice in monostotic FD is observation unless symptomatic (e.g., pathological fracture, interference with function), and then treatment is individualized. Curettage with packing with or without metallic stabilization is frequent [306]. Polyostotic fibrous dysplasia presents uniquely complex problems in relationship to symptoms, cosmetics, and functions.

As already indicated, FD can be monostotic or polyostotic. Polyostotic frequency ratio is estimated between 8:1 and 10:1 [304]. FD can be isolated to one side or a single region (monomelic polyostotic FD) or scattered throughout the skeleton (polymelic polyostotic FD) [1, 268]. Polyostotic fibrous dysplasia is associated with café au lait pigmentation and endocrinopathies in McCune-Albright syndrome [303, 304], while the association of polyostotic FD with soft tissue myxomas constitutes Mazabraud syndrome. Fibrous dysplasia is also one of the lesions that may be associated with secondary aneurysmal bone cyst formation.

Secondary malignancies occur in <1.0% of FD [20, 304, 307]. Roughly half occur spontaneously and half following radiation exposure. Osteosarcoma accounts for two-thirds of cases followed by fibrosarcoma and chondrosarcoma. The jaws and femur are most frequent sites of origin. Incomplete reporting negates unequivocal statements regarding survival; however, it appears that long-term disease survival is somewhat less than their counterparts not associated with FD [307].

FD appears to be a genetic disease resulting from a postzygotic mutation in the GNAS1 gene that codes the alpha-subunit of the stimulatory G-protein (Gs[alpha]) [1, 22]. The mutation ultimately results in interference with normal osteoblast differentiation and function. The histological manifestation is the proliferation of spindle cells with aberrant bone forming characteristics rather than normal osteoblasts. The timing of this embryonic phenomenon is thought to contribute to the pattern and severity of FD.

FD has also been associated with structural changes involving chromosomes 3, 8, 10, 12, and 15 suggesting to some that fibrous *dysplasia* is actually a form of neoplasia [1].

Histopathology

The histological findings in FD are those of a spindle-cell proliferation accompanied by randomly oriented woven bone trabecula (Fig. 3.153a–d). The lesional cells are inconspicuous spindle cells with nondescript, round to oval to polygonal nuclei with finely divided chromatin, rare inconspicuous nucleoli, and rare if any mitoses. Their cytoplasm is ill-defined, pink to clear, and fibrillar to vacuolated. From low power, the poorly staining cytoplasm imparts an "edematous" optical quality to the non-matrix component. The neoplastic cells are organized in a whirling pattern that seems to "flow" around and merge with the embedded bone trabecula (Fig. 3.153a–d). The woven bone varies from round, psammomatous, or cementicle-like structures to longer, randomly branching, curvilinear trabecular, which have been likened to so-called alphabet soup or Chinese letters. The spindle cells extend to the trabecular surfaces. There is no evidence of activated osteoblasts normally associated with bone formation, lining the bone trabecula, i.e., the so-called "absence of osteoblastic rimming" (Fig. 3.153a–d). At times there is a "zonation phenomenon" in which the spindle cells on the convex aspect of bone trabecula are more numerous and closer together (i.e., hypercellular) than those on the concave aspect where they may be less numerous and less concentrated, i.e., hypocellular.

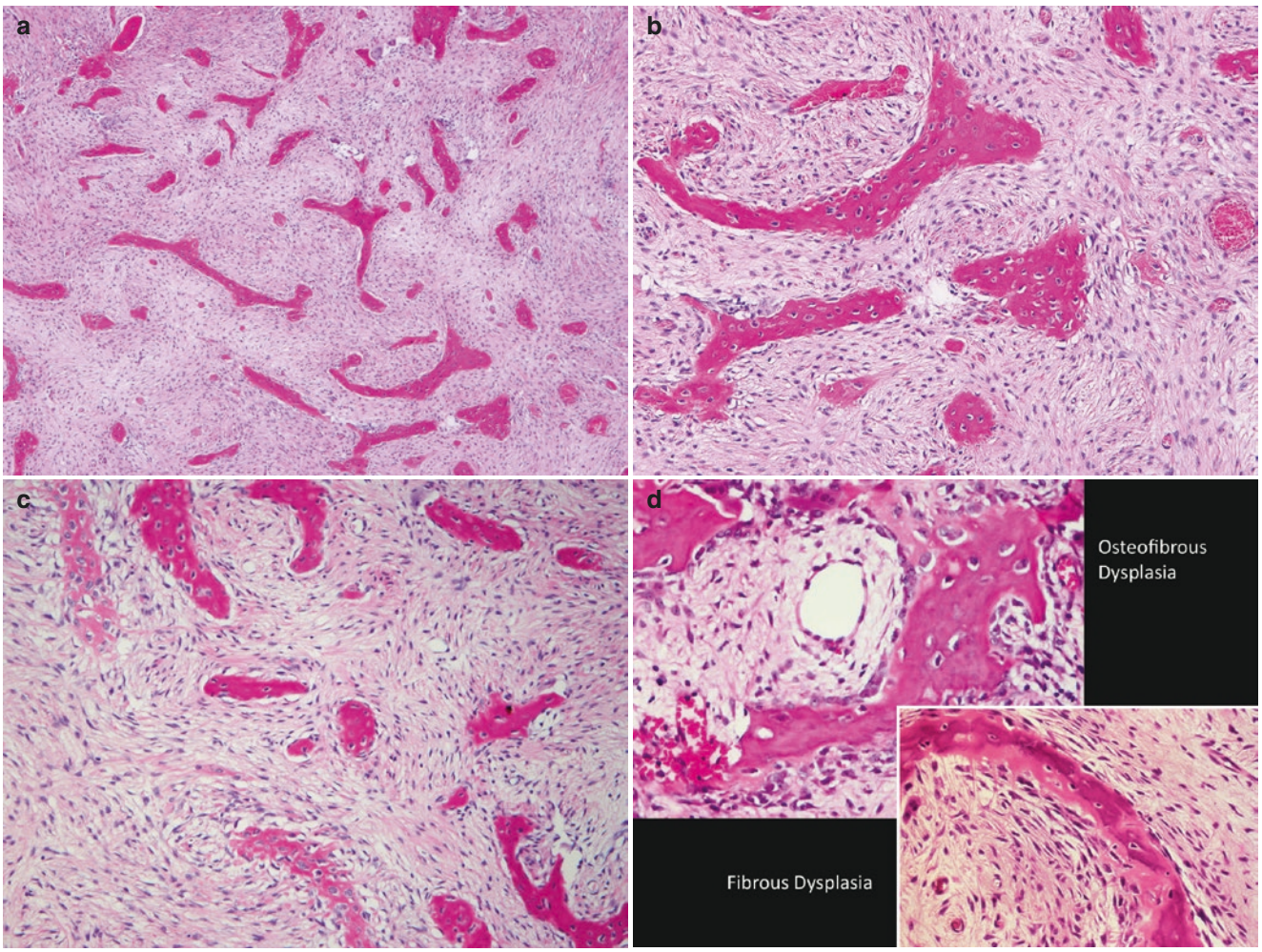

Fig. 3.153 Fibrous dysplasia. (**a**) Innocuous spindle cells and randomly disposed spicules of woven bone with random orientation and so-called *alphabet soup* appearance. Note faint staining of cell cytoplasm and intercellular areas (H&E, 40×). (**b**) Innocuous spindle cells swirling around short randomly shaped woven bone trabecular. Note the lack of osteoblasts on the surface of the lesion-produced bone surfaces, *lack of osteoblastic rimming* (H&E, 100×). (**c**) Innocuous spindle cells swirling around short randomly shaped woven bone trabecula. Note the lack of osteoblasts on the surface of the lesion-produced bone surfaces, *lack of osteoblastic rimming* (H&E, 200×). (**d**) Comparison of fibrous dysplasia and osteofibrous dysplasia. Note the absence of osteoblasts with the fibrous dysplasia woven bone trabecula. As opposed to a near-continuous rim of activated osteoblasts on the surface of the osteofibrous dysplasia woven bone trabecula (H&E, 200×). (Courtesy of A. Kevin Raymond, M.D.)

On occasion there may be abundant cartilage present, (Fig. 3.154a–c) the so-called fibrocartilaginous dysplasia [268, 305, 308]. Histologically, these are lobules of benign-appearing hyaline cartilage that may undergo endochondral ossification. Although this alters the gross and radiographic features, it does not impact prognosis.

Gross Pathology

Grossly, the name "fibrous dysplasia" would seem to imply a soft or perhaps firm soft tissue mass. In contrast to expectations, FD lesions are rock-hard and have a compact, finely granular cut surface reflecting the high content of mineralized woven bone (Figs. 3.155a, b and 3.156). Lesional color is

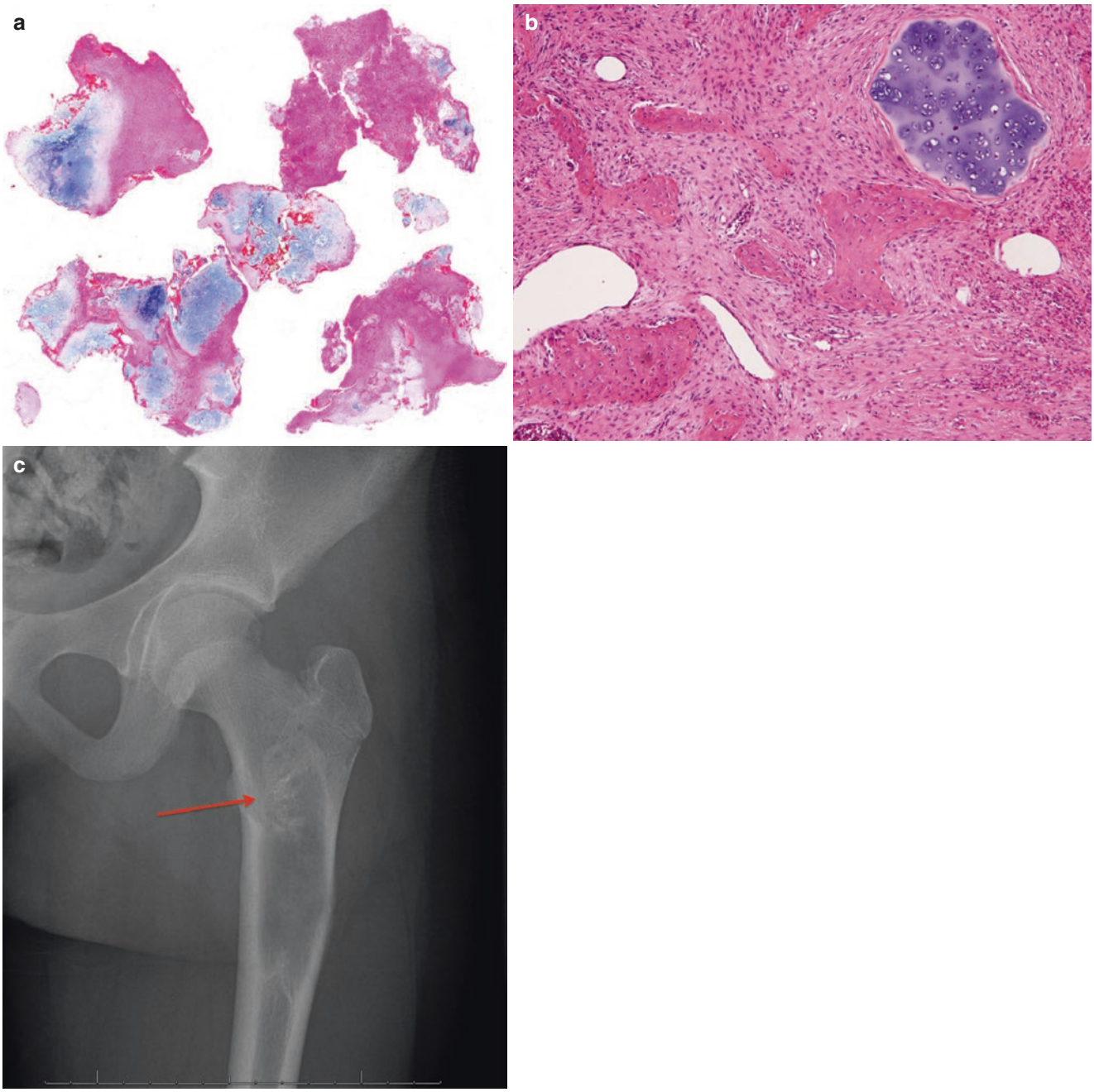

Fig. 3.154 Fibrous dysplasia with hyaline cartilage (i.e., fibrocartilaginous dysplasia). (**a**) Fragments of with lobules of blue cartilage with adherent pink "stroma." Whole mount scanned (H&E, 40×). (**b**) Innocuous sheets of typical fibrous dysplasia with associated lobules of benign hyaline cartilage (H&E, 100×). (**c**) Plane film (AP) of proximal femur. There is a well-defined "hazy" osteoblastic lesion involving the proximal femur, *ground glass appearance*. The lesion is well-defined with a sclerotic interface with normal and has resulted in distortion and expansion of the femur. Note there is a focus of chondroid popcorn-like calcification toward the proximal end of the lesion (red arrow). (Courtesy of A. Kevin Raymond, M.D.)

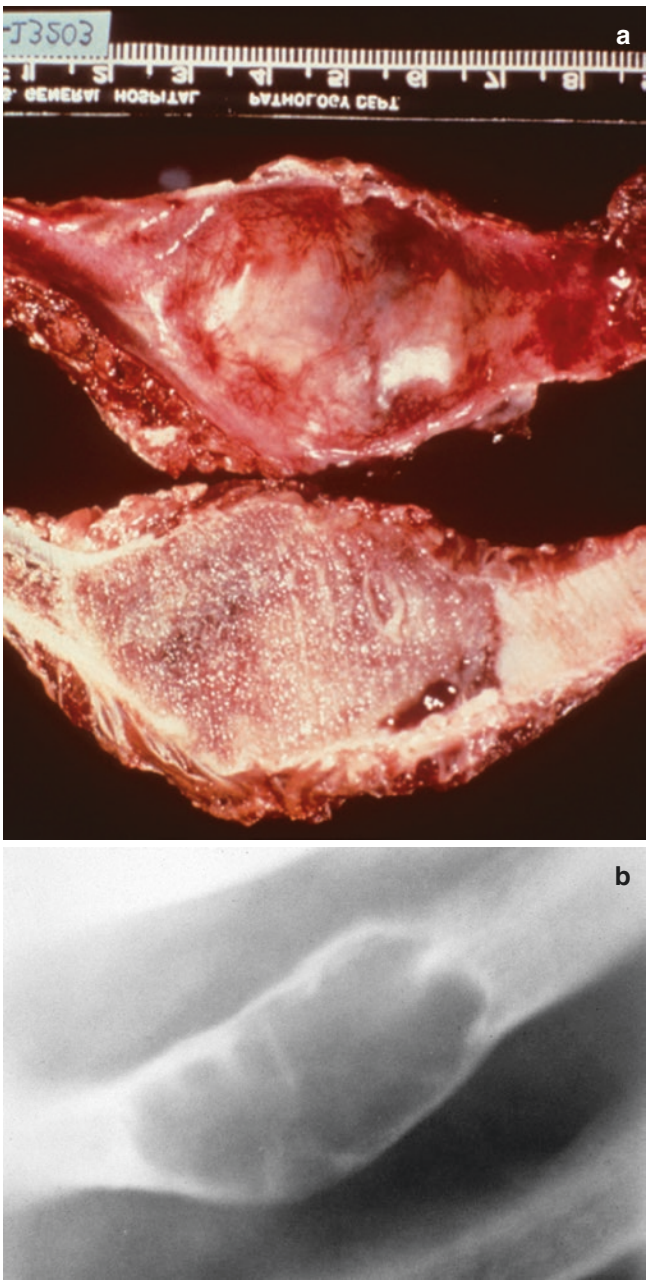

Fig. 3.155 Fibrous dysplasia. (**a**) Resected rib segment with a well-defined, rock-hard, expansile beige to tan lesion. The cut surface consists of a finely granular cut surface that has resulted in granular distortion of reflected light (gross specimen). (**b**) Plane file (AP) of chest wall showing an expansile radiolucent lesion. Overall, the lesion has a soap bubble architecture and a ground glass quality. (Courtesy of A. Kevin Raymond, M.D.)

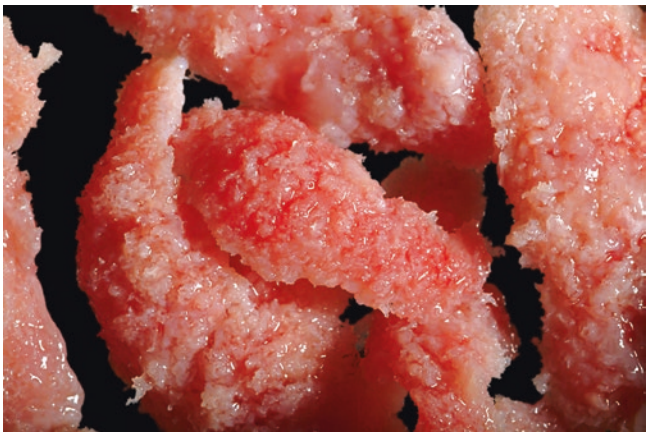

Fig. 3.156 Fibrous dysplasia. Washed curettings from fibrous dysplasia lesion. The bone does not have the normal bridging architecture expected of cancellous bone. Rather normal bone has been replaced by densely granular randomly oriented bone. (Courtesy of A. Kevin Raymond, M.D.)

highly variable, from pink-tan to gray-tan to white, and may be a function of secondary phenomena (e.g., hyperemia, hemorrhage). Lesions tend to be relatively well-demarcated and may thin and expand overlying cortex. When foci of cartilage are present, they appear as typical lobules of gray-blue hyaline cartilage. Aneurysmal bone cyst-like change may be present (Fig. 3.157).

Radiology

The radiographic watchword for FD is "*ground glass*." Lesions tend to occur in the metaphysis or meta-diaphysis and are relatively well-defined but have a hazy radiopaque appearance (Fig. 3.158). The overall radiographic appearance may have a cystic appearance (Fig. 3.155a, b), but nevertheless the ground glass quality is retained. In long bones the limits of disease may be defined by a sclerotic interface with normal bone, the so-called *ring sign* [304]. Extent of disease may be better evaluated through the use of CT and MRI. FD tends to be hypointense with both T1- and T2-weighted lesions. Cyst formation may alter this appearance. When cartilage is present, it may appear as localized, lobulated areas of typical cartilage punctate calcifications [309].

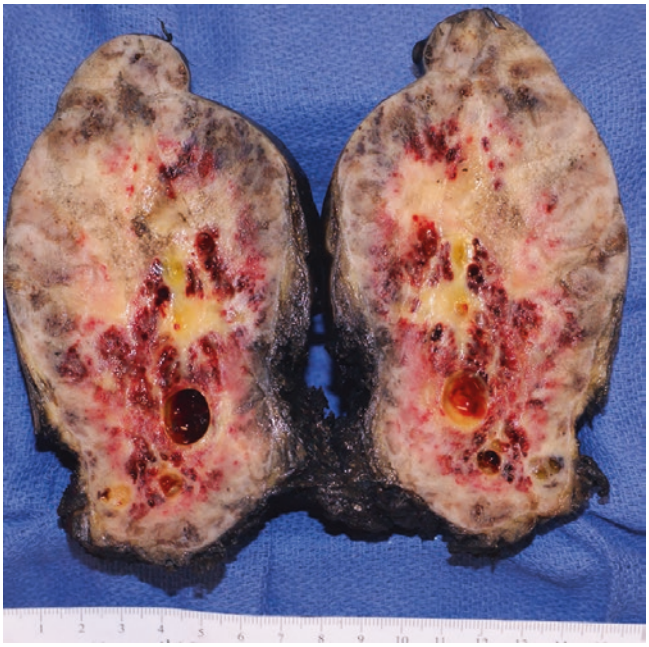

Fig. 3.157 Fibrous dysplasia with aneurysmal bone cyst-like change. The rib has been replaced by a massive expansile lesion. There are multiple areas containing blood-filled cysts; secondary aneurysmal bone cyst. (Courtesy of NingXing Chen, D.O.)

Osteofibrous Dysplasia

Definition

Osteofibrous dysplasia (OFD) is a benign fibro-osseous lesion arising within cortex with unusual clinical, radiographic, and histological features.

Clinical

As currently understood, OFD was described as a clinical, radiological, and histological entity by Campanacci in 1976 [1, 268, 310, 311]. Until then, the lesion had been viewed from a number of perspectives using a variety of terms: osteogenic fibroma, monostotic cortical fibrous dysplasia, variant fibrous dysplasia, and ossifying fibroma [312, 313].

The demographics of OFD are somewhat unique. Typically, it occurs in children under the age of 10 years and males somewhat more frequently than females, with male to female ratio of 4:3. OFD is almost exclusively a disease of the tibia, in particular the anterior metadiaphyseal tibial cortex and to a much lesser degree the fibula. It may be multifocal within the host bone, and both the tibia and ipsilateral fibula are involved in some 20% of cases [310, 314]. With the accrual of larger numbers of cases, rare examples in older patients and involvement of other bones have been described [19, 315].

Fig. 3.158 Fibrous dysplasia. The plane films (AP): the intertrochanteric proximal femur has been replaced and distorted by radiopaque lesions with typical ground glass appearance. (Courtesy of A. Kevin Raymond, M.D.)

Initially, patients are typically asymptomatic. However, with time anterior bowing of the tibia is frequent. Pain is generally a function of pathological fracture. The natural history of OFD is one of slow, progressive growth. With larger lesions there may be mass, deformity, and pathological fracture, and pseudoarthrosis may ensue.

The natural history of OFD is unpredictable. There are reported cases of spontaneous involution at skeletal maturity. More often, it is a disease of slow progression with lesions increasing in size resulting in pain, deformity, and potential pathological fracture with potential pseudoarthrosis [310, 312].

The treatment of OFD is generally a function of clinical setting and patient age [316]. In younger patients (less than 5 years) who are largely asymptomatic, observation is recommended with hopes of shepherding the patient to

skeletal maturity and potential tumor maturation. Incomplete surgery (e.g., simple curettage) is usually followed by local relapse and potential local progression [317]. Therefore, when treatment is required, complete surgical extirpation is recommended, extended curettage or wide local resection.

Pathology

The cytological/histological features of OFD are similar to fibrous dysplasia; OFD is a spindle-cell lesion accompanied by woven bone formation (Fig. 3.159a–c). The neoplastic cells are slender, innocuous spindle cells. The nuclei vary from round to oval with chromatin varying from finely divided to hyperchromatic. There may be small inconspicuous nucleoli and mitoses may be seen. Tumor cell cytoplasm is "wispy" and ill-defined. The cells have a loose whirling orientation within a "myxoid" or edematous background. Embedded within the loose sheets of spindle cells are irregular trabeculae of woven bone that with one exception are similar to those seen in fibrous dysplasia. In contrast to fibrous dysplasia, the woven bone trabecula is lined by activated osteoblasts (Fig. 3.160). There may be a "zonation" pattern with central spindle cells with slender osteoid trabecula and increasingly thickening woven and lamellar bone toward the lesion periphery merging with peripheral sclerotic normal and reactive bone.

Immunohistochemical studies are largely noncontributory. However, single cells and very small groups of cells that cannot be discriminated from the overall spindle-cell population on H&E staining may show immunoreactivity for cytokeratin in OFD. These same cells fail to stain with EMA. When these cytokeratin-positive cells are more

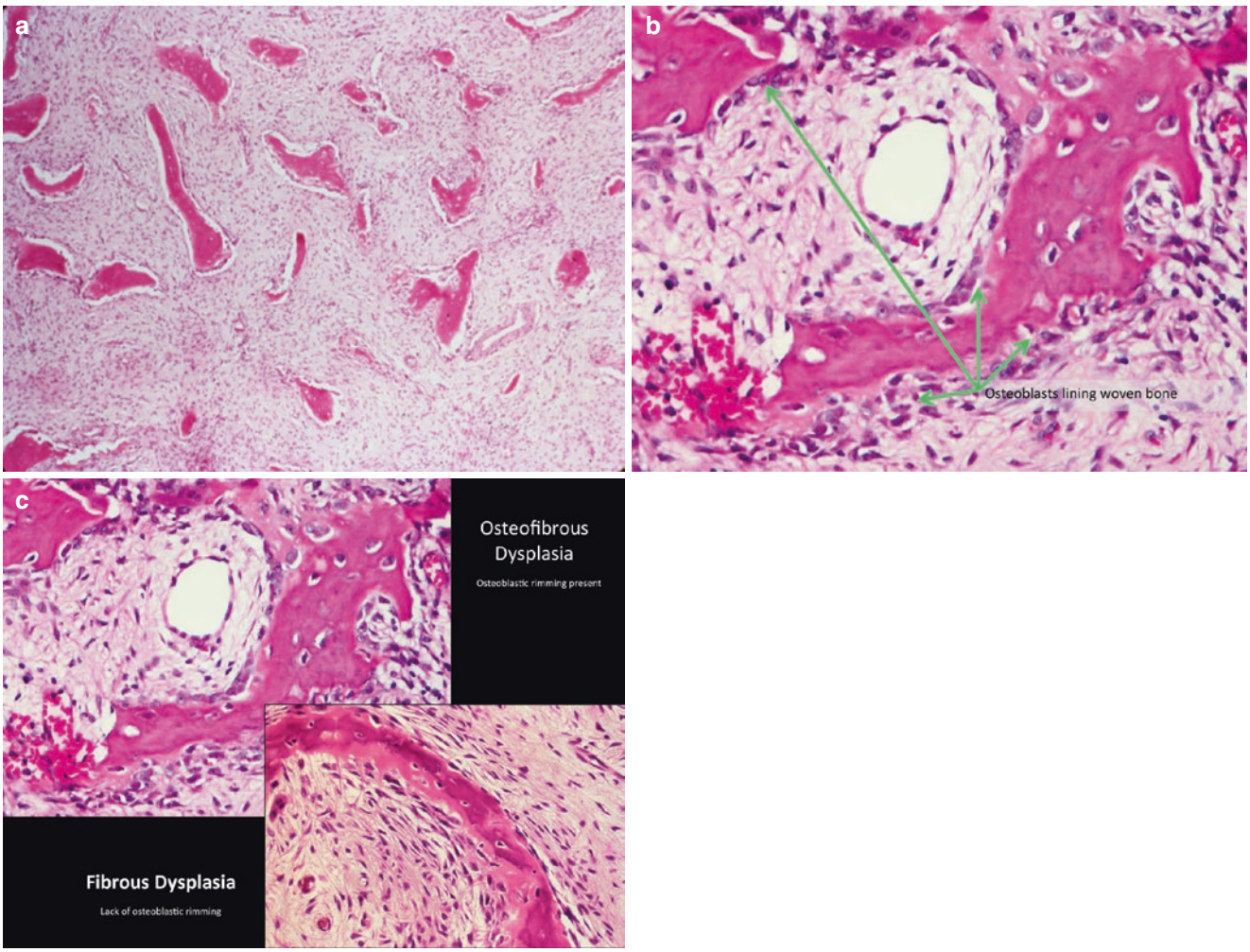

Fig. 3.159 Osteofibrous dysplasia. (**a**) Innocuous spindle cells surround randomly shaped and oriented wove bone trabecula set in a pale *"edematous"* background. The overall appearance is reminiscent of fibrous dysplasia. However, even from low power, a rim of cells can be seen lining the bone trabecula (H&E. 40×). (**b**) Higher magnification of woven bone trabecula of osteofibrous dysplasia shows that they are lined by a near-continuous layer of *activated osteoblasts* (green arrows) (H&E. 200×). (**c**) Comparison of fibrous dysplasia and osteofibrous dysplasia. In osteofibrous dysplasia, woven bone is lined by activated osteoblasts. In contrast, there are no activated osteoblasts lining the woven bone of fibrous dysplasia (H&E. 200×). (Courtesy of A. Kevin Raymond, M.D.)

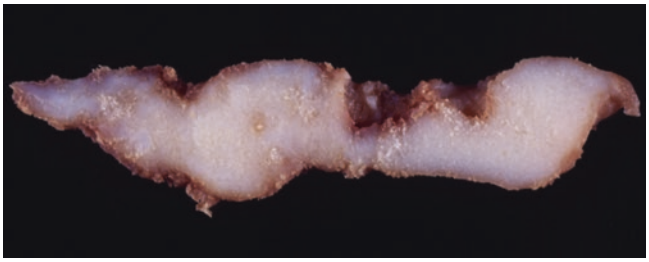

Fig. 3.160 Osteofibrous dysplasia, gross. The cut surface of the resected gray-white to white, rubbery specimen is firm, granular, and gritty. (Courtesy of A. Kevin Raymond, M.D.)

Fig. 3.161 Osteofibrous dysplasia. Plane films (AP and lateral). There is a lytic lesion involving the proximal tibial cortex. The lesion has a soap bubble configuration and a sclerotic interface with normal structures. There is *anterior bowing* of the tibia. (Courtesy of A. Kevin Raymond, M.D.)

numerous and form small groups, the diagnosis of osteofibrous dysplasia-like adamantinoma should be considered. Ultimately, with the emergence of a significant epithelial component, present in both H&E and immunohistochemical studies, merits a diagnosis of adamantinoma [1, 22, 311, 314, 316, 318].

The gross appearance of OFD is one of yellow-to-white rubbery to rock-hard granular tissue (Figs. 3.161 and 3.162). In resection specimens this merges with adjacent dense reactive bone and normal cortex.

Radiology

Radiographically, early OFD presents on plane films (Fig. 3.162) as an eccentric, cortical defect involving the meta-diaphysis or diaphysis. The lesion itself consists of multiple lytic foci within dense sclerotic surrounding bone. When involving the tibia, the lesion almost always involves the anterior cortex and is accompanied by anterior bowing. With increasing size and extension into the medullary cavity, OFD may involve a considerable portion of the involved bone and takes on a soap bubble appearance accompanied by peripheral sclerosis together with cortical thinning, distortion, and possible pathological fracture. CT and MRI provide more detail as well as better evaluation of extent of disease. OFD lesions tend to have a low to intermediate signal on T1-weighted images. In contrast, T2-weighted images appear as intermediate- to high-signal intensity lesions with internal low-signal bands and are multilocular in 91% of cases [319].

Comment

The clinical, radiographical, and histological features of OFD are such that a potential relationship with adamantinoma has long been questioned [1, 268, 310, 311, 318, 320–325]. That is, OFD has the same site specificity as adamantinoma, a similar radiographic appearance and affects patients approximately 10 years younger than those with adamantinoma. In addition, the presence of a loose spindle-cell "stroma" accompanied by woven bone production in both lesions begs the question of OFD being a precursor to adamantinoma. Although, there has not been a documented case of progression of OFD to adamantinoma, the question remains.

Cytogenetic studies have shown trisomies of chromosomes 7, 8, and 12 present in the spindle-cell components of OFD, a subset of adamantinoma (i.e., OFD-like adamantinoma) as well as conventional adamantinoma. These findings suggest that OFD represents a neoplastic phenomenon while at the same time reinforcing the concept of a potential interrelationship between the entities [320, 326].

There is no evidence that either OFD or adamantinoma have a mutation in the GNAS-gene. Thus despite histological similarities, this would strongly suggest a different underlying genetic mechanism from that present in fibrous dysplasia [327].

Of interest, there is evidence in cell culture studies that the spindle cells of OFD and adamantinoma produce osteo-

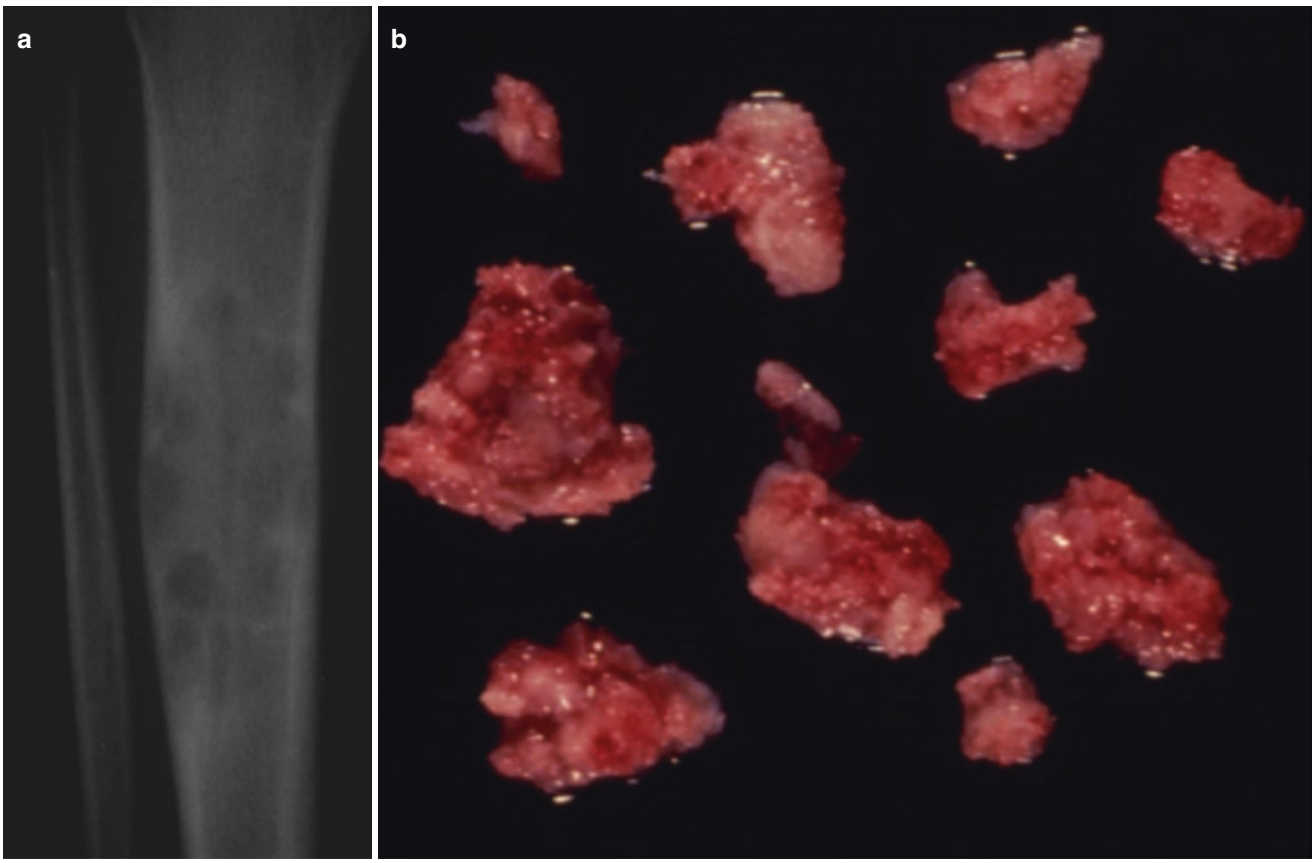

Fig. 3.162 Osteofibrous dysplasia. (**a**) Plane film (AP) shows a destructive lytic lesion with a sclerotic interface involving the tibial diaphysis consistent with osteofibrous dysplasia (H&E, 40×). (**b**) Higher gross curetting specimen. The lesion consists of granular, pink-tan osseous tissue adherent to normal bone of spindle cells (H&E, 200×). (Courtesy of A. Kevin Raymond, M.D.)

calcin, osteonectin, osteopontin, osterix, and collagen type I. At the same time, there is evidence that the spindle cells may induce osteoclast formation via a RANK-L pathway. Taken together, these findings suggest that the spindle-cell component of OFD processes osteoblast-like function [314, 328–332].

Vascular Neoplasia

Introduction

The understanding of primary vascular tumors of the bone has long stood in defiance of bone pathologists. One of the most basic issues has been terminology. We are dealing with tumors that are functions of cell type (i.e., endothelium), but we frequently only speak in terms of structure (i.e., vessels); an active integration of both is necessary.

However, with the accrual of increasing case numbers, the pooling of resources, and the focused attention of dedicated investigators, greater understanding has come to this historically frustrating arena. As with other areas of pathology, this increased understanding has also been a function of ever-increasingly sophisticated investigatory techniques.

Bovée et com have proposed a tentative classification system that seems to answer many past questions. The system divides osseous vascular tumors into benign, intermediate, and malignant categories. In turn, each of the three categories is divided into specific diagnostic entities (Table 3.10).

Hemangioma

Definition

Hemangiomas are benign vasoformative tumors of endothelial origin.

Clinical

Hemangiomas occur in patients over a broad age spectrum in a more or less “bell-shaped” distribution, with a peak in the fifth decade [1, 19, 333, 334]. Women are more frequently

Table 3.10 Vascular neoplasia: proposed classification system

Benign vascular tumors of bone
Hemangioma
Cavernous
Capillary
Hemangiomatosis
Nonaggressive, regional
Nonaggressive, disseminated (cystic angiomatosis)
Aggressive/massive osteolysis (i.e., Gorham-stout disease)
Intermediate vascular tumors of bone
Epithelioid hemangioma
Pseudomyogenic hemangioendothelioma
Malignant vascular tumors of bone
Epithelioid hemangioendothelioma
Angiosarcoma
Primary
Secondary
Postradiation
Bone infarct associated

affected than men, male to female ratio of 2:3. The most frequently involved sites are the craniofacial flat bones and vertebra. When involving long tubular bones (e.g., femur), hemangioma tends to preferentially involve metaphyses. As with all vascular tumors, hemangioma may be multifocal, 5–18% of cases [10].

In surgery-based series [19, 20], hemangioma constitutes some 1% of bone tumors. However, in autopsy-based series, 10% of autopsied patients had incidental spinal hemangioma [3, 10], suggesting that hemangioma may be much more common than clinically appreciated.

Many hemangiomas are asymptomatic and are incidental radiographic findings in imaging studies performed for other reasons. When symptomatic pain is the cardinal symptom, pain may be due to tumor growth and fracture including vertebral compression fracture or secondary to mass effect. Considering the frequency of vertebral lesions, cord compression resulting in pain and/or a variety of neurological symptoms may be in the forefront.

The potential uncertainty of the incidence of hemangioma draws to question any definitive statement concerning the natural history of this tumor; the possibility of a high percentage of clinically insignificant asymptomatic, undetected cases remains a possibility. However, based on experience with clinically relevant lesions, we are forced to consider hemangioma a benign tumor with potential for local growth but without intrinsic capacity for metastasis. This local growth has the consequence of interfering with structural and functional bone integrity resulting in symptoms and consequences secondary to bone destruction and/or mass effect.

When therapy is required, the treatment of choice in hemangioma is largely a function of tumor location and size. Ideally, complete removal with normal margins would be optimal. However, locational parameters may dictate a less aggressive approach with curettage or low-dose external beam radiation therapy proving adequate and associated with a low incidence of local relapse. Others espouse stratifying patients into protocols using various combinations of transarterial embolization and surgery. The utility of targeted systemic agents is under investigation: AGM-1470, angiostatin, matrix metalloproteinase inhibitor batimastat, and interleukin-12 [4, 10].

Histopathology

The cytological/histological features of hemangioma are those of a proliferation of thin-walled vessels that are lined by a single layer of essentially normal endothelial cells (Fig. 3.163a–c). These endothelial cells may be somewhat larger than normal, but they remain a monolayer, do not protrude into vessel lumens, or have cellular/nuclear atypia. Although cavernous hemangiomas are much more common, both cavernous and capillary patterns occur in bone, as do mixed forms.

The vascular spaces of hemangiomas are intertwined with underlying adipose tissue and infiltrate between residual bone trabecula. Tumor infiltration results in expansion of intertrabecular marrow spaces. The remaining bone trabecula are generally thickened, resulting in alternating areas of soft tissue and marked bone sclerosis. The trabecula are frequently lined by activated osteoblasts, and the histological picture can be confused with osteoblastoma.

Immunohistochemical studies can be used to confirm the endothelial differentiation of the neoplastic cells and help discriminate vascular lesions and nonvascular cysts: factor VIII, *Ulex europaeus*, CD31, CD34, Fli-1, and in some cases cytokeratin and EMA [3, 10].

Analysis of vascular lesions can present a number of problems intrinsic to histology of blood vessels. As pointed out by Unni [19], unequivocal distinction between hemangioma and lymphangioma of bone can be difficult since the current discriminating feature is the presence or absence of intraluminal blood elements. Unfortunately, during specimen management blood vessels can be emptied of blood and lymphatics filled with blood. In addition, absolute distinction between hemangiomas and other benign vascular lesions (e.g., hamartoma, arteriovenous malformation) may not be possible in all cases at the histopathological level; radiographical and clinical correlation may be necessary.

Gross Pathology

Grossly, bone involved by hemangioma has an overall "honeycomb" appearance resulting from the contrasting presence of expanded blood-filled intratrabecular spaces juxtaposed to thickened sclerotic residual normal bone (Fig. 3.163a–c). Tumor itself appears as blood-tinged membranes adherent to residual bone (Fig. 3.164a, b). Lesions arising in flat bones

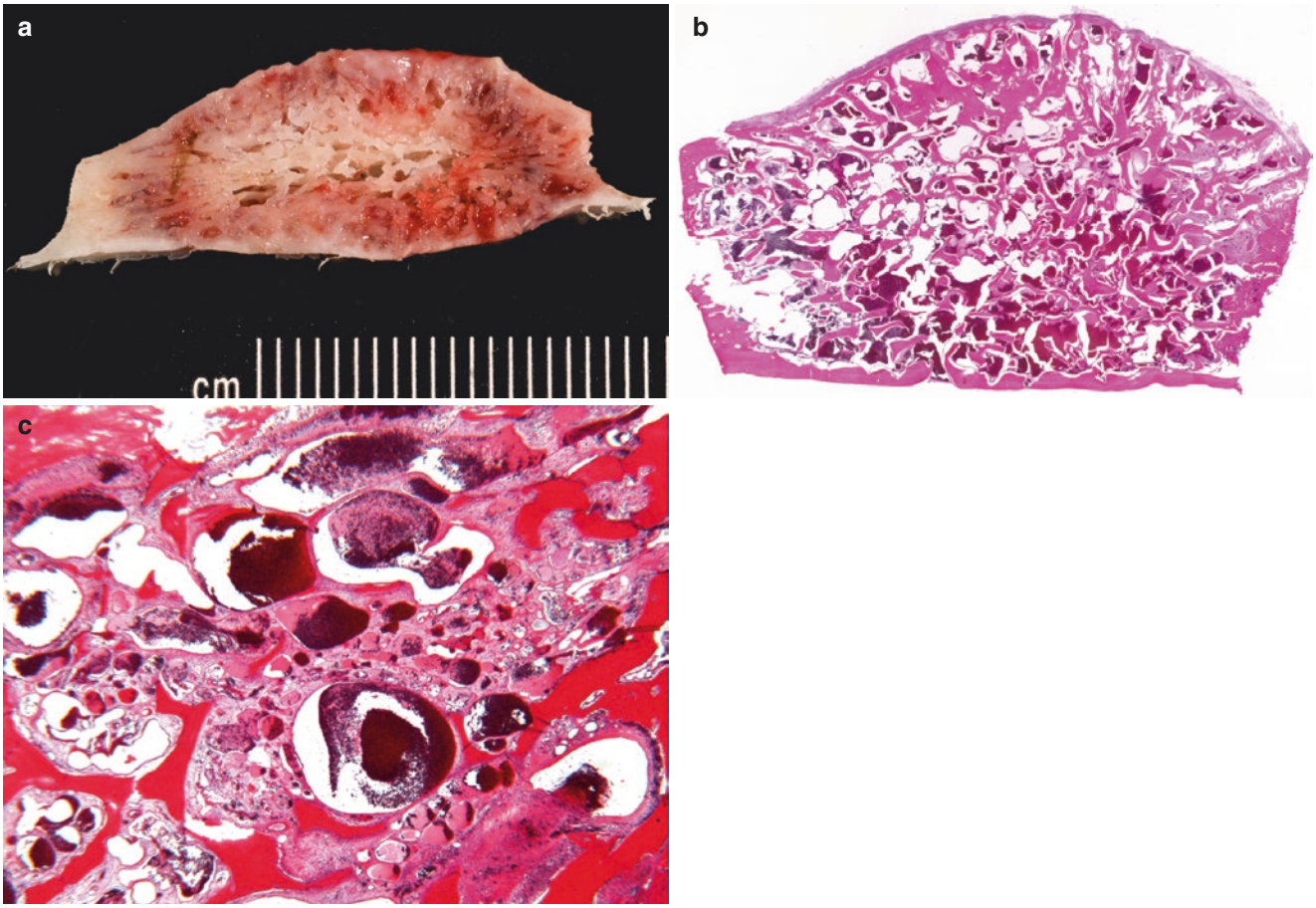

Fig. 3.163 Hemangioma. (**a**) Resected segment of calvarium. The cut surface shows sclerosis and accentuation of the reduced number of residual trabecula. In turn, the enlarged intertrabecular spaces are lined by gray-tan membranes, and contain blood. (**b**) Whole mount showing thickening of reduced number residual trabecula. The remaining intertrabecular spaces are replaced by a thin covering of endothelial lined vascular spaces filled with blood; cavernous hemangioma (H&E. 1×). (c) Low-power view of same case confirming the presence of hemangioma (H&E. 2×). (Courtesy of Michael Klein, M.D.)

tend to be accompanied by large amounts of reactive bone that may be speculated and result in "hair-on-end" or "sunburst" architecture. Any large areas of solid tumor must be viewed with suspicion of malignancy [20].

Radiology

The radiographic features of hemangioma arising in the vertebra, craniofacial bones, and flat bones of the pelvis are relatively consistent (Fig. 3.164a–c). They are well-circumscribed radiolucent lesions accompanied by dense trabeculations of reactive bone. When viewing plane films of vertebral lesions, the juxtaposition of radiolucent tumor infiltration and reactive bone results in vertical striations, the so-called *corduroy* or *jailhouse* appearance. Transaxial CT views of these alternating vertebral changes cut crosswise imparts and overall "polka dot" pattern. Of interest, hemangioma in the vertebra is one of the few lesions to increase MRI signal intensity in both T1 and T2 imagery, a feature attributed to the presence of tumor, adipose tissue, and sclerotic bone [335]. Lesions arising in flat bones are generally well-circumscribed lytic lesions accompanied by sclerotic intralesional trabeculation and may also be accompanied by exuberant periosteal new bone formation corresponding the speculated sunburst bone seen grossly. Lesions in long bones of the appendicular skeleton appear as well-defined areas of radiolucency with or without peripheral sclerosis (Fig. 3.165).

Angiomatosis

Skeletal hemangiomatosis is a rare family of disorders and defined as multiple cystic bone hemangiomas that may or may not be associated with soft tissue hemangiomas. It is estimated that 60–70% of cases have soft tissue involvement. Angiomatosis may be further classified by biological behavior (i.e., aggressive versus nonaggressive forms) and by pattern of involvement [1, 4, 333].

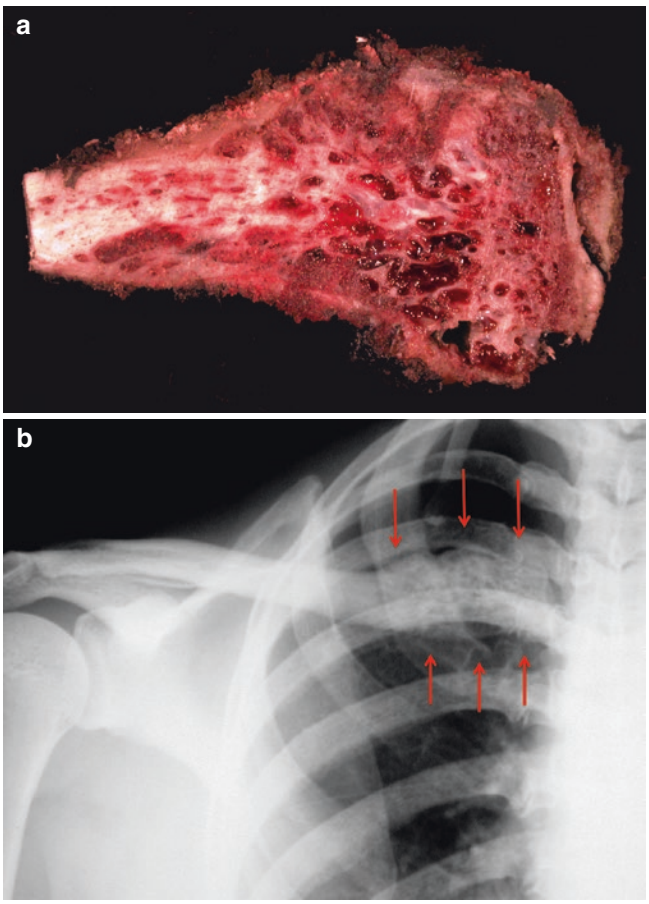

Fig. 3.164 Hemangioma. (**a**) Resected segment of medial clavicle. The clavicle is replaced by a sponge-like lesion resulting from enlargement of intertrabecular spaces by hemangioma and sclerosis of the remaining otherwise normal cancellous bone. (**b**) Plane film of chest (AP). There is an expansile, destructive mixed lytic/blastic lesion involving the medial clavicle (red arrows). (Courtesy of Michael Klein, M.D.)

Nonaggressive angiomatosis occurs in regional and systemic patterns of involvement. Regional forms are identified by multiple lesions occurring within a given anatomic region. In contrast, systemic angiomatosis has more general skeletal involvement and shows a propensity for non-appendicular core skeleton. The clinical presentation varies from unsuspected imaging finding to localized pain, swelling, and pathological fracture. Treatment is aimed toward relieving symptoms and correcting functional impairment. Prognosis is generally a function of the extent and complications of soft tissue lesions.

Other than multifocality and more extensive involvement of affected bones, the lesions of nonaggressive angiomatosis are histologically, grossly, and radiographically similar to their monostotic counterparts.

Fig. 3.165 Hemangioma. Tibia, plane films (AP and lateral) shows a well-defined destructive, osteolytic lesion involving the tibial diaphysis. (Courtesy of Michael Klein, M.D.)

Aggressive angiomatosis is Gorham-Stout disease also referred to as disappearing bone disease, vanishing bone disease, and phantom bone disease [1, 333]. Lesions start as areas of radiolucency eventually growing to include large parts of the involved bone resulting in pain, functional instability, and pathological fracture. The lesion frequently extends to involve contiguous bones. Treatment is aimed at eliminating the pathological process. Radiographically, lesions appear as ill-defined, geographic, and purely lytic. Cortex is resorbed and has a characteristic tapering quality. Histologically, the pathological process consists of a proliferation of delicate, capillary-sized vessels.

In addition, angiomatosis may be associated with a number of systemic syndromes including Osler-Weber-Rendu syndrome, von Hippel-Lindau syndrome, Klippel-Trenaunay syndrome, Kasabach-Merritt syndrome, Parkes-Weber syndrome, and Maffucci's syndrome [11, 336].

Epithelioid Hemangioma

Definition

Epithelioid hemangioma (HE) is a hemangioma variant in which the characteristic neoplastic element is the *epithelioid* endothelial cell. It is zonated heterogeneous form of benign vascular neoplasia that may be locally aggressive or multifocal but lacks the inherent capacity for metastasis. HE is also

referred to as angiolymphoid hyperplasia with eosinophilia and histiocytoid hemangioma [337].

Clinical

Vested in controversy, the concept of HE is a classic example of vascular neoplasia evolution. To some investigators the definition and diagnostic criteria failed to provide a means of unequivocally distinguishing HE from other atypical vascular neoplasms, in particular epithelioid hemangioendothelioma (EHE). However, the identification of a recurrent translocation present in EHE that is not in HE or other vascular neoplasms has added an additional component to our diagnostic armamentarium, the t(1;3)(p36;q25) chromosomal translocation resulting in the WWTR1-CAMTA1 fusion product. This discovery has allowed the identification of a group of vasoproliferative lesions that fulfill the histological criteria of HE while allowing confident, cytogenetic exclusion of EHE [338].

HE affects patients over a wide age range with a peak in the third and fourth decades. Males are affected more frequently than females: male to female ratio 3:2. The bones of the appendicular skeleton are more frequently involved than the central skeleton, in particular the short tubular bones of the hands and feet, followed by the tibia, humerus, and femur. However, the spine and pelvis account for some 25% of cases. When involving tubular bones, the metaphysis is preferentially affected.

HE may be asymptomatic and detected as an incidental radiographic finding. However, more often patients present with localized pain with or without swelling. The natural history of HE of the bone is one of local growth that may include extension into overlying soft tissue. HE is multifocal in some 18% of cases and on occasion involves regional lymph nodes. However, tumor does not appear to have the intrinsic capacity for systemic dissemination. In light of its limited potential behavior, treatment is directed toward local control; complete excision would be ideal, but therapy choice is largely dictated by tumor size and location, and curettage has proven adequate in the majority of cases. In one series of 50 cases, local relapse occurred in 4 of 36 patients for whom follow-up was available. There were no examples of systemic dissemination, and no patients died of disease [339].

Histopathology

Histologically, EH is a zonated, lobular lesion. There is a dominant *hyper*cellular central mass that merges with a hypocellular infiltrative vascular periphery. The peripheral component radiates between reactive and residual normal bone trabecula [10, 17, 340, 341].

The lobule centers are composed of large, polyhedral, epithelioid endothelial cells forming either rudimentary, compact, vascular lumens or tightly packed sheets (Fig. 3.166a–d). Most lesions have at least an element of well-formed vessels that are lined by epithelioid cells that protrude into the lumen imparting a "tombstone" appearance. In some cases solid sheets predominate. The central tumor cells have large, round to oval nuclei with well-defined nuclear membranes and finely distributed chromatin. There may be nuclear grooves imparting a kidney-bean or hyperlobated appearance (Fig. 3.166a–d). Epithelioid endothelial cytoplasm is abundant, deeply eosinophilic and may contain one or more round, clear, eccentric, thin-walled vacuoles that may contain red blood cells or RBC debris. In some instances, vacuolated cells aggregate together resulting in an appearance in which the intracytoplasmic vacuoles from adjacent cells appear to coalesce to form vascular lumens. Mitoses are few and normal. The background stroma is composed of lose connective tissue which may have a fairly significant inflammatory infiltrate rich in eosinophils (Fig. 3.166a–d). Importantly, there should be no hyalinized or myxoid extracellular matrix present. Occasionally, there may be small foci of necrosis as well as hemorrhage.

In contrast to the center, the lesion periphery consists of loose connective tissue through which arteriolar vessels infiltrate. Although the lining endothelial cells tend to be relatively flat, their nuclei may bulge the cytoplasm. The background consists of loose edematous connective tissue with a minimal inflammatory infiltrate.

Infrequent findings associated with EH include the presence of osteoclast-like giant cells within the lesion proper, reactive bone compartmentalizing the lesion into small lobules, and large dilated epithelioid endothelial-lined blood vessels.

The neoplastic cells of EH show immunoreactivity for factor VIII, CD31, ERG, and Fli-1. There may be variable immunoreactivity with CD34. In addition about half of cases show positive staining with keratin and EMA [17].

Gross Pathology

Grossly lesions are solid, red, and hemorrhagic. In curettage cases the lesions appear as areas of hemorrhage of soft tissue or hemorrhage within bone trabecula. When resected intact, the parent bone may be expanded [10]. The cut surface of the tumor is that of a well-circumscribed, dark red, hemorrhagic mass that appears to be solid tumor in the center and has a narrow zone in which it blends with pre-exiting normal bone trabecula. Tumor erodes or destroys adjacent cortex and extend into overlying soft tissue.

Radiology

Radiographically, plane films and CT show EH as a relatively well-circumscribed tumor (Fig. 3.167), purely lytic or having pseudotrabeculations that impart a cystic quality to the lesion [339, 342]. In some cases there may be cortical expansion, particularly lesion arising in the small tubular

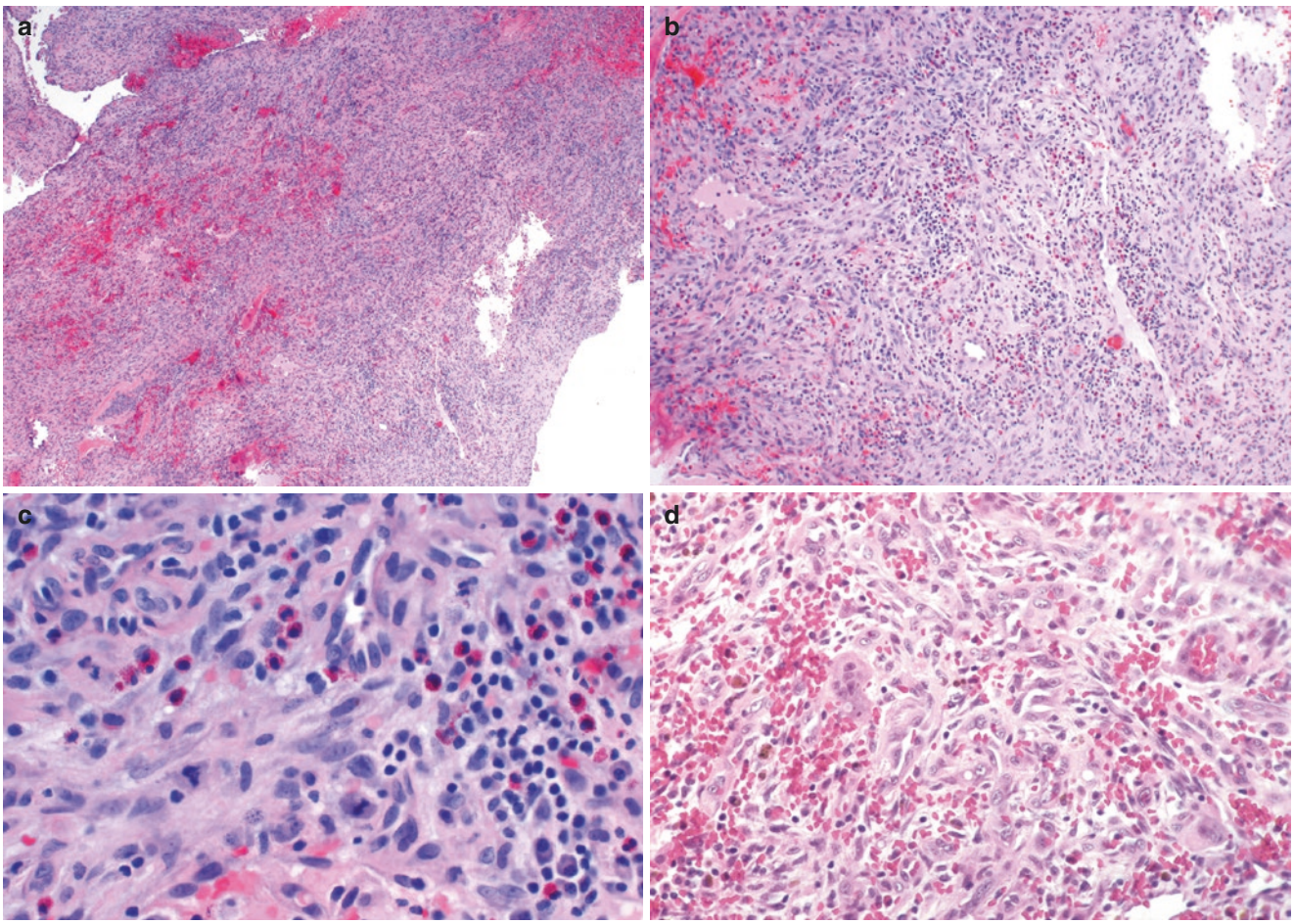

Fig. 3.166 Epithelioid hemangioma. (**a**, **b**) Cellular center of lobular lesion. Tumor consists of mixture of elements. There are vascular spaces lined by epithelioid cells surrounded by spindle cell and an inflammatory infiltrate with prominent eosinophils (H&&E. 40×, 100×). (**c**) Higher-power view of lesion center. The epithelioid cells have round to cigar-shaped nuclei, some with nuclear grooves. Epithelioid cells line vascular structures. Many of the neoplastic cells have intracytoplasmic vacuoles. The stroma also contains lymphocytes and eosinophils (H&E, 200×). (**d**) Periphery of lesion with anastomosing vessels with an arteriolar aura lined by epithelioid cells (H&E, 200×) (Courtesy of Michael Klein, M.D.)

bones of the hands and feet. Cortex may be eroded and destroyed, and tumor may extent into soft tissue. MRI is again a good indicator of extent of disease where EH appears as a hypointense lesion on T1-weighted images and hyperintense on T2-weighted imaging [1, 4].

Epithelioid Hemangioendothelioma

Definition

Epithelioid hemangioendothelioma (EHE) is considered a low-grade malignant tumor of endothelial origin that has minimal if any evidence of vessel formation. Tumor is locally aggressive, is frequently multifocal, and has the capacity for metastasis. EHE is associated with a specific genetic aberration; the t(1;3)(p36.3;q25) translocation resulting in the WWTR1-CAMTA1 fusion product.

Clinical

EHE affects patients over a wide spectrum, with almost 60% occurring in the second through fourth decades and a peak incidence in the second decade (i.e., 25%). Males and females are affected equally. EHE most frequently arises in the bones of the appendicular skeleton as a whole, in particular the femur. The pelvis and spine are the second and third most frequently affected sites. Over 50% of cases have multifocal bone involvement, and that involvement has some propensity for being regional, e.g., bones of the knee or shoulder. In addition, some 18% also have visceral involvement [343].

Although some lesions are identified as incidental finding discovered in the course of imaging studies carried out for unrelated indications, the majority of cases present with localized pain that may be accompanied by swelling. Occasionally patients present with pathological fracture.

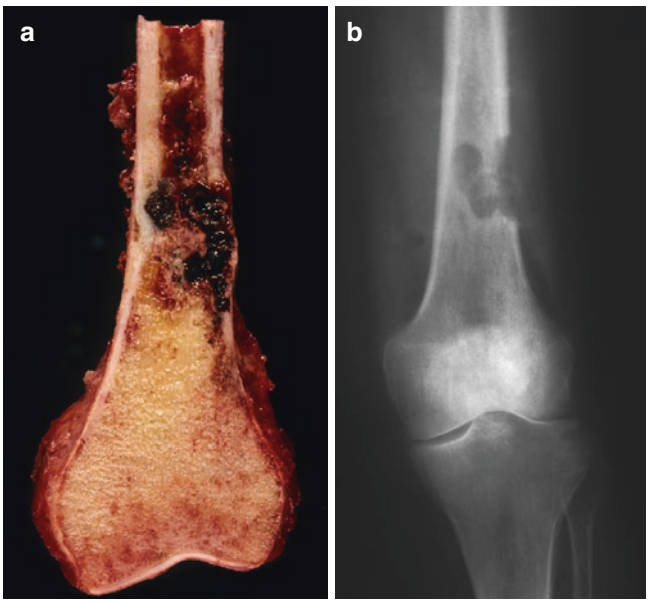

Fig. 3.167 Epithelioid hemangioma. (**a**) Distal femur, resection. Tumor forms a largely hemorrhagic mass involving the meta-diaphysis. The cut surface of the tumor itself appears to be pink-tan and overshadowed by large amounts of hemorrhage. The intramedullary tumor has eroded the lateral cortex. (**b**) Plane film (AP): tumor forms a destructive radiolucent mass involving the distal femoral meta-diaphysis with destruction of the lateral cortex. (Courtesy of Michael Klein, M.D.)

EHE is considered a form of low-grade malignancy. Locally aggressive tumor growth is routine. Multicentricity occurs in at least 55% of cases. This may be multifocal disease in a single bone or multiple bones. When multiple bones are involved, they tend to be regional, e.g., bones around the knee or shoulder. Metastases to lymph nodes and visceral organs occur inasmuch as 30% of cases. The overall mortality rate in EHE of the bone is 20%, which is somewhat higher than its soft tissue counterpart. Correlation of specific histological features (e.g., grade) with ultimate prognosis has been largely unsuccessful. Older data that indicated a better prognosis for patients with multifocal disease has not been borne out by updated information [20, 343]. However, EHE associated with visceral involvement appears to have a worse prognosis; in one series, seven of eight such patients were dead of disease.

Complete surgical extirpation of tumor is the ideal. However, the possibility of multicentric disease may complicate surgery. The rarity of this disease precludes unequivocal statements regarding the role of radiation therapy and chemotherapy.

Histopathology

At low power, EHE is a lobulated mass. Tumor is composed of epithelioid endothelial cells that are present as single cells, clusters, nests, or cords of variable length that are embedded in an amorphous background stroma. The stroma may appear hyalinized pink, pale-blue myxoid, or combinations of both (Fig. 3.168a–d). Although they may occur, vessel-like organization of neoplastic cells is not generally a prominent feature of EHE. The epithelioid neoplastic cells are round to oval, cuboidal, or polyhedral. The eccentric nuclei are round- to cigar-shaped with well-defined nuclear membranes, finely distributed chromatin, and may be grooved. Neither nucleoli nor mitoses are generally a prominent feature. The cytoplasm is abundant eosinophilic or amphophilic with one or more prominent, thin-walled intracytoplasmic vacuoles that represent intracytoplasmic lumina. The vacuoles may result in nuclear pseudo-inclusions or in some cases coalesce to recapitulate primitive vessel formation. The cytoplasmic vacuoles frequently contain red blood cells or RBC fragments.

The presence of vacuolated epithelioid cells in nests and cords together with the hyalinized or myxoid stroma leads to a broad differential diagnosis that includes other epithelioid vascular lesions, chondromyxoid fibroma, and most importantly metastatic carcinoma.

The lack of specific immunoreactivity mandates a battery of studies. Immunohistochemical studies frequently positive in EME include factor VIII-related antigen, *Ulex europaeus*, CD31, CD34, and Fly-1. Cytokeratin and EMA help in the identification of metastatic carcinoma [344, 345].

Admittedly there is overlap between the histological appearances of epithelioid hemangioendothelioma and other epithelioid vascular tumors: epithelioid hemangioma and epithelioid angiosarcoma. As indicated earlier, the t(1;3)(p36.3;q25) translocation resulting in the WWTR1-CAMTA1 fusion product has been found to be a unique genetic aberration associated with EME and not found in other vascular tumors [4, 10, 346].

Gross

The gross appearance of EME is a limited spectrum. Lesions generally range from 1 to 10 cm. Unaltered, EME appears as a nodular, gray-white to tan, firm to rubbery mass [17]. If there is intralesional necrosis and bleeding, the mass appears as a red to red-black, soft hemorrhagic mass.

Radiology

Radiographically, EHE appears as a destructive, lytic intramedullary lesion on plane films and CT (Fig. 3.169). The interface between tumor and normal bone can be either well-circumscribed or ill-defined. With increasing size, tumor may expand and/or erode cortex and extend into overlying soft tissue. On MRI lesions are generally hypointense with T1-weighted imaging and hyperintense with T2-weighted images. In general, imaging studies are

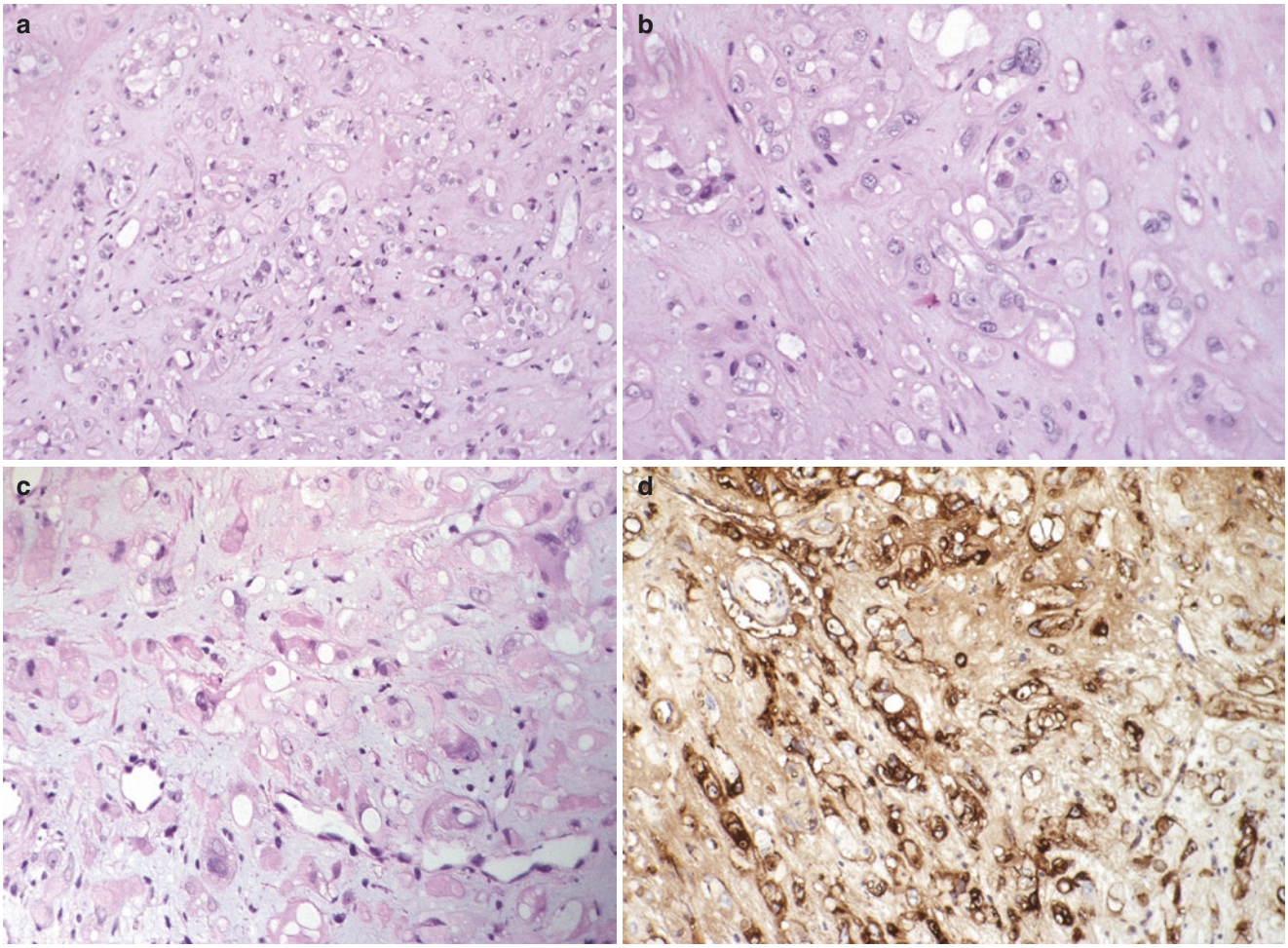

Fig. 3.168 Epithelioid hemangioendothelioma. (**a**–**c**) Sequential views of EHE. Tumor is formed by small clusters, groups, and individual cells in a pink-blue background myxoid matrix. Most of the cells in this case have an epithelioid quality; however, spindle cells are present. The cells have round to oval to angulated nuclei with variably staining nuclear membranes. The chromatin tends to be finely dispersed, and nucleoli are not uncommon. The cytoplasm of tumor cells tends to be abundant and pink, in some cases imparting a rhabdoid quality to the neoplastic cells. Many cells have intracytoplasmic vacuoles, some of which are so large as to obscure other cytoplasmic detail. (Courtesy of Michael Klein, M.D.)

interpreted as malignant. Because of the high propensity for multicentricity, a skeletal survey is indicated in all cases of EME [334].

Angiosarcoma

Definition

Angiosarcoma (AS) is a rare primary malignant tumor of the bone in which the neoplastic cells exhibit endothelial differentiation and have vasoformative capacity.

Introduction

Making up <1.0–1.5% of primary malignant bone tumors, AS of bone is a rare tumor. It appears to have been described in the early twentieth century, and confusion regarding origin, diagnostic criteria, clinical significance, and terminology has since been in flux as documented by Carter [1, 347].

Although the underlying concepts are relatively straightforward, a lack of agreement among investigators as to definitions and diagnostic criteria has led to terminology surrounding angiosarcoma that is extremely confused [11, 12, 347–350]. Terms used to refer to this group of tumor include angiosarcoma, hemangiosarcoma, hemangioendothelioma, and hemangioendothelial sarcoma.

Clinical

AS affects patients over a broad age range with a rough bell-shaped distribution and a relative peak in the fourth and fifth decades. Males are affected somewhat more often than females, with male to female ratio of 6:5. The tubular bones of the appendicular skeleton (e.g., femur, humerus, tibia) constitute 74% of cases, while some 25% involve the spine

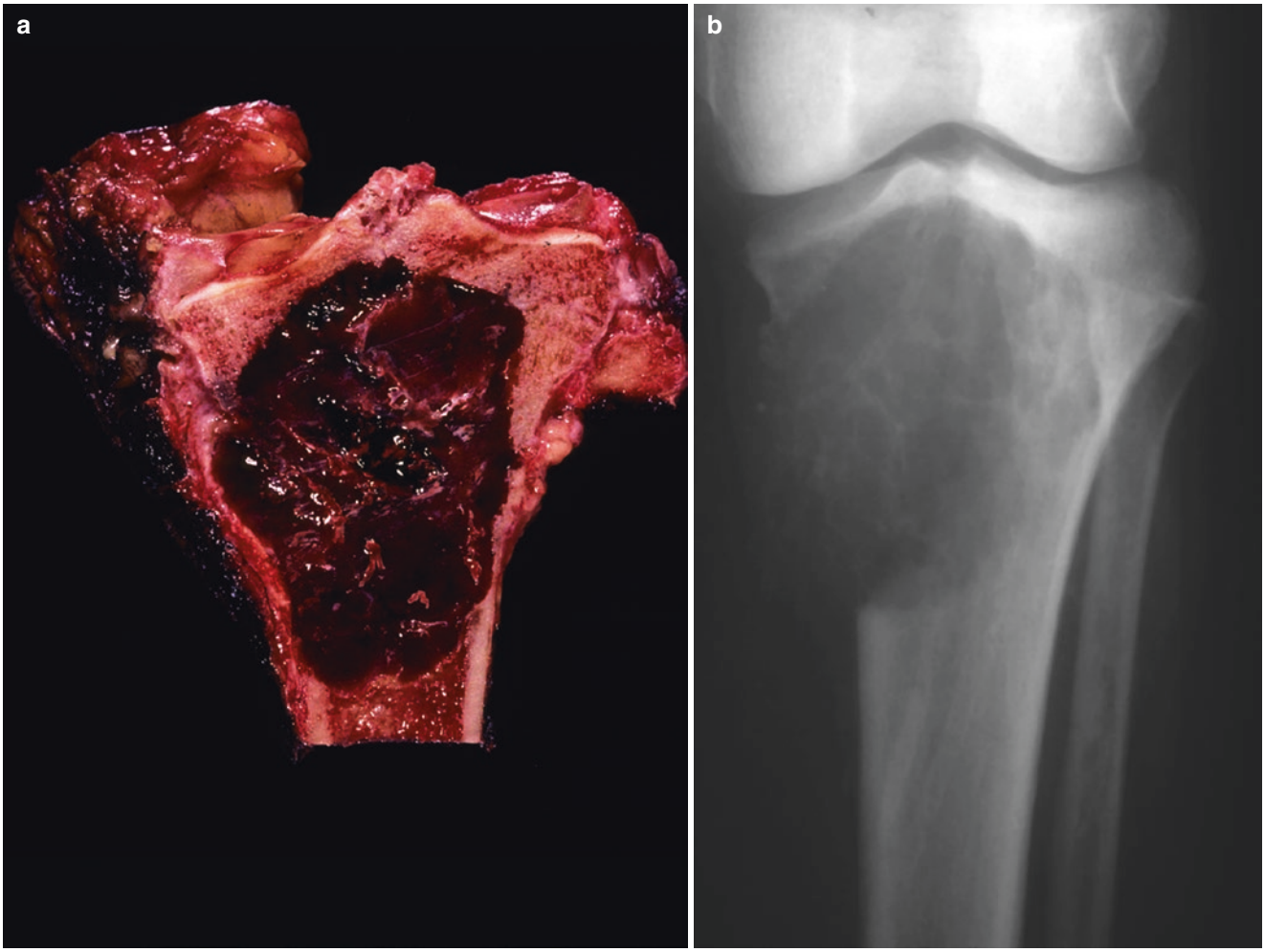

Fig. 3.169 Epithelioid hemangioendothelioma. (**a**) The proximal tibia is replaced by a reddish-black, grossly hemorrhagic tumor. Tumor involves the proximal metaphysis as well as the adjacent epiphysis (gross specimen). (**b**) Knee plane film (AP): the proximal tibia has been replaced by a destructive, purely lytic tumor that appears to have started and destroyed the medial and central portions of the proximal metaphysis, extended into adjacent epiphysis. The medial cortex overlying tumor is destroyed; soft tissue extension cannot be excluded. (Courtesy of Michael Klein, M.D.)

and pelvis. Tumor involving the tubular bones tends to occur in the metaphysis or meta-diaphysis. The etiology and underlying genetic mechanisms remain obscure. However, a small percentage occurs as postradiation sarcomas or complicating chronic osteomyelitis with draining sinuses [347, 351, 352]. At least one-third of cases are multicentric, and of these 64% arise as a regional phenomenon in contiguous bones. The remaining 36% of cases involve distant bones [268].

Symptoms are relatively non-specific with patient presentation generally a consequence of pain, mass, and/or pathological fracture. Other than those lesions arising as a long-term consequence of radiation exposure [352], the etiology of AS is poorly understood. The natural history of AS is unpredictable but tends to be that of a high-grade locally aggressive tumor with the capacity for early systemic dissemination [1, 12, 268, 349, 353].

In one 31-patient study, the overall survival was 55%, 43%, and 33% at 1 year, 2 years, and 5 years, respectively [354]. Histological features associated with a poor prognosis were the presence ≥3 mitoses per 10 HPF, macro-nucleoli, and low percentage of eosinophils. In another study there was a 50% mortality rate [355]. At the same time, there has been a general feeling that prognosis is a direct reflection of grade [268, 349].

Surgery is the mainstay of treatment; complete surgical extirpation is a prerequisite to successful therapy, complete resection with a rim of normal tissue or amputation. Systemic agents are employed with mixed results.

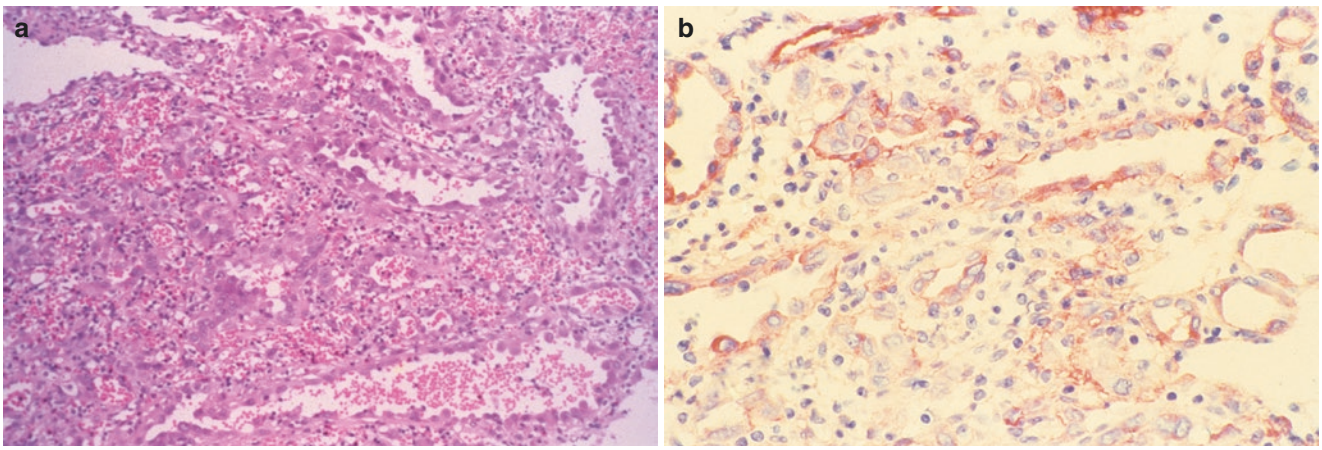

Fig. 3.170 Angiosarcoma. (**a**) A case of angiosarcoma in which intralesional hemorrhage has reduced this portion of the tumor to a membrane-bound blood-filled cyst. The neoplastic cells are highly anaplastic and in areas have an epithelioid aura that imparts a tombstone appearance to parts of the tumor (H&E. 100×). (**b**) Angiosarcoma: the neoplastic cells show strong cytoplasmic immunoreactivity for endothelial markers (Factor VIII. 200×). (Courtesy of A. Kevin Raymond, M.D.)

Histopathology

AS is composed of cytologically malignant cells that frequently have an epithelioid appearance [268, 353]. Although tumor may grow in seemingly disorganized sheets, there are usually areas with tumor-lined vascular channels (Fig. 3.170a, b). Tumor cell nuclei tend to be vesicular with one or more small nucleoli; but macronuclei can be present. Tumor cell cytoplasm tends to be deeply eosinophilic or amphophilic, and there are frequent intracytoplasmic vacuoles. Occasionally, red blood cells can be identified within intracytoplasmic vacuoles. Mitotic activity is generally present and may be brisk, and atypical forms may be identified. Hemorrhage is frequent, and blood breakdown products may be identified together with inflammatory elements, e.g., PMNs, lymphocytes, and eosinophils [353, 356, 357]. Reactive bone is a frequent finding and may be proportional to the changes of pathological fracture.

Immunohistochemical studies can be of paramount importance, particularly when evidence of vasoformative capacity is questionable [17, 268, 353, 357]. In particular, CD31, CD34, and factor VIII are most contributory (immunoreactive in 95%, 40%, and 60%, respectively) together with ERG and Fli-1. Relatively non-specific immunoreactivity may also been seen with SMA, D2-40, EMA, and cytokeratin. Interestingly, cytokeratins seem particularly reactive in case of AS with epithelioid features [17].

Cytogenetic as yet offers limited diagnostic assistance. Although its significance is not completely understood, a translocation, t(1;14)(p21;q24), has been described [348, 358]. MYC amplification has been described in association with postradiation angiosarcoma [359].

Gross

Lesions of AS are generally larger than 5 cm and described as friable. The color tends to be a function of overt hemorrhage. Tumor itself may be tan with hyperemia, or it may be reddish-black with frank hemorrhage. There may be extensive necrosis hidden by superimposed hemorrhage [17, 19, 268, 353].

Radiology

On plane films and CT, AS tends to be a destructive, purely radiolucent lesion with little reactive bone formation in the absence of overt pathological fracture (Fig. 3.171). The lytic tumor foci may be relatively well-defined or frankly infiltrative. Intramedullary lesions erode and destroy cortex while extending into overlying soft tissues. MRI remains the mainstay for evaluation of extent of disease. It tends to show a heterogeneous lesion with variable imaging characteristics that may enhance with contrast [17, 20, 21, 360–362].

Notochord Neoplasia

Introduction

In the not too distant past notochord pathology consisted of notochordal rests and chordoma. However, we have come to understand that the pathology is somewhat more complex (Tables 3.11 and 3.12).

Benign lesions include the historically recognized remnant of notochord in the intervertebral discs and vertebral bodies, *notochordal rests*. Larger collections have been

Fig. 3.171 Angiosarcoma. The plane films show a destructive, purely radiolucent lesion replacing the proximal humeral metaphysis. (Courtesy of A. Kevin Raymond, M.D.)

Table 3.11 Notochord neoplasia: proposed classification system

Notochordal rest
Simple notochordal rest
Ecchordosis physaliphora vertebralis
Giant notochordal hamartoma
Benign notochordal cell tumor
Chordoma
Conventional chordoma
Chondroid chordoma
Dedifferentiated chordoma
Primary
Secondary
Postradiation
Spontaneous

Table 3.12 Chordoma vs BNCT. Comparison of morphological features

Parameter	BNCT	Chordoma
Bone trabecula	Preserved	Destructive, smaller, and inconspicuous
Growth pattern	Embedded in bone trabecula	Infiltrative and lobular configuration
Cell morphology	Polygonal Large vacuolated adipocyte-like	Syncytial cords or strands of physaliphorous cells Abundant eosinophilic cytoplasm
Nuclear atypia	Absent or minimal	Mild to intermediate
Mitoses	None	Occasional
Necrosis	None	Present
Extracellular myxoid matrix	None	Present

Courtesy of A. Kevin Raymond, M. D.
BNCT benign notochordal cell tumor

variously referred to as *giant notochordal rests* and *(giant) notochordal hamartoma*. Similar lesions at the clivus and base of the brain have long been referred to by the term *ecchordosis physaliphora*. More recently a distinct benign lesion has been identified within vertebra alone and associated with chordoma, benign notochordal cell tumor.

On the other hand, malignancy of notochord is chordoma, in three subtypes. Conventional chordoma is what has been historically referred to as chordoma. Chondroid chordoma is a histological subtype with elements of both chordoma and chondrosarcoma and of arguable clinical significance. The third subtype is the lethal dedifferentiated chordoma. It is similar to other "dedifferentiated" tumors: typical histologically indolent chordoma with superimposed high-grade sarcoma (e.g., osteosarcoma, malignant fibrous histiocytoma) and associated with a poor prognosis.

Benign Notochordal Cell Tumor

Definition

Benign notochordal cell tumor (BNCT) is a slow-growing, indolent benign notochordal cell proliferation.

Clinical

BNCT is a recently described entity [10, 363, 364] virtually exclusive to the axial skeleton. The term represents a reinterpretation of benign notochordal lesions in light of recent observations and may also include those entities previously referred to as *giant notochordal rest* and *giant notochordal hamartoma* [17, 363, 365]. However, there remains some disagreement as to appropriate classification of lesions referred to as *ecchordosis physaliphora* which at least appear to have clinico-pathological features justifying separation.

Although multifocal lesions have been described, BNCT tends to be monostotic [17, 366]. Lesions tend to be small and growth is self-limited. Although there is a report of whole vertebra involvement, the vast majority of BNCT forms lesions that are <1 cm in diameter and generally closer to 0.2–0.4 cm.

So far, BNCT has been described over a broad age range, without statement concerning gender predominance. The skeletal distribution approximates that of conventional chordoma [364].

BNCT is almost always asymptomatic. To date, the vast majority have been incidental findings discovered either at autopsy or during imaging studies for unrelated reasons [367]. Cases subject to sequential imaging show it to be a very slow-growing lesion. Its skeletal distribution together with rare cases with coexisting chordoma suggests that BNCT may predispose patients to the development of chordoma.

The prognosis of BNCT is excellent. Although treatment of BNCT is not indicated, follow-up imaging studies to mon-

itor for the development of secondary chordoma is recommended [364, 368].

Histology

Histologically BNCT is composed of relatively well-defined intertrabecular sheets and aggregates of polyhedral cells. Tumor does not erode or destroy cancellous bone. Rather, tumor is surrounded by dense, sclerotic reactive bone (Fig. 3.172a–d).

A variety of features associated with chordoma are absent in BNCT. Extracellular mucin is not present in BNCT, and therefore chords or chains of neoplastic cells draped over and through mucin is not present. Tumors do not have a lobular configuration or the fibrous bands subdividing tumor.

The neoplastic cells present a biphasic population. The dominant population mimics fat cells (i.e., *adipocytes*) having abundant well-defined clear cytoplasm with either a single large clear vacuole or multiple vacuoles imparting a spider weblike appearance. The alternate population consists of cells has a more epithelioid quality. The latter have abundant pale pink cytoplasm, some of which have large PAS-positive (diastase-resistant) intracytoplasmic hyaline globules. In either case, nuclei tend to be small, round, and well-defined. The chromatin may be finely dispersed or hyperchromatic. Atypia is minimal, and mitoses are not a feature.

The immunohistochemical profile of BNCT as well as ecchordosis physaliphora is similar to chordoma. There is immunoreactivity for cytokeratin, S-100, EMA, CAM 5.2, and brachyury.

Chordoma may arise in patients with BNCT. Therefore, knowledge of BNCT and care in histological interpretation are necessary to avoid over- or under-calling chordoma.

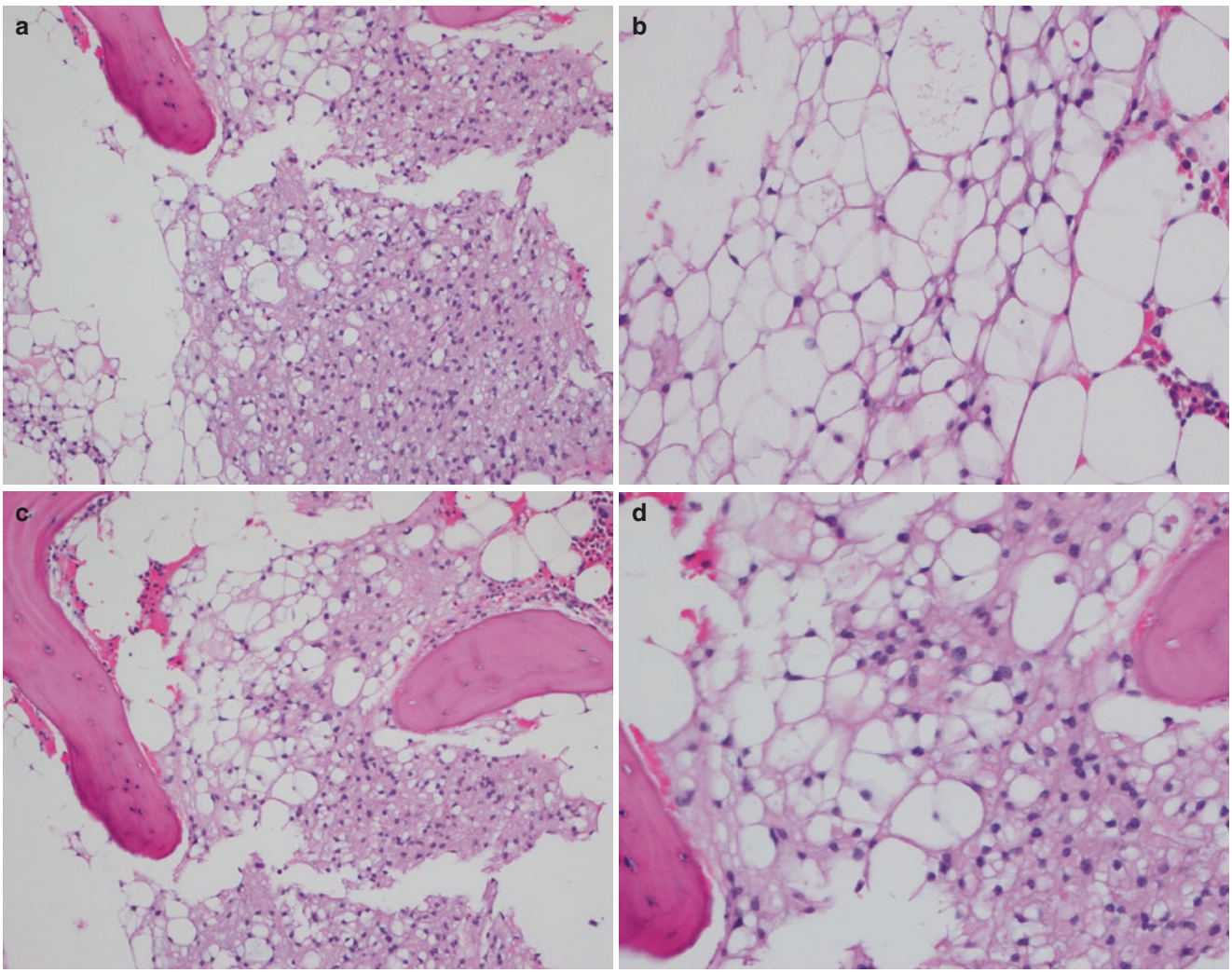

Fig. 3.172 Benign notochordal cell tumor. (**a**) Lesional cells of BNCT tumor aggregate between trabecula of cancellous bone. The cells are large and well-defined and have abundant pink cytoplasm. The nuclei are round to oval and are not atypical. The lesional cells have an overall epithelial quality (H&E). (**b**) In another area of the tumor the lesional cells are large, vacuolated, and polyhedral. The nuclei are small and inconspicuous. The lesional cells in this area have features similar to adipocytes (H&E). (**c**) Innocuous in another area of this BNCT, there is a mixture of the two morphological forms of the BNCT cells (H&E). (**d**) In another area of this BNCT, there is a mixture of the two morphological forms of the BNCT cells. This is a higher magnification of the previous area of tumor (H&E). (Courtesy of Fiona Bonar, M.D. and Michael Klein, M.D.)

Gross Pathology

The gross hallmark of BNCT is the absence of tumor-specific pathology. Rather, the lesional hallmark is focal sclerosis. Cancellous bone is thickened by appositional new bone deposition on pre-existing normal bone. The result is an area of gray-white to yellow-white bone production. Despite the histological appearance of the tumor, neither fish-flesh nor gelatinous material is grossly identified (Fig. 3.173a–c).

Radiology

BNCT is frequently undetectable on plane film. Bone destruction is not a feature of BNCT handcuffing radiographic detection. However, the associated reactive bone formation frequently results in an ill-defined radiopaque area confined within bone. In general this is a relatively small focus; however, entire bone involvement can occur. On CT BNCT consists of a small, ill-defined, circumscribed focus of sclerosis (Figs. 3.174 and 3.175). On MRI, the BNCT appears as a focus of low-signal intensity on T1-weighted imaging and hyperintense on T2 [369, 370].

Conventional Chordoma

Definition

Chordoma is a primary malignant tumor of the bone in which the neoplastic cells are phenotypically similar to those of notochord. There are three histological subtypes: conventional chordoma, chondroid chordoma, and dedifferentiated chordoma.

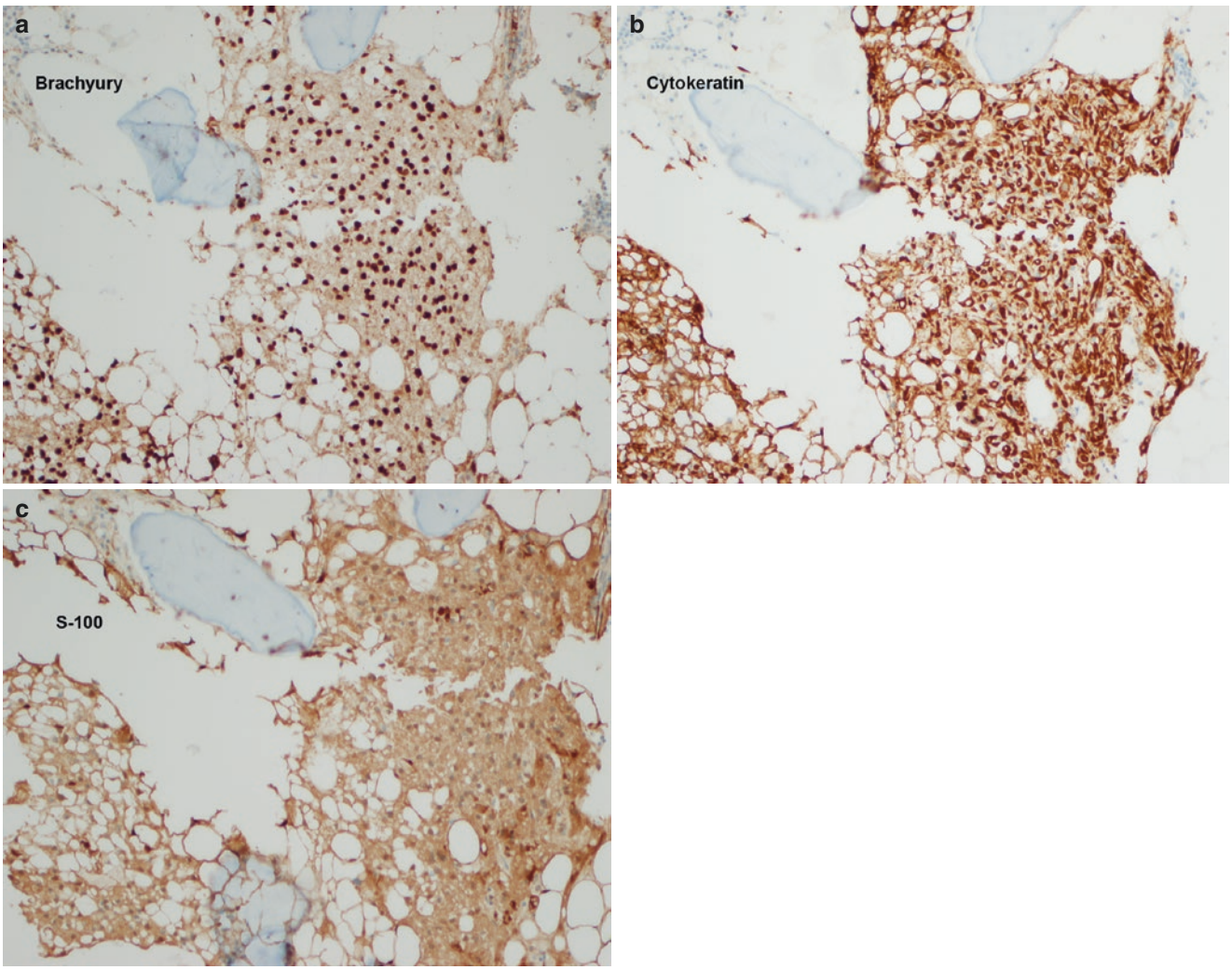

Fig. 3.173 Benign notochordal cell tumor. Sections corresponding to Fig. 3.172**.** (**a**) Strong intranuclear immunohistochemical staining for brachyury within neoplastic cells. (**b**) Strong intracytoplasmic immunohistochemical staining for cytokeratin within neoplastic cells. (**c**) Strong intranuclear and cytoplasmic immunohistochemical staining for S-100 protein within neoplastic cells. (Courtesy of Fiona Bonar, M.D. and Michael Klein, M.D.)

Demographics

With an incidence of 0.08 per 100,000 population, chordoma comprises some 5–6% of primary malignant bone tumors [17]. Although it can arise in patients of virtually any age, chordoma is rare in patients under 30 years of age and most frequently affects patients in the fifth through seventh decades of life. Chordoma is more common in men than women, with male to female ratio of 2:1.

Chordoma is, for all intents and purposes, unique to the spine. In most series the base of skull and sacrococcygeal mechanism accounts for a vast majority (i.e., 90%) of cases with much lesser representation in the mobile spine. An exception to this is found in the SEER data that indicates a relatively uniform distribution throughout the spine [1]. Tumors that arise in the skull base do so approximately one decade earlier than sacrococcygeal lesions, probably a function of a slow-growing tumor with varying spatial restrictions. Interestingly, at least one series shows a gender bias by location: 55% of skull base tumors are male, while 71% of patients with sacral tumors are male [20]. Recently, well-documented examples of chordoma arising in bones outside of the axial skeleton, and even soft tissues, have been described, *chordoma peripheric ium* [17]. Chordoma is rare in black Africans, but more or less equally affects all other races.

The unique epithelioid histology and localization to the axial skeleton, in particular the extremes of the spine, have resulted in much speculation as to the origin of chordoma. Historically, in light of the similarities of histology and skeletal distribution, it was taught that chordoma arose from notochordal remnants. Recently, this direct linage has been questioned and is the subject of at least one detailed discussion [371]. As to precursor lesions, some chordomas arise in association with benign notochordal cell tumors [17]. A few are familial and associated with a specific genetic aberration: duplication of the brachyury gene, a transcription factor necessary for notochord development [10]. Occasionally, they have been associated with tuberous sclerosis. However, at this time it is currently held that most chordomas arise as sporadic events, of which at least 7% are associated with amplification of the brachyury gene. Notochord remnants, hamartomas, benign notochord cell tumors, and chordoma may represent differing evolution and expression of some distant primitive event, but defining origin is at best speculative at this time.

Fig. 3.174 Benign notochordal cell tumor. Co-existent chordoma and BNCT. The chordoma is the focally hemorrhagic, cystic mass extending into anterior soft tissue. The area of yellow-white sclerotic bone (red arrows) corresponds to the BNCT. (Courtesy of Fiona Bonar, M.D. and Michael Klein, M.D.)

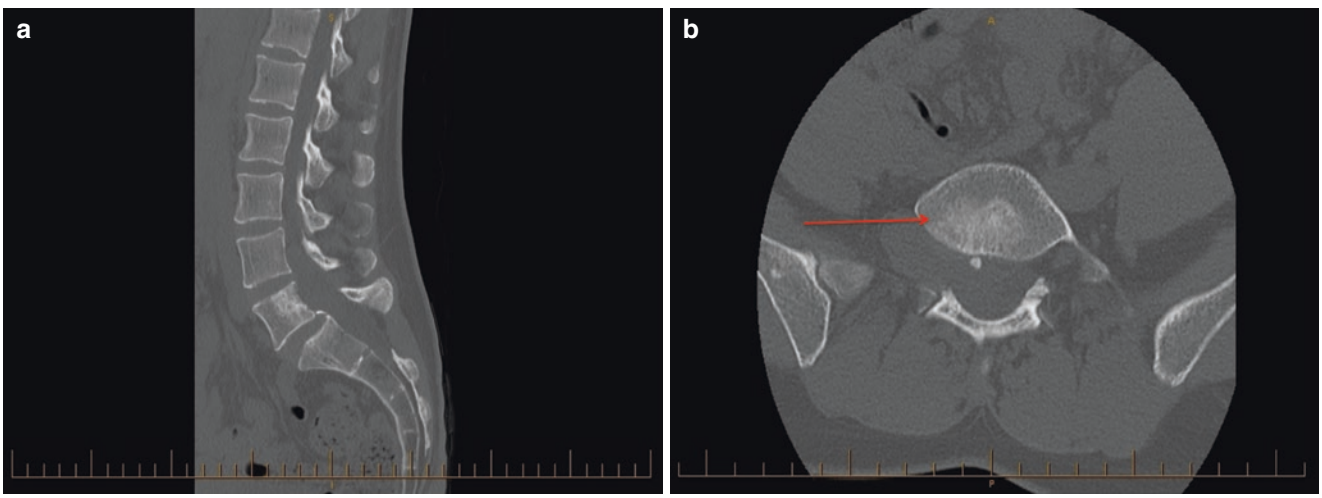

Fig. 3.175 Benign notochordal cell tumor with superimposed chordoma. (**a**) Plane film of the whole spine shows an isolated area of sclerosis involving a sacral vertebra (red arrow) corresponding to the BNCT. (**b**) CT shows an isolated area of sclerosis involving a sacral vertebra (red arrow) corresponding to the BNCT. (Courtesy of Fiona Bonar, M.D. and Michael Klein, M.D)

Clinical

Initial chordoma presentation is largely a function of tumor site and size. Arising in the spine, tumor growth with resulting mass effect results in a diversity of symptoms resulting from local nerve and/or cord compression; cranial nerves with base of skull lesions and spinal nerves in the remainder.

Skull base chordoma frequently presents with headache, neck pain, and symptoms referable to cranial nerve compression or destruction, e.g., diplopia, visual field defects, or facial nerve palsy. Local growth may impinge upon the sella turcica resulting in pituitary dysfunction. Inferior growth may result in nasopharyngeal mass.

Sacrococcygeal lesions are generally associated with pelvic pain that may involve the coccyx tip (i.e., coccydynia). Local growth may be in any direction and involve adjacent vertebrae, spinal canal, nerves, and/or soft tissues. But anterior growth into the posterior retroperitoneum generally predominates and may result in an enormous mass that may be palpable on rectal examination. Mass effect may result in cord, nerve, or organ compression resulting in bowel, bladder, or sexual dysfunction.

The natural history of chordoma is one unrelenting local growth with a relatively low incidence of systemic dissemination. Metastases occur in 5–43% of patients [20] but have been largely overshadowed by local relapse. The lung, bone, and skin are the usual sites of metastases.

Surgery was and is the treatment of choice. Until recently, surgery was almost always incomplete resulting in residual disease and local relapse, in essence *debulking* procedures. In general, repeated surgeries could add several functional years of survival with the patient ultimately succumbing to the complications of local disease.

However, recent developments in surgical technique now allow a higher probability of complete tumor removal in the majority of vertebral and sacrococcygeal tumors. However, the potential sacrifice of normal structures necessitated by some of these techniques makes the "rate-limiting element" of surgery the amount of loss of function (e.g., bladder, bowel, sexual and/or mobility) patients are willing to endure. Whenever margins are close, external beam radiation therapy becomes part of treatment. Currently available chemotherapeutic agents have not been affective in the treatment of chordoma.

Employing contemporary therapy the overall 5- and 10-year survival for patients with sacrococcygeal chordoma has been reported as 60–95% and 40–60% [1]. Survival in the mobile spine is reported at 55% with local relapse occurring in 62–75%.

With the use of surgery and proton beam radiation therapy, the survival in skull base chordoma has improved. However, 41–46% suffer local progression within 69 months. Poor prognostic factors are large tumors, female gender, and patient age >40 years [20].

Historically, the near-uniformly lethal nature of chordoma in which death due to local disease was the norm, systemic metastases were largely relegated to the status of medical curiosity. However, with the increasing success of surgery-dominated multimodality therapy and what appears to be predictable durable local control of non-skull base chordoma, the biological consequences of chordoma metastases may take on greater significance.

A word of warning: Sacrococcygeal chordoma may closely approximate the rectum and present a tempting target for transrectal needle biopsy; after-all, transrectal prostate needle biopsy is a routine procedure. However, there are anatomic considerations that abrogate posterior transrectal needle biopsy. Anteriorly, the rectal-prostate interface consists of a continuum of dense connective tissue allowing contained prostate needle biopsy; any contamination is confined to poorly vascularized dense connective tissue. Posteriorly, the rectum is covered by visceral peritoneum that separates it from the peritoneal cavity, while the posterior retroperitoneal-based chordoma is covered by parietal peritoneum. Any posterior transrectal biopsy results in a peritoneal defect that may provide a source of tumor leak and intra-abdominal contamination and give rise to a clinical situation analogous to ovarian cancer with peritoneal *chondromatosis*. Therefore, transrectal biopsy can only be discouraged in the strongest terms! All biopsies should be performed from the posterior, utilizing a percutaneous route where contaminated soft tissue can be removed at the time of definitive surgery.

Histopathology

From low power, chordoma appears as lobulated sheets of cells infiltrating between normal bone trabecula, surrounding and then engulfing trabecula. Cortex is infiltrated, invaded, and destroyed resulting to pathological fracture as tumor extends into subperiosteal and ultimately true soft tissue. Bone destruction tends to be extensive, while reactive bone changes tend to be negligible.

Tumor is crisscrossed by arcades of fibrovascular septa dividing tumor into lobules of varying sizes (Fig. 3.176a–d). The smaller lobules appear to be solid spheres of neoplastic cells with minimal mucin. The overall appearance suggests that with tumor growth, there is increasing mucin production and collection within tumor lobules, imparting a myxoid quality to chordoma. The mucin is insubstantial, gray-blue, and appears wispy and/or "frothy."

Characteristically epithelioid, the neoplastic cells of chordoma are typically columnar or tall cuboidal and mildly atypical (Fig. 3.176a–d). The nuclei are dark, round to oval,

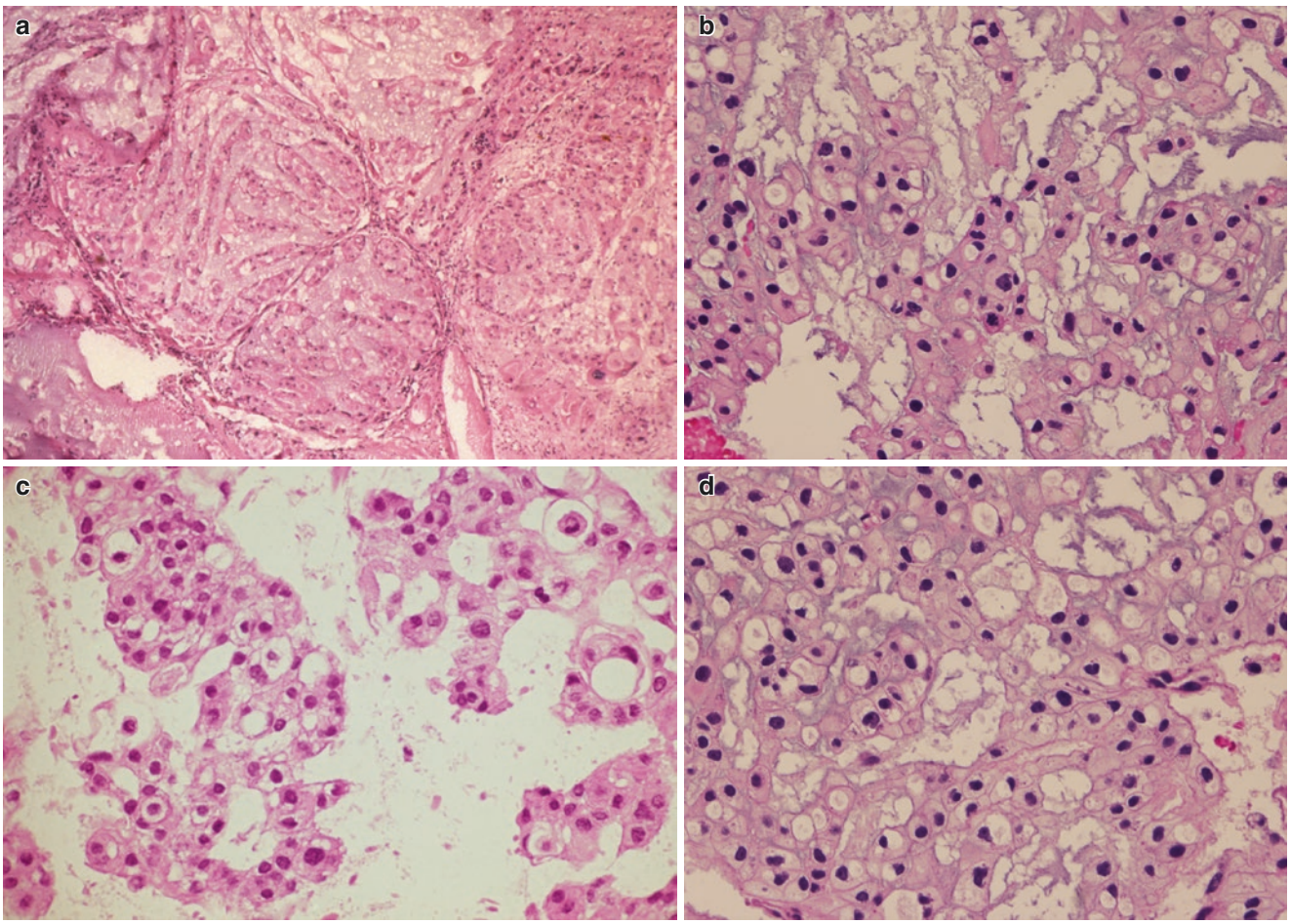

Fig. 3.176 Chordoma. (**a**) Chordoma forms mucin-filled lobules lined by fibrovascular septa. Cords and chains of neoplastic cells arch over and through the mucin (H&E. 40×). (**b**) Chains of vacuolated neoplastic cells form chains within the mucin (H&E. 100×). (**c**) Smaller clusters of "free-floating" neoplastic cells in wispy, ill-defined mucin. These highly vacuolated cells are referred to as *physaliferous cells* (H&E. 200×). (**d**) In lobules with minimal mucin, the neoplastic cells frequently appear more cohesive and have a plate-like arrangement (H&E. 200×). (Courtesy of A. Kevin Raymond, M.D.)

relatively small, with well-defined irregular nuclear membranes and highly variable chromatin ranging from finely dispersed to vesicular, but an element of chromatin condensation along the nuclear membrane is frequently present. *Smudgy* chromatin indicative of degenerative (so-called "ancient" or "pseudomalignant" appearance) changes may be present. Nucleoli may be present, but are small. Mitoses are infrequent.

Cytoplasm is generally abundant and may be deeply eosinophilic or variably vacuolated. The clear vacuoles may be large and solitary and result in peripheral displacement of the nucleus resulting in a signet ring cell appearance. Vacuoles may be smaller and multiple and cause the cells to mimic adipocytes. But most cells tend to have numerous small vacuoles imparting a bubbly appearance, so-called *physaliferous* cells. At lobule peripheries there may be cellular compression imparting a spindle-cell quality to the neoplastic cells.

Tumor cells appear to be mutually adherent and have syncytial growth pattern resulting in the formation of nests, strands, or ribbons. In smaller lobules, with only minimum mucin, the neoplastic cells may take on a plate-like organization mimicking hepatic architecture (Fig. 3.176a–d). In the larger lobules, much of the increased size is the result of substantial centrolobular mucin pools, which in turn cause displacement of neoplastic cells into a peripheral layer and chains or cords coursing through and apparently draped across the mucin.

In the larger lobules, neoplastic cells are found in two positions: condensation of neoplastic cells toward the lobule

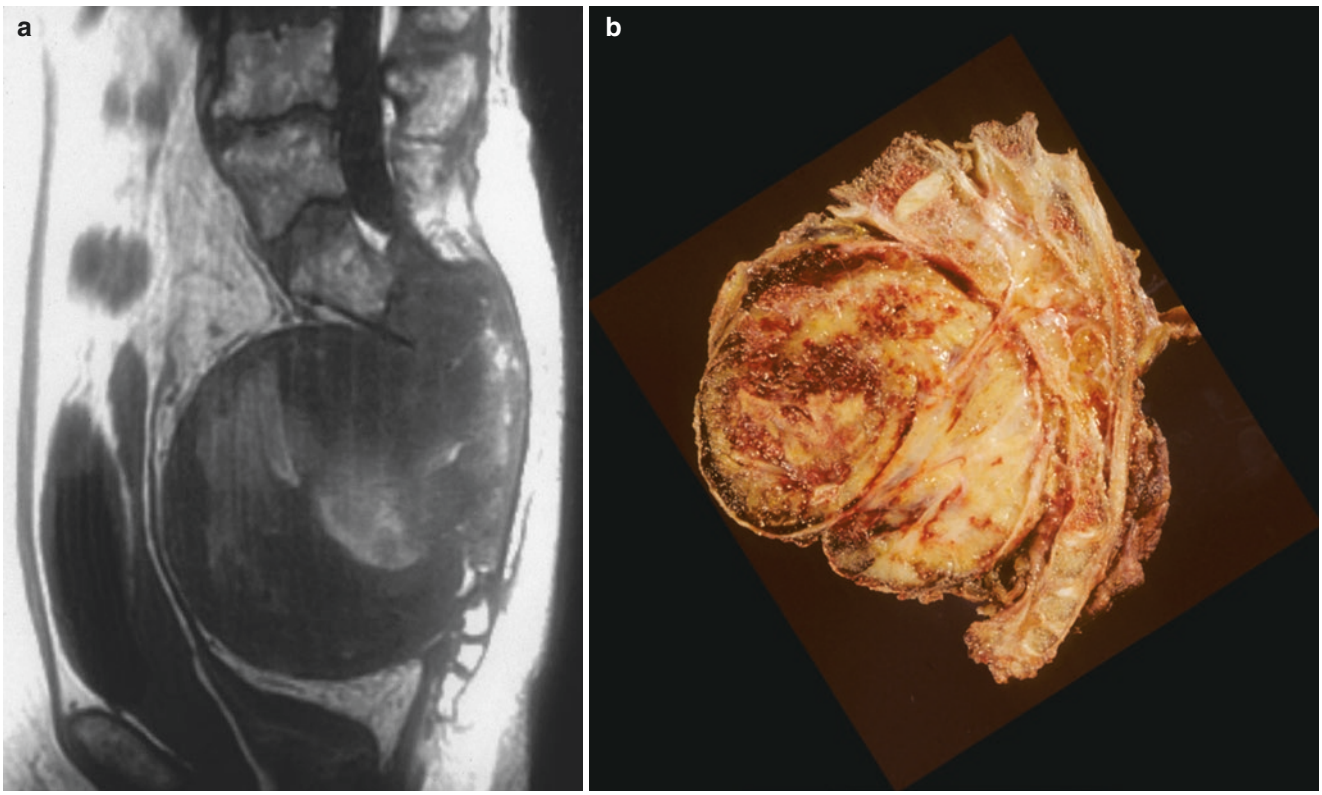

Fig. 3.177 Chordoma. (**a**) MRI shows destruction of the majority of the sacrococcygeal mechanism by tumor that extends into overlying soft tissue and spine. (**b**) Gross specimen shows extensive tumor destruction of the sacrum and coccyx with significant tumor extension into the posterior peritoneum. The S-2 nerve is encased by tumor. Chordoma has also invaded into and extended up the spinal canal. (Courtesy of A. Kevin Raymond, M.D.)

periphery and cells forming chains and cords coursing through and apparently draped across the mucin.

There are almost always extensive secondary changes of hemorrhage, necrosis, inflammation, and fibrosis. Tumor invasion results in pathological fracture, osteonecrosis, osteoclast migration, and small amounts of reactive bone formation.

The epithelioid cells of chordoma routinely show immunoreactivity for epithelial markers, i.e., CK AE1/AE3, CK8 and CK19, and EMA. Immunoreactivity for brachyury is both sensitive and specific for notochordal differentiation. Some investigators report that S-100 protein is positive in many cases of chordoma. Other markers that may show nondiagnostic immunoreactivity include CEA, GFAP, and INI1.

Special stains are non-specific but are positive for intracytoplasmic glycogen (i.e., PAS) and extracellular acid mucopolysaccharides (i.e., Alcian Blue), pretty slides, but non-specific.

Gross

Grossly, chordoma is nodular tumor composed of superimposed and interlocking lobules varying from millimeters to centimeters in diameter (Fig. 3.177a, b). Intact, the lobules are firm though compressible. With sectioning and loss of confinement, chordoma is found to be a semisolid tumor with variable amounts of expressible mucin. Lobular tumor replaces and fills the medullary cavity of the parent bone, infiltrating and then destroying cancellous bone and cortex while gaining access to adjacent bone(s) and overlying soft tissues. Tumor may extend superior or inferior to involved skeletal elements. It may extend posteriorly to involve spinal canal, vertebral arch, and overlying soft tissues.

However, the cut surface is a smooth, semitranslucent gray to blue-gray glistening mass subdivided by delicate septa into mucin-filled lobules and cysts. The color of chordoma is highly variable and largely a function of secondary changes. Degenerative changes impart a yellow-green granu-

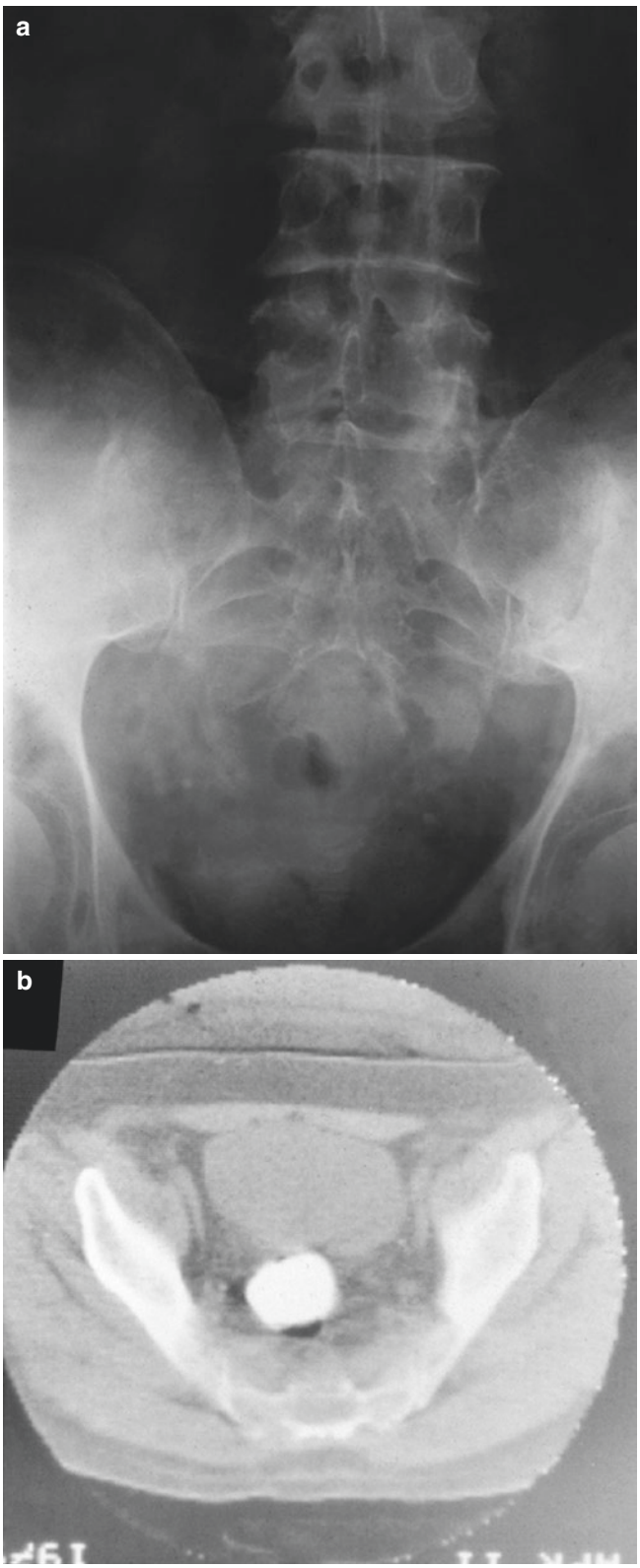

Fig. 3.178 Chordoma. (**a**) Plane film (AP) of the pelvis is difficult to interpret. There is a suggestion of some destruction of the sacrum but overlying soft tissue changes and bowel gas obscure details. (**b**) CT (same case) shows a radiolucent mass destroying much of the sacral body and ala with extension into overlying retroperitoneum. Despite proximately to colon, the high probability of peritoneal contamination contraindicates transrectal biopsy

lar quality to parts of tumors. Areas of hemorrhage are red, black, or shades of yellow and brown depending on the status of blood breakdown products and inflammation. Tumor/normal soft tissue interfaces almost inevitably consist of compressed fibrous connective tissue.

Radiology

Regardless of the location, chordoma forms a destructive, radiolucent mass. However, the anatomical peculiarities of the spine/axial extremes can complicate imaging interpretation. Sacrococcygeal lesions are generally >10 cm, while skull base lesions tend to be small (i.e., 2–5 cm).

The AP plane film appearance of sacral lesions is notoriously deceptive; soft tissue and intestinal gas patterns can mask even large lesions (Fig. 3.178a). Lateral plane film views are frequently better. But CT and MRI have become the standard of sacrococcygeal imaging evaluation (Fig. 3.178b). Chordoma is hypointense on T1-weighted images, while T2-weighted images show a lobulated hyperintense lesion with internal septation. CT shows a destructive, lobulated nonhomogeneous mass, with cortical thinning, destruction, and tumor extension into overlying soft tissues; in particular anterior extension into the posterior retroperitoneum may be overwhelming. The subtleties and specifics of soft tissue extension and extent of disease are best evaluated with MRI.

The relatively small skull base lesions may involve relatively subtle changes in the spheno-occipital, hypophyseal, and/or sella turcica regions [17]. There may be destruction of the clivus. There may be soft tissue extension along the skull base and into the nasopharynx. Again, CT and MRI are best suited for these inquiries (Fig. 3.179) [10].

Lesions involving the mobile spine tend to be mixed lytic/blastic but otherwise non-specific. The tumor itself is radiolucent. Radiodensities correspond to entrapped normal bone and reactive bone at the tumor/normal interface [4, 372–374].

Chondroid Chordoma

Definition

Chondroid chordoma (Ch-Cd) is a biphasic subset of chordoma in which there is histological evidence of both histologically typical chordoma together with conventional chondrosarcoma.

Clinical

Ch-Cd was originally described by Heffelfinger and Dahlin in 1973 as an outgrowth of an inquiry concerning an unexpected long-term survivor with skull base chordoma and the resulting review of that institution's chordoma experience [374].

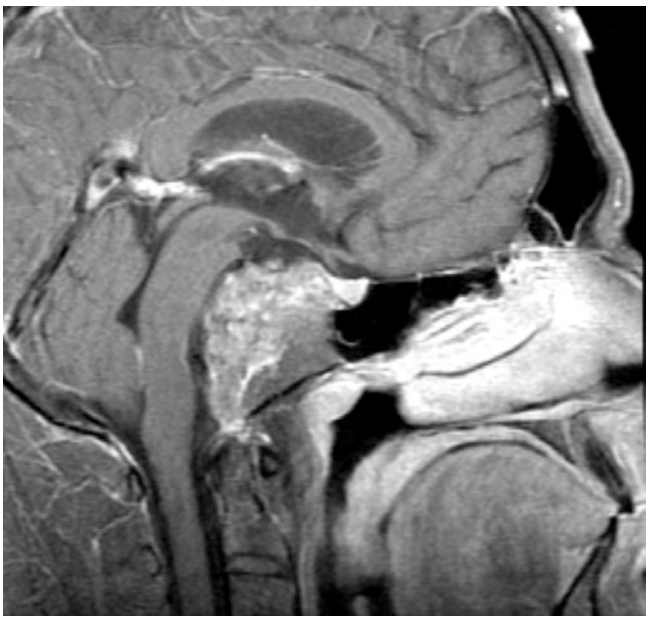

Fig. 3.179 Chordoma. MRI of skull (T2-weighted image) shows a hyperintense lesion in the region of the skull base

The overwhelming majority of patients with Ch-Cd have lesions arising in the skull base, 19 of 22 in the largest series [375]. Women are affected somewhat more frequently than men, with male to female ratio approximating 2:3. When compared with the entire chordoma family, Ch-Cd appears to involve a somewhat younger group of patients. However, when compared to only those cases arising in the skull base, Ch-Cd and c-Cd affect a similar age group.

Signs and symptoms of Ch-Cd are similar to other skull base lesions and largely a consequence of increased intracranial pressure and compression of regional structures, in particular cranial nerve compression. Frequent findings include diplopia, visual field defects, and headache. On occasion local growth can result in intranasal or pharyngeal mass.

The treatment of choice is surgery with postoperative radiation therapy.

The initial data showed a surprising survival advantage of Ch-Cd versus c-Cd. The ultimate prognosis with Ch-Cd is poor secondary to the critical location of a locally aggressive tumor that denies unfettered surgical access, resulting in an inevitable sequence of events: incomplete surgery, local relapse, repeated surgery/surgeries, and ultimately patient death due to uncontrolled local growth. However, it appeared that the time between initial presentation and ultimate patient demise is unexpectedly protracted in Ch-Cd. In the initial series, there were no survivors with skull base c-Cd after 7 years, and the mean survival was 4 years. In contrast 60% of Ch-Cd patients survived 15 years with a mean survival of 15.8 years [20, 372, 374, 375].

Subsequently, the existence of Ch-Cd as a distinct clinicopathological entity was brought to question with authors suggesting that Ch-Cd actually represents a form of chondrosarcoma [376, 377]. Over the decades, the topic has been a source of significant contention among pathologists with discussions bordering on the acerbic. Although disagreement continues, most investigators currently hold that Ch-Cd is a distinct histological entity with at least some suggestion of survival advantage [375].

Histopathology

Histologically, Ch-Cd is a biphasic lesion with areas of chondrosarcoma juxtaposed to chordoma. Discrimination between cartilage matrix and extracellular mucin is critical (Fig. 3.180).

There are areas of low- to intermediate-grade *hyaline* cartilage differentiation. The identification of hyaline cartilage adds confidence to the discrimination between chondroid matrix and the myxoid elements of chordoma. Juxtaposed to this are areas in which there are chains and cords of the epithelioid *physaliferous* cells appended to a myxoid background (Fig. 3.181) [1, 372].

Immunohistochemical studies are as expected for the respected tissues. Unfortunately, SOX 9 appears to be expressed in chordoma as well as cartilage neoplasia.

Gross

Arising at the skull base, Ch-Cd specimens are seldom more than small fragments of curetted tissue. In general these consist of small fragments of shiny, semitranslucent, gray-white to silver semisolid tissue that may be independently submitted. Frequently, tumor is adherent to the interstices of cancellous bone fragments.

Radiology

The radiographic appearance of Ch-Cd is similar to conventional skull base chordoma. Tumor presents as an expansile radiolucent mass that erodes and destroys contiguous bone while compressing adjacent vital structures. Occasionally, small flecks of punctate calcification can be identified and are presumed to correspond to areas of the cartilage component of Ch-Cd. Tumor may grow anteriorly and inferiorly resulting in a nasopharyngeal mass [17].

Dedifferentiated Chordoma

Definition

Dedifferentiated chordoma (dd-Cd) is a biphasic tumor in which there are elements of conventional chordoma juxtaposed to high-grade sarcoma.

Clinical

dd-Cd is a rare, relatively recently described aggressive subset of chordoma [10, 378, 379]. The demographics (age, gen-

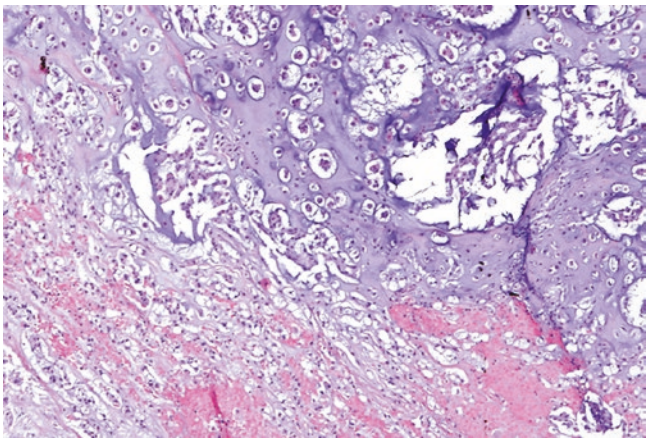

Fig. 3.180 Chondroid chordoma. Tumor is a biphasic lesion: the upper right contains lobules of gray-blue hyaline cartilage (low-grade chondrosarcoma). (**b**) In contrast, the lower left is composed of ribbons and chains of otherwise typica

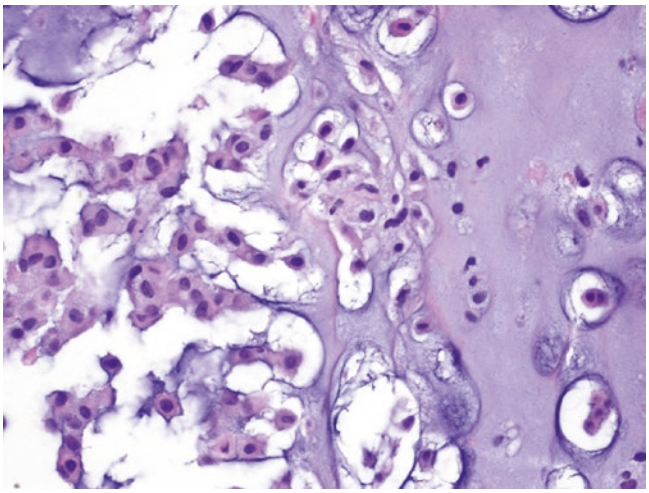

Fig. 3.181 Chondroid chordoma. Biphasic with low-grade chondrosarcoma on the right side of the field. The left side of the field is replaced by mucin with small groups and short chains of *physaliferous* cells of chordoma (H&E, 200×). (Courtesy of A. Kevin Raymond, M.D.)

der, and skeletal distribution) of dd-Cd are similar to conventional chordoma. dd-Cd occurs in both primary and secondary forms. In the rare primary form, both typical chordoma and a superimposed high-grade sarcoma are present in the initial, untreated, presenting lesion. The secondary form consists of high-grade sarcoma occurring in either systemic or local relapse of an otherwise typical conventional chordoma. The vast majority of dd-Cd arise after external beam radiation therapy for a conventional chordoma that may or may not have undergone prior incomplete or questionably complete surgery and therefore represent a form of postradiation sarcoma [378, 380].

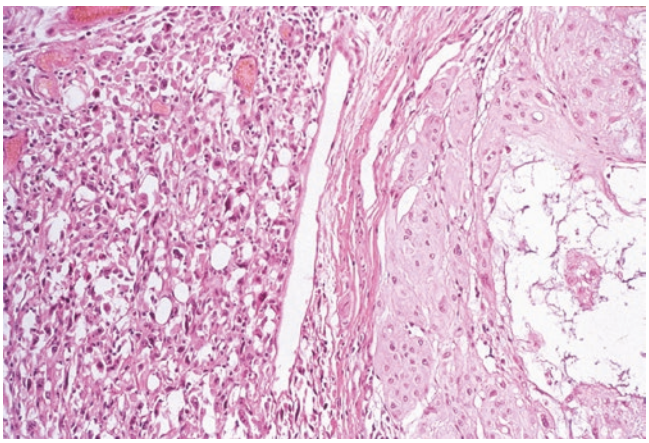

Fig. 3.182 Dedifferentiated chordoma. This is a biphasic tumor. The right side of the slide has an area of compact conventional chordoma. The left side of the slide is replaced by a high-grade pleomorphic sarcoma (H&E, 100×). (Courtesy of A. Kevin Raymond, M.D.)

The natural history of dd-Cd is one of local relapse and systemic dissemination with uniform mortality in less than 2 years. Treatment is usually multimodal and unsuccessful. No form of systemic therapy has thus far been found effective in dd-Cd [378, 381, 382].

Histopathology

As with other dedifferentiated sarcomas, dd-Cd is a biphasic tumor. Much of the tumor is composed of the typical cords and chains of physaliferous cells coursing through, draping across, and encasing mucin-filled lobules (Fig. 3.182). Juxtaposed to chordoma without gradual transition or mixing, but, a sharp interface is high-grade sarcoma; most frequently high-grade osteosarcoma, unclassified spindle-cell sarcoma (i.e., malignant fibrous histiocytoma), fibrosarcoma and on rare occasion other sarcoma (e.g., rhabdomyosarcoma) [383, 384]. High-grade sarcoma is generally present in large amounts but on occasion may be scattered small foci.

The results of immunohistochemical studies are those expected for chordoma and high-grade sarcoma.

Gross

As a result of its rarity, there is little specific information pertaining to the details of gross specimens. In the two examples seen at MD Anderson Cancer Center, there were large areas of typical lobular shiny, semitranslucent, silver-gray to yellow-brown, mucoid chordoma juxtaposed to typical tan to off-white osteosarcoma and MFH. Mineralized bone production was evident in the case with osteosarcoma. Superimposed were secondary changes of necrosis and hemorrhage, together with reactive and inflammatory elements and blood breakdown products.

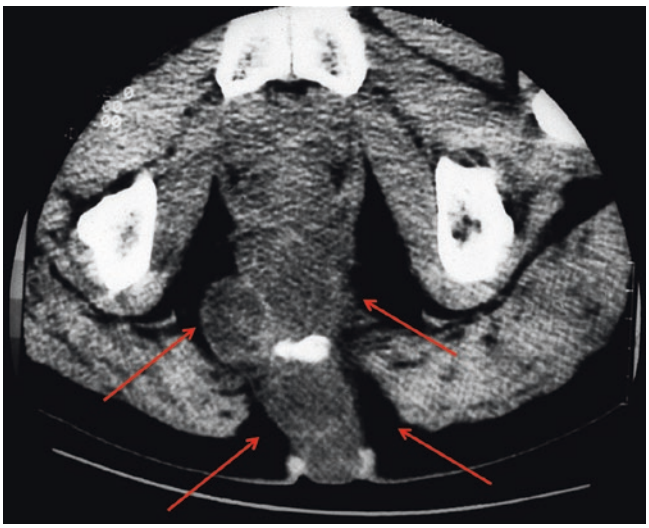

Fig. 3.183 Dedifferentiated chordoma. CT of pelvis: there is virtual complete destruction of only minute radiopaque fragments of bone remain. Tumor is extending anteriorly into the retroperitoneum. Posteriorly, tumor has extended into soft tissue and formed an intergluteal mass. (Courtesy of A. Kevin Raymond, M.D.)

Radiology

Plane film, CT, and MRI imaging studies for dd-Cd are similar to those of conventional chordoma (Fig. 3.183). However, the lobular, homogeneous hyperintense picture seen on T2-weighted imaging is absent. Instead, areas of high-grade sarcoma result in a heterogeneous picture with alternating and mixing areas of hyperintensity and hypointensity [17, 385].

Adamantinoma

Definition

Adamantinoma has long been viewed as an unusual low-grade biphasic malignant tumor composed of both bland spindle-cell and epithelioid components. It is a tumor with a penchant for local relapse and low probability of potentially lethal metastases.

Clinical

Adamantinoma has long been recognized as a distinct entity primarily affecting long bones. With the accrual of larger numbers of cases and experience, it has been suggested that "adamantinoma" does not represent a single entity but rather a family of related diseases with a potential linkage with osteofibrous dysplasia. This adamantinoma family includes differentiated or osteofibrous dysplasia-like adamantinoma, conventional adamantinoma, and dedifferentiated adamantinoma. The precise relationship and significance of these "entities" are still a matter of investigation.

Conventional adamantinoma (c-Ad) is the lesion originally described by Mair in 1900 [386] and subsequently the subject of extensive literature [387, 388]. c-Ad occurs at any age, but there is a profound peak in the second decade of life and a lesser peak in the third decade, together 70% of cases. Males and females are affected in roughly equal numbers. Although virtually any bone may be the primary site, c-Ad shows a profound predilection for the tibia (i.e., >80%) and to a much lesser extent the fibula. Tumor is frequently multifocal within the primary bone and may involve both the tibia and ipsilateral fibula in some 10% of cases. Intraosseous skip metastases may be present. When involving the tibia, c-Ad almost inevitably arises within the anterior, diaphyseal tibial cortex.

c-Ad is a slow-growing tumor, and minimal symptoms may be disregarded for prolonged periods of time. The natural history is one of aggressive local growth, first within the bone and then extension into soft tissue. Despite the frequently voiced misconception that c-Ad's aggressive behavior is confined to local extension, c-Ad is a fully malignant tumor. Metastatic disease occurs in 25–30% of patients involving the regional lymph nodes, lung, and/or bone [322]. Clinically evident metastases may be a long-term phenomenon and become apparent as many as 17 years after the primary diagnosis [389].

With no form of effective systemic therapy, treatment is a surgical. Incomplete surgery (i.e., curettage, marginal excision) virtually guarantees local relapse and puts the patient at greater risk for systemic metastases [322, 389]. Currently, the treatment of choice is wide resection or amputation with a cuff of normal tissue, i.e., negative resection margins [322, 324, 389, 390]. The current expected long-term survival is estimated to be 80%.

Histopathology

c-Ad forms a mass or masses that consist of sheets of neoplastic cells centered within cortex, infiltrating adjacent medullary cavity; skip metastases may be present, and tumor may invade overlying soft tissues. c-Ad is a biphasic tumor with both epithelial and spindle-cell components (Fig. 3.184a–d). The epithelial cells are variable in numbers and concentrations appearing as islands within the edematous fibrous or fibro-osseous stroma. The epithelial elements may be present in one or more histological patterns: basaloid, tubular, squamous, spindle cell, or osteofibrous dysplasia-like [268, 322, 391]. The spindle cells have small, round, oval, or fusiform nuclei with either euchromatin or heterochromatin. The eosinophilic cytoplasm is abundant but varies from dense to ill-defined. The

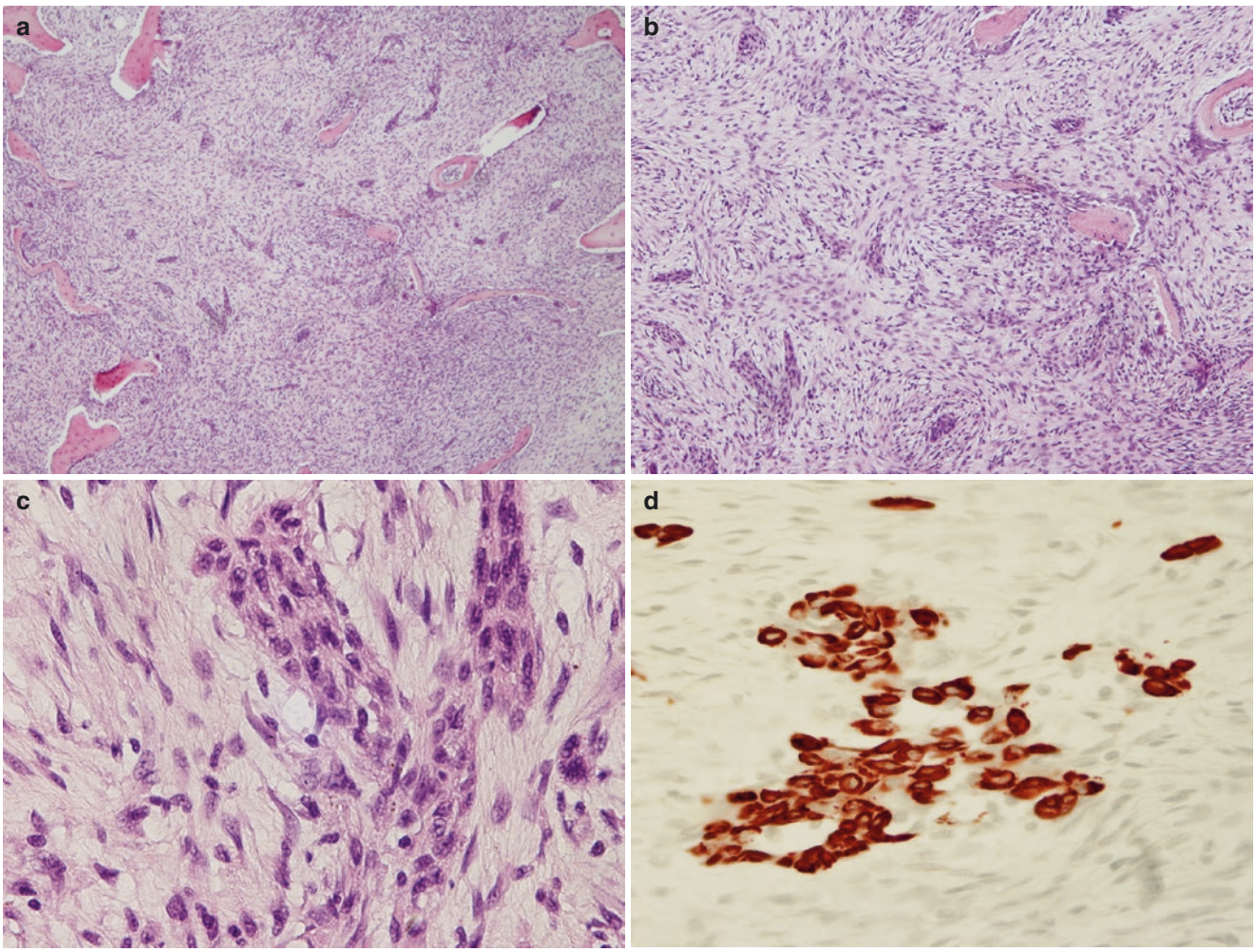

Fig. 3.184 Adamantinoma. (**a**) Tumor is composed of sheets of innocuous spindle cells with round to oval nuclei and abundant eosinophilic cytoplasm. The spindle cells may have a storiform pattern. In addition, there are randomly disposed and shaped trabecula of woven bone lined by larger cells mimicking the findings of osteofibrous dysplasia. More importantly there are islands of what appear, even at low power, to be epithelial elements (H&E, 20×). (**b**) Higher magnification confirms the triphasic nature of the tumor: swirling spindle cells, osteoblast-lined bone, and islands of epithelial cells (H&E, 100×). (**c**) Large nest of epithelioid cells with features suggestive of squamous differentiation. Background of innocuous spindle cells with wispy cytoplasm and stroma imparting an impression of edema (H&E, 200×). (**d**) Epithelial cells have strong intracytoplasmic immunoreactivity for cytokeratin (CK AE1/AE3. 200×). (Courtesy of A. Kevin Raymond, M.D.)

spindle cells frequently exhibit a storiform pattern. Tumor may be zonated with the epithelial component more pronounced at the center with gradual transition to a spindle-cell-dominant periphery that may transition with reactive bone. There may be secondary changes of necrosis, inflammation, fibroxanthomatous change, and/or cyst formation.

The epithelial components show immunoreactivity for a number of cytokeratins (CK AE 1/CK AE 3, CK 14, CK 19) and EMA while being negative for others, e.g., CK8 and CK18 [268, 386, 392]. The spindle-cell component does not stain with cytokeratin. Both epithelioid and spindle-cell elements stain for vimentin.

The origin of the epithelioid component has been a point of contention since c-Ad was first described.

Gross

The gross appearance of adamantinoma is largely a function of secondary features. The tumor itself is a fairly typical fish-flesh cream white to beige, soft, and rubbery. However, adamantinoma is frequently accompanied by large amounts of bone formation. In the latter case, the tumor takes on a sclerotic gray-white to tan appearance consistent with sclerotic bone (Fig. 3.185). There may be degenerative changes or pathological fracture superimposed. Larger lesions frequently extend into and may replace large portions of the medullary cavity. Skip metastases may be present; multifocality may be confined to the parent bone (e.g., tibia) or may involve the tibia and fibula.

Fig. 3.185 Adamantinoma. (**a**) Tumor forms an eccentric cortical-based mass on the medial aspect of the mid-tibia. The soft parts of the tumor are off-white and opalescent. There is focal hemorrhage and extensive bone formation. (**b**) Plane film (AP) shows a cortical-based radiolucent lesion with an overall soap bubble configuration. There is sclerotic bone formation at the tumor/normal interface. (Courtesy of A. Kevin Raymond, M.D.)

Tumor in local soft tissue relapses, and pulmonary metastases tend to be off-white, beige to tan. In the limited number of cases seen by the author, the bone component has not been present in a non-osseous relapse (Fig. 3.186).

Radiology

Adamantinoma begins as an intracortical lesion where it forms a destructive radiolucent mass. With time there are variable amounts of reactive bone formation that is frequently concentrated on the medullary cavity side of the lesions (Fig. 3.185). CT and MRI both add to detailed analysis of the lesion, and MRI best evaluates extent of disease and the possibility of multifocal disease [1, 328, 393–400].

Fig. 3.186 Adamantinoma. Pulmonary metastasis from a patient who had been diagnosed with adamantinoma 3 years earlier. (Courtesy of A. Kevin Raymond, M.D.)

Giant Cell Lesions

Introduction

Giant cell tumor of bone (GCT) has a long and complex differential diagnosis (Table 3.13). In many ways, the differential can be summarized as anything with an aneurysmal bone cyst component. The vast majority of this differential represents primary bone tumors with degenerative changes, secondary aneurysmal bone cyst. Identification of the original underlying primary pathological process is the key to diagnostic specificity and appropriate therapy. Diagnosis will almost inevitably include complete integration of clinical and pathology evidence.

Historically the most difficult discrimination is between GCT, brown tumor hyperparathyroidism, aneurysmal bone cyst, and giant cell reparative granuloma. While histological features can largely exclude ABC and giant cell reparative granuloma, clinical integration makes the task easier.

On the other hand, GCT and brown tumor can be histologically indistinguishable. The clinical parameters are paramount for correct diagnosis. GCT shows a profound localization predilection for secondary growth centers, epiphyses. Brown tumor does not; it tends to be a metadiaphyseal lesion. In contrast, patients with hyperparathyroidism show unique bone resorption in unusual sites, e.g., terminal tufts of digits. Considering the etiology of brown tumor, the results of serum analysis for calcium and parathyroid hormone are of paramount importance.

Table 3.13 The differential diagnosis of giant cell tumor of bone

Tumor	Age (decades)	Gender (M/F)	Location	Radiology	Gross	Histopathology	
						Giant cells	Stromal cells
GCT	3 and 4 2 and 5	2:3	Epiphysis epiph-metaph	Eccentric: lytic expansile soap bubble, infiltrative	Fleshy, soft, fawn brown ± hemorrhagic: red-black	Evenly distributed	Uniform "mononuclear stromal cells" Naked nuclei, nuclear identity w GCs
Brown tumor (hyperparathyroidism)	6 and 7 > 5 and 8	1:2	Anywhere (digits, clavicle, L = spine, pelvis)	Any, lytic, expansile	Fleshy, cystic ± hemorrhagic ±	Focal, around hemosiderin and hemorrhage	Fibroblasts
ABC	2 and 1 > 3	1:1.1	Metaphysis	Eccentric lytic expansile, soap bubble	Blood-filled cysts	Focal, around hemorrhage	Variable "mononuclear stromal cells," fibroblasts
Giant cell rep gran	2 and 3	2:3	Maxilla, mandible	Lucent	Soft, fleshy, brown	Abundant around hemosiderin or hemorrhage	Fibroblasts
NOF	2 and 1	5:4	Metaphysis	Eccentric: subcortical, soap bubble	Fleshy, soft, brown, hemorrhagic ±	Focal, small, hemorrhage	Slender, spindle cells, little cytoplasm
Chondroblastoma	2	2:1	Epiphysis	Lucent, w ring and fleck Ca++	Pebbles on the beach	Few, focal ± around hemorrhage	"Fried egg" w abundant pink cytoplasm
CMF	3 and 2 >1	3:2	Metaphysis	Lytic w thinned expanded cortices	Gelatin + Ca++	Focal random	Zonated spindle cells
UBC	1 and 2	Equal	Metaphysis	Lucent w trabeculations	Membranes clear fluid	Focal around cholesterol clefts	Cyst walls
Fibrous dysplasia	2 >2.3 and 4	1:1	Metaphysis	Ground glass	Firm, rock-hard, gritty to granular	Few, focal around hemorrhage	Short spindle cells in "edematous" background
Ossifying fibroma	2 and 3	2:3	Maxilla, mandible	Mixed lytic, blastic	Bony	Few and focal	Lamellar bone in fibrous stroma
Osteoblastoma	2	3:1	Vertebra, posterior elements	Mixed lytic, blastic	Granular, gray-white, hyperemic	Random with osseous matrix	Osteoblasts lining osteoid
Osteosarcoma	2 and 3	3:2	Metaphysis, any	Any, mixed lytic, blastic	Any ± Ca ++	Random, adjacent hemorrhage	Anaplastic cells produce osteoid

Giant Cell Tumor of Bone

Definition

Historically, conventional giant cell tumor of bone (GCT or c-GCT) has been viewed as a histologically biphasic tumor of unknown etiology. GCT tends to arise in secondary ossification centers and when appropriately treated has a relatively indolent albeit unpredictable biological behavior.

Clinical

In the USA, GCT comprises an estimated 22% of benign bone tumors and 6.6% of all bone tumors [1]. In contrast, it is the most common bone tumor in China [401].

GCT most frequently affects patients in the third and fourth decades of life, as well as the second half of the second decade, i.e., the skeletally mature. Women are affected more frequently than men, with 2:3 male to female ratio. The most frequently involved sites are the distal femur, proximal tibia, and distal radius. Somewhat less frequently involved are the sacrum, spine, distal tibia, and pelvis. For the most part, tumor selectively involves secondary ossification centers (i.e., epiphyses, apophyses) of the effected bones. When originating in the spine, GCT tends to involve the vertebral bodies as opposed to the posterior elements that are preferentially involved by osteoblastoma. Of interest, the rare pediatric cases of GCT tend to originate in metaphyses.

Pain is the most common presenting complaint. However, depending on location, pain may be accompanied by swelling, enlarging mass, range of motion limitation, and pathological fracture in 5–10% of patients.

In the overwhelming majority (>95%) of cases, GCT behaves as a benign, locally aggressive tumor with a propensity for local relapse following incomplete treatment. Metastases occur in a small proportion of cases, and their behavior is unpredictable; some behave as indolent, nonaggressive lung lesions, while others follow a progressive, malignant course [402]. A small percentage of cases are multicentric, and an equally small number are associated with evidence of high-grade sarcoma [20].

The treatment of choice is complete surgical extirpation, with the form of that surgery undergoing evolution over the last several decades. Initially, curettage was considered adequate treatment. However, there was a >75% incidence of local relapse following simple curettage. In contrast the recurrence rate after curettage *and* packing is variously reported as being 25–50%.

Wide resection with metallic endoprosthesis placement is an alternative. Although providing maximum potential for complete tumor extirpation and virtually eliminating local relapse, prostheses pose different consequences. By any of a number of mechanisms, prostheses eventually fail and require replacement, e.g., fracture, loosening, infection, etc. In the older population originally targeted for endoprostheses, prosthetic failure is less of a problem as a function of life expectancy vs prosthesis half-life; prostheses tend to outlive patients. However, in younger patients there is not just the issue of failure but a high probability of multiple failures over time, each followed by prosthesis replacement and consequent tissue sacrifice. Eventually, there is the possibility of reaching a juncture at which time replacement is no longer anatomically feasible and more debilitating surgery must be carried out, arthrodesis or amputation. Therefore, despite the successes of metallic endoprosthetics, we would like to avoid their use when possible, and this has resulted in the investigation of alternative forms of therapy to avoid the consequences of sequential prosthesis failure.

In the vast majority of cases, post-curettage relapse is a function of residual microscopic disease within the interstices of cancellous and cortical bone. A variety of approaches have been investigated with the goal of *extending* the curettage process to eradicate this residual tumor burden: sequential curettings utilizing decreasing caliber curettes, high-speed bone burring, liquid nitrogen washing, and phenol installation. Many, if not most, surgeons incorporate all, or most, of these techniques to ensure eradication of residual tumor.

At the same time, it was recognized that GCT relapse can be radiologically indistinguishable from the reorganizing bone chips of "packing" that occurs during graft incorporation and contributes to delayed recognition of local relapse. To avoid this problem, packing with bone chips is abandoned in favor of using methyl methacrylate to fill the surgical defect and provide a functional bone. This has several advantages: *first*, relapse must occur outside the methyl methacrylate which in turn provides a radiopaque background against which relapse can be easily monitored, and *second*, the exothermic reaction generated by combining the methyl methacrylate ingredients provides thermal extension of the curettage.

As indicated, a small number of GCTs are multicentric. Although multicentricity has some preference for younger GCT patients, it is otherwise clinically similar to c-GCT. Each lesion is treated as a primary lesion, and the prognosis is similar to c-GCT [17, 403].

In the past, external beam radiation therapy was used to treat GCT. Although relatively effective, there is a high incidence of postradiation sarcoma following the treatment of GCT; in 1 series 21 of 30 GCT patients treated with radiation developed postradiation sarcoma. Therefore, whenever possible radiation therapy is avoided, and surgery remains the treatment of choice. However, there are situations (e.g., tumor size, location, or other medical factors) that preclude surgery, and radiation therapy provides the only therapeutic option [20].

A special association deserves mention. For as yet unknown reasons, GCT arising in Paget's disease of bone is an unusually aggressive neoplasm and has a mortality rate approaching 50%.

It has been recently recognized that GCT is functionally dependent on the RANK/RANK-L signaling system. Attempts to treat with a RANK-L inhibitor (e.g., denosumab) have met with variable degrees of success [22, 404]. While surgery remains the treatment of choice for surgically accessible tumors, agents such as denosumab may have a place in the treatment of lesions in which surgery is not a viable option.

Histology

At low power, tumor forms a relatively homogeneous, destructive, hypercellular blue/purple sheet of neoplastic cells. Little, if any, residual normal tissue can be identified with the tumor. However, variability is imparted by alternating areas of tumor, hemorrhage, necrosis, and reactive/inflammatory changes. Tumor infiltrates cortex and insinuates between bone trabecula at the tumor/normal interface.

Histologically, GCT is a biphasic tumor composed of multinucleated osteoclast-like giant cells and mononuclear cells. Whether numerous or few, the giant cells tend to be evenly distributed throughout any given tumor. However, giant cells may be more numerous around areas of hemor-

rhage and decreased in number in areas with degenerative changes, necrosis, or fibrosis. The mononuclear cells have round to oval nuclei with well-defined nuclear membranes, finely distributed chromatin, and small, inconspicuous nucleoli. The minimal cytoplasm tends to be wispy and ill-defined; mononuclear cells are essentially naked nuclei. The nuclei of the mononuclear cells and multinucleated giant cells (i.e., osteoclasts) are for all intents and purposes the same, so-called *nuclear identity*. When present mitoses are present in the mononuclear cells and absent in the multinucleated giant cells (Fig. 3.187a–d).

Additional superimposed histological features may be extensive and reflect hemorrhage, inflammation, cyst formation, necrosis, or degeneration. Hemorrhage may be massive imparting an appearance mimicking aneurysmal bone cyst, i.e., ABC (Fig. 3.188a, b). Inflammatory and degenerative changes may result in a picture mimicking nonossifying fibroma, infection, degeneration, or infarction. These histological features generally do not hinder the interpretation of major surgical specimens. On the other hand, secondary pathology may impede evaluation of small biopsies, thus emphasizing the need for incorporation of clinical and radiographic findings in the histopathological diagnostics. However, secondary changes may be so extensive as to require extensive sampling to identify viable, diagnostic GCT.

Gross

In the absence of significant degenerative changes, the gross appearance of GCT is that of a relatively soft, homogeneous, well-defined, somewhat lobulated mass with infiltrating

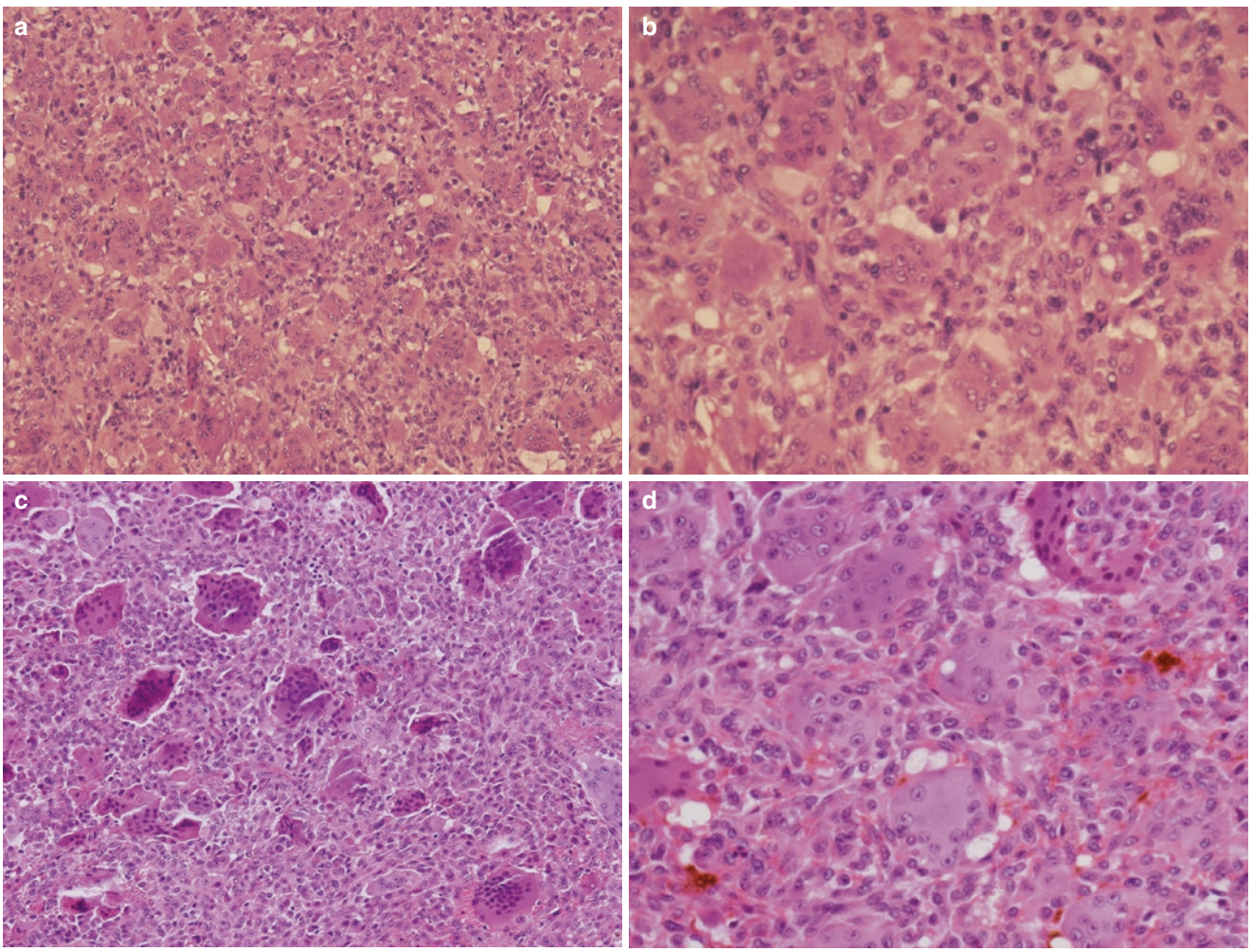

Fig. 3.187 Giant cell tumor of bone. (**a**) GCT is a bimorphic tumor composed of multinucleated osteoclast-like giant cells and mononuclear stromal cells. The osteoclasts tend to be evenly distributed throughout the lesion (H&E, 40×). (**b**) Bimorphic tumor in which the mononuclear cells have minimal ill-defined cytoplasm, the so-called naked nuclei. The nuclei of the mononuclear cells and osteoclasts look the same, the so-called nuclear identity (H&E, 200×). (**c**) GCT is a bimorphic tumor composed of multinucleated osteoclast-like giant cells and mononuclear stromal cells. The osteoclasts tend to be evenly distributed throughout the lesion (H&E, 40×). (**d**) GCT is a bimorphic neoplasm in which the mononuclear cells have minimal ill-defined cytoplasm; so-called naked nuclei. The nuclei of the mononuclear cells and osteoclasts look the same; so-called nuclear identity (H&E, 200×). (Courtesy of A. Kevin Raymond, M.D.)

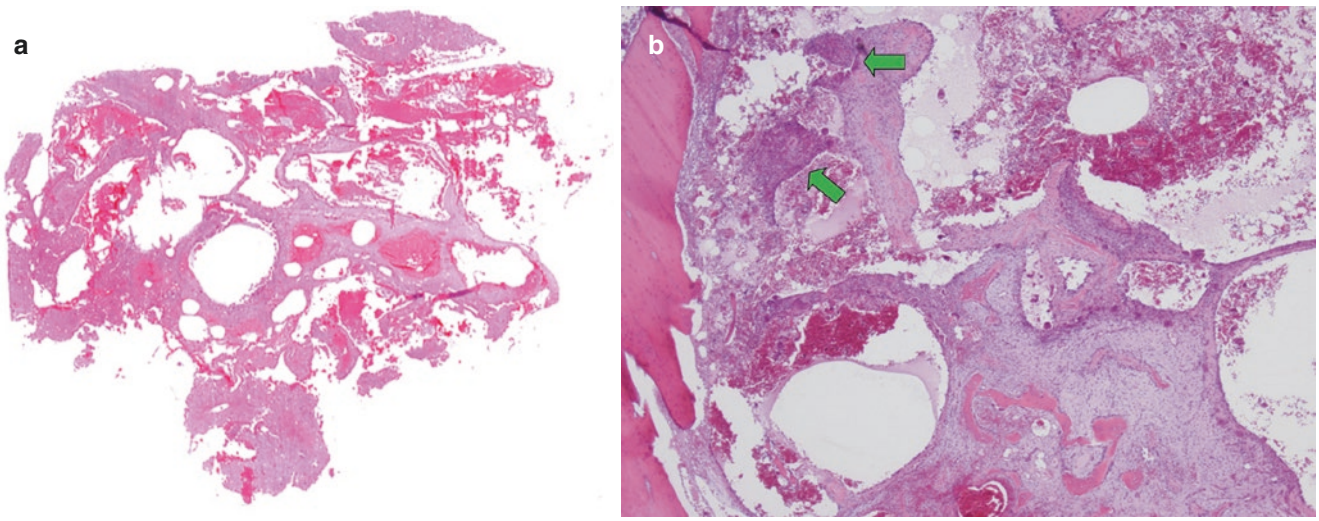

Fig. 3.188 Giant cell tumor of bone. (**a**) Aneurysmal bone cyst-like change is frequent in GCT and can be extensive. Since the ultimate form of therapy is determined by any underlying primary tumor, it is critical to search the specimen for residual primary pathology. In most cases this is relatively straightforward (H&E, scanned whole mount 1×). (**b**) Bimorphic: in this case, residual primary tumor was confined to small foci (green arrows) within membranes (H&E, 20×). (Courtesy of A. Kevin Raymond, M.D.)

interfaces. The color is pale brown or "*fawn*" *brown* similar to parathyroid tissue (Fig. 3.188). The frequently referenced red to red-black tumors are those with significant amounts of hemorrhage and ABC-like change. Hemorrhage and reactive changes frequently obscures the underlying GCT. Again, extensive sampling may be required to identify histologically diagnostic GCT.

The appearance of local relapse is generally similar to the primary tumor. However, there is a spectrum and local soft tissue masses take on a lobular configuration with egg shell-like calcification and the lobule periphery. The cut surface of the tumor itself is fawn brown. However, the edge at the normal/tumor interface is mineralized (Fig. 3.189).

Radiology

Radiographically, GCT forms a destructive osteolytic lesion with a marked propensity for the involvement of secondary ossification centers, which in tubular bones means involvement of epiphyses and apophyses at the "ends of the bones." Lesions tend to be lobulated and frequently have a "soap bubble" appearance. The tumor/normal bone interface tends to be infiltrative, as opposed to other mimicking lesions (e.g., ABC) that have well-defined interfaces that may be sclerotic. These features, together with better analysis of the extent of disease and fluid layering within tumor, are better viewed with CT and MRI (Fig. 3.190).

Molecular

Historically, GCT has been categorized as a tumor of unknown origin. Recent work suggests that the neoplastic mononuclear *spindle cells* represent preosteoblasts [10, 17]. The cells have been found to express collagen type I, alkaline phosphatase, osteocalcin, matrix metalloproteinases, and osteoprotegerin, factors associated with osteoblast differentiation. In addition, neoplastic cells utilize the RANK/

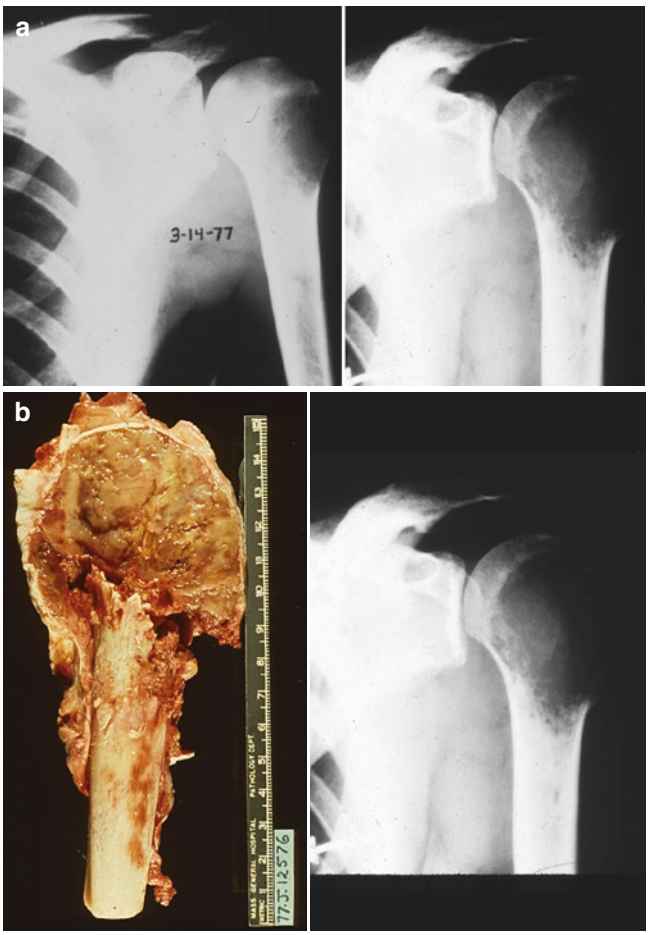

Fig. 3.189 Giant cell tumor of bone. Although considered benign, GCT can be locally aggressive: (**a**) Plane film (AP) on the left: initial presentation. Lytic lesion involving the greater tuberosity. X-ray on the right: 6 weeks later, follow-up, plane film shows virtual complete destruction of the entire proximal humerus. (**b**) Right: resection proximal humerus. GCT replaces the entire proximal humeral metaphysis and epiphysis. There is thinning of the cortices and pathological fracture. GCT cut surface is typical fawn-brown color

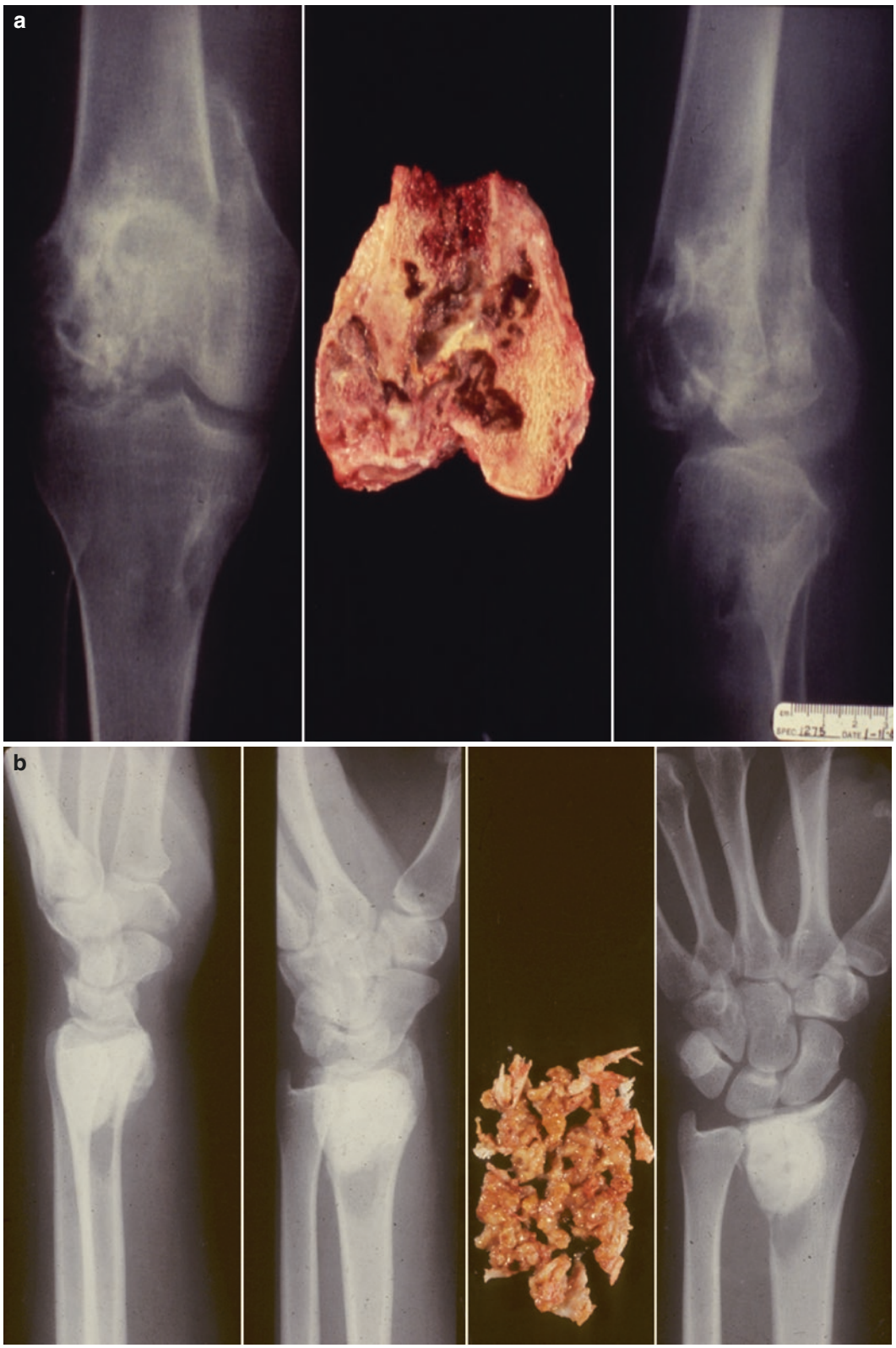

Fig. 3.190 Giant cell tumor of bone, local relapse. Plane films (AP and lateral) and gross specimen. (**a**) Although GCT has relapsed following curettage and packed with bone chips; relapse had not been suspected. The imaging studies were interpreted as consistent with incorporating graft. The resection was performed because of the intercondylar fracture. GCT is present as tan and pink foci of tumor admixed with the incorporating bone chips. (**b**) Relapse following extended curettage and cementation. Tumor relapse cannot occur within the methyl methacrylate, so it must occur in the adjacent tissues. The contrast between lytic tumor and radiopaque methyl methacrylate simplifies reviewing for relapse and allows for earlier and more confident identification of relapsing tumor

RANK-L signaling system, resulting in recruitment of appropriate histiocytes and stimulation of osteoclast formation, differentiation, and maturation [17, 22, 404–406]. In essence, what we recognize as the histological appearance of GCT is largely a response to signaling from the largely unnoticed underlying neoplastic cells. There is evidence suggesting that the presence of p63 may help distinguish between GCT and other elements of the GCT differential diagnosis.

"Malignant" Giant Cell Tumor of Bone

Definition

A malignant tumor biologically associated with giant cell tumor of bone.

Clinical

The concept of "malignant giant cell tumor of bone" (i.e., m-GCT) is elusive and seemingly shrouded in contention and confusion while utilizing a term that borders on misnomer. The term/phenomenon m-GCT, or malignancy *in* GCT, is more of a colloquialism or "short-hand term" that refers to a number of clinico-pathological scenarios [1, 20].

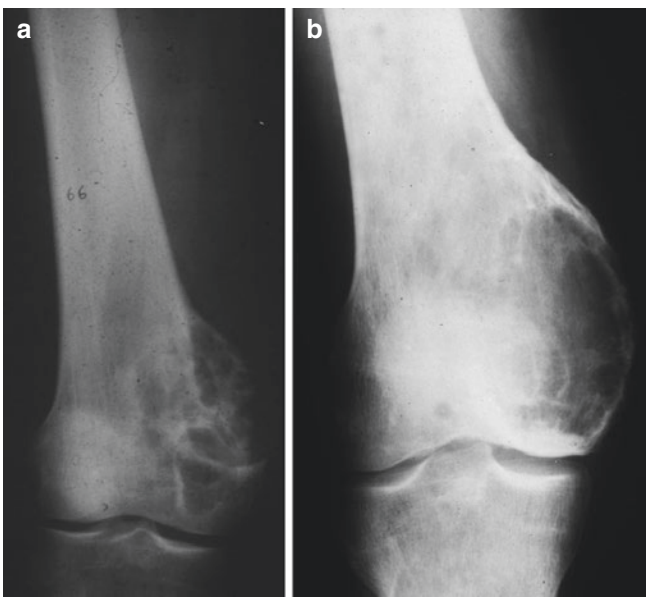

Fig. 3.191 Giant cell tumor of bone. (**a**) Plane film (AP) femur: the distal femur is replaced by an eccentric osteolytic lesion with a soap bubble appearance consistent with giant cells tumor of bone. Following multiple local relapses following curettage and packing of GCT, the lesion was treated with high-dose external beam radiation therapy. (**b**) Plane film (AP) femur: 12 years after completing radiation therapy, the patient present with new pain. Plane film shows a mixed lytic/blastic destructive lesion involving the distal femur. Surgical specimens confirmed a diagnosis of post-radiation osteosarcoma. (Courtesy of A. Kevin Raymond, M.D.)

In the vast majority of cases, m-GCT is actually a secondary phenomenon and represents a form of *postradiation sarcoma.* In this scenario an otherwise typical GCT is treated with radiation therapy. In the majority of cases, the GCT is located in an anatomical area, which together with tumor size negates the possibility of complete surgical removal. In some cases patients refuse surgery. After a latency period, usually of several years, postradiation sarcoma develops in as many as one-third of these patients (Fig. 3.191). Tumor manifests as a local "relapse," and high-grade sarcoma (e.g., osteosarcoma, fibrosarcoma) is present in the local "relapse" or subsequent metastases. The biological behavior, therapy, and ultimate prognosis are a function of the high-grade sarcoma.

Dedifferentiation analogous to that seen in chondrosarcoma and parosteal osteosarcoma can occur with GCT. In the majority of cases, the malignant element is a form of high-grade sarcoma (e.g., osteosarcoma, spindle-cell sarcoma) that arises in association with an otherwise typical conventional GCT (Fig. 3.192a–c). This spontaneous high-grade component may arise in conjunction with the primary tumor, within local relapse or as systemic metastases.

The so-called benign metastasizing giant cell tumor of bone: A small percentage (i.e., <5%) of otherwise, histologically, typical GCTs give rise to systemic metastases that are histologically indistinguishable from typical, conventional GCT (Fig. 3.193a, b). In many cases these pulmonary metastases are biologically indolent and do not influence prognosis, in essence a vascular transport phenomenon rather than true, aggressive metastases. However, in a small percentage of these cases, the metastases do pursue an aggressive course similar to that seen in more typically malignant tumors.

Aneurysmal Bone Cyst

Definition

Aneurysmal bone cyst is a destructive benign bone tumor composed of a multiloculated cyst formed by blood-filled, membrane-bound cysts.

Clinical

Aneurysmal bone cyst (ABC), first described by Jaffe in 1950 [407], has two significant divisions, primary and secondary ABC [17, 22, 408, 409]. Primary ABC is a fairly specific clinico-pathological entity associated with rearrangement of the USP6 gene in some 70% of cases. Secondary ABC consists of components histologically similar to primary ABC superimposed on an underlying primary bone tumor, effectively a hemorrhagic degenerative process. The underlying lesions are usually benign (e.g., giant cell tumor of bone, osteoblastoma, chondroblastoma, fibrous dysplasia). However, ABC changes may be associated with osteosarcoma. Secondary ABC is not associated with any recognized ABC-related genetic aberra-

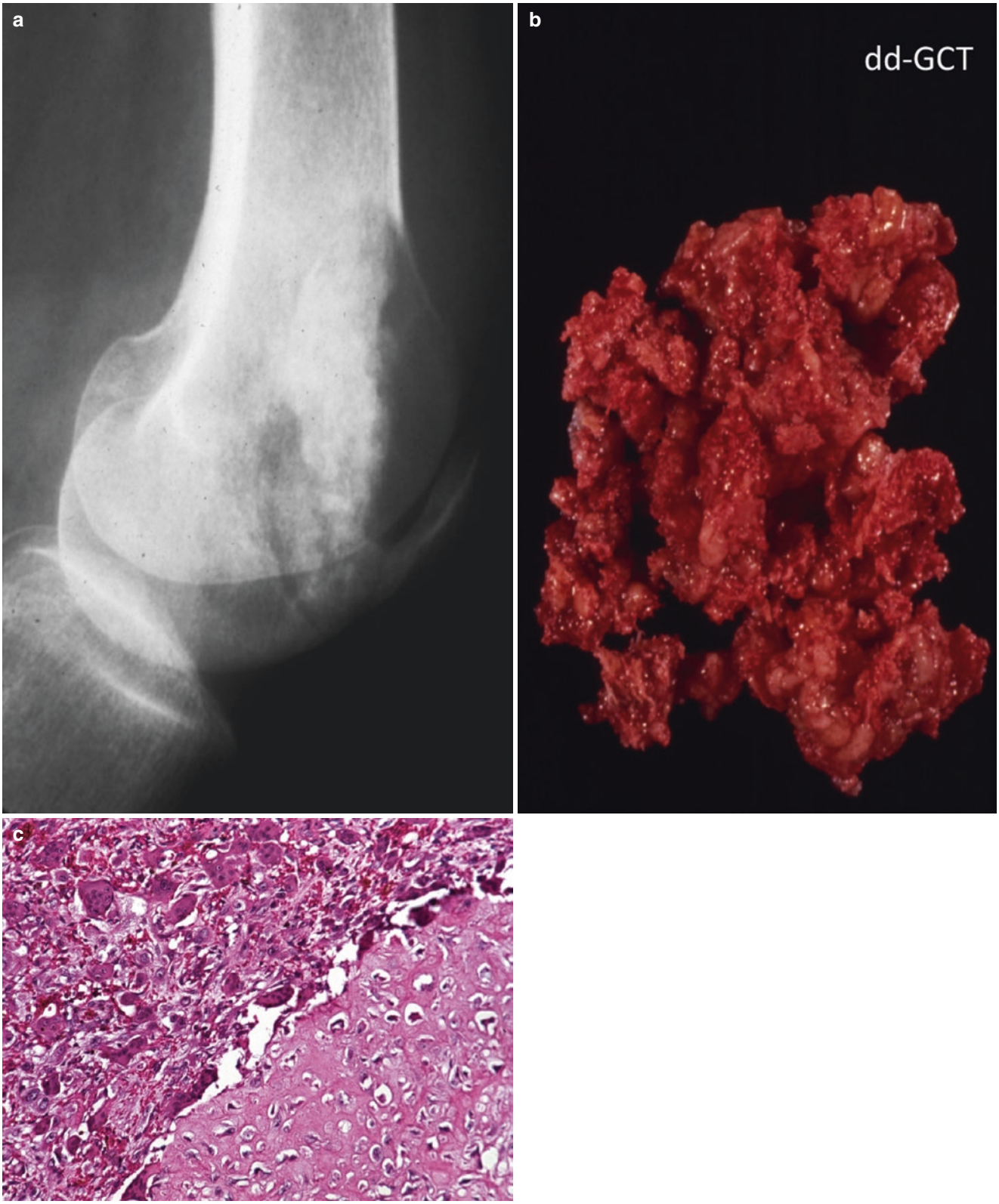

Fig. 3.192 Malignant giant cell tumor of bone: dedifferentiated giant cell tumor of bone. (**a**) Plane film (lateral) of knee. There is a mixed lytic/blastic lesion involving the distal femur. The patient had undergone prior curettage and grafting. The specimen was diagnostic of giant cell tumor of the bone. (**b**) Gross specimen: the lesion relapsed and the patient underwent a second curettage. (**c**) The lesion consisted of giant cell tumor of bone with superimposed osteosarcoma: dedifferentiated giant cell tumor of the bone. (Courtesy of A. Kevin Raymond, M.D.)

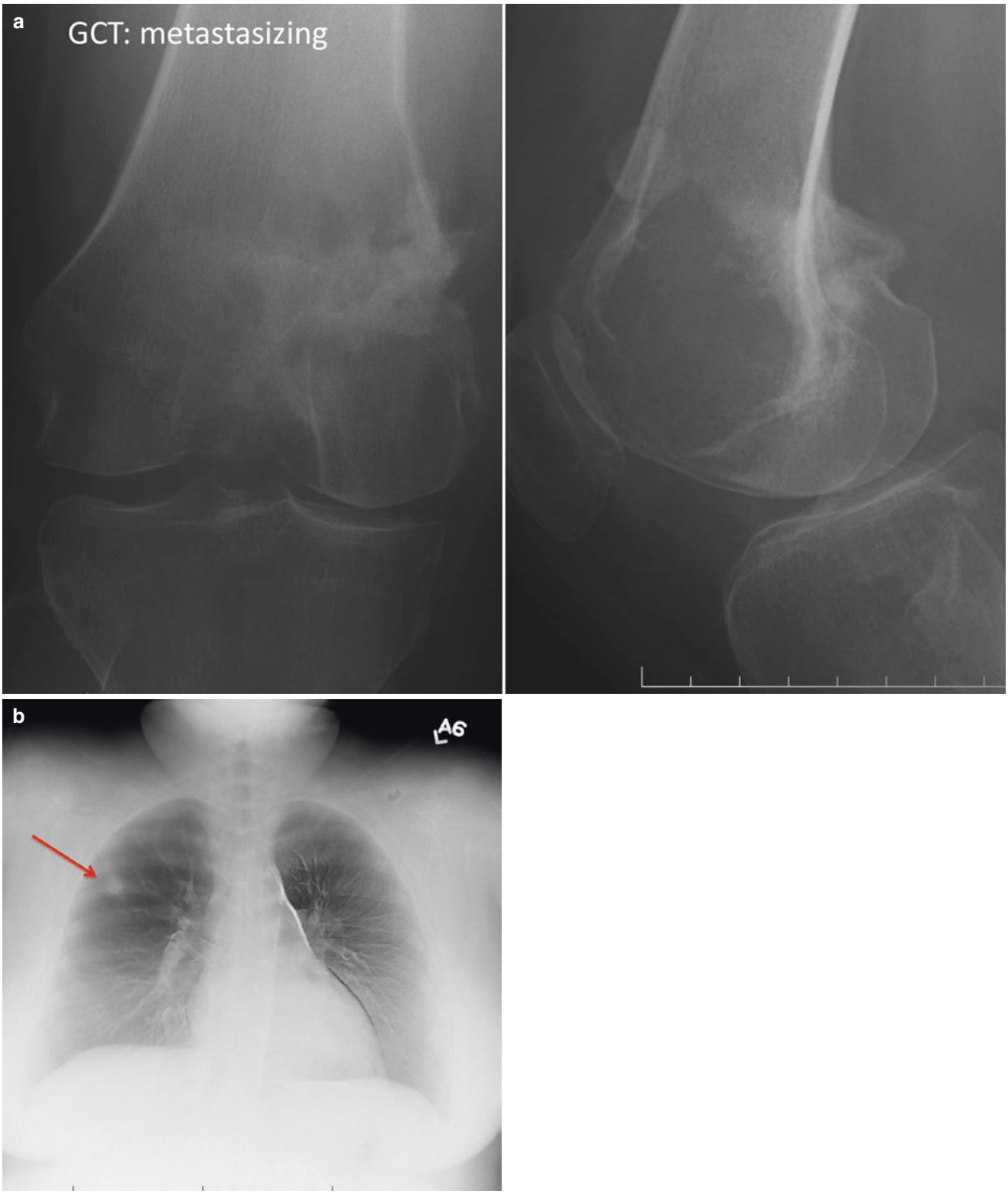

Fig. 3.193 Malignant giant cell tumor of bone: the so-called benign metastasizing giant cell tumor of bone. (**a**) Plane film (AP and lateral) knee. Other than changes of pathological fracture, the lesion is typical of giant cell tumor of bone. (**b**) Chest plane film (AP) shows metastatic disease resected and histologically confirmed as conventional giant cell tumor of bone. (Courtesy of A. Kevin Raymond, M.D.)

tion. Close correlation of clinical, radiological, and histological disciplines is a prerequisite of bone pathology; it is particularly useful in giant cell or ABC-like lesions since a significant proportion of secondary ABC cases retain the radiological features of the underlying primary pathology.

ABC may be seen over a broad age range but most frequently affects patients in their second decade and to a lesser extent the first decades of life, males and females equally. It may affect any part of any bone, both intramedullary and cortical surface, but most frequently arises within the femur, tibia, spine, and humerus. Vertebral involvement is more frequent in the posterior elements, i.e., spinous and transverse processes.

Patients most frequently present with pain that may or may not be associated with mass. Pathological fracture may occur. Additional symptoms are generally a function of lesion size, soft tissue involvement, and location. Vertebral lesions may be associated with diverse symptomatology secondary to spinal cord or nerve compression. The natural history of ABC is progressive growth, potential organ instability, and fracture. A range of treatment options have been offered; however, curettage with packing or cementation appears to offer the best chance of cure. Local relapse may occur in as many as 10–30% of cases and is virtually always cured with recurettage [17, 410, 411].

Histopathology

ABC is composed of membrane-bound, blood-filled cysts (Fig. 3.194a, b). The membranes are composed of mononuclear cells embedded in a background stroma that varies from "edematous" to fibrous. The mononuclear cells have round to oval to spindle-shaped nuclei with chromatin ranging from finely divided to heterochromatin. They have variable amounts of pink to clear cytoplasm. The underlying neoplastic cell is felt to be among the relatively non-specific appearing spindle cells. Osteoclasts may be numerous and generally most concentrated in areas of hemorrhage. Small numbers of histiocytes and lymphocytes are frequent. The spindle cells and mononuclear cells, together with osteoclasts, extend to the cyst membrane surfaces. ABC cysts are not line by endothelial cells. Degenerative changes (e.g., necrosis with inflammatory response) are generally a function of fracture.

The ABC membranes frequently contain small amounts of osteoid and bone, generally slender ramifications. Mineralized matrix with a mixed osseous/chondroid aura may be present. The latter is frequently referred to as the *blue bone* of ABC.

There may be solid areas present in ABC and these deserve special consideration. The solid areas may merely concentrations of the already described cellular elements. However, these are the areas most suspected for any underlying primary non-ABC pathology.

The differential diagnosis of ABC is similar to giant cell tumor of bone. It should also be noted that there are examples of ABC in which cyst formation is either minimal or absent. Such cases are referred to as the *solid variant of ABC*. These cases share histological properties with *giant cell reparative granuloma*, and some argue that there may be a relationship between these two pathological processes. So far, molecular analysis suggests that at least some of the lesion involving bones of the hands and feet may represent ABC.

Gross Pathology

Grossly, ABC consists of a complex mass of blood-filled cysts. With resection specimens, the overall appearance is *spongelike* imparting an appearance akin to a *bag of blood*

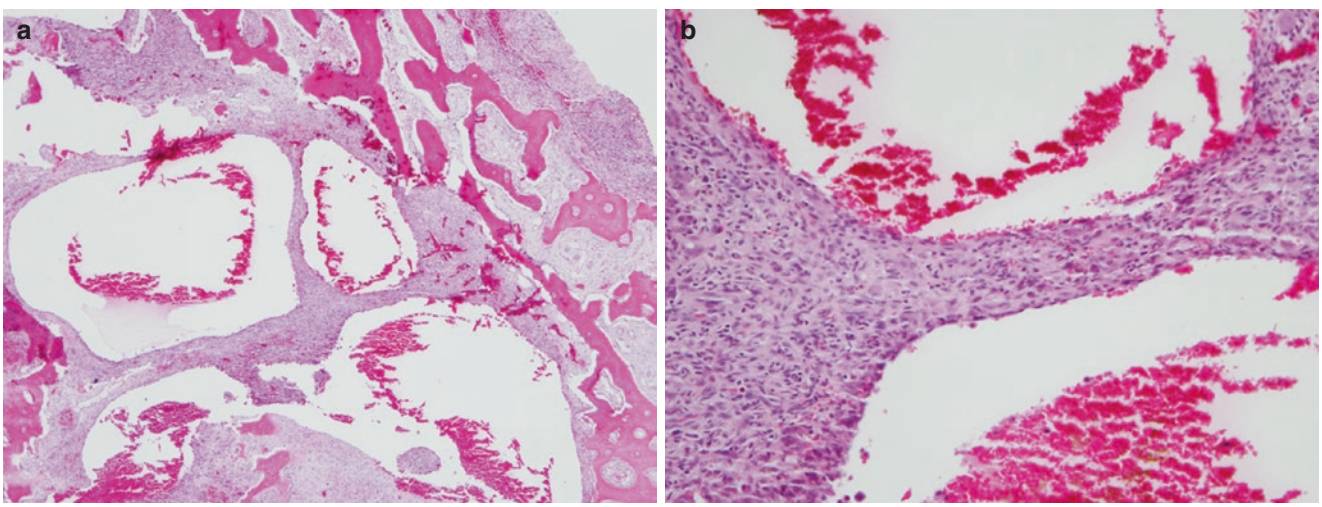

Fig. 3.194 Aneurysmal bone cyst. (**a**) ABC is a made up of undulating membranes lining blood-filled cyst (H&E 20×). (**b**) The membranes are composed of innocuous mononuclear cells and fibroblasts in a collagen background. Osteoclasts are found in areas of hemorrhage, in particular lining the interface between membranes and blood-filled cyst (H&E, 40×). (Courtesy of A. Kevin Raymond, M.D.)

(Fig. 3.195). The cysts are bound by thin, delicate, tan membranes surrounding red to red-black blood and clot. Residual cortex frequently consists of not much more that eggshell thin bone at the tumor periphery. These features may be difficult to appreciate in curetting specimens.

Again, solid areas deserve special consideration since they are the most likely sites of any underlying primary pathology in a secondary ABC.

Of interest, it has been an operating room observation that ABC does not spurt blood when surgically unroofed. The latter observation suggesting that the underlying pathological process is not vascular in origin.

Radiology

The plane film appearance of ABC is that of an eccentric occasionally central, destructive, osteolytic lesion (Fig. 3.195). The vast majority of lesions arise within the medullary cavity, but there is a small subset of tumor arising atop the cortex and beneath the periosteum. In long bones ABC tends to be a metaphyseal lesion, while vertebral lesions show preference for the posterior elements, transverse and spinous processes. ABC tends to be radiolucent, well-defined lesion with an overall *soap bubble* configuration. As opposed to giant cell tumor of the bone, which tends to have an infiltrative tumor/normal interface, the transition zone of ABC tends to be narrow, well-defined, and frequently sclerotic. The overall appearance of ABC is often described imparting a ballooned or *aneurysmal dilatation* of the tumor/normal bone [21].

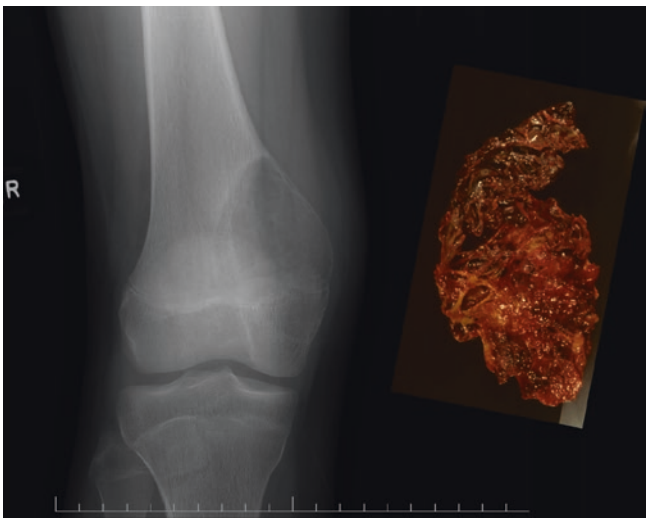

Fig. 3.195 Aneurysmal bone cyst. The plane film (AP) shows and expansile radiolucent lesion involving the distal femoral metaphysis of this skeletally immature patient. The tumor/normal interface (i.e., transition zone) is narrow, and there is sclerosis at the interface, suggesting that this is a benign or very slow-growing process and spontaneous involution and healing. (Courtesy of A. Kevin Raymond, M.D.)

CT allows greater imaging detail including analysis of the ABC internal structure and tumor/normal interface. Together with MRI, CT allows identification of solid areas within the cysts of ABC as well as defining extent of disease. MRI also allows identification of *fluid levels* within the ABC cysts (Fig. 3.196). The latter are a function of differential fluid densities and may require a period of inactivity to appear [412–414].

Giant Cell Reparative Granuloma

Definition

Giant cell reparative granuloma (GCRG) is a mixed giant cell/spindle cell lesion preferentially involving the jaw and bones of the hands and feet. Conceptualization pertaining to this family of lesions is in transition, GCRG ABC and solid ABC.

Clinical

GCRG was first described in relation to jaw lesions by Jaffe in 1953 [415]. In 1980, Lorenzo and Dorfman expanded the concept to include lesions arising in the hands and feet [416]. Interestingly, the latter authors took pains to underscore the morphological similarities between GCRG and ABC suggesting a potential common etiology. Occasional lesions

Fig. 3.196 Aneurysmal bone cyst. MRI of spine (sagittal plane). ABC has destroyed much of the sacrum. Note the linear fluid levels within the lesion

involve long bones [417]. More recently, there has been a suggestion that the extra-gnathic lesions be better classified as a form of solid aneurysmal bone cyst [10, 17, 418].

GCRG can occur as a spontaneous monostotic form or as part of a number of syndromes. The monostotic form affects patients over very broad age range, with something of a peak in the second decade. Jaws lesions tend to involve a somewhat younger population than lesions involving the hands and feet. Patients tend to present with pain and swelling. Jaw lesions tend to grow rapidly resulting in cosmetic facial deformity tooth displacement and interference with function. Regardless of site, the natural history is one of increasing size, interference with function and pathological fracture.

Where surgically accessible, curettage is the treatment of choice. Local relapse may occur and controlled with recurettage. In sites with limited surgical inaccessibility, alternative forms of treatment are (e.g., radiation therapy and rank ligand inhibitors) employed with some frequency.

Lesions morphologically similar to GCRG can be seen in a number of syndromes: cherubism (mutation in SH3BP2 gene), neurofibromatosis type 1 (mutation in NF1 gene), Noonan syndrome (mutation PTPN11 gene), and Jaffe-Campanacci syndrome [17].

Histopathology

From low power, GCRG forms a relatively well-defined cohesive mass with minimal permeation of adjacent normal bone. The predominant elements are bland spindle cells, non-specific mononuclear cells, and osteoclasts set in a collagenous background. Osteoclasts tend to be smaller and with fewer nuclei than those of giant cell tumor of the bone. In addition, osteoclasts may aggregate around areas of hemorrhage. Reactive bone is inevitably present. Secondary changes of mild chronic inflammation and hemosiderin deposition are frequent [10, 17, 415–418].

The histological differential diagnosis includes the differential diagnosis of GCT or ABC: giant cell tumor of bone, ABC, brown tumor of hyperparathyroidism, nonossifying fibroma, and ossifying fibroma.

Gross Pathology

Curettings are the expected specimen, while resection specimens are exceptional. Grossly, GCRG forms a hemorrhagic brown to tan relatively well-defined lesion (Fig. 3.197). The cut surface is friable and gritty reflecting the underlying and surrounding reactive bone and admixed normal bone. Intralesional cyst formation is frequent.

Radiology

On plane films, jaw lesions are well-defined radiolucent lesions with well-defined margins that are frequently somewhat sclerotic. Lesions may have trabeculation or septation resulting in a multiloculated lesion. With larger lesions, there is tooth displacement. CT and MRI give added detail to this cystic lesion [419].

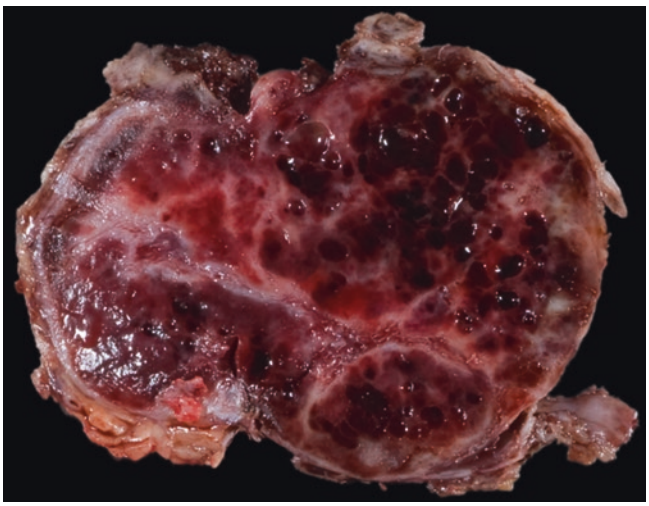

Fig. 3.197 Giant cell reparative granuloma. Tumor forms a soft red-brown to tan mass with internal partial septation. There are multiple foci of hemorrhage. (Courtesy of A. Kevin Raymond, M.D.)

References

1. Czerniak B. Dorfman and Czerniak's Bone Tumors. 2nd ed. Philadelphia: Saunders an imprint of Elsevier; 2016.
2. Raymond AK, Lazar AJ. Orthopedic Oncologic Surgical Specimen Management and Surgical Pathology. In: Lin PP, Patel S, editors. Bone Sarcoma. New York: Springer; 2013. p. 43–75.
3. Adler C-P. Bone diseases. Macroscopic, histological, and radiological diagnosis of structural changes in the skeleton. Berlin: Springer; 2000.
4. Bovée VMG, editor. Bone tumor pathology. Surgical pathology clinics. Clinics Review Articles. 2017;10(3):513–764.
5. Bullough PG. Atlas of orthopedic pathology: with clinical and radiologic correlations. Philadelphia: Lippincott Williams & Wilkins; 1992.
6. Dahlin DC. Bone tumors: general aspects and data on 6221 cases. 3rd ed. Springfield: Charles C Thomas; 1978.
7. Campanacci M, Bertoni F, Bacchini P. Bone and soft tissue tumors. New York: Springer-Verlag; 1990.
8. Fechner RE, Mills SE. AFIP Atlas of Tumor Pathology. Series 3. Washington, DC: American Registry of Pathology; 1993.
9. Fletcher CDM, Unni KK, Mertens F. In: Mertens F, editor. WHO classification of tumours of soft tissue and bone. 4th ed. Geneva: WHO Press; 2002.
10. Fletcher CDM, Bridge JA, Hogerndoorn PCW. In: Mertens F, editor. WHO classification of tumours of soft tissue and bone. 4th ed. Geneva: WHO Press; 2013.
11. Folpe AL, Inwards CY. Bone and soft tissue pathology. Foundations in diagnostic pathology. Philadelphia: Saunders Elsevier; 2010.
12. Huvos AG. Bone tumors: diagnosis, treatment, prognosis. 2nd ed. Philadelphia: W.B. Saunders; 1990.
13. Jaffe HL, Selin G. Tumors of bones and joints. Bull N Y Acad Med. 1951;27(3):165–74. PMID: 14812254.

14. Jaffe HL. Tumors and tumorous conditions of the bones and joints. Philadelphia: Lea & Febiger; 1972.
15. Klein MJ, Bonar SF, Freemont T, Vinh TN, Lopez-Ben R, Siegel HJ, Siegal GP. Atlas of nontumor pathology. Non-neoplastic diseases of bones and joints. Washington, DC: American Registry of Pathology; 2011.
16. Mirra JM, Picci P, Gold RH. Bone tumors. Clinical, radiologic, and pathologic correlations. Philadelphia: Lea & Febiger; 1998.
17. Nielsen GP, Rosenberg AE. Diagnostic pathology: bone. Philadelphia: Elsevier; 2017.
18. Spjut HJ, Fechner RE, Ackerman LV. Tumors of bone and cartilage. In: Hartmann WH, editor. Atlas of tumor pathology, series 2, fascicle 5, supplement. Washington, DC: Armed Forces Institute of Pathology; 1981.
19. Unni KK, Inwards CY, Bridge JA, Kindblom L-G, Wold LE. Tumors of the bones and joints, AFIP atlas of tumor pathology. Series 4. Washington, DC: American Registry of Pathology; 2005.
20. Unni KK, Inwards CY. Dahlin's bone tumors. General aspects and data on 10,165 cases. 6th ed. Philadelphia: Lippincott, Williams, and Wilkins; 2010.
21. Wold LE, Adler C-P, Sim FH, Unni KK. Atlas of orthopedic pathology. 2nd ed. Philadelphia: Saunders-Elsevier; 2003.
22. Garcia RA, Inwards CY, Unni KK. Benign bone tumors—recent developments. Semin Diagn Pathol. 2011;28:73–85. PMID: 21675379.
23. Bovée JV, Hogendoorn PC, Wunder JS, et al. Cartilage tumours and bone development: molecular pathology and possible therapeutic targets. Nat Rev Cancer. 2010;10:481–8.
24. Hameetman L, Bovée JV, Taminiau AH, et al. Multiple osteochondromas: clinicopathological and genetic spectrum and suggestions for clinical management. Hered Cancer Clin Pract. 2004;2:161–73.
25. Hameetman L, Szuhai K, Yavas A, et al. The role of EXT1 in nonhereditary osteochondroma: identification of homozygous deletions. J Natl Cancer Inst. 2007;99:396–406.
26. Romeo S, Hogendoorn PCW, Dei Tos AP. Benign cartilaginous tumor of bone. From morphology to somatic and germ-line genetics. Adv Anat Pathol. 2009;16:307–15.
27. Unni KK, Inwards CY, editors. Dahlin's bone tumors: general aspects and data on 10,165 cases. 6th ed. Philadelphia: Lippincott Williams & Wilkins Publishers; 2010.
28. Bell WC, Klein MJ, Pitt MJ, et al. Molecular pathology of chondroid neoplasms: part 1, benign lesions. Skeletal Radiol. 2006;35:805–13.
29. Bovée JV, van den Broek LJ, Cleton-Jansen AM, et al. Up-regulation of PTHrP and Bcl-2 expression characterizes the progression of osteochondroma towards peripheral chondrosarcoma and is a late event in central chondrosarcoma. Lab Investig. 2000;80:1925–34.
30. Fletcher CDM, Bridge JA, Hogendoorn PCW, Mertens F, Unni KK, Mertens F, editors. WHO classification of tumors of soft tissue and bone. Lyon: IARC Press; 2013.
31. Wicklund CL, Pauli RM, Johnston D, Hecht JT. Natural history study of hereditary multiple exostoses. Am J Med Genet. 1995;55(1):43–6.
32. Wuyts W, Schmale GA, Chansky HA, Raskind WH. Hereditary multiple osteochondromas. In: Pagon RA, Adam MP, Ardinger HH, Wallace SE, Amemiya A, Bean LJH, Bird TD, Fong CT, Mefford HC, Smith RJH, Stephens K, editors. Source GeneReviews® [Internet]. Seattle: University of Washington, Seattle; 1993–2016; 2000. Aug 03 [updated 2013 Nov 21].
33. Schmale GA, Conrad EU 3rd, Raskind WH. The natural history of hereditary multiple exostoses. J Bone Joint Surg Am. 1994;76(7):986–92.
34. Choi BB, Jee WH, Sunwoo HJ, Cho JH, Kim JY, Chun KA, Hong SJ, Chung HW, Sung MS, Lee YS, Chung YG. MR differentiation of low-grade chondrosarcoma from enchondroma. Clin Imaging. 2013;37(3):542–7.
35. Fletcher CDM, Unni KK, Mertens F, editors. Pathology and genetics: tumours of soft tissue and bone. Lyon: IARC Press; 2002.
36. Tallini G, Dorfman H, Brys P, Dal Cin P, de Wever I, Fletcher CD, Jonson K, Mandahl N, Mertens F, Miltelman F, Rosai J, Rydholm A, Samson I, Sciot R, van den Berghe H, Vanni R, Willén H. Correlation between clinicopathological features and karyotype in 100 cartilaginous and chordoid tumours. A report from the Chromosomes and Morphology (CHAMP) Collaborative Study Group. J Pathol. 2002;196:194–203.
37. Lichtenstein L, Hall JE. Periosteal chondroma; a distinctive benign cartilage tumor. J Bone Joint Surg Am. 1952;24 A(3):691–7.
38. Rabarin F, Laulan J, Saint Cast Y, Césari B, Fouque PA, Raimbeau G. Focal periosteal chondroma of the hand: a review of 24 cases. Orthop Traumatol Surg Res. 2014;100(6):617–20.
39. Boriani S, Bacchini P, Bertoni F, Campanacci M. Periosteal chondroma. A review of twenty cases. J Bone Joint Surg Am. 1983;65(2):205–12.
40. Nojima T, Unni KK, McLeod RA, Pritchard DJ. Periosteal chondroma and periosteal chondrosarcoma. Am J Surg Pathol. 1985;9(9):666–77.
41. Bauer TW, Dorfman HD, Latham JT Jr. Periosteal chondroma. A clinicopathologic study of 23 cases. Am J Surg Pathol. 1982;6(7):631–7.
42. deSantos LA, Spjut HJ. Periosteal chondroma: a radiographic spectrum. Skelet Radiol. 1981;6(1):15–20.
43. Nishio J, Arashiro Y, Mori S, Iwasaki H, Naito M. Periosteal chondroma of the distal tibia: computed tomography and magnetic resonance imaging characteristics and correlation with histological findings. Mol Clin Oncol. 2015;3(3):677–81. Epub 2015 Jan 22.
44. Varma DG, Kumar R, Carrasco CH, Guo SQ, Richli WR. MR imaging of periosteal chondroma. J Comput Assist Tomogr. 1991;15(6):1008–10.
45. Fletcher CDM, Bridge JA, Hogerndoorn PCW, Mertens F. In: Mertens F, editor. WHO classification of tumours of soft tissue and bone. 4th ed. Geneva: WHO Press; 2013.
46. Pansuriya TC, Kroon HM, Bovée JV. Enchondromatosis: insights on the different subtypes. Int J Clin Exp Pathol. 2010;3(6):557–69. Review.
47. Liu J, Hudkins PG, Swee RG, Unni KK. Bone sarcomas associated with Ollier's disease. Cancer. 1987;59(7):1376–85.
48. Pansuriya TC, van Eijk R, d'Adamo P, van Ruler MA, Kuijjer ML, Oosting J, Cleton-Jansen AM, van Oosterwijk JG, Verbeke SL, Meijer D, van Wezel T, Nord KH, Sangiorgi L, Toker B, Liegl-Atzwanger B, San-Julian M, Sciot R, Limaye N, Kindblom LG, Daugaard S, Godfraind C, Boon LM, Vikkula M, Kurek KC, Szuhai K, French PJ, Bovée JV. Somatic mosaic IDH1 and IDH2 mutations are associated with enchondroma and spindle cell hemangioma in Ollier disease and Maffucci syndrome. Nat Genet. 2011;43(12):1256–61.
49. Amary MF, Damato S, Halai D, Eskandarpour M, Berisha F, Bonar F, McCarthy S, Fantin VR, Straley KS, Lobo S, Aston W, Green CL, Gale RE, Tirabosco R, Futreal A, Campbell P, Presneau N, Flanagan AM. Ollier disease and Maffucci syndrome are caused by somatic mosaic mutations of IDH1 and IDH2. Nat Genet. 2011;43(12):1262–5. https://doi.org/10.1038/ng.994.
50. Fanburg JC, Meis-Kindblom JM, Rosenberg AE. Multiple enchondromas associated with spindle-cell hemangioendotheliomas. An overlooked variant of Maffucci's syndrome. Am J Surg Pathol. 1995;19(9):1029–38.

51. Pellegrini AE, Drake RD, Qualman SJ. Spindle cell hemangioendothelioma: a neoplasm associated with Maffucci's syndrome. J Cutan Pathol. 1995;22(2):173–6.
52. Schaison F, Anract P, Coste F, Pinieux G, Forest M, Tomeno B. [Chondrosarcoma secondary to multiple cartilage diseases. Study of 29 clinical cases and review of the literature].Rev Chir Orthop Reparatrice Appar Mot. 1999;85(8):834–45.
53. Schwartz HS, Zimmerman NB, Simon MA, Wroble RR, Millar EA, Bonfiglio M. The malignant potential of enchondromatosis. J Bone Joint Surg Am. 1987;69(2):269–74.
54. Verdegaal SH, Bovée JV, Pansuriya TC, Grimer RJ, Ozger H, Jutte PC, San Julian M, Biau DJ, van der Geest IC, Leithner A, Streitbürger A, Klenke FM, Gouin FG, Campanacci DA, Marec-Berard P, Hogendoorn PC, Brand R, Taminiau AH. Incidence, predictive factors, and prognosis of chondrosarcoma in patients with Ollier disease and Maffucci syndrome: an international multicenter study of 161 patients. Oncologist. 2011;16(12):1771–9.
55. Lichtenstein L, Jaffe HL. Chondrosarcoma of bone. Am J Pathol. 1943;19(4):553–89.
56. Pritchard DJ, Lunke RJ, Taylor WF, Dahlin DC, Medley BE. Chondrosarcoma: a clinicopathologic and statistical analysis. Cancer. 1980;45(1):149–57.
57. Dahlin DC, Henderson ED. Chondrosarcoma, a surgical and pathological problem; review of 212 cases. J Bone Joint Surg Am. 1956;38-A(5):1025–38.
58. Evans HL, Ayala AG, Romsdahl MM. Prognostic factors in chondrosarcoma of bone. *A clinicopathologic analysis with emphasis on histologic grading*. Cancer. 1977;40(2):818–31.
59. Eefting D, Scharage YM, Geirnaerdt MJ, Le Cessie S, Taminiau AH, Bovée JV, Hogendoorn PC, EroBoNeT consortium. Assessment of interobserver variability and histologic parameters to improve reliability in classification and grading of central cartilaginous tumors. Am J Surg Pathol. 2009;33(1):50–7.
60. Wang W-L, Hilliard NJ, Deavers MT, Lewis VO, Raymond AK. Chondrosarcomas: skip metastasis. Lab Invest. 2009;89(Suppl 1):25A.
61. Björnsson J, McLeod RA, Unni KK, Ilstrup DM, Pritchard DJ. Primary chondrosarcoma of long bones and limb girdles. Cancer. 1998;83(10):2105–19.
62. Henderson ED, Dahlin DC. Chondrosarcoma of bone—a study of two hundred and eighty-eight cases. J Bone Joint Surg Am. 1963;45:1450–8. No abstract available.
63. Lichtenstein L. Tumors of periosteal origin. Cancer. 1955;8:1060–9.
64. Bertoni F, Boriani S, Laus M, Campanacci M. Periosteal chondrosarcoma and periosteal osteosarcoma: two distinct entities. J Bone Joint Surg Br. 1982;64:370–6.
65. Chaabane S, Bouaziz MC, Drissi C, Ladeeb MF. Periosteal chondrosarcoma. AJR Am J Roentgenol. 2009;192:1–6.
66. Matsumoto K, Hukuda S, Ishizawa M, Saruhashi Y, Okabe H, Asano Y. Parosteal (juxtacortical) chondrosarcoma of the humerus associated with regional lymph node metastasis. A case report. Clin Orthop Relat Res. 1993;290:168–73.
67. Papagelopoulos PJ, Galanis EC, Mavrogenis AF, Savvidou OD, Bond JR, Unni KK, Sim FH. Survivorship analysis in patients with periosteal chondrosarcoma. Clin Orthop Relat Res. 2006;448:199–207.
68. Schajowicz F. Juxtacortical chondrosarcoma. J Bone Joint Surg. 1977;59B:473–80.
69. Kumta SM, Griffith JF, Chow LT, Leung PC. Primary juxtacortical chondrosarcoma dedifferentiating after 20 years. Skeletal Radiol. 1998;27:569–73.
70. Vanel D, De Paolis M, Monti C, Mercuri M, Picci P. Radiological features of 24 periosteal chondrosarcomas. Skeletal Radiol. 2001;30:208–12.
71. Ahmed AR, Tan TS, Unni KK, Collins MS, Wenger DE, Sim FH. Secondary chondrosarcoma in osteochondroma: report of 107 patients. Clin Orthop Relat Res. 2003;411:193–206.
72. Garrison RC, Unni KK, McLeod RA, Pritchard DJ, Dahlin DC. Chondrosarcoma arising in osteochondroma. Cancer. 1982;49(9):1890–7.
73. Lichtenstein L, Bernstein D. Unusual benign and malignant chondroid tumors of bone. Cancer. 1959;12:1142–57.
74. Bertoni F, Picci P, Bacchini P. Mesenchymal chondrosarcoma of bone and soft tissues. Cancer. 1983;52:533–41. http://www.ncbi.nlm.nih.gov/pubmed/6861090
75. Cesari M, Bertoni F, Bacchini P, et al. Mesenchymal chondrosarcoma. An analysis of patients treated at single institution. Tumori. 2007;93:423–7. http://www.ncbi.nlm.nih.gov/pubmed/18038872
76. Huvos AG, Rosen G, Dabska M, et al. Mesenchymal chondrosarcoma: a clinicopathologic analysis of 35 patients with emphasis on treatment. Cancer. 1983;51:1230–7.
77. Xu J, Li D, Lu X, Tang S, Guo W. Mesenchymal chondrosarcoma of bone and soft tissue: a systematic review of 107 patients in the past 20 years. PLoS One. 2015;10(4):e0122216.
78. Nakashima Y, Unni KK, Shives TC, et al. Mesenchymal chondrosarcoma of bone and soft tissue: a review of 111 cases. Cancer. 1986;57:2444–53.
79. Swanson PE, Lillemoe TJ, Manivel JC, et al. Mesenchymal chondrosarcoma: an immunohistochemical study. Arch Pathol Lab Med. 1990;114:943–8.
80. Wehrli BM, Huang W, DeCrombrugghe B, Ayala AG, Czerniak B. Sox9, a master regulator of chondrogenesis, distinguishes mesenchymal chondrosarcoma from other small blue round cell tumors. Hum Pathol. 2003;34:263–9.
81. Lee AF, Hayes MM, Lebrun D, et al. FLI-1 distinguishes Ewing sarcoma from small cell osteosarcoma and mesenchymal chondrosarcoma. Appl Immunohistochem Mol Morphol. 2011;19:233–8.
82. Wang L, Motoi T, Khanin R, Olshen A, Mertens F, Bridge J, Dal Cin P, Antonescu CR, Singer S, Hameed M, Bovee JV, Hogendoorn PC, Socci N, Ladanyi M. Identification of a novel, recurrent HEY1-NCOA2 fusion in mesenchymal chondrosarcoma based on a genome-wide screen of exon-level expression data. Genes Chromosomes Cancer. 2012;51(2):127–39. https://doi.org/10.1002/gcc.20937.
83. Damato S, Alorjiani M, Bonar F, et al. IDH1 mutations are not found in cartilaginous tumours other than central and periosteal chondrosarcomas and enchondromas. Histopathology. 2012;60:363–5.
84. Frassica FJ, Unni KK, Beabout JW, Sim FH. Dedifferentiated chondrosarcoma: a report of the clinicopathological features and treatment of seventy-eight cases. J Bone Joint Surg. 1986;68A:1197–205.
85. Mirra JM, Marcove RC. Fibrosarcomatous dedifferentiation of primary and secondary chondrosarcoma. J Bone Joint Surg. 1974;56A:285–96.
86. Sanerkin NG, Woods CG. Fibrosarcomata and malignant fibrous histiocytomata arising in relation to enchondromata. J Bone Joint Surg. 1979;61B:366–72.
87. Dahlin DC, Beabout JW. Differentiation of low-grade chondrosarcomas. Cancer. 1971;28:461–6.
88. Staals EL, Bacchini P, Bertoni F. Dedifferentiated central chondrosarcoma. Cancer. 2006;106(12):2682–91.
89. Munk PL, Connell DG, Quenville NF. Dedifferentiated chondrosarcoma of bone with leiomyosarcomatous mesenchymal component: a case report. Can Assoc Radiol J. 1988;39:218–20.
90. Niezabitowski A, Edel G, Roessner A, Grundmann E, Timm C, Wuisman P. Rhabdomyosarcomatous component in dedifferentiated chondrosarcoma. Pathol Res Pract. 1987;182:275–82.
91. Okada K, Hasegawa T, Tateishi U, Endo M, Itoi E. Dedifferentiated chondrosarcoma with telangiectatic osteosarcoma-like features. J Clin Pathol. 2006;59:1200–2.

92. Estrada EG, Ayala AG, Lewis V, Czerniak B. Dedifferentiated chondrosarcoma with a noncartilaginous component mimicking a conventional giant cell tumor of bone. Ann Diagn Pathol. 2002;6:159–63.
93. Bierry G, Feydy A, Larousserie F, Pluot E, Guerini H, Campagna R, Dufau-Andreu C, Anract P, Babinet A, Dietemann JL, Chevrot A, Drapé JL. Dedifferentiated chondrosarcoma: radiologic-pathologic correlation. J Radiol. 2010;91(3 Pt 1):271–9.
94. Unni KK, Dahlin DC, Beabout JW, Sim FH. Chondrosarcoma: clear-cell variant—a report of 16 cases. J Bone Joint Surg. 1976;58A:676–83.
95. Bjornsson J, Unni KK, Dahlin DC, Beabout JW, Sim FH. Clear cell chondrosarcoma of bone: observations in 47 cases. Am J Surg Pathol. 1984;8:223–30.
96. Campanacci M, Bertoni F, Laus M. Clear cell chondrosarcoma. Ital J Orthop Traumatol. 1980;6(3):365–72.
97. van Oosterwijk JG, Meijer D, van Ruler MA, van den Akker BE, Oosting J, Krenács T, Picci P, Flanagan AM, Liegl-Atzwanger B, Leithner A, Athanasou N, Daugaard S, Hogendoorn PC, Bovée JV. Screening for potential targets for therapy in mesenchymal, clear cell, and dedifferentiated chondrosarcoma reveals Bcl-2 family members and TGFβ as potential targets. Am J Pathol. 2013;182(4):1347–56.
98. Wang LT, Liu TC. Clear cell chondrosarcoma of bone: a report of three cases with immunohistochemical and affinity histochemical observations. Pathol Res Pract. 1993;189:411–5.
99. Collins MS, Koyama T, Swee RG, Inward CY. Clear cell chondrosarcoma: radiographic, computed tomographic, and magnetic resonance findings in 34 patients with pathologic correlation. Skelet Radiol. 2003;32:687–94.
100. Codman EA. Epiphyseal chondromatous giant cell tumors of the upper end of the humerus. Surg Gynecol Obstet. 1931;52:543–8.
101. Dahlin DC, Ivins JC. Benign chondroblastoma: a study of 125 cases. Cancer. 1972;30:401–13.
102. Jaffe HL, Lichtenstein L. Benign chondroblastoma of bone: a reinterpretation of the so-called calcifying or chondromatous giant cell tumor. Am J Pathol. 1942;18(6):969–91.
103. Lin PP, Thenappan A, Deavers MT, Lewis VO, Yasko AW. Treatment and prognosis of chondroblastoma. Clin Orthop Relat Res. 2005;438:103–9.
104. Green P, Whittaker RP. Benign chondroblastoma: case report with pulmonary metastasis. J Bone Joint Surg. 1975;57A:418–20.
105. Mirra JM, Ulich TR, Eckardt JJ, Bhuta S. “Aggressive” chondroblastoma: light and ultramicroscropic findings after en bloc resection. Clin Orthop. 1983;178:276–84.
106. Dancer JY, Henry SP, Bondaruk J, Lee S, Ayala AG, de Crombrugghe B, Czerniak B. Expression of master regulatory genes controlling skeletal development in benign cartilage and bone forming tumors. Hum Pathol. 2010;41:1788–93.
107. Swarts SJ, Neff JR, Johansson SL, Nelson M, Bridge JA. Significance of abnormalities of chromosomes 5 and 8 in chondroblastoma. Clin Orthop Relat Res. 1998;349:189–93.
108. Brecher ME, Simon MA. Chondroblastoma: an immunohistochemical study. Hum Pathol. 1988;19:1043–7.
109. Konishi E, Nakashima Y, Iwasa Y, Nakao R, Yanagisawa A. Immunohistochemical analysis for Sox9 reveals the cartilaginous character of chondroblastoma and chondromyxoid fibroma of the bone. Hum Pathol. 2010;41:208–13.
110. Jaffe HL, Lichtenstein L. Chondromyxoid fibroma of bone: distinctive benign tumor likely to be mistaken especially for chondrosarcoma. Arch Pathol. 1948;45:541–51.
111. Dahlin DC. Chondromyxoid fibroma of bone, with emphasis on its morphological relationship to benign chondroblastoma. Cancer. 1956;9:195–203.
112. Kyriakos M. Soft tissue implantation of chondromyxoid fibroma. Am J Surg Pathol. 1979;3:363–72.
113. Rahimi A, Beabout JW, Ivins JC, Dahlin DC. Chondromyxoid fibroma: a clinicopathologic study of 76 cases. Cancer. 1972;30:726–36.
114. Söder S, Inwards C, Müller S, Kirchner T, Aigner T. Cell biology and matrix biochemistry of chondromyxoid fibroma. Am J Clin Pathol. 2001;116:271–7.
115. Wu CT, Inwards CY, O’Laughlin S, Bock MG, Geaubout JM, Unni KK. Chondromyxoid fibroma of bone: a clinicopathologic review of 278 cases. Hum Pathol. 1998;29:438–46.
116. Sim FH, Dahlin CD, Beabout JW. Osteoid-osteoma: diagnostic problems. J Bone Joint Surg Am. 1975;57(2):154–9.
117. Akhlaghpoor S, Ahari AA, Shabestari AA, Alinaghizadeh MR. Radiofrequency ablation of osteoid osteoma in atypical locations: a case series. Clin Orthop Relat Res. 2010;468:1963–70.
118. Baruffi MR, Volpon JB, Neto JB, Casartelli C. Osteoid osteomas with chromosome alterations involving 22q. Cancer Genet Cytogenet. 2001;124:127–31.
119. Mylona S, Patsoura S, Galani P, Karapostolakis G, Pomoni A, Thanos L. Osteoid osteomas in common and technically challenging locations treated with computed tomography- tomography-guided percutaneous radiofrequency ablation. Skelet Radiol. 2010;39:443–9.
120. Rosenthal DI. Radiofrequency treatment. Orthop Clin North Am. 2006;37:475–84.
121. Hasegawa T, Hirose T, Sakamoto R, Seki K, Ikata T, Hizawa K. Mechanism of pain in osteoid osteomas: an immunohistochemical study. Histopathology. 1993;22:487–91.
122. Mungo DV, Zhang X, O’Keefe RJ, Rosier RN, Puzas JE, Schwarz EM. COX-1 and COX-2 expression in osteoid osteomas. J Orthop Res. 2002;20:159–62.
123. Cantwell CP, Obyrne J, Eustace S. Current trends in treatment of osteoid osteoma with an emphasis on radiofrequency ablation. Eur Radiol. 2004;14:607–17.
124. Dahlin DC. Johnson EW Jr Giant osteoid osteoma. J Bone Joint Surg Am. 1954;36-A(3):559–72.
125. Jaffe H. Benign osteoblastoma. Bull Hosp Joint Dis. 1956;17(2):141–51.
126. Lichtenstein L. Benign osteoblastoma: a category of osteoid-and bone-forming tumors other than classical osteoid osteoma, which may be mistaken for giant-cell tumor or osteogenic sarcoma. Cancer. 1956;9(5):1044–52.
127. Bettelli G, Tigani D, Picci P. Recurring osteoblastoma initially presenting as a typical osteoid osteoma: report of two cases. Skelet Radiol. 1991;20:1–4.
128. Bruneau M, Polivka M, Cornelius JF, George B. Progression of an osteoid osteoma to an osteoblastoma. Case report. J Neurosurg Spine. 2005;3:238–41.
129. Chotel F, Franck F, Solla F, Dijoud F, Kohler R, Berard J, Abelin Genevois K. Osteoid osteoma transformation into osteoblastoma: fact or fiction? Orthop Traumatol Surg Res. 2012;98(6):S98–S104.
130. Bertoni F, Unni KK, McLeod RA, Dahlin DC. Osteosarcoma resembling osteoblastoma. Cancer. 1985;55(2):416–26.
131. Lucas DR, Unni KK, McLeod RA, O’Conner MI, Sim FH. Osteoblastoma: clinicopathologic study of 306 cases. Hum Pathol. 1994;25:117–34.
132. Lucas DR. Osteoblastoma. Arch Pathol Lab Med. 2010;134:1460–6.
133. Mirra JM, Kendrick RA, Kendrick RE. Pseudomalignant *os*teoblastoma versus arrested osteosarcoma: a case report. Cancer. 1976;37:2005–14.
134. Bertoni F, Unni KK, Lucas DR, McLeod RA. Osteoblastoma with cartilaginous matrix. An unusual morphologic presentation in 18 cases. Am J Surg Pathol. 1993;17(1):69–74.
135. McLeod RA, Dahlin DC, Beabout JW. The spectrum of osteoblastoma. Am J Roentgenol. 1976;126:321–35.
136. Berry M, Mankin H, Gebhardt M, Rosenberg A, Hornicek F. Osteoblastoma: a 30-yearstudy of 99 cases. J Surg Oncol. 2008;98:179–83.
137. Giannico G, Holt GE, Homlar KC, Johnson J, Pinnt J, Bridge JA. Osteoblastoma characterized by a three-way transloca-

tion: report of a case and review of the literature. Cancer Genet Cytogenet. 2009;195:168–71.
138. Coventry MB, Dahlin DC. Osteogenic sarcoma; a critical analysis of 430 cases. J Bone Joint Surg Am. 1957;39-A(4):741–57; discussion, 757–8.
139. Huvos AG. Clinicopathologic spectrum of osteogenic sarcoma. Recent observations. Pathol Annu. 1979;14 Pt 1:123–44.
140. Jaffe N, Frei E 3rd, Traggis D, Bishop Y. Adjuvant methotrexate and citrovorum-factor treatment of osteogenic sarcoma. N Engl J Med. 1974;291(19):994–7. No abstract available.
141. Dahlin DC, Unni KK. Osteosarcoma of bone and its important recognizable varieties. Am J Surg Pathol. 1977;1(1):61–72. Review.
142. Eilber F, Giuliano A, Eckardt J, Patterson K, Moseley S, Goodnight J. Adjuvant chemotherapy for osteosarcoma: a randomized prospective trial. J Clin Oncol. 1987;5(1):21–6.
143. Klein MJ, Siegal GP. Osteosarcoma: anatomic and histologic variants. Am J Clin Pathol. 2006;125(4):555–81.
144. Link MP, Goorin AM, Miser AW, Green AA, Pratt CB, Belasco JB, Prichard J, Malpas JS, Baker AR, Kirpatrick JA, et al. The effect of adjuvant chemotherapy on relapse-free survival in patients with osteosarcoma of the extremity. N Engl J Med. 1986;314(25):1600–6.
145. Raymond AK, Chawala SP, Carrasco CH, Ayala AG, Fanning TV, Grice B, Armen T, Plager C, Papadopoulos NEJ, Edeiken J, Wallace S, Jaffe N, Murray JA, Benjamin RS. Osteosarcoma chemotherapy effect: a prognostic factor. Semin Diagn Pathol. 1987;4:212–36.
146. Taylor WF, Ivins JC, Dahlin DC, Edmonson JH, Pritchard DJ. Trends and variability in survival from osteosarcoma. Mayo Clin Proc. 1978;53(11):695–700.
147. Campanacci M, Bacci G, Bertoni F, Picci P, Minutillo A, Franceschi C. The treatment of osteosarcoma of the extremities: twenty year's experience at the Istituto Ortopedico Rizzoli. Cancer. 1981;48(7):1569–81.
148. Rosen G, Murphy ML, Huvos AG, Gutierrez M, Marcove RC. Chemotherapy, en bloc resection, and prosthetic bone replacement in the treatment of osteogenic sarcoma. Cancer. 1976;37(1):1–11.
149. Bacci G, Ferrari S, Forni C, Mercuri M, Picci P, Bertoni F, Capanna R, Manfrini M, Donati D, Brach Del Prever A, Baldini N. The effect of intra-arterial versus intravenous cisplatinum in the neoadjuvant treatment of osteosarcoma of the limbs: the experience at the Rizzoli Institute. Chir Organi Mov. 1996;81(4):369–82. English, Italian.
150. Rosen G, Marcove RC, Caparros B, Nirenberg A, Kosloff C, Huvos AG. Primary osteogenic sarcoma: the rationale for preoperative chemotherapy and delayed surgery. Cancer. 1979;43(6):2163–77.
151. Rosen G, Caparros B, Groshen S, Nirenberg A, Cacavio A, Marcove RC, Lane JM, Huvos AG. Primary osteogenic sarcoma of the femur: a model for the use of preoperative chemotherapy in high risk malignant tumors. Cancer Investig. 1984;2:181–92.
152. Rosen G, Caparros B, Huvos AG, Kosloff C, Nirenberg A, Cacavio A, Marcove RC, Lane JM, Mehta B, Urban C. Preoperative chemotherapy for osteogenic sarcoma: selection of postoperative adjuvant chemotherapy based on the response of the primary tumor to preoperative chemotherapy. Cancer. 1982;49(6):1221–30.
153. Picci P, Bacci G, Campanacci M, Gasparini M, Pilotti S, Cerasoli S, Bertoni F, Guerra A, Capanna R, Albisinni U, Galletti S, Gherlinzoni F, Calderoni P, Sudanese A, Baldini N, Bernini M, Jaffe N. Histologic evaluation of necrosis in osteosarcoma induced by chemotherapy: regional mapping of viable and nonviable tumor. Cancer. 1985;56:1515–21.
154. Raymond AK, Ayala AG. Specimen management after osteosarcoma chemotherapy. In: Unni KK, editor. Bone tumors. New York: Churchill Livingstone; 1988.
155. Raymond AK, Ayala AG, Carrasco H, Jaffe N, Romsdahl MM, Martin RG, Murray JA, Benjamin R. Osteosarcoma preoperative chemotherapy: specimen management. Cancer Bulletin. 1990;42:317–31.
156. Raymond AK. Surface osteosarcoma. Clin Orthop Relat Res. 1991;270:140–8.
157. Raymond AK, Simms W, Ayala AG. Osteosarcoma: management following primary chemotherapy. Hematol Oncol Clin North Am. 1995;9:841–66.
158. Weatherby RP, Unni KK. Practical aspects of handling orthopedic specimens in the surgical pathology laboratory. Pathol Annu. 1982;17:1–31.
159. Cahan WG, Woodard HQ, Higinbotham NL, Stewart FW, Coley BL. Sarcoma arising in irradiated bone: report of eleven cases. Cancer. 1948;1:3–29.
160. Huvos AG, Woodard HQ, Cahan WG, Higinbotham NL, Stewart FW, Butler A, Bretsky SS. Postradiation osteogenic sarcoma of bone and soft tissues. A clinicopathologic study of 66 patients. Cancer. 1985;55(6):1244–55.
161. Inoue YZ, Frassica FJ, Sim FH, Unni KK, Petersen IA, McLeod RA. Clinicopathologic features and treatment of postirradiation sarcoma of bone and soft tissue. J Surg Oncol. 2000;75(1):42–50.
162. Lewis VO, Raymond K, Mirza AN, Lin P, Yasko AW. Outcome of postradiation osteosarcoma does not correlate with chemotherapy response. Clin Orthop Relat Res. 2006;450:60–6.
163. Sim FH, Cupps RE, Dahlin DC, Ivins JC. Postradiation sarcoma of bone. J Bone Joint Surg Am. 1972;54(7):1479–89.
164. Weatherby RP, Dahlin DC, Ivins JC. Postradiation sarcoma of bone: review of 78 Mayo Clinic cases. Mayo Clin Proc. 1981;56(5):294–306.
165. Deyrup AT, Montag AG, Inwards CY, Xu Z, Swee RG, Krishnan UK. Sarcomas arising in Paget disease of bone: a clinicopathologic analysis of 70 cases. Arch Pathol Lab Med. 2007;131(6):942–6.
166. McKenna RJ, Schwinn CP, Soong KY, Higinbotham NL. Osteogenic sarcoma arising in Paget's disease. Cancer. 1964;17:42–66.
167. Mirabello L, Troisi RJ, Savage SA. Osteosarcoma incidence and survival rates from 1973 to 2004: data from the surveillance, epidemiology, and end results program. Cancer. 2009;115(7):1531–43. https://doi.org/10.1002/cncr.24121.
168. Porretta CA, Dahlin DC, Janes JM. Sarcoma in Paget's disease of bone. J Bone Joint Surg Am. 1957;39-A(6):1314–29.
169. Seitz S, Priemel M, Zustin J, Beil FT, Semler J, Minne H, Schinke T, Amling M. Paget's disease of bone: histologic analysis of 754 patients. J Bone Miner Res. 2009;24(1):62–9. https://doi.org/10.1359/jbmr.080907.
170. Hansen MF, Seton M, Merchant A. Osteosarcoma in Paget's disease of bone. J Bone Miner Res. 2006;21 Suppl 2:P58–63. Review.
171. Greditzer HG 3rd, McLeod RA, Unni KK, Beabout JW. Bone sarcomas in Paget disease. Radiology. 1983;146(2):327–33.
172. Wick MR, Siegal GP, Unni KK, McLeod RA, Greditzer HG 3rd. Sarcomas of bone complicating osteitis deformans (Paget's disease): fifty years' experience. Am J Surg Pathol. 1981;5(1):47–59.
173. Hadjipavlou A, Lander P, Srolovitz H, Enker IP. Malignant transformation in Paget disease of bone. Cancer. 1992;70(12):2802–8.
174. Moore TE, King AR, Kathol MH, el-Khoury GY, Palmer R, Downey PR. Sarcoma in Paget disease of bone: clinical, radiologic, and pathologic features in 22 cases. AJR Am J Roentgenol. 1991;156(6):1199–203.
175. Haibach H, Farrell C, Dittrich FJ. Neoplasms arising in Paget's disease of bone: a study of 82 cases. Am J Clin Pathol. 1985;83(5):594–600.
176. Jattiot F, Goupille P, Azais I, Roulot B, Alcalay M, Jeannou J, Bontoux D, Valat JP. Fourteen cases of sarcomatous degeneration in Paget's disease. J Rheumatol. 1999;26(1):150–5.
177. Nellissery MJ, Padalecki SS, Brkanac Z, Singer FR, Roodman GD, Unni KK, Leach RJ, Hansen MF. Evidence for a novel osteo-

sarcoma tumor-suppressor gene in the chromosome 18 region genetically linked with Paget disease of bone. Am J Hum Genet. 1998;63(3):817–24.
178. Bertoni F, Dallera P, Bacchini P, Marchetti C, Campobassi A. The Istituto Rizzoli-Beretta experience with osteosarcoma of the jaw. Cancer. 1991;68(7):1555–63.
179. Clark JL, Unni KK, Dahlin DC, Devine KD. Osteosarcoma of the jaw. Cancer. 1983;51(12):2311–6.
180. Bennett JH, Thomas G, Evans AW, Speight PM. Osteosarcoma of the jaws: a 30-year retrospective review. Oral Surg Oral Med Oral Pathol Oral Radiol Endod. 2000;90(3):323–32.
181. Doval DC, Kumar RV, Kannan V, Sabitha KS, Misra S, Vijay Kumar M, Hegde P, Bapsy PP, Mani K, Shenoy AM, Kumarswamy SV. Osteosarcoma of the jaw bones. Br J Oral Maxillofac Surg. 1997;35(5):357–62.
182. Garrington GE, Scofield HH, Cornyn J, Hooker SP. Osteosarcoma of the jaws. Analysis of 56 cases. Cancer. 1967;20(3):377–91. No abstract available.
183. Goepfert H, Raymond AK, Spires JR, Chawla SP, Wolf PF, Lee Y-Y, Batsakis JG. Osteosarcoma of the head and neck. Cancer Bulletin. 1990;42:347–54.
184. Guadagnolo BA, Zagars GK, Raymond AK, Benjamin RS, Sturgis EM. Osteosarcoma of the jaw/craniofacial region: outcomes after multimodality treatment. Cancer. 2009;115(14):3262–70. https://doi.org/10.1002/cncr.24297.
185. Demicco EG, Deshpande V, Nielsen GP, Kattapuram SV, Rosenberg AE. Well-differentiated osteosarcoma of the jaw bones: a clinicopathologic study of 15 cases. Am J Surg Pathol. 2010;34(11):1647–55.
186. Silverman G. Multiple osteosarcoma. Arch Pathol. 1936;21:88–95.
187. Mahoney JP, Spanier SS, Morris JL. Multifocal osteosarcoma: a case report with review of the literature. Cancer. 1979;44:1897–907.
188. Parham DM, Pratt CB, Parvey LS, Webber BL, Champion JC. Childhood multifocal osteosarcoma. Clinicopathologic and radiologic correlates. Cancer. 1985;55:2653–8.
189. Corradi D, Wenger DE, Bertoni F, Bacchini P, Bosio S, Goldoni M, Unni KK, Sim FH, Inwards CY. Multicentric osteosarcoma: clinicopathologic and radiographic study of 56 cases. Am J Clin Pathol. 2011;136(5):799–807.
190. Unni KK, Dahlin DC, McLeod RA, Pritchard DJ. Intraosseous well-differentiated osteosarcoma. Cancer. 1977;40:1337–47.
191. Campanacci M, Bertoni F, Capanna R, Cervellati C. Central osteosarcoma of low grade malignancy. Ital J Orthop Traurnatol. 1981;7:71–8.
192. Kurt AM, Unni KK, McLeod RA, Prichard DJ. Low-grade intraosseous osteosarcoma. Cancer. 1990;65(6):1418–28.
193. Okada K, Nishida J, Morita T, Kakizaki H, Ishikawa A, Hotta T. Low-grade intraosseous osteosarcoma in northern Japan: advantage of AgNOR and MIB-1 staining in differential diagnosis. Hum Pathol. 2000;31(6):633–9.
194. Xipell JM, Rush J. Case report. 340. Well- differentiated intraosseous osteosarcoma of the left femur. Skelet Radiol. 1985;14:312–6.
195. Yoshida A, Ushiku T, Motoi T, et al. Immunohistochemical analysis of MDM2 and CDK4 distinguishes low-grade osteosarcoma from benign mimics. Mod Pathol. 2010;23:1279–88.
196. Farr GH, Huvos AG, Marcove RC, Higinbotham NL, Foote FW Jr. Telangiectatic osteogenic sarcoma. A review of twenty-eight cases. Cancer. 1974;34(4):1150–8.
197. Matsuno T, Unni KK, McLeod RA, Dahlin DC. Telangiectatic osteogenic sarcoma. Cancer. 1976;38:2538–47.
198. Bacci G, Ferrari S, Ruggieri P, Biagini R, Fabbri N, Campanacci L, Bacchini P, Longhi A, Forni C, Bertoni F. Telangiectatic osteosarcoma of the extremity: neoadjuvant chemotherapy in 24 cases. Acta Orthop Scand. 2001;72:167–72.
199. Chawla SP, Benjamin RS. Effectiveness of chemotherapy in the management of metastatic telangiectatic osteosarcoma. Am J Clin Oncol. 1988;11:177–80.
200. Huvos AG, Rosen G, Bretsky SS, Butler A. Telangiectatic osteogenic sarcoma: a clinicopathologic study of 124 patients. Cancer. 1982;49:1679–89.
201. Larsson SE, Lorentzon R, Boquist L. Telangiectatic osteosarcoma. Acta Orthop Scand. 1978;49:589–94.
202. Weiss A, Khoury JD, Hoffer FA, Wu J, Billups CA, Heck RK, Quintana J, Poe D, Rao BN, Daw NC. Telangiectatic osteosarcoma: the St. Jude Children's Research Hospital's experience. Cancer. 2007;109:1627–37.
203. Rosen G, Huvos AG, Marcove R, Nirenberg A. Telangiectatic osteogenic sarcoma: improved survival with combination chemotherapy. Clin Orthop. 1986;207:164–73.
204. Murphey MD, wan Jaovisidha S, Temple HT, Gannon FH, Jelinek JS, Malawer MM. Telangiectatic osteosarcoma: radiologic-pathologic comparison. Radiology. 2003;229:545–53.
205. Sangle NA, Layfield LJ. Telangiectatic osteosarcoma. Arch Pathol Lab Med. 2012;136:572–6.
206. Sim FH, Unni KK, Beabout JW, Dahlin DC. Osteosarcoma with small cells simulating Ewing's tumor. J Bone Joint Surg Am. 1979;61(2):207–15.
207. Righi A, Gambarotti M, Longo S, Benini S, Gamberi G, Cocchi S, Vanel D, Picci P, Bertoni F, Simoni A, Franchi A, Dei Tos AP. Small cell osteosarcoma: clinicopathologic, immunohistochemical, and molecular analysis of 36 cases. Am J Surg Pathol. 2015;39(5):691–9. https://doi.org/10.1097/PAS.0000000000000412.
208. Ayala AG, Ro JY, Raymond AK, Jaffe N, Chawla S, Carrasco H, Link M, Jimenez J. Small cell osteosarcoma. A clinicopathologic study of 27 cases. Cancer. 1989;64(10):2162–73.
209. Noguera R, Navarro S, Triche TJ. Translocation (11;22) in small cell osteosarcoma. Cancer Genet Cytogenet. 1990;45(1):121–4. No abstract available.
210. Edeiken J, Raymond AK, Ayala AG, Benjamin RS, Murray JA, Carrasco HC. Small cell osteosarcoma. Skelet Radiol. 1987;16(8):621–8. Review.
211. Bertoni F, Present D, Bacchini P, Pignatti G, Picci P, Campanacci M. The Istituto Rizzoli experience with small cell osteosarcoma. Cancer. 1989;64(12):2591–9. Review.
212. Dickersin GR, Rosenberg AE. The ultrastructure of small-cell osteosarcoma with a review of the light microscopy and differential diagnosis. Hum Pathol. 1991;22(3):267–75.
213. Martin SE, Dwyer A, Kissane JM, Costa J. Small-cell osteosarcoma. Cancer. 1982;50(5):990–6.
214. Geschickter CF, Copeland MM. Parosteal osteoma of bone: a new entity. Ann Surg. 1951;133:790–807.
215. Dwinnell LA, Dahlin DC, Ghormley RK. Parosteal (juxtacortical) osteogenic sarcoma. J Bone Joint Surg. 1954;36A:732–44.
216. Edeiken J, Farrell C, Ackerman LV, Spjut HJ. Parosteal sarcoma. Am J Roentgenol Radium Ther Nucl Med. 1971;111(3):579–83.
217. Kaste SC, Fuller CE, Saharia A, Neel MD, Rao BN, Daw NC. Pediatric surface osteosarcoma: clinical, pathologic, and radiologic features. Pediatr Blood Cancer. 2006;47(2):152–62.
218. Campanacci M, Picci P, Gherlinzoni F, Guerra A, Neff JR. Parosteal osteosarcoma. J Bone Joint Surg Br. 1984;66:313–21.
219. Picci P, Campanacci M, Bacci G, Capanna R, Ayala A. Medullary involvement in parosteal osteosarcoma. J Bone Joint Surg Am. 1987;69(1):131–6.
220. Campanacci M, Capanna R, Stilli S. Posterior hemiresection of the distal femur in parosteal osteosarcoma. Ital J Orthop Traumatol. 1982;8(1):23–8.
221. Laitinen M, Parry M, Albergo JI, Jeys L, Abudu A, Carter S, Sumathi V, Grimer R. The prognostic and therapeutic factors which influence the oncological outcome of parosteal osteosarcoma. Bone Joint J. 2015;97-B(12):1698–703.
222. Duhamel LA, Ye H, Halai D, Idowu BD, Presneau N, Tirabosco R, Flanagan AM. Frequency of Mouse Double Minute 2 (MDM2) and Mouse Double Minute 4 (MDM4) amplification in paros-

teal and conventional osteosarcoma subtypes. Histopathology. 2012;60(2):357–9.
223. Heidenblad M, Hallor KH, Staaf J, Jönsson G, Borg Å, Höglund M, Mertens F, Mandahl N. Genomic profiling of bone and soft tissue tumors with supernumerary ring chromosomes using tiling resolution bacterial artificial chromosome microarrays. Oncogene. 2006;25:7106–16.
224. Ahuja SC, Villacin AB, Smith J, Bullough PG, Huvos AG, Marcove RC. Juxtacortical (parosteal) osteogenic sarcoma: histological grading and prognosis. J Bone Joint Surg Am. 1977;59(5):632–47.
225. Stevens GM, Pugh DG, Dahlin DC. Roentgenographic recognition and differentiation of parosteal osteogenic sarcoma. Am J Roentgenol Radium Ther Nucl Med. 1957;78(1):1–12.
226. Bertoni F, Present D, Hudson T, Enneking WF. The meaning of radiolucencies in parosteal osteosarcoma. J Bone Joint Surg. 1985;67A:901–10.
227. Sheth DS, Yasko AW, Raymond AK, Ayala AG, Carrasco CH, Benjami RS, Jaffe N, Murray JA. Conventional and dedifferentiated parosteal osteosarcoma. Cancer. 1996;78(10):2136–45.
228. Lindell MM Jr, Shirkhoda A, Raymond AK, Murray JA, Harle TS. Parosteal osteosarcoma: radiologic-pathologic correlation with emphasis on CT. AJR Am J Roentgenol. 1987;148(2):323–8.
229. Wold LE, Unni KK, Beabout JW, Sim FH, Dahlin DC. Dedifferentiated parosteal osteosarcoma. J Bone Joint Surg Am. 1984;66(1):53–9.
230. Bertoni FI, Bacchini P, Staals EL, Davidovitz P. Dedifferentiated parosteal osteosarcoma: the experience of the Rizzoli institute. Cancer. 2005;103(11):2373–82.
231. Azura M, Vanel D, Alberghini M, Picci P, Staals E, Mercuri M. Parosteal osteosarcoma dedifferentiating into telangiectatic osteosarcoma: importance of lytic changes and fluid cavities at imaging. Skelet Radiol. 2009;38(7):685–90. https://doi.org/10.1007/s00256-009-0672-3. Epub 2009 Mar 7.
232. Cardona DM, Knapik JA, Reith JD. Dedifferentiated parosteal osteosarcoma with giant cell tumor component. Skelet Radiol. 2008;37(4):367–71. https://doi.org/10.1007/s00256-007-0440-1. Epub 2008 Feb 7.
233. Shuhaibar H, Friedman L. Dedifferentiated parosteal osteosarcoma with high-grade osteoclast-rich osteogenic sarcoma at presentation. Skelet Radiol. 1998;27(10):574–7. Review.
234. Dönmez FY, Tüzün U, Başaran C, Tunaci M, Bilgiç B, Acunaş G. MRI findings in parosteal osteosarcoma: correlation with histopathology. Diagn Interv Radiol. 2008;14(3):142–52.
235. Unni KK, Dahlin DC, Beabout JW. Periosteal osteogenic sarcoma. Cancer. 1976;37:2476–85.
236. Campanacci M, Giunti A. Periosteal osteosarcoma review of 41 cases, 22 with long-term follow-up. Ital J Orthop Traumatol. 1976;2:23–35.
237. Spjut HJ, Ayala AG, deSantos LA, et al. Periosteal osteosarcoma. In: Management of primary bone and soft tissue tumors. St. Louis: Mosby; 1977.
238. Grimer RJ, Bielack S, Flege S, Cannon SR, Foleras G, Andreeff I, Sokolov T, Taminiau A, Dominkus M, San-Julian M, Kollender Y, Gosheger G, European Musculo Skeletal Oncology Society. Periosteal osteosarcoma—a European review of outcome. Eur J Cancer. 2005;41:2806–11.
239. Ritts GD, Pritchard DJ, Unni KK, Beabout JW, Eckardt JJ. Periosteal osteosarcoma. Clin Orthop. 1987;219:299–307.
240. Cesari M, Albergini M, Vanel D, Palmerini E, Stalls EL, Longhi A, Abate M, Ferrari C, Balladelli A, Ferrari S. Periosteal osteosarcoma: a single-institution experience. Cancer. 2011;117(8):1731–5.
241. Rose PS, Dickey ID, Wenger DE, Unni KK, Sim FH. Periosteal osteosarcoma: long-term outcome and risk of late recurrence. Clin Orthop Relat Res. 2006;453:314–7.
242. Murphey MD, Jelinek JS, Temple HT, Flemming DJ, Gannon FH. Imaging of periosteal osteosarcoma: radiologic-pathologic comparison. Radiology. 2004;233:129–38.
243. Righi A, Gambarotti M, Benini S, Gamberi G, Cocchi S, Picci P, Bertoni F. MDM2 and CDK4 expression in periosteal osteosarcoma. Hum Pathol. 2015;46(4):549–53.
244. deSantos LA, Murray JA, Finklestein JB, Spjut HJ, Ayala AG. The radiographic spectrum of periosteal osteosarcoma. Radiology. 1978;127:123–9.
245. Wold LE, Unni KK, Raymond AK, Dahlin DC. High grade surface osteosarcoma. Lab Invest. 1983;48:94A. (abstract).
246. Wold LE, Unni KK, Beabout JW, Pritchard DJ. High grade surface osteosarcomas. Am J Surg Pathol. 1984;8:181–6.
247. Abe K, Kumagai K, Hayashi T, Kinoshita N, Shindo H, Uetani M, Ishida T. High-grade surface osteosarcoma of the hand. Skeletal Radiol. 2007;36(9):869–73.
248. Staals EL, Bacchini P, Bertoni F. High-grade surface osteosarcoma: a review of 25 cases from the Rizzoli Institute. Cancer. 2008;112(7):1592–9.
249. Okada K, Unni KK, Swee RG, Sim FH. High grade surface osteosarcoma: a clinicopathologic study of 46 cases. Cancer. 1999;85(5):1044–54.
250. Hoshi M, Matsumoto S, Manabe J, et al. Report of four cases with high-grade surface osteosarcoma. Jpn J Clin Oncol. 2006;36:180–4.
251. Sonneland PR, Unni KK. Case report 258: high-grade "surface" osteosarcoma arising from the femoral shaft. Skelet Radiol. 1984;11:77–80.
252. Vanel D, Picci P, De Paolis M, Mercuri M. Radiological study of 12 high-grade surface osteosarcomas. Skelet Radiol. 2001;30(12):667–71.
253. Lichtenstein L, Jaffe HL. Eosinophilic granuloma of bone: with report of a case. Am J Pathol. 1940;16(5):595–604.
254. Lichtenstein L. Histiocytosis X; integration of eosinophilic granuloma of bone, Letterer-Siwe disease, and Schüller-Christian disease as related manifestations of a single nosologic entity. AMA Arch Pathol. 1953;56(1):84–102.
255. Lieberman PH, Jones CR, Steinman RM, Erlandson RA, Smith J, Gee T, Huvos A, Garin-Chesa P, Filippa DA, Urmacher C, Gangi MD, Sperber M. Langerhans cell (eosinophilic) granulomatosis. A clinicopathologic study encompassing 50 years. Am J Surg Pathol. 1996;20(5):519–52.
256. Wester SM, Beabout JW, Unni KK, Dahlin DC. Langerhans' cell granulomatosis (histiocytosis X) of bone in adults. Am J Surg Pathol. 1982;6(5):413–26.
257. Zeng K, Ohshima K, Liu Y, Zhang W, Wang L, Fan L, Li M, Li X, Wang Z, Guo S, Yan Q, Guo Y. BRAFV600E and MAP2K1 mutations in Langerhans cell histiocytosis occur predominantly in children. Hematol Oncol. 2017;35(4):845–51. https://doi.org/10.1002/hon.2344. Epub 2016 Sep 6.
258. Oberling C. Les reticulosarcomes et les reticuloendotheliosarcomes de la moelle osseuse (sarcomes d'Ewing). Bull Assoc Fr Cancer. 1928;17:259–96.
259. Boston HC, Dahlin DC, Ivans JC, Cupps RE. Malignant lymphoma (so-called reticulum cell sarcoma) of bone. Cancer. 1974;34(4):1131–7.
260. Dosoretz DE, Raymond AK, Murphy GF, Doppke KP, Schiller AL, Wang CC, Suit HD. Primary lymphoma of bone: the relationship of morphologic diversity to clinical behavior. Cancer. 1982;50(5):1009–14.
261. Ivins JC, Dahlin DC. Malignant lymphoma (reticulum sarcoma) of bone. Proc Staff Meet Mayo Clin. 1963;38:375–85. No abstract available.
262. Parker F, Jackson H. Primary reticulum cell sarcoma of bone. Surg Gynecol Obstet. 1939;68:45–53.

263. Heyning FH, Hogendoorn PC, Kramer MH, Hermans J, Kluin-Nelemans JC, Noordijk EM, Kluin PM. Primary non-Hodgkin's lymphoma of bone: a clinicopathological investigation of 60 cases. Leukemia. 1999;13(12):2094–8.
264. Mertens F, Romeo S, Bovée JV, Tirabosco R, Athanasou N, Alberghini M, Hogendoorn PC, Dei Tos AP, Sciot R, Domanski HA, Aström K, Mandahl N, Debiec-Rychter M. Reclassification and subtyping of so-called malignant fibrous histiocytoma of bone: comparison with cytogenetic features. Clin Sarcoma Res. 2011;1(1):10.
265. Li X, Xu-Monette ZY, Yi S, Dabaja BS, Manyam GC, Westin J, Fowler N, Miranda RN, Zhang M, Ferry JA, Medeiros LJ, Harris NL, Young KH. Primary bone lymphoma exhibits a favorable prognosis and distinct gene expression signatures resembling diffuse large B-cell lymphoma derived from centrocytes in the germinal center. Am J Surg Pathol. 2017;41(10):1309–21.
266. Ewing J. The classic: diffuse endothelioma of bone. Proceedings of the New York Pathological Society. 1921;12:17. Clin Orthop Relat Res. 2006;450:25–7.
267. Ewing J. Diffuse endothelioma of bone. Proc NY Pathol Soc. 1921;21:17–24.
268. Fletcher CDM, Bridge JA, Hogerndoorn PCW. WHO classification of Tumours of soft tissue and bone. 4th ed. Geneva: Editors Fredrik Mertens. WHO Press; 2013.
269. Wilkins RM, Pritchard DJ, Burgert EO Jr, Unni KK. Ewing's sarcoma of bone. Experience with 140 patients. Cancer. 1986;58(11):2551–5.
270. Bacci G, Longhi A, Barbieri E, Ferrari S, Mercuri M, Briccoli A, Versari M, Pignotti E, Picci P. Second malignancy in 597 patients with Ewing sarcoma of bone treated at a single institution with adjuvant and neoadjuvant chemotherapy between 1972 and 1999. J Pediatr Hematol Oncol. 2005;27(10):517–20.
271. Park YK, Chi SG, Park HR, Yang MH, Unni KK. Detection of t(11;22)(q24;q12) translocation of Ewing's sarcoma in paraffin embedded tissue by nested reverse transcription-polymerase chain reaction. J Korean Med Sci. 1998;13(4):395–9.
272. Nascimento AG, Unii KK, Pritchard DJ, Cooper KL, Dahlin DC. A clinicopathologic study of 20 cases of large-cell (atypical) Ewing's sarcoma of bone. Am J Surg Pathol. 1980;4(1):29–36.
273. Dahlin DC, Coventry MB, Scanlon PW. Ewing's sarcoma. A critical analysis of 165 cases. J Bone Joint Surg Am. 1961;43-A:185–92.
274. Romeo S, Bovée JV, Kroon HM, Tirabosco R, Natali C, Zanatta L, Sciot R, Mertens F, Athanasou N, Alberghini M, Szuhai K, Hogendoorn PC, Dei Tos AP. Malignant fibrous histiocytoma and fibrosarcoma of bone: a re-assessment in the light of currently employed morphological, immunohistochemical and molecular approaches. Virchows Arch. 2012;461(5):561–70. https://doi.org/10.1007/s00428-012-1306-z. Epub 2012 Sep 22.
275. Inwards CY, Unni KK, Beabout JW, Sim FH. Desmoplastic fibroma of bone. Cancer. 1991;68(9):1978–83.
276. Jaffe HL. Tumors and tumorous conditions of the bones and joints. In: Lea&Febiger, editor. Tumors and tumorous conditions of the bones and joints. Philadelphia: Lea & Febiger; 1958.
277. Nedopil A, Raab P, Rudert M. Desmoplastic fibroma: a case report with three years of clinical and radiographic observation and review of the literature. Open Orthop J. 2013;8:40–6.
278. Hauben EI, Jundt G, Cleton-Jansen AM, Yavas A, Kroon HM, Van Marck E, Hogendoorn PC. Desmoplastic fibroma of bone: an immunohistochemical study including beta-catenin expression and mutational analysis for beta-catenin. Hum Pathol. 2005;36(9):1025–30.
279. Frick MA, Sundaram M, Unni KK, Inwards CY, Fabbri N, Trentani F, Baccini P, Bertoni F. Imaging findings in desmoplastic fibroma of bone: distinctive T2 characteristics. AJR Am J Roentgenol. 2005;184(6):1762–7.
280. Gebhardt MC, Campbell CJ, Schiller AL, Mankin HJ. Desmoplastic fibroma of bone. A report of eight cases and review of the literature. J Bone Joint Surg Am. 1985;67(5):732–47.
281. Papagelopoulos PJ, Galanis E, Frassica FJ, Sim FH, Larson DR, Wold LE. Primary fibrosarcoma of bone. Outcome after primary surgical treatment. Clin Orthop Relat Res. 2000;373:88–103.
282. Papagelopoulos PJ, Galanis EC, Trantafyllidis P, Boscainos PJ, Sim FH, Unni KK. Clinicopathologic features, diagnosis, and treatment of fibrosarcoma of bone. Am J Orthop (Belle Mead NJ). 2002;31(5):253–7. Review.
283. Bertoni F, Capanna R, Calderoni P, Patrizia B, Campanacci M. Primary central (medullary) fibrosarcoma of bone. Semin Diagn Pathol. 1984;1(3):185–98.
284. Jaffe HL, Lichtenstein L. Non-osteogenic fibroma of bone. Am J Pathol. 1942;28:205–21.
285. Campanacci M, Laus M, Boriani S. Multiple non-ossifying fibromata with extraskeletal anomalies: a new syndrome? J Bone Joint Surg Br. 1983;65:627–32.
286. Mirra JM, Gold RH, Rand F. Disseminated nonossifying fibromas in association with café-au-lait spots (Jaffe-Campanacci syndrome). Clin Orthop Relat Res. 1982;168:192–205.
287. Arata MA, Peterson HA, Dahlin DC. Pathological fractures through nonossifying fibromas: review of the Mayo Clinic experience. J Bone Joint Surg Am. 1981;63:980–8.
288. Mankin HJ, Trahan CA, Fondren G, Mankin CJ. Non-ossifying fibroma, fibrous cortical defect and Jaffe-Campanacci syndrome: a biologic and clinical review. Chir Organi Mov. 2009;93:1–7.
289. Betsy M, Kupersmith LM, Springfield DS. Metaphyseal fibrous defects. J Am Acad Orthop Surg. 2004;12:89–95.
290. Bhagwandeen SB. Malignant transformation of a non-osteogenic fibroma of bone. J Pathol Bacteriol. 1966;92:562–4; Glockenberg A, Sobel E, Noel JF. Nonossifying fibroma. Four cases and review of the literature. J Am Podiatr Med Assoc. 1977;87:66–9.
291. Nelson M, Perry D, Ginsburg G, Sanger WG, Neff JR, Bridge JA. Translocation (1;4)(p31;q34) in nonossifying fibroma. Cancer Genet Cytogenet. 2003;142:142–4.
292. Jee WH, Choe BY, Kang HS, Suh KJ, Ryu KN, Lee YS, Ok IY, Kim JM, Choi KH, Shinn KS. Nonossifying fibroma: characteristics at MR imaging with pathologic correlation. Radiology. 1998;209:197–202.
293. Ritschl P, Hajek PC, Pechmann U. Fibrous metaphyseal defects: magnetic resonance imaging appearances. Skeletal Radiol. 1989;18:253–9. PMID: 2781323.
294. Ponset IV, Friedman B. Evolution of metaphyseal fibrous defects. J Bone Joint Surg. 1949;31:582.
295. Moser RP Jr, Sweet DE, Haseman DB, et al. Multiple skeletal fibroxanthomas: radiologic-pathologic correlation of 72 cases. Skelet Radiol. 1987;16:353–9. PMID: 3629279.
296. Capanna R, Bertoni F, Bacchini P, Bacci G, Guerra A, Campanacci M. Malignant fibrous histiocytoma of bone. The experience at the Rizzoli Institute: report of 90 cases. Cancer. 1984;54(1):177–87.
297. Dahlin DC, Unni KK, Matsuno T. Malignant (fibrous) histiocytoma of bone-fact or fancy? Cancer. 1977;39(4):1508–16.
298. Feldman F, Norman D. Intra- and extraosseous malignant histiocytoma (malignant fibrous xanthoma). Radiology. 2013;1972:497–9.
299. Huvos AG, Heilweil M, Bretsky SS. The pathology of malignant fibrous histiocytoma of bone. A study of 130 patients. Am J Surg Pathol. 1985;9(12):853–71.
300. Papagelopoulos PJ, Galanis EC, Sim FH, Unni KK. Clinicopathologic features, diagnosis, and treatment of malignant fibrous histiocytoma of bone. Orthopedics. 2000;23(1):59–65; quiz 66–7.
301. Nooij MA, Whelan J, Bramwell VH, Taminiau AT, Cannon S, Hogendoorn PC, Pringle J, Uscinska BM, Weeden S, Kirkpatrick A, Glabbeke M, Craft AW, European Osteosarcoma Intergroup. Doxorubicin and cisplatin chemotherapy in high-grade spindle cell sarcomas of the bone, other than osteosarcoma or malignant fibrous histiocytoma: a European Osteosarcoma Intergroup Study. Eur J Cancer. 2005;41(2):225–30.

302. Bacci G, Ferrari S, Bertoni F, Mercuri M, Forni C, Sottili S, Gasbarrini A, Tienghi A, Cesari M, Campanacci M. Neoadjuvant chemotherapy for osseous malignant fibrous histiocytoma of the extremity: results in 18 cases and comparison with 112 contemporary osteosarcoma patients treated with the same chemotherapy regimen. J Chemother. 1997;9(4):293–9.
303. Lichtenstein L, Jaffe HL. Fibrous dysplasia of a bone: condition affecting one, several or many bones, graver cases of which may present abnormal pigmentation of skin, premature sexual development, hyperthyroidism or still other extraskeletal abnormalities. Arch Pathol. 1942;33:777.
304. Dorfman HD. New knowledge of fibro-osseous lesions of bone. Int J Surg Pathol. 2010;18(3 Suppl):62S–5S.
305. Lichtenstein L. Polyostotic fibrous dysplasia. Arch Surg. 1938;36:874–98.
306. DiCaprio MR, Enneking WF. Fibrous dysplasia. Pathophysiology, evaluation, and treatment. J Bone Joint Surg Am. 2005;87:1848–64.
307. Ruggieri P, Sim FH, Bond JR, Unni KK. Malignancies in fibrous dysplasia. Cancer. 1994;73:1411–24.
308. Morioka H, Kamata Y, Nishimoto K, Susa M, Kikuta K, Horiuchi K, Sasaki A, Kameyama K, Nakamura M, Matsumoto M. Fibrous dysplasia with massive cartilaginous differentiation (fibrocartilaginous dysplasia) in the proximal femur: a case report and review of the literature. Case Rep Oncol. 2016;9(1):126–33.
309. Dal Cin P, Sciot R, Brys P, et al. Recurrent chromosome aberrations in fibrous dysplasia of the bone: a report of the CHAMP study group. CHromosomes And MorPhology. Cancer Genet Cytogenet. 2000;122:30–2.
310. Campanacci M. Osteofibrous dysplasia of long bones a new clinical entity. Ital J Orthop Traumatol. 1976;2(2):221–37.
311. Park YK, Unni KK, McLeod RA, Pritchard DJ. Osteofibrous dysplasia: clinicopathologic study of 80 cases. Hum Pathol. 1993;24(12):1339–47.
312. Campbell CJ, Hawk T. A variant of fibrous dysplasia (osteofibrous dysplasia). J Bone Joint Surg Am. 1982;64(2):231–6.
313. Kempson RL. Ossifying fibroma of the long bones. A light and electron microscopic study. Arch Pathol. 1966;82(3):218–33.
314. Sweet DE, Vinh TN, Devaney K. Cortical osteofibrous dysplasia of long bone and its relationship to adamantinoma. A clinicopathologic study of 30 cases. Am J Surg Pathol. 1992;16(3):282–90.
315. Kamineni S, Briggs TW, Saifuddin A, Sandison A. Osteofibrous dysplasia of the ulna. J Bone Joint Surg Br. 2001;83(8):1178–80.
316. Most MJ, Sim FH, Inwards CY. Osteofibrous dysplasia and adamantinoma. J Am Acad Orthop Surg. 2010;18(6):358–66.
317. Nakashima Y, Yamamuro T, Fujiwara Y, Kotoura Y, Mori E, Hamashima Y. Osteofibrous dysplasia (ossifying fibroma of long bones). A study of 12 cases. Cancer. 1983;52(5):909–14.
318. Ishida T, Iijima T, Kikuchi F, Kitagamwa T, Imamura T, Machinami R. A clinicopathological and immunohistochemical study of osteofibrous dysplasia, differentiated adamantinoma, and adamantinoma of long bones. Skelet Radiol. 1992;21(8):493–502.
319. Jung JY, Jee WH, Hong SH, Kang HS, Chung HW, Ryu KN, Kim JY, Im SA, Park JM, Sung MS, Lee YS, Hong SJ, Jung CK, Chung YG. MR findings of the osteofibrous dysplasia. Korean J Radiol. 2014;15(1):114–22. https://doi.org/10.3348/kjr.2014.15.1.114.
320. Bridge JA, Dembinski A, DeBoer J, Travis J, Neff JR. Clonal chromosomal abnormalities in osteofibrous dysplasia. Implications for histopathogenesis and its relationship with adamantinoma. Cancer. 1994;73(6):1746–52.
321. Gleason BC, Liegl-Atzwanger B, Kozakewich HP, Connolly S, Gebhardt MC, Fletcher JA, Perez-Atayde AR. Osteofibrous dysplasia and adamantinoma in children and adolescents: a clinicopathologic reappraisal. Am J Surg Pathol. 2008;32(3):363–76. https://doi.org/10.1097/PAS.0b013e318150d53e.
322. Hazelbag HM, Taminiau AH, Fleuren GJ, Hogendoorn PC. Adamantinoma of the long bones. A clinicopathological study of thirty-two patients with emphasis on histological subtype, precursor lesion, and biological behavior. J Bone Joint Surg Am. 1994;76(10):1482–99.
323. Simoni P, Scarciolla L, Mutijima E, Zobel BB. Osteofibrous dysplasia: a case report and review of the literature. Radiol Case Rep. 2011;6:1–3.
324. Hazelbag HM, Hogendoorn PC. Adamantinoma of the long bones: an anatomo-clinical review and its relationship with osteofibrous dysplasia. Ann Pathol. 2001;21(6):499–511.
325. Ueda Y, Roessner A, Bosse A, Edel G, Böcker W, Wuisman P. Juvenile intracortical adamantinoma of the tibia with predominant osteofibrous dysplasia-like features. Pathol Res Pract. 1991;187(8):1039–43; discussion 1043–4.
326. Bridge JA, Swarts SJ, Buresh C, Nelson M, Degenhardt JM, Spanier S, Maale G, Meloni A, Lynch JC, Neff JR. Trisomies 8 and 20 characterize a subgroup of benign fibrous lesions arising in both soft tissue and bone. Am J Pathol. 1999;154(3):729–33.
327. Sakamoto A, Oda Y, Iwamoto Y, et al. A comparative study of fibrous dysplasia and osteofibrous dysplasia with regard to Gs-alpha mutation at the Arg201 codon: polymerase chain reaction-restriction fragment length polymorphism analysis of paraffin-embedded tissues. J Mol Diagn. 2000;2:67–72.
328. Springfield DS, Rosenberg AE, Mankin HJ, Mindell ER. Relationship between osteofibrous dysplasia and adamantinoma. Clin Orthop Relat Res. 1994;309:234–44.
329. Taylor RM, Kashima TG, Ferguson DJ, Szuhai K, Hogendoorn PC, Athanasou NA. Analysis of stromal cells in osteofibrous dysplasia and adamantinoma of long bones. Mod Pathol. 2012;25(1):56–64. https://doi.org/10.1038/modpathol.2011.141.
330. Nakahara H, Kunisada T, Noda T, Ozaki T. Minimally invasive plate osteosynthesis for osteofibrous dysplasia of the tibia: a case report. J Orthop Surg (Hong Kong). 2010;18(3):374–7.
331. Lee RS, Weitzel S, Eastwood DM, Monsell F, Pringle J, Cannon SR, Briggs TW. Osteofibrous dysplasia of the tibia. Is there a need for a radical surgical approach? J Bone Joint Surg Br. 2006;88(5):658–64.
332. Hahn SB, Kang ES, Jahng JS, Park BM, Choi JC. Ossifying fibroma. Yonsei Med J. 1991;32(4):347–55.
333. Ross JS, Masaryk TJ, Modic MT, Carter JR, Mapstone T, Dengel FH. Vertebral hemangiomas: MR imaging. Radiology. 1987;165(1):165–9.
334. Verbeke SLJ, Bovée JVMG. Review article: primary vascular tumors of bone: a spectrum of entities? Int J Clin Exp Pathol. 2011;4(6):541–51.
335. Matsumoto K, Ishizawa M, Okabe H, Taniguchi I. Hemangioma of bone arising in the ulna: imaging findings with emphasis on MR. Skelet Radiol. 2000;29(4):231–4.
336. Wold LE, Adler CP, Sim FH, Unni KK. Atlas of orthopedic pathology. 2nd ed. Philadelphia: Saunders; 2002.
337. Rosai J, Gold J, Landy R. The histiocytoid hemangiomas. A unifying concept embracing several previously described entities of skin, soft tissue, large vessels, bone, and heart. Hum Pathol. 1979;10(6):707–30.
338. Errani C, Zhang L, Panicek DM, Healey JH, Antonescu CR. Epithelioid hemangioma of bone and soft tissue: a reappraisal of a controversial entity. Clin Orthop Relat Res. 2012;470(5):1498–506.
339. Nielsen GP, Srivastava A, Kattapuram S, Deshpande V, O'Connell JX, Mangham CD, Rosenberg AE. Epithelioid hemangioma of bone revisited: a study of 50 cases. Am J Surg Pathol. 2009;33(2):270–7.
340. Verbeke SL, Bovée JV. Primary vascular tumors of bone: a spectrum of entities? Int J Clin Exp Pathol. 2011;4(6):541–51.
341. O'Connell JX, Kattapuram SV, Mankin HJ, Bhan AK, Rosenberg AE. Epithelioid hemangioma of bone. A tumor often mistaken for low-grade angiosarcoma or malignant hemangioendothelioma. Am J Surg Pathol. 1993;17(6):610–7.

342. Ling S, Rafii M, Klein M. Epithelioid hemangioma of bone. Skelet Radiol. 2001;30(4):226–9.
343. Kleer CG, Unni KK, McLeod RA. Epithelioid hemangioendothelioma of bone. Am J Surg Pathol. 1996;20(11):1301–11.
344. Gill R, O'Donnell RJ, Horvai A. Utility of immunohistochemistry for endothelial markers in distinguishing epithelioid hemangioendothelioma from carcinoma metastatic to bone. Arch Pathol Lab Med. 2009;133(6):967–72.
345. Kulkarni KR, Jambhekar NA. Epithelioid hemangioendothelioma of bone--a clinicopathologic and immunohistochemical study of 7 cases. Indian J Pathol Microbiol. 2003;46(4):600–4.
346. Errani C, Zhang L, Sung YS, Hajdu M, Singer S, Maki RG, Healey JH, Antonescu CR. A novel WWTR1-CAMTA1 gene fusion is a consistent abnormality in epithelioid hemangioendothelioma of different anatomic sites. Genes Chromosomes Cancer. 2011;50(8):644–53.
347. Davies JD, Rees GJ, Mera SL. Angiosarcoma in irradiated postmastectomy chest wall. Histopathology. 1983;7(6):947–56.
348. Antonescu C. Malignant vascular tumors – an update. Mod Pathol. 2014;27 Suppl 1:S30–8.
349. Campanacci M, Boriani S, Giunti A. Hemangioendothelioma of bone: a study of 29 cases. Cancer. 1980;46(4):804–14.
350. O'Connell JX, Nielsen GP, Rosenberg AE. Epithelioid vascular tumors of bone: a review and proposal of a classification scheme. Adv Anat Pathol. 2001;8(2):74–82.
351. Mittal S, Goswami C, Kanoria N, Bhattacharya A. Post-irradiation angiosarcoma of bone. J Cancer Res Ther. 2007;3(2):96–9.
352. Nakanishi K, Yoshikawa H, Ueda T, Araki N, Tanaka H, Aozasa K, Nakamura H. Postradiation sarcomas of the pelvis after treatment for uterine cervical cancer: review of the CT and MR findings of five cases. Skelet Radiol. 2001;30(3):132–7.
353. Wold LE, Unni KK, Beabout JW, Ivins JC, Bruckman JE, Dahlin DC. Hemangioendothelial sarcoma of bone. Am J Surg Pathol. 1982;6(1):59–70.
354. Verbeke SL, Bertoni F, Bacchini P, Sciot R, Fletcher CD, Kroon HM, Hogendoorn PC, Bovée JV. Distinct histological features characterize primary angiosarcoma of bone. Histopathology. 2011;58(2):254–64.
355. Volpe R, Mazabraud A. Hemangioendothelioma (angiosarcoma) of bone: a distinct pathologic entity with an unpredictable course? Cancer. 1982;49(4):727–36.
356. Deshpande V, Rosenberg AE, O'Connell JX, Nielsen GP. Epithelioid angiosarcoma of the bone: a series of 10 cases. Am J Surg Pathol. 2003;27(6):709–16.
357. Miettinen M, Lindenmayer AE, Chaubal A. Endothelial cell markers CD31, CD34, and BNH9 antibody to H- and Y-antigens – evaluation of their specificity and sensitivity in the diagnosis of vascular tumors and comparison with von Willebrand factor. Mod Pathol. 1994;7(1):82–90.
358. Dunlap JB, Magenis RE, Davis C, Himoe E, Mansoor A. Cytogenetic analysis of a primary bone angiosarcoma. Cancer Genet Cytogenet. 2009;194(1):1–3.
359. Manner J, Radlwimmer B, Hohenberger P, Mössinger K, Küffer S, Sauer C, Belharazem D, Zettl A, Coindre JM, Hallermann C, Hartmann JT, Katenkamp D, Katenkamp K, Schöffski P, Sciot R, Wozniak A, Lichter P, Marx A, Ströbel P. MYC high level gene amplification is a distinctive feature of angiosarcomas after irradiation or chronic lymphedema. Am J Pathol. 2010;176(1):34–9.
360. Wenger DE, Wold LE. Malignant vascular lesions of bone: radiologic and pathologic features. Skelet Radiol. 2000;29(11):619–31. Review.
361. Palmerini E, Maki RG, Staals EL, Alberghini M, Antonescu CR, Ferrari C, Ruggieri P, Mavrogenis A, Bertoni F, Cesari M, Paioli A, Marchesi E, Picci P, Ferrari S. Primary angiosarcoma of bone: a retrospective analysis of 60 patients from 2 institutions. Am J Clin Oncol. 2014;37(6):528–34.
362. Evans HL, Raymond AK, Ayala AG. Vascular tumors of bone: a study of 17 cases other than ordinary hemangioma, with an evaluation of the relationship of hemangioendothelioma of bone to epithelioid hemangioma, epithelioid hemangioendothelioma, and high-grade angiosarcoma. Hum Pathol. 2003;34(7):680–9.
363. Mirra JM, Brien EW. Giant notochordal hamartoma of intraosseous origin: a newly reported benign entity to be distinguished from chordoma. Report of two cases. Skelet Radiol. 2001;30(12):698–709. Epub 2001 Oct 16. Review. Erratum in: Skeletal Radiol 2002 Apr;31(4):251.
364. Yamaguchi T, Suzuki S, Ishiiwa H, Ueda Y. Intraosseous benign notochordal cell tumours: overlooked precursors of classic chordomas? Histopathology. 2004;44(6):597–602.
365. Kyriakos M, Totty WG, Lenke LG. Giant vertebral notochordal rest: a lesion distinct from chordoma: discussion of an evolving concept. Am J Surg Pathol. 2003;27(3):396–406. Review.
366. Deshpande V, Nielsen GP, Rosenthal DI, Rosenberg AE. Intraosseous benign notochord cell tumors (BNCT): further evidence supporting a relationship to chordoma. Am J Surg Pathol. 2007;31:1573–7.
367. Nishiguchi T, Mochizuki K, Tsujio T, Nishita T, Inoue Y. Lumbar vertebral chordoma arising from an intraosseous benign notochordal cell tumour: radiological findings and histopathological description with a good clinical outcome. Br J Radiol. 2010;83:e49–53.
368. Yamaguchi T, Yamato M, Saotome K. First histologically confirmed case of a classic chordoma arising in a precursor benign notochordallesion: differential diagnosis of benign and malignant notochordallesions. Skelet Radiol. 2002;31:413–8.
369. Yamaguchi T, Suzuki S, Ishiiwa H, Shimizu K, Ueda Y. Benign notochordal cell tumors: a comparative histological study of benign notochordal cell tumors, classic chordomas, and notochordal vestiges of fetal intervertebral discs. Am J Surg Pathol. 2004;28(6):756–61.
370. Yamaguchi T, Watanabe-Ishiiwa H, Suzuki S, Igarashi Y, Ueda Y. Incipient chordoma: a report of two cases of early-stage chordoma arising from benign notochordal cell tumors. Mod Pathol. 2005;18:1005–10.
371. Kyriakos M. Benign notochordal lesions of the axial skeleton: a review and current appraisal. Skelet Radiol. 2011;40(9):1141–52. https://doi.org/10.1007/s00256-011-1167-6. Review.
372. Dahlin DC, MacCarty CS. Chordoma. Cancer. 1952;5(6):1170–8.
373. Dahlin DC, Unni KK. Chordoma. Arch Pathol Lab Med. 1994;118(6):596–7.
374. Heffelfinger MJ, Dahlin DC, MacCarty CS, Beabout JW. Chordomas and cartilaginous tumors at the skull base. Cancer. 1973;32(2):410–20.
375. Forsyth PA, Cascino TL, Shaw EG, Scheithauer BW, O'Fallon JR, Dozier JC, Piepgras DG. Intracranial chordomas: a clinicopathological and prognostic study of 51 cases. J Neurosurg. 1993;78(5):741–7.
376. Brooks JJ, Trojanowski JQ, LiVolsi VA. Chondroid chordoma: a low-grade chondrosarcoma and its differential diagnosis. Curr Top Pathol. 1989;80:165–81.
377. Brooks JJ, LiVolsi VA, Trojanowski JQ. Does chondroid chordoma exist? Acta Neuropathol. 1987;72(3):229–35.
378. Meis JM, Raymond AK, Evans HL, Charles RE, Giraldo AA. "Dedifferentiated" chordoma. A clinicopathologic and immunohistochemical study of three cases. Am J Surg Pathol. 1987;11(7):516–25.
379. Smith J, Reuter V, Demas B. Case report 576. Anaplastic sacrococcygeal chordoma (dedifferentiated chordoma). Skelet Radiol. 1989;18(7):561–4. No abstract available.
380. Frankl J, Grotepas C, Stea B, Lemole GM, Chiu A, Khan R. Chordoma dedifferentiation after proton beam therapy:

a case report and review of the literature. J Med Case Rep. 2016;10(1):280. Review.
381. Fleming GF, Heimann PS, Stephens JK, Simon MA, Ferguson MK, Benjamin RS, Samuels BL. Dedifferentiated chordoma. Response to aggressive chemotherapy in two cases. Cancer. 1993;72(3):714–8. Review.
382. Zhou J, Sun J, Bai HX, Huang X, Zou Y, Tan X, Zhang Z, Tang X, Tao Y, Xiao B, Zhang PJ, Yang L. Prognostic factors in patients with spinal chordoma: an integrative analysis of 682 patients. Neurosurgery. 2017;81(5):812–23.
383. Chan AC, Tsang WY, Chan GP, Lam YL, Chan MK. Dedifferentiated chordoma with rhabdomyoblastic differentiation. Pathology. 2007;39(2):277–80. No abstract available.
384. Choi YJ, Kim TS. Malignant fibrous histiocytoma in chordoma – immunohistochemical evidence of transformation from chordoma to malignant fibrous histiocytoma. Yonsei Med J. 1994;35(2):239–43.
385. Chou WC, Hung YS, Lu CH, Yeh KY, Sheu S, Liaw CC. De novo dedifferentiated chordoma of the sacrum: a case report and review of the literature. Chang Gung Med J. 2009;32(3):330–5. Review.
386. Deepali J, Jain VK, Vassishta RK, Ranjan P, Kumar Y. Adamantinoma: a clinicopathological review and update. Diagn Pathol. 2008;3:8.
387. Baker PL, Dockerty MB, Coventry MB. Adamantinomas (so called) of long bones: review of literature and report of three new cases. J Bone Joint Surg. 1954;36A:704–20.
388. Weiss SW, Dorfman HD. Adamantinoma of long bone: an analysis of nine new cases with emphasis on metastasizing lesions and fibrous dysplasia–like changes. Hum Pathol. 1977;8:141–53.
389. Keeney GL, Unni KK, Beabout JW, Pritchard DJ. Adamantinoma of long bones. A clinicopathologic study of 85 cases. Cancer. 1989;64:730–7.
390. Huvos AG, Marcove RC. Adamantinoma of long bones. Clinicopathological study of fourteen cases with vascular origin suggested. J Bone Joint Surg Am. 1975;57(2):148–54.
391. Sarita-Reyes CD, Greco MA, Steiner GC. Mesenchymal-epithelial differentiation of adamantinoma of long bones: an immunohistochemical and ultrastructural study. Ultrastruct Pathol. 2012;36:23–30.
392. Benassi MS, Campanacci L, Gamberi G, Ferrari C, Picci P, Sangiorgi L, Campanacci M. Cytokeratin expression and distribution in adamantinoma of the long bones and osteofibrous dysplasia of tibia and fibula: an immunohistochemical study correlated to histogenesis. Histopathology. 1994;25:71–6.
393. Bridge JA, Fidler ME, Neff JR, Degenhardt J, Wang C, Dorfman HD, Baker KS, Seemayer TA. Adamantinoma-like Ewing's sarcoma: genomic confirmation, phenotypic drift. Am J Surg Pathol. 1999;23(2):159–65.
394. Cohen DM, Dahlin DC, Pugh DG. Fibrous dysplasia associated with adamantinoma of the long bones. Cancer. 1962;15:515–21.
395. Eisenstein W, Pitcock JA. Adamantinoma of the tibia: an eccrine carcinoma. Arch Pathol Lab Med. 1984;108:246–50.
396. Hauben E, van den Broek, Van Marck E, Hogendoorn PC. Adamantinoma-like Ewing's sarcoma and Ewing's-like adamantinoma. The t(11;22), t(21;22) status. J Pathol. 2001;195(2):218–21.
397. Hazelbag HM, Laforga JB, Roels JH, Hogendoorn PC. Dedifferentiated adamantinoma with revertant mesenchymal phenotype. Am J Surg Pathol. 2003;27:1530–7.
398. Izquierdo FM, Ramos LR, Sanchez-Herraez S, Hernández T, de Alava E, Hazelbag HM. Dedifferentiated classic adamantinoma of the tibia: a report of a case with eventual complete revertant mesenchymal phenotype. Am J Surg Pathol. 2010;34:1388–92.
399. Kahn LB. Adamantinoma, osteofibrous dysplasia and differentiated adamantinoma. Skelet Radiol. 2003;32(5):245–58.
400. Kuruvilla G, Steiner GS. Osteofibrous dysplasia-like adamantinoma of bone: a report of five cases with immunohistochemical and ultrastructural studies. Hum Pathol. 1998;29(8):809–14.
401. Sung HW, Kuo DP, Shu WP, Chai YB, Liu CC, Li SM. Giant-cell tumor of bone: analysis of 208 cases in Chinese patients. J Bone Joint Surg. 1982;64A:755–61.
402. Bertoni F, Present D, Sudanese A, Baldini N, Bacchini P, Campanacci M. Giant-cell tumor of bone with pulmonary metastases: six case reports and a review of the literature. Clin Orthop. 1988;237:275–85.
403. Hoch B, Inwards C, Sundaram M, Rosenberg AE. Multicentric giant cell tumor of bone. Clinicopathologic analysis of thirty cases. J Bone Joint Surg Am. 2006;88:1998–2008.
404. Thomas D, Henshaw R, Skubitz K, Chawla S, Staddon A, Blay JY, Roudier M, Smith J, Ye Z, Sohn W, Dansey R, Jun S. Denosumab in patients with giant-cell tumour of bone: an open-label, phase 2 study. Lancet Oncol. 2010;11:275–80.
405. Roux S, Amazit L, Meduri G, Guiochon-Mantel A, Milgrom E, Mariette X. RANK (receptor activator of nuclear factor kappa B) and RANK ligand are expressed in giant cell tumors of bone. Am J Clin Pathol. 2002;117:210–6.
406. Jaffe HL, Lichtenstein L, Portis RB. Giant cell tumor of bone: its pathologic appearance, grading, supposed variants and treatment. Arch Pathol. 1940;30:993–1031.
407. Jaffe HL. Aneurysmal bone cyst. Bull Hosp Joint Dis. 1950;11(1):3–13.
408. Kransdorf MJ, Sweet DE. Aneurysmal bone cyst: concept, controversy, clinical presentation, and imaging. AJR Am J Roentgenol. 1995;164(3):573–80. Review.
409. Martinez V, Sissons HA. Aneurysmal bone cyst. A review of 123 cases including primary lesions and those secondary to other bone pathology. Cancer. 1988;61(11):2291–304.
410. Mankin HJ, Hornicek FJ, Ortiz-Cruz E, Villafuerte J, Gebhardt MC. Aneurysmal bone cyst: a review of 150 patients. J Clin Oncol. 2005;23(27):6756–62. Review.
411. Vergel De Dios AM, Bond JR, Shives TC, McLeod RA, Unni KK. Aneurysmal bone cyst. A clinicopathologic study of 238 cases. Cancer. 1992;69(12):2921–31.
412. Dahlin DC, McLeod RA. Aneurysmal bone cyst and other non-neoplastic conditions. Skelet Radiol. 1982;8(4):243–50.
413. Gipple JR, Pritchard DJ, Unni KK. Solid aneurysmal bone cyst. Orthopedics. 1992;15(12):1433–6.
414. Mascard E, Gomez-Brouchet A, Lambot K. Bone cysts: unicameral and aneurysmal bone cyst. Orthop Traumatol Surg Res. 2015;101(1 Suppl):S119–27.
415. Jaffe HL. Giant-cell reparative granuloma, traumatic bone cyst, and fibrous (fibro-osseous) dysplasia of the jaw bones. Oral Surg Oral Med Oral Pathol. 1953;6(1):159–75.
416. Lorenzo JC, Dorfman HD. Giant-cell reparative granuloma of short tubular bones of the hands and feet. Am J Surg Pathol. 1980;4(6):551–63.
417. Ilaslan H, Sundaram M, Unni KK. Solid variant of aneurysmal bone cysts in long tubular bones: giant cell reparative granuloma. AJR Am J Roentgenol. 2003;180(6):1681–7.
418. Bertoni F, Bacchini P, Capanna R, Ruggieri P, Biagini R, Ferruzzi A, Bettelli G, Picci P, Campanacci M. Solid variant of aneurysmal bone cyst. Cancer. 1993;71(3):729–34.
419. Agaram NP, LeLoarer FV, Zhang L, Hwang S, Athanasian EA, Hameed M, Antoescu CR. USP6 gene rearrangements occur preferentially in giant cell reparative granulomas of the hands and feet but not in gnathic location. Hum Pathol. 2014;45(6):1147–52.